The role of lamin A and emerin in mediating genome organisation

A thesis for the degree of Doctor of Philosophy

by

Lauren Sarah Godwin

School of Health Sciences and Social Care

Brunel University

July 2010

Abstract

The nuclear matrix (NM) is proposed to be a permanent network of core filaments underlying thicker fibres, present regardless of transcriptional activity. It is found to be both RNA and protein rich; indeed, numerous important nuclear proteins are components of the structure. In addition to mediating the organisation of entire chromosomes, the NM has also been demonstrated to tether telomeres via their TTAGGG repeats.

In order to examine telomeric interactions with the NM, a technique known as the DNA halo preparation has been employed. Regions of DNA that are tightly attached to the structure are found within a so-called residual nucleus, while those sequences forming lesser associations produce a halo of DNA. Coupled with various FISH methodologies, this technique allowed the anchorage of genomic regions by the NM, to be analysed. In normal fibroblasts, the majority of chromosomes and telomeres were extensively anchored to the NM. Such interactions did not vary significantly in proliferating and senescent nuclei. However, a decrease in NM-associated telomeres was detected in quiescence.

Since lamin A is an integral component of the NM, it seemed pertinent to examine chromosome and telomere NM-anchorage in Hutchinson-Gilford Progeria Syndrome (HGPS) fibroblasts, which contain mutant forms of lamin A. Indeed, genome tethering by the NM was perturbed in HGPS. In immortalised HGPS fibroblasts, this disrupted anchorage appeared to be rescued; the implications of this finding will be discussed. This study also suggested that telomere-NM interactions are aberrant in X-linked Emery-Dreifuss Muscular Dystrophy (X-EDMD), which is caused by mutant forms of emerin, another NM-associated protein.

The positioning of selected genes in control and X-EDMD cell lines was examined in un-extracted nuclei using 2D and 3D FISH. Subtle shifts in the organisation of these genes were detected in diseased cells; however, their expression levels remained unaltered. Furthermore, in order to examine the architectural integrity of the nuclear lamina in lamin A and emerin mutant cell lines, scanning electron microscopy (SEM) was

employed. This work revealed that such structures were indeed compromised in disease.

The findings presented in this thesis highlight the importance of lamin A and emerin in mediating the organisation of the genome and taken together, promote the hypothesis that dysfunctional NM dynamics may well contribute to disease pathology.

Declaration

I declare that all the work presented within this thesis was produced by me except from where stated.

Lauren Godwin

Acknowledgements

First and foremost, I am extremely grateful for the encouragement, direction and support of my PhD supervisor, Dr. Joanna Bridger. Throughout my studies, she has allowed me to fulfil my potential as a PhD scientist. I would also like to thank Dr. Ian Kill, my second supervisor, for his help, training and guidance.

I am highly thankful to Dr. Joanna Bridger for arranging the financial support which funded my PhD research. In terms of funding, I would like acknowledge and thank the EU FP6 Programme (Eurolaminopathies), Brunel University and the Progeria Research Fund.

I would like to thank Professor Christopher Hutchison and Dr. Martin Goldberg for welcoming me into their laboratories as a visiting scientist. Dr. Martin Goldberg's electron microscopy training was invaluable; without which, I could not have produced the data presented in chapter 6 of this thesis. I am grateful to numerous scientists for providing a number of cell lines which I have used during my PhD: Professor CJ Hutchison (AP, KK, TR, 99P0598, 99P0599, Y259X), Professor Manfred Wehnert (G12660), Professor Glenn Morris (ED5364), Professor Richard Faragher (TAG06297) and Dr. Christopher Parris (UACC 903).

I would like to acknowledge the laboratory support I received during my PhD studies. Firstly to Dr. Ishita Mehta, who assisted in the maintenance of various HGPS cultures. I would also like to thank Miss Elisa Garimberti for showing me how to generate single-gene probes. For general laboratory support during my studies, I am grateful to Dr. Helen Foster, Ms. Denise May and Ms. Helen Cox.

I could not have survived my PhD without the support of my friends at Brunel, especially Dr. Helen Foster, Miss Elisa Garimberti and Mr Andrew McVean. Last, but by no means least, I would like to thank my family for providing infinite love and support throughout my PhD studies. In particular, I will always be endebted to my husband, David, for putting up with my erratic working hours and moods! Thank you.

Abbreviations

2D = 2 dimensional

3D = 3 dimensional

4C = Chromosome conformation capture-on-chip

53BP1 = p53 binding protein 1

A = Adenine

AD = Autosomal dominant

APC = Adenomatous polyposis coli

APD = Accumulated population doublings

APL = Acquired Partial Lipodystrophy

BAC = Bacterial Artificial Chromosome

BAF = Barrier to autointegration

BCIP = 5-bromo-4-chloro-3-indolyl-phosphate

Biotin-16-dUTP = Biotin-16-2'-deoxy-uridine-5'-triphosphate

bp = Base pair

BrdU = Bromodeoxyuridine

BSA = Bovine serum albumin

Btf = Bcl-2-associated transcription factor

C = Cytosine

CCD = Charge-coupled device

cDNA = Complementary DNA

ChiP = Chromatin immunoprecipitation

CMT = Charcot-Marie Tooth

CT = Chromosome territory

CTE = Chromosome territory edge

Cy3 = Indocarbocyanine

DAPI = 4', 6-diamidino-2-phenylindole

DEPC = Diethyl pyrocarbonate

DHB = DNA halo buffer

DMEM = Dulbecco's Modified Eagle Medium

DNA = Deoxyribonucleic acid

DNase = Deoxyribonuclease

dNTP = Deoxynucleoside-triphosphate

DOP-PCR = Degenerate oligonucleotide primed polymerase chain reaction

DSB = Double strand breaks

E = Exon

EDMD = Emery-Dreifuss Muscular Dystrophy

EDTA = Ethylenediaminetetra-acetic acid

EM = Electron microscopy

ER = Endoplasmic reticulum

FACE = Farnesylated protein-converting enzyme 2

FBS = Fetal bovine serum

feSEM = Field emission scanning electron microscopy

FISH = Fluorecence *in situ* hybridisation

FITC = Fluorescein isothiocyanate

FLPD = Dunnigan-Type Familial Partial Lipodystrophy

FrdU = Fluorodeoxyuridine

FT/FTase = Farnesyltransferase

FTI = Farnesyltransferase inhibitor

HGPS = Hutchinson-Gilford progeria syndrome

g = g-force

G = Guanine

G_0 = Quiescence

GCL = Germ cell-less

GFP = Green fluorescent protein

GGT = Geranylgeranyltransferase

GGTI = Geranylgeranyltransferase inhibitor

HDF = Human dermal fibroblast

HIV = Human immunodeficiency virus

HP1 = Heterochromatin protein 1

HSC = Haematopoetic stem cell

ICD = Interchromatin domain

INM = Inner nuclear membrane

kb = Kilobase

LAD = Lamina-associated domain

LAP = Lamina-associated polypeptide

LBR = Lamin B Receptor

LEM = LAP2-emerin-MAN1

LINC = linker of nucleoskeleton and cytoskeleton

LIS = Lithium di-iodosalicylic acid

MAD = Mandibuloacral Dysplasia

MAPK = Mitogen-activated protein kinase

MAR = Matrix attachment region

MEF = Mouse embryonic fibroblast

MMCT = Microcell-mediated chromosome transfer

mRNA = Messenger ribonucleic acid

MSC = Mesenchymal stem cells

n = Number

NBP = Aminobisphosphonate

NCS = Newborn calf serum

NCT = Nitroblue tetrazolium

NE = Nuclear envelope/ edge

NHEJ = Non-homologous end joining

NL = Nuclear lamina

nm = Nanometer

NM = Nuclear matrix

NMP = Nuclear matrix protein

NPC = Nuclear pore complex

NS = Nucleoskeleton

OsO_4 = Osmium tetroxide

ONM = Outer nuclear membrane

PBS = Phosphate buffered saline

PCR = Polymerase chain reaction

PFA = Paraformalydehyde

PHA = Pelger-Huet Anomaly

PNA = Peptide nucleic acid

pRb = Retinoblastoma protein

RD = Restrictive Dermopathy

RIDGE = Regions of increased gene expression

RNA = Ribonucleic acid

RNase = Ribonuclease

rRNA = Ribosomal RNA

RT= Revese transcription

SAF-A = Scaffold attachment factor-A

SAF-B = Scaffold attachment factor-B

SAR = Scaffold attachment region

SDS = Sodium dodecyl sulphate

SEM = Scanning electron microscopy/ Standard error mean

snRNA = Small nuclear ribonucleic acid

SREBP1 = Sterol response element binding protein 1

SSC = Saline sodium citrate

TBE = Tris-borate EDTA

TBS = Tris-buffered saline

T = Thymine

TIFF = Tagged Image File Format

TRITC = Tetramethylrhodamine isothiocyanate

TRF1 = Telomere repeat binding factor 1

tRNA = Transfer RNA

UV = Ultraviolet

VSMC = Vascular smooth muscle cells

v/v = Volume/ volume

WS = Werner's Syndrome

w/v = Weight/ volume

X-EDMD = X-linked Emery-Dreifuss Muscular Dystrophy

Table of Contents

Table of Figures

Chapter 1

Chapter 2

Chapter 3

Chapter 4

Chapter 5

Chapter 6

Table of Tables

1. Introduction

(Partially published in Elcock and Bridger, 2008; Elcock and Bridger, 2010)

1.1 INTRODUCTION

Since the discovery that inner nuclear membrane proteins could cause disease, interest in nuclear structures and their functions has increased tremendously. As a result, evidence has accumulated which demonstrate that these structures participate in a multitude of cellular processes and indeed, are required for them to proceed accurately and efficiently. However, although considerable progress has been made in this field in the last decade, there are still substantial gaps in our knowledge. This fact is highlighted by our understanding of the nuclear lamina; many of its functions have been documented and detailed, yet, comprehension of how a defective lamina can lead to the array of lamina-associated diseases observed is poor. In light of this, this review intends to provide an overview of nuclear structure, highlighting specific diseases caused by lamin mutations; subsequently, potential disease mechanisms will be discussed, considering those therapeutic options available.

1.2 NUCLEAR STRUCTURE

1.2.1 Nuclear Envelope

In the eukaryotic cell, nuclear and cytoplasmic activities are separated by the nuclear envelope (NE); between the two membranes of this structure sits the perinuclear space. The outer nuclear membrane (ONM) is continuous with the endoplasmic reticulum (ER) while the inner nuclear membrane (INM) is lined by the nuclear lamina (NL), which is instrumental in organising nuclear pore complex (NPC) localisation (Aebi et al., 1986; Gerace and Burke, 1988; Goldberg and Allen, 1996; Ris, 1997). A model of lamina organisation was originally proposed by Aebi and colleagues (1986), who using *Xenopus* oocytes, suggested that 2 sets of parallel 10 nm lamin filaments, with a repeat distance of 50 nm, are orthogonally arranged along the inner face of the NE. While this has been the accepted model for many years, Goldberg et al. (2008a) have recently put forward a modified version. They propose that the NL comprises of a single set of parallel filaments, 8–10 nm in diameter which are linked by 5 nm uncharacterised cross connections. Unlike the Aebi model, the filaments are predicted to be more tightly packed, with a repeat distance of 15 nm instead of 50 nm (Goldberg et al.,

2008a). It is primarily composed of the intermediate filament type V proteins known as nuclear lamins (McKeon et al., 1986). Following the discovery that these were nuclear-based (Aaronson and Blobel, 1975), immunolabeling identified them as INM proteins (Gerace et al., 1978).

1.2.2 Nuclear Lamins

1.2.2.1 Introduction

Both A-type and B-type lamins exist; while A-type lamins are expressed mainly in differentiated somatic cells, B-type lamins are generally ubiquitous (Lehner et al., 1987). Historically, it has been suggested that A-type lamin expression correlates with the onset of differentiation pathways (Lehner et al., 1987; Rober et al., 1989; Goldman et al., 2002; Hutchison and Worman, 2004). However, it is becoming clear that these proteins are present early in embryogenesis; this has been shown in murine (Schatten et al., 1985), sea urchin (Schatten et al., 1985) and porcine embryos (Foster et al., 2007). In contrast, the necessity for B-type lamins is not disputed; they have been identified as essential. Their loss induces apoptosis and prevents cell growth; however, *lmna*$^{-/-}$ mice develop normally (Sullivan et al., 1999; Harbourth et al., 2001). Nuclear lamins are evolutionarily conserved and as a result, are seen in an array of phylogenies (for review, see Hutchison, 2002).

1.2.2.2 Lamin encoding genes

The major A-type lamins are lamin A and C; in humans, these are encoded at equal frequency by the *LMNA* gene through alternate splicing. It is the activation of an alternate splice site in intron 10 which leads to lamin C's production (Fisher et al., 1986). While the two isoforms share the primary 566 residues, their C-termini differ (Lin and Worman, 1993). It is not yet understood why, in evolutionary terms, these two isoforms are produced since mice producing exclusively lamin C are apparently healthy and fertile. This finding indicates that lamin A is perhaps dispensable (Fong et al., 2006).

Two other proteins, lamin C2 and lamin AΔ10, can also be encoded by this gene locus. However, their expression is somewhat restricted to certain cell types; meiosis-specific lamin C2 is found only in spermatocytes whereas, AΔ10 is confined to a few carcinoma cell lines (Alsheimer and Benavente, 1996). Interestingly, the latter product results from the deletion of exon 10, through alternate splicing (Hutchison, 2002) and is found to localise at the NE (Broers et al., 1999). In contrast, the human B-type lamins are generated by two separate genes. *LMNB1* produces lamin B1 (Lin and Worman, 1995), while lamin B2 and B3 are the products of *LMNB2* (Biamonti et al., 1992).

For years, it was assumed that lamin proteins were restricted to the nuclear periphery of the interphase nucleus (e.g. Gerace et al., 1978) however, this appears not to be the case. Immunofluorescence has revealed the presence of an internal, diffuse lamin network; these speckles are absent from nucleolar regions and most prominent during nuclear growth (Goldman et al., 1992; Bridger et al., 1993; Hozak et al., 1995; Broers et al., 1999; Barboro et al., 2002).

1.2.2.3 Post-translation modifications of lamin proteins

Lamin proteins consist of 3 domains; an amino terminal head domain, a central helical rod domain and lastly, a carboxy-terminal globular domain. The central rod domain is divided into 4 sub-domains, denoted 1A, 1B, 2A and 2B; these are separated by the linkers, L1, L12 and L2 (Parry and Steinert, 1999). L1 and L2 are highly conserved, indicating their potential significance in lamin function and structure (Conway and Parry, 1988). These polypeptides go on to form parallel, coiled-coil dimers; the two molecules interact through their alpha-helical rod domains. Subsequently, these dimers assemble into polar, head-to-tail polymers (Strelkov et al., 2004; for review, see Herrmann et al., 2007).

Present at the C-terminus is a highly conserved CAAX motif (c, cysteine; aa, 2 aliphatic residues; x, any amino acid) which is absent in both lamin C and C2 (see figure 1.1). This sequence acts as a signal to indicate that farnesylation can proceed. Indeed, during post-translational modifications, a farnesyl group is added to the cysteine residue by a farnesyltransferase (Beck et al., 1990). This farnesyl group is required for

pre-lamin A's integration into the inner nuclear membrane (Lutz et al., 1992; Hennekes and Nigg, 1994). Following this, cleavage of the terminal AAX residues occurs; which is catalysed by the zinc metalloproteinase, ZMPSTE24, also denoted as FACE1 in humans (Sinensky et al., 1994). This event exposes the farnesylated cysteine which subsequently undergoes carboxymethylation; a step catalysed by isoprenylcysteine carboxyl methyl transferase (ICMT). To produce mature lamin A, this aforementioned cysteine plus the other terminal 14 amino acids must be removed by a second cleavage event; this again requires ZMPSTE24 (see figure 1.1). If the farnesyl group is not cleaved, the protein remains associated with the NE and is not released and inserted into the NL (Holtz et al., 1989; Hennekes and Nigg, 1994). Since lamin C lacks this specific CAAX motif, it does not undergo these post-translational modifications (Fisher et al. 1986).

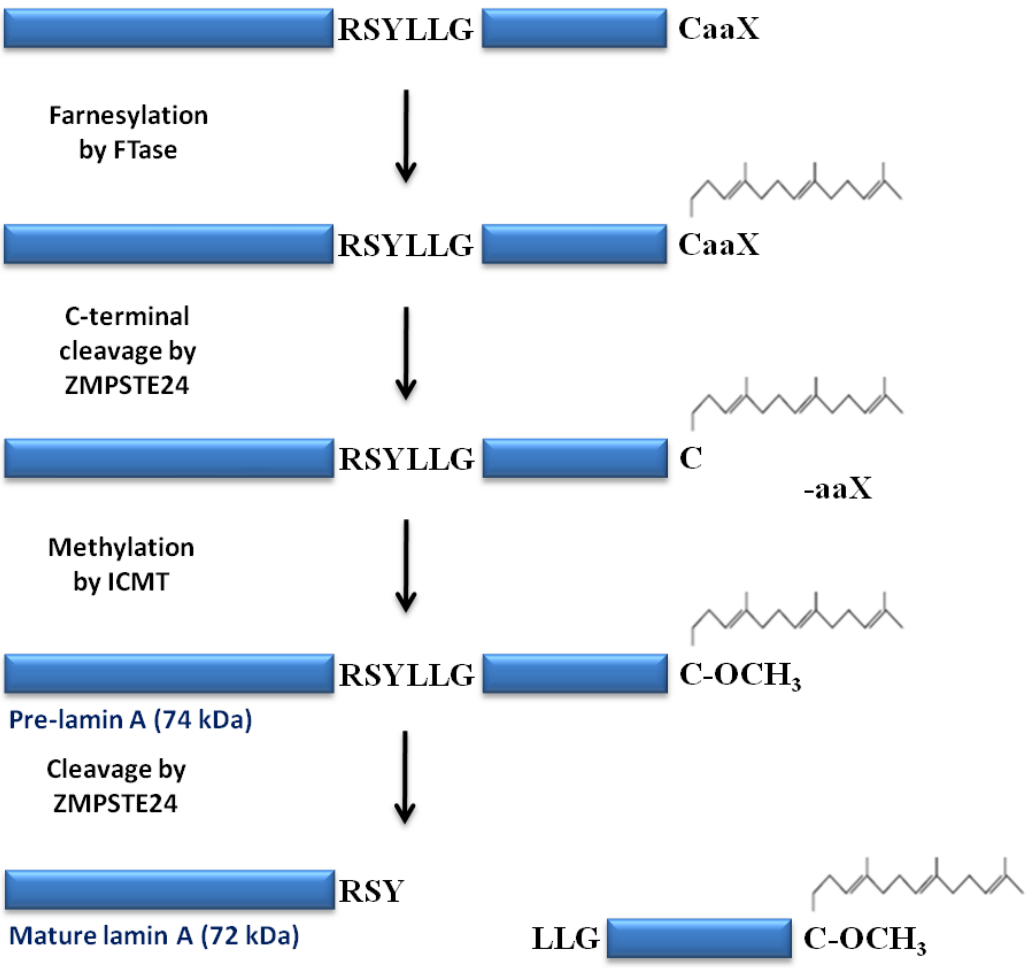

Figure 1.1: Lamin A processing in normal cells

FTase = farnesyltransferase; ICMT = isoprenylcysteine carboxyl methyl transferase.

1.2.2.4 Functions of nuclear lamins

1.2.2.4.1 Genome organisation

In addition to the structural properties of the NL, lamins are implicated in numerous other important nuclear functions. Perhaps most significantly is their role in mediating chromatin organisation; A- and B- type lamins have been demonstrated to bind DNA *in vitro* (Shoeman and Traub, 1990; Luderus et al., 1992; Stierle et al., 2003) and core histones (Taniura et al., 1995). Indeed, around 500 genes have been shown to interact with the NL in *Drosophila* (Pickersgill et al., 2006). Research using human fibroblasts reveals that over 1,300 distinct genomic sites associate with this peripheral structure; such regions have thus been termed lamina-associated domains (LADs; Guelen et al., 2008). These LADs are generally characterised by low expression levels (Guelen et al., 2008) which concurs with the observation that NL-associated genes in *Drosophila* are found to be transcriptionally silent (Pickersgill et al., 2006). Taken together, the findings suggest that the NL is an area of transcriptional repression.

1.2.2.4.2 Signalling pathways: transcription, proliferation and differentiation factors

Both A- and B-type lamins also sequester transcription factors to the nuclear periphery, thus regulating their transcriptional activity. One such protein is c-fos; this protein is a member of the AP-1 transcription factor complex, a dimeric complex which regulates gene transcription. Significantly, c-fos is recruited to the NE through lamin A/C binding; importantly, this tethering is found to suppress the onset of c-fos mediated transcription (Ivorra et al., 2006; Gonzalez et al., 2008). Phosphorylation of c-fos by the mitogen activated protein kinase (MAPK), ERK1/2, is demonstrated to release c-fos from its inhibitory interaction with lamin A/C which, in turn induces the transcription of AP-1 target genes (Gonzalez et al., 2008). A similar role for B-type lamins has also been demonstrated; lamin B1 is found to sequester Oct-1, a transcription factor which regulates the expression of genes involved in oxidative stress response pathways (Malhas et al., 2009). Further strengthening their role in signalling pathways, reports have revealed that nuclear lamins also interact with the kinase, JIL-1 (Bao et al., 2005), the transcription factor, MOK2 (Dreuillet et al., 2002; Dreuillet et al., 2008), the tumour suppressor, ING1 (Han et al., 2008) and also the

enzyme, 12-lipoxygenase (12-LOX; Tang et al., 2000). In addition, lamin A associates with lamina-associated polypeptide 2 alpha (LAP2α; described later) and the retinoblastoma protein (pRb) to form a complex, which prevents the degradation of the latter (Ozaki et al., 1994; Johnson et al., 2004). This is significant since pRb is a key tumour suppressor protein which acts to regulate cell cycle progression.

Lamin A is also demonstrated to interact with factors involved in cellular differentiation. Indeed, the sterol response element binding protein 1 (SREBP1) is found to bind to both mature and immature lamin A (Lloyd et al., 2002; Capanni et al., 2005). This is of interest since SREBP1 regulates the expression of genes involved in adipocyte differentiation, such as the peroxisome proliferator-activated receptor gamma (PPARγ; Fajas et al., 1998). Furthermore, lamin A participates in muscle differentiation pathways; the ectopic expression of lamin A leads to a transient increase in the transcription of muscle-specific genes (Lourim and Lin, 1989). Additionally, the protein is present in the speckles of proliferating skeletal-muscle cells, while absent in those actively differentiating (Muralikrishna et al., 2001). Moreover, A-type lamins interact with both cyclin D3, a cyclin involved in muscle differentiation (Mariappan et al., 2007).

1.2.2.4.3 Transcription and DNA replication

The activity of RNA polymerase II, an enzyme which catalyzes transcription, is inhibited by the presence of a dominant negative lamin mutant. This highlights the need for intact lamin organisation during mRNA synthesis (Spann et al., 2002). Since this finding was demonstrated using *Xenopus* cell free extracts, it has been suggested that the inhibitory effect observed results from lamin B loss as this amphibian only expresses B-type lamins (Stick et al., 1985). Lamin A has also been implicated in supporting RNA splicing (Jagatheesan et al., 1999).

Various studies demonstrate a link between lamin proteins and DNA replication; indeed, their highly conserved tail motifs directly bind to proliferating cell nuclear antigen (PCNA; Shumaker et al., 2008), which acts to mediate the interaction between DNA polymerase and DNA (Lee and Hurwitz, 1990). Furthermore, B-type lamins are

necessary for efficient DNA replication; this has been mainly proven by the manipulation of *Xenopus* egg extracts (Newport et al., 1990; Meier et al., 1991; Goldberg et al., 1995; Ellis et al., 1997). When lamin B_3 is depleted from egg extracts, the initiation of DNA replication is inhibited until its re-introduction (Goldberg et al., 1995). Furthermore, lamin B is seen to co-localise with replication sites (Moir et al., 1994; Philimonenko et al., 2006). Ellis et al. (1997) report that lamin proteins are required for the production of replication foci; they propose elongation can proceed in their absence. Despite this finding, other studies demonstrate that this is not the case (Moir et al., 1994; Moir et al., 2000).

1.2.3 Other INM Proteins

1.2.3.1 LEM domain proteins

Numerous other INM proteins have been identified, many of which interact with lamins and/or chromatin (figure 1.2). Several of these belong to the LAP2-emerin-MAN1 (LEM) domain family; a group of proteins which share a conserved motif, ~40 amino acids in length (Lin et al., 2000; Cai et al., 2001; Laguri et al., 2001; Wolff et al., 2001). In mammalian cells, 4 such LEM proteins have been characterised: LAP2, emerin, MAN1 and NET25/LEM2 (Schirmer et al., 2003; Wilson and Foisner, 2010). The LEM domain binds the 10 kDa barrier-to-autointegration factor (BAF), a DNA cross-linking protein and thus mediates chromatin interactions (Lee and Craigie, 1998; Segura-Totten and Wilson, 2004; Margalit et al., 2005). Importantly, lamin A also interacts with BAF, although the avidity of such binding is less than that seen for BAF-LEM complexes (Holaska et al., 2003; Margalit et al., 2007).

1.2.3.2 Emerin

Emerin is an integral INM protein (Nagano et al., 1996) whose expression is almost ubiquitous; it is detected in all human cells apart from those non-myocytes found in the heart (Manilal et al., 1996). Its correct nuclear localisation requires A-type lamins since they are found to anchor emerin at the NE; indeed, in cells lacking functional A-type lamins, the protein is mislocalised to the ER (Sullivan et al., 1999; Burke and Stewart, 2002; Holaska et al., 2002; Muchir et al., 2003). In agreement with these

findings, emerin colocalises with lamin proteins *in vitro* and *in vivo* (Manilal et al., 1998; Clements et al., 2000; Vaughan et al., 2001; Lee et al., 2001; Goldman et al., 2005).

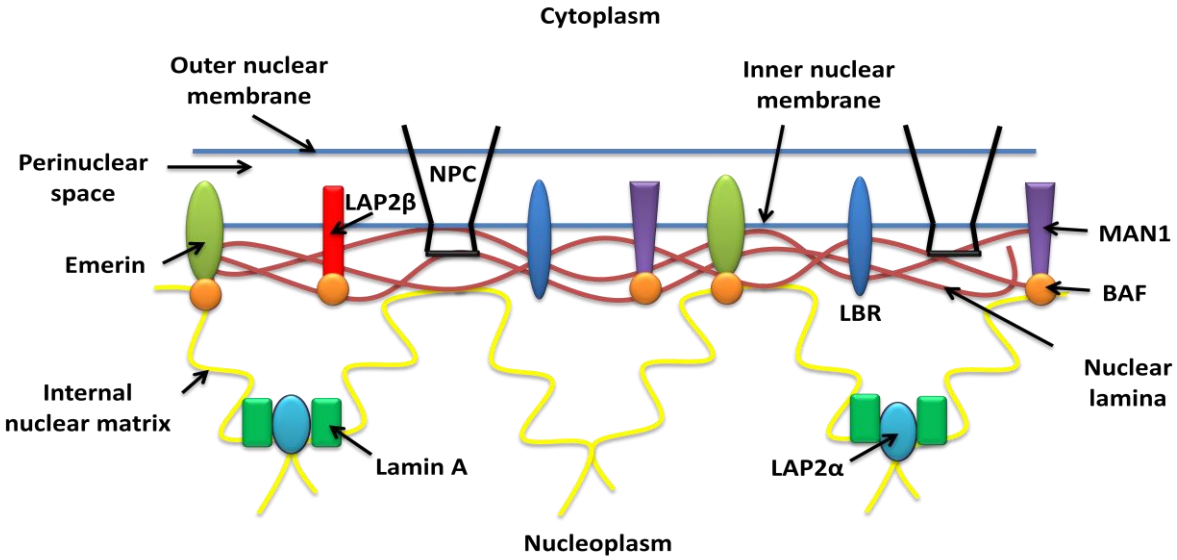

Figure 1.2: An overview of the nuclear envelope

Evidence is building to suggest that emerin has a role in regulating gene expression, however, studies showing this are still few and far between (Holaska and Wilson, 2006). Emerin binds Bcl-2-associated transcription factor (Btf; Haraguchi et al., 2004) and germ cell-less (GCL; Holaska et al., 2003), both of which are repressors of transcription. Interestingly, Btf is a pro-apoptotic factor, which associates with the NE following the initiation of apoptosis (Haraguchi et al., 2004). GCL, on the other-hand, is involved in E2F signalling (Holaska et al., 2003). Additionally, emerin is thought to be involved in mRNA processing; this stems from the observation that the protein interacts with the splicing factor, YT521-B, *in vivo* (Wilkinson et al., 2003).

1.2.3.3 Lamina-associated polypeptide 2 (LAP2) family

The alternate splicing of the *LAP2* produces six LAP2 isoforms, each of which exhibit varying functions and localisation; while LAP2α is found dispersed throughout the nucleus, LAP2-β, -δ, -γ, -ε are bound to the INM (Harris et al., 1994; Berger et al., 1996; Dechat et al., 1998; Vlcek et al., 1999). Of the isoforms, LAP2α and β are documented

to participate in regulating gene expression. Indeed, LAP2α-lamin A complexes anchor pRb to the nuclear edge, which thus affects the transcription of S-phase genes and influences cell cycle progression (Markiewicz et al., 2002). LAP2β can repress transcription either through GCL binding or via its recruitment of the histone deacetylase (Nili et al., 2001; Somech et al., 2005). LAP2β also binds to HA95, a chromatin-associated factor (Martins et al., 2003).

1.2.3.4 Lamin B Receptor

Another protein of note is the lamin B receptor (LBR). This 58 kDa protein, also known as p58, harbours two significant, functional domains; the N-terminus confers the ability to bind both lamin B and chromatin, while, the C-terminus exhibits sterol Δ^{14}-reductase activity (Silve et al., 1998). LBR also interacts with the heterochromatin protein 1 alpha (HP1α; Ye and Worman, 1996); a factor which is thought to participate in gene silencing (Nielsen et al., 1999). Importantly, mutations in *LBR* have been found to result in two phenotypically distinct diseases; these disorders will be discussed later in the review.

1.2.4 Nuclear Matrix

1.2.4.1 Overview

Significantly, the NL forms part of a larger nuclear structure, the nuclear matrix (NM; figure 1.2). The NM is composed of two main constituents; the peripheral NL and the internal NM (Nickerson, 2001). The term NM was first coined by Berezney and Coffey in 1974 and was at the time, used to describe a newly isolated nuclear fraction. The authors had achieved this by treating nuclei with both high salt molarities and DNase I, which functioned to extract the soluble proteins present and remove the DNA (Berezney and Coffey, 1974). Since then, criticism over the technique has been rife; some suggest that the structure is an artefact resulting from harsh, non-physiological extraction methods (Hancock, 2000). As a consequence of this, numerous modifications to this biochemical technique have been made resulting with nuclei being subjected to more physiologically accurate conditions; as a result, the term nucleoskeleton has been adopted (Jackson and Cook, 1988; Philimonenko et al., 2001).

There is a general consensus in the field that the NM or nucleoskeleton is a proteinaceous, RNA-rich network of thick polymorphic fibres, underlying which are thinner core filaments (Jackson and Cook, 1988; He et al., 1990; Philimonenko et al., 2001). It is also found to be present regardless of transcriptional activity (Philimonenko et al., 2001).

1.2.4.2 Functional relevance of the NM

1.2.4.2.1 Genome organisation

Within the interphase nucleus, chromosomes are non-randomly organised (Foster and Bridger, 2005). Although it is uncertain which nuclear elements mediate such arrangement, the most likely candidate for doing so is the NM (de Lange, 1992; Gerdes et al., 1994; Luderus et al., 1996; Ma et al., 1999; Croft et al., 1999; Elcock and Bridger, 2008; Elcock and Bridger, 2010). Indeed, the genome is reported to interact with the NM at specific DNA sequences, known as matrix-attachment regions (MARs); although thousands of these regions exist, they are, in general, poorly characterised (Bode et al., 2000). Telomeres which serve as caps at the extreme ends of chromosomes (Blackburn, 1994; Zakian, 1995) are anchored to the NM via their TTAGGG repeats, throughout the nuclear volume and not just at the periphery (de Lange, 1992; Luderus et al., 1996). Indeed, these repetitive elements are found to contain one MAR every 1 kb (Luderus et al. 1996). Telomeres are of great interest since they shorten with each cell cycle; once they have reached a critical length, the cell enters a state termed replicative senescence (Allsopp et al., 1992; Bodnar et al., 1998). Telomeres can be replaced by the activity of telomerase; however this enzyme is switched off in somatic cells (Greider and Blackburn, 1989; Bodnar et al., 1998).

Although it is not fully understood which NM proteins mediate genome interactions with the NM, it is becoming apparent that A-type lamins are involved in such associations. This is in light of their DNA binding properties (Shoeman and Traub, 1990; Taniura et al., 1995; Stierle et al., 2003) and recognition as MAR-binding proteins (Luderus et al., 1992; Bode et al., 2003). Furthermore, A-type lamins are shown to associate with telomeres (Raz et al., 2008); indeed, the loss of such proteins

significantly disrupts telomere localisation and maintenance (Gonzalez-Suarez et al., 2009).

1.2.4.2.2 DNA replication

There is an abundance of research which demonstrates that the NM is required for efficient DNA replication. Indeed, newly synthesised DNA is found to associate with the structure (Berezney and Coffey, 1975; Hassan and Cook, 1993). Several enzymes which participate in DNA replication are also attached to the NM: DNA polymerase alpha (DNA pol α), DNA primase, 3'–5' exonuclease, RNase H and DNA methylase (Smith and Berezney, 1980, 1982, 1983; Foster and Collins, 1985; Tubo and Berezney, 1987a, b, c; Martelli et al., 1998). Furthermore, primer recognition proteins, such as annexin II and the glycolytic enzyme, 3-phosphoglycerate kinase (PGK), exhibit NM attachment (Vishwanatha et al., 1992). In line with these observations, other studies reveal that replication factories, the discrete sites at which replication is demonstrated to occur, are anchored to the NM (Hassan and Cook, 1993; Hozak et al., 1993; Hozak et al., 1994; Djeliova et al., 2001a, 2001b; Radichev et al., 2005). Replication forks are also associated with the structure (Vaughn et al., 1990). The attachment of replication factories to the NM is important for the initiation of replication (Djeliova et al., 2001a; Radichev et al., 2005). However, origins of replication are not associated with the NM throughout the cell cycle; they associate with the structure in late G1 and are released following initiation in S-phase (Djeliova et al., 2001a; Djeliova et al., 2001b).

1.2.4.2.3 Transcription and splicing

Importantly, the NM provides the foundation upon which transcription factories operate. The sites of RNA polymerase I and II mediated-transcription are attached to this nuclear substructure (Dickinson et al., 1990; Jackson et al., 1993; Iborra et al., 1996). Actively transcribing DNA is fed through fixed RNA polymerase molecules (Iborra et al., 1996); in line with this, transcriptionally active genomic regions are found associated with the NM, while inactive regions are not (Ciejek, 1983; Jackson and Cook, 1993; Gerdes et al., 1994). Transcription factors such as the estrogen receptor (Alexander et al., 1987; Metzger and Korach, 1990), steroid hormone receptor

(Barrack, 1987), corticosteroid receptor (Van steensel et al., 1991) and vitamin D receptor (Bidwell et al., 1994) are NM-associated. Furthermore, elements required for ribosomal assembly, pre-mRNA processing and splicing, including nucleophosmin/B23, hnRNPs and spliceosomes, are also attached to the NM (Zeitlin et al., 1987, 1989; Mattern et al., 1996).

A fully functional NM is required to support transcription; if lamin proteins are missing or mutant, this process is perturbed. Spann et al. (2002) reported that the presence of mutant lamin A inhibits the activity of RNA polymerase. Furthermore, depleting lamin B1 levels by interference technology significantly disrupts RNA synthesis (Tang et al., 2008).

1.2.4.2.4 DNA repair

In addition to its role in chromatin modelling, replication and transcription, the NM is thought to serve as a platform for the regulation of cell cycle progression and DNA repair. Indeed, DNA repair occurs at the NM (McCready and Cook, 1984; Harless and Hewitt, 1987) and NM-associated DNA is preferentially repaired following genotoxic stress (Mullenders et al., 1988). However, such repair is not exclusively a NM-associated event (Mullenders et al., 1988). Furthermore, DNA is recruited to the NM following genotoxic stress (Koehler and Hanawalt, 1996). The CSA (Cockayne syndrome group A) protein, which is important for transcription-coupled repair (TCR), is translocated to the NM following ultraviolet (UV) irradiation, in a CSB-dependent manner (Kamiuchi et al., 2002). A significant relationship exists between the NM and p53; this major tumour suppressor protein initiates an array of key cellular responses. Concomitant with an increase in p53 levels, p53 binding to the NM augments in response to DNA damage (Jiang et al., 2001). It has thus been suggested that this interaction is vital for the correct and efficient activation of p53-related pathways, following genotoxic stress (Jiang et al., 2001). By creating structural mutants, it was demonstrated that residues 67–98, located in the protein's N-terminus, mediate this binding (Jiang et al., 2001). Further adding to the view that the NM has a role in co-ordinating DNA damage signalling, Rad51, a key homologous recombination protein, is reported to be a NM protein (Mladenov et al., 2006, 2007, 2009). Such binding is

mediated by a putative NM targeting signal in Rad51; in response to DNA damage, this interaction facilitates the formation of NM-associated nuclear foci. Indeed, when Rad51 is mutated to eliminate NM binding, these foci no longer assemble (Mladenov et al., 2009). Other DNA damage response proteins, such as Brca1, Brca2, ATM, also associate with the NM (Gately et al., 1998; Huber and Chodosh, 2005).

1.3 GENOME ORGANISATION

1.3.1 Introduction

Over the past decade, much progress has been made in order to elucidate the nuclear organisation of the genome. The positioning of chromosomes in the interphase nucleus is shown to be non-random; each occupies a specific domain, known as a 'chromosome territory' (Cremer et al., 1982; Strasburger, 1905, cited in Rothmann et al., 1997, p1105; Boveri, 1909, cited in Bridger and Foster, 2005, p213). These territories can be visualised by using fluorescence *in situ* hybridisation (FISH) on fixed cells, however, it is also possible to view these structures in living cells via the incorporation of labelled nucleotides (Zink et al., 1998; Visser and Aten, 1999). Historically, the interchromatin domain (ICD) model has been accepted, whereby little, if any, intermingling between neighbouring chromosome sites exists (Cremer et al., 1993; Zirbel et al., 1993; Visser et al., 2000; Cremer et al., 2000; Kosak and Groudine, 2002). However, recent evidence suggests that this is not the case. Branco and Pombo (2006) used high-resolution *in situ* hybridisation to demonstrate significant intermingling between territories; indeed, the degree of interaction correlated with translocation frequency.

Interestingly, this spatial arrangement of chromosomes appears to alter both upon differentiation (Solovei et al., 2004; Foster et al., 2005) and exit from the cell cycle (Bridger et al., 2000; Mehta et al., 2010). Studies have shown that individual chromosomes have preferential neighbours in nuclei (Nagele et al., 1999); an organisation which appears to be cell type specific (Marella et al., 2009). Several studies have demonstrated that, within interphase nuclei, chromosome territories are radially organised (Croft et al., 1999; Bridger et al., 2000; Boyle et al., 2001); however, the basis of such positioning has caused much debate. Boyle et al. (2001) suggest that

it is driven by gene density while others (Sun et al., 2000; Bolzer et al., 2005) propose that chromosome organisation is size-dependent. Unfortunately, the study of chicken cells has done little to clarify the situation since the organisation of their macro- and micro-chromosomes fits both hypotheses (Habermann et al., 2001; Parada and Mistelli, 2002).

Certain groups report that transcriptionally active sequences tend to be positioned either towards the territory edge or outside the territory altogether (Scheuermann et al., 2004; Morey et al., 2009). Indeed, gene-rich chromatin loops radiating away from chromosome territories have been reported (Volpi et al., 2000; Mahy et al., 2002; Ragoczy et al., 2003). However, in some cases, these gene-rich regions are found at the chromosome territory edge regardless of transcription status (Mahy et al., 2002). It is thus possible that such gene-rich sequences are poised in these peripheral positions to enhance transcription factory accessibility. Recent research suggests that both GC content and replication timing could also be important for positioning chromatin domains within nuclear space (Hepperger et al., 2008; Grasser et al., 2008).

1.3.2 Nuclear periphery: an area of repression?

Historically, the nuclear edge has been regarded as an area of transcriptional inactivity. Indeed, constitutive heterochromatin is consistently found to associate with both the nuclear periphery and nucleoli, while the early-replicating, transcriptionally active, euchromatin occupies a more internal position (for review, see Deniaud and Bickmore, 2009). This observation concurs with the apparent gene-density dependent radial positioning of chromosomes revealed by FISH studies (Boyle et al., 2001). Unfortunately, however, the picture is not as straightforward as perhaps once imagined; work is continually being published which makes the transcriptional distinction between the nuclear edge and interior increasingly less certain.

Research shows that the nuclear interior is unquestionably, a hot-bed of transcriptional activity. Regions of increased gene expression (RIDGEs) are found located within the nuclear interior, while anti-RIDGEs, transcriptionally inactive genomic regions, are often observed at the periphery (Caron et al., 2001; Versteeg et

al., 2003; Goetze et al., 2007; Gierman et al., 2007). Indeed, Kosak et al. (2007) report that the majority of transcribed genes are positioned within the nuclear interior. In line with this, Takizawa et al. (2008) demonstrated that the transcriptionally active allele tends to cluster within the nuclear interior, unlike its inactive counterpart.

As mentioned previously, the genome interacts with the NL at multiple sites, known as LADs (Guelen et al., 2008). Importantly, such domains are found to be regions of low levels of gene expression (Guelen et al., 2008). Is the nuclear periphery, however, incompatible with transcription? By tracking nascent RNA production, it is evident that transcription occurs throughout the nucleus, both within the nuclear interior and at the nuclear edge (Wansink et al., 1993). Work performed using mice demonstrates that the *IFNγ* locus is located at the nuclear periphery regardless of whether the gene is active or inactive (Hewitt et al., 2004). A study involving the human immunodeficiency virus (HIV) further strengthens the opinion that the nuclear edge is not unsuited to gene expression (Dieudonne et al., 2009). Recently, three groups have focussed on the transcriptional consequences of artificially tethering regions of the genome to the nuclear edge. Reddy et al. (2008) reported that while *cxcl5* and *cxcl1* were significantly down-regulated as a result of such anchorage to the nuclear periphery, no noteworthy changes were observed in any of the other genes examined. Conclusions from the studies of Bickmore and Spector appear to confirm this, in that targeting to the nuclear edge represses some, but not all genes (Finlan et al., 2008; Kumaran and Spector, 2008). To further complicate matters, it is emerging that NPCs are in fact areas of high transcriptional activity; this view is, in part, formed by observing events occurring in both yeast and *Drosophila* (Akhtar and Gasser, 2007). Indeed, this chimes with Blobel's early gene-gating hypothesis where he suggested that high levels of gene transcription at NPCs would logically facilitate mRNA export (Blobel, 1985).

1.3.3 What is the functional relevance of gene repositioning?

Specific genes are found to be repositioned from the nuclear periphery to the interior during their activation (Chuang et al., 2006; Dundr et al., 2007; Lanctot et al., 2007). Other studies demonstrate that when expression is increased, loci move towards the

nuclear interior, while when repressed they preferentially associate with the nuclear edge (Brown et al., 2001; Kimura et al., 2002; Zink et al., 2004; Szczerbal et al., 2009). However, it is becoming apparent that rather than nuclear repositioning dictating transcriptional activity, it is expression that drives repositioning. Indeed, purely relocating the *Mash1* locus from the periphery to a more interior position was not sufficient to activate transcription (Williams et al., 2006). Furthermore, the looping out of a gene from its chromosome territory, into a more interior position, was insufficient to up-regulate gene expression (Morey et al., 2009). Taken together, these conclusions infer that an internal nuclear position is more important for attaining high transcriptional activity, than for the actual activation event *per se* (Ragoczy et al., 2006).

1.3.4 Gene positioning and transcription factories

It is generally accepted that transcription occurs in discrete foci known as transcription factories, which are found to be distributed throughout the nucleus, attached to an underlying nucleoskeleton (figure 1.3; Iborra et al., 1996). Contrary to popular belief, mRNA is generated from active genes during infrequent bursts rather than continual periods of transcription (Raj et al., 2006). The majority of active genes reside within transcription factories, while inactive loci are found outside these structures (Osborne et al., 2007). There is some evidence to indicate that certain genes preferentially co-transcribe. Using RNA FISH, Osborne et al. (2007) demonstrated that in mouse B-lymphocytes, the proto-oncogene, *Myc*, preferentially shares the same transcription factory as the highly transcribed, *Igh*; a significant finding since the two gene loci are frequently involved in lymphoma-related translocation events. Importantly, it appears that functionally-related genes come together in order to be transcribed (figure 1.4).

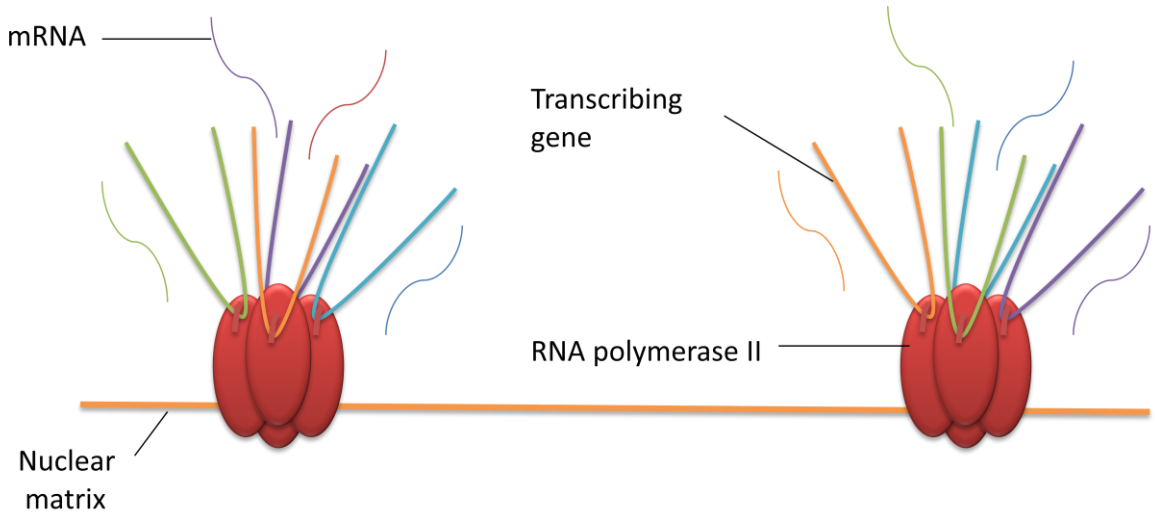

Figure 1.3: Nuclear matrix-associated RNA polymerase II transcription factories

Genes are proposed to be transcribed in nuclear matrix-associated transcription factories; these factories are found to be immobile and composed of numerous RNA polymerase II molecules. DNA is fed through these RNA polymerase II complexes and transcribed.

The mouse β-globin gene co-localises, at high frequency, to the same transcription factory as other erythroid-specific genes; an observation which has been proven by both RNA FISH and 4C (chromosome conformation capture-on-chip) studies (Osborne et al., 2004; Simonis et al., 2006). In yeast, tRNA genes, which are generally scattered throughout the genome, are reported to cluster into nucleolar-based factories when transcribed (Thompson et al., 2003). Furthermore, the transcription of specific snRNA genes is found to occur at coiled bodies (Frey et al., 1999). Recent work by Peter Cook's group suggests that such factories appear to specialize in the production of certain transcript species. Plasmids were introduced into cells, which subsequently assembled into minichromosomes; the transcription of these elements was tracked using FISH. Interestingly, only ~ 20 transcription factories were employed to transcribe the 8000 minichromosomes present per cell; this indicates (1) that factory specificity exists and (2) that one factory can process multiple transcripts simultaneously. The study reported that this selectivity was driven by intronic status and promoter type (Xu and Cook, 2008). This implies that specific sequences are transcribed by selected factories; thus, surely if this is the case, the distribution of different transcription factory types would influence the position of genes within the nucleus. Perhaps some genes are positioned within the vicinity of necessary factories, which contain the

required transcription factors, while other genes need to migrate some distance in order to be expressed or repressed. This begs the question: which particular elements target gene sequences to specific transcription factories? Elucidating such factors will also aid in understanding the basis of genome organisation.

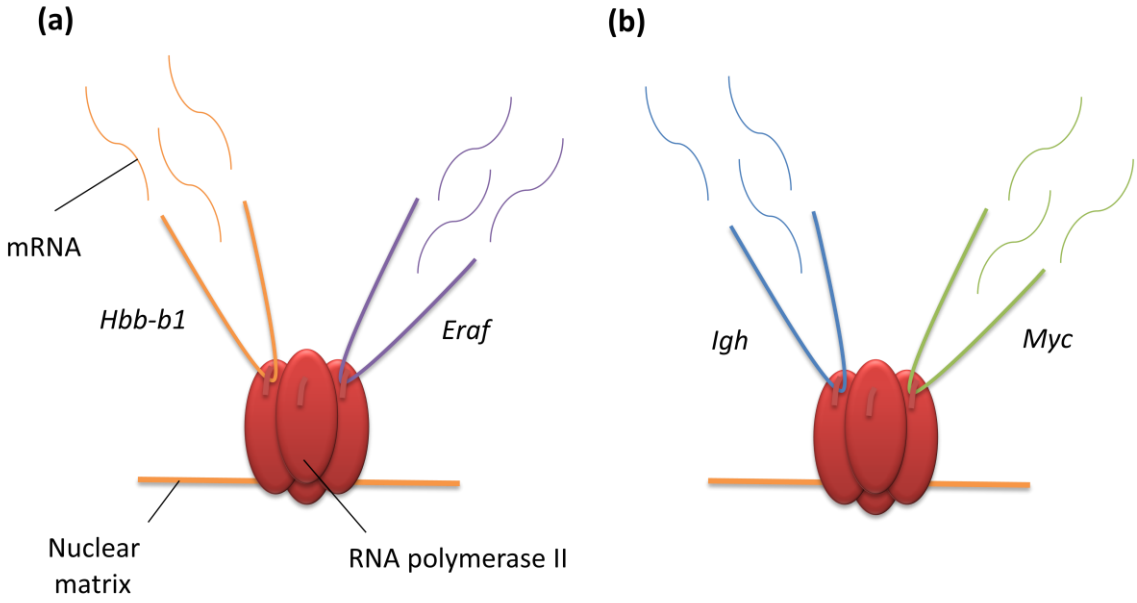

Figure 1.4: The co-transcription of specific genes

(a) The mouse β-globin gene co-localises to the same transcription factory as other erythroid-specific genes (Osborne et al.,2004).
(b) In mouse B lymphocytes, the proto-oncogene, *Myc*, preferentially shares the same transcription factory as the highly transcribed, *Igh* (Osborne et al., 2007).

1.3.5 What can evolution tell us?

Perhaps one of the most thought-provoking articles on genome organisation in recent years has been that published by Solovei et al. (2009). The group investigated and compared the nuclear architecture of rod photoreceptor cells in both nocturnal and diurnal mammals. Significantly, the results questioned the widely accepted theory; that the heterochromatic rich regions of the periphery are a staple in nuclear organisation. The study discovered that, in rod photoreceptor cells of the mouse, this typical arrangement is in fact reversed; gene-dense regions decorate the nuclear edge, while gene-poor regions localise in the interior. In line with this, the majority of transcription machinery is also found peripherally. Interestingly, all genes, regardless of transcriptional activity, were located towards the nuclear edge. The authors

reported that this 'inverse' pattern of organisation in the retina was indeed associated with nocturnal vision; diurnal mammals have conventionally arranged rod photoreceptor nuclei. This finding has led to many questions; one of which centres around evolution. The demonstration that an 'inverse' version of the 'conventional' genome organisation exists, suggests that each must confer an evolutionary advantage to the corresponding organisms. Solovei et al. (2009) suggest that this inverse arrangement facilitates, in some way, the transmission of photons. Whether or not this is the sole reason, the study reveals the flexibility of the organisation and indicates that it remains unchanged through evolution for a purpose. Evidently, this 'purpose' will be inextricably linked to transcriptional regulation; however, for the time being, the answer remains elusive. It will be extremely fruitful to identify those elements which encode the global organisation of the genome.

1.3.6 Closing remarks

Over the past decade, major advances have been made in terms of elucidating the organisation of the genome. It is now becoming increasingly apparent that the functional relevance of this organisation is somewhat complex; indeed, the transcriptional distinction between the nuclear periphery and nuclear interior is not as straightforward as once imagined. The repositioning of certain genes correlates with changes in expression; however, with other loci, it does not. It is likely that gene repositioning is used in order to regulate the expression of specific genes; it is probably not representative of a blanket genomic response. Furthermore, the significance and role of transcription factories in mediating this organisation should not be overlooked. As our understanding of these factories increases, so too will our comprehension of genome organisation and the nuclear structures which dictate it.

1.4 LAMINOPATHIES

1.4.1 Introduction

The laminopathies are a collection of human diseases that result primarily from mutations in lamin-encoding genes, namely *LMNA*; this genomic region is found to harbour over 180 different disease-causing mutations (Hutchison and Worman, 2004;

Gruenbaum et al., 2005; Jacob and Garg, 2005; Capell and Collins, 2006). Interestingly, mutations in *LMNA* can produce clinically distinct disorders, which exhibit tissue specificity; unfortunately, this presents a huge problem when attempting to understand the disease mechanisms involved. In addition, other lamin-binding proteins such as emerin and LAP2α, when defective, are seen to produce so called 'secondary laminopathies' (Jacob and Garg, 2006). In this respect, several disorders have both primary and secondary causes. A fact which highlights how inextricably interconnected these proteins have become throughout evolution. Taking this into account, the section will aim to provide an overview of the laminopathy diseases, discuss the proposed disease mechanisms involved and briefly touch on potential future therapies.

1.4.2 Premature Ageing Syndromes

1.4.2.1 Hutchinson-Gilford Progeria Syndrome (HGPS)

Hutchinson-Gilford Progeria Syndrome (HGPS) is an extremely rare premature ageing disease, which affects 1 in 4–8 million live births (Capell and Collins, 2006). It was first reported in 1886 by Hutchinson and then, later by Gilford in 1904. Patients with the disease invariably exhibit micrognathia, alopecia, short stature, insulin resistance, delayed dentition and absent sexual maturation; these features become noticeable after the first twelve months of life (DeBusk, 1972). The mean age of HGPS patients at death is 13.4 years (DeBusk, 1972) when cardiovascular disease i.e. atherosclerosis, is usually the cause (Baker et al., 1981).

In 2003, Eriksson et al. produced a seminal paper which showed that of the 20 classical HGPS patients studied, 18 of these exhibited a G608G mutation in exon 11 of the *LMNA* gene. Although, this mutation was a silent C>T transition at position 1824, it was demonstrated that the single nucleotide substitution activated a cryptic splice site. As a result of this activation, there was found to be a 150 bp deletion at the mRNA level from the carboxy terminus of lamin A. This event produced a mutant protein lacking its pre-terminal 50 amino acids (Eriksson et al., 2003). Simultaneously, De Sandre-Giovannoli et al. (2003) also demonstrated the occurrence of lamin A truncation in HGPS patients. It was found that this deletion interferes significantly with the protein's

post-translational modifications; it removes a cleavage site required by *ZMPSTE24,* the zinc metalloproteinase. As a result, it abnormally remains associated with the NE. This farnesylated, truncated version of lamin A has been termed progerin or LAΔ50 (figure 1.5; Goldman et al., 2004). Interestingly, in another study, which involved 3 HGPS patients, it was observed that the *de novo LMNA* mutations were paternally-derived (D'Apice et al., 2004).

The mode of inheritance can also be autosomal recessive; Plasilova et al. (2004) reported homozygotes harbouring a missense mutation in *LMNA* at residue 1626 (K542N). This resulted in the replacement of a charged lysine molecule with an uncharged asparagine, an event which did not activate a cryptic splice site, as previously described (e.g. Eriksson et al., 2003). The authors thus suggested that this mutation interferes with docking sites for emerin, LAP2α and DNA interaction (Plasilova et al., 2004). Furthermore, compound heterozygosity has been observed in a patient with both R471C and R527C *LMNA* mutations (Cao and Hegele, 2003). A somatic and gonadal mosaic form has also been noted in an unaffected parent, whose child suffers from HGPS (Wuyts et al., 2005).

1.4.2.2 Werner's Syndrome (WS)

Another disorder which displays progeroid features is Werner's syndrome (WS); this is a rare, autosomal recessive disease caused by mutations in the *WRN* gene, which encodes a RecQ-type DNA/RNA helicase (Yu et al., 1996). Interestingly, it is found that in 70% of cases, the patient is the result of a consanguineous marriage (Goto et al., 1981). The symptoms observed in WS overlap somewhat with those seen in HGPS: short stature, alopecia, bilateral cataracts, atrophic skin, hypogonadism and low body weight (Goto et al., 1997). Malignancy and atherosclerosis are the two main causes of death with 50% of patients dying before the age of 40 (Goto et al., 1997). Significantly, of the 1100 WS patients reported worldwide, 810 of these originate in Japan (Goto et al., 1997).

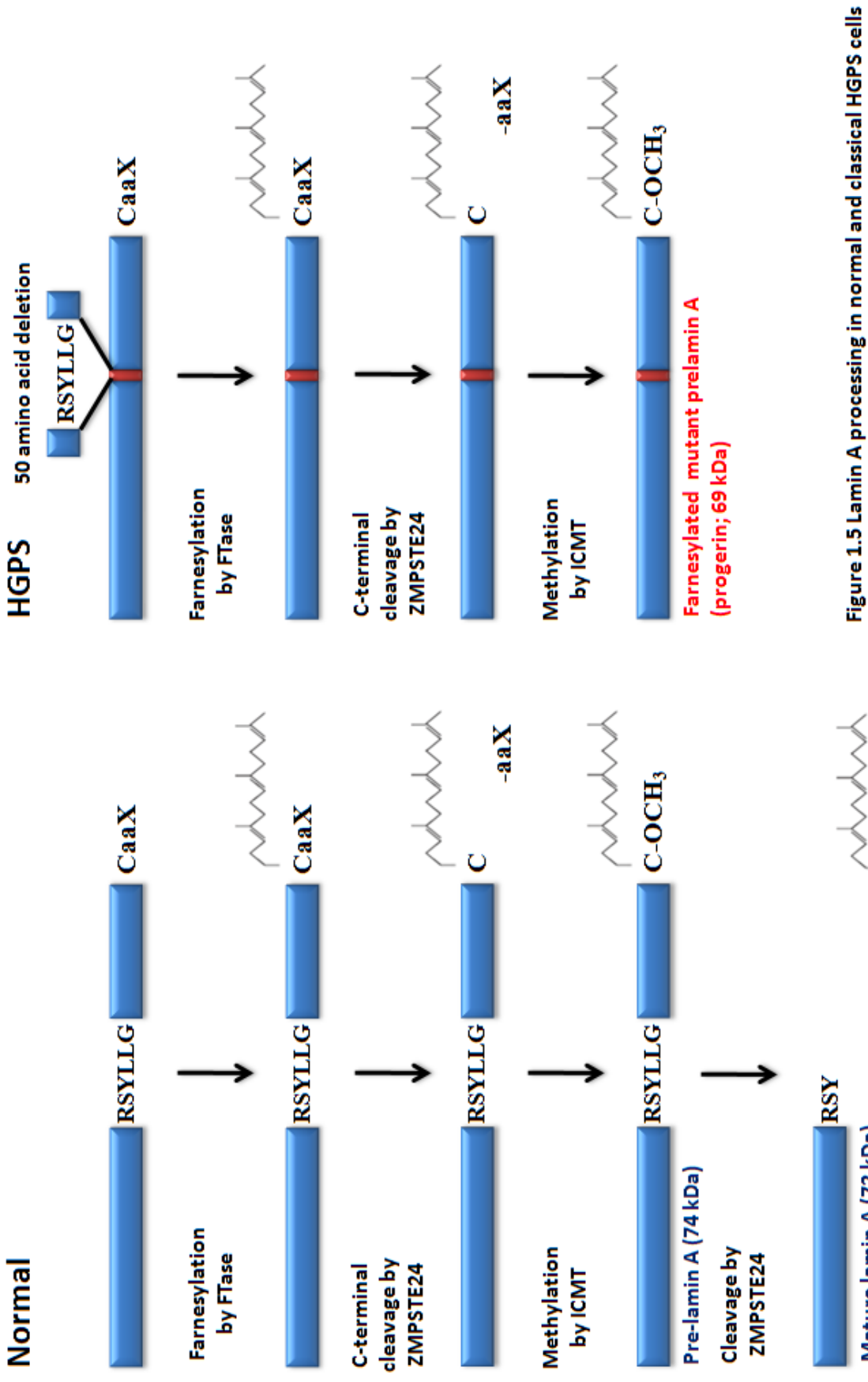

Figure 1.5 Lamin A processing in normal and classical HGPS cells

Figure 1.5: Lamin A processing in normal and classical HGPS cells
In normal cells, which harbour wildtype *LMNA,* mature and functional lamin A is generated. However, in classical HGPS, the 50 amino acid deletion removes the site required for the final cleavage step. Consequently, prelamin A remains farnesylated. FTase = farnesyltransferase; ICMT = isoprenylcysteine carboxyl methyl transferase. This has been influenced by a figure presented by Young et al. (2006).

Of the 129 samples sent for molecular diagnosis from patients presenting with WS symptoms, 26 lacked a *WRN* mutation. Subsequently, *LMNA* was sequenced; it was found that of these 26, 15% carried novel heterozygous, missense mutations in this gene. Accordingly, this phenotype has been termed atypical WS; adding it to the increasing list of laminopathies (Chen et al., 2003).

1.4.3 Myopathies and Neuropathies

1.4.3.1 Emery-Dreifuss Muscular Dystrophy (EDMD)

Emery-Dreifuss Muscular Dystrophy (EDMD) was first described as an X-linked disorder by Emery and Dreifuss, in 1966; it was found to be a recessive trait, occurring only in males. Sufferers of X-EDMD share symptoms such as muscle weakness, early contractures of the elbows, cardiac disorders and shortening of the Achilles tendons (Emery and Dreifuss, 1966). Years later, the disease's molecular cause was mapped to Xq 28, the home of the *STA* or *EMD* gene. It emerged that the encoded 34kDa protein, emerin, was defective in the five X-EDMD patients studied (Bione et al., 1994). This was a significant finding since previous to this discovery, defects in inner nuclear membrane proteins had not been seriously considered as a viable source of human disease. In the majority of cases, there is loss of emerin expression rather than the generation of a defective product (Yates et al., 1999).

Subsequently, a paper documented *LMNA* mutations as the cause of autosomal dominant EDMD (Bonne et al., 1999). Numerous studies have confirmed these observations (Raffaele di Barletta et al., 2000; Brown et al., 2001) and in addition, it has been shown that an autosomal recessive form of EDMD exists (Raffaele di Barletta et al., 2000). These studies were the first to show that mutations in this gene could cause a disease phenotype in humans. As is the case in many laminopathies, the symptoms displayed in autosomal EDMD can vary dramatically from patient to patient

(Raffaele di Barletta et al., 2000); however, the sex-linked form is usually less severe (Bonne et al., 2000).

Linking the disease phenotype to the mutation site is not as straightforward as expected; the analysis of numerous AD-EDMD patients showed no significant correlation between the two (Bonne et al., 2000). As a result, the involvement of a modifier gene has been postulated (Bonne et al., 2000). Nonetheless, a study conducted by Brown et al. (2001) did observe that the majority of *LMNA* exons affected in EDMD shared a common feature; the mutations disrupt residues in the protein's central rod domain. Perhaps unsurprisingly, it was revealed that the disease-causing mutations altered those evolutionarily conserved residues. Consequently, the authors suggested a functional or structural importance of these sites (Brown et al., 2001). Significantly, dominant mutations in *SYNE1* and *SYNE2,* which encode the proteins nesprin-1 and nesprin-2, respectively, are also a cause of EDMD (Zhang et al., 2007; Puckelwartz et al., 2009).

1.4.3.2 Dilated Cardiomyopathy (DCM)

Dilated cardiomyopathy (DCM) is characterised by the presence of systolic dysfunction and cardiac dilation; it is a leading cause of congestive heart failure worldwide (Kasper et al., 1994). Although DCM can result from a plethora of disorders (Kasper et al., 1994), evidence has shown that in certain patients, a *LMNA* mutation is the source (Fatkin et al., 1999; Song et al., 2007). Significantly, Taylor et al., (2005) provided the first evidence to show that a mutant form of LAP2α is sufficient to produce disease in humans; they revealed an Arg690Cys *LAP2* mutation in a DCM patient. Mutations in *EMD* also cause X-linked familial atrial fibrillation (Karst et al., 2008).

1.4.3.3 Limb-Girdle Muscular Dystrophy (LGMD)

Mutations in *LMNA* are also found to be responsible for Limb-Girdle Muscular Dystrophy 1B; this is a slow, progressive disease characterised by cardiac involvement (Van der Kooi et al., 1996). Evidence for this was first provided by Muchir et al. (2000); they identified missense, codon deletion and splice donor site mutations in patients

with the disease. In addition to these, LGMD1B can result from synonymous codon changes in *LMNA* which act to perturb mRNA splicing. In one published case, although the substitution (AAG>AAA) did not change the encoded amino acid (lysine), it activated a cryptic splice site. This resulted in the insertion of a string of 15 amino acids into the protein (Muchir et al., 2000). More recently, it has been demonstrated that mutations in *EMD* also cause LGMD (Ura et al., 2007).

1.4.3.4 Charcot-Marie Tooth (CMT) Type 2 B1

In addition, homozygous *LMNA* mutations are the cause of the periphery axonopathy, Charcot-Marie Tooth (CMT) type 2 B1 (De Sandre-Giovannoli et al., 2002). In a study involving several Algerian families, a novel mutation (892C>T) was identified in exon 5 of the *LMNA* gene, resulting in a R298C amino acid substitution. Research performed using *Lmna*$^{-/-}$ mice show that they exhibit axonal enlargement, a reduction in axonal density and nerve demyelination; concurrently, similar manifestations are observed in human CMT2 patients (De Sandre-Giovannoli et al., 2002).

1.4.4 Lipodystrophies

1.4.4.1 Dunnigan-Type Familial Partial Lipodystrophy (FLPD)

LMNA mutations are also found to cause the autosomal dominant disorder, Dunnigan-Type Familial Partial Lipodystrophy (FLPD; Cao et al., 2000; Shackleton et al., 2000; Speckman et al., 2000). Sufferers of the disease display symmetrical lipodystrophy of the trunk and extremities as well as insulin-resistant diabetes and type V hyperlipidemia (Dunnigan et al., 1974). Although the majority of FLPD patients harbour missense mutations, the incorrect splicing of the gene is demonstrated to cause disease too (Morel et al., 2006). It was found that a novel G>C mutation led to intron 8's inclusion in the mRNA; this resulted in a truncated lamin A isoform, 516 residues in length (Morel et al., 2006).

1.4.4.2 Mandibuloacral Dysplasia (MAD)

Two categories of Mandibuloacral Dysplasia (MAD) exist, type A and type B; these diseases are caused by mutations in *LMNA* or *ZMPSTE24,* respectively (Novelli et al., 2002; Agarwal et al., 2003). MAD-A results from a homozygous *LMNA* missense mutation (R527H; Novelli et al., 2002) while heterozygous, usually compound, *ZMPSTE24* defects lead to type B disease (MAD-B; Agarwal et al., 2003). Patients with MAD display characteristic features: mandibular hypoplasia, cutaneous atrophy, insulin resistance, diabetes mellitus and lipodystrophy (Young et al., 1971; Freidenberg et al., 1992; Simha and Garg, 2002).

1.4.5 Additional Laminopathies

1.4.5.1 Restrictive Dermopathy (RD)

First reported by Witt et al. (1986), restrictive dermopathy (RD) is characterised by tight, translucent, dysplasic skin; this is documented to severely compromise physical movement and to impact on other bodily functions. As a result, the disorder is fatal (Verloes, 1992). The disease is caused by mutations in either *LMNA* or *ZMPSTE24,* although most cases result from the latter (Navarro et al., 2004; Navarro et al., 2005). In *LMNA*, a heterozygous splicing mutation leads to the partial or complete loss of exon 11, an event which causes RD. In contrast, the activation of a premature stop codon, caused by the insertion of a single nucleotide is what mutates the *ZMPSTE24* gene in the disease (Navarro et al., 2004). As a consequence of both events, farnesylated pre-lamin A accumulates in the nucleus and thus, exerts its dominant-negative effects (Navarro et al., 2004; Navarro et al., 2005). Significantly, in one reported case, the disease phenotype of a homozygous *ZMPSTE24* mutation was rescued by the presence of a heterozygous mutation in *LMNA,* in the same patient (Denecke et al., 2006). This finding acts to emphasize the deleterious effects of pre-lamin A on the nucleus and how it leads to cellular pathology.

1.4.5.2 Lamin B Mutants

Only recently, has it been demonstrated that mutations in B-type lamin proteins cause viable disease in humans; interestingly, the disorders produced are phenotypically distinct (Worman and Bonne, 2007). Padiath et al. (2006) produced the first evidence of this; *LMNB1* duplications were discovered in patients with autosomal dominant leukodystrophy. This disorder, first noted in 1984 (Eldridge et al., 1984), is characterised by slow, progressive neurological wasting which has striking similarities with chronic progressive multiple sclerosis (Eldridge et al., 1984). There is prominent symmetrical loss of myelin from nerve cells in the central nervous system (Schiffmann and van der Knaap, 2004). Indeed, Lamin B1 is required for correct oligodendrocyte maturation and the formation of myelin (Lin and Fu, 2009). In addition, by sequencing the *LMNB2* gene in patients with Acquired Partial Lipodystrophy (APL), known also as Barraquer-Simons Syndrome, a novel heterozygous mutation was discovered (Hegele et al., 2006).

As a review by Worman and Bonne (2007) highlighted, our grasp on how mutations in B-type lamins cause pathology is limited; this is understandable since research into lamins and disease has been predominantly focussed on lamin A/C.

1.4.5.3 Lamin B Receptor (LBR) Mutants

Mutations in the lamin B receptor (LBR) are found to produce three distinct clinical phenotypes known as Greenberg Dysplasia (Waterham et al., 2003), Pelger-Huet Anomaly (PHA; Hoffman et al., 2002) and Reynolds Syndrome (Gaudy-Marqueste et al., 2010). Greenberg Dysplasia, also referred to Hydrops-ectopic calcification-moth-eaten skeletal dysplasia, is an autosomal recessive, fatal disorder (Waterham et al., 2003). Patients display a number of severe symptoms: short limbs, post axial polydactyly (both hands), abnormal chondro-osseous calcification, chondrodystrophy and fetal hydrops (Chitayat et al., 1993; Waterham et al., 2003). The cause of the disease is a substitution mutation in exon 13 of the *LBR* gene (Waterham et al., 2003). *LBR* encodes the enzyme, 3β-hydroxysterol Δ^{14}-reductase; when active, it catalyses the reduction of the C_{14}-C_{15} double bond of cholesterol-8-14-dien-3β-ol, producing cholesterol-8-en-3β-

ol. An *LBR* mutant allele thus generates a truncated, non-functional version of this enzyme (Waterham et al., 2003).

In contrast, PHA has an autosomal dominant mode of inheritance, characterised by the hypolobulation of granulocyte nuclei (Hoffman et al., 2002). It usually results from heterozygous *LBR* mutations and is a far more benign disorder. However, a homozygote PHA sufferer has been identified; this child exhibited mild congenital abnormalities (Oosterwijk et al., 2003). It cannot go unnoticed that the very same genetic abnormality i.e. a homozygous *LBR* mutation, produces two significantly different phenotypes, PHA and Greenberg Dysplasia. Consequently, it has been postulated that the two disorders be seen as part of a continuous phenotypic spectrum rather than as two discrete entities, since the inconsistency could be as a result of allelic heterogeneity (Oosterwijk et al., 2003).

1.5 DISEASE MECHANISMS

1.5.1 Introduction

The fact that different *LMNA* mutations can lead to an array of diseases, each with tissue-specific phenotypes, highlights the importance of the gene in normal nuclear functioning. Unfortunately, there is no clear correlation between mutation position and the resulting phenotypes. Thus, it is proposed that the various laminopathy pathologies should be placed along a continuous phenotypic spectrum rather than being categorised as distinct, individual diseases (Capell and Collins, 2006). This next section proposes that it is not the activity of just one disease mechanism that causes pathology in this collection of disorders, but the amalgamation of several.

1.5.2 The Mechanical Role of the INM proteins

It has been found that the accumulation of mutant lamin A induces changes in nuclear morphology; these modifications are observed to worsen with age (Bridger and Kill, 2004; Goldman et al., 2004). They include the thickening of the NL, nuclear stiffness, the mislocalisation of NPCs, nuclear blebbing and aberrant nuclear shape (Fidzianska and Hausmanowa-Petrusewicz, 2003; Goldman et al., 2004; Columbaro et al., 2005;

Scaffidi and Misteli, 2005; Filesi et al., 2005; Capell et al., 2005; Yang et al., 2005; Wang et al., 2006; Meaburn et al., 2007; Verstraeten et al., 2008; Park et al., 2009). In agreement, the lack of functional A-type lamins in EDMD was found to severely compromise the integrity of the nuclear envelope (Sullivan et al., 1999).

Perhaps an obvious result of perturbed lamin A is a compromised NL; indeed, numerous studies have produced evidence to support this hypothesis. Dahl et al. (2004) used *Xenopus* oocyte nuclei to prove the NL's role as a 'molecular shock absorber'. In this study, the lamina was observed to be elastic and compressible; however, both these features exhibited thresholds. In addition to disrupting the nuclear architecture, the authors suggested that defective *LMNA* products could in fact weaken responses to mechanical stimuli, thus perturbing nuclear integrity (Dahl et al., 2004).

In agreement, mice lacking A-type lamins are found to have defective nuclear mechanics (Lammerding et al., 2004; Broers et al., 2004); when such *Lmna*$^{-/-}$ mouse embryonic fibroblasts (MEFs) are subjected to mechanical strain, their ability to cope is significantly compromised (Lammerding et al., 2004; Broers et al., 2004). Indeed, nuclei are extremely prone to bursting (Broers et al., 2004) and more susceptible to apoptosis (Lammerding et al., 2004). Importantly, the activation of transcription in response to mechanical stress is perturbed in lamin A/C-deficient cells; it is thus proposed that this is the cause of the increase in apoptosis observed (Lammerding et al., 2004). Indeed, more recent work by Lammerding's group demonstrates that HGPS patient fibroblasts also exhibit nuclear stiffness (which increases with passage number) and marked reductions in cell viability and wound healing responses, when compared to normal cells (Verstraeten et al., 2008). In line with mouse models, HGPS cells are also more susceptible to apoptosis when subjected to repetitive mechanical strain (Verstraeten et al., 2008).

Research has highlighted the problem with viewing cytoplasmic and nuclear activities separately; loss of dialogue between the two is proposed to greatly affect nuclear behaviour (Broers et al., 2004). Indeed, protein structures known as LINC (linker of nucleoskeleton and cytoskeleton) complexes are found to connect the nucleus with

the cytoplasm (Crisp et al., 2006). These complexes are composed of a protein family known as nesprins, which are tethered to the outer nuclear membrane by SUN proteins (Padmakumar et al., 2005; Haque et al., 2006). Importantly, SUN1 and SUN2 interact with A-type lamins (Padmakumar et al., 2005; Haque et al., 2006). It is thus possible to envisage how mutations in lamin A may impact on the dialogue between the nucleus and cytoskeleton. Using mouse embryonic fibroblasts (MEFs), the resilience of *Lmna*$^{-/-}$ and *Lmna*$^{+/+}$ cells were compared. In *Lmna*$^{-/-}$ cells, interactions between cytoskeletal actin, tubilin and vimentin structures were perturbed, in addition to reductions in mechanical stiffness (Broers et al., 2004). Indeed, a study by Nikolova et al. (2004) reported that cytoskeletal desmin became detached from nuclear surfaces in lamin A/C deficient mice; again evidence of disrupted associations between the two cellular compartments. In contrast, Piercy et al. (2007) reported no disruption of desmin networks in AD-EDMD.

While A-type lamins are expressed in many human tissue-types, EDMD appears to affect primarily muscle. Why this selectivity? It has been proposed that since these tissues are most likely to be subjected to mechanical strain via muscle contractions, they are in all probability, highly susceptible to the nuclear fragility caused by a disrupted lamina (Hutchison et al., 2002; Capell and Collins, 2006). In addition, concomitant with the fact that HGPS patients suffer fatal cardiovascular traumas, evidence shows that vascular cells are severely compromised by the presence of progerin. As a result, these cells have a reduced proliferative capacity and prematurely senesce (McClintock et al., 2006).

1.5.3 Chromatin organisation

Numerous groups have reported changes in genome organisation that occur as a consequence of mutant lamin A or accumulated pre-lamin A (Sewry et al., 2001; Fidzianska and Hausmanowa, 2003; Goldman et al., 2004; Filesi et al., 2005; Maraldi et al., 2006; Meaburn et al., 2007; Lattanzi et al., 2007; Hakelien et al., 2008; Park et al., 2009). Indeed, the peripheral loss or abnormal distribution of heterochromatin has been repeatedly documented in such cells (Sabatelli et al., 2001; Goldman et al., 2004; Filesi et al., 2005; Columbaro et al., 2005; Meaburn et al., 2007; Lattanzi et al., 2007).

In line with this, modifications to heterochromatin markers such as HP1α and trimethyl-K9-histone 3 have been frequently observed in these mutant cells (Filesi et al., 2005; Scaffidi and Misteli, 2005; Shumaker et al., 2006; Lattanzi et al., 2007; Hakelien et al., 2008). The reduction or loss of lamin species in *Drosophila* (Gurudatta et al., 2010), *C. elegans* (Liu et al., 2000) and mice (Sullivan et al., 1999; Nikolova et al., 2004; Arimura et al., 2005; Yang et al., 2006) reveal similar perturbations in chromatin organisation. Research also demonstrates that other INM proteins have a role in mediating chromatin organisation; however, such evidence is far less extensive. Chromosome 18 is found to be mis-localised in *Lmnb1*$^{-/-}$ knockout murine cells (Malhas et al., 2007) and neutrophils from LBR mutants exhibit chromatin disorganisation (Hoffmann et al., 2002). Furthermore, mutations in *EMD* are shown to perturb correct chromatin localisation in patient muscle and skin cells (Fidzianska et al., 1998; Ognibene et al., 1999) and chromosome positioning in dermal fibroblasts (Meaburn et al., 2007). Since the NL is shown to interact with and tether chromatin to the nuclear edge (Pickersgill et al., 2006; Guelen et al., 2008), it is unsurprising that mutations affecting its protein components, lead to the loss of peripheral heterochromatin. The disruption of complexes involving the DNA-bridging protein, BAF, is also most probably responsible, in part, for the perturbation of chromatin organisation reported in *LMNA* and *EMD* mutants (Margalit et al., 2007). Similarly, such disorganisation in PHA cells is likely to result from interrupted interactions between HP1α and LBR.

1.5.4 Gene Expression

Since chromatin disorganisation has been repeatedly observed in laminopathy-based disease, it is logical to question whether this leads or contributes to aberrant gene expression. Indeed, studies have investigated gene activity in X-EDMD (Tsukahara et al., 2002), MAD-A (Amati et al., 2004) and HGPS (Ly et al., 2000; Csoka et al., 2004; Marji et al., 2010) patients; the consensus was significant alteration in gene expression. Tsukahara et al. (2002) demonstrated that the introduction of emerin into X-EDMD cells, rescued the expression of almost half of the genes affected. Thus, the authors hypothesized that as a way of compensating for emerin loss, cells modify the activity of various genes (Tsukahara et al., 2002). In one study examining gene activity in HGPS, alterations were seen most frequently in genes involved in cell division and

RNA/DNA synthesis (Ly et al., 2000). In another, by Csoka et al. (2004), 1.1% of the genes tested exhibited at least a 2-fold change. Of those genes affected, the most significant groups included those that encoded transcription factors and extracellular matrix proteins (Csoka et al., 2004). It was found that the *MEOX2/GAX* gene displayed a major shift in expression; this is noteworthy since its product is a homebox transcription factor which negatively regulates mesodermal cell proliferation. The fact that the prominent cell types displaying pathology in HGPS are of mesodermal and mesenchymal origin, is surely of some importance (Csoka et al., 2004; Hutchison and Worman, 2004). Furthermore, the introduction of GFP-progerin into normal immortalised fibroblasts results in the misregulation of 194 and 1013 genes, respectively, after 5 and 10 days of expression. The extent to this misregulation ranged from −14-fold to +17.3-fold. Significantly, the over-expression of wild-type lamin A also led to aberrant gene expression, however, the severity of such mis-regulation was considerably less severe than that seen for progerin's presence (Scaffidi and Misteli, 2008). While the majority of evidence linking lamins and gene expression focuses on A-type lamins, the NE sequestration of the transcription factor, Oct-1 is perturbed in lamin B mutant cells, which leads to the deregulated expression of down-stream genes (Malhas et al., 2009).

The analysis of hearts from *Lmna* knock-in and *Emd* knock-out mice also reveal changes in gene expression (Muchir et al., 2007a; Muchir et al., 2007b). Significantly, these mouse models provided evidence of the inappropriate activation of the ERK1/2 branch of the MAPK pathway; a pathway which is postulated to contribute to the pathogenesis of cardiomyopathy. Thus, it is hypothesised that the hyperactivation of ERK1/2 signalling is involved in the cardiac disease observed in both autosomal and X-linked EDMD (Muchir et al., 2007a; Muchir et al., 2007b). Indeed, the expression of several MAPK pathway components is considerably altered prior to the development of heart disease (Muchir et al., 2007a; Muchir et al., 2007b). Furthermore, there appears to be a dosage effect of MAPK activation; the onset of cardiomyopathy in these mice appears earlier in homozygotes (Muchir et al., 2007a; Muchir et al., 2007b). In line with this, a recent paper by Emerson et al. (2009) reports the deregulation of ERK1/2 signalling in lamin A mutant patient fibroblasts. The observation that

mutations in *LMNA* and *EMD* can affect convergent pathways goes someway to explaining how they induce similar disease phenotypes in humans.

Also implicated in the pathogenesis of *EMD*-related disease is the Wnt-signalling pathway. Emerin is found to interact with the transcriptional coactivator, β-catenin, and regulate its activity; this binding is mediated by an APC-like domain harboured by emerin (Markiewicz et al., 2006). In fibroblasts lacking emerin, β-catenin accumulates in the nucleus; an event which results in the deregulated transcriptional activation of β-catenin downstream target genes (Markiewicz et al., 2006). This is a significant finding since Wnt signalling is involved in cardiac muscle formation (Eisenberg and Eisenberg, 2006) and as a result, it was suggested that the disruption of this pathway could possibly play a role in the cardiomyopathy seen in emerin null patients (Markiewicz et al., 2006). Indeed, a recent study confirms that emerin-β-catenin complexes also exist in cardiomyocytes; significantly, these are important for the structure of intercalated discs in such cells (Wheeler et al., 2010). However, Wheeler et al. (2010) suggest that the role of β-catenin in cardiomyocytes appears to be Wnt-independent. Taken together, these studies have begun to unravel the multi-faceted nature of emerin's function within the cell and also contribute to our understanding of how mutations in *EMD* can contribute to the pathogenesis, particularly of cardiac tissue, seen in EDMD and other *EMD*-related diseases.

1.5.5 Role in DNA Repair

Liu et al. (2005) produce evidence to suggest that both unprocessed prelamin A and truncated lamin A act in a dominant-negative manner to perturb DNA damage and repair pathways. The authors show that the accumulation of both truncated lamin A (seen in HGPS) and unprocessed prelamin A (seen in *Zmpste24* deficient mice) leads to delayed checkpoint response, partly through the inefficient recruitment of p53 binding protein 1 (53BP1) and Rad51. This could contribute to the high levels of aneuploidy and micronuclei reported in the *Zmpste24* null mice. Indeed, various chromosomal aberrations have been previously reported in several HGPS cell lines (Mukherjee and Costello., 1998; Corso et al., 2005). In addition, increased γ-H2AX concentrations were observed in these cells, indicating that DNA damage was rife. The *Zmpste24* deficient

mice were also overly sensitive when exposed to DNA damaging agents. Moreover, this revealed elevated susceptibility to double strand breaks (DSBs). Another finding worthy of note was that the frequency of non-homologous end joining (NHEJ) in these mice was raised; NHEJ is a DNA repair process which functions to rescue DSBs. Further experiments uncovered that this possibly occurred to compensate for the impairment of another DSB repair response, homologous recombination (HR; Liu et al., 2005). Taken together, this study proposes that in some way, mutant lamin A perturbs those pathways involved in sensing and responding to DNA damage. Indeed, Liu et al. (2005) suggests that this reduced capacity to recruit DNA repair proteins is related to the fact that the truncated form of lamin A localises more intensely at the NE and ER, than mature lamin A (Pendas et al., 2002).

In agreement with these findings, Varela et al. (2005) demonstrated that p53 signalling is involved in the accelerated ageing phenotype displayed by Zmpste24$^{-/-}$ mice. Using microarray analysis, the group revealed that in these mice, there was an up-regulation in various down-stream targets of p53, the tumour suppressor protein. These included *p21* and *Gadd45a*. Significantly, they reported similar results for *Lmna* deficient mice. Varela et al. (2005) hypothesize that mutant lamin A perturbs nuclear integrity and as a result, a so-called structural checkpoint is activated. Consequently, the initiation of DNA damage responses occurs, such as an increase in p53 transcription. In theory, this could lead to a 'senescence-like programme' which induces the premature ageing phenotype exhibited by laminopathy patients (Varela et al., 2005, p.566). Indeed, symptoms reminiscent of accelerated ageing are observed in mice who have p53 hyperactivity (Tyner et al., 2002).

1.5.6 Role in Proliferation and Differentiation

It is becoming increasingly obvious that the nuclear roles emerin and lamin A/C play are both multi-faceted and complex; in addition to those previously aforementioned, these proteins are found to regulate cell proliferation and/or differentiation. Very significantly, A-type lamins, along with LAP2α, are seen to form a complex with pRb; in fact, they prevent its targeted degradation by the proteosome (Johnson et al., 2004). This stabilisation of pRb by lamin A is necessary for p16-mediated cell cycle arrest at G_1

(Nitta et al., 2006). In support of this, Pekovic et al. (2007) later demonstrated that both lamin A and LAP2α play a part in regulating the phosphorylation and localisation of pRb. They also found that a mutant variant of either protein could perturb this control, leading to a disruption in proliferative checkpoints (Pekovic et al., 2007). In agreement, Bridger and Kill (2004) reported an increased capacity for proliferation in HGPS fibroblasts. Taken together, this evidence shows a direct, undisputable link between A-type lamins and a key factor involved in cell proliferation and differentiation. Importantly, pRb's hypo-phosphorylated form, which functions to prohibit cell cycle progression in non-proliferating cells, binds to the NM (Mittnacht and Weinberg, 1991; Mancini et al., 1994).

Interestingly, when mutant lamin A is ectopically expressed in C2C12 murine myoblasts, muscle differentiation is perturbed (Favreau et al., 2004; Markiewicz et al., 2005). Markiewicz et al. (2005) hypothesised that it is the disruption of these aforementioned complexes that impairs pRb function and thus affects muscle differentiation. Subsequently, Frock et al. (2006) pondered the influence of A-type lamins and emerin on skeletal muscle satellite cell differentiation. Using *Lmna*$^{-/-}$ myoblasts, the authors demonstrated that these cells in fact have a reduced differentiation potential and also exhibit decreased levels of pRb, MyoD and desmin; significantly, these proteins are required for successful muscle differentiation. To confirm this, the artificial expression of MyoD or desmin in *Lmna*$^{-/-}$ cells returned their differentiation potentials to normal (Frock et al., 2006).

These findings indicate that reductions in a myoblast's ability to differentiate could lead to the disease phenotype experienced in EDMD (Frock et al., 2006). Furthermore, disruptions to pRb1/E2F and MyoD pathways plus impaired differentiation kinetics have been documented in emerin null mice. This is consistent with the perturbed muscle regeneration noted in these animals (Melcon et al., 2006). Additionally, cyclin D3, a factor proposed to be required for muscle differentiation, has been identified as a novel partner of lamin A/C (Mariappan et al., 2007). Furthermore, the interaction which exists between A-type lamins and the adipocyte differentiation factor, SREBP1 is reduced in FPLD patients (Lloyd et al., 2002).

It is found that the two main types of stem cells exhibit different profiles of lamin expression; the majority of mesenchymal stem cells (MSC) express lamin A, while in many haematopoetic stem cell (HSC) lineages the protein is absent (Rober et al., 1990; Weissman et al., 2001). Since the primary tissues affected in laminopathy-based diseases are derived from MSCs, it is logical to suggest that lamin mutations could disrupt aspects of their development such as their differentiation, repair and maintenance (Wilson, 2000). Concurrently, lymphoblastoid cells which are of HSC origin do not appear to require A-type lamins for survival (Hornbeck et al., 1988). Indeed, the exogenous expression of progerin, in both normal immortalised fibroblasts and hMSCs, is found to aberrantly activate components of the Notch signalling pathway; a pathway which is important for the regulation of stem cell differentiation (Scaffidi and Misteli, 2008). Similarly, the analysis of HGPS patient cell lines demonstrated a perturbation of Notch signalling. Thus, Scaffidi and Misteli (2008) propose that progerin disrupts hMSC differentiation and cell fate which may contribute to the tissue-specific deterioration seen in HGPS patients. Furthermore, in light of the observation that low levels of the protein are generated in normal individuals (Scaffidi and Misteli, 2006; McClintock et al., 2007), progerin accumulation may also be implicated in the tissue degeneration exhibited during physiological ageing (Scaffidi and Misteli, 2008).

In line with this, pre-lamin A accumulation has recently been reported in the vascular smooth muscle cells (VSMCs) of aged individuals and in those with athersclerosis; significantly, such accumulation was absent in samples from the young and healthy (Ragnauth et al., 2010). This phenomenon was also observed in VSMCs that were aged i*n vitro* (Ragnauth et al., 2010). Taken together, the findings of these studies (Scaffidi and Misteli, 2006; McClintock et al., 2007; Scaffidi and Misteli, 2008; Ragnauth et al., 2010) suggest that HGPS could be a model for normal ageing.

1.5.7 Summarising the similarities and differences between laminopathy-based disease in mice and humans

Mice engineered to lack emerin display a mild clinical phenotype and while such mice demonstrate reduced motor co-ordination, they do not exhibit muscle weakness, joint

contractures or significant cardiac problems. Furthermore, the life-spans of these mice are not significantly different to wild-type (Ozawa et al., 2005). These findings suggest that emerin loss in mice does not induce a comparable phenotype to that seen in human X-EDMD patients. Thus, it has been suggested that these discrepancies are due to interspecies differences and possibly due to the fact that emerin's absence may be compensated by other INM proteins such as MAN1 (Ozawa et al., 2005).

In contrast to the *Emd*$^{-/-}$ mouse model, *Lmna* mutant mice display severer phenotypes and generally mimic human disease more accurately. Lamin A/C null mice exhibit skeletal and cardiac disorders which are characteristic of human EDMD; their growth rate is retarded and they die at 8 weeks (Sullivan et al., 1999). *Lmna*$^{L530P/L530P}$ mice display a phenotype similar to HGPS in humans; indeed, they die prematurely at 4 weeks (Mounkes et al., 2003). This is very interesting since, in humans, this mutation is known to cause AD-EDMD (Mounkes et al., 2003). The mouse model which investigated the effect of *Lmna*$^{N195K/N195K}$ mutations revealed that such mice develop similar cardiac dysfunction to the DCM caused by the heterozygous form of this mutation in humans (Mounkes et al., 2005). Similarly, homozygous *Lmna*^{H222P} mice exhibit a phenotype comparable to their human counterparts (Arimura et al., 2005). Taken together, *Lmna* mouse models serve as a good platform to study *LMNA*-mediated human disease; however, the study by Mounkes et al. (2003) demonstrates that genotype-phenotype correlations are not always translated from human to mice. Furthermore, the disease phenotypes exhibited in these mice result from homozygous *Lmna* mutations as opposed to the heterozygous disease-causing mutations in *Homo sapiens*. Indeed, *Lmna*$^{-/+}$ mice are generally indistinguishable from wild-type counterparts (Sullivan et al., 1999; Arimura et al., 2005; Mounkes et al., 2005).

1.5.8 Potential Therapies

1.5.8.1 Farnesyltransferase inhibitors (FTIs)

The majority of HGPS cases result from a point mutation that activates a cryptic splice site in exon 11 of *LMNA*; this creates a truncated protein, termed progerin, which lacks the terminal 50 amino acids. The loss of these residues removes the cleavage site required by the endoprotease, ZMPSTE24 (Eriksson et al., 2003). As a result, the

necessary cleavage cannot occur and thus, the protein remains both carboxymethylated and farnesylated. The presence of this farnesyl group causes the protein to remain anchored to the NE and thus, is prevented from being incorporated into the NL (Hennekes and Nigg, 1994). The loss of *ZMPSTE24* activity in humans, which causes the disease, RD, also prevents lamin A maturation and thus, retention of the farnesyl group (Navarro et al., 2005). Progerin is shorter than and thus, distinct from, the resulting pre-lamin A molecule in RD.

Experiments using farnesyltransferase inhibitors (FTI) have been instrumental in understanding the detrimental effects associated with the retention of this farnesyl group (figure 1.6). Since this farnesyl group is involved in the targeting of pre-lamin A/progerin to the INM, by preventing the addition of this group by FTI treatment, the immature protein cannot associate with the NE and thus, remains in the nucleoplasm (Toth et al., 2005). In this way, pre-lamin A/progerin's disruption of nuclear shape can be largely reduced. Indeed, FTI treatment of typical HGPS and RD cells has been shown to reverse and reduce abnormal nuclear morphology (Toth et al., 2005; Mallampalli et al., 2005; Glynn and Glover, 2005; Capell et al., 2005; Yang et al., 2005). Significantly, FTIs also ameliorate misshapen nuclei in atypical HGPS cells, which harbour missense mutations that do not result in pre-lamin A/progerin accumulation (Toth et al., 2005; Verstraeten et al., 2006). This alleviation of nuclear abnormalities is likely to be a consequence of a reduction in the incorporation of mutant lamin A generated by such *LMNA* mutations, into the INM (Toth et al., 2005). The demonstration that the introduction of GFP-progerin into normal fibroblasts induced a significant rise in nuclear aberrations confirms progerin's dominant negative-effect as a protein (Glynn and Glover, 2005).

The treatment of *Lmna*$^{HG/-}$ mice with FTIs is shown to improve survival and ameliorate other disease symptoms such as body weight and spontaneous bone fractures (Yang et al., 2008). It can also prevent the onset as well as progression of cardiovascular disease (Capell et al., 2008). Interestingly, treatment with FTI-277 has been shown to reverse the incorrect localisation of nucleolar proteins seen in HGPS fibroblasts (Mehta et al., 2010). The treatment of human fibroblasts with this same drug resulted in the redistribution of heterochromatin (Mattioli et al., 2008). FTI therapy has also been

demonstrated to rescue the perturbed gene expression observed in HGPS cultured cells (Marji et al., 2010). Furthermore, the morphological defects induced by the accumulation of pre-lamin A in aged VSMCs, are reversed by FTIs (Ragnauth et al., 2010).

The use of FTIs does not constitute a cure; indeed, HGPS mice still die prematurely (Yang et al., 2008). While treating ageing *C. elegans* with these drugs is documented to restore perturbed nuclear shape and improve motility, it cannot extend the life-span of the worms (Bar et al., 2009). In addition, incubation of HGPS fibroblasts in FTIs is shown to reverse nuclear stiffness and improve responses in wound healing assays; however, the sensitivity of such cells to mechanical strain is not ameliorated (Verstraeten et al., 2008). Evidently, not all elements of the disease phenotype are improved or rescued after treatment with FTIs. While Liu et al. (2006) demonstrated that abnormal nuclear shape could be reversed in HGPS and RD cells by using FTIs, the aberrant levels of DNA damage and constant activation of DNA damage pathways could not be alleviated. Thus, it has been suggested that abnormal nuclear morphology and the elevation in DNA damage possibly represent two distinct and unrelated phenotypes which result from the accumulation of pre-lamin A. Consequently, its use as a single therapy has been questioned (Liu et al., 2006).

Significantly, it has been demonstrated that in the presence of FTIs, prelamin A and progerin prenylation can occur via an alternative pathway involving geranylgeranyltransferase (GGT; Varela et al., 2008). The activity of this additional enzyme (GGT) is suggested to partially counteract the FTI treatment of prelamin A and progerin accumulation (figure 1.6). Thus, it is thought to account for the incomplete success of FTI therapy in mouse models (Varela et al., 2008).

1.5.8.2 Combination therapy: statins and aminobisphosphonates

In addition to FTIs, there are two other classes of drugs, statins and aminobisphosphonates, which affect lamin biosynthesis. Statins work by preventing the activity of HMG-CoA reductase (Sinensky et al., 1990), while aminobisphosphonates target farnesyl-pyrophosphate synthase (Amin et al., 1992;

Keller and Fliesler, 1999). Historically, statins and aminobisphosphonates have been used to treat high cholesterol levels and bone disease, respectively. However, since these drugs interfere with the pathway involved in the production of farnesyltransferase, they can also be employed to prevent prelamin A's farnesylation and thus, maturation (Pereira et al., 2008; see figure 1.6). Indeed, Varela et al. (2008) demonstrated that the combination therapy of statins and aminobisphosphonates ameliorated progerin/pre-lamin A specific defects in HGPS and *Zmpste24*$^{-/-}$ cells. Furthermore, improvements to body weight, reductions in subcutaneous fat levels and extended lifespans were observed in *Zmpste24*$^{-/-}$ mice undergoing statin-aminobisphosphonate treatment (Varela et al., 2008).

1.5.8.3 Morpholino oligonucleotides

Scaffidi and Misteli (2005) took a different approach to reversing the cellular phenotype in HGPS. Instead, the experiment involved the use of a modified oligonucleotide; this small anti-sense molecule was targeted to the cryptic splice site commonly activated in HGPS. Since the molecule has a sequence that is complementary to this site, it is able to sterically inhibit the splicing activity. The group successfully prevented the production of 90% of progerin from the mutant allele and furthermore, the treated HGPS cells showed vast improvements in their nuclear morphology. Nuclear behaviour, such as histone modifications and the expression of select genes were also rescued. Another interesting point to note was that the improvements in nuclear shape occurred without entering mitosis. Importantly, they demonstrated that merely introducing wild type lamin A into HGPS cells did not reverse the cellular phenotype; this was true even at high concentrations for prolonged periods (Scaffidi and Misteli, 2005).

However, there is evidence to suggest that the activation of the cryptic splice site is not 100% efficient (Reddel and Weiss, 2004). The authors examined the transcript levels of lamin A produced from both alleles (mutant and normal) in HGPS heterzygotes. They discovered that the splicing event is in fact incomplete and that the mutant allele can still produce fully functional lamin A; this is possible since the silent mutation does not alter the amino acid encoded (Reddel and Weiss, 2004).

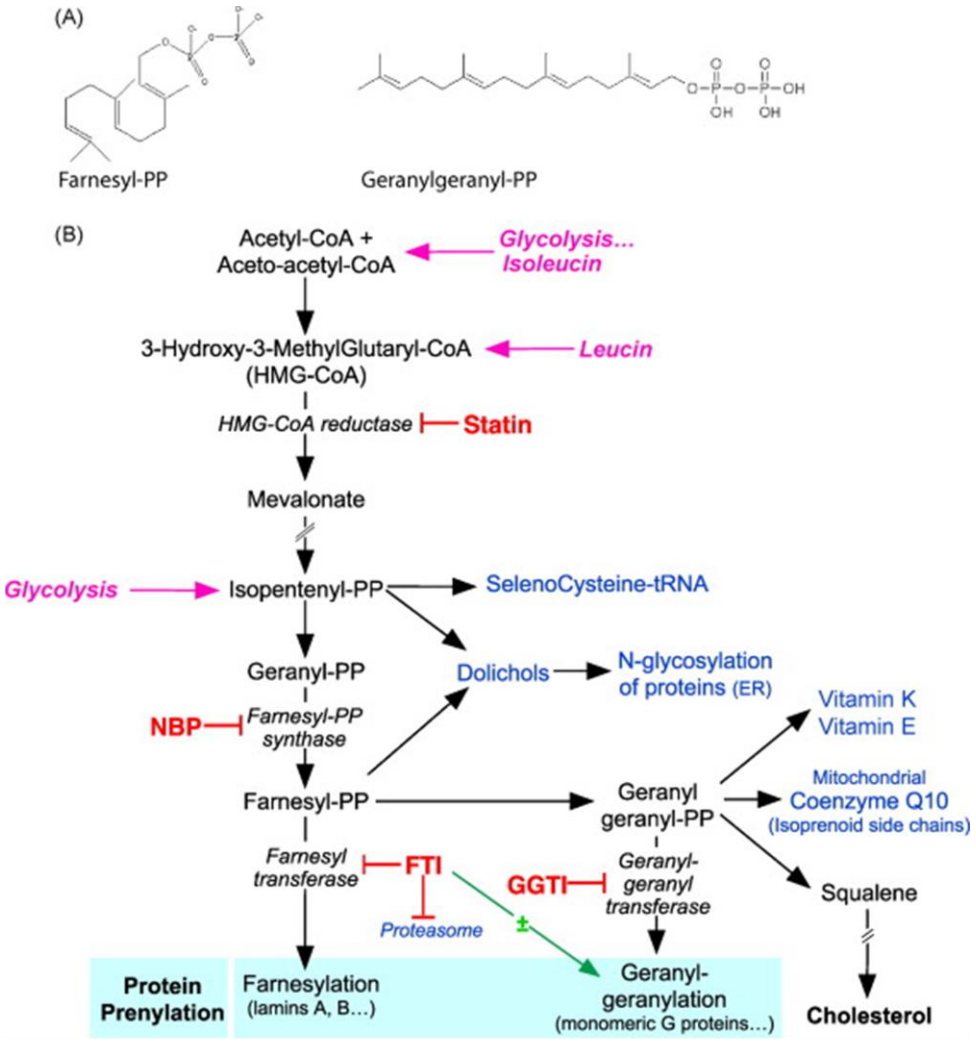

Figure 1.6: Inhibitors of isoprenoids and cholesterol biosynthetic pathways.

(A) Chemical structures of farnesyl-PP and geranylgeranyl-PP used in protein prenylation. **(B)** The isoprenoid pathway can be arrested at different steps (red): statins inhibit HMG-CoA reductase, a polytopic protein inserted into the ER membrane. The rate-limiting enzyme of the synthesis of these farnesyl-PP and geranylgeranyl-PP is the farnesyl-PP synthase, selectively inhibited by amino-bisphosphonates (NBPs). The farnesyl-transferase (FT) and geranylgeranyl-transferase (GGT, type 1) are the targets of their respective inhibitors (FTI and GGTI). Figure (including legend) sourced in its entirety from Pereira et al. (2008).

1.5.9 Consolidating the roles of INM proteins: a model for laminopathy-based disease

This review has highlighted the need for an intact NL in cellular integrity; indeed, the wide array of disease phenotypes described adds credence to this observation. However, this overview has also drawn attention to the fact that the scientific community have a long way to go in terms of determining those mechanisms involved in the manifestation of disease. In the future, it is likely that additional NE proteins will be discovered, bringing along with them new laminopathy disorders. Indeed, the recent discovery of lamin B mutations in human disease supports this prediction. All in all, this will contribute to the rapidly progressing, exciting field of research that is NE proteins.

1.6 CONCLUSION

This review of the literature has highlighted the importance of NE and NM proteins, especially lamin A, in maintaining the correct functioning of the nucleus. Indeed, the plethora of diseases which arise from mutant or absent forms of these proteins, further strengthen this view. Since the organisation of the genome is perturbed in a number of these disorders, it is necessary to ponder how and why this occurs and whether it has an effect on nuclear processes such as transcription and DNA repair. As the NM is demonstrated to mediate genome organisation, it seems pertinent to examine these interactions in cells which harbour mutant NM proteins. This should hopefully reveal the importance of such proteins in NM function.

2. Using the DNA halo assay to examine the role of the nuclear matrix in mediating genome organisation

(Partially published in Elcock and Bridger, in press)

2.1 INTRODUCTION

2.1.1 What is the NM?

The NM is a proteinaceous and RNA-rich network which spans the nucleus; it is proposed to consist of thick polymorphic fibres, underlying which are 10 nm filaments that connect this internal NM to the peripheral NL (Jackson and Cook, 1998; He et al., 1990; Nickerson et al., 2001). Originally, the term NM was used to describe the residual nuclear structure which remained following DNA digestion and extraction using high salt molarities (Berezney and Coffey, 1974). On the other hand, the phrase nucleoskeleton refers to the nuclear structure which is isolated using a gentler, more physiological method (Jackson and Cook, 1988). In addition to the terms NM and nucleoskeleton, nuclear scaffold has also been assigned by some to describe the nuclear structure isolated using the detergent, lithium di-iodosalicylic acid (LIS; Mirkovitch et al., 1984). However, to avoid confusion, much of the field use such terms interchangeably (Nickerson, 2001). Although research shows that at least 300 NM-associated proteins exist (Mika and Rost, 2005), the structural composition of the NM has not yet been fully determined (Nickerson, 2001). The NM provides a platform for replication and transcription; indeed, factories for both processes are associated with the structure (Jackson and Cook, 1985; Hozak et al., 1993; Cook, 1999; Anachkova et al., 2005).

2.1.2 The isolation and visualisation of the inner NM

Different methodologies have been employed to isolate and visualise the inner NM. In general, a detergent, usually Triton X-100 is used to extract plasma and nuclear membranes. Such treatment removes the majority of phospholipids and a proportion of both cellular and nuclear proteins (Aaronson and Blobel, 1974). In order to remove the chromatin which obscures the view of the underlying inner NM, the residual structures are subjected to nucleases/DNase I, which partially digest the DNA. The primary dissimilarities between different NM preparations revolve around the elution of this DNA; some methodologies employ 2M NaCl (Berezney and Coffey, 1974), while others use lower salt concentrations (Capco et al., 1982; Fey et al., 1986; He et al., 1990; Nickerson et al., 1992). Conversely, the procedure used to isolate the

nucleoskeleton involves agarose beads, physiological buffers and electro-elution (Jackson and Cook, 1988).

A protocol which employs 0.25 M ammonium sulphate followed by 2M NaCl has been used to visualise NM structure (He et al., 1990; see figure 2.1.1). The elution of digested chromatin is achieved by using 0.25M ammonium sulphate; along with the DNA, the bulk of histones and other soluble proteins are also removed. Such treatment uncovers the outer NM, which is composed of non-uniformly-arranged, polymorphic fibres which run throughout the nuclear interior. Between these fibres, there are large gaps of differing sizes. Further extraction by 2M NaCl removes the outer NM proteins and in the process of doing so, reveals thinner, regular filaments which are 9–13 nm in diameter (He et al., 1990; Nickerson et al., 1992). It is proposed that these filaments, termed the core filaments of the NM, are both protein and RNA rich and the framework on which the aforementioned polymorphic fibres are built (He et al., 1990). Indeed, approximately 70% of total nuclear RNA remains after this high-salt extraction (He et al., 1990). The treatment of this framework with RNase A, results in the almost complete removal of core filaments, leaving the nucleus as an empty shell; significantly, the NL remains intact and is largely unaffected. This provides evidence that intact RNA is an essential component of the inner NM (He et al., 1990).

In order to improve the preservation of NM ultrastructure, this methodology used by He et al. (1990) has been subject to modifications. Nickerson et al. (1997) employed the cross-linking agent, formaldehyde, to stabilise the structure of the NM before the removal of attached chromatin. Importantly, following this use of formaldehyde, digested chromatin could be removed without the use of non-physiological salt concentrations. Later, Wan et al. (1999) demonstrated that by chemically modifying nucleosomal amine groups, which are thought to complicate the removal of digested material, chromatin could be removed easily without the need for non-physiological salt concentrations. In this same study, three methodologies were tested and compared: (1) original (He et al., 1990), (2) formaldehyde-cross linking (Nickerson et al., 1997) and (3) amine modification (Wan et al., 1999). Significantly, the visualisation of the nuclear interior using these different protocols revealed that the internal NM is

indeed built upon a highly-branched network of filaments approximately 10 nm in diameter (Wan et al., 1999).

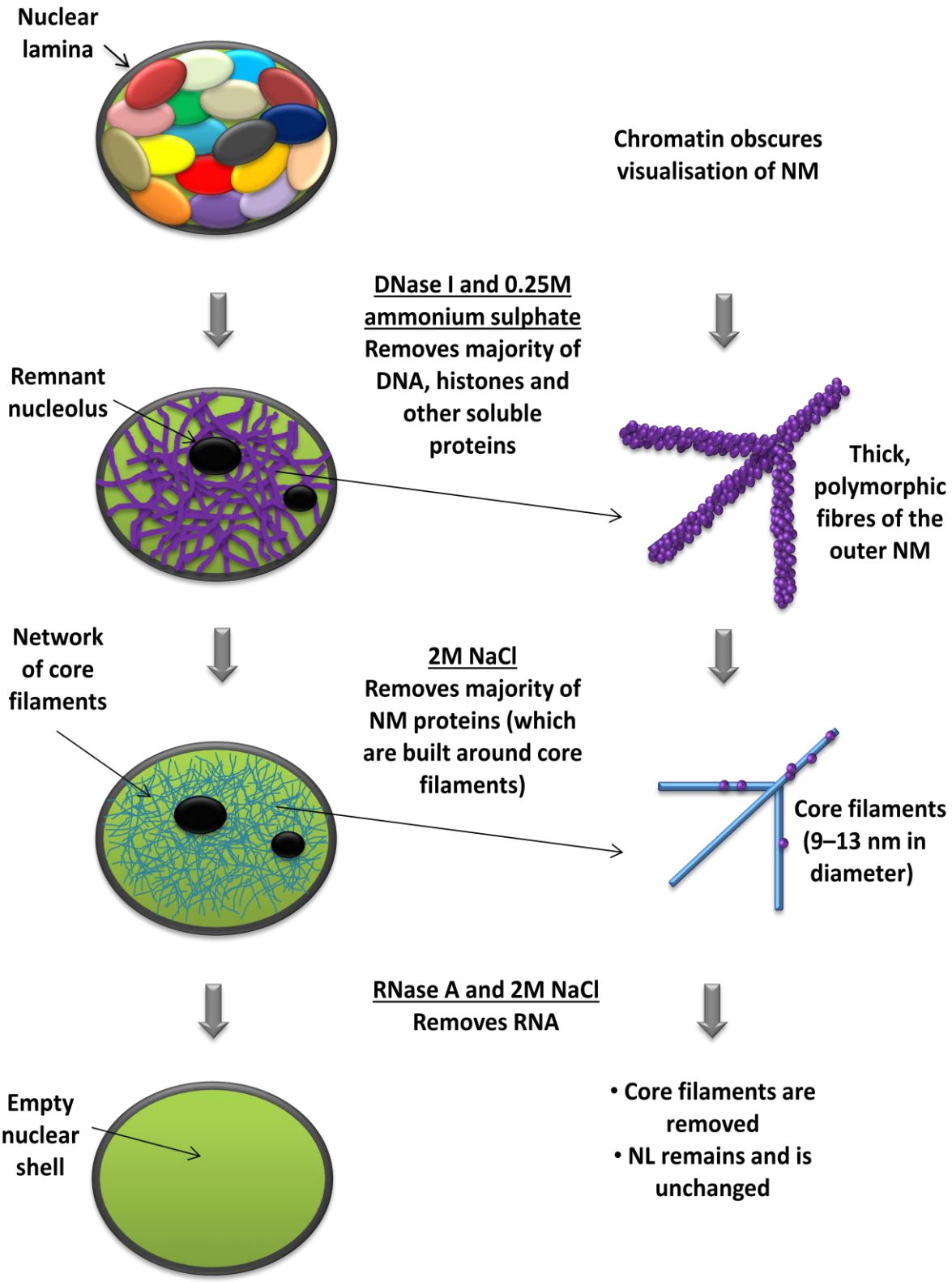

Figure 2.1.1: A summary of the methodology employed to visualise the structure of the NM

2.1.3 The role of the NM in organising the genome

2.1.3.1 Overview

Within the interphase nucleus, chromosomes are non-randomly organised (Foster and Bridger, 2005). It is uncertain whether the positioning of these chromosomes is driven by gene density (Croft et al., 1999; Bridger et al., 2000; Boyle et al., 2001; Meaburn et al., 2005, 2007) or size (Sun et al., 2000; Bolzer et al., 2005; Mora et al., 2006); indeed, some groups provide evidence to suggest that it is a combination of the two (Habermann et al., 2001; Tanabe et al., 2002; Mayer et al., 2005; Mora et al., 2006; Neusser et al., 2007). Since this radial positioning of chromosomes appears to change according to cellular state (Bridger et al; 2000; Meaburn et al., 2007; Mehta et al., 2010) and differentiation (Galiova et al., 2004; Kim et al., 2004), much debate surrounds its functional relevance.

Importantly, the NM appears to mediate the organisation of the genome; the structure is involved in tethering chromatic regions within the interphase nucleus (de Lange, 1992; Gerdes et al., 1994; Ma et al., 1999; Weipoltshammer et al., 1999). Indeed, the genome interacts with the NL at multiple sites named LADs; these are typically characterised by low levels of gene expression (Guelen et al., 2008). It is hypothesised that the NM organises chromatin into repeating loops, approximately 50–200 kb in length; the DNA sequences at the base of these loops, which interact with the NM are termed MARs (matrix attachment regions; Cockerill and Gerrard, 1986) or SARs (scaffold attachment regions; Gasser and Laemmli, 1986), depending on the nuclear extraction procedure used for their examination (Bode et al., 1992; Heng et al., 2004). From this point onwards, the term MAR will refer to both MARs and SARs. MARs function as *cis*-acting elements which are involved in transcriptional regulation (Laemmili et al., 1992; Boulikas, 1995; Schubeler et al., 1996; Bode et al., 2000; Martins et al., 2004). They are shown to function as both transcriptional enhancers (Blasquez et al., 1989; Bode et al., 1992; Allen et al., 1996) and insulators (Kalos and Fournier, 1995; Namciu et al., 1998; Antes et al., 2001; Farrell et al., 2002; Yusafzai and Felsenfeld, 2004; Goetze et al., 2005). Importantly, MARs demarcate transcriptionally active chromatin domains (Bode and Maass, 1988); however, they are also found within intronic DNA (Kas and Chasin, 1987). MARs bind to an number of proteins

including: scaffold attachment factor-A (SAF-A; Romig et al., 1992; Fackelmayer et al., 1994; Fackelmayer and Richter, 1994; Gohring and Fackelmayer, 1997; Kipp et al., 2000), scaffold attachment factor-B (SAF-B; Renz and Fackelmayer, 1996), DNA topoisomerase II (Adachi et al., 1989), lamin B1 (Luderus et al., 1992), A-type lamins (Luderus et al., 1994), NuMa (Luderus et al., 1994), nucleolin (Dickinson and Kohwi-Shigematsu, 1995) and CTCF (Dunn et al., 2003).

Although approximately 100,000 MARs are estimated to exist within the genome (Bode et al., 1996), the characterisation of these sequences to date has not been extensive (Bode et al., 2000; Nickerson, 2001). A consensus element is yet to be reported and in line with this, it has been suggested that the interactions are more dependent on the structural conformation of MARs than the DNA sequences alone (Bode et al., 1998). However, MARs are typically AT rich; the weak bonds between AT bases are predicted to facilitate the binding of MAR-associated proteins (Platts et al., 2006). Indeed, MAR-like regions of AT-rich sequences, known as 'AT islands' are found to be thermodynamically unstable, highly flexible and susceptible to base unpairing (Woynarowski et al., 2001). It is proposed that MARs and DNA topoisomerases may work together to regulate the topology of chromatin regions, thus facilitating transcriptional processes (Bode et al., 1992).

2.1.3.2 DNA halo preparations

NM preparations involving the use of DNase I are extremely useful for visualising and characterising the structural morphology and composition of the inner NM, however, they are not appropriate for examining NM-DNA interactions. In order to examine such genomic associations, a methodology known as the DNA halo preparation was developed; while many variations of this technique exist, the majority of methodologies employ detergents and salt or LIS to extract histones, other non-soluble proteins and non-NM associated DNA (Wiegant et al., 1992; Tocharoentanaphol et al., 1994; Luderus et al., 1996; Ma et al., 1999; Ratsch et al., 2002; Iarovaia et al., 2004). Once interphase nuclei have been subjected to such preparation, residual structures known as nuclear or DNA halos are found to remain. These structures are composed of a residual nucleus, surrounded by a halo of DNA; the residual nucleus is composed of

the NM and NM-associated DNA, while the halo contains extracted DNA. The coupling of DNA halo preparations with FISH, thus termed HALO-FISH (Volpi and Bridger, 2008), has been used for genomic mapping and the study of genomic interactions with the NM (Elcock and Bridger, 2010b). Indeed, the spatial resolution achieved with these DNA halos is significantly higher than that attained using FISH on metaphase chromosomes or interphase chromatin (Wiegant et al., 1992; Heng et al., 1992). The organisation of the human dystrophin gene into loop domains has been studied extensively at such high resolution using HALO-FISH (Tocharoentanaphol et al., 1994; Iarovaia et al., 2004); importantly, the results correspond to those generated using biochemical approaches (Iarovaia et al., 2004). Indeed, using this technique, it has been demonstrated that one of the gene's loop attachment regions is a major deletion hotspot (Iarovaia et al., 2004). Similarly, Repping et al. (2003) employed a variation of HALO-FISH (named sperm HALO-FISH) to accurately determine the copy number of *DAZ* (Deleted in AZoospermia), a gene associated with spermatogenic failure.

2.1.3.3 Examining genomic interactions with the NM

2.1.3.3.1 Chromosome territories (CT)

In addition to its use as a tool for high resolution mapping, HALO-FISH has been frequently employed to examine genome interactions with the NM. Ma et al. (1999) demonstrated that CTs remain intact after extraction using 2M NaCl. Thus, despite the loss of histones and other soluble proteins, CT organisation is still maintained. The combination of RNase A and 2M NaCl is found to disrupt such CT organisation; this implicates the involvement of the NM's core filaments in mediating such genome arrangements. This disruption of CTs was accompanied by the extraction of a subset of nuclear proteins, which could be implicated in the mediation of CT organisation. However, significantly, despite this perturbation of CT structure, the majority of chromosome mass remained within the periphery of the residual nucleus. An additional study by Croft et al. (1999) revealed that the anchorage of chromosomes 18 and 19 differed according to gene density; gene-rich HSA-19 was found to be tightly associated with the NM, while gene-poor HSA-18 was extracted into the surrounding DNA halo.

2.1.3.3.2 Telomeric DNA

Using telomere specific probes for HALO-FISH, Luderus et al. (1996) examined telomere anchorage by the NM; DNA halos were produced using either LIS or NaCl extraction methodologies. Significantly, both protocols revealed that the majority of telomeres are attached to the NM; thus, concurring with previous biochemical data produced previously (de Lange, 1992). More recent work also concurs with this notion (Ratsch et al., 2002). Furthermore, it was demonstrated that the internal NM rather than the peripheral NL, was responsible for this telomere anchorage (Luderus et al., 1996). Telomeres are found throughout the nuclear volume and exhibited no significant clustering; the exception to this was in late telophase/early G1, when a ring of telomeres around the nuclear periphery, was reported (Luderus et al., 1996).

2.1.3.3.3 Genes and other specific genomic regions

Gerdes et al. (1994) used HALO-FISH to study the interactions of specific genes with the residual nucleus. Strikingly, transcriptionally active genes were observed to tightly associate with the NM, whereas transcriptionally inactive genes were extracted into the DNA halo and thus, assumed to be non-NM associated (Gerdes et al., 1994). Furthermore, HALO-FISH has been used to determine whether *MYC* and *IGK* exhibit different interactions with the NM when involved in a Burkitt's lymphoma (BL) translocation event (Ratsch et al., 2002). In normal monocytes, *MYC* and *IGK* were associated with the residual nucleus, in 40% and 8% of cases, respectively. In the BL-derived cells, there were differences between those genes found on translocated chromosomes and those on non-translocated chromosomes. Significantly, the majority of the activated *MYC* (78%) and *IGK* (88%) alleles were associated with the NM. In contrast, the non-translocated *MYC* and *IGK* alleles were attached to the residual nucleus in 50% and 62% of cases, respectively (Ratsch et al., 2002). In line with Gerdes et al. (1994), these findings also demonstrate a correlation between transcriptional activity and NM-association. Providing further evidence that NM interactions are functional, Iarovaia and colleagues (Iarovaia et al., 2005) studied the interaction of a ~170 kb region of HSA-19 with the NM, in both proliferating and differentiated cells. Significantly, in these two states, the anchorage of this region differed; in proliferating

nuclei, it was extracted into the DNA halo while upon differentiation, it was found to be attached to the NM (Iarovaia et al., 2005).

2.1.4 Using DNA halo preparations as a platform to analyse genomic interactions with the nuclear matrix

2.1.4.1 Chromosomes

Since it has been demonstrated that the NM is involved in mediating the organisation of CTs (Ma et al., 1999), it seemed pertinent to question whether different chromosomes have varying levels of interactions with the structure in human fibroblasts. In order to do this, HALO-FISH was performed using whole chromosome probes for HSA-1, -13, -15, -17 and -18. In light of the observation that the organisation of CTs in interphase nuclei changes according to proliferative state (Bridger et al; 2000; Meaburn et al., 2007; Mehta et al., 2010), the interaction of these chromosomes with the NM was examined in both proliferating and senescent (in 10% serum) nuclei. The marker of proliferation, pKi67, was used to differentiate between these populations (Kill, 1996).

2.1.4.2 Telomeres

Telomere interactions with the NM were also investigated in three distinct cellular states: proliferation, quiescence (G_0) and senescence. In order to do this, the DNA halo preparation has been coupled with telomere PNA FISH (Peptide Nucleic Acid Fluorescence *in situ* Hybridisation); this allowed us to differentiate between those telomeres that are tightly attached to the NM and those which are not. Proliferating and senescent populations (in 10% serum) were distinguished by the use of either bromodeoxyuridine (BrdU) incorporation and detection or anti-pKi67 staining. Control HDFs were induced into quiescence using serum-starvation and their proliferative status verified using anti-pKi67. Importantly, the results demonstrate that in all 3 cellular states, the majority of telomeres remain associated with the NM in human dermal fibroblasts. Interestingly, no significant differences in telomere anchorage by the NM were observed when comparing proliferating and senescent populations; however, significantly fewer were associated with the structure in quiescence.

2.1.4.3 Genes

In order to investigate whether the anchorage of specific genes by the NM changes on entry into senescence, *CCND1*, *C-MYC* and *CTNNA1* were examined in proliferating (pKi67+) and senescent (in 10% serum; pKi67−) HDFs using the DNA halo assay. Significantly, the binding of each gene to the NM did not differ statistically between pKi67+ and pKi67− extracted nuclei. However, importantly, the extent to which specific genes were anchored by the NM did vary. These results demonstrate that different genes are bound with varying avidities to the NM and importantly, such binding does not change detectably on entry into senescence.

Taken together, the findings presented in this chapter reveal that genome interactions do not differ significantly in proliferating and senescent cells using the DNA halo assay.

2.2 MATERIALS AND METHODS

2.2.1 Cell Culture

Primary human dermal fibroblasts were grown in Dulbecco's Modified Eagle Medium (DMEM; Gibco, Invitrogen) containing 10% (v/v) newborn calf serum (NCS), 2% (v/v) penicillin/streptomycin (Invitrogen) and L-glutamine (v/v) (Invitrogen); the cells were kept at 37°C, in an atmosphere containing 5% $C0_2$. Cells were passaged twice weekly. At pre-confluence, the medium was removed and the cells were rinsed with versene (phosphate buffered saline (PBS; 137 mM NaCl, 2.7 mM KCl, 10 mM Na_2HPO_4, 2 mM KH_2PO_4; pH7.4) with 0.2% (w/v) ethylenediaminetetra-acetic acid; EDTA). Following this, the culture was treated with 0.25% trypsin (2.5% stock solution ((Gibco)) 1:10 dilution in versene (v/v)); the cells were continually checked using an Olympus CK2 light microscope until complete cell detachment from the substratum. The cell suspension was then added to a 15 cm^2 centrifuge tube and the flask rinsed using 5 ml medium. The completion of the trypsin reaction was initiated by the addition of the medium containing the remaining cells. This cell suspension was centrifuged for 5 minutes at 200 g; following this, the supernatant was removed, leaving only the pellet, which was then re-suspended in fresh medium. Using a haemocytometer, the number of cells was counted (viewed with a light microscope; 20x lens) and the cell density was calculated using the following equation:

Number of cells/Number of squares on haemocytometer grid x Volume in tube x 10^4

The cells were then seeded at a density of 5 x 10^5 per 75 cm^2 flask or 2 x 10^5 per 10 cm^2 dish, along with an appropriate volume of medium and grown as aforementioned. For DNA halo preparations, the cells were grown for 2 days on SuperFrost® (Fisher Scientific) slides, in QuadriPERM™ chambers (Greiner Bio One), at a starting density of 1 x 10^5. In order to arrest cells in G_0, cells were twice washed with serum-free medium after 24 hours of growth and then fed with 0.5% NCS medium; cells were then left for 7 days.

2.2.2 BrdU Labelling

Cells were seeded on SuperFrost® slides (Fisher Scientific) in QuadriPERM™ chambers at a density of 1 x 10^5 and were left to grow for 24 hours. The medium was then removed and replaced with medium containing BrdU and FrdU (3 µg/µl) (Sigma Aldrich). After 24 hours, the media was removed, cells were washed once with medium (10% NCS) and then re-fed with medium (10% NCS). Following an additional 24 hours, the slides were taken through the DNA halo preparation.

2.2.3 DNA Halo Preparation

The methodology used to create DNA halos is the same as that published by Bridger and Lichter (1999). After two days of growth, the medium was removed and the slides were placed in Coplin jars, on ice, containing CSK buffer (10 mM Pipes pH 7.8, 100 mM NaCl, 0.3 M sucrose, 3 mM $MgCl_2$, 0.5% (v/v) Triton-X 100) for 15 minutes. The slides were then washed three times in 1 x DNA halo buffer (DHB; 140 mM NaCl, 27 mM KCl, 110 M $NaPO_4$, 15 mM KH_2 PO_4). Following this, they were placed in extraction buffer (2 M NaCl, 10 mM Pipes pH 6.8, 10 mM EDTA, 0.1% (w/v) digitonin (Sigma Aldrich), 0.05 mM (v/v) spermine (Sigma Aldrich), 0.125 mM (v/v) spermidine (Sigma Aldrich)) for 4 minutes. The slides were rinsed consecutively in 10 x DHB (1.4 M NaCl, 270 mM KCl, 1.1 M $NaPO_4$, 150 mM KH_2PO_4) , 5 x DHB, 2 x DHB and 1 x DHB, for 1 minute each. They were then taken through an ethanol series of 10%, 30%, 70% and 95% (v/v), respectively. The slides were then air dried and stored at −80°C until FISH was performed.

2.2.4 Directly labelled total human chromosome probes

Chromosome probes were made in-house via the amplification of flow sorted chromosomes (a kind gift from Professor M. Bittner) by DOP-PCR (degenerate oligonucleotide primed polymerase chain reaction; Telenius et al., 1992; Cheung and Nelson, 1996). Subsequently, these were labelled using Biotin-16-2'-deoxy-uridine-5'-triphosphate (Biotin-16-dUTP). FISH probes were prepared by making the following solution: 8 µl PCR product, 7 µl $C_O t$-1 DNA (Roche), 3 µl herring sperm, with 1/20th

volume of 3M sodium acetate (pH 5.4) and 2 volumes of 100% ethanol, per slide. This probe solution was then incubated at −80°C for at least 30 minutes. Following this, it was centrifuged at 13,700 g at 4°C for 15 minutes and then washed with 70% ethanol. The centrifugation and washing procedure was repeated once more, finishing with a final centrifugation. The DNA pellet was subsequently dried; to which 12 µl of hybridisation buffer (50% formamide, 10% dextran sulphate (Helena Biosciences), 10% 20 x saline sodium citrate (SSC; 3M NaCl, 0.3M tri-sodium citrate; pH 7.0), 1% (v/v) Polyoxyethylene sorbitan monolaurate (Tween-20 (Sigma-Aldrich)) per slide, was added. This solution was mixed and left at 37°C for at least 2 hours, overnight in some cases.

2.2.5 Directly labelled human single gene probes

2.2.5.1 DNA Isolation from BAC clones

Bacterial Artificial Chromosomes (BACs) were obtained from Invitrogen. A small portion of glycerol stock from the respective BAC clone was streaked onto a Luria-Bertani (LB) agar plate (1% (w/v) NaCl; 1% (w/v) tryptone, 0.5% (w/v) yeast extract, 1.5% (w/v) Agar Technical (Oxoid, Fisher Scientific); 12.5 µg/ml (w/v) chloramphenicol (Sigma)). The plate was then incubated at 37°C overnight. Next, a single colony from the plate was used to inoculate 10 ml of LB broth (1% (w/v) NaCl; 1% (w/v) bactotryptone, 0.5% (w/v) yeast extract (Oxoid, Fisher Scientific); 12.5 µg/ml (w/v) chloramphenicol (Sigma)); this solution was left in a shaking incubator at 37°C overnight.

In order to make glycerol stocks of the BAC clone, 0.5 ml of the bacterial culture was placed in an eppendorf with 0.5 ml glycerol, mixed and then stored at −80°C. The remainder of the culture was centrifuged at 1,700 g for 10 minutes at room temperature. The supernatant was discarded and 300 µl of P1 solution (15 mM Tris (pH 8), 10 mM EDTA, 100 µg/ml RNase A) was added to the pellet. After vigorous vortexing, the cells were transferred into a 2 ml eppendorf. Next, 300 µl of P2 solution (0.2 M NaOH, 1% (w/v) sodium dodecyl sulphate (SDS) was added to the cells in a dropwise manner; following this, the tube was inverted 5 times and left at room temperature for a maximum of 5 minutes. 300 µl of P3 (3 M CH_3COOK) was then

added slowly and after gentle mixing, the eppendorf was placed on ice for 10 minutes. Next, the tube was centrifuged at 8,100 g for 10 minutes at 4°C; the supernatant was then transferred into a tube containing 800 µl of ice-cold isopropanol and inverted several times before being placed at −20°C overnight.

Following the overnight incubation, the tube was centrifuged at 8,100 g for 15 minutes at 4°C. The supernatant was removed and 500 µl of ice-cold 70% ethanol was added. The tube was inverted several times and then centrifuged for 5 minutes at 4°C (8,100 g). The supernatant was then removed and the pellet was left to dry at room temperature. When dry, the pellet was re-suspended in 40 µl of diethyl pyrocarbonate-treated water (DEPC-treated) and left at 4°C overnight. Once fully re-suspended, 5 µl of the solution was loaded onto a 1% agarose gel, in order to check for the presence of DNA.

2.2.5.2 Single probe preparation

The respective DNA was then labelled using a Nick Translation kit (Invitrogen). Each mix contained: 5 µl dNTP mix (minus dTTP), 1 µl Biotin-16-dUTP (Roche), 5 µl Pol I/DNase I Mix, DEPC-treated water (Fisher Scientific) and DNA. Once mixed and centrifuged briefly, the solution was incubated at 15°C overnight. To verify the fragment sizes, 5 µl of the solution was loaded onto a 2% agarose gel.

In order to remove the unincorporated nucleotides, Illustra MicroSpin G-50 Columns (GE Healthcare) were used. Initially, the column was placed into the collection tube and centrifuged at 3,200 g for 1 minute. The collection tube was discarded and the column placed into a sterile eppendorf. After adding the DNA solution, the column was again centrifuged at 3,200 g for 1 minute. The column was then discarded; to the DNA solution in the tube, 5 µl herring sperm DNA (10 mg/ml), 10 µl 3M NaAC and 2.25 V of 100% ice cold ethanol was added. After gentle mixing, the solution was incubated at −80°C for 1 hour. Following this, the tube was centrifuged at 13,700 g for 30 minutes at 4°C. The supernatant was discarded and the pellet washed with 200 µl of ice cold 70% ethanol. Again, the tube was centrifuged at 13,700 g for 15 minutes at 4°C. The supernatant was discarded and the pellet was dried for approximately 15 minutes

using the Speed Vac® Plus SC110A (Savant). The pellet was re-suspended in 20 µl of DEPC-treated water (at room temperature for several hours or overnight at 4°C) and then stored at -20°C.

For each slide, 5 µl probe DNA was mixed with 5 µl C_0t-1 DNA and then dried for 15 minutes using the Speed Vac® Plus SC110A. Once the pellet had dried, it was re-suspended in 12 µl of hybridisation mix (detailed previously).

2.2.6 2-Dimensional Fluorescence *in situ* Hybridisation

The DNA probes were denatured at 75°C for 10 minutes. Following this, the probes were kept at 37°C for 30 minutes to 2 hours; after this incubation, 12 µl of probe was added to the appropriate slide, covered by a coverslip secured using rubber glue (Halfords). Next, the slides were left at 37°C in a humid hybridisation chamber for at least 18 hours.

After removing the slides from the hybridisation chamber, the rubber was carefully taken off. The slides were then washed in buffer A (50% formamide, 2 x SSC (pH 7.0)), pre-warmed to 45°C, for 15 minutes, with 3 changes of buffer. Subsequently, the same procedure was performed with buffer B (0.1 x SSC (pH 7.0)) but instead incubated at 60°C. The slides were then plunged into 4 x SSC at room temperature. Following the post-hybridisation wash procedures, 100 µl of blocking solution, 4% bovine serum albumin (BSA) (Sigma Aldrich) was added to the slides, which were covered by parafilm; these were then incubated at room temperature for 10 minutes. In order to detect the labelled probe, each slide was incubated in 100 µl of a 1:200 dilution (made up in 1% BSA) of streptavidin-Cy3 antibody (Amersham Life Sciences Ltd) for 1 hour at room temperature. After which, the slides were washed with 4 x SSC (0.5% Tween-20) 3 times, for 5 minutes per wash. At this point, the slides were mounted in counterstain, Vectashield (Vector Laboratories) containing 4', 6-diamidino-2-phenylindole (DAPI).

2.2.7 Telomere PNA FISH

Telomeres were detected using a Telomere PNA FISH Kit/FITC (Dako); the protocol was carried out according to manufacturer's instructions. The procedure was performed at room temperature, unless stated otherwise. Slides were immersed in tris-buffered saline (TBS, pH 7.5) for 2 minutes and then placed in 3.7% formaldehyde (in TBS; v/v) for exactly 2 minutes. Following this, slides were washed in TBS twice for 5 minutes at a time. They were immersed in pre-treatment solution for 10 minutes and then washed twice with TBS for 5 minutes per wash. Next, the slides were taken through an ice cold ethanol series comprising of 70%, 85% and 95% (v/v) ethanol for 2 minutes per concentration. After this, the slides were air dried and then 10 µl of Telomere PNA Probe/FITC (or Cy3) was added to each slide and covered with a coverslip. The slides were placed in a pre-heated oven set at 80°C for 5 minutes and then put in the dark for approximately 1 hour. In order to remove the coverslips, the slides were immersed in the 'Rinse Solution' for 1 minute and then placed in the 'Wash Solution' for 5 minutes at 65°C. Following this, the slides were taken through the ice-cold ethanol series (70%, 85% and 95% (v/v)) for 2 minutes per concentration and then air dried. At this point, slides were mounted with Vectashield (Vector Laboratories) containing DAPI.

2.2.8 Indirect Immunofluorescence

Slides were washed 3 times in PBS and incubated at room temperature for 1 hour in the necessary primary antibody (rabbit anti-human pKi67 (Novocastra) diluted 1:1500; BrdU mouse anti-human diluted 1:100 (BD Pharmingen); all dilutions made using 1% (v/v) NCS). Cells were then washed 3 times in PBS and incubated at room temperature for 1 hour in a fluorochrome-conjugated secondary antibody (pKi67: swine anti-rabbit TRITC diluted 1:30 (Dako); BrdU: donkey anti-mouse Cy3 diluted 1:100 (Jackson Laboratory)). Following 3 more washes with PBS, slides were mounted with Vectashield (Vector Laboratories) containing DAPI.

2.2.9 Image Capture

DNA halo prepared nuclei were visualised using one of 3 different microscope systems and respective lenses; grey-scale images of randomly selected nuclei were captured using various cameras. Images were pseudocoloured and merged using various versions of Digital Scientific software (table 2.2.1).

Microscope system	Lens	Camera	Imaging Software
Leica fluorescence microscope	Leica Plan Fluoropar 100x oil immersion lens	Cooled charge-coupled device (CCD) camera (Sensys, Photometrics)	Smart Capture VP V1.4 (Digital Scientific)
Olympus BX41 fluorescence microscope	Olympus UPlanFL N 100x oil immersion lens	Model viewpoint GS digital camera (Digital Scientific)	Smart Capture V3.0 (Digital Scientific)
Zeiss Axioplan 2 fluorescence microscope	Zeiss Ph3 Plan-NEOFLUAR 100x oil immersion lens	Cooled charge-coupled device (CCD) camera (Sensys, Photometrics)	Smart Capture V2.0 (Digital Scientific)

Table 2.2.1: An overview of the microscopes, lenses, cameras and software used to visualise, capture and process DNA halo prepared nuclei.

2.2.10 Image Analysis

2.2.10.1 Chromosome territories

The images were converted into TIFFs and then the colour balance modified using IP Lab Spectrum Software. Using Adobe Photoshop, the images were cropped and split into individual colour channels i.e. red, blue and green; each channel was saved separately. Next, the residual nucleus was identified and selected using NIH Image/ Scion Image; following this, the colour of the residual nucleus was modified and density threshold and binary functions were performed (figure 2.2.1).

This allowed the centre of the nucleus to be determined. The distance from the nuclear centre to each furthest chromosome territory edge (CTE) was determined. These distances were divided by the distance from the nuclear centre to each respective nuclear edge (NE). Results were presented as a CTE/NE ratio. This process was performed for at least 50 nuclei, from which an average CTE/NE ratio was established, for each chromosome and cell line. For an overview of the analysis process, see figure 2.2.2. Using this data, bar charts were plotted and error bars were added which corresponded to the ± standard error mean (SEM) (SEM: standard deviation/ square root of n, where n is the sample size).

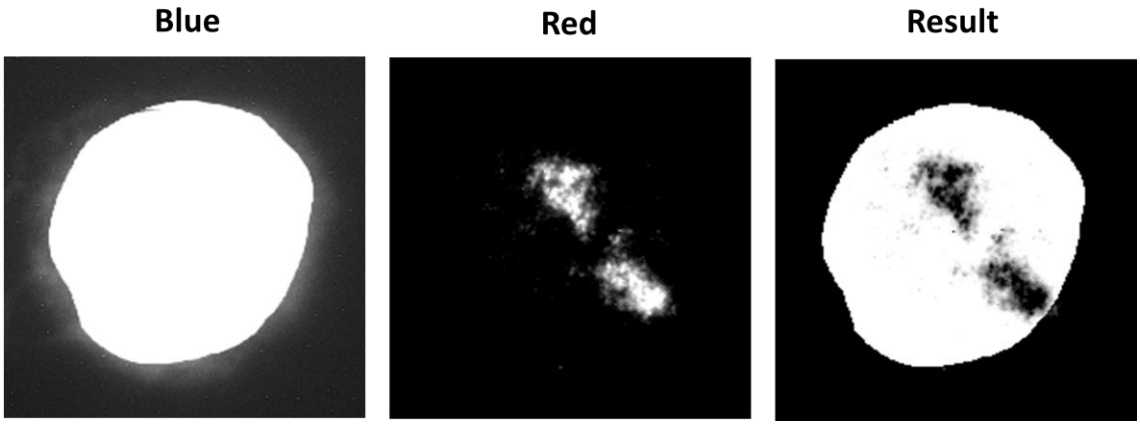

Figure 2.2.1: An overview of the analysis method used to examine chromosome anchorage by the NM

The blue channel captures the DAPI-stained nucleus and surrounding DNA, while the red channel detects the probe signal. The residual nucleus is selected and removed using NIH image/ Scion Image (see resultant 'Blue' channel). The image denoted 'Result' is the outcome of superimposing the red channel on the blue channel image; this allows the aforementioned distances to be calculated.

2.2.10.2 Telomeres

30 nuclei were analysed per dataset. The images were opened in Photoshop 5.0.2 and analysed manually; the number of telomeres within (1) the residual nucleus and (2) within the DNA halo, were counted. BrdU or pKi67 staining was used to differentiate between proliferating (BrdU/pKi67+) and senescent (BrdU/pKi67−) nuclei. Using this data, bar charts were plotted and error bars were added which corresponded to the ± SEM.

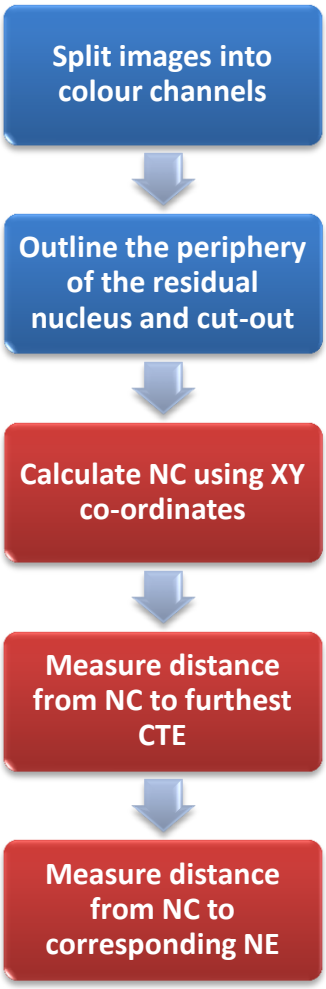

Figure 2.2.2: An overview of the analysis procedure employed to measure CT extraction following HALO-FISH. NC = nuclear centre; CTE = chromosome territory edge; NE = nuclear edge.

2.2.11 Statistical Analysis

The Student's *t*-test (unpaired) was used to statistically compare the results; $p < 0.05$ was considered significant.

2.3 RESULTS

2.3.1 Using DNA halo preparations to examine chromosome interactions with the nuclear matrix

2.3.1.1 An assay to examine chromosome anchorage by the nuclear matrix

In order to examine chromosome interactions with the NM, control HDFs were subjected to the DNA halo preparation. As a consequence of the permeabilisation and extraction stages, the residual nucleus should only theoretically consist of the inextractable NM and any NM-associated DNA and protein (Gerdes et al., 1994). Conversely, the DNA halo is composed of extracted DNA (figure 2.3.1a). It is thus possible to differentiate between those sequences which were attached to the NM at the point of fixation and those which were not (or were very loosely associated with the structure). 2D FISH was then employed to visualise specific chromosomes and to investigate whether different chromosomes interact with the NM to varying extents. 5 chromosomes were studied: HSA-1, -13, -15, -17 and -18 (figure 2.3.1). HSA-1 was chosen since it is the largest chromosome; HSA-13 was selected due to the fact that it is acrocentric and thus, associates with nucleoli (Henderson et al., 1972; Sullivan et al., 2001) and has a similar gene density to HSA-18. HSA-15 was selected since it is significantly more gene dense than HSA-13 but is of a comparable size and is also acrocentric (Deloukas et al., 1998). HSA-17 and HSA-18 were chosen since although they are similar in size, HSA-17 is gene-rich, while HSA-18 is gene-poor (Deloukas et al., 1998). Furthermore, they are not acrocentric chromosomes.

In order to compare chromosome anchorage by the NM, the distance from the nuclear centre to each furthest chromosome territory edge (CTE) was determined. These distances were divided by the distance from the nuclear centre to each respective nuclear edge (NE). At least 50 nuclei were analysed per dataset and the collation of these results was presented as an average CTE/NE ratio.

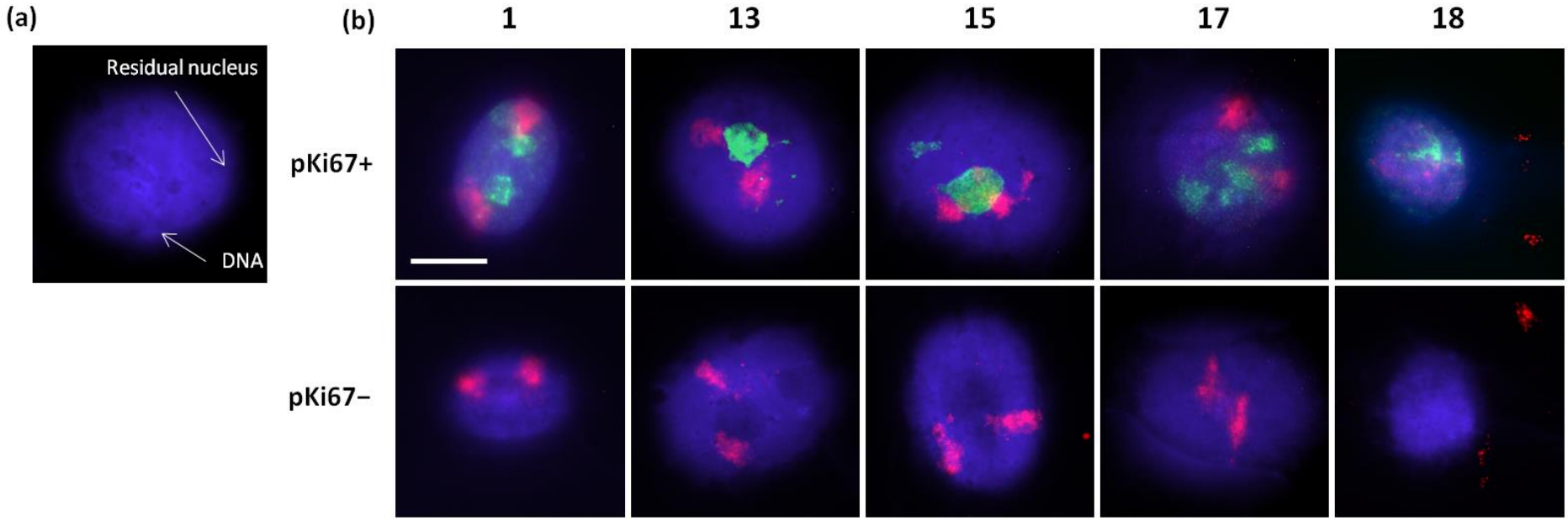

Figure 2.3.1: Analysing NM-chromosome interactions using HALO-FISH

(a) A control HDF which has been extracted using the DNA halo preparation; NM-associated DNA is anchored to the residual nucleus, while extracted, non-NM associated DNA forms the faint halo surrounding the structure. DNA has been stained using DAPI and can be seen in blue. **(b)** Control HDFs were subjected to the DNA halo preparation and 2D-FISH. Specific probes were used for chromosomes 1, 13, 15, 17 and 18. Chromosome paints are depicted in red (Cy3). In order to differentiate between proliferating (pKi67+) and senescent nuclei (pKi67–), HALO-FISH nuclei were also stained with anti-pKi67, which can be seen in green (FITC).

2.3.1.2 The majority of chromosome mass is attached to the NM regardless of cellular state

In order to test whether chromosomes form different interactions with the NM in proliferative and non-proliferative states, HALO-FISH was coupled with anti-pKi67 staining (figure 2.3.1b). pKi67 is a nucleolar antigen which exists only in proliferating cells (Gerdes et al., 1984; 1986; Kill, 1996). Therefore, it can be used to differentiate between proliferating and senescent cells. Nuclei positive for pKi67 were scored as proliferative, while those negative were deemed senescent. Significantly, all chromosomes except for HSA-18 were largely attached to the residual nucleus. This suggests that, typically, many MARs exist within chromosomes 1, 13, 15 and 17 which anchor the chromosomes to the residual nucleus, thus preventing their extraction. On the other hand, since HSA-18 was frequently extracted into the DNA halo as a whole chromosome, this indicates that far fewer MARs are located within chromosome 18. However, this data for HSA-18 is tentative since the number of nuclei examined per population was less than half (n = 24) than that analysed for the other 4 chromosomes (n = 50). This was due to technical difficulties with the HSA-18 probe DNA. Nevertheless, it is likely that the extraction trend for HSA-18 is correct since it concurs with previous data by Croft et al. (2001). The anchorage of all chromosomes analysed did not change according to cellular state; indeed, statistical; analysis demonstrated that NM-chromosome interactions were similar in both proliferating and senescent nuclei (figure 2.3.2; 2.3.3). The CTE/NE ratios for each chromosome indicate that, on average, the chromosome territory edge barely exceeded that of the corresponding nuclear periphery. However, there were statistical differences between chromosomes (figure 2.3.2b), suggesting that although there is a mass anchorage of these 5 chromosomes, there are variations in the levels of NM attachment.

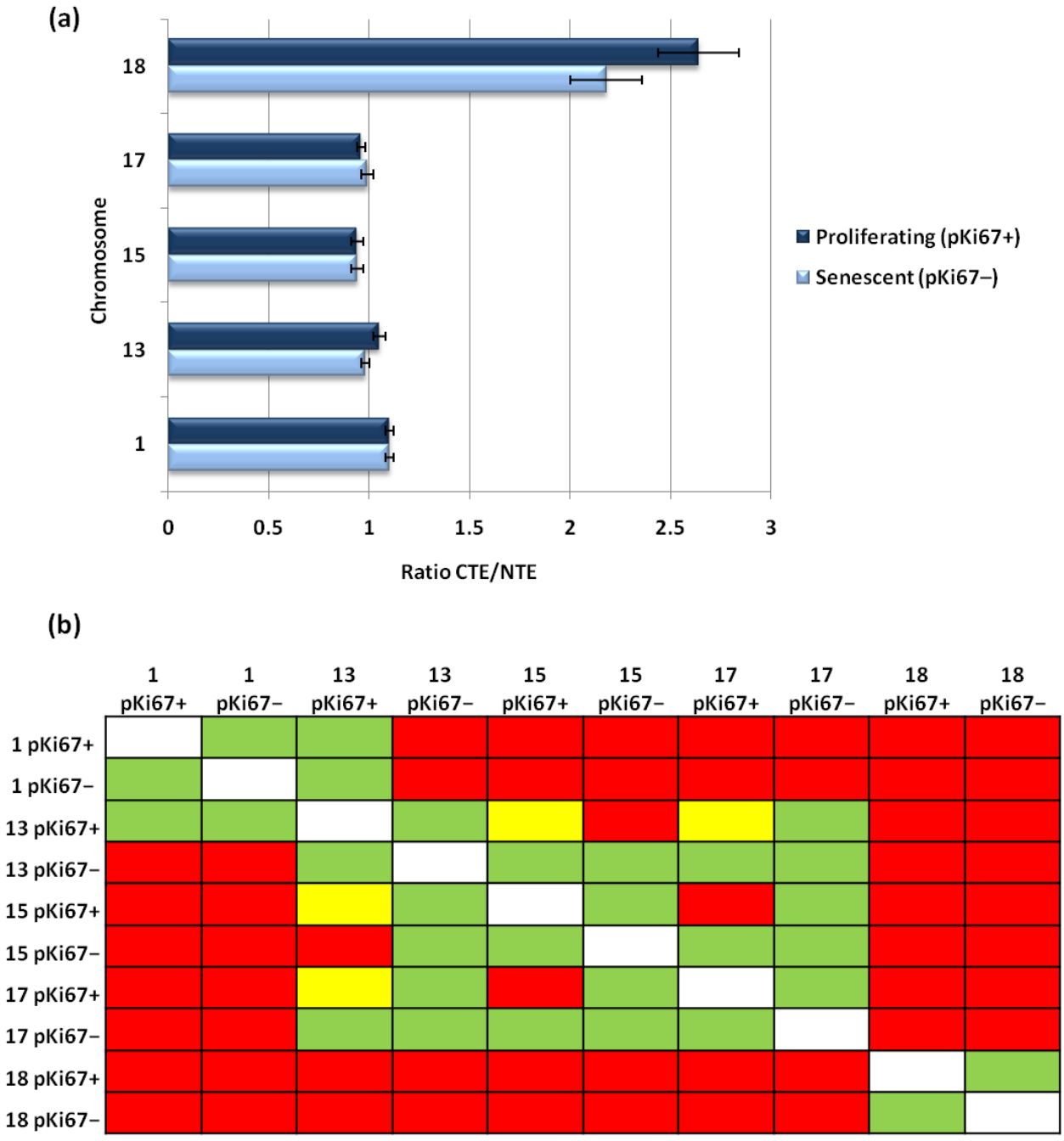

Figure 2.3.2: Examining chromosome anchorage by the NM in proliferating and senescent control HDFs using the DNA halo assay

(a) The ratio of furthest chromosome territory edge (CTE) to respective nuclear edge (NE) for specific chromosomes in pKi67+ and pKi67– nuclei. Error bars represent ± SEM. **(b)** Statistical analysis of NM-chromosome interactions using the Student's *t*-Test. + = pKi67+; – = pKi67–. Green shading indicates no significant difference between the populations, yellow shading depicts a *p*-value < 0.05 and red shading represents *p*-value < 0.01.

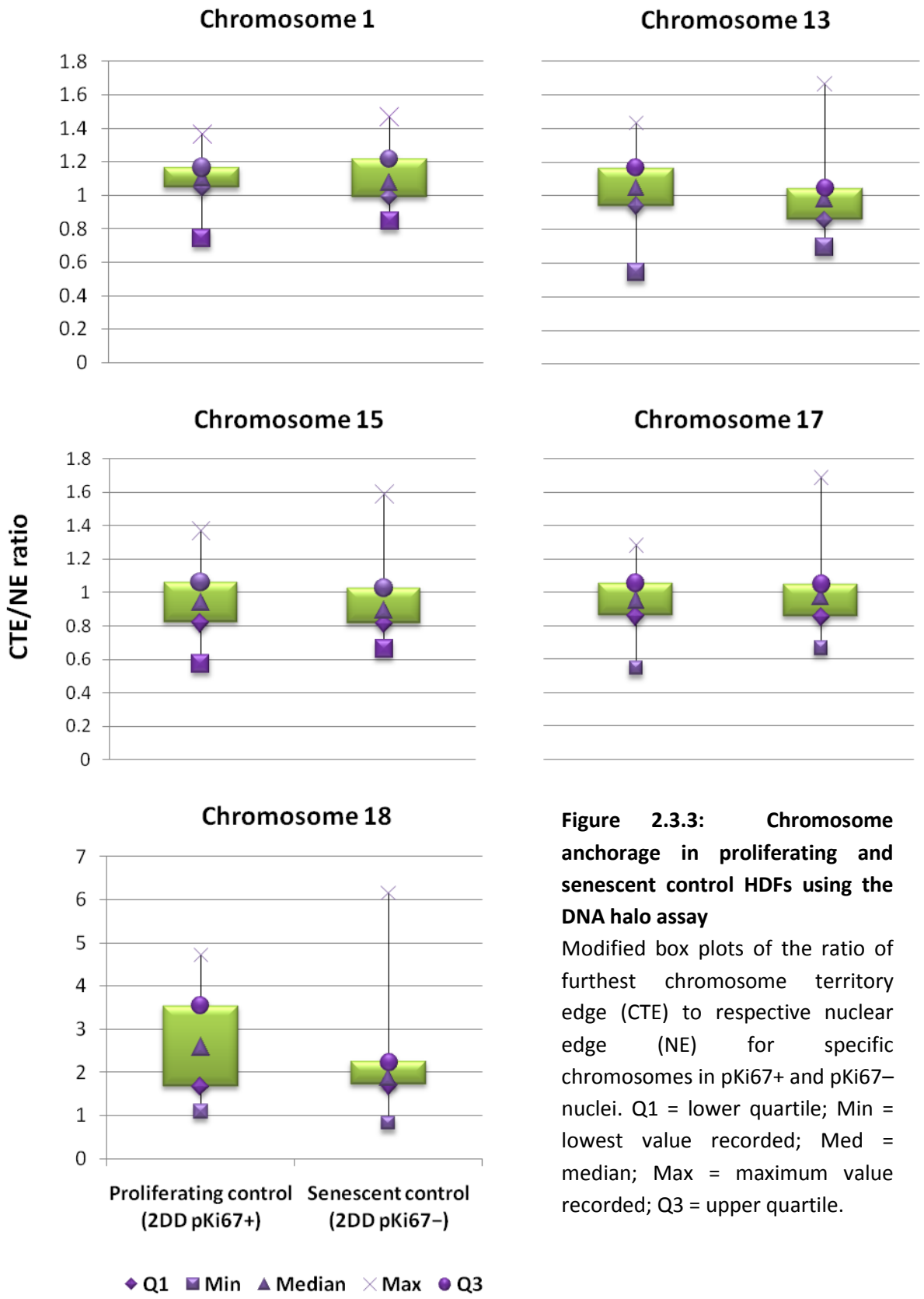

Figure 2.3.3: Chromosome anchorage in proliferating and senescent control HDFs using the DNA halo assay

Modified box plots of the ratio of furthest chromosome territory edge (CTE) to respective nuclear edge (NE) for specific chromosomes in pKi67+ and pKi67– nuclei. Q1 = lower quartile; Min = lowest value recorded; Med = median; Max = maximum value recorded; Q3 = upper quartile.

2.3.2 Using DNA halo preparations to examine telomere interactions with the NM

2.3.2.1 An assay to examine telomere anchorage by the NM

I have coupled the DNA halo preparation with telomere PNA FISH, in order to examine telomere interactions with the NM in control HDFs. Resulting images were analysed by scoring the number of telomere signals within the residual nucleus and the number of telomeres in the DNA halo (figure 2.3.4). From these values, the percentage of telomeres extracted into the DNA halo was calculated.

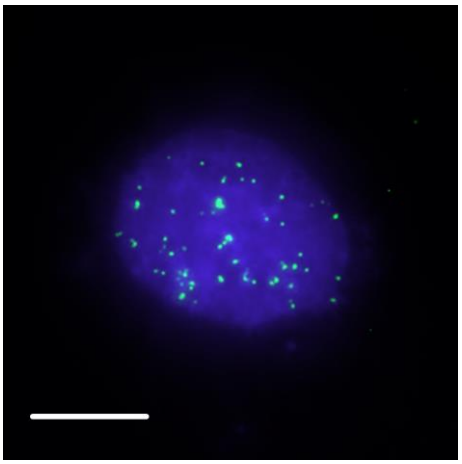

Figure 2.3.4: Telomere anchorage in a control HDF using the DNA halo preparation.
The residual nucleus and surrounding DNA halo have been counterstained using DAPI (blue) while telomere signals can be seen in green (FITC). Magnification = x100; scale bar = 10 μm.

To check the consistency of the results (within a slide), 3 sets of 30 nuclei were analysed. In each of the three data sets, on average approximately 15% of telomeres were extracted into the DNA halo (figure 2.3.5). When comparing the three data sets (nuclei = 30), no statistical differences were observed, suggesting that the results produced by the assay are consistent and reproducible. Furthermore, these data indicate that the analysis of a population of 30 nuclei provides an accurate representation of telomere anchorage in this control population.

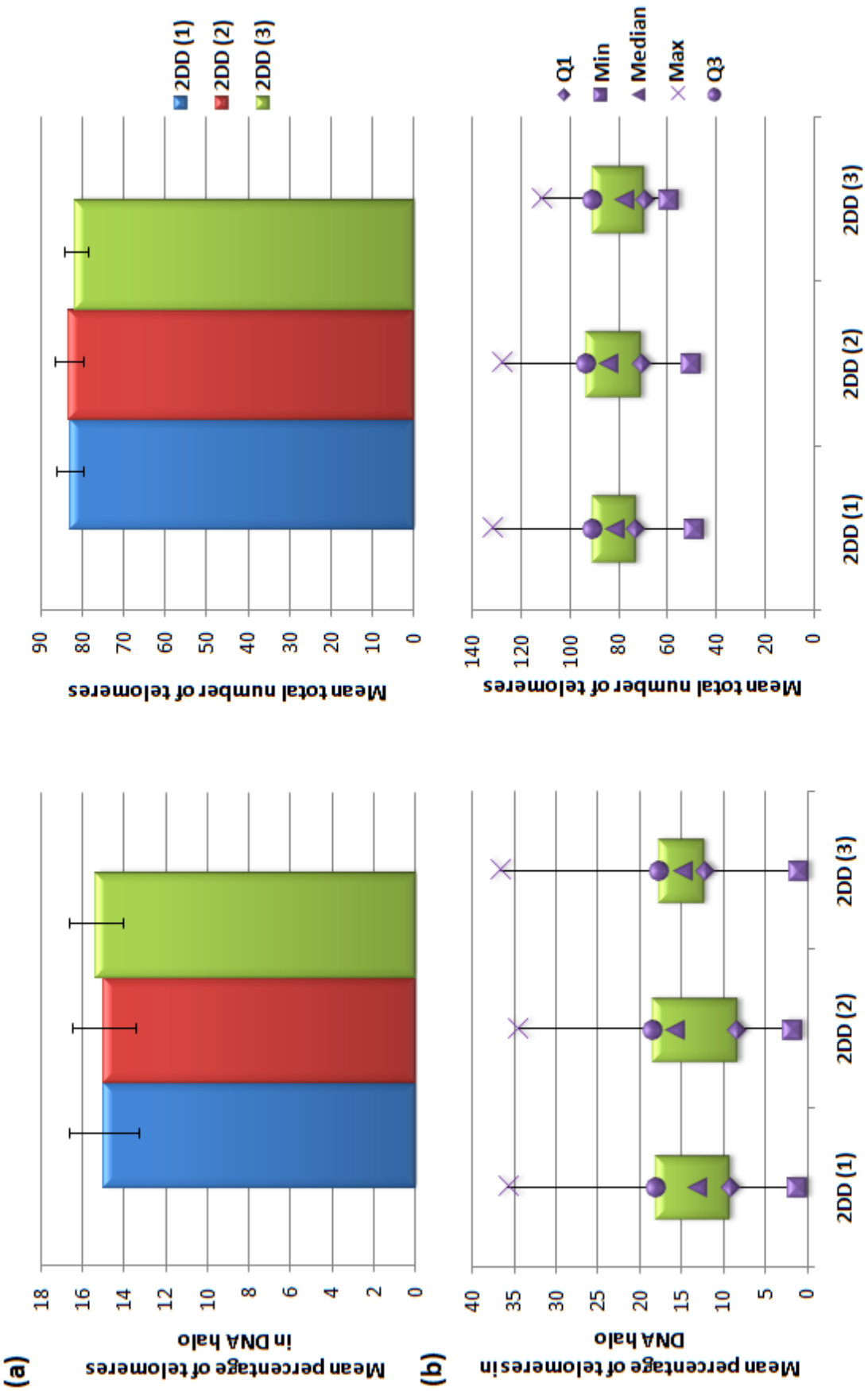

Figure 2.3.5: Examining NM-telomere interactions in control HDFs using the DNA halo assay. (a) Mean percentage of telomeres extracted into DNA halo and mean total number of telomeres scored for control HDFs. Error bars represent ± SEM. **(b)** Modified box plots (Q1 = lower quartile; Min = lowest value recorded; Med = median; Max = maximum value recorded; Q3 = upper quartile).

2.3.2.2 Examining telomere anchorage by the NM in proliferating and senescent (senescent) HDFs using the DNA halo assay

To determine whether telomere associations with the NM vary between different cellular states, we determined the percentage of telomeres in the DNA halo for proliferating and senescent cell populations. Control HDFs were grown on glass slides in QuadriPERM^{TM} chambers and then incubated in a mixture of BrdU/fluorodeoxyuridine (FrdU) for 24 hours. Following another 24 hours growth, the cells were subjected to the DNA halo preparation. In order to differentiate between those cells which had incorporated the thymidine analogue (BrdU) and those which had not, residual nuclei were stained with anti-BrdU. Proliferating nuclei stained positive for the presence of BrdU (BrdU+), while senescent nuclei were BrdU negative (BrdU−; figure 2.3.6).

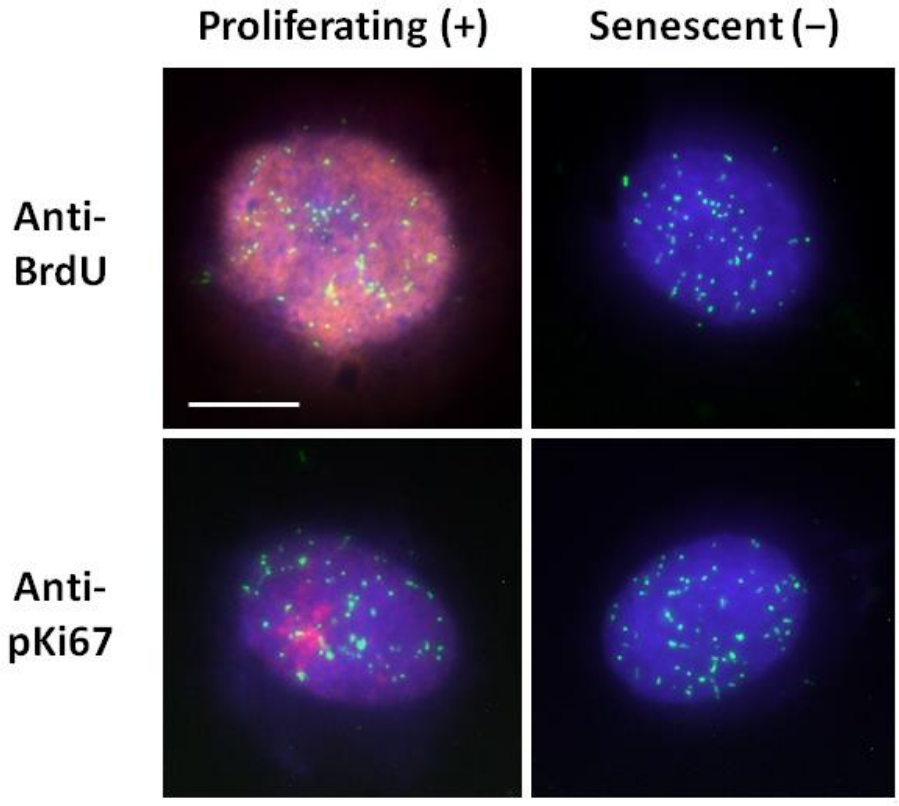

Figure 2.3.6: Examining telomere anchorage by the NM in proliferating and senescent HDFs using the DNA halo assay.
Control HDFs were subjected to the DNA halo preparation and telomere PNA-FISH. The residual nucleus and surrounding DNA halo have been counterstained using DAPI (blue) while telomere signals are green (FITC). Proliferating nuclei have been detected using anti-BrdU or anti-pKi67 staining (red; TRITC). Magnification = x100; scale bar = 10 μm.

For proliferating (BrdU+) nuclei, an average of 14.1% (± 7.8 (± standard deviation); nuclei = 90) of telomeres were extracted into the DNA halo, while for senescent (BrdU−) nuclei, this value was 16.5% (± 7.7; nuclei = 90; see figure 2.3.7). Importantly, when comparing these results to the pooled HDF population presented in the previous section (2.3.2.1), which exhibited 15.1% (± 8.1; nuclei = 90) of telomeres in the DNA halo, there were no statistical differences. This is significant since it demonstrates that DNA halo preparations performed separately produce statistically similar levels of telomere anchorage by the NM. When statistically comparing BrdU+ and BrdU− nuclei, a significant difference was detected using $p < 0.05$; however, there was no difference with $p < 0.01$. Thus, this suggests that there may be a small difference between telomere interactions with the NM in proliferating and senescent nuclei using the DNA halo assay.

Since the use of BrdU in living cells is documented to induce a senescent-like phenotype, in terms of gene expression and the number of MARs that exist (Michishita et al., 1999; Suzuki et al., 2001; Suzuki et al., 2002), it seemed necessary to examine telomere anchorage in proliferating and senescent nuclei using another method to differentiate between the two populations. Therefore, anti-pKi67 was employed; cells grown in the absence of BrdU preceding the DNA halo preparation were stained with anti-pKi67 (figure 2.3.6). Importantly, there was no significant statistical difference between the pKi67 populations; in pKi67+ residual nuclei, an average of 10.9% (± 4.9; nuclei = 30) of telomeres were extracted into the DNA halo, while in pKi67− nuclei, a mean of 9.3% (± 5.1; nuclei = 30) were scored in the DNA halo (nuclei = 30; figure 2.3.8).

Thus, while nuclei grown in the presence of BrdU demonstrated that senescent nuclei exhibited an increase in telomeres in the DNA halo; pKi67-differentiated nuclei displayed the reverse trend. When statistically comparing BrdU+ and pKi67+ nuclei, no significant difference was detected. However, BrdU− and pKi67− were statistically different. This could suggest that telomere anchorage does not differ between proliferating and senescent nuclei and therefore, the discrepancy between the results represents a variation which is either inherent with the assay. Therefore, taken together, these findings suggest that on average, 9–17% of telomeres are not

anchored by the NM in control HDFs. This concurs with the results of a biochemical study performed by de Lange (1992), which reported that at least 80% of telomeric DNA is attached to the NM.

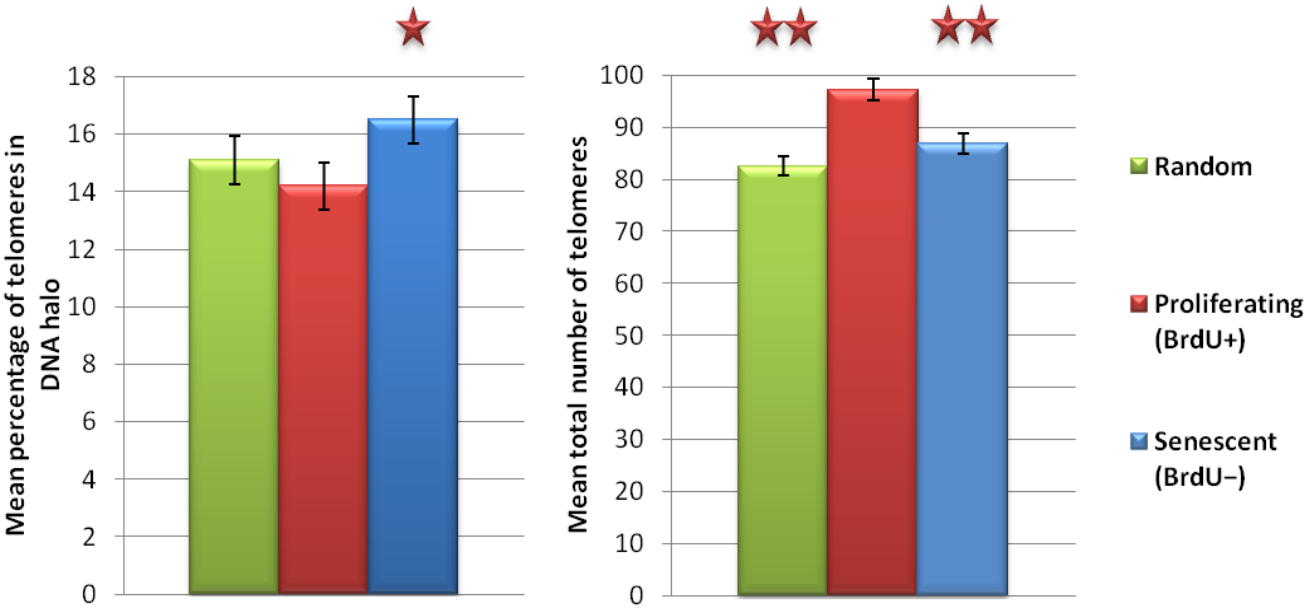

Figure 2.3.7: Examining telomere anchorage by the NM in proliferating (BrdU+) and senescent (BrdU−) nuclei using the DNA halo assay

The random population refers to the initial dataset analysed without differentiating between proliferating and senescent nuclei. Proliferating and senescent populations were distinguished by the presence or absence, respectively, of BrdU incorporation. For each population, n = 90. Significant differences between BrdU+ vs. BrdU− and random populations are denoted by stars (1 = $p < 0.05$; 2 = $p < 0.01$). Error bars represent ± SEM.

2.3.2.3 The number of detectable telomeres is reduced in senescence

Theoretically, it should be possible to detect almost all telomeres within in a normal diploid human nucleus using PNA FISH (Thisted et al., 1999). Although the visualisation of all telomeres is possible in metaphase (using telomere PNA FISH), this is not true of interphase nuclei; a maximum of 92 telomeres has been reported in cultured human haematopoietic cells (Lansdorp et al., 1996). In our study, the average number of telomeres scored per nucleus using the DNA halo assay was statistically lower in senescent populations; indeed, this was demonstrated when either anti-BrdU or anti-pKi67 was used to differentiate between proliferating and senescent states (figure 2.3.7 and 2.3.8). Thus, there was an 11% difference when comparing BrdU+ and BrdU− populations and almost a 20% difference between pKi67+ and pKi67− nuclei.

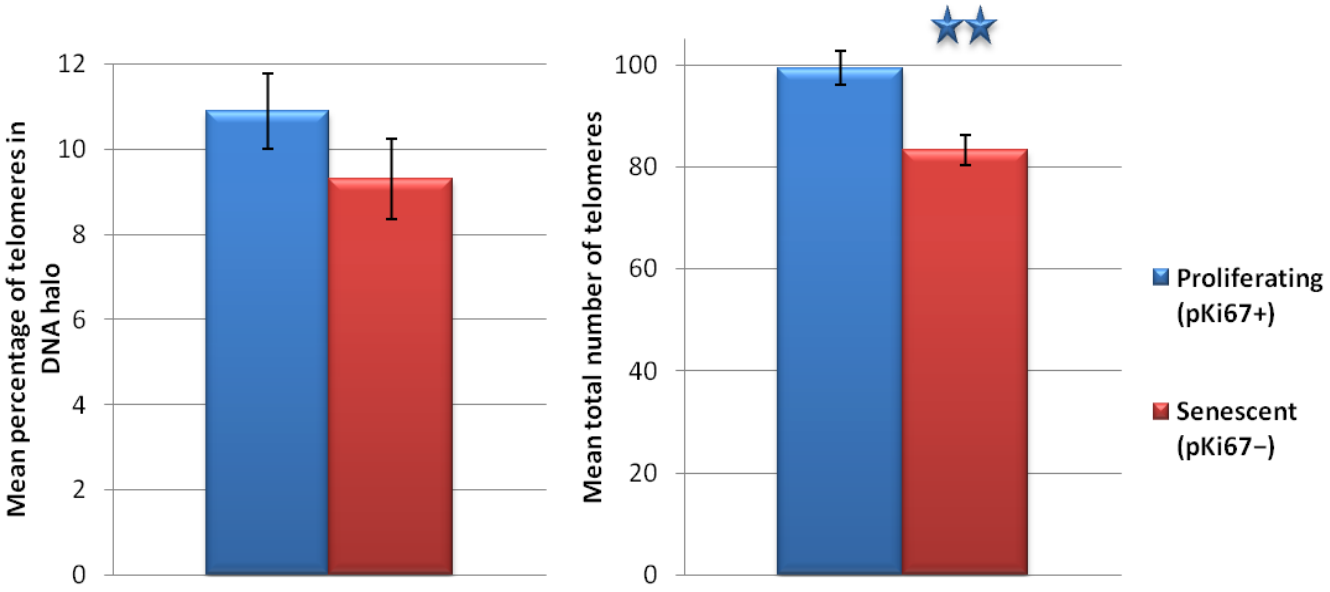

Figure 2.3.8: Examining telomere anchorage by the NM in proliferating (pKi67+) and senescent (pKi67−) nuclei using the DNA halo assay
Proliferating and senescent populations were distinguished by the presence or absence, respectively, of anti-pKi67 staining. For each population, 30 nuclei were analysed. Significant differences between pKi67+ and pKi67− populations are denoted by stars ($p < 0.01$). Error bars represent ± SEM.

2.3.2.4 Examining telomere anchorage by the NM in quiescent HDFs using the DNA halo assay

In order to examine telomere anchorage in quiescent HDFs using the DNA halo assay, cells were induced to enter quiescence by serum-starvation (0.5% NCS for 7 days), subjected to the DNA halo preparation and telomere PNA FISH. To confirm that the majority of the culture was quiescent, nuclei were stained with anti-Ki67 (figure 2.3.9). This methodology was performed on two separate occasions in order to confirm any detectable trends. The difficulty with analysing quiescent populations of cells is that there is no way to differentiate between the already senescent cells and newly quiescent populations. However, since approximately 60–70% of cells were proliferating in the control cultures at the point of serum-starvation induced quiescence, an equal proportion should be susceptible to quiescence induction. Thus, if quiescent cells exhibit a different pattern of telomere anchorage by this NM, this should be detected in a shift in the percentage of telomeres in the DNA halo. Significantly, the mean percentage of telomeres extracted into the DNA halo was 16.6% (± 5.8; nuclei = 30) in experiment 1 and 18.4% (± 6.0; nuclei = 30) in experiment

2, which were not statistically different (figure 2.3.10a). Importantly, both quiescent datasets were significantly different to proliferating (pKi67+) and senescent (pKi67−; senescent) populations (figure 2.3.9b). These results suggest that telomere anchorage is reduced in quiescence.

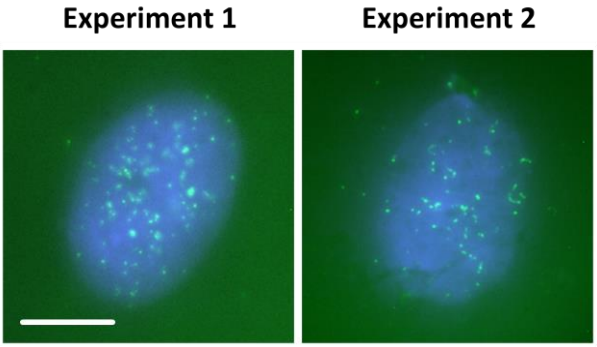

Figure 2.3.9: Examining telomere anchorage by the NM in quiescent HDFs using the DNA halo assay.
Control HDFs were grown in low-serum for 7 days in order to induce entry into quiescence. This was performed on two separate occasions. The cells were then subjected to the DNA halo preparation and telomere PNA-FISH. Slides were also stained with anti-pKi67 to ensure that the nuclei were non-proliferating. The residual nucleus and surrounding DNA halo have been counterstained using DAPI (blue), while telomere signals can be seen in green (FITC). Magnification = x100; scale bar = 10 μm.

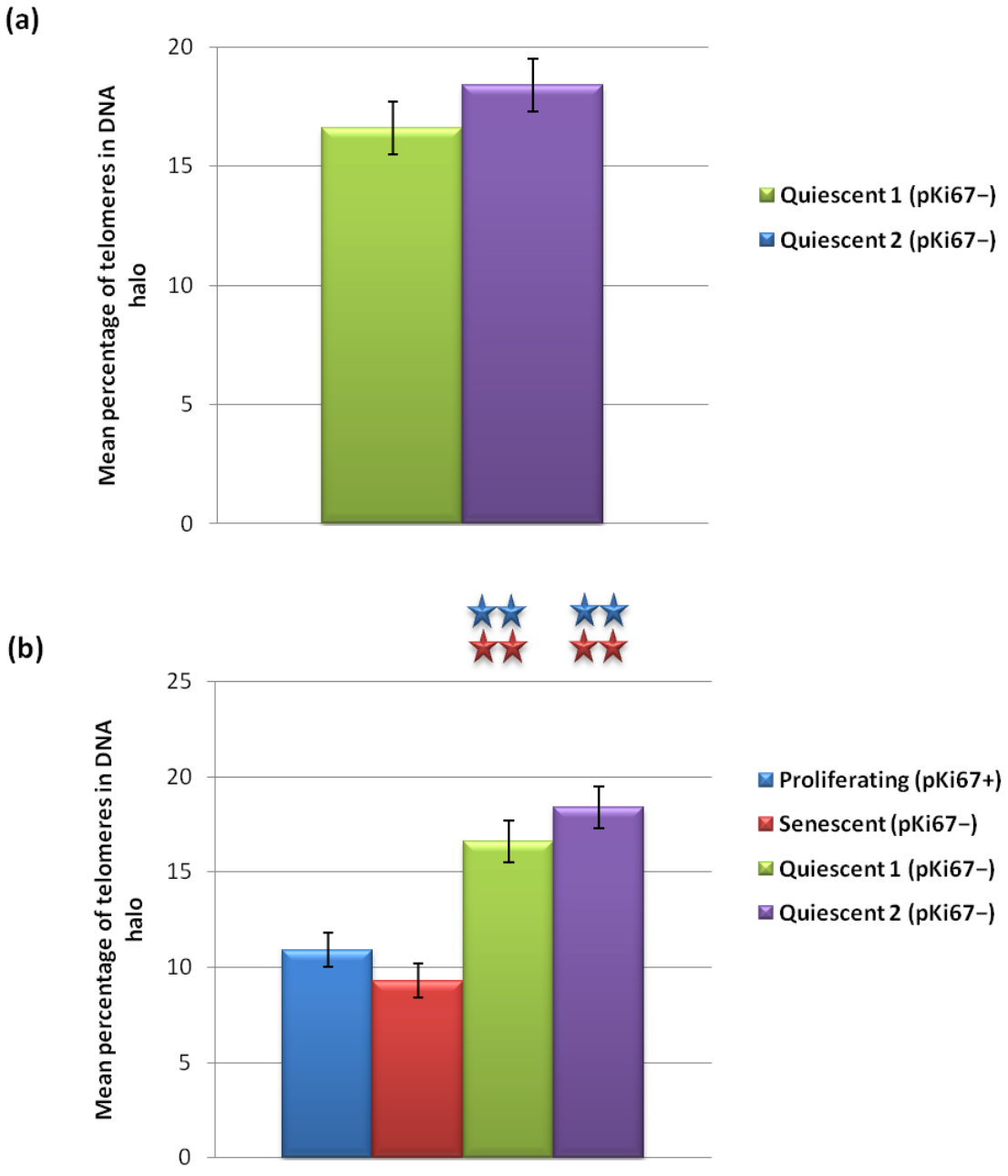

Figure 2.3.10: Examining telomere anchorage by the NM in quiescent HDFs using the DNA halo assay

Control HDFs were grown in low-serum for 7 days in order to induce entry into quiescence. This was performed on two separate occasions. Significant differences between the populations are denoted by stars ($p < 0.01$); the colour of the stars refers to the specific dataset. **(a)** Mean percentage of telomeres in the DNA halo in two quiescent datasets; **(b)** Comparing the mean percentage of telomeres extracted into the DNA halo in proliferating, senescent and quiescent populations. Error bars represent ± SEM.

2.3.3 Examining the interaction of specific genes with the NM

In order to determine whether genes interact differently with the NM in different cellular states, the NM anchorage of 3 genes, *CCND1*, *C-MYC* and *CTNNA1* was examined in proliferating (pKi67+) and senescent (pKi67−) control HDFs using the DNA halo assay (figure 2.3.11). Interestingly, in both pKi67+ and pKi67− populations, *CCND1* alleles were observed within the residual nucleus in over 95% of cases (nuclei = 30; figure 2.3.11; 2.3.12). Thus, regardless of cellular state, *CCND1* appears to be tightly bound to the NM. In proliferating nuclei, approximately 75% of *C-MYC* alleles were found within the residual nucleus, while the remaining 25% were extracted into the DNA halo (nuclei = 30; figure 2.3.12). These extracted alleles were observed as loops emanating from the residual nucleus rather than discrete spots in the DNA halo. In senescent nuclei, the anchorage of *C-MYC* by the NM increased slightly, although this was not statistically significantly. Similarly, 80% of *CTNNA1* alleles were associated with the NM in pKi67+ nuclei; this increased to 88% in pKi67− nuclei (nuclei = 30; figure 2.3.12). Importantly, *CCND1* signals were more condensed than those for *C-MYC* and *CTNNA1*. In conclusion, these findings demonstrate that the anchorage of selected genes by the NM did not change on entry into senescence using our DNA halo assay. However, differences in the level of gene packaging were observed.

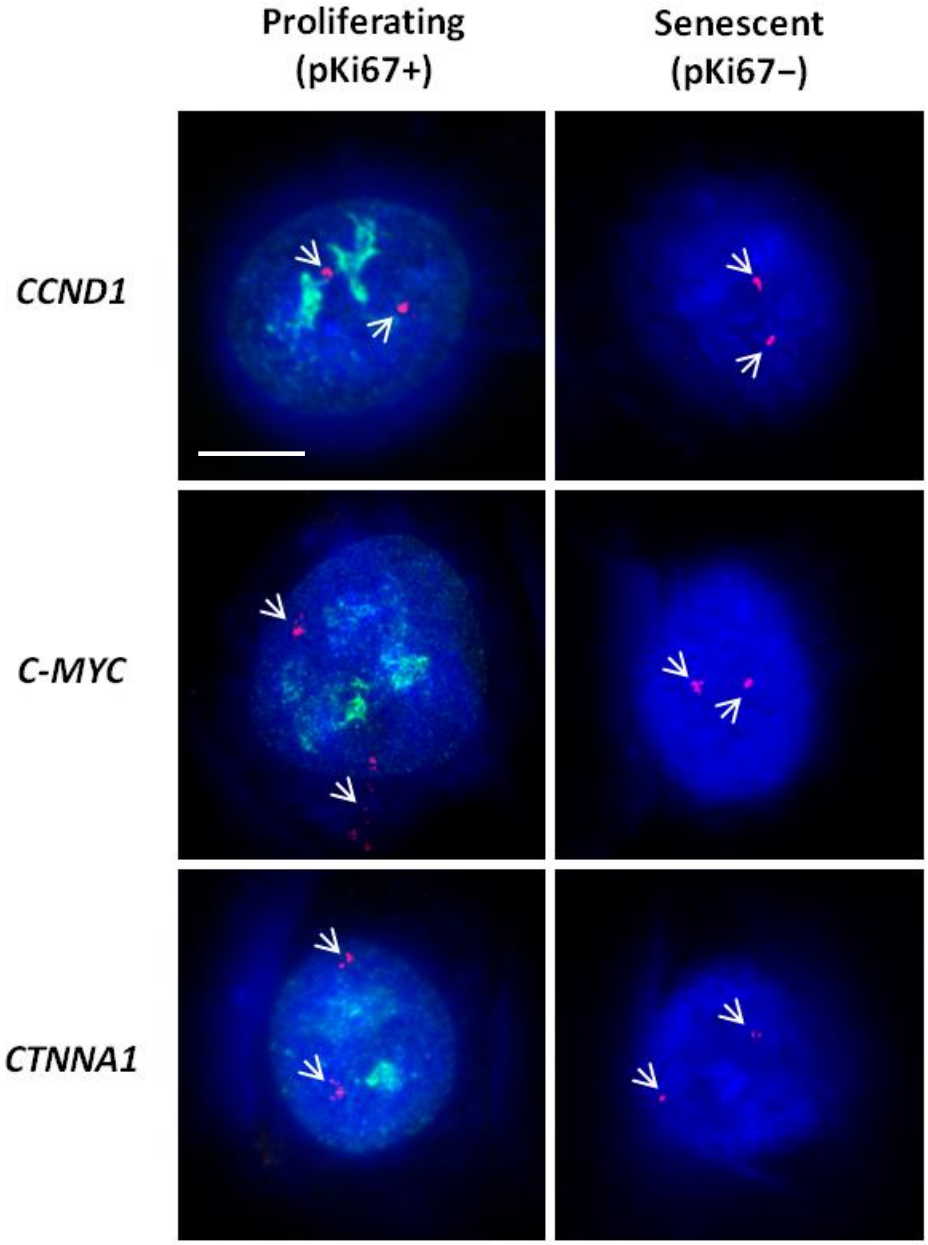

Figure 2.3.11: Examining NM-gene interactions in control HDFs using the DNA halo assay

The residual nucleus and surrounding DNA halo have been counterstained using DAPI (blue). Gene specific probes (*CCND1*, *C-MYC* and *CTNNA1*) have been used to investigate the anchorage of certain genes by the NM. Gene signals are depicted in red (Cy3), while anti-pKi67 can be seen in green (FITC). Magnification = x100; scale bar = 10 µm.

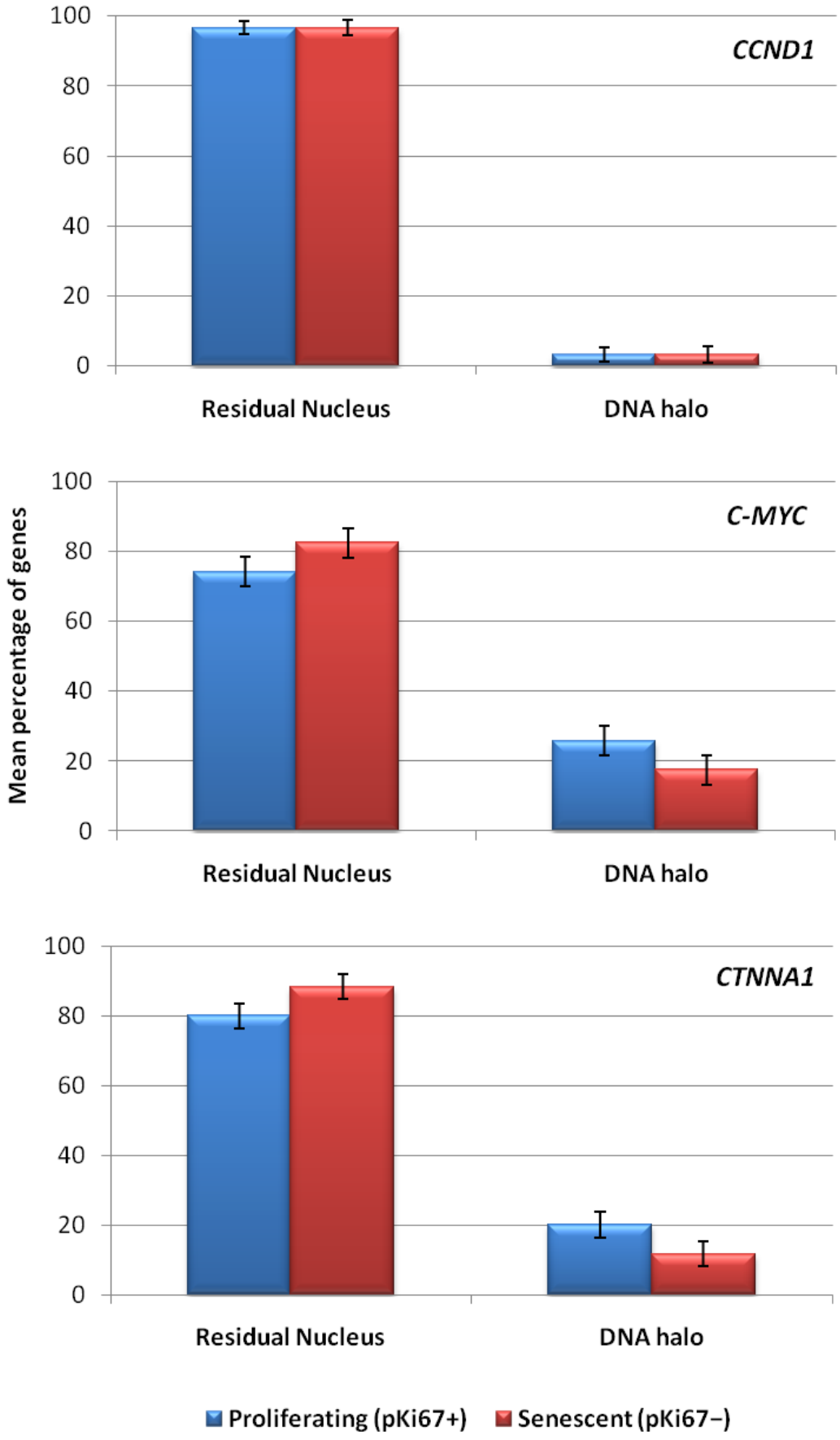

Figure 2.3.12: Examining NM-gene anchorage in proliferating and senescent control HDFs using the DNA halo assay. Error bars represent ± SEM.

2.4 DISCUSSION

2.4.1 Using DNA halo preparations as a platform to analyse genomic interactions with the nuclear matrix

The NM consists of an internal NM and a peripheral NL (Nickerson et al., 2001). This internal NM is composed of thick polymorphic fibres built around core filaments approximately 10 nm in diameter (He et al., 1990). Significantly, the NM complex is proposed to organise eukaryotic DNA into loops of 50–200 kb in length (Heng et al., 1992; 2001). The DNA sequences which anchor the base of these loops to the NM, in interphase and metaphase cells have been termed MARs or SARs, respectively (Mirkovitch et al., 1984; Cockerill and Gerrard, 1986; and Laemmli, 1986; Bode et al., 1992). These loops can be visualised following the extraction of histones and other soluble proteins in DNA halo preparations (Vogelstein et al., 1980; Gerdes et al., 1994). The use of such extraction procedures to study genome interactions with the NM have revealed that chromosomes (Ma et al., 1999; Croft et al., 1999), telomeres (Luderus et al., 1996; Ratsch et al., 2002), genes (Gerdes et al., 1994; Ratsch et al., 2002) and other genomic regions (Iarovaia et al., 2005) are indeed anchored by this nuclear structure.

2.4.2 Chromosome anchorage by the NM in normal fibroblasts in the DNA halo assay

Previous work performed demonstrates that following such preparations involving 2M NaCl, the majority of CTs remain within the residual nucleus and are not extracted into the DNA halo; this is true of HSA-1, -2, -4, -7, -9, -11, -14, -19 and -22 (Ma et al., 1999; Croft et al., 1999). However, HSA-18 is the one documented exception to this rule; this chromosome is consistently extracted into the DNA halo, which suggests that not all CTs are anchored to the NM to the same extent (Croft et al., 1999). Thus, it seemed pertinent to examine the associations of selected chromosomes with the NM in human HDFs. The anchorage of HSA-1 and HSA-18 by the NM have been studied by Ma et al. (1999) and Croft et al. (2001), respectively; however, to the best of my knowledge, NM associations with HSA-13, -15 and -17, have not been investigated elsewhere. In line with Ma et al. (1999), HSA-1 resisted extraction and remained tightly anchored to the residual nucleus, which suggests that it interacts with the NM at numerous sites. In line with this hypothesis, HSA-1 was observed to be the most structured of the

chromosomes examined in this study. The other 3 chromosomes (HSA-13, -15 and -17) were also demonstrated to be avidly associated with the NM. Previous work by Croft et al. (1999) suggested that there may be a correlation between gene-density and NM-attachment; indeed, gene-poor HSA-18 was loosely anchored by the NM, while gene-rich HSA-19 exhibited tight associations with the structure. The preliminary HSA-18 data presented in this study appears to confirm this trend. However, HSA-13, which is also of similar gene density to HSA-18 (Deloukas et al., 1998), remained tightly attached to the NM. It is likely that HSA-13's anchorage by the nucleolus was partly responsible for its ability to resist extraction. In line with the fact that both HSA-13 and -15 are acrocentric and are tethered by the nucleolus (Henderson et al., 1972; Sullivan et al., 2001), both chromosomes were seen to decorate the edges of remnant nucleoli. Therefore, these findings do not negate the possibility of a relationship between gene-density and NM anchorage; instead, they suggest that although gene-poorer chromosomes such as HSA-13 and HSA-18 are likely to interact at far fewer sites than gene-richer chromosomes, HSA-13 remains within the residual nucleus due to its association with the nucleolus, while HSA-18, which lacks such anchorage, is extracted into the DNA halo. The findings also indicate that chromosome size is probably not a determinant of NM-association since HSA-17 and HSA-18 are of a similar size (Deloukas et al., 1998) but are anchored to differing extents by the NM (this study; Croft et al., 1999). However, the different cell types used in these separate studies must be taken into account; HDFs were used in this current investigation while Croft et al. (1999) employed lymphoblasts and Ma et al. (1999) used both dermal and lung fibroblasts. It is possible that chromosome anchorage by the NM differs according to cell type; indeed, while the positioning of chromosomes is largely similar in both human fibroblasts and lymphoblasts, some differences have been reported (Boyle et al., 2001).

There is evidence to suggest that there is a correlation between transcriptional activity and NM-binding (Gerdes et al., 1994; Ratsch et al., 2002; Iarovaia et al., 2005). Indeed, active genes are found in smaller loops whereas inactive regions form part of much larger DNA loops (Bode et al., 2000). In line with this, Croft et al. (2001) demonstrated that the gene-rich chromosome, HSA-19 is tightly associated with the NM while gene-poor HSA-18 is loosely anchored by the structure. This study also indicates that HSA-18

has a loose association with the NM. Since chromosome positioning appears to alter on exit from the cell cycle (Bridger et al., 2000; Meaburn et al., 2007; Mehta et al., 2010), it seemed pertinent to examine and compare chromosome anchorage by the structure in normal proliferating and non-proliferating (senescent) nuclei. Our results demonstrate that global chromosome interactions with the NM do not appear to differ in the two proliferative states. These findings are certainly not incompatible with observations that the genome is rearranged on cell cycle exit (Bridger et al., 2000; Meaburn et al., 2007; Mehta et al., 2010); however, they do suggest that NM-MARs attachments are released and reformed in order to allow shifts in chromosome positioning. These data confirm earlier accounts that the CTs are anchored by the NM (Ma et al., 1999; Croft et al., 1999). The results also demonstrate that there are no obvious differences in chromosome attachment to the NM in proliferating and non-proliferating nuclei. However, performing HALO-FISH with chromosome-specific probes cannot reveal any changes in NM interactions occurring at a more local scale. Indeed, it is likely that the nature of specific NM-MARs interactions differ between the two proliferative states as a result of their differing transcriptional profiles (Gerdes et al., 1994).

2.4.3 Telomere anchorage by the NM in normal fibroblasts in the DNA halo assay

2.4.3.1 Proliferating vs. senescent nuclei

In order to examine telomere interactions with the NM, we have coupled the DNA halo preparation (as per Bridger and Lichter, 1999) with telomere PNA FISH. When examining such interactions in HDFs using this assay, the results consistently reveal that approximately 85–90% of telomeres are anchored by the NM. Significantly, this concurs with previous biochemical data which demonstrates that at least 80% of telomeric DNA is attached to this nuclear structure (de Lange, 1992). The results also confirm earlier HALO-FISH experiments using telomere-specific probes (Luderus et al., 1996; Ratsch et al., 2002). Although the study of NM-telomere interactions using HALO-FISH is not novel, the consistent results of this study demonstrate that we have produced a reliable and reproducible assay which generates quantitative data. Therefore, this assay can now be used to compare telomere anchorage in different cell and disease states.

Human fibroblasts have a limited lifespan *in vitro*; their maximum replicative capacity is known as the Hayflick limit (Hayflick and Moorhead, 1961). Indeed, telomere length is found to be an indicator of such proliferative capacity (Allsopp et al., 1992). Telomeres are shortened with each cell division due to the end replication problem; once telomere length reaches a critical length, the cells enter replicative senescence (Bodnar et al., 1998; Stewart and Weinberg, 2006). This can be achieved in culture by passaging cells repeatedly until this state is achieved. It has been demonstrated that such eroded telomeres trigger DNA damage checkpoint responses which in turn leads to this irreversible G1/S cell cycle arrest (d'Adda di Fagagna et al., 2003). In light of these facts, we thought it pertinent to investigate and compare telomeric interactions with the NM in senescence with those in a proliferating population of HDFs.

Interestingly, our results demonstrate that the majority of telomeres associate with the NM, regardless of cellular state. There was a significant difference ($p < 0.05$) between telomere anchorage when BrdU was used to differentiate between proliferating and senescent nuclei. However, the fact that BrdU is documented to induce changes in gene expression and MAR anchorage (Michistuta et al., 1999; Suzuki et al., 2001; Suzuki et al., 2002), this difference should be interpreted with caution. When anti-pKi67 staining was used to distinguish proliferating and senescent nuclei, no difference was detected. Thus, taken together, these data suggest that telomere anchorage does not change on entry into senescence. Telomeres are found to contain a MAR every 1 kb of telomeric DNA, which is far more frequent than the genome as a whole (Luderus et al. 1996). Since telomeres in cultured human fibroblasts are observed to shorten approximately 50–150 bp per division (Harley et al., 1990; Levy et al., 1992; Wright et al., 1997; Londono-Vallejo et al., 2001), this suggests a 2.5–7.5 kb loss of telomeric DNA after 50 divisions. Thus, this translates into the elimination of 2–7 MARs in human fibroblasts over a lifetime of 50 divisions. Considering that the mean telomere length of chromosomes in such cells is 6–9 kb (Allsopp et al., 1992; Decker et al., 2009), this indicates the possible loss of a large proportion of telomeric MARs. The results suggest that even with the probable reduction in MARs anchoring a telomere to the NM, the telomere remains attached to the residual nucleus in our assay. However, obviously, since telomeres are predicted to be shorter in senescence cells, this does mean that there is less telomeric DNA to anchor. Therefore, the findings suggest that

telomere length does not influence the avidity of telomere binding to the NM, which is in fact in agreement with previous work performed by Luderus et al., (1996).

2.4.3.2 The number of detectable telomeres decreases in senescence

The mean number of telomeres detected in the senescent cells was significantly less than the average number observed in the proliferating population. This is unsurprising since telomere length is reduced with every cell division and thus, it would be expected that the senescent telomeres would be shorter than telomeres in proliferating cells (Allsopp et al., 1992). Since PNA signal intensity is directly correlated with telomere length (Lansdorp et al., 1996), those telomeres that were critically short could have possibly avoided detection. However, in a study which employed Q-FISH to detect telomere length in metaphases, signal-free telomeric ends were not reported for control human fibroblasts, although they were present in those derived from HGPS patients (Decker et al., 2009). This probably reflects the differences between the ease of signal detection in interphase and metaphase cells. Is it possible that this reduction in detectable telomeres in senescence distorted the results regarding NM-telomere binding in proliferating versus senescent cells? This would only be the case if the majority of short telomeres were not associated with the NM and thus, were extracted into the DNA halo. However, since there appears to be no relationship between telomere length and the avidity of NM binding (this study; Luderus et al., 1996), this is not likely to be of concern.

2.4.3.3 Quiescence

Although both quiescence and senescence are non-dividing states, they represent two very distinct phases; the former is reversible under physiological conditions while the latter is not. Furthermore, quiescent cells are considerably less metabolically active than senescent populations (Blomen and Boonstra, 2007). Within the laboratory, quiescence can be induced in three ways; by serum starvation, contact inhibition and by loss of adhesion (Coller et al., 2006).

Furthermore, as quiescence is distinctly different to both proliferation and senescence, it seemed logical to examine telomere anchorage by the NM in quiescent cells. These investigations are of particular relevance since radial chromosome positioning in interphase nuclei changes according to cellular state (Bridger et al; 2000; Meaburn et al., 2007; Mehta et al., 2010) and differentiation (Galiova et al., 2004; Kim et al., 2004). Significantly, the proportion of telomeres associated with the NM decreased significantly in both quiescent populations. This could suggest that the binding of certain telomeres to the structure is weaker in quiescence. However, since the initial study (which did not differentiate between proliferative state) demonstrated that approximately 15% of telomeres are extracted into the DNA halo, it is possible that there is no general difference between NM-telomere interactions in proliferating, senescent and quiescent cells. Therefore, this suggests that in control HDFs, regardless of proliferative state, 9–19% of telomeres are not associated with the residual nucleus when using the DNA halo assay. Indeed, this chimes with biochemical work by de Lange (1992), which reported that at least 80% of telomeres are anchored by the NM. Thus, this range is likely to represent biological differences between individual cells.

2.4.4 Gene anchorage by the NM

Research demonstrates that transcriptionally active genes tend to remain attached to the residual nucleus, while transcriptionally inactive genes are generally extracted into the DNA halo (Gerdes et al., 1994; Ratsch et al., 2002). Indeed, alpha-satellite sequences, which are non-transcribed, form part of DNA loops rather than associate with the NM (Yaron et al., 1998). Other genomic regions also have a cell-state specific relationship with the structure (Iarovaia et al., 2005). Thus, the anchorage of genes by the NM appears to have a functional importance (Gerdes et al., 1994; Ratsch et al., 2002; Iarovaia et al., 2005). In order to determine whether the anchorage of specific genes changes on entry into senescence, NM associations with *CCND1*, *CTNNA1* and *C-MYC* were examined in control HDFs using the DNA halo assay. These genes (*CCND1*, *CTNNA1* and *C-MYC*) are found on chromosomes 11 (Motokura et al., 1991), 5 (Furukawa et al., 1994) and 8 (Leder, 1982; Taub et al., 1982; Dalla-Favera et al., 1982; Takahashi et al., 1991), respectively. Apart from HSA-11 (Ma et al., 1999), the NM

anchorage of these parent chromosomes has not been examined in this or any previous study.

Significantly, *CCND1* was typically attached to the NM in both proliferating and non-proliferating nuclei. This is important since *CCND1* is a key regulator of the G1/S phase transition; it associates with the cyclin-dependent kinase, CDK4, to form a holoenzyme, which in turn functions to phosphorylate pRb (Dowdy et al., 1993; Ewen et al., 1993). This hyperphosphorylation of pRb causes the release of E2F; an event which leads to the transcriptional activation of S-phase genes and thus, cell cycle progression (Bartek et al., 1996). In G1 and G2 phase fibroblasts, cyclin D1 levels are high while in S-phase, *CCND1* expression is reduced (Yang et al., 2006). Thus, *CCND1* expression occurs throughout the cell cycle to varying extents (Stacey, 2003), thus concurring with the demonstration by our assay that *CCND1* is consistently associated with the NM.

Interestingly, in senescent cells, *CCND1* alleles were also typically anchored by the NM. In line with this, *CCND1* is highly expressed in senescent human fibroblasts (Fukami et al., 1995; Fukami-Kobayashi and Mitsui, 1998) and in fact, expression levels are higher than those seen in young fibroblasts (Fukami et al., 1995). Taken together, the findings of our study indicate that *CCND1* remains associated with the NM in both cell cycle states. Furthermore, the results appear to fit with the previously proposed correlation between transcriptional activation and NM association (Gerdes et al., 1994).

C-MYC is a transcription factor which influences the expression of numerous genes; *C-MYC* target genes are involved in many cellular processes including cell cycle regulation and differentiation (for review, see Riggelen et al., 2010). The association of *C-MYC* with the NM has been previously examined in human monoctyes; indeed, in that particular study, 40% of signals were associated with the residual nucleus while 60% were extracted into the DNA halo (Ratsch et al., 2002). This is interesting since *C-MYC* is expressed at low levels in resting human monocytes (Lee et al., 1987). Importantly, these findings support the correlation between transcriptional activity and NM-association (Gerdes et al., 1994). In contrast to the results reported by Ratsch et al. (2002), my study demonstrated that the large majority of *C-MYC* signals were associated with the residual nucleus. However, this is likely to be due to differences in

cell type (dermal fibroblast vs. monocyte) and proliferation status (proliferating/senescent vs. quiescent). While *C-MYC* is low in resting monocytes (Lee et al., 1987), the gene is expressed at high levels in a proliferating HDF culture (see chapter 4.3). Although *C-MYC* expression in a senescent HDF culture was not examined in this thesis, there is evidence to suggest that *C-MYC* expression is reduced in senescent human fibroblasts (Dean et al., 1986). Since *C-MYC* was associated with the residual nucleus in both proliferating and senescent HDFs to similar extents, this does not necessarily correlate with the gene activity/NM-association hypothesis. However, to investigate this fully, total RNA would ideally be extracted from a senescent culture of HDFs on the same day as the DNA halo preparation. This would allow a fairer analysis of *C-MYC* expression and NM-binding.

2.4.5 How does the NM organise the genome within interphase nuclei?

The findings presented here in this chapter do indeed indicate that the organisation of the genome is mediated by the NM. In line with previous data, CTs remained attached to the residual nucleus following extraction with 2M NaCl (Ma et al., 1999). The results presented in this chapter demonstrate that the NM is involved in anchoring CTs within interphase nuclei. Since the components of the outer NM are proposed to be removed by 2M NaCl treatment (He et al., 1990; Nickerson et al., 1992), this suggests that it is the core filaments of the inner NM and the peripheral component of the NM, the NL, which mediate such organisation. The removal of RNA species by RNase A is shown to destroy the integrity of core filaments (He et al., 1990); importantly, after such treatment, although CT structure is disrupted, the majority of CT mass remains within the residual nucleus (Ma et al., 1999). This is very significant since it suggests that even when core filaments are lost, chromosomes are still tethered inside the nucleus. Although these filaments are not resistant to RNase A, the NL is found to remain intact (Ma et al., 1999). Thus, it is likely that the NL is responsible for the overall anchorage of CT within the nucleus, while the core filaments of the inner NM are important for mediating specific, more local interactions. Indeed, the NL is found to interact with the genome at over a 1000 sites known as LADs (Guelen et al., 2008).

While the peripheral component of the NM (NL) is implicated in organising interphase chromosomes, it appears that the internal NM is responsible for the overall tethering of telomeres. The evidence for this comes from Luderus et al. (1996) who demonstrated that telomeres do not generally associate with the NL; indeed, telomeres were found throughout the nuclear volume. Since telomeres are found to remain attached to the residual nucleus after 2M NaCl extraction (this study; Luderus et al., 1996), it is likely that the core filaments of the inner NM (rather than outer NM proteins) mediate telomere anchorage. Taken together, the results of this suggest that different elements of the NM have a role to play in organising different genomic regions. The obvious question is: how are these MARs tethered by the core filaments of the NM? Furthermore, what are the proteinaceous elements of these core filaments?

2.4.6 How are MARs tethered by the NM?

Unfortunately, the structural composition of the internal NM has not been fully characterised. The proteins of the internal NM can be categorised according to their release during NM preparations; indeed, 0.25 M ammonium sulphate extraction appears to reveal thick polymorphic fibres of the NM, while 2M NaCl removes the outer layer of NM proteins and exposes the core filaments of the NM (He et al., 1990). Since the methodology used in this chapter employs 2M NaCl to extract histones, other soluble proteins and non-NM associated DNA, this suggests that both the core filaments and peripheral NL are responsible for organising the genome. This also indicates that while this outer layer of NM proteins may contribute to mediating NM-MAR associations, it is not instrumental; indeed, this study and others (Ma et al., 1999) demonstrate that in spite of their removal, DNA is still held in place. As a result, this leaves few characterised candidates for this role. While A-type lamins and the nuclear mitotic apparatus protein (NuMA) have been identified as minor components of these core filaments (Zeng et al., 1994; He et al., 1995; Hozak et al., 1995), much of their composition remains uncharacterised (for review, see Nickerson, 2001).

2.4.7 Conclusion

Although the NM has been repeatedly visualised and isolated using various methodologies, the exact protein composition of the structure is still not fully understood (Nickerson, 2001). This is despite the fact that hundreds of NM associated proteins have been identified (Mika and Rost, 2005). It is uncertain which elements of the NM mediate telomere tethering, however, some NM proteins, such as the lamin protein family, are reported to bind telomeric DNA. In light of this study, it will be interesting to investigate whether mutations in certain NM associated proteins affect telomere anchorage by the NM.

3. Mutations in lamin A and emerin disrupt nuclear matrix-genome interactions

(Partially published in Elcock and Bridger, 2008)

3.1 INTRODUCTION

3.1.1 The composition of the NM

Although research demonstrates that at least 300 NM-associated proteins exist (Mika and Rost, 2005), the structural composition of the NM has not yet been fully characterised (Nickerson, 2001). While the peripheral component of the structure is well understood, the protein constituents of the internal portion require further elucidation. The most abundant proteins of this inner NM are found to be hnRNP proteins and numatrin/nucleophospmin (Mattern et al., 1996). Other important inner NM proteins include NuMA (Zeng et al., 1994; He et al., 1995) and A-type lamins (Hozak et al., 1995; Barboro et al., 2002).

However, it appears that there are two categories of internal NM proteins: those that are released by 2M NaCl treatment and those that resist such extraction (He et al., 1990). The elution of digested chromatin by 0.25 M ammonium sulphate reveals a network of polymorphic fibres (He et al., 1990). The subsequent addition of 2M NaCl to this structure further extracts these fibres to expose thinner, less heterogeneous filaments which have been termed the core filaments of the internal NM (He et al., 1990). Therefore, 2M NaCl extracts a layer of 'outer' NM proteins; this is important since it implicates core filaments, rather than the complete NM, in being the primary mediator of DNA anchorage. Proteome analysis demonstrates that lamin A/C forms part of the insoluble nuclear fraction which remains after 2M NaCl extraction (Takata et al., 2009). Since the peripheral NL is also present within this pellet, this alone cannot provide evidence of the protein within the 2M NaCl-resistant internal nuclear matrix. Research confirming lamin's internal nuclear localisation after 2M NaCl is not abundant.

The use of electro-elution to remove partially digested chromatin (Jackson and Cook, 1988) is also shown to reveal core filaments of similar morphology and size to those reported by He et al. (1990). In places, these filaments appear to underlie polymorphic fibres (Hozak et al., 1995), which again is an observation consistent with He et al. (1990). Using this method, Hozak et al (1995) demonstrated that anti-lamin A antibodies react, albeit weakly, with these core filaments; although, the intensity of staining was stronger at the 'knobs' and 'clumps' polymorphic fibres. Thus, this

suggests that although lamin A proteins are components of the core filaments, they are not the major constituents (Hozak et al., 1995). Therefore, although the method used to localise lamin A to the core filaments is different (i.e. salt- vs electro-elution), it does suggest that the protein is also likely to remain as part of the internal network following 2M NaCl extraction.

Significantly, the lamin-associated INM, emerin, is also found to be part of the high-salt resistant insoluble nuclear fraction (Squarzoni et al., 1998; Ellis et al., 1998; Takata et al., 2009). However, so far, it has only been visualised at the nuclear periphery; a localisation mainly mediated by its interaction with the A-type lamins of the NL (Squarzoni et al., 1998).

3.1.2 Which proteins mediate the NM's role at organising the genome?

As demonstrated and discussed in chapter 2, the organisation of the genome is mediated by the NM (de Lange, 1992; Gerdes et al., 1994; Luderus et al., 1996; Ma et al., 1999; Croft et al., 1999; Elcock and Bridger, 2008). The NM is composed of a peripheral NL and an internal network of fibres and filaments (inner NM; Jackson and Cook, 1988; He et al., 1990; Nickerson et al., 1997; Wan et al., 1999). The NL's role in organising the genome is well characterised (Pickersgill et al., 2006; Guelen et al., 2008) and this is partly aided by the knowledge of its constituents. Since the NM is proposed to arrange the genome into repeating loops of 50–200 kb, the peripheral component of the NM alone cannot be responsible for mediating such organisation. While the MARs which mediate the formation of these loops exist in their thousands, their characterisation is poor (Bode et al., 2000).

A number of MAR-binding proteins have been identified and examined (Adachi et al., 1989; Luderus et al., 1992; Romig et al., 1992; Luderus et al., 1994; Fackelmayer et al., 1994; Fackelmayer and Richter, 1994; Dickinson and Kohwi-Shigematsu, 1995; Renz and Fackelmayer, 1996; Gohring and Fackelmayer, 1997; Kipp et al., 2000; Dunn et al., 2003) and significantly, a few, including A-type lamins and NuMa (Luderus et al., 1994), are also recognised as constituents of the inner NM (Zeng et al., 1994; He et al., 1995; Hozak et al., 1995). Logically, this implicates the involvement of such proteins in tethering DNA to the inner NM. Indeed, A-type lamins have DNA binding properties

(Shoeman and Traub, 1990; Taniura et al., 1995; Stierle et al., 2003) and are demonstrated to associate with telomeres (Raz et al., 2008); in line with this, the loss of such proteins significantly disrupts telomere localisation and maintenance (Gonzalez-Suarez et al., 2009).

3.1.3 How can studying human disease aid our understanding of the NMPs?

The composition of the NM is reported to be modified in various human diseases; this is especially true of certain cancer types (Sjakste et al., 2004). As a result, NM-associated proteins are useful as diagnostic biomarkers for cancers such as those affecting the prostate, colon and bladder (Leman and Getzenberg, 2008). Significantly, the lamin composition of the NM is also disrupted in human prostate cancer (Coradeghini et al., 2006). It is likely that in disease cells, a number of MAR-binding proteins are also displaced and as a result, their ability to organise the genome correctly, is perturbed. Indeed, chromatin disorganisation has been reported in cancer (Bartova et al., 2000; Cremer et al., 2003; Bartova et al., 2005; Wiech et al., 2005; Harnicarova et al., 2006; Murata et al., 2007; Meaburn and Misteli, 2008; Weich et al., 2009; Meaburn et al., 2009).

Therefore, since both lamin A and emerin are shown to form part of the inner NM, it is logical to question whether mutant forms of these proteins affect the NM's ability to tether genomic regions effectively. This is especially relevant to A-type lamins which have been extensively implicated in mediating genome organisation (Shoeman and Traub, 1990; Luderus et al., 1992; Taniura et al., 1995; Stierle et al., 2003; Bode et al., 2003). Emerin's role in tethering chromatin within the interphase nucleus is less well characterised and is indirect. There is no evidence that emerin binds DNA directly; however, the protein probably exerts its effect via its binding to the highly conserved chromatin factor, BAF (Lin et al., 2000; Lee et al., 2001; Segura-Totten and Wilson, 2004). While research using non-extracted cells demonstrates that chromatin disorganisation can result from mutations in *LMNA* (Sewry et al., 2001; Fidzianska and Hausmanowa, 2003; Goldman et al., 2004; Filesi et al., 2005; Maraldi et al., 2006; Meaburn et al., 2007; Lattanzi et al., 2007; Hakelien et al., 2008; Park et al., 2009) and

EMD (Fidzianska et al., 1998; Ognibene et al., 1999; Meaburn et al., 2007), the nature of NM-genomic interactions in such mutants has not been examined.

As discussed in 1.4, HGPS is caused by *LMNA* mutations; the classical and most common form of the disease, results from a *de novo* mutation affecting codon 608 (GGC>GGT; G608G). A number of other mutations in *LMNA* also result in HGPS; this is known as atypical HGPS. This term is also applied to patients who exhibit an HGPS phenotype, in spite of the fact that *LMNA* is wildtype (see chapter 5.1; Bridger and Kill, 2004). These latter atypical patients (referred to as atypical type 2) are of great interest since eventually their cells will reveal another genetic cause of HGPS. Mutations in *LMNA* can also result in autosomal EDMD (Bonne et al., 1999; Raffaele Di Bartletta et al., 2000). An X-linked version of EDMD exists; this disease results from mutations in *EMD*, the gene encoding emerin (Bione et al., 1994). Unlike autosomal EDMD, most cases of X-EDMD involve the absence of emerin rather than the presence of a mutant protein (Yates et al., 1999). Interestingly, a phenotype combining both HGPS and myopathy has been reported in a patient harbouring a point mutation at S143F in lamin A/C (Kirschner et al., 2005).

3.1.4 Using DNA halo preparations to examine NM-genome interactions in laminopathy fibroblasts

In light of the observation that both lamin A and emerin are components of the NM and that in cells expressing mutant forms of these proteins, the genome displays evidence of disorganisation (Ognibene et al., 1999; Sullivan et al., 1999; Sabatelli et al., 2001; Sewry et al., 2001; Capanni et al., 2003; Fidzianska & Hausmanowa-Petrusewicz, 2003; Goldman et al., 2004; Nikolova et al., 2004; Columbaro et al., 2005; Filesi et al 2005; Scaffidi and Misteli, 2005; Arimura et al., 2005; Meaburn et al., 2007), it seemed pertinent to test whether genome interactions with the NM are perturbed in disease. In order to do this, a multi-faceted approach was adopted.

Firstly, chromosome interactions with the NM were examined in cells derived from classical and atypical HGPS cell lines and compared with controls. Interestingly, the interactions of certain chromosomes were perturbed in HGPS cell lines. Secondly, in

order to determine whether telomere anchorage by the NM is disrupted in disease, three diseases were studied: HGPS, X-EDMD and cutaneous malignant melanoma. The effect of telomerase activation on telomere interactions with the NM was also examined by comparing mortal and immortalised HGPS fibroblasts. Significantly, it was observed that telomere anchorage by the NM was disrupted, to varying extents, by the presence of mutant lamin A as well as in the absence of emerin. Attempts were made to rescue perturbed telomere interactions in X-EDMD; however, these were not successful. Interestingly, the activation of telomerase in classical HGPS cells appeared to completely rescue perturbed telomere interactions.

Taken together, the results of this chapter confirm that lamin A and emerin are important for mediating genome organisation. Importantly, they further strengthen the link between A-type lamin proteins and telomere biology.

3.2 MATERIALS AND METHODS

3.2.1 Cell Culture

Primary HDFs were maintained in conditions aforementioned in 2.2.1. ED5364 (X-EDMD carrier), G12660 (HGPS + Myopathy) and AP (X-EDMD patient) (provided by Professor Glenn Morris, Professor Manfred Wehnert and Professor Chris Hutchison, respectively) were grown in 10% (v/v) fetal bovine serum (FBS), while AG06297 and AG08466 were grown in 15% (v/v) FBS.

3.2.2 DNA Halo Preparation

As per chapter section 2.2.3.

3.2.3 Directly labelled total human chromosome probes and 2D FISH

As per chapter sections 2.2.4 and 2.2.6.

3.2.4 Telomere PNA FISH

As per chapter 2.2.7.

3.2.5 Transient transfection

Emerin cDNA was cloned into the *Hind*III and *Bam*HI sites of the vector pEGFP-C2 (Clontech; figure 3.2.1; Fairley et al., 1999). The resulting construct, emerin-pEGFP-C2 (referred to as *EMD-GFP* from this point onwards) which encodes emerin-green fluorescent protein (GFP), was generated previously to this study and was a kind gift from J. Ellis (Kings College, London). Cells were transfected with *EMD-GFP* using GeneJuice® Transfection Reagent (Novagen®). Cells were seeded in QuadriPERM™ chambers at a density of 1 x 10^5 per slide and then left to grow for 24 hours. After this time, cells were transfected according to the manufacturer's protocol; following a series of optimisation experiments (which are detailed in section 3.3), 5 µg of *EMD-GFP* and 15 µl of GeneJuice® Transfection Reagent were selected as the optimal

transfection conditions. Following another 24 hours, slides were either taken through the DNA halo preparation or fixed with methanol: acetone for 10 minutes on ice.

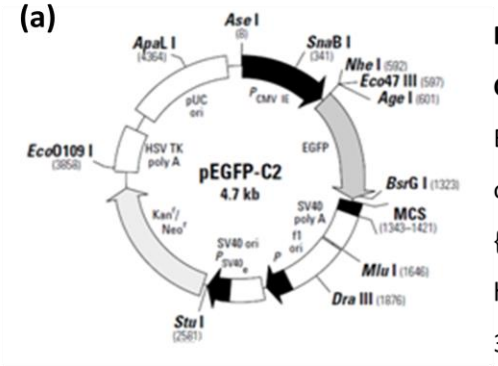

Figure 3.2.1: (a) Restriction Map and (b) Multiple Cloning Site of pEGFP-C2.

Emerin cDNA was inserted into the *Hind*III – *Bam*HI of the pEGFP-C2 mammalian expression vector {Clontech}. Images for this figure were sourced from http://www.clontech.com/images/pt/dis_vectors/PT3051-5.pdf

(b)

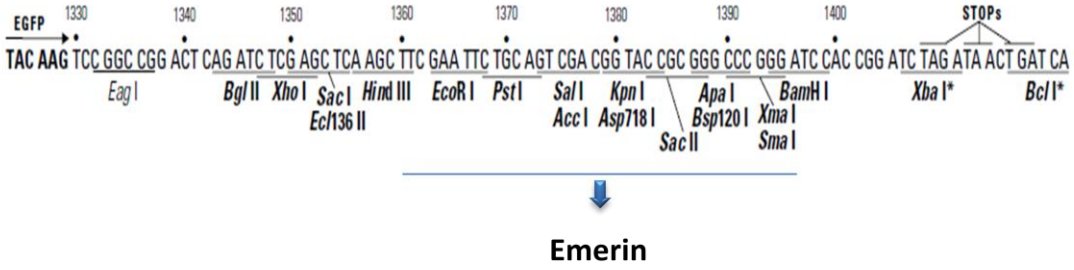

3.2.6 Indirect immunofluorescence

In order to detect the presence of lamin A/C, emerin and pKi67 following the DNA halo preparation, slides were washed 3 times in PBS and incubated at room temperature for 1 hour (or overnight at 4°C) in primary antibody (rabbit anti-human pKi67 (Novocastra) diluted 1:1500; mouse monoclonal anti-human lamin A/C (Novocastra) diluted 1:10; mouse monoclonal anti-human emerin (Novocastra) diluted 1:20; all dilutions made using 1% (v/v) NCS). Cells were then washed 3 times in PBS and incubated at room temperature for 1 hour in a fluorochrome-conjugated secondary antibody (Lamin A/C and emerin: rabbit anti-mouse FITC/TRITC diluted 1:30 (Dako); pKi67: swine anti-rabbit TRITC diluted 1:30 (Dako)). Following 3 more washes with PBS, slides were mounted with Vectashield (Vector Laboratories) containing DAPI.

In order to detect the presence of GFP in DNA halo prepared nuclei following transfection, slides were washed 3 times in PBS and incubated at room temperature for 1 hour in primary antibody (polyclonal rabbit anti-human GFP diluted 1:1000 (eBiosciences)). Slides were again washed 3 times in PBS and then incubated for 1 hour

in a secondary antibody (swine anti-rabbit diluted 1:30 (Dako)). Following this incubation, slides were washed 3 times in 2 x SSC and fixed with 4% paraformaldehyde (in PBS; v/v) for 10 minutes at room temperature. The slides were then taken through telomere PNA FISH.

3.2.7 Image capture and analysis

As per chapter 2.2.9 and 2.2.10.

3.3 RESULTS

3.3.1 Lamin A/C is revealed to be an inner NM protein using the DNA halo preparation

Research has demonstrated that lamin A is an inner NM protein (Hozak et al., 1995; Barbaro et al., 2002), which is retained within the inextractable nuclear structure following 2M NaCl (Ma et al., 1999). Thus, it seemed pertinent to investigate whether lamin A/C remains within the residual nucleus after the DNA halo preparation, which also employs high-salt. In methanol:acetone fixed control (2DD) HDFs, anti-lamin A/C staining was seen as a rim decorating the nuclear periphery; in addition, the antibody reacted with some foci within the nucleoplasm (figure 3.3.1). Indeed, such anti-lamin A foci have been detected previously; however, their appearance is reported to be cell-cycle dependent (Goldman et al., 1992; Bridger et al., 1993).

Significantly, after the DNA halo preparation, the pattern of anti-lamin A/C staining was considerably different; the strong rim staining was lost and instead, anti-lamin A/C reacted at sites throughout the nucleoplasm, in addition to the prominent foci observed in non-extracted nuclei (figure 3.3.1). This is an important finding since it confirms earlier work which proves that lamin A resists extraction using 2M NaCl (Ma et al., 1999). These staining patterns also suggest that lamin A/C forms a network that runs throughout the nucleoplasm, which is not normally observable in non-extracted nuclei. In methanol:acetone fixed nuclei, the antibodies to lamin A/C probably cannot access the epitopes buried deep within nucleoplasm, likely due to obscuring chromatin. However, in DNA halo preparations, such accessibility is greatly improved as a result of the less dense nucleoplasmic environment formed by extracting non NM-associated protein and DNA.

3.3.2 Mutant lamin A is mis-localised in the NM using the DNA halo assay

Since antibody staining demonstrates that lamin A/C is highly associated with the salt-resistant structure which remains following the DNA halo preparation, it seemed logical to investigate such staining in HDFs derived from HGPS patients. 3 HGPS patient HDF lines were selected; AG06297, AG08466 and G12660. AG06297 is termed a

classical HGPS cell line since it harbours the G608G (GGC>GGT) splice-site mutation in *LMNA*, while the patient from which AG08466 was derived exhibited atypical (type 2) HGPS. As aforementioned, such atypical patients display an HGPS phenotype, however, they do not harbour a mutation in *LMNA* (Dr. N. Levy; personal communication) and the affected gene is yet to be determined (see chapter 5). Finally, G12660 originates from a patient presenting with HGPS symptoms as well as myopathy (Kirschner et al., 2005); these cells contain a missense mutation in *LMNA* (c428>t, p.S143F) which is predicted to result in a protein that exerts a dominant negative effect (Kandert et al., 2007).

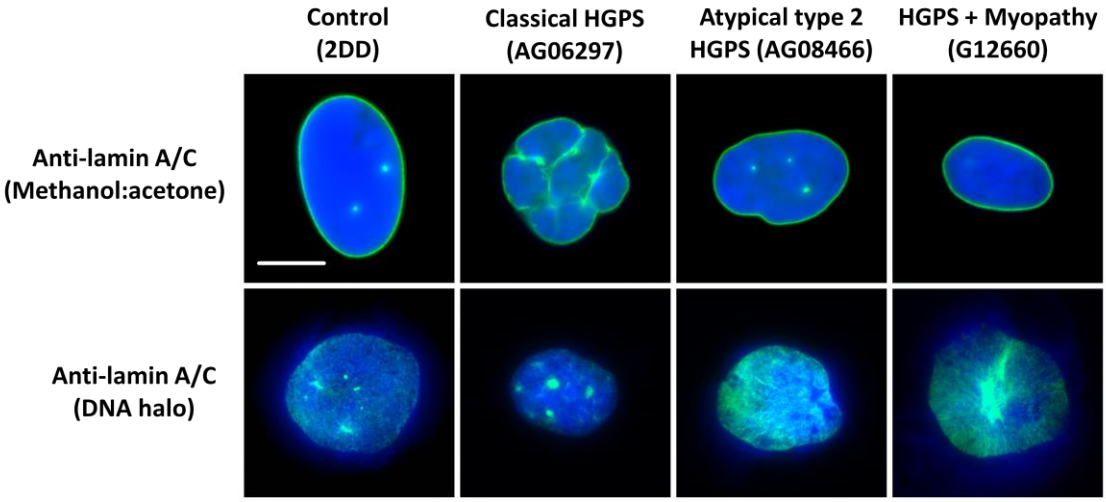

Figure 3.3.1: Lamin A/C staining in control and HGPS HDFs before and after the DNA halo preparation. DNA has been counterstained in blue (DAPI), while anti-lamin A/C can be seen in green (FITC). Scale bar = 10 μm.

In non-extracted nuclei, the pattern of anti-lamin A/C staining at the nuclear rim in AG08466 and G12660 HDFs was very similar to that found in control HDFs. However, in the classical HGPS cell line, anti-lamin A/C invaginations were observed in addition to the peripheral staining (figure 3.3.1). When comparing anti-lamin A/C localisation in cells subjected to the DNA halo preparation, there were differences between control and HGPS cell lines. For both AG08466 (atypical HGPS) and G12660 (HGPS plus myopathy), the anti-lamin staining displayed in these cells appeared different to controls, in terms of intensity and pattern. While this is perhaps unsurprising for G12660, since it produces a mutant lamin A protein, it was unexpected for AG08466, which produce wild-type lamin A (Dr. N. Levy; personal communication). One possible explanation for this is that the disease-causing mutant protein in AG08466, in some way, affects lamin A localisation. Most strikingly, large aggregates of anti-lamin A/C

were detected in residual nuclei of classical HGPS HDFs (AG06297; figure 3.3.1); indeed, these nucleoplasmic structures were seen in the majority of AG06297 cells. Conversely, these aggregates were not observed in AG08466 nor G12660 (figure 3.3.1). This is a significant finding since classical HGPS cells generate a truncated version of lamin A, known as progerin (Eriksson et al., 2003; De Sandre-Giovannoli et al., 2003) and thus, it appears that such aggregates were unique to cells producing progerin.

3.3.3 Examining chromosome associations with the NM in HGPS HDFs using the DNA halo assay

In order to determine whether NM-chromosome interactions are perturbed in laminopathy-based disease, the anchorage of selected chromosomes by the NM was examined in both classical (AG06297) and atypical (type 2; AG08466) HGPS HDFs. The results presented in chapter 2 demonstrate that DNA halo preparations generate reproducible inextractable nuclear structures, which can be coupled with various FISH procedures to study NM-genome associations. Therefore, it seemed logical to examine chromosome anchorage in HGPS using the DNA halo assay. Since the interactions of HSA-1, -13, -15 and -17 with the NM in control HDFs were examined in chapter 2, these chromosomes were selected for investigation in this study (figure 3.3.2). Furthermore, as the data in chapter 2 revealed no differences between such chromosome anchorage in proliferating and senescent control HDFs, proliferation status was not considered in this analysis of HGPS cells. Results (see figure 3.3.3 and 3.3.4) were then compared to those reported in chapter 2.3 for control HDFs. Significantly, for all chromosomes and cell lines, the majority of chromosome mass was observed within the periphery of the residual nucleus. The full extraction of chromosome territories into the DNA halo was not observed. In both classical (AG06297) and atypical (type 2; AG08466) HGPS nuclei, the anchorage of chromosomes 1 and 13 by the NM was disrupted; however, no differences were observed for chromosomes 15 and 17 (see figure 3.3.3). When comparing NM-chromosome interactions in the 2 HGPS cell lines, only one statistical difference was detected; this was with chromosome 13. Taken together, the findings of this section reveal that the anchorage of selected chromosomes by the NM is perturbed in HGPS.

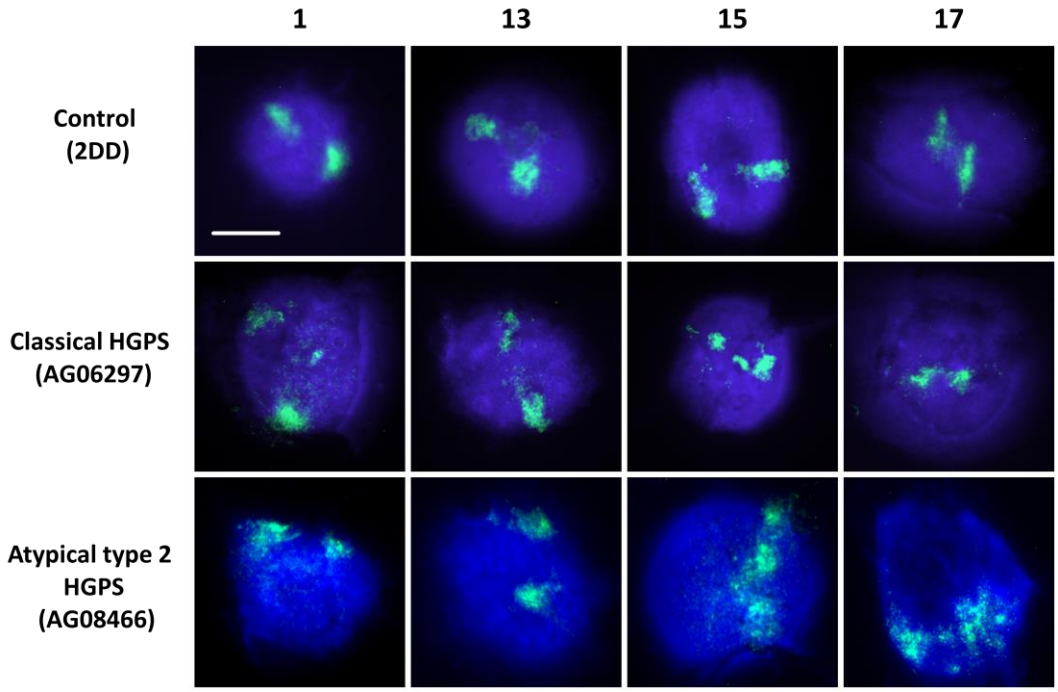

Figure 3.3.2: Investigating chromosome anchorage by the NM in HGPS using the DNA halo assay.

Control and HGPS HDFs were subjected to the DNA halo preparation and 2D-FISH. Specific probes were used for chromosomes 1, 13, 15 and 17. DNA has been stained using DAPI and can be seen in blue, while chromosome paints are depicted in green (FITC). Magnification = x100; scale bar = 10 µm.

(a)

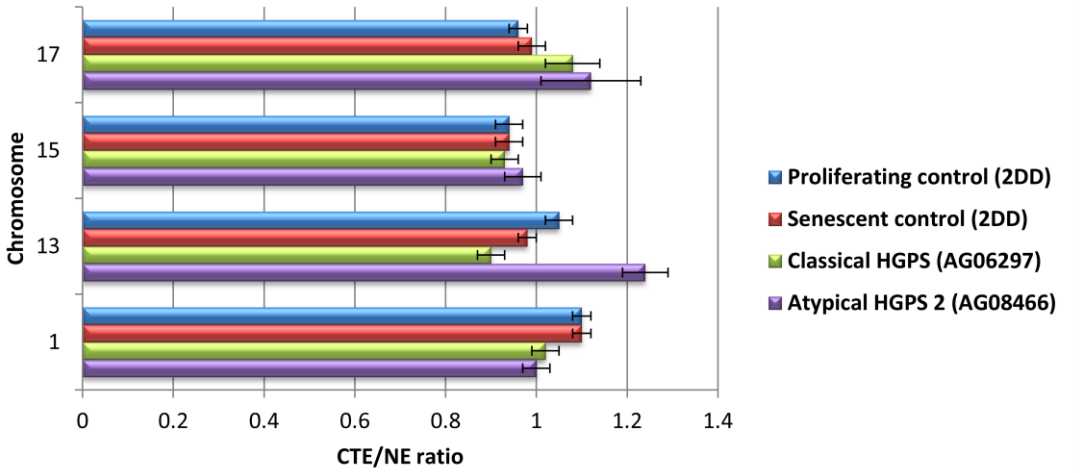

(b)

Statistical comparisons

Chromosome	2DD (P) vs AG06297 (R)	2DD (S) vs AG06297 (R)	2DD (P) vs AG08466 (R)	2DD (S) vs AG08466 (R)
1				
13				
15				
17				

Figure 3.3.3: Examining NM-chromosome interactions in HGPS using the DNA halo assay

(a) Mean chromosome territory edge (CTE)/nuclear edge (NE) ratio for 4 chromosomes; a ratio below 1 denotes that the furthest CTE lies within the corresponding NE, while a ratio above 1 signifies that the furthest CTE lies outside the corresponding NE. Error bars represent ± SEM. **(b)** Statistical analysis of NM-chromosome interactions in control and X-EDMD using the Student's *t*-Test. Green shading indicates no significant difference between the populations, yellow shading depicts a $p < 0.05$ and red shading represents $p < 0.01$. P = pKi67+, proliferating; S = pKi67−, senescent; R = random.

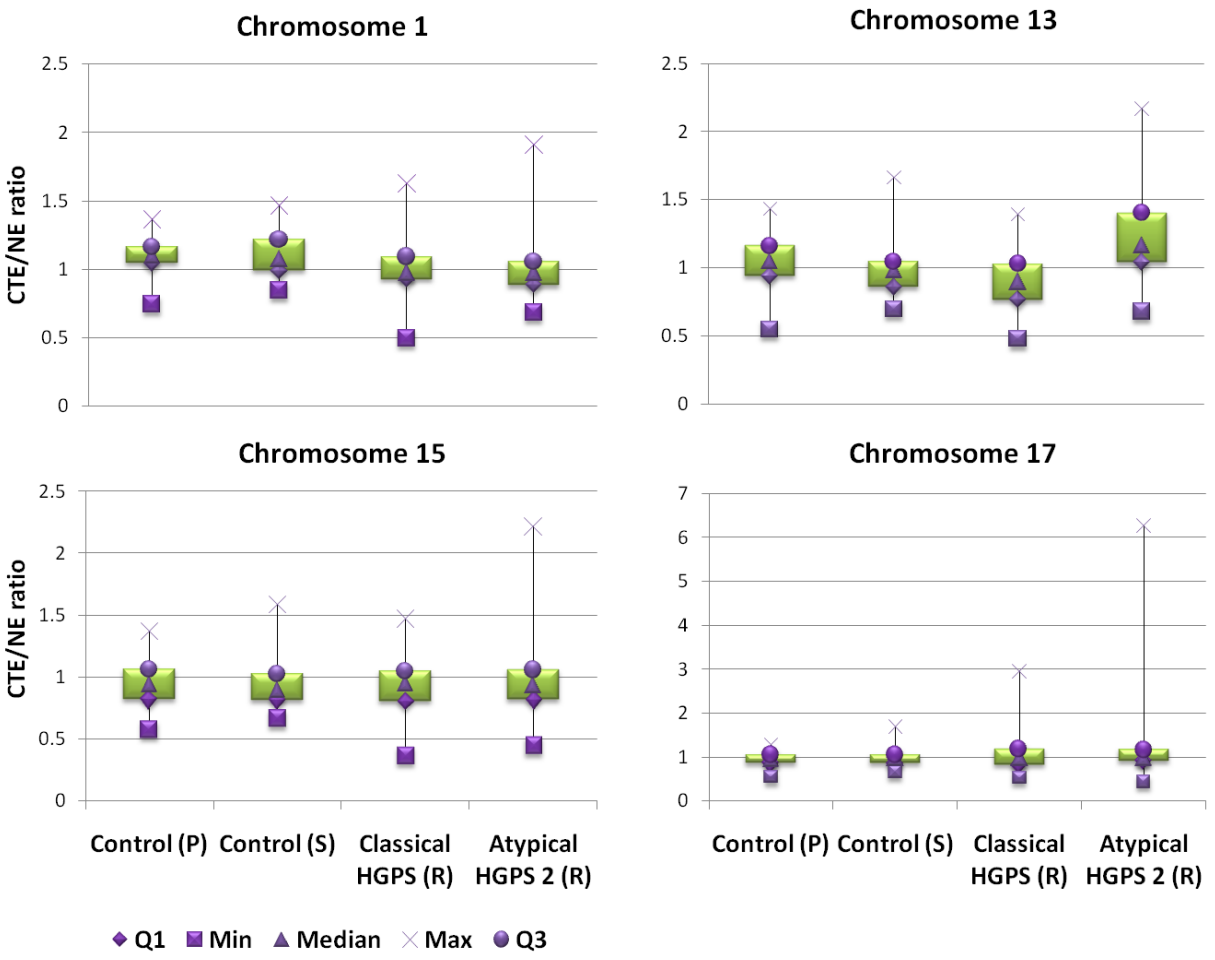

Figure 3.3.4: Chromosome anchorage by the NM is perturbed in HGPS
Chromosome anchorage by the NM was examined in 2 HGPS cell lines: Classical (AG06297) and Atypical (AG08466) and compared to proliferating (P) and senescent (S) control (2DD) populations. Modified box plots for control and HGPS populations for each chromosome (Q1 = lower quartile; Min = lowest value recorded; Med = median; Max = maximum value recorded; Q3 = upper quartile).

3.3.4 Examining telomere associations with the NM in HGPS HDFs using the DNA halo assay

3.3.4.1 Telomere anchorage by the NM in HGPS

3.3.4.1.1 Telomere anchorage by the NM is disrupted in HGPS

Lamin A is demonstrated to be a component of the internal NM (Hozak et al., 1995) and is found to associate with telomeric DNA (Shoeman and Traub, 1990; Raz et al., 2008). Therefore, it seemed pertinent to examine whether mutant lamin A affects the capacity of the NM to anchor telomeric DNA. To do this, NM-telomere associations

were analysed in 3 HGPS cell lines (AG08466, AG06297 and G12660) using the DNA halo assay (see figure 3.3.5).

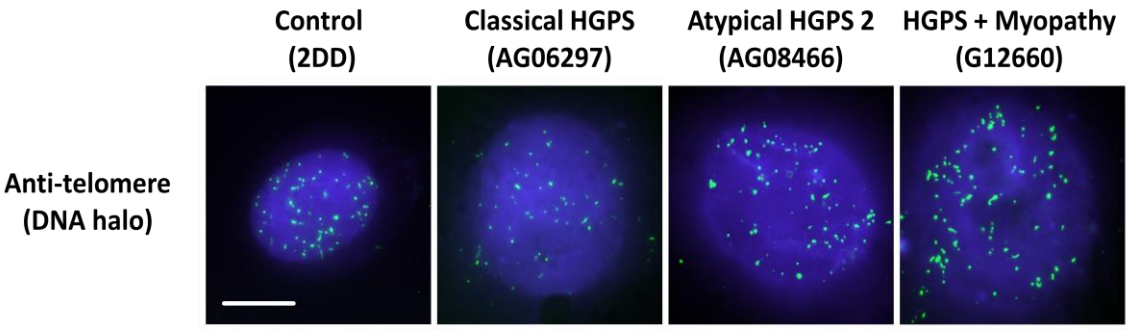

Figure 3.3.5: Investigating telomere anchorage in HGPS HDFs using the DNA halo assay
The residual nucleus and surrounding DNA halo have been counterstained using DAPI (blue) while telomere signals can be seen in green (FITC). Magnification = 100x; scale bar = 10 µm.

Interestingly, the mean percentage of telomeres extracted into the DNA halo was significantly higher in all HGPS cell lines when compared to the control; however, the severity of the differences varied between the HGPS cell lines (figure 3.3.6). In the atypical (type 2) HGPS cell line, AG08466, approximately 20% (± 11.9 (± standard deviation); nuclei = 90) of telomeres were, on average, extracted into the DNA halo. This was statistically different to the 15% (± 8.1; nuclei = 90) observed in control HDFs, using $p > 0.05$ not $p > 0.01$. Taking into account the slight variation inherent within an assay such as this (as shown in chapter 2), it is thus likely that telomere anchorage by the NM in AG08466 is only slightly perturbed, if not normal. Indeed, this cell line generates wild-type lamin A. In the cell lines (AG06297 and G12660) harbouring *LMNA* mutations, NM-telomere interactions were significantly perturbed ($p > 0.0001$). In the classical HGPS cell line (AG06297), 30% (± 9.1; nuclei = 90) of telomeres were, on average, extracted into the DNA halo, which was twice the fraction reported for control cells in chapter 2. Surprisingly, the highest mean percentage, 37% (± 10.9; nuclei = 90) was seen in G12660, the cell line derived from a patient suffering from a combination of HGPS and myopathy. This is interesting since unlike AG06297, which produces a truncated version of lamin A (progerin), G12660 expresses full-length lamin A containing a point mutation. Regarding the spread of results within each dataset, all 3 HGPS cell lines exhibited a greater variance than control; furthermore, the maximum value recorded for all HGPS cell lines was approximately 60%, while in control cells, the

highest noted was below 40% (figure 3.3.6b). Taken together, these findings suggest that telomere anchorage is disrupted considerably in *LMNA* mutants.

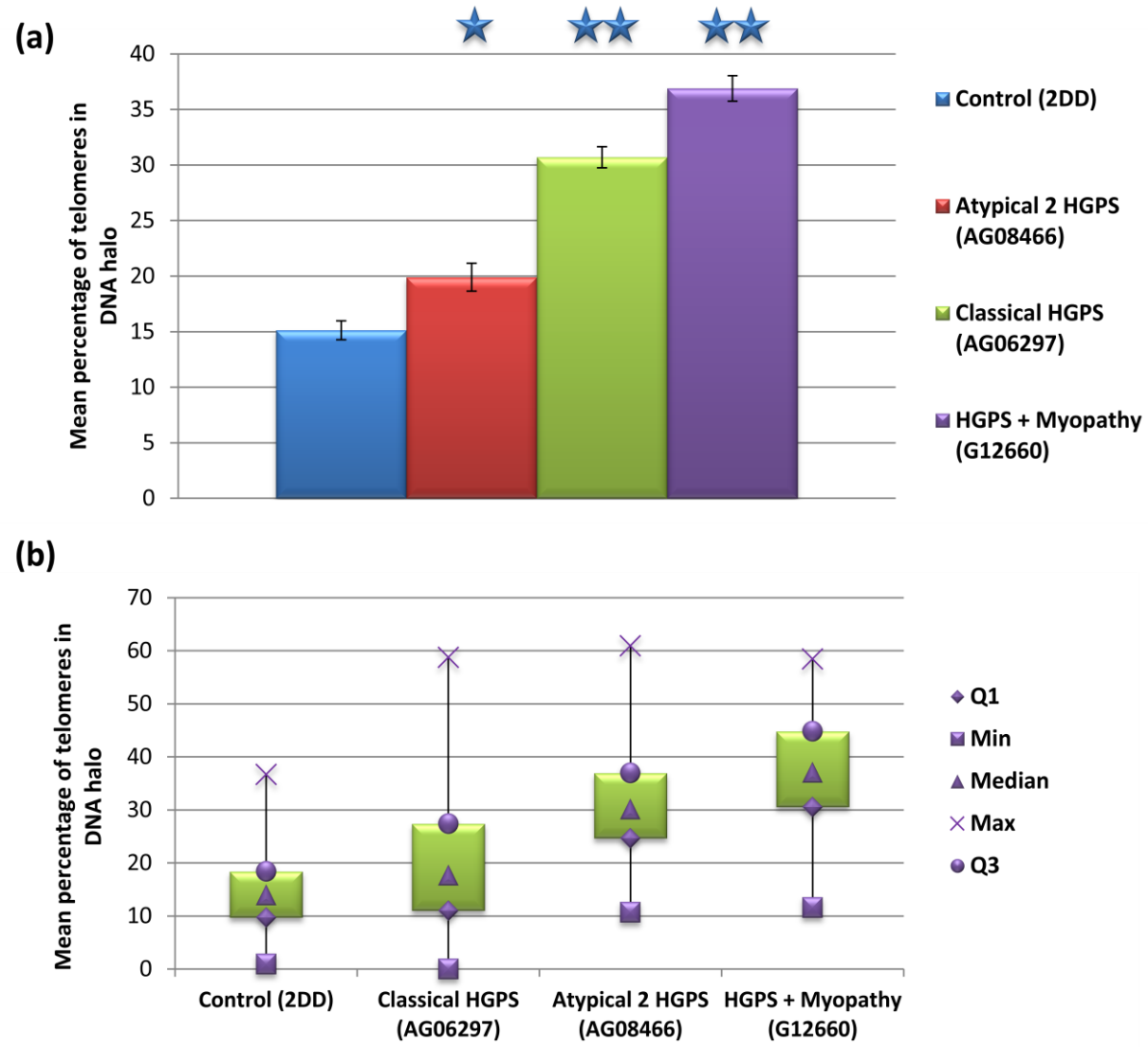

Figure 3.3.6: Telomere anchorage by the NM is perturbed in HGPS using the DNA halo assay

Telomere-NM interactions were examined in 3 HGPS cell lines: atypical HGPS (AG08466), classical HGPS (AG06297) and HGPS + Myopathy (G12660). **(a)** Mean percentage of telomeres extracted into DNA halo in control versus 3 different HGPS cell lines (samples were random with regards to proliferation status). Statistical differences between control and HGPS cell lines have been determined by the Student's *t*-test and are denoted by stars (1 = $p < 0.05$; 2 = $p < 0.01$). Error bars represent ± SEM. **(b)** Modified box plots for control and HGPS populations (Q1 = lower quartile; Min = lowest value recorded; Med = median; Max = maximum value recorded; Q3 = upper quartile).

3.3.4.1.2 Proliferating vs. senescent HGPS

pKi67 is a nucleolar antigen which exists only in proliferating cells (Kill, 1996). Therefore, it can be used to differentiate between proliferating (Ki67+) and senescent (pKi67−) cells. Importantly, no difference between the two populations was observed when comparing NM-telomere associations in control HDFs using the DNA halo assay (chapter 2). In order to examine whether this is also the case in *LMNA* mutant HGPS HDFs (AG11513 and G12660), telomere PNA FISH was coupled with pKi67 staining. Since AG06297 was no longer available to use, another classical HGPS cell line, AG11513, was employed (figure 3.3.7). Significantly, in both pKi67+ and pKi67− AG11513 HDFs, a mean 30% (nuclei = 30) of telomeres were extracted into the DNA halo. This is an important finding for 2 reasons; firstly, it suggests that telomere anchorage by the NM does not change on entry into senescence using the DNA halo assay, in classical HGPS. Secondly, it demonstrates that 2 individual cell lines harbouring the same mutation (AG06297 and AG11513) exhibit very similar NM-telomere interactions. This is significant since it reinforces the notion presented in chapter 2, that the DNA halo assay produces reproducible results.

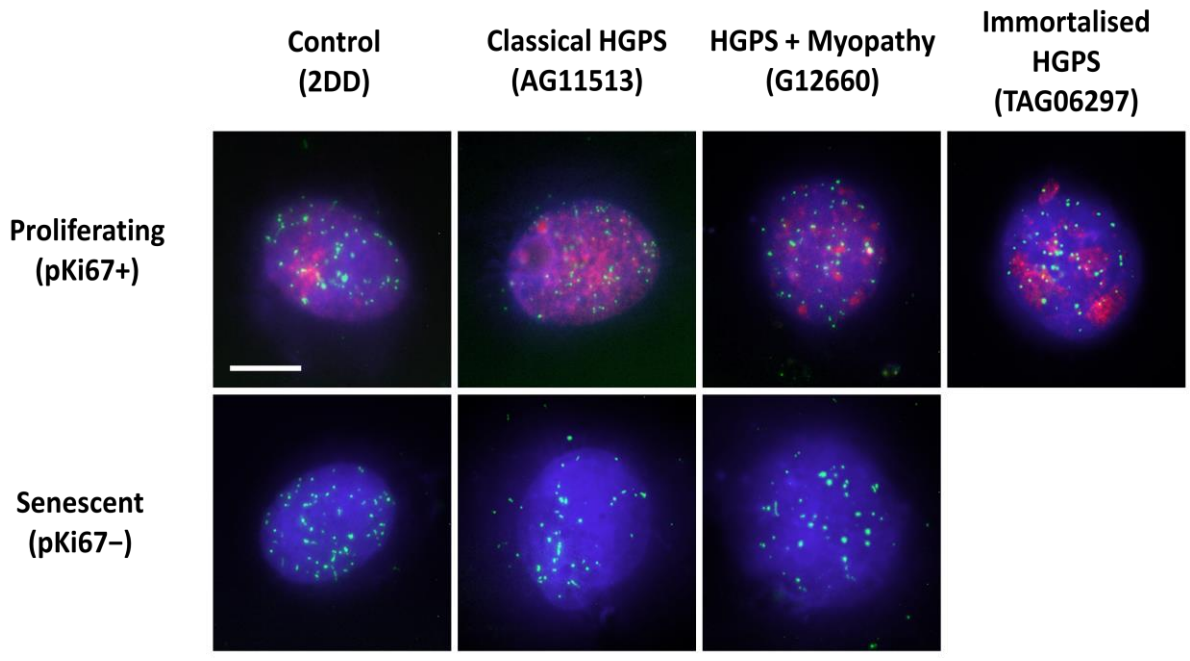

Figure 3.3.7: Telomere anchorage by the NM in proliferating, senescent and hTERT immortalised HGPS HDFs using the DNA halo assay.
The residual nucleus and surrounding DNA halo have been counterstained using DAPI (blue). Anti-telomere signals can be seen in green (FITC), while anti-pKi67 is pseudo-coloured red (TRITC). Magnification = x100; scale bar = 10 µm.

While there was no significant difference in the mean percentage of telomeres in the DNA halo, when comparing pKi67+ and pKi67− populations in classical HGPS, this was not the case for G12660. In senescent G12660 nuclei, nearly 40% (± 16.7; nuclei = 30) of telomeres were extracted into the DNA halo, whereas, this value was 30% (± 11.6; nuclei = 30) in the pKi67+ population (figure 3.3.8a). The higher variance observed inpKi67− HDFs suggests that a proportion of nuclei are more susceptible to extraction than others (figure 3.3.b). Indeed, for one G12660 pKi67− nucleus, approximately 80% of telomeres were detected in the DNA halo. In contrast, the maximum value in the AG11513 pKi67− population was below 60% and in control HDFs, this was less than 40%.

Significantly, these data suggest the absence of a clear-cut correlation between telomere-NM associations and proliferative state using the DNA halo assay in HGPS. However, there was an obvious reduction in the mean total number of telomeres scored in senescent nuclei for both HGPS cell lines. Importantly, this decrease was concomitant with that observed for control HDFs (figure 3.3.8a).

3.3.4.1.3 Telomere anchorage in hTERT immortalised HGPS cells

To examine the impact of telomerase activation on telomere anchorage by the NM, hTERT-immortalised classical HGPS fibroblasts (TAG06297; Wallis et al., 2004) were studied using the DNA halo assay (figure 3.3.7). TAG06297 was generated by expressing a retroviral vector encoding the catalytic subunit of telomerase (hTERT) in the HGPS HDF cell line, AG06297 (Wallis et al., 2004). On average, 13.8% (± 11%; nuclei = 30) telomeres were extracted into the DNA halo in the hTERT-immortalised HGPS cell line, TAG06297 (figure 3.3.9). This was statistically different ($p < 0.001$) to the percentage of 30% (± 9.1; nuclei = 90) recorded for AG11513; however, it was very similar to the value recorded for proliferating control HDFs (figure 3.3.9). Furthermore, there was a statistical difference between the average total number of telomeres scored for immortal and mortal HGPS populations; far fewer (69.4 ± 20.3; nuclei = 30) telomeres were observed in the immortalised HGPS cells (figure 3.3.9).

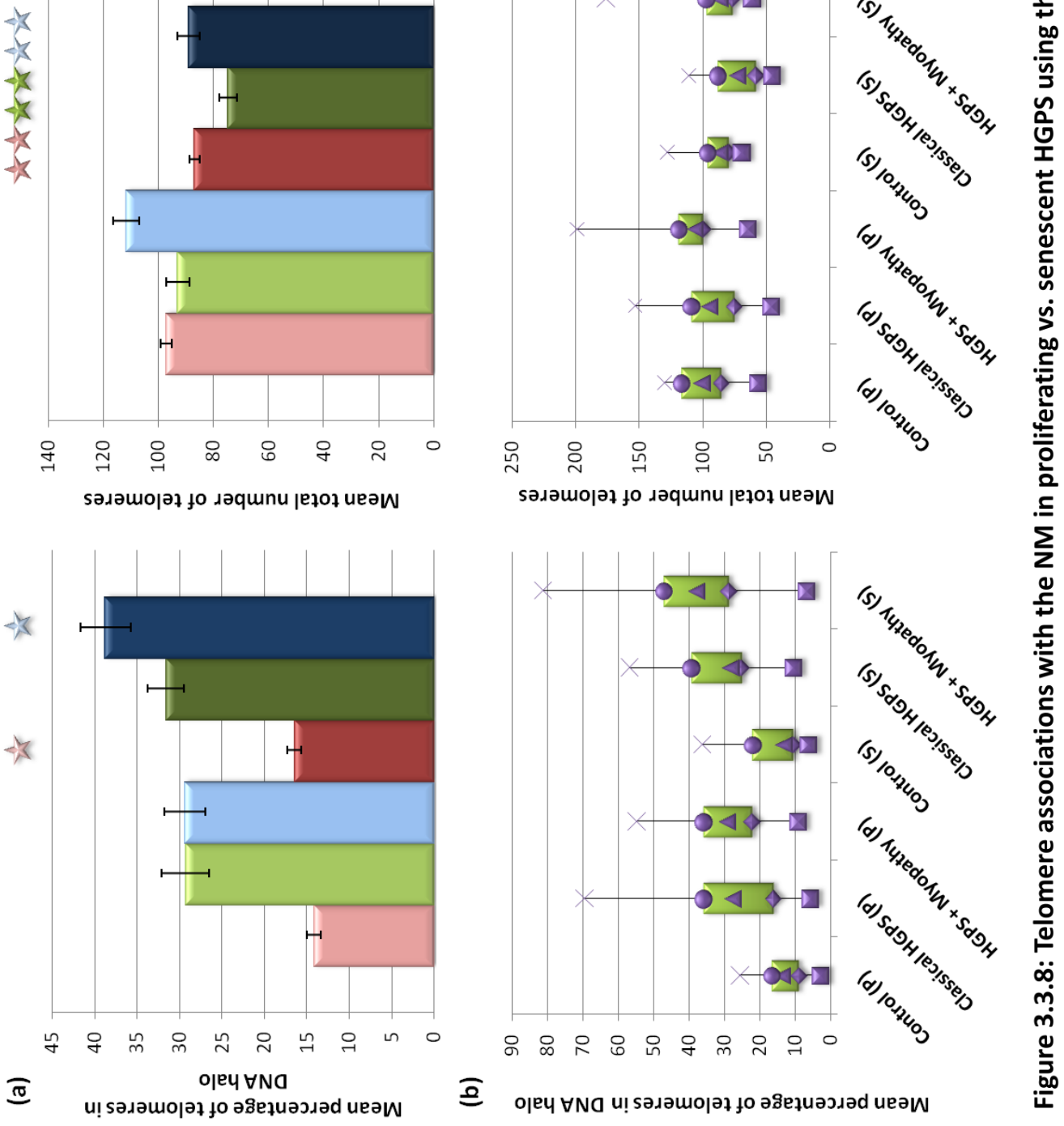

Figure 3.3.8: Telomere associations with the NM in proliferating vs. senescent HGPS using the DNA halo assay

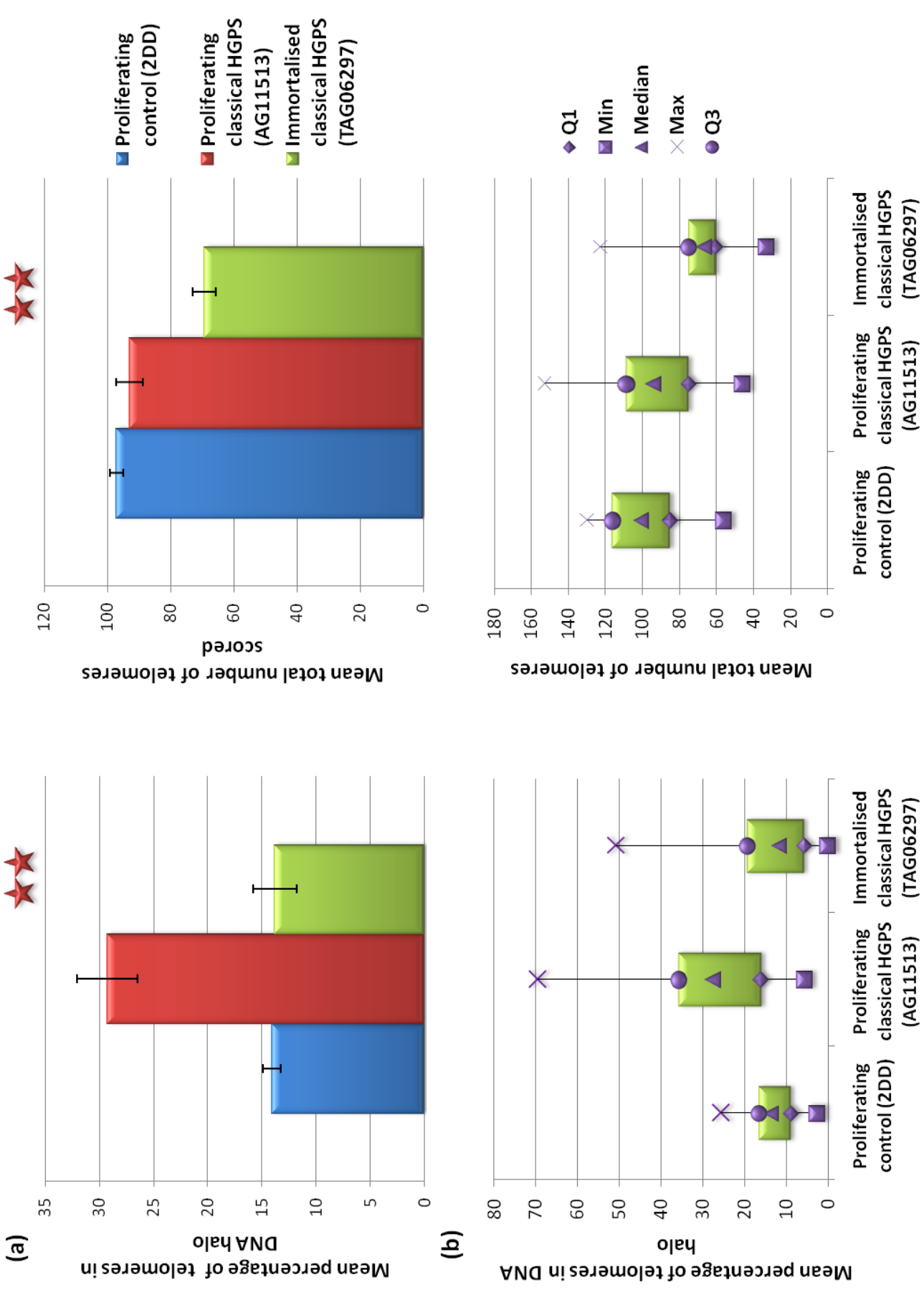

Figure 3.3.9: Telomere anchorage in immortalised classical HGPS HDFs

Figure 3.3.8: Telomere associations with the NM in proliferating vs. senescent HGPS using the DNA halo assay

(a) Mean percentage of telomeres extracted into DNA halo and mean total number of telomeres scored for proliferating (P; pKi67+) and senescent (S; pKi67−) HGPS HDFs. Statistical differences between proliferating and senescent populations for each cell line have been determined by the Student's *t*-test and are denoted by stars (1 = $p < 0.05$; 2 = $p < 0.01$). Error bars represent ± SEM. **(b)** Modified box plots for mean percentage of telomeres extracted into DNA halo and mean total number of telomeres scored (Q1 = lower quartile; Min = lowest value recorded; Med = median; Max = maximum value recorded; Q3 = upper quartile).

Figure 3.3.9: Telomere anchorage in immortalised classical HGPS HDFs

(a) Mean percentage of telomeres extracted into DNA halo and mean total number of telomeres scored for proliferating mortal and immortalised classical HGPS populations compared with control. Statistical differences between mortal and immortalised HGPS populations have been determined by the Student's *t*-test and are denoted by stars ($p < 0.01$). Error bars represent ± SEM. **(b)** Modified box plots for mean percentage of telomeres extracted into DNA halo and mean total number of telomeres scored (Q1 = lower quartile; Min = lowest value recorded; Med = median; Max = maximum value recorded; Q3 = upper quartile).

3.3.5 Emerin is revealed to be a NM-protein using the DNA halo assay

Previous research demonstrates that emerin is a NM protein (Squarzoni et al., 1998; Ellis et al., 1998; Takata et al., 2009)**;** however, its association with the NM appears limited to periphery of salt-extracted nuclei (Squarzoni et al., 1998). To test whether emerin remains following the extraction procedure used in this current study, control HDFs were subjected to the DNA halo preparation and stained with anti-emerin (figure 3.3.10). In methanol:acetone fixed nuclei, anti-emerin decorates the nuclear edge (figure 3.3.10). However, in DNA halo prepared HDFs, the intensity of rim staining decreased; instead, emerin is found throughout the nucleoplasm. Indeed, this difference between anti-emerin staining patterns in non-extracted and extracted nuclei is very similar to that seen for anti-lamin A/C (section 3.3.1).

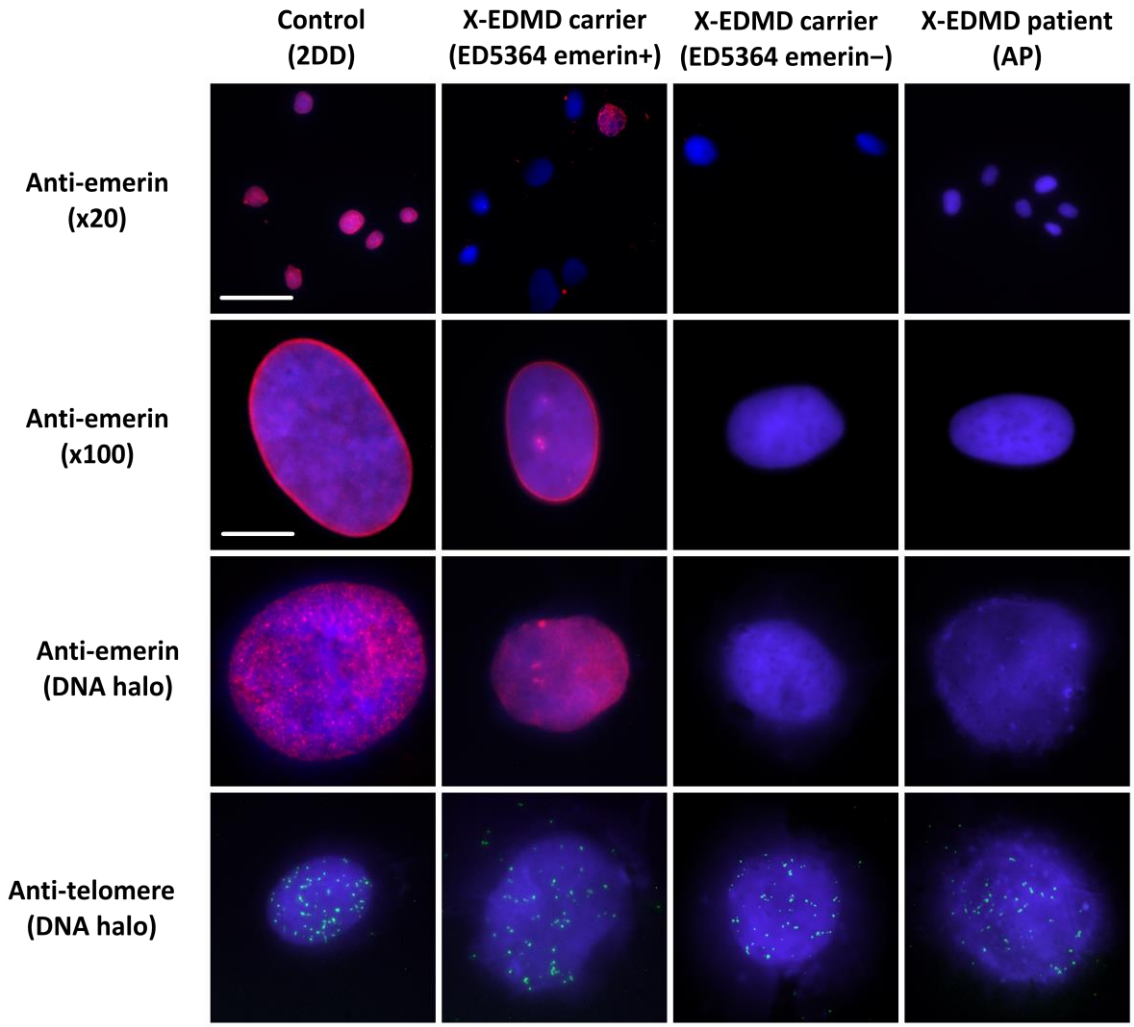

Figure 3.3.10: Emerin is revealed to be a NM protein using the DNA halo assay
Anti-emerin staining was employed to detect the protein's localisation and presence in methanol:acetone (2D) fixed and DNA halo prepared control and X-EDMD nuclei. Since the carrier X-EDMD cell line (ED5364) has a mixed population of emerin positive and negative nuclei, both categories are depicted in this figure. DNA is counterstained using DAPI (blue), while anti-emerin can be visualised in red (TRITC). Telomere PNA FISH (FITC; green) was used to paint telomeres in DNA halo prepared cells (bottom panel). Scale bar = 50 µm (x20); 10 µm (x100).

3.3.6 Telomere anchorage by the NM in X-EDMD HDFs

3.3.6.1 Mutations in *EMD* disrupt telomere associations with the NM using the DNA halo assay

Since emerin resisted extraction during the DNA halo preparation, this confirmed that it is indeed associated with the NM (Squarzoni et al., 1998; Ellis et al., 1998; Takata et al., 2009). In light of the observation that *EMD* mutant cells exhibit perturbed genome organisation (Fidzianska et al., 1998; Ognibene et al., 1999; Meaburn et al., 2007), it

seemed logical to investigate the effect of emerin loss on NM function. To do this, NM-telomere associations were examined in cells derived from both an X-EDMD carrier (ED5364) and patient (AP). The carrier cell line, ED5364, originated from the mother of a child with X-EDMD; DNA sequencing of *EMD* in this cell line revealed the presence of a heterozygous point mutation (c.315T>G/ p.Tyr105X) in exon 4 (chapter 5), which results in the formation of a premature stop codon. This mutation, which has previously been reported in another case, produces an unstable mutant protein, leading to an absence of emerin in all affected nuclei (Muntoni et al., 1998). Within the carrier, it is expected that one population of cells express functional emerin while the remaining cells are emerin null; this is expected to be random due to the nature of X chromosome inactivation (Lyon, 1961). However, deviations from this expected 50:50 ratio of normal to mutant protein, have been observed in X-EDMD carriers (Manilal et al., 1997; 1998). Once in culture, the majority of ED5364 cells were emerin-negative (~90%; figure 3.3.10); this is unsurprising since emerin null cells appear to be hyperproliferative (Markiewicz et al., 2006). In contrast, all AP cells were negative for emerin, as a result of an *EMD* mutation (figure 3.3.10; previously reported by Markiewicz et al., 2002).

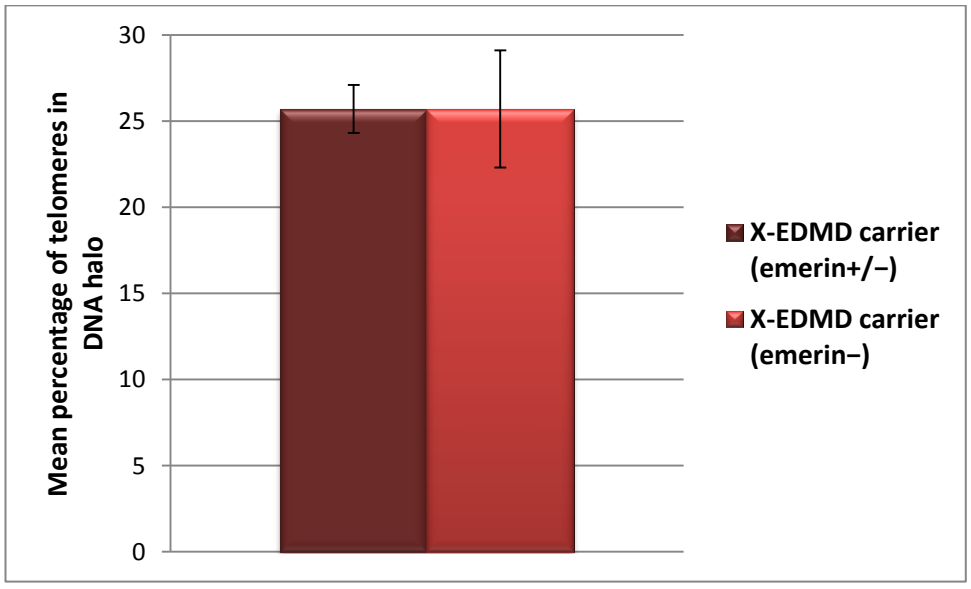

Figure 3.3.11: Examining telomere anchorage in X-EDMD carrier HDFs using the DNA halo assay. Error bars represent ±SEM.

In order to confirm that the ED5364 sample analysed contained mostly emerin null cells, residual nuclei were stained using anti-emerin; only those negative for emerin were included (figure 3.3.10). There was no significant difference between the ED5364 emerin negative population and the ED5364 sample analysed at random (figure 3.3.11). Interestingly, there was a statistically significant increase ($p < 0.01$) in the mean percentage of telomeres extracted into the DNA halo, in both ED5364 (emerin−) and AP cell lines (figure 3.3.12). On average, 25.7% (± 13.6; nuclei = 90) telomeres were not associated with the residual nucleus in emerin -ED5364 HDFs. This figure was only slightly higher in AP (28% ± 7.4; nuclei = 30). The variation present within the ED5364 sample was considerably higher than for control and AP cells (figure 3.3.12); this is further highlighted by the huge difference between the minimum and maximum values recorded for ED5364. The variation within the AP sample was similar to the control. Perhaps unexpectedly, the highest percentage was detected in a nucleus derived from the ED5364 cell line (figure 3.3.12). In spite of these differences in variation, it can still be concluded that telomere anchorage is disrupted in both carrier and patient X-EDMD cell lines.

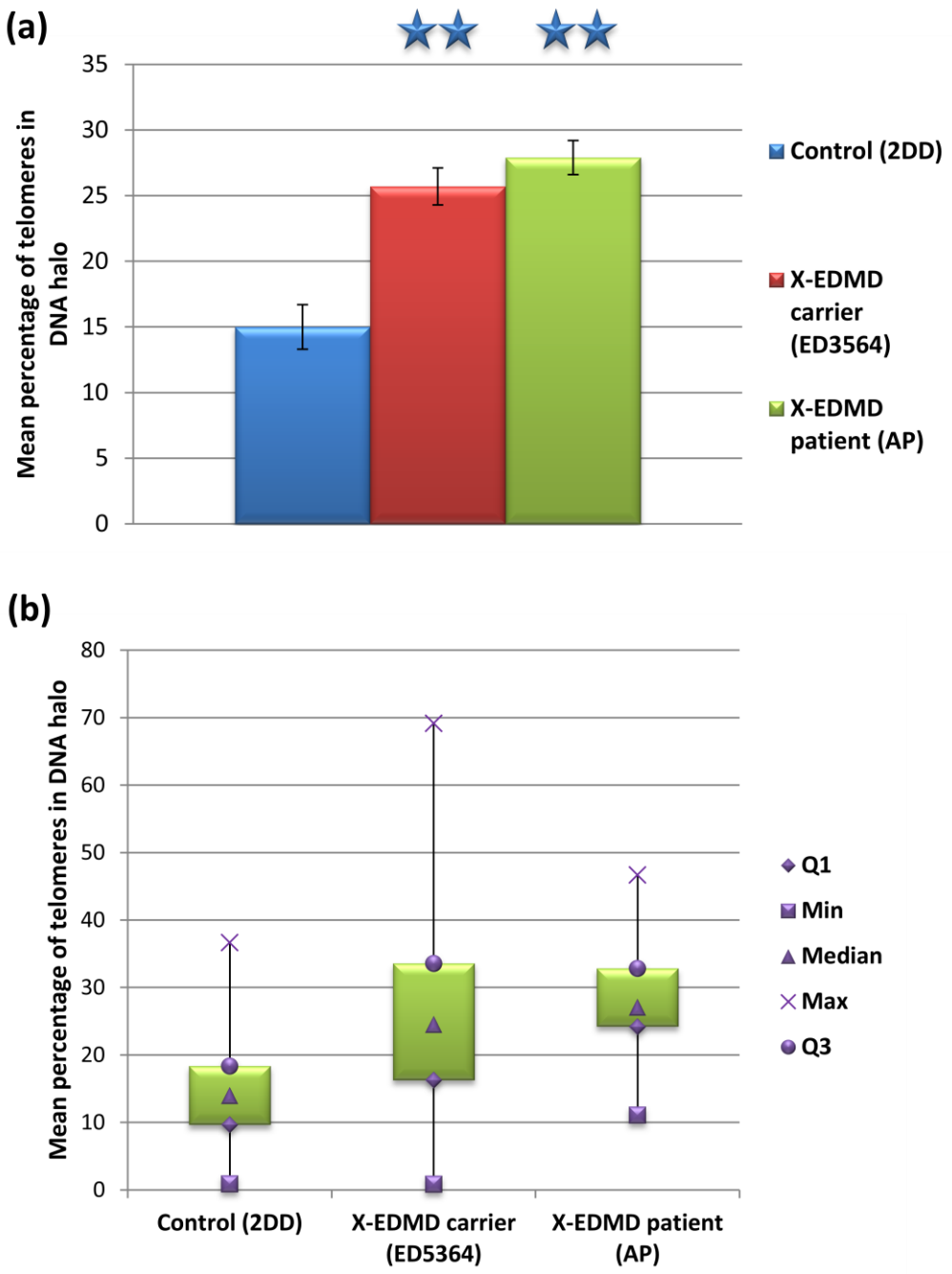

Figure 3.3.12: Telomere anchorage by the NM is perturbed in X-EDMD.

Telomere-NM interactions were examined in 2 X-EDMD cell lines: an X-EDMD carrier (c; ED5364) and patient (p; AP). **(a)** Mean percentage of telomeres extracted into DNA halo in control versus X-EDMD carrier (ED5364) and X-EDMD patient (AP; samples were random with regards to proliferation status). Statistical differences between control and X-EDMD cell lines have been determined by the Student's *t*-test and are denoted by stars ($p < 0.01$). Error bars represent ± SEM. **(b)** Modified box plots for control and X-EDMD populations (Q1 = lower quartile; Min = lowest value recorded; Med = median; Max = maximum value recorded; Q3 = upper quartile).

3.3.6.2 Attempting to rescue perturbed telomere-NM associations in X-EDMD fibroblasts

3.3.6.2.1 Overview

Since the absence of emerin appears to perturb telomere anchorage by the NM, attempts were made to rescue this function of the NM by introducing *EMD-GFP* into ED5364 cells. In order to do this, cells were transiently transfected with emerin-GFP using GeneJuice (Novagen) (figure 3.3.13).

3.3.6.2.2 Optimisation

In order to determine the most optimal conditions for transfection, several optimisation experiments were performed (table 3.3.1). Control HDFs were seeded in QuadriPERM dishes at a density of ~0.9 x 10^5; after 24 hrs of growth, the transfection was performed using GeneJuice. The optimisation process was started by using the GeneJuice to DNA ratio of 3:1, which is recommended by the manufacturers (Novogen). However, since the guidelines did not cover cells grown in QuadriPERM chambers, the manufacturer's protocol was slightly modified and a higher starting concentration of 2 µg *EMD*-GFP DNA was used per slide. Following the execution of the transfection procedure, cells were left for 48 hrs and then fixed using methanol:acetone or taken through the DNA halo preparation. However, visualisation of the slides using UV microscopy revealed the absence of signal and thus indicated that the transfection was unsuccessful. Indeed, DAPI staining detected a high amount of DNA on the slide, confirming that the majority of DNA did not enter the cell.

Following this unsuccessful attempt to transfect the HDFs with *EMD*-GFP, the experiment was repeated using control and ED5364 fibroblasts. Both the volume of serum-free medium and amount of DNA used per slide was increased to 300 µl and 2.7 µg respectively. Since the volume of GeneJuice remained the same as before, the ratio of GeneJuice to plasmid DNA was reduced to 2.2:1. After 48 hrs, the slides were prepared accordingly and checked; the transfection was successful and emerin-GFP was visualised at the NE in both 2D-fixed and DNA halo nuclei. This demonstrated that the emerin-GFP survived the DNA halo preparation and also confirmed that emerin is

Experiment	Slide	Cell line	Volume			Amount of plasmid DNA (µg; GeneJuice: DNA ratio)	Duration of transfection (hrs)	Preparation	Successful?
			Complete growth medium (ml)	Serum-free medium in transfection mixture (µl)	GeneJuice Transfection reagent (µl)				
1	1	2DD	6	200	6	2 (3:1)	48	M:A	No
	2	2DD	6	200	6	2 (3:1)	48	DNA halo	
2	1(C)	2DD	6	0	0	0	N/A	M:A	N/A
	2 (C)	2DD	6	0	0	0	N/A	DNA halo	
	3	2DD	6	300	6	2.7 (2.2:1)	48	M:A	Yes
	4	2DD	6	300	6	2.7 (2.2:1)	48	DNA halo	
	5 (C)	ED5364	6	0	0	0	N/A	DNA halo	N/A
	6	ED5364	6	300	6	2.7 (2.2:1)	48	M:A	Yes
	7	ED5364	6	300	6	2.7 (2.2:1)	48	DNA halo	
3	1 (C, 24 hrs)	2DD	5	0	0	0	N/A	M:A	N/A
	2 (C, 24 hrs)	2DD	5	0	0	0	N/A	M:A	
	3	2DD	5	150	7.5	2.5 (3:1)	24	M:A	Yes
	4	2DD	5	300	15	5 (3:1)	24	M:A	
	5 (C, 48 hrs)	2DD	5	0	0	0	N/A	M:A	N/A
	6 (C, 48 hrs)	2DD	5	0	0	0	N/A	M:A	N/A
	7	2DD	5	150	7.5	2.5 (3:1)	48	M:A	Yes
	8	2DD	5	300	15	5 (3:1)	48	M:A	
4	1 (C)	ED5364	5	0	0	0	N/A	M:A	N/A
	2	ED5364	5	300	15	5 (3:1)	24	M:A	Yes
	3	ED5364	5	300	20	5 (4:1)	24	M:A	Yes
	4	ED5364	5	300	25	5 (5:1)	24	M:A	
	5	ED5364	5	300	30	10 (3:1)	24	M:A	

Table 3.3.1: An overview of the transient transfection experiments performed in order to determine optimal conditions. M:A = methanol:acetone; C = control.

indeed associated with the inextractable NM. However, the transfection efficiency was low (~5%) and thus, I proceeded with the optimisation.

The aim of the next step of the process was to increase the transfection efficiency and also to determine whether the length of exposure to the transfection reagent augmented such efficiency. In order to do this, the transfections were performed using 2 different DNA concentrations: 2.5 and 5 μg and 2 different exposure times (24 and 48 hrs); the GeneJuice:DNA ratio was constant at 3:1. All slides were fixed using methanol:acetone after 24 or 48 hrs; since this was an optimisation procedure, it was illogical to take the slides through the DNA halo preparation due the procedure's expense. The results of this experiment demonstrated that by doubling the DNA concentration, the transfection efficiency was increased to 10–15%. The findings also revealed that such efficiency was similar in cells transfected for 24 and 48 hrs; thus, suggesting that an incubation of 24 hrs is sufficient for such a transfection.

Although transfection efficiency was increased when the DNA concentration used doubled, the percentage of transfected cells was still low. In light of this, a different optimisation approach was employed; instead, 3 different GeneJuice:DNA ratios were used: 3:1, 4:1 and 5:1. In addition, a higher concentration of DNA (10 μg) was tested at a ratio of 3:1. The visualisation of the slides using UV microscopy revealed that the use of a GeneJuice to DNA ratio of 3:1 using 5 μg were the most efficient transfection conditions (figure 3.3.13).

3.3.6.2.3 Transfection experiments

Although, at best, the transfection efficiency was low (10–15% emerin-GFP positive), this still allowed for a sufficient number of nuclei to be analysed. Thus, the use of this transfection method was continued with the aim to correct the perturbed telomere anchorage observed in the ED5364 HDFs. Alongside the cells exposed to the transfection reagent and DNA, non-exposed ED5364 cells were used as a control. The transfection was repeated three times on three different days to test the accuracy and reproducibility of the results. Following the first transfection experiment, telomere PNA FISH was performed using one of the slides. Importantly, the FISH procedure

appeared to destroy the fluorescence of the GFP, which was present beforehand. Therefore, in order to differentiate between the transfected and non-transfected cells, anti-GFP staining was used; GFP-positive cells were deemed transfected while GFP-negative were categorised as non-transfected.

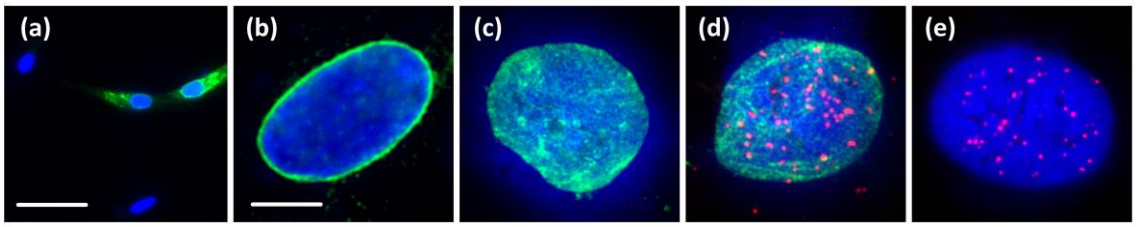

Figure 3.3.13: Using transient transfections to introduce *EMD-GFP* into X-EDMD carrier HDF
Representative images of **(a)** Methanol:acetone fixed HDFs (x20); emerin-GFP is green, **(b)** Methanol:acetone fixed HDFs (x100); emerin-GFP is green, **(c)** DNA halo prepared nucleus (x100); emerin-GFP is green, **(d)** DNA halo prepared nucleus (x100); anti-GFP is green (FITC), **(e)** DNA halo prepared nucleus (x100); anti-telomere signals are red (Cy3). Scale bar = 50 µm (x20); 10 µm (x100).

For each experiment, the mean percentage of telomeres recorded in the DNA halo was between 20–25% for control (non-exposed) ED5364 nuclei, while this value rose to 29–34% for cells transfected with emerin-GFP. Thus, transfecting the cells with emerin-GFP led to a decrease, not the expected increase, in the number of NM-telomere interactions; in short, correct telomere anchorage was not restored (figure 3.3.14). One limitation of a transient transfection is that the transcription of the exogenous DNA cannot be regulated; therefore, it is likely that varying amounts of emerin-GFP were generated during the transfections.

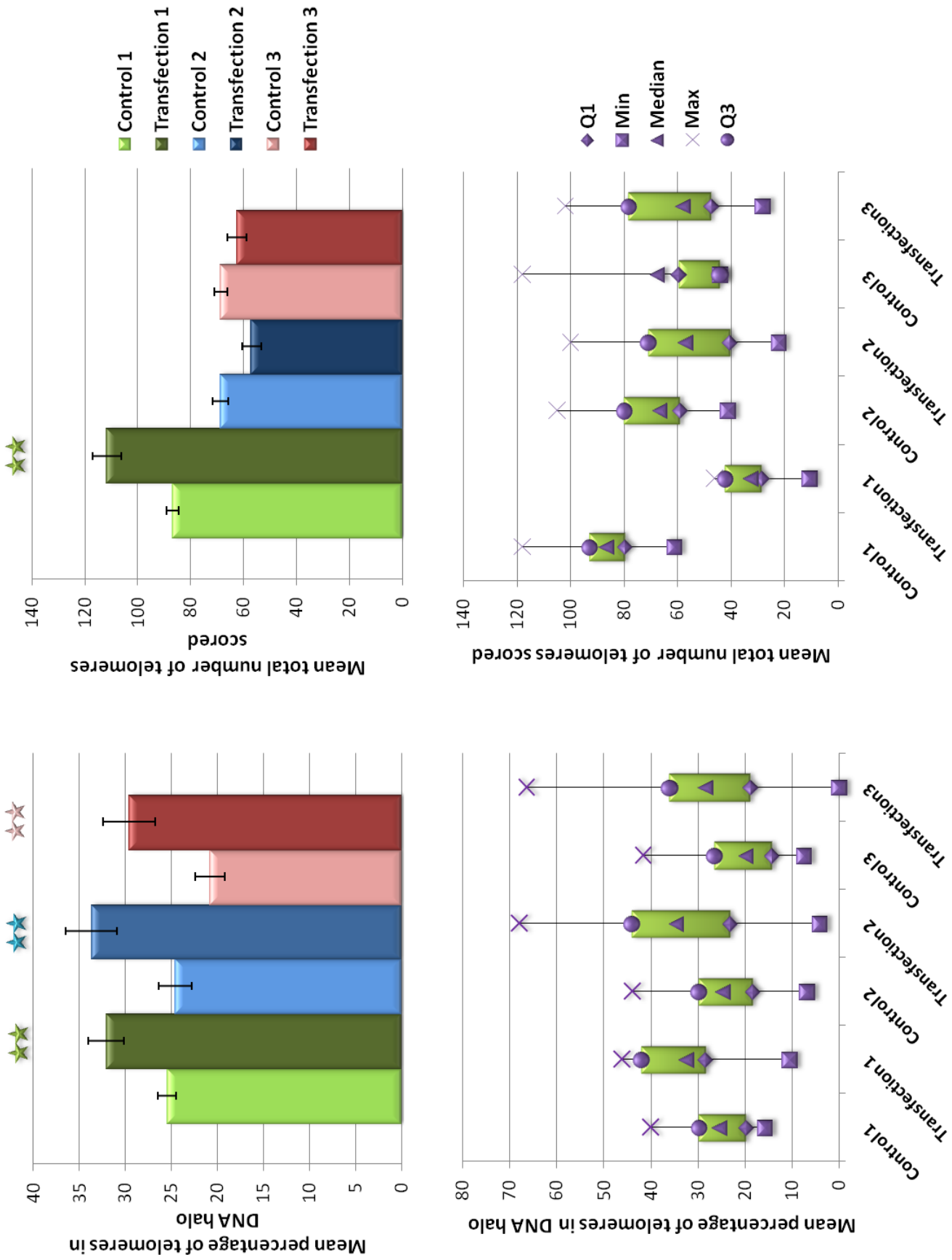

Figure 3.3.14: Attempting to rescue perturbed telomere-NM associations in X-EDMD

Figure 3.3.14: Attempting to rescue perturbed telomere-NM associations in X-EDMD
(a) Mean percentage of telomeres extracted into DNA halo and mean total number of telomeres scored; samples were random with regards to proliferation status. Statistical differences between normal and transfected X-EDMD cell lines have been determined by the Student's *t*-test and are denoted by stars (1 = $p < 0.05$; 2 = $p < 0.01$). Error bars represent ± SEM. **(b)** Modified box plots for mean percentage of telomeres extracted into DNA halo and mean total number of telomeres scored for normal and transfected X-EDMD cell lines (Q1 = lower quartile; Min = lowest value recorded; Med = median; Max = maximum value recorded; Q3 = upper quartile).

3.3.7 Examining telomere anchorage by the NM in Melanoma cells using the DNA halo assay

3.3.7.1 Telomere anchorage in tumourigenic and non-tumourigenic melanoma

To investigate whether telomere-NM associations are disrupted in cutaneous malignant melanoma, 2 cell lines were employed (figure 3.3.15). The first, UACC 903 Parental, is a highly tumourigenic human metastatic cell line. The second was a non-tumourigenic version of UACC 903 which had been rescued by the addition of chromosome 10 by microcell fusion (named UACC 903 Clone 3); both cell lines were created previously by Parris et al. (1999). These cells presented an opportunity to test firstly, whether telomere interactions with the NM are disrupted in cancer and secondly, to examine whether the tumourigenic potential of a cell line alters telomere anchorage.

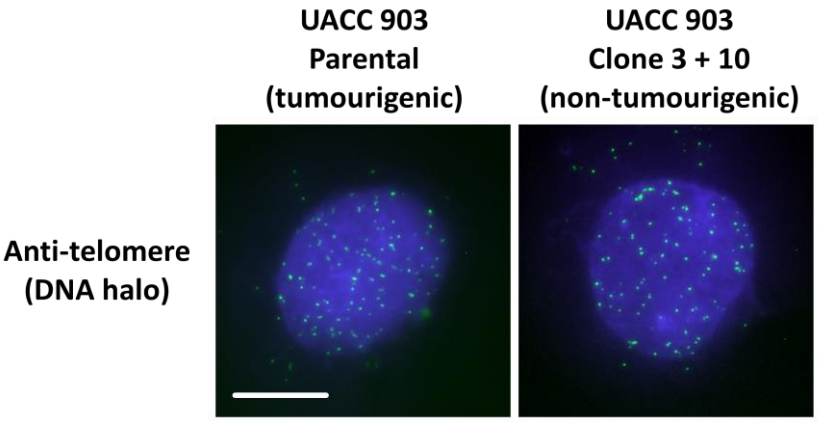

Figure 3.3.15: Telomere anchorage in tumourigenic and non-tumourigenic melanoma cell lines using the DNA halo assay.
The residual nucleus and surrounding DNA halo have been counterstained using DAPI (blue) while telomere signals can be seen in green (FITC). Magnification = x100; scale bar = 10 μm.

There was no significant difference in the mean number of telomeres attached to the residual nucleus halo when comparing the highly tumourigenic and rescued melanoma cells (figure 3.3.16a). In both cell lines, approximately 9% of telomeres were extracted into the DNA halo (figure 3.3.16b). Variance was greater in the non-tumourigenic cell line, which could suggest that the addition of the chromosome 10 had rescued telomere anchorage for some but not all cells. Since telomere anchorage in control melanocytes has not been examined in this or any other study, it was not possible to determine whether the average value of 9% was different to that of normal, un-transformed melanocytes. When comparing the telomere anchorage in these cell lines with that observed in control HDFs, the difference between the two was not as vast as that for control vs. HGPS. However, one factor which makes comparisons difficult is that both the tumourigenic and rescued melanoma cell lines were immortalised at the time of analysis. It is possible that the activation of telomerase alone influenced telomere anchorage by the NM irrespective of disease-state. Interestingly, there was a significant increase in the total number of telomeres recorded for the rescued, UACC 903 Clone 3 cell line. Since these cells contain an additional copy of chromosome 10, a slight rise (i.e. of 4) would be expected. However, the increase recorded was 34%.

Figure 3.3.16: Telomere anchorage in tumourigenic and non-tumourigenic melanoma cell lines using the DNA halo assay.

(a) Mean percentage of telomeres extracted into DNA halo and mean total number of telomeres scored for proliferating (P; pKi67+) and senescent (S; pKi67−) HGPS HDFs. Statistical differences between proliferating and senescent populations for each cell line have been determined by the Student's *t*-test and are denoted by stars (1 = $p < 0.05$; 2 = $p < 0.01$). Error bars represent ± SEM. **(b)** Modified box plots for mean percentage of telomeres extracted into DNA halo and mean total number of telomeres scored (Q1 = lower quartile; Min = lowest value recorded; Med = median; Max = maximum value recorded; Q3 = upper quartile).

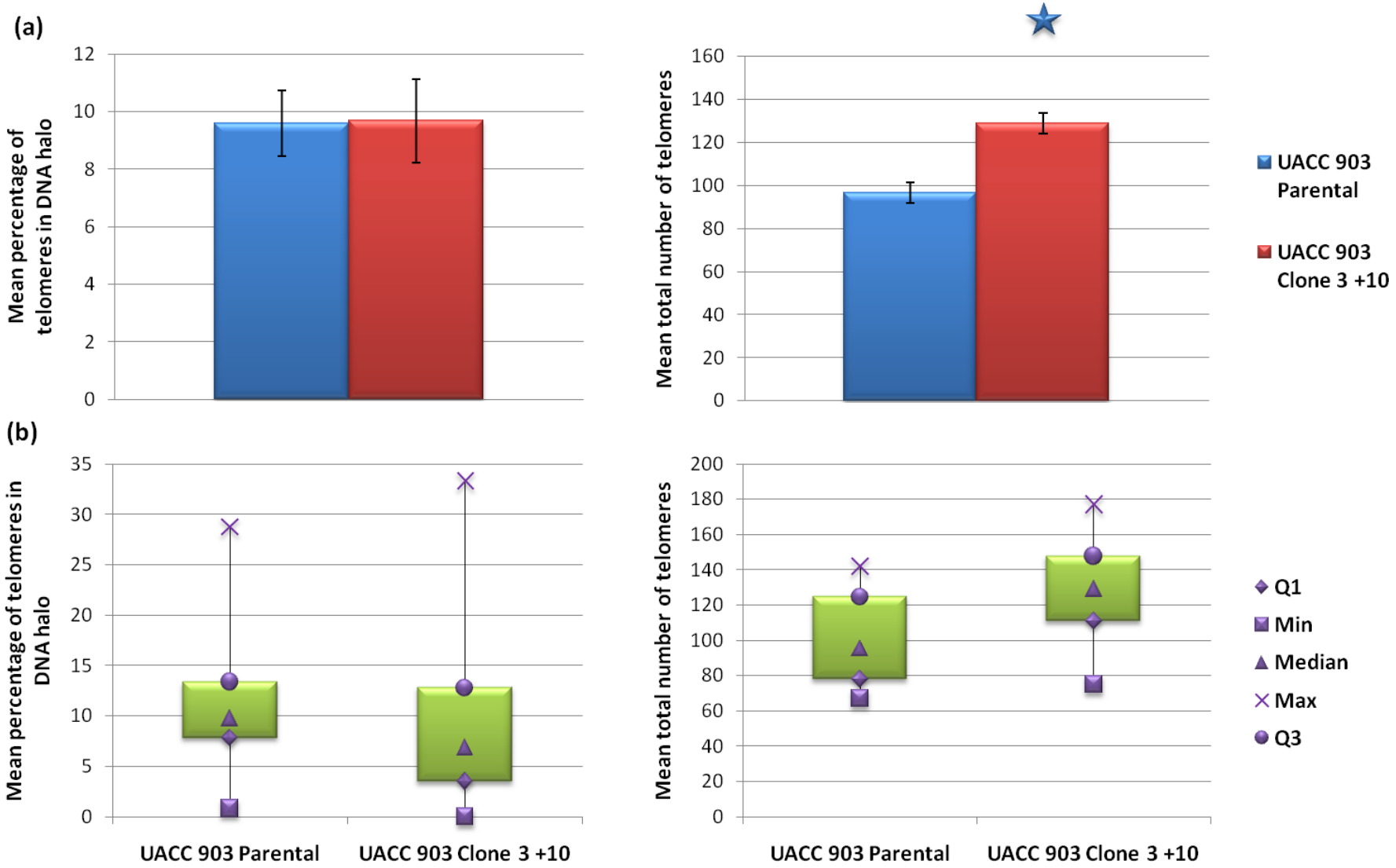

Figure 3.3.16: Telomere anchorage in tumourigenic and non-tumourigenic melanoma cell lines using the DNA halo assay

3.4 DISCUSSION

3.4.1 Chromosome anchorage in HGPS

While it is uncertain which specific NM-proteins are involved in anchoring the genome to the NM, A-type lamins are likely participants since they are shown to bind DNA (Shoeman and Traub, 1990; Taniura et al., 1995; Stierle et al., 2003). In order to investigate the effect of mutant lamin A (progerin) on such interactions, chromosome anchorage in classical HGPS fibroblasts was examined. Furthermore, to test whether perturbed NM associations are a common occurrence in HGPS, nuclei derived from an atypical HGPS patient producing normal lamin A, were also analysed.

The results demonstrate that the interaction of some chromosomes with the NM is perturbed in HGPS. Importantly, however, not all chromosome interactions were disrupted in the cell lines studied. The majority of the chromosome mass was found within the residual nucleus; this was generally true for all chromosomes studied. This indicates that despite progerin's presence in classical HGPS cells, the anchorage of whole chromosomes is still able to occur. Since the *LMNA* mutation in AG06297 is heterozygous, on one allele *LMNA* is wild-type while on the other, *LMNA* is mutated. However, due to the fact that the mutation is dominant-negative, the transcriptional processing of the normal *LMNA* is thought to be affected (De Sandre-Giovannoli et al., 2003). Thus, it could be assumed that in AG06297, the majority of protein generated by *LMNA* is aberrant. How does the presence of progerin and the lack of normal lamin A affect telomere anchorage by the NM? It is unlikely that the G608G *LMNA* mutation directly disrupts lamin A's ability to interact with DNA since the protein's DNA binding site is situated between amino acids 411–553 (Stierle et al., 2003). It is more plausible that progerin disrupts telomere anchorage due to its inability to integrate into the NM correctly. If lamin A was largely responsible for anchoring all MARs to the NM in control nuclei, it would be expected that in HGPS, the majority of chromosome mass would be extracted into the surrounding DNA halo. However, this evidently did not occur. The results from the study suggest that lamin A is involved in the anchorage of a sub-set of MARs as opposed to entire chromosomes. The observation that interactions with the NM are disrupted for specific chromosomes indicates that A-type lamins are not alone in mediating these associations; there are likely to be numerous other NM-

proteins which participate in maintaining MAR-NM complexes. Since this section of the study concentrated on global chromosome organisation, events occurring on a more local scale have not been determined. While the global anchorage of only certain chromosomes is perturbed, it is possible that the interactions of specific MARs with the NM are more significantly disrupted.

Our findings concur with previous research which indicates that chromatin organisation is disrupted in *LMNA* mutant cells (Sullivan et al., 1999; Sabatelli et al., 2001; Sewry et al., 2001; Capanni et al., 2003; Fidzianska & Hausmanowa-Petrusewicz, 2003; Goldman et al., 2004; Nikolova et al., 2004; Arimura et al., 2005; Columbaro et al., 2005; Filesiet al 2005; Scaffidi & Misteli, 2005). However, the observation that only certain chromosomes are affected agrees with earlier data produced by our laboratory (Meaburn et al., 2007). Therefore, it would be pertinent to investigate the anchorage of specific MARs in disease.

3.4.2 Telomere anchorage by the NM is disrupted in HGPS

Significantly, we have demonstrated that telomere anchorage by the NM is disrupted, to varying extents, in all three HGPS cell lines. A spectrum of severity existed; telomere anchorage was least perturbed in the atypical HGPS cell line (AG08466; whose mutation status is unknown), while the highest disruption was observed in the cell line derived from a patient exhibiting both HGPS and myopathy symptoms (G12660). In line with this trend, although AG08466 and AG06297 have similar growth potentials, the fraction of nuclei exhibiting abnormal nuclear morphology in AG06297 is considerably higher than in AG08466 (Bridger and Kill, 2004). Furthermore, the percentage of such nuclei for AG08466 is much more similar to control than to AG06297 (Bridger and Kill, 2004). Interestingly, there was no clear correlation between proliferative state and telomere anchorage in HGPS; this is a relevant observation since the radial positioning of certain chromosomes appears to change according to cellular state (Bridger et al; 2000; Meaburn et al., 2007; Mehta et al., 2010).

Combined with the mutation status of each HGPS cell line, the results indicate several interesting points. The atypical HGPS cell line (AG08466), which harbours no mutation

in *LMNA* and hence produces functional lamin A, is least affected in terms of telomere anchorage by the NM. In contrast, telomere-NM interactions in AG06297, which produces a mutant form of lamin A (progerin), are more severely affected. Taken together, these observations suggest that the protein affected in AG08466 is not as important for maintaining correct anchorage by the NM as lamin A.

More significantly, telomere anchorage was most perturbed in cells derived from the patient exhibiting both HGPS and myopathy symptoms. G12660 harbours a missense mutation in the *LMNA* gene (c428>t, p.S143F) which is predicted to generate a dominant negative protein (Kandert et al., 2007). This specific mutation leads to the substitution of a serine residue with phenylalanine; importantly, serine 143 is highly conserved and situated within the coiled region 1B of lamin A/C's rod domain (Kirschner et al., 2005). Kandert et al. (2007) suggest that the S143F mutation would likely disrupt lamin assembly and dynamics. How could this mutation impinge on telomere-NM associations? Again, as is the case with the classical HGPS cell line, AG06297, it is likely that the mutation affects the integration of lamin A into the NM, rather than DNA binding *per se*. Furthermore, it is feasible that S143 is an important phosphorylation site which is involved in lamin assembly or is required for some unknown process. Indeed, lamin phosphorylation is reported be necessary for the breakdown of the NL during mitosis (Lee et al., 2001). The phosphorylation of lamins is performed by protein kinase C in interphase and by cyclin-dependent kinases during mitosis (CDKs; Buendia et al., 2001).

In line with our study which has demonstrated that telomere binding to the NM is reduced in HGPS, De Vos et al. (2010) reported that the absence of lamin A resulted in increased telomere and nuclear mobility. Indeed, the authors suggest that lamin A is integral for maintaining 'internal inertia' (De Vos et al., 2010). They also propose that intranuclear lamin molecules are important for correct telomere localisation within the nucleus (De Vos et al., 2010). In fact, this concurs with the observation of another recent study which demonstrated that the loss of functional lamin A is concomitant with a migration of telomeres towards the nuclear periphery (Gonzalez-Suarez et al., 2009). These results indicate that when wild-type lamin A is absent, telomeres are no

longer correctly anchored by the NM via lamin A-containing complexes and thus, telomere mobility is increased.

However, the presence of progerin in HGPS nuclei has been reported to reduce telomere mobility rather than increase it (De Vos et al., 2010). Raz et al. (2008) also demonstrate that lamin-telomere binding is augmented in lamin mutants. Significantly, treatment of HGPS cells with FTIs is able to rescue perturbed telomere motility (De Vos et al., 2010). These studies both report a stiffening of the NL in HGPS nuclei and as a result, a reduction in nuclear mobility (Raz et al., 2008; De Vos et al., 2010).

What could account for the discrepancies in findings between our study and these two studies? Firstly, in Raz et al. (2009), the *LMNA* mutations disrupted different residues (R133L and R220Q) to those used in our current study (S143F, G608G). The HGPS cell line used by De Vos and colleagues harboured a G608C mutation, which should in theory produce the same progerin molecule as G608G. We have shown in our study that different lamin mutants vary in their capacity to disrupt telomere-NM interactions. Thus it is possible that these particular mutations increase rather than reduce telomere binding. Furthermore, the use of such distinct methodologies makes it difficult to directly compare the respective results. Raz and colleagues (2008) employed chromatin immunoprecipitation (ChiP) and quantitative PCR, while De Vos et al. (2010) used transfection biology to track telomere mobility. In contrast, our investigation involved a NM extraction followed by telomere PNA FISH. The nature of the non-physiological NM extraction dictates that the results must be considered within the context of the investigation and thus do not assume to be representative of processes occurring *in vivo*. However, nonetheless, the data generated from all three studies do highlight the significance of lamin A in telomere biology.

3.4.3 The hTERT-immortalisation of HGPS cells appears to rescue disrupted NM-telomere interactions

On average, telomeres in HGPS fibroblasts are significantly shorter than those found in controls (Allsopp et al., 1992; Decker et al., 2009) and as a result, it has been suggested that lamin A has a direct influence over telomere length (Decker et al., 2009). Indeed,

telomeres in fibroblasts which express mutant lamin A or over-express the wild-type form are shown to have an accelerated rate of shortening (Huang et al., 2008). In light of this, it seemed pertinent to assess telomere-NM interactions in hTERT-immortalised HGPS cells. Indeed, telomere anchorage by the NM was significantly increased in hTERT-immortalised HGPS fibroblasts and was comparable to that found in controls. This suggests that the activation of telomerase in HGPS cells enables the restoration of correct telomere-NM associations. However, it must be noted that while the proportion of telomeres detected in the DNA halo was reduced in the hTERT-immortalised HGPS nuclei, so too was the overall number of telomeres scored per nucleus. In fact, one would expect there to be increase in the number of detectable telomeres since the telomeres were theoretically longer (and signal intensity correlates with telomere length). It is possible that telomeres cluster together in response to telomerase activation; this would account for the observed reduction in individual telomeres. However, there is no scientific basis for this hypothesis.

Nonetheless, this increase in telomere anchorage by the NM in hTERT immortalised HGPS is revealing since it implies that the interactions can be rescued in spite of progerin's presence. In fact, this chimes with the earlier demonstration that the expression of hTERT can rescue the proliferation defects associated with the expression of progerin (Kudlow et al., 2008). This poses the question: does telomerase activation ameliorate progerin-induced deficiencies via telomere elongation? Kudlow and colleagues (2008) suggest that this is not the case since in their study, improvements were observed almost immediately following hTERT expression. It is also unlikely that the increased NM-telomere interactions in hTERT-immortalised HGPS reported in this chapter are as a direct result of increased telomere length. Indeed, Luderus et al. (1996) demonstrate that the avidity of telomere binding to the NM is not correlated to telomere length. The role of telomere biology in HGPS pathology is becoming more apparent; telomeres in cells over-expressing wild-type lamin A enter senescence at a similar length to controls, while those in cells expressing mutant lamin A senesce at lengths much shorter (Huang et al., 2008). As a result, Huang and colleagues (2008) suggest that mutant lamin may suppress signals from shortened telomeres, thus allowing telomeres to continue to shorten in these diseased cells.

The telomere repeat binding factor 1 (TRF1) is demonstrated to bind to telomeric repeats (Chong et al., 1995). Importantly, the availability of TRF1 is critical for *de novo* telomere formation; it is thus suggested that TRF1 availability as well as the status of telomerase activation, are together determinants of proliferative capacity in HDFs (Okabe et al., 2000; 2004). Indeed, TRF1 is upregulated in immortalised human fibroblasts and the amount of TRF1 correlates with proliferative lifespan (Okabe et al., 2000, 2004). Significantly, TRF1 is found to tether telomeres to the NM (Luderus et al., 1996). In line with this, far higher numbers of TRF1-NM complexes are observed in immortalised cells than in mortal cells (Okabe et al., 2004). This concurs with the increase in NM-telomere associations observed in our immortalised HGPS nuclei. It is logical to hypothesize that TRF1's function is perturbed in mortal HGPS cells in some way by the presence of progerin. When these cells are immortalised and TRF1 is upregulated, it is possible that this restores some aspects of previously disrupted telomere biology.

Interestingly, the proliferative capacity of normal HDFs can be extended and thus, cellular senescence delayed, by expressing exogenous TRF1. However, TRF1's influence over proliferative lifespan is limited; it is not able to support prolonged proliferation or *de novo* telomere formation (Okabe et al., 2004). Okabe and colleagues (2004) also discovered that TRF1 in immortal cells forms greater associations with the NM than the protein present in mortal cells. This indicates that mortal cells may lack the specific factors required for such NM-TRF1 binding and thus, may limit the ability of exogenous TRF1 to participate correctly in telomere dynamics (Okabe et al., 2004). If TRF1 is restricted from interacting with the NM in mortal HGPS, telomere maintenance could also be affected.

3.4.4 The effect of mutations in *EMD* on telomere anchorage by the NM

Several studies demonstrate that emerin forms part of the high-salt resistant insoluble nuclear fraction, otherwise referred to as the NM (Squarzoni et al., 1998; Ellis et al., 1998; Takata et al., 2008). Furthermore, the protein has been observed at intranuclear sites in complexes with A- and B-type lamins (Manilal et al., 1998). The fact that emerin has a hydrophobic C-terminus which anchors it to the inner nuclear membrane

(Manilal et al., 1996) poses certain questions: would emerin be able to anchor telomeres in the internal NM or does another isoform of the protein exist? While emerin interacts with the chromatin factor, BAF (Lin et al., 2000; Lee et al., 2001; Segura-Totten and Wilson, 2004), there is also no evidence that the protein binds telomeric DNA; however, we have demonstrated that telomere anchorage is perturbed in both X-EDMD patient and carrier cell lines.

With the aim of correcting the disrupted telomere anchorage demonstrated in X-EDMD, emerin-GFP was transiently transfected into X-EDMD carrier HDFs. Although this was performed on 3 separate occasions, the trend was the same each time; in transfected nuclei, there was an increase in the percentage of telomeres unattached to the NM. Although the disrupted interactions were not rescued, the results suggest that emerin does indeed contribute to telomere anchorage by the NM. Furthermore, the data suggest that the amount of emerin required for this function lies within a restricted range; too little or too much of the protein is detrimental to the cell. Thus, it is possible that a proportion of the nuclei generated emerin within this range and as a result, perturbed telomere anchorage was rescued. However, in the remaining population, nuclei were under- or over-loaded with emerin-GFP and hence, NM-telomere associations remained unchanged or were further disrupted.

Ideally, it would have been more useful to perform a stable transfection with these cells, however, in culture, the cell line tends to stop growing after approximately 11 passages. To confirm emerin's involvement in tethering telomeres to NM, the next logical step would be to knock-down emerin in normal cells using siRNA technology.
While the results presented here do suggest that emerin is important for tethering telomeres to the NM, a study by Markiewicz et al. (2002) indicates another possible explanation. The authors demonstrated that the solubility of both A and B type lamins was increased in X-EDMD cells; thus, it is possible that the perturbed telomere anchorage observed in X-EDMD is due to this increased solubility of lamins rather than the absence of emerin.

3.4.5 Telomere anchorage by the NM is unaffected in Melanoma

Since the composition of the NM is repeatedly perturbed in cancer (Lemen and Getzenberg, 2008; Lever and Sheer, 2010) and lamin organisation is disrupted in certain cancer types (Kaufmann et al., 1991; Broers et al., 1993; Moss et al., 1999; Willis et al., 2008; Sun et al., 2010), it seemed pertinent to examine telomere anchorage in cancerous cells. Indeed, certain elements of the genome are reported to be disorganised in cancer (Cremer et al., 2003; Bartova et al., 2005 and 2005; Harnicarova et al., 2006; Murata et al., 2007; Meaburn and Mistelli, 2008; Wiech et al., 2009). In this study, no significant differences were found when comparing telomere-NM interactions in highly tumourigenic and non-tumourigenic melanoma cell lines. However, the rescued (non-tumourigenic) cell line retained its immortality. As previously discussed, the activation of telomerase in cells appears to influence telomere anchorage by the NM.

Interestingly, although telomere anchorage by the NM was very high (>90%) in the two melanoma cell lines, the amount of DNA extracted into the DNA halo was also much higher than observed for any of the other cell lines studied. This could be interpreted as the existence of fewer stable MAR-NM interactions in melanoma. Furthermore, this significant increase in halo DNA could be accounted for by an increase in single-stranded DNA breaks; indeed, genomic instability is constantly reported in cancer (Negrini et al., 2010). It also indicates that any increases in telomere extraction reported do not simply correlate with the efficiency of the extraction.

3.4.6 What do these studies suggest about the involvement of the NM in disease pathology?

We have demonstrated that genome organisation is disrupted in both HGPS and X-EDMD; however, what possible implications could this have for the functioning of the disease cell? The observation that the telomere-NM interactions are perturbed by mutant lamin or absent emerin, suggests firstly, that the NM is dysfunctional. This indicates that other NM-related processes could also be disordered in these diseased cells. Indeed, the NM is involved in both transcription and DNA replication (Jackson

and Cook, 1985; Hozak et al., 1993; Cook, 1999; Djeliova et al., 2001a, 2001b; Radichev et al., 2005; Anachkova et al., 2005). The nuclear structure also provides a platform for DNA damage response pathways (Jiang et al., 2001). Furthermore, the key tumour suppressor protein, pRb, associates with the NM (Mittnacht and Weinberg, 1991; Mancini et al., 1994).

Our results infer the disorganisation of telomeres within the nuclear volume; it is possible that this disorganisation could negatively affect the maintenance and correct functioning of telomeres. In human fibroblasts, telomere shortening is demonstrated to trigger senescence through a p53 dependent pathway (Herbig et al., 2004). It has been suggested that in cells expressing mutant lamin A, this pathway is inefficient and thus, telomeres continue to shorten in such cells, creating problems for the cell (Huang et al., 2008). Taken together, our results suggest that the effect of mutant lamin A on telomere biology, within the context of NM function, is likely to be multi-faceted. The presence of mutant lamin A appears to interfere with correct telomere anchorage by the NM. However, since lamin A's interaction with DNA is mediated by residues 411–553 of the protein (Stierle et al., 2003), it is unlikely that the lamin mutations presented in this study directly disrupt the protein's ability to bind DNA. Instead, it is more probable that lamin assembly, structure and integration into the NM is disrupted when such mutations are present, thus, perturbing lamin-associated processes. Furthermore, in cells expressing mutant lamin A, the NM's involvement in DNA damage response pathways could be compromised.

It is possible that the activation of telomerase and all associated consequences, in some way compensates for the lack of functional A-type lamins. Indeed, as aforementioned A-type lamins are involved in regulating telomere structure, length and function (Gonzalez-Suarez et al., 2009). Lamin A also functions to stabilise the DNA-damage response protein, 53BP1 (Gonzalez-Suarez et al., 2009). Thus, perhaps only when telomeres are extended in a manner independent of lamin A, does the absence of functional lamin A become less of a problem for the cell. Obviously, to answer the question of how telomerase activation appears to rescue disrupted NM-telomere associations in HGPS, an investigation of a far greater scale than this current one would have to be performed.

The findings from this study also indicate that lamin A and emerin are not necessarily important for maintaining the anchorage of all MARs by the NM. This is especially evident from the observation that not all telomeres are extracted into the DNA halo in HGPS and X-EDMD nuclei. Indeed, this concurs with the aforementioned results produced by studying chromosome-NM interactions in HGPS. This, therefore, points to the involvement of other proteins, such as TRF1 (Chong et al., 1995; Luderus et al., 1996), in the maintenance of these interactions. This poses several questions: are lamin A and emerin present at all NM-MAR complexes at varying loads or are the proteins restricted to the particular regions of certain chromosomes? What factors dictate which MARs associate with which proteins? Further investigation is required to increase our comprehension of these NM-associated proteins and their role in disease pathology.

Although telomere anchorage did not appear to be perturbed in melanoma cells, even though lamin distribution was observed to be disrupted, the results concur with observations of immortalised HGPS fibroblasts. Indeed, taken together, these findings indicate that telomerase activation alone has the ability to influence telomere interactions with the NM and thus analysing disease cells which are immortalised complicates the interpretation of results.

3.4.7 Model

The studies presented here in this chapter demonstrate that correct genome organisation is disrupted in human disease. Furthermore, the capacity for the NM to mediate such organisation appears to be perturbed in cells lacking functional lamin A and emerin. Therefore, I have thus proposed a model of disease pathology in HGPS and X-EDMD. Figure 3.4.1 summarises how such interactions can be examined using the DNA halo preparation while figure 3.4.2 predicts how mutations in lamin A and emerin affect genome organisation in disease.

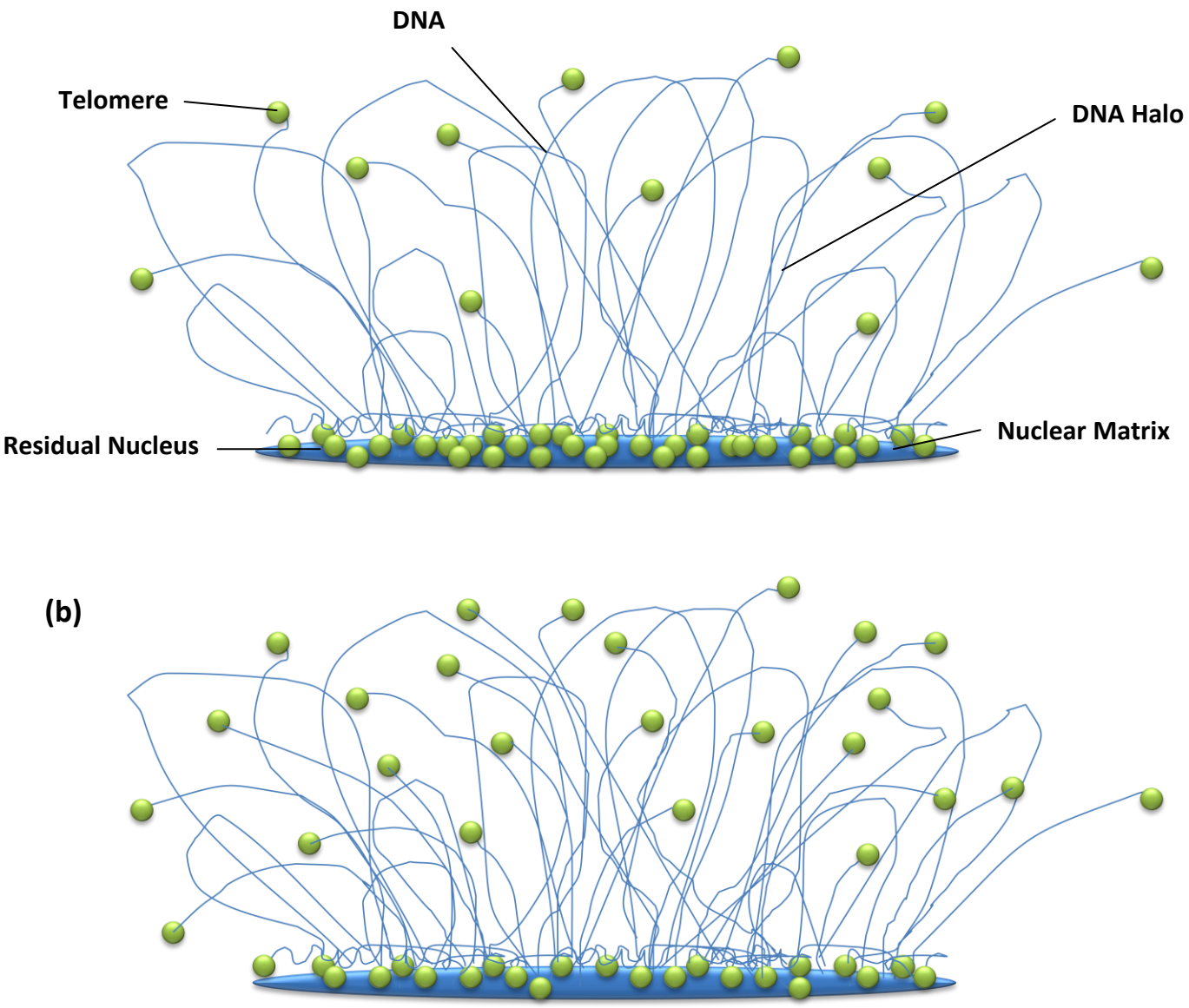

Figure 3.4.1: Telomere anchorage is perturbed in cells lacking functional lamin A and emerin

(a) Normal cells: Through their MARs, certain sequences are anchored by the NM; these would be resistant to extraction during the DNA halo preparation and thus, would be found in the residual nucleus. Those sequences less-tightly associated with the NM would be subject to extraction and as a result, become part of the surrounding DNA halo.

(b) Lamin A deficient/mutant cells: When lamin A is missing or mutated, NM-MAR associations are disrupted; consequently, regions of DNA which normally form strong interactions with the NM are released into the DNA halo.

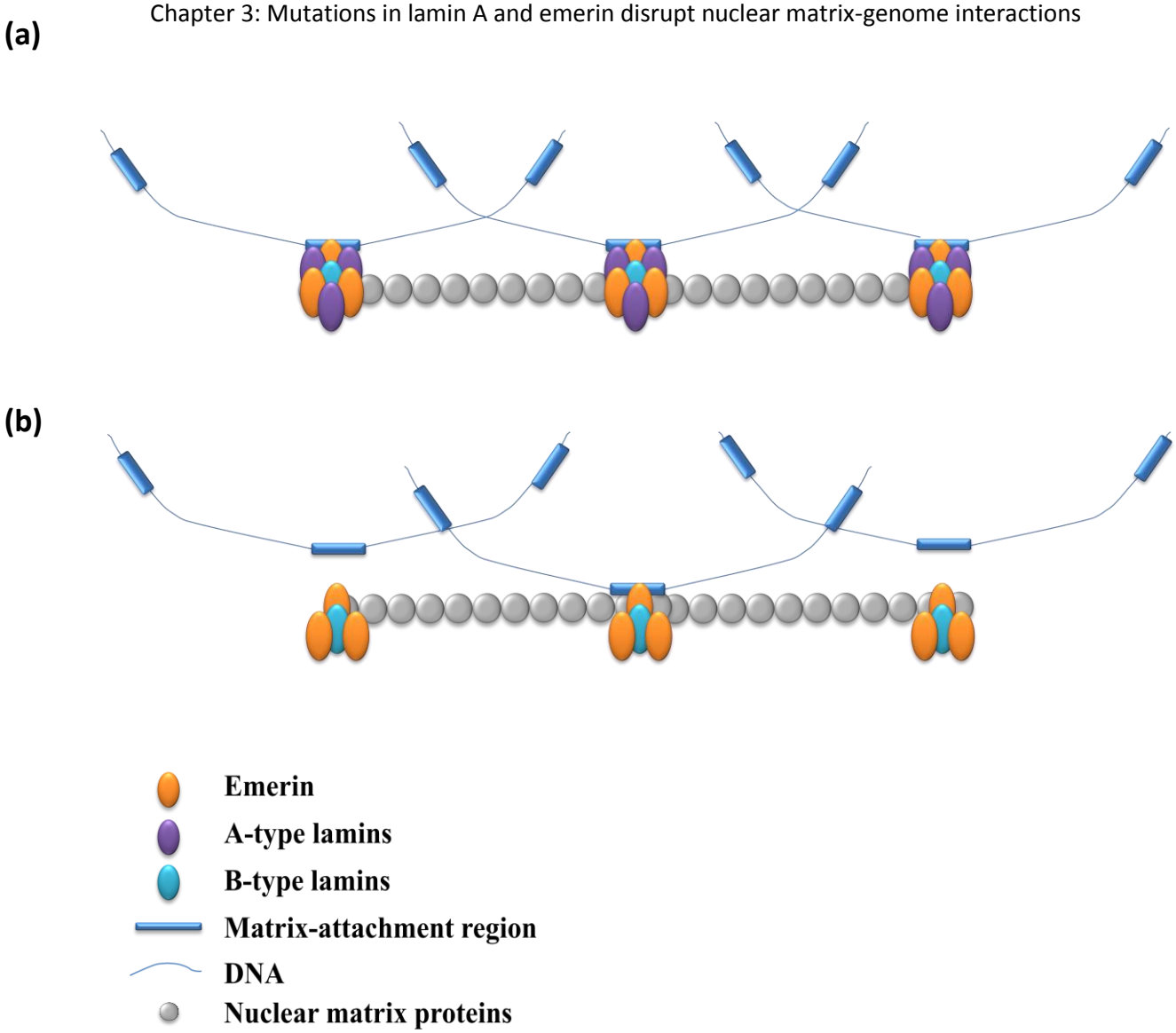

Figure 3.4.2: The role of lamin and emerin proteins in the maintenance of NM-MAR interactions

(a) Normal cells: A and B-type lamin proteins form complexes with emerin at NM filament junctions; these complexes are then involved in anchoring MARs.

(b) Lamin A deficient/mutant cells: When lamin A is mutant or missing, these MAR-NM associations are disrupted.

4. Examining interphase gene positioning and transcriptional regulation in X-EDMD fibroblasts

4.1 INTRODUCTION

4.1.1 The role of emerin in the nucleus

It is not fully understood why mutations in *EMD* specifically affect tendons, skeletal muscles and the cardiac conduction system. Originally, two main hypotheses were proposed in order to explain the tissue-type specificity observed in X-EDMD. Firstly, it was suggested that nuclei lacking functional emerin suffered from both increased fragility and impaired mechanics; thus, this could theoretically account for why mechanically strained tissues were primarily affected. In line with this hypothesis, nuclear architecture is disrupted in the myonuclei of X-EDMD patients (Fidzianska and Hausmanowa-Petrusewicz, 2003) and emerin-deficient murine fibroblasts display abnormal nuclear shape (Lammerding et al., 2005). Furthermore, emerin is found to associate with a number of important structural proteins including lamin A/C and certain nesprin isoforms (Clements et al., 2000; Lee et al., 2001; Mislow et al., 2002; Wheeler et al., 2007). It also caps the pointed ends of actin filaments (Holaska et al., 2004). However, research performed in mice indicates that it is the cell's inability to respond transcriptionally to mechanical strain rather than an abnormality in nuclear mechanics that significantly contributes to the pathogenesis of X-EDMD (Lammerding et al., 2005). In agreement, evidence is building to suggest that emerin has a role in regulating gene expression. Indeed, microarray analysis has indicated that at least 60 genes are abnormally expressed in X-EDMD fibroblasts (Tsukahara et al., 2002).

Significantly for this study, emerin is found to interact, via an APC-like domain, with β-catenin, a key mediator of the Wnt signalling pathway (Markiewicz et al., 2006). Through this association, emerin is able to regulate the flux of β-catenin into the nucleus and thus, β-catenin activity. The β-catenin/TCF-4 transcription complex results in the up-regulation of numerous down-stream target genes (van de Wetering et al., 2002). The loss of interaction between emerin and β-catenin leads to an accumulation of β-catenin within the nucleus and consequently, influences the expression of β-catenin response genes (Markiewicz et al., 2006). Indeed, in X-EDMD cells which are emerin null, β-catenin activity is significantly elevated along with the expression of the β-catenin target gene, *C-MYC* (Markiewicz et al., 2006).

4.1.2 Examining the role of emerin in gene positioning and transcriptional regulation

In light of this link between emerin and the regulation of gene expression, it seemed pertinent to investigate both the position and expression of 4 β-catenin down-stream target genes (*CCND1*, *CDH1*, *CTNNA1* and *C-MYC*; as reported by van de Wetering et al., 2002) in X-EDMD and control fibroblasts. In this way, several hypotheses could be tested. Firstly, whether the loss of an INM protein disrupts the organisation of the genome; secondly, how (and if) the absence of emerin impacts on the expression of β-catenin target genes and lastly, whether there is a relationship between gene expression and interphase nuclear positioning. Indeed, numerous studies suggest a correlation between gene positioning and transcriptional regulation (for review, see Elcock and Bridger, 2010). It also allows for a comparison of gene positioning in proliferating versus non-proliferating nuclei; relevant since some chromosomes appear to change their nuclear positions on entry into quiescence and senescence (Bridger et al., 2000; Meaburn et al., 2007; Mehta et al., 2010).

The results of this chapter reveal the selected genes are aberrantly positioned in X-EDMD; importantly, such organisation was more disrupted in senescent X-EDMD nuclei. However, these differences in gene positioning were observed as subtle rather than major shifts in location. Both *CTNNA1* and *CCND1* were located more interiorly in proliferating and senescent X-EDMD nuclei, respectively. There were also other statistically significant differences between emerin null and control cells. Interestingly, in control and X-EDMD nuclei, *CCND1* was positioned differently in proliferating and senescent nuclei; in proliferating nuclei, the alleles occupied an interior/intermediate location, while in senescent nuclei, the alleles were positioned more peripherally. With the exception of this and *C-MYC* in AP nuclei, the other genes generally occupied statistically similar locations in both proliferating and senescent nuclei within each cell line. The observation that the shift in *CCND1* position is still able to occur in X-EDMD fibroblasts suggests that gene positioning is not massively disrupted in the absence of emerin. Furthermore, using RT-PCR to examine mRNA levels of these particular genes, no changes in expression were detected. Taken together, these findings demonstrate that while gene positioning is subtlety disrupted in X-EDMD, the transcriptional

regulation of such genes in these cells is not perturbed. Furthermore, this study highlights the complexity of emerin's structural and regulatory roles in the nucleus.

4.2 MATERIALS AND METHODS

4.2.1 Cell Culture

Control (2DD) and emerin null (AP, KK and TR) primary HDFs were grown as per 2.2.1. The emerin null cells were provided by Professor Chris Hutchison.

4.2.2 2-Dimensional Fluorescence *in situ* Hybridisation (2D FISH)

4.2.2.1 Cell Fixation

Cells were harvested as per usual; the resulting cell suspension was centrifuged for 5 minutes in order to produce a pellet. To this pellet, hypotonic buffer (0.075M KCl (0.7 g in 125 ml)) was added drop-wise with agitation. This cell suspension was then left for 15 minutes at room temperature and centrifuged for 5 minutes. The buffer was discarded and the cells resuspended in a small volume of solution remaining. At this point, the fixative 3:1 (v/v) methanol:acetic acid was added drop-wise with agitation. The cells were next placed on ice for at least an hour, spun, with the fixation procedure being repeated at least 5 times more. However, the cells were only left on ice for 5–15 minutes at a time.

4.2.2.2 Slide Preparation

The cells were resuspended in fresh fixative, producing a slightly opaque solution. These cells were then dropped from a height onto SuperFrost® slides, made humid by the steam of the water bath. The density and spread of the cells were next assessed using the light microscope (20x) and if satisfactory, the slides were aged for at least two days at room temperature or by baking the slides in an oven at 70°C for one hour. The slides were then dehydrated using an ethanol row (70%, 90% and 100% ethanol; five minutes per concentration). Following this, the slides were air dried.

4.2.2.3 Probe Preparation

As per chapter section 2.2.5.

4.2.2.4 Probe and Slide Denaturation and Hybridisation

As per chapter section 2.2.6.

4.2.2.5 Washing

As per chapter section 2.2.6.

4.2.3 3-Dimensional Fluorescence *in situ* Hybridisation (3D FISH)

4.2.3.1 Cell Fixation and Preparation

Cells were seeded at 1 x 10^5 on SuperFrost slides in QuadriPERM chambers and grown for 2 days. The slides were then washed 3 times in PBS and placed in 4% paraformaldehyde (v/w; in PBS) for 10 minutes. Following this, the slides were washed with PBS three times and then placed in 0.5% Triton X-100/Saponin (v/w; in PBS) for 20 minutes. Again, the slides were washed three times using PBS; next, they were placed in 20% glycerol (v/v; in PBS) for at least 30 minutes. Slides were then dipped into liquid nitrogen and removed after several loud cracking sounds were heard. At this point, the slides were stored at -80°C until required. Once thawed, the slides were taken through 4 –7 additional freeze-thaw (liquid nitrogen-thaw-glycerol) cycles.

Following these freeze-thaw cycles, the slides were placed in PBS for 30 minutes, with 2 changes of PBS. After this, the slides were left in 0.1N HCl (v/v) for 10 minutes; they were then washed twice with 2 x SSC (v/v) for 3 minutes per wash. Slides were then left in buffer B (50% formamide, 2 x SSC (v/v) (pH 7.0)) overnight.

4.2.3.2 Probe Preparation

As per chapter section 2.2.5.

4.2.3.3 Slide Denaturation

The slides were incubated at 73°C in buffer A (70% formamide, 2 x SSC (pH 7.0) (v/v)) for 3 minutes and then buffer B (50% formamide, 2 x SSC (pH 7.0) (v/v)) for 1 minute. During the remaining minute, 12 µl of probe was pipetted onto a pre-warmed coverslip. After this minute, the slides were removed quickly from the denaturation buffer and gently placed on top of the coverslip. The slide and coverslip were sealed using rubber cement and then placed at 37°C for at least 48 hours.

4.2.3.4 Washing

As per chapter section 2.2.6.

4.2.4 Indirect Immunofluorescence

100 µl of primary anti-pKi67 antibody (1:1500) (Novocastra Laboratories Ltd) was added to a coverslip, onto which a slide was placed. The slides were then incubated at room temperature for 1 hour. After which, the slides were washed in 1 x PBS for 15 minutes, with 3 changes of buffer. 100 µl of secondary antibody (Swine anti-rabbit antibody (1:30 dilution (TRITC) or 1:50 dilution (FITC)(Dako)) was applied to each slide in a manner identical to the primary; at this point, slides were incubated for 1 hour at room temperature. All antibodies used were diluted in 1% (v/v) newborn calf serum (NCS; previously diluted in 1 x PBS). Next, they were washed in 1 x PBS for 15 minutes, again with 3 changes of buffer. Following this, the slides were mounted in DAPI.

4.2.5 Image capture and analysis

4.2.5.1 2D images

Randomly selected nuclei were visualised using an Olympus UPlanFL N 100x oil immersion lens on an Olympus BX41 fluorescence microscope. Grey-scale images of the nuclei were captured using a Model viewpoint GS digital camera (Digital Scientific); these were pseudocoloured and merged using Smart Capture V3.0 software (Digital Scientific). Images were converted into PICTs and using IP Lab Spectrum Software, the

colour balance of these PICTs were optimised. The enhanced versions of the images then underwent a simple erosion analysis, whereby the nucleus was divided into 5 shells, using a script originally written by P. Perry, as previously described (Croft et al., 1999; Bridger et al., 2000). The script determines the pixel intensity of DAPI and chromosome probe. The background was eliminated from the FISH signal by subtracting mean pixel intensity within the segment nucleus. The normalisation of probe signal distribution was achieved by dividing probe % by DAPI signal % in each shell. This was calculated for 5 shells in all 50 nuclei and from these data, a graph was plotted using Microsoft Excel software. Standard error bars were added which correspond to the ± SEM. The Student's *t* test was used to statistically compare datasets; a *p*-value of < 0.05 was considered significant.

4.2.5.2 3D image capture and analysis

3D z stacks were obtained using a Nikon Eclipse confocal microscope TE 2000 with a 100x oil immersion lens and C1 (EZ-C1) software version 3.00. An optical step size of 0.2 µm was used; the pixel dwell was 4.56 and 8 averages were taken for each image. Measurements were acquired and 3D reconstructions performed using Imaris 5.7.0 software (Bitplane). The distance from the gene signal to the nearest nuclear edge was presented as a percentage of the approximate radius (0% = nuclear periphery, 100% = nuclear interior). 40 signals were analysed per dataset and the Student's *t* test was used to compare datasets; a *p*-value of < 0.05 was considered significant. The explanation of this analysis process is expanded in section 4.3.1.3.

4.2.6 Reverse transcription-polymerase chain reaction (RT-PCR)

4.2.6.1 RNA extraction

Total RNA was extracted from cells using the GenElute^{TM} Mammalian Total RNA Miniprep Kit (Sigma-Aldrich). Before starting, 10 µl of 2-mercaptoethanol (2-ME) was mixed with 990 µl of lysis solution. The cells were then harvested as per usual to produce a pellet; to this, 250 µl of the lysis Solution/2-ME was added. This cell solution was then vortexed to remove all clumps. The lysed cells were added to a GenElute Filtration column and centrifuged at a maximum speed (13,700 g) for 2 minutes. The

Filtration column was then discarded and 250 µl of 70% ethanol was added to the lysate. This lysate/ethanol solution was placed into a GenElute Binding column and centrifuged at maximum speed for 15 seconds. The flow-through liquid was discarded. To the collection tube, 500 µl of Wash Solution 1 was added and then the tube was centrifuged at maximum speed for 15 seconds. The Binding column was next transferred into a fresh 2 ml collection tube and to this, 500 µl of Wash Solution 2 was added. Following centrifugation for 15 seconds (maximum speed), the resulting flow-through liquid was discarded and a second 500 µl of Wash Solution 2 was placed into the column. The column was centrifuged for 2 minutes, the flow-through discarded and then centrifuged for another 1 minute. The Binding column was transferred into a fresh 2 ml collection tube; 40 µl of Elution Solution then added. The RNA solution was collected following centrifugation of 1 minute at maximum speed.

4.2.6.2 DNase I treatment

The resulting RNA solution was next treated with DNase I (Amplification Grade; Sigma) in order to remove any contaminating DNA. To 40 µl of total RNA, 5 µl 10x Reaction Buffer and 5 µl of Amplification Grade DNase I (1 unit/µl) were added. This solution was then gently mixed and incubated at room temperature for 15 minutes. Following this period, 5 µl of Stop Solution was added to the RNA solution and heated at 70°C for 10 minutes. Using a Nanodrop (2000c, Thermo Scientific), the quality and concentration of the RNA samples were then tested.

4.2.6.3 Reverse transcription

Complementary DNA (cDNA) was generated from total RNA using SuperScript™ III Reverse Transcriptase (Invitrogen). 3 µg of total RNA was mixed with 100 ng of random primers and 1 µl 10 mM dNTP mix; sterile, DEPC-treated water was added to 13 µl. The solution was heated to 65°C for 5 minutes and then incubated on ice for at least 1 minute. After a brief centrifugation, 4 µl 5X First-Strand Buffer, 1 µl 0.1M DTT, 1 µl SuperScript™ III RT (200 units/ µl) and 1 µl sterile, DEPC-treated water was added to the tube. The solution was mixed gently using a pipette and then incubated at 25°C for 5 minutes. Following this period, the solution was incubated at 50°C for 30–60

minutes. To inactivate the reaction after this time, the solution was heated to 70°C for 15 minutes.

4.2.6.4 Polymerase chain reaction

Using specific primers (table 4.2.1), 5 genes were amplified using the cDNA generated by RT. In order to do this, the KAPAHiFi^{TM} kit (KAPA Biosystems) was used; the components of each reaction can be seen in table 4.2.2, while the cycling parameters are detailed in 4.2.3.

Gene	Primer Sequences	T_A (°C)	Product size (bp)
CCND1	F1: 5'-TGT TTG CAA GCA GGA CTT TG-3' R1: 5'-CCT TCC GGT GTG AAA CAT CT-3'	60	264
CDH1	F1: 5'-GGC TCA AGC TAT CCT TGC AC-3' R1: 5'-CTT GAG CCC AGG AGT TTG AG-3'	60	140
	F2: 5'-TGC CCC CAA TAC CCC AGC GT-3' R2: 5'-ACG GTG GCT GTG GAG GTG GT-3'	65	213
CTNNA1	F1: 5'-GGG ACT TGC GTA GAC AGC TC-3' R1: 5'-GCT TGC AGA CAT TCG AAC AA-3'	60	239
C-MYC	F1: 5'-TTC GGG TAG TGG AAA ACC AG-3' R1: 5'-CAG CAG CTC GAA TTT CTT CC-3'	60	203
	F2: 5'-TCC ACC TCC AGC TTG TAC CTG-3' R2: 5'-CGC CTC TTG ACA TTC TCC TCG-3'	62	557
GAPDH	F1: 5'-ACA GTC AGC CGC ATC TTC TT-3' R1: 5'-GAC AAG CTT CCC GTT CTC AG-3'	60	259

Table 4.2.1: The primer pairs employed to amplify *CCND1*, *CDH1*, *CTNNA1*, *C-MYC* and *GAPDH*.
T_A refers to the annealing temperature used.

4.2.6.5 Agarose gel electrophoresis

Amplification products from the PCR reactions were visualised using agarose gel electrophoresis. A 1% agarose gel solution containing 2% (v/v) ethidium bromide (Sigma) was poured into a sealed gel casting platform; to this, a gel comb was inserted. When the gel had set, it was placed inside a tank, which was pre-filled with 1 X Tris-Borate EDTA (TBE; 89 mM Tris, 89 mM borate, 2 mM EDTA) buffer. Following this, the PCR samples were loaded into the wells. The resultant gel was visualised using a UV-

transilluminator. Band intensities were analysed and compared using AlphaEaseFC software.

Component	Volume
PCR grade water	Up to 25.0 µl
5x KAPAHiFi Buffer	5.0 µl
dNTP mix (10 mM each dNTP; final concentration 0.3 mM)	0.75 µl
Forward primer (10 µM; final concentration 0.3 µM)	0.75 µl
Reverse primer (10 µM; final concentration 0.3 µM)	0.75 µl
Template cDNA	1.0 µl
KAPAHiFi DNA Polymerase (1 U/µl)	0.5 µl
Final Volume	25.0 µl

Table 4.2.2: The PCR reaction components employed to amplify *CCND1*, *CDH1*, *CTNNA1*, *C-MYC* and *GAPDH*. As per manufacterer's instructions (KAPA Biosystems).

Phase	Temperature	Duration	Cycles
Initial denaturation	95°C	3 m	1
Denaturation	98°C	20 s	35
Annealing	As per 4.2.1	15 s	
Extension	72°C	30 s	
Final extension	72°C	3 m	1

Table 4.2.3: The cycling parameters used to amplify *CCND1*, *CDH1*, *CTNNA1*, *C-MYC* and *GAPDH*. As per manufacterer's instructions (KAPA Biosystems). s = seconds; m = minutes.

4.3 RESULTS

4.3.1 Using 2D and 3D FISH to examine interphase gene positioning in control and emerin null nuclei

4.3.1.1 Overview

In order to determine whether interphase gene positioning is disrupted in X-EDMD, HDFs from 3 X-EDMD cell lines (AP, KK and TR) and 1 control (2DD) were prepared for 2D or 3D FISH. To verify that the X-EDMD cell lines were emerin null as predicted, anti-emerin staining was performed; indeed, control HDFs were positive for anti-emerin while such staining was absent in all 3 of the X-EDMD cell lines (figure 4.3.1). Probes specific to 4 genes (*CCND1* (cyclin D1), *CDH1* (E-cadherin), *CTNNA1* (alpha catenin) and *C-MYC* (C-MYC)) were generated and then used for 2D and 3D FISH. To differentiate between proliferating and senescent nuclei, anti-pKi67 staining was employed.

4.3.1.2 2D FISH analysis

Approximately 50 2D nuclei were captured per cell line, per gene and per proliferation status; representative images can be seen in figure 4.3.2. Subsequently, the positioning of genes within interphase 2D nuclei was assessed using erosion analysis software (Croft et al., 1999; Bridger et al., 2000; Boyle et al., 2001; Meaburn et al., 2005; Meaburn et al., 2007). This software divides the flattened DAPI-stained 2D nucleus into 5 concentric shells of equal area and individually measures the intensity of DAPI and probe signal in each shell. To normalise the data for each shell, the percentage of probe signal was divided by the percentage of DAPI signal. From this data, histograms were generated, with the mean normalised signal for each shell presented along the Y-axis while the X-axis depicts shell number; shell 1 is the most interior and shell 5 is the most peripheral. Such histograms for all 4 cell lines and genes in both proliferating (green bars) and senescent (purple bars) nuclei can be observed in figure 4.3.3. Statistical differences between datasets were determined using the Student's *t* test; a *p*-value below 0.05 was deemed significant. The outcome of statistical tests using data from 2D FISH assays is summarised in figure 4.3.4.

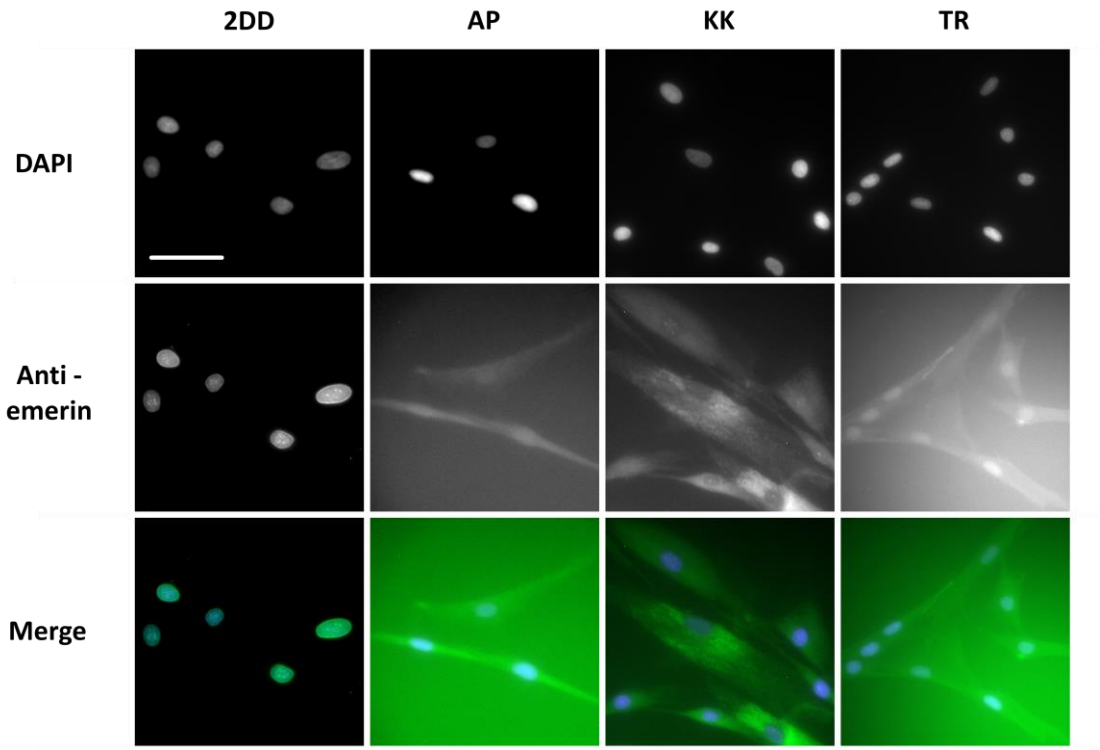

Figure 4.3.1: Anti-emerin staining in control and X-EDMD HDFs

In order to confirm that HDFs derived from X-EDMD cell lines were indeed emerin null, methanol:acetone fixed control and X-EDMD nuclei were subjected to anti-emerin staining. DAPI (blue) is used to counterstain the nucleus, while anti-emerin is pseudocoloured green (FITC). As expected, in control HDFs, anti-emerin reacted with the periphery of the nucleus and also at foci within the nucleoplasm. Conversely, in all 3 X-EDMD cell lines, no anti-emerin staining was observed. Magnification = x20; scale bar = 50 µm.

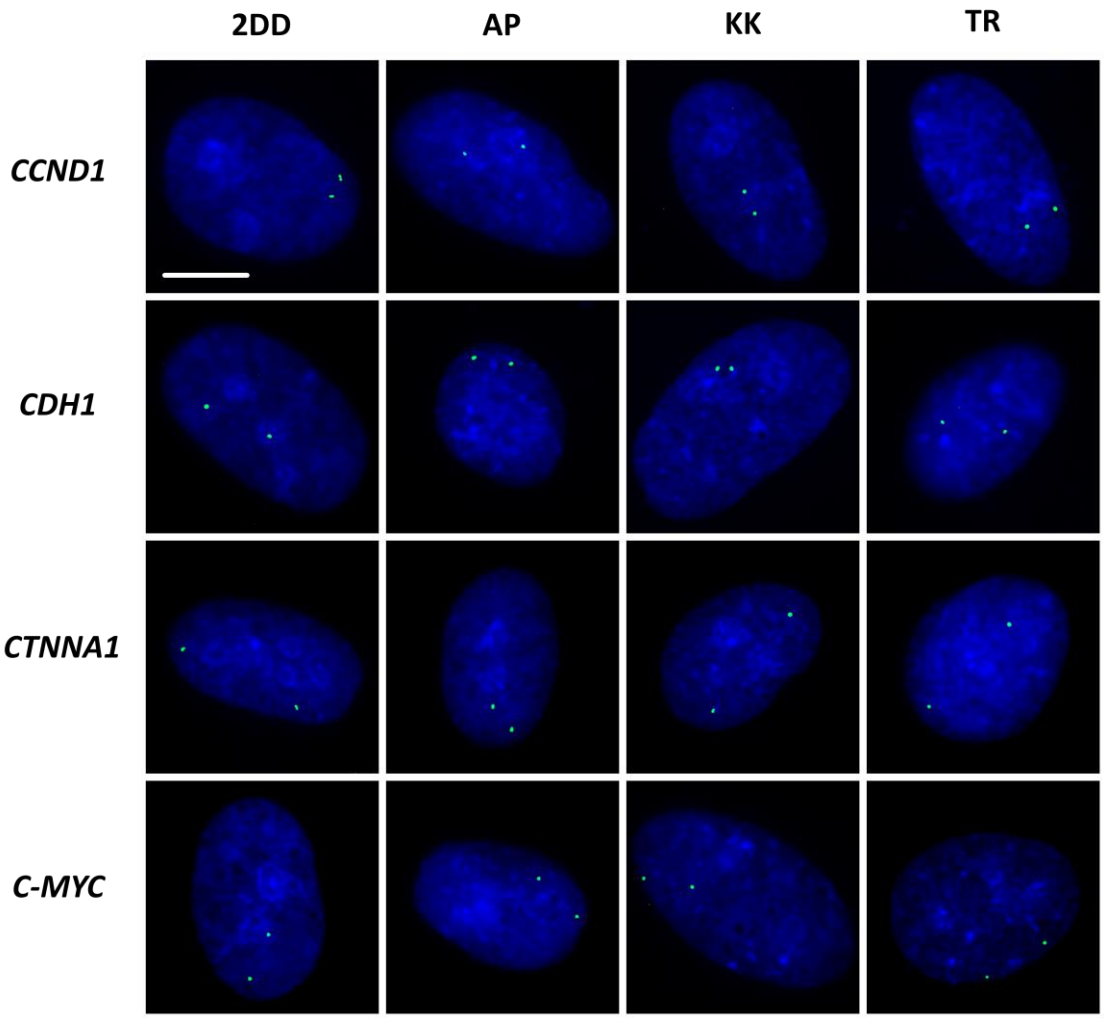

Figure 4.3.2: Using 2D-FISH to analyse the position of *CCND1*, *CHD1*, *CTNNA1* and *C-MYC* in control and X-EDMD HDFs

DNA has been counterstained using DAPI (blue), while gene signals can be seen in green (FITC). Magnification = x100; scale bar = 10 µm.

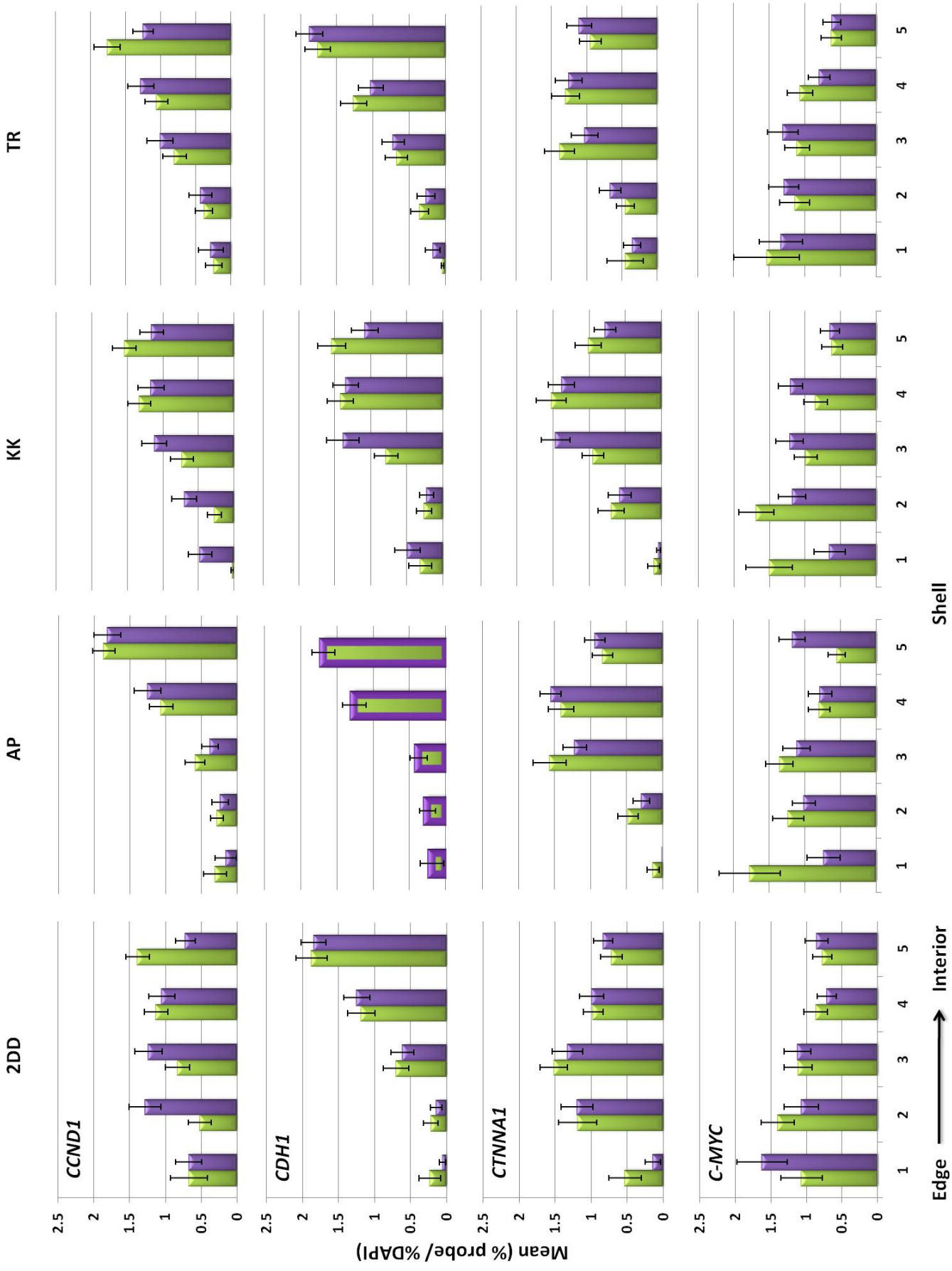

Figure 4.3.3: Gene positioning in proliferating and senescent control and X-EDMD nuclei using 2D FISH analysis

Figure 4.3.3: Gene positioning in proliferating and senescent control and X-EDMD nuclei using 2D FISH analysis

Mean proportion (%) of hybridization signals for each of the 4 genes in eroded shells of control and X-EDMD nuclei. Using an erosion script, nuclei were divided into five concentric shells of equal area; shell 1 being nearest to the nuclear periphery while shell 5 was the most interior (Croft et al., 1999; Bridger et al., 2000; Boyle et al., 2001; Meaburn et al., 2007). The % of signal in each shell was divided by the corresponding % of DAPI signal; the graphs represent the normalised signals. Green bars refer to proliferating (pKi67+) data, while purple bars denote signal distribution in senescent (pKi67−) nuclei. 50 nuclei were analysed per dataset with 3 exceptions (2DD *CTNNA1* (47); KK *CTNNA1* (48); AP *C-MYC* (49)); error bars are representative of SEM. For AP *CDH1*, the graph presents data from a pKi67 random population.

4.3.1.3 3D FISH analysis

In order to verify the accuracy of the data produced by the 2D FISH assay, the position of these genes were analysed using 3D FISH. Since a consistent difference in *CCND1* location was observed between pKi67+ and pKi67− populations in control and X-EDMD HDFs using the 2D FISH assay, this gene was examined in all cell lines. For the other 3 genes, only control and 1 X-EDMD (AP) cell line was examined with 3D FISH. 20 nuclei were captured per population and the gene position assessed manually using Imaris: an example of a reconstructed 3D nucleus can be seen in 4.3.5. The distance from each gene signal to the nearest nuclear periphery (X-, Y- or Z-axis) was measured and then normalised by dividing this distance by the radius of the nucleus. The radius was calculated by dividing the width (rather than the length) of the nucleus by 2. As a result, the normalised gene distance from the nuclear periphery is presented as a percentage of the nuclear radius in frequency distribution line charts.

For each nucleus, the distance of the gene signals from the nearest nuclear edge has been analysed either as individual alleles or as an average of the two; the mean distance for each allele or the average can be seen in 4.3.6a and b, respectively. The allele closest to the nuclear periphery was categorised as allele 1, while the remaining allele was classified as allele 2. Statistical differences between datasets were calculated as per the 2D analysis; see figure 4.3.7 for an overview.

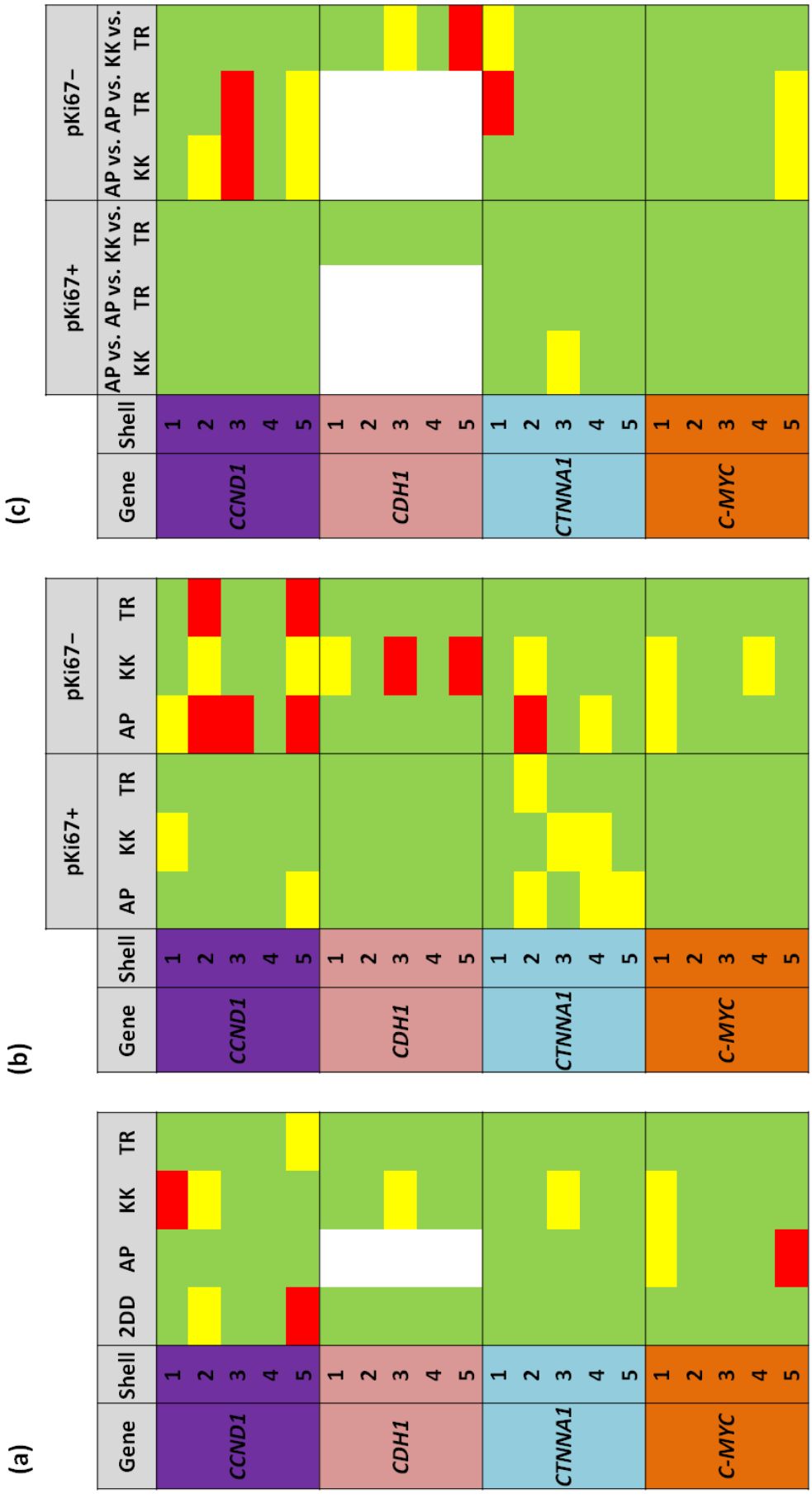

Figure 4.3.4: Statistical tests for 2D analysis positioning data

Figure 4.3.4: Statistical tests for 2D analysis positioning data
The tables contain the results of statistical tests (Student's *t*-test; unpaired; two-tailed distribution) comparing interphase gene positioning in control and X-EDMD nuclei using the 2D FISH analysis. The results have been colour-coded; green represents no statistical difference (ND; $p > 0.05$); yellow denotes a statistical difference (*; $p < 0.05$, > 0.01); red represents a statistical difference of higher significance (**; $p < 0.01$). **(a)** Proliferating (pKi67+) versus senescent nuclei, **(b)** Control versus emerin null nuclei, **(c)** Emerin null versus emerin null nuclei.

4.3.1.4 *CCND1*

Using the 2D FISH assay, the nuclear position occupied by *CCND1* in proliferating nuclei (pKi67+) was similar in all 4 cell lines (3 emerin null plus 1 control). *CCND1* was positioned towards the interior in proliferating control and X-EDMD nuclei (figure 4.3.3). While the mean location of *CCND1* in TR pKi67+ nuclei did not differ significantly from the control, the gene alleles were statistically more interior (than the control) in AP (shell 5; $p < 0.05$) and KK (shell 1; $p < 0.05$) pKi67+ populations (figure 4.3.4b). 3D positioning confirmed that in AP proliferating nuclei, *CCND1* alleles were located more interiorly than in control. In contrast, *CCND1* in TR pKi67+ nuclei was reported to be positioned more interiorly than in control 3D preserved nuclei; this was not detected in 2D nuclei. While no statistical differences were observed when comparing this gene's position within X-EDMD cell lines (pKI67+) using the 2D FISH assay, disparities were observed in 3D (figures 4.3.6 and 4.3.7c).

When comparing the datasets for senescent (pKi67−) populations, many more differences were observed. 2D analysis data demonstrated that in all 3 X-EDMD cell lines (pKi67−), *CCND1* occupied a different location to control (figure 4.3.4b). *CCND1* occupied an intermediate position in control 2D nuclei, while in AP, KK and TR, the alleles were generally found in interior locations (figure 4.3.3). However, there were disparities within X-EDMD; *CCND1* was positioned more interiorly in AP than KK or TR (figures 4.3.3) and indeed, this was demonstrated statistically (figure 4.3.4c). In 3D, *CCND1* alleles were located more peripherally than control in KK, while in AP and TR, the gene alleles were positioned no differently to controls (figure 4.3.7b). As a result, the 3D location of *CCND1* in KK is significantly different to the other 2 X-EDMD cell lines (figure 4.3.7c).

For control, KK and TR, *CCND1* shifted from an interior position in proliferating nuclei to an intermediate location in senescent nuclei, using the 2D FISH assay (figures 4.3.3 and 4.3.4a). This was confirmed using 3D positioning (figure 4.3.7a). The 2D analysis demonstrated no significant statistical difference between the position of these alleles in pKi67+ and pKi67− AP nuclei; *CCND1* remained interior in pKi67− nuclei (figure 4.3.4a). However, 3D positioning detected a change in position in AP senescent nuclei which was not evident using 2D FISH (figures 4.3.6 and 4.3.7a).

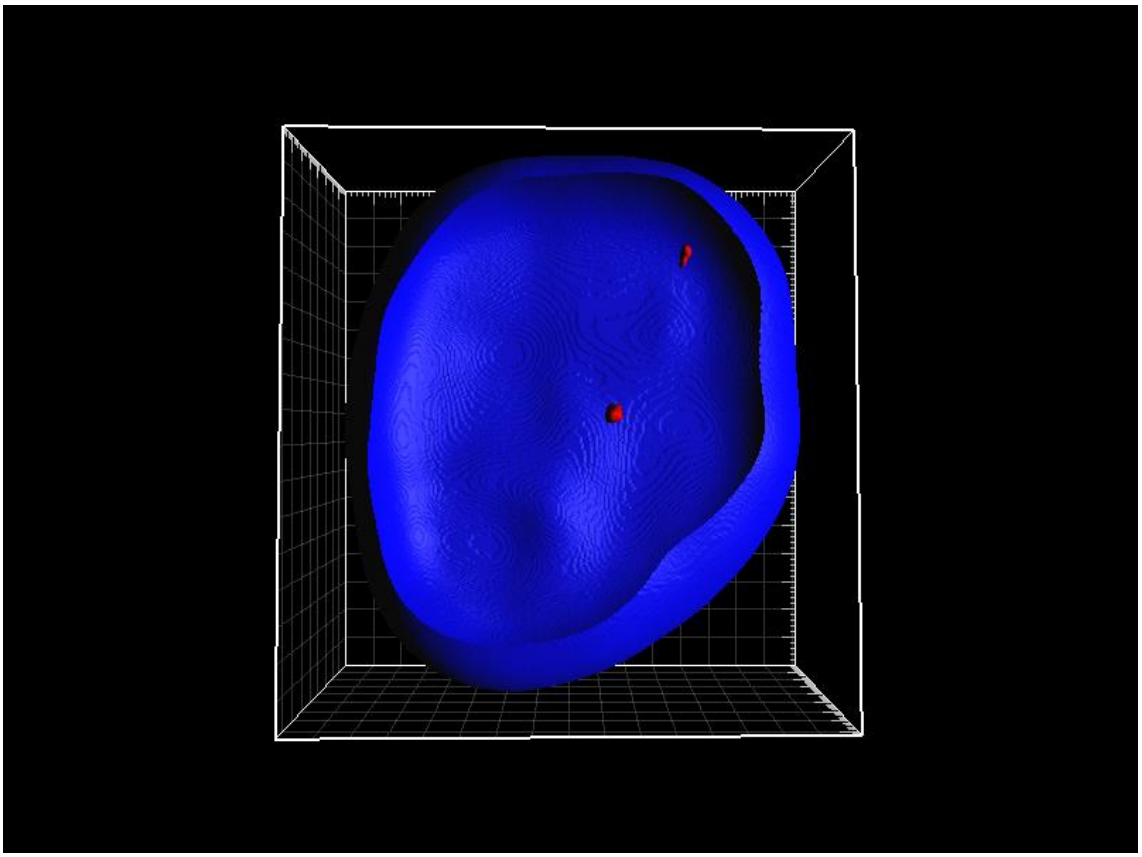

Figure 4.3.5: An example of a reconstructed 3D nucleus.
Control and X-EDMD HDFs were subjected to 3D FISH. This is an example of a control 3D reconstructed nucleus; the DNA is counterstained using DAPI (blue), while *CTNNA1* gene signals can be seen in red (Cy3).

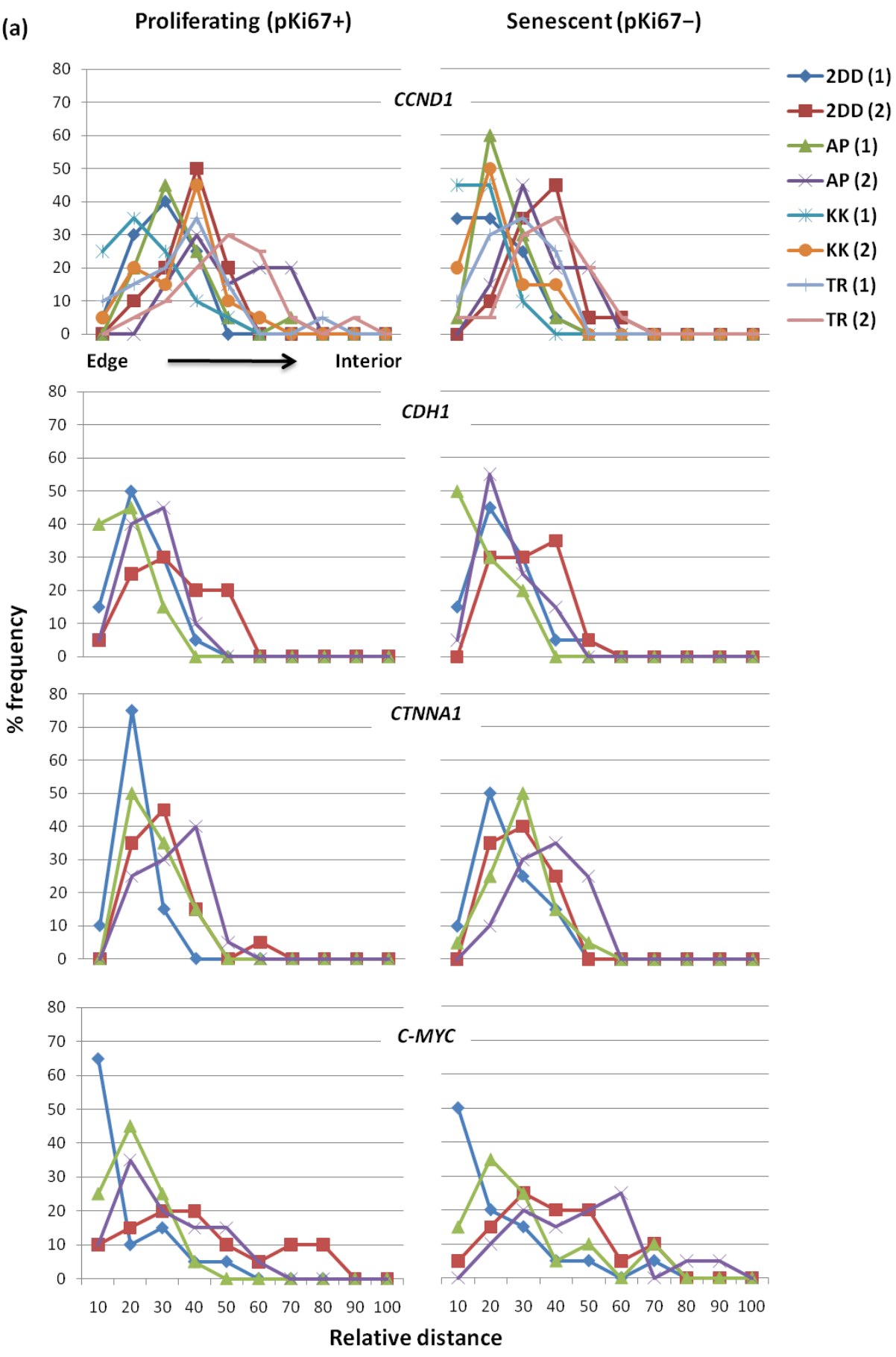

Figure 4.3.6a: Gene positioning in 3D-preserved nuclei (individual alleles)

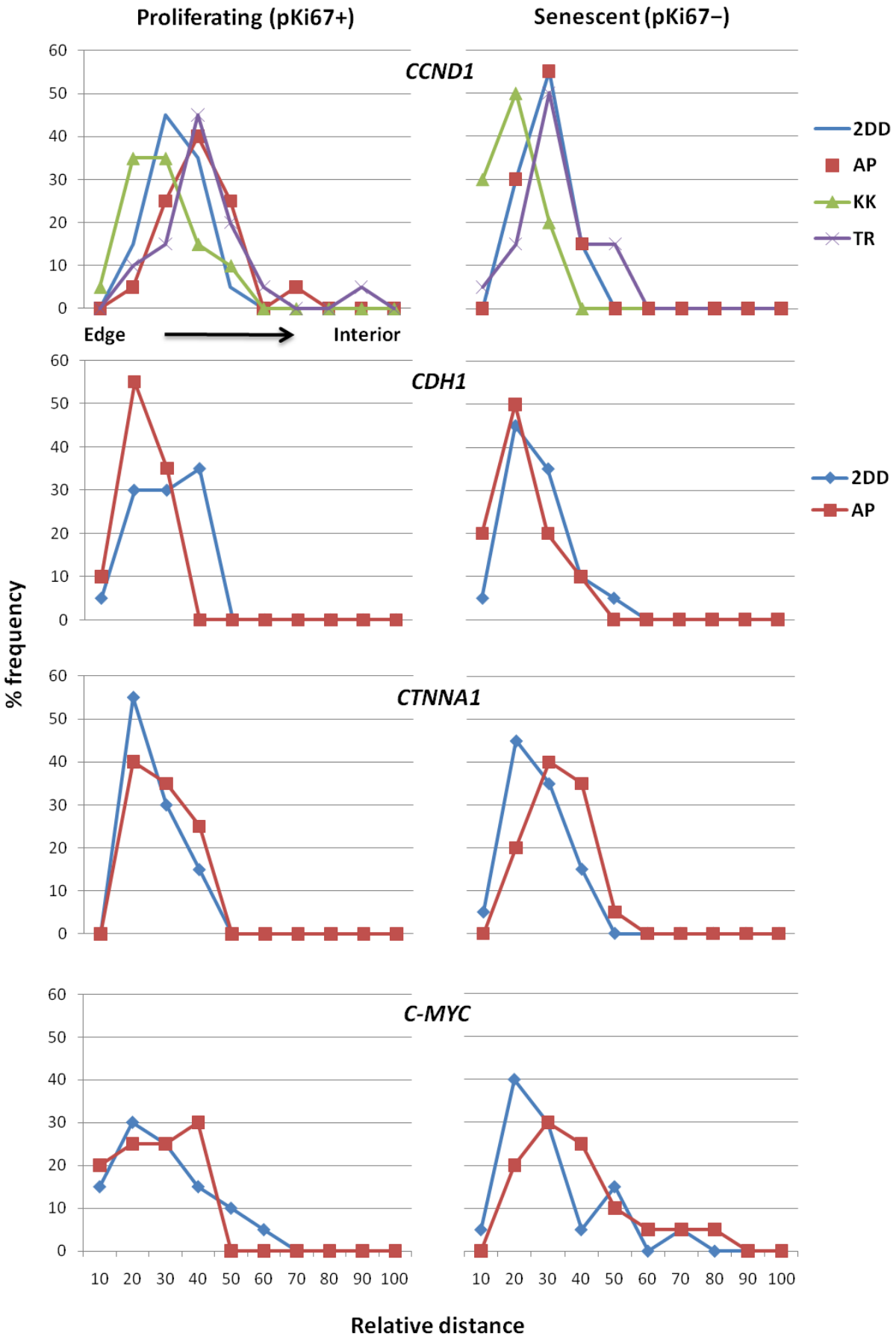

Figure 4.3.6b: Gene positioning in 3D-preserved nuclei (average)

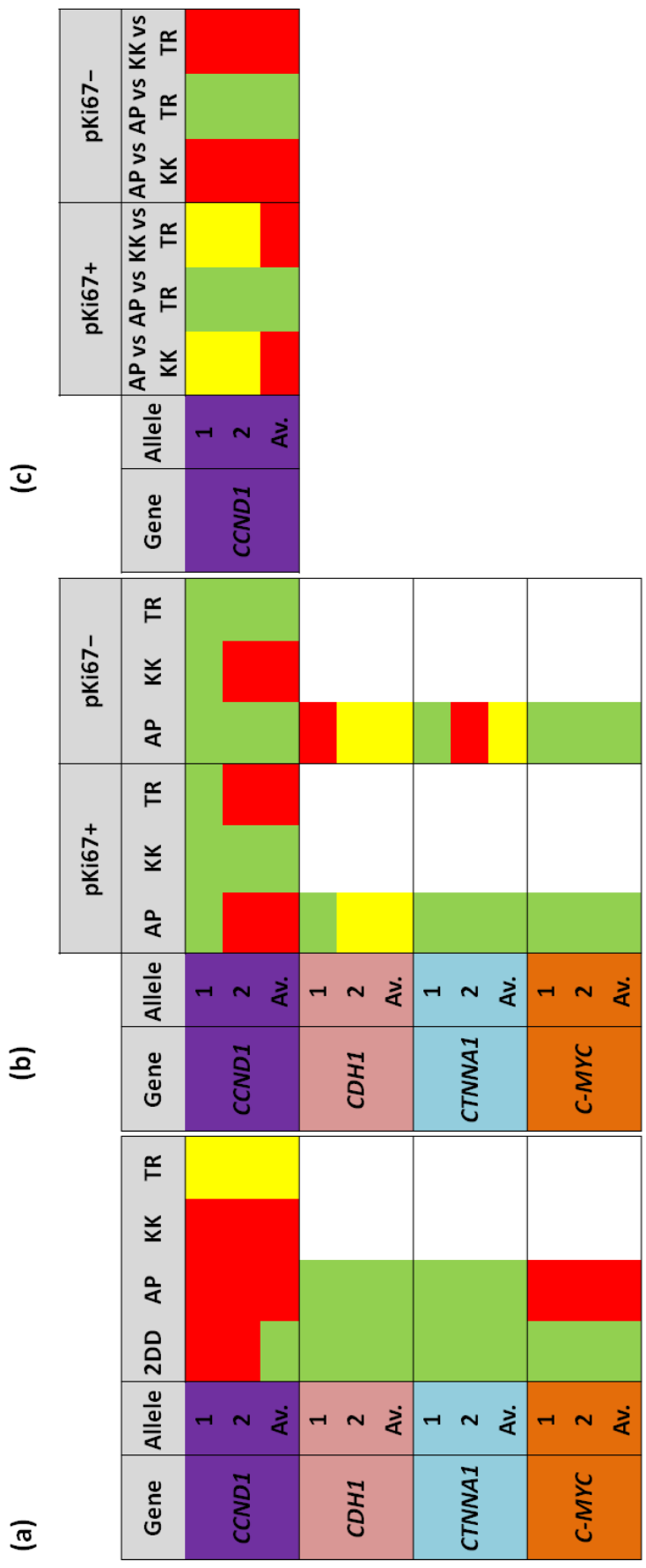

Figure 4.3.7: Statistical tests for 3D positioning data

Figure 4.3.6: Gene positioning in 3D-preserved nuclei
Frequency distribution plots of the position of 4 genes within proliferating (pKi67+) and senescent (pKi67−) control and X-EDMD nuclei. Measurement data have been normalised by dividing the distance from the nuclear edge by the approximate radius and are reported as percentages; 0% represents the nuclear edge while 100% denotes the nuclear interior. Results are presented for **(a)** individual alleles or **(b)** as an average of the two alleles. For **(a)** allele 1 refers to the allele closest to the nuclear periphery.

Figure 4.3.7: Statistical tests for 3D positioning data
The tables contain the results of statistical tests (Student's *t*-test; unpaired; two-tailed distribution) comparing gene positioning in 3D-preserved control and X-EDMD nuclei. The results have been colour-coded; green represents no statistical difference (ND; $p > 0.05$); yellow denotes a statistical difference (*; $p < 0.05$, > 0.01); red represents a statistical difference (**; $p < 0.01$). **(a)** Proliferating (pKi67+) versus senescent (pKi67−) nuclei, **(b)** Control versus emerin null nuclei, **(c)** Emerin null versus emerin null.

4.3.1.5 *CDH1*

When comparing the position of *CDH1* in control and emerin null proliferating nuclei using the 2D FISH assay, there were no significant differences (figure 4.3.4b). In all cell lines (pKi67+), the gene alleles occupied an interior position (figure 4.3.3). In senescent nuclei, *CDH1* occupied a similar interior location in control and TR nuclei, while in KK the gene alleles were statistically positioned more intermediately (figures 4.3.3 and 4.3.4b). 3D FISH demonstrated that *CDH1* was significantly closer to the nuclear edge in AP nuclei (proliferating and senescent) than in the control (figures 4.3.6 and 4.3.7); a difference which was not detected by the 2D analysis (figure 4.3.4b).

CDH1 occupied statistically similar positions in pKi67+ and pKi67− control and TR 2D nuclei (figures 4.3.3 and 4.3.4a). For KK, there was one significant difference (shell 3; $p < 0.05$) when comparing pKi67+ and pKi67− nuclei. A comparison between *CDH1* positioning in pKi67 + and pKi67− AP 2D nuclei could not be performed since anti-pKi67 staining was unsuccessful; however, in a proliferation-random population, *CDH1* was interior (figure 4.3.3). In contrast, *CDH1* was positioned towards the periphery in AP pKi67+ and pKi67− 3D nuclei (figure 4.3.6); a location which was significantly different to control (figure 4.3.b).

4.3.1.6 *CTNNA1*

2D analysis revealed that there were statistically significant differences when comparing the position of *CTNNA1* in proliferating control and X-EDMD HDFs (figure 4.3.4b). *CTNNA1* occupied an intermediate location in control nuclei while in emerin null nuclei, the gene alleles were intermediate and interior (figure 4.3.3). Within the proliferating X-EDMD cell lines, there was one significant difference for AP vs. KK (shell 3; $p < 0$ .05, figure 4.3.4c).

The nuclear positions of *CTNNA1* in senescent nuclei were similar in control, KK and TR cell lines (figure 4.3.3); when comparing these 3 cell lines, only one difference was detected (KK vs. TR; shell 1; $p < 0.05$, figure 4.3.4). The location of the gene in pKi67− AP nuclei was different to that found in control (shells 2 ($p < 0.01$) and 4 ($p < 0.05$)) and TR (shell 1; $p < 0.01$) nuclei. 3D analysis demonstrated that *CTNNA1* occupied a similar position in proliferating control and AP nuclei, however, the gene alleles were more interiorly positioned in senescent AP nuclei (figures 4.3.6 and 4.3.7b). Apart from shell 3 (*) in KK, no significant differences were detected for *CTNNA1* when comparing pKi67+ and pKi67− populations by 2D analysis (figure 4.3.4a); this concurred with the data produced for control and AP HDFs by 3D FISH (figure 4.3.7).

4.3.1.7 *C-MYC*

No statistical differences were observed when comparing the position of *C-MYC* in the proliferating nuclei of control and emerin null nuclei using the 2D FISH assay (figure 4.3.4b); in all cell lines, *C-MYC* occupied a peripheral position (figure 4.3.3). In control and TR pKi67− nuclei, the gene alleles were peripheral, while for AP and KK, *C-MYC* had bimodal and intermediate distributions, respectively (figure 4.3.3). Indeed, the locations of *C-MYC* alleles in AP and KK pKi67− were statistically different to those found in control pKi67− nuclei (2DD vs. AP, shell 1, $p < 0.05$; 2DD vs. KK, shells 1 and 4, $p < 0.05$; figure 4.3.4b).

For both control and TR populations, no statistically significant differences were found between proliferating and senescent populations (figure 4.3.4a), which is in agreement

with control 3D data (figures 4.3.6 and 4.3.7). However, there were changes in the signal intensity in shell 1 ($p < 0.05$) for KK and AP and in shell 5 ($p < 0.01$) for AP, when comparing pKi67+ and pKi67− 2D nuclei (figure 4.3.4a). This concurs with 3D data for AP nuclei, which demonstrated that *C-MYC* alleles were located more interiorly in senescent nuclei (figure 4.3.7a).

4.3.1.8 Overview of positioning results

4.3.1.8.1 Control vs. X-EDMD

The 2D analysis results demonstrate that the interphase positioning of selected genes are perturbed in X-EDMD. Interestingly, the organisation of such genes was most affected in senescent X-EDMD nuclei. Significantly, *CCND1* was located more interiorly in senescent X-EDMD than in control HDFs. *CDH1* was positioned similarly to controls in all X-EDMD populations (pKi67+ and pKi67−) apart from senescent KK nuclei. Furthermore, *CTNNA1* location was disrupted in the majority of proliferating and senescent X-EDMD datasets. Significantly, in two-thirds of the X-EDMD cell lines, *C-MYC* was positioned incorrectly in senescent nuclei.

4.3.1.8.2 Proliferating vs. senescent

By combining the findings from both 2D and 3D FISH assays, it is evident that the position of *CCND1* shifts from an interior position in proliferating (pKi67+) nuclei to a more intermediate location in senescent (pKi67−) nuclei. In the control cell line, none of the other genes demonstrated a change in location according to proliferative state; however, this was not true for the X-EDMD cell lines. A shift in the position of *CDH1* and *CTNNA1* was observed in senescent KK nuclei. Furthermore, C-*MYC* appeared to move away from the periphery in senescent AP and KK nuclei; for AP this was shown using both 2D and 3D analysis. An overview of these findings can be observed in table 4.3.1.

4.3.1.8.3 2D vs. 3D analysis

In general, 3D analysis detected similar shifts in gene positioning between proliferating and senescent nuclei as the 2D FISH assay. However, the differences observed when comparing control and X-EDMD populations were not so similar when using 2D and 3D analysis. Furthermore, 3D positioning demonstrated that genes were far closer to the nuclear periphery than the 2D assay suggested. This was particularly true of *CDH1*; while 2D analysis revealed that the gene alleles were interior in both proliferating and senescent populations, the 3D assay showed that the genes were significantly more peripheral. Interestingly, in the 3D analysis, all gene alleles (regardless of proliferation status) were observed to be in the bottom half of the nucleus; this suggests that genes are not only radially organised but also exhibit polarity within the nucleus.

	CCND1		***CDH1***		***CTNNA1***		***C-MYC***	
	P	**S**	**P**	**S**	**P**	**S**	**P**	**S**
2DD (control)	I	IM**	I	I	IM	IM	P	P
AP	I	I	I		IM	IM	P	B**
KK	I	I**	I	I*	IM	IM*	P	IM*
TR	I	I*	I	I	IM	I	P	P

Table 4.3.1: Interphase gene positioning in control and X-EDMD HDFs using the 2D FISH assay

I = interior, IM = intermediate, P = peripheral, B = bimodal. Significant differences between proliferating (P) and senescent (S) nuclei are denoted by stars (*, $p < 0.05$; **, $p < 0.01$).

4.3.2 Using RT-PCR to examine gene expression

The expression levels of the 4 genes (*CCND1*, *CDH1*, *CTNNA1* and *C-MYC*) were investigated using RT-PCR; *GAPDH* was used as an internal control. Total RNA was extracted from control and 3 X-EDMD cell lines; this RNA was then used to produce cDNA, which was consequently employed for PCR (figure 4.3.8). To determine whether the proliferative state of the culture influenced expression, RNA was extracted from the control cell line at 2 different passages (Ki67+: P10 = 71.1%; P19 = 56.5%). The percentage of pKi67 positive cells within the emerin null cell lines varied at the time of extraction; 77.9% (TR), 62.6% (AP) 52.1% (KK) cells (figure 4.3.9). The primer pairs

employed can be seen in section 4.2. In order to verify *C-MYC*'s expression level, 2 primer sets were employed; the first were designed independently while the second pair was employed as per Markiewicz et al. (2006). Difficulty was experienced with *CDH1* since many unrelated PCR products were amplified along with the gene's cDNA; thus, in order to verify expression levels, two different primer pairs were used (figure 4.3.8). *C-MYC* expression levels were lowest in TR; this was shown using both sets of primers (figure 4.3.9). Since the *GAPDH* band intensity for this cell line was very similar to the other cell lines, it is likely that the reduced *C-MYC* levels are correctly reflective of expression in TR. Apart from *C-MYC*, no obvious differences were detected when comparing the band intensities (using AlphaEaseFC software) of the other 4 genes in the 5 cell lines (figure 4.3.9).

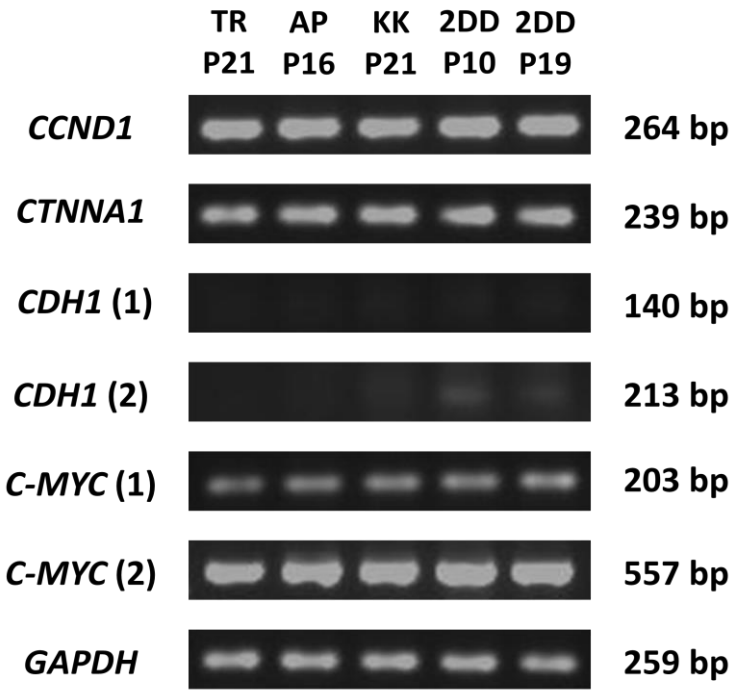

Figure 4.3.8: Analysing the expression of *CCND1*, *CDH1*, *CTNNA1*, *C-MYC* and *GAPDH* using RT-PCR.

Gene specific primers were employed to amplify regions of *CCND1*, *CDH1*, *CTNNA1*, *C-MYC* and the positive control, *GAPDH*. In order to confirm *CDH1* and *C-MYC* expression levels, two different primer pairs were used. RT-PCR products were separated and visualised using agarose gel electrophoresis.

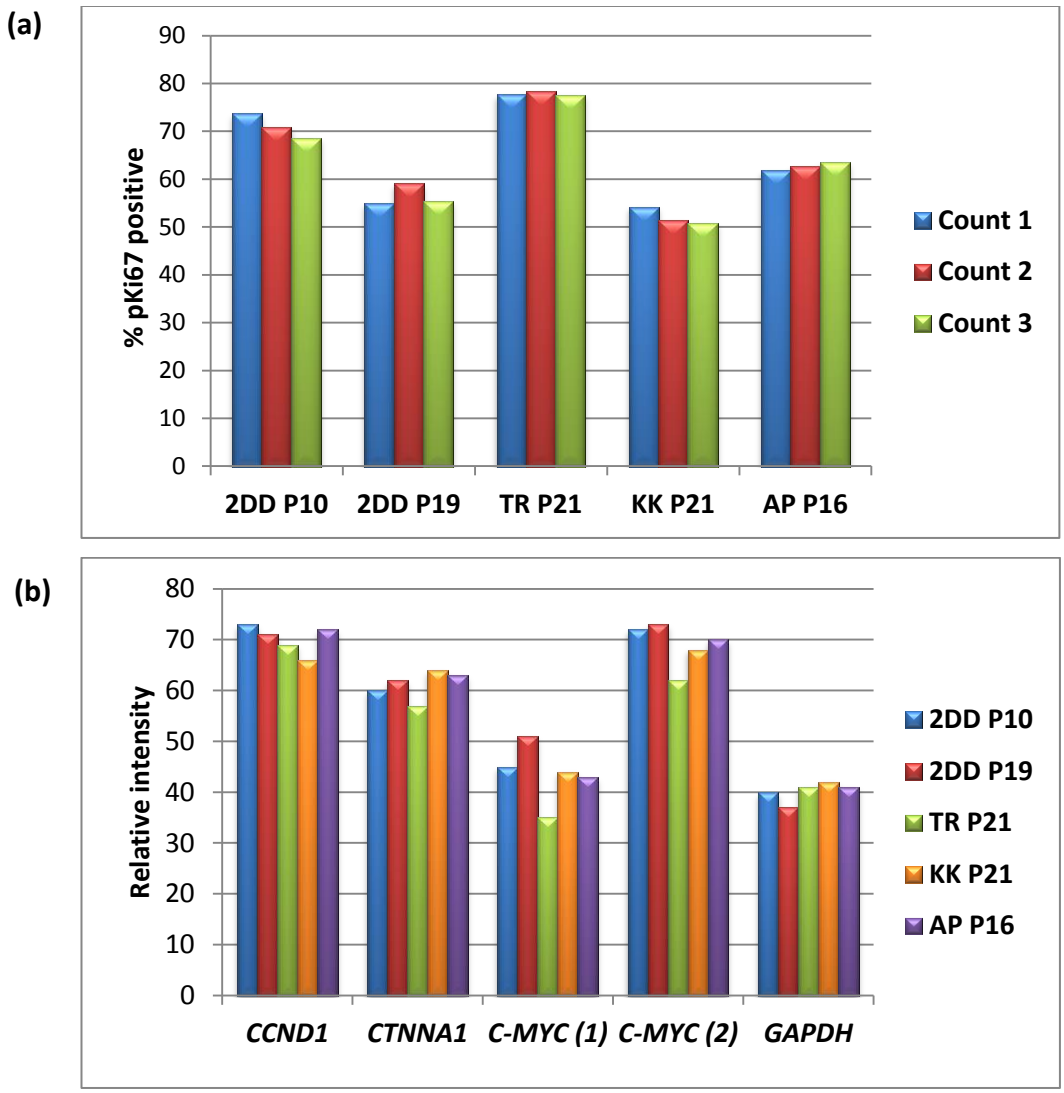

Figure 4.3.9: Analysing the expression and proliferative capacity of control and X-EDMD HDFs.

(a) The proliferative capacities of 3 X-EDMD and 2 control cultures were determined using anti-Ki67 staining. At least 200 pKi67+ nuclei were scored per separate count for each cell line. **(b)** PCR was performed using primers specific to *CCND1*, *CDH1*, *CTNNA1*, *C-MYC* and *GADPH*; the RNA used to generate cDNA was derived from 3 X-EDMD and 2 control HDF cultures. The control RNA extractions were derived from the same cell line; however, the proliferative capacity of each culture differed (see **(a)**). The relative intensities of PCR bands following RT-PCR and gel electrophoresis (see figure 4.3.8) were measured and compared using AlphaEaseFC software.

4.4 DISCUSSION

4.4.1 Overview

In order to investigate the effect of emerin's absence on genome organisation, the positions of 4 genes (*CCND1*, *CDH1*, *CTNNA1* and *C-MYC*) were determined in control and emerin null nuclei. This was performed using primarily 2D FISH on interphase nuclei; 3D gene positioning was employed to validate 2D analysis data. The basis of the study was multi-faceted. It was performed to investigate whether the absence of a protein which forms part of the inner nuclear membrane and NM, would disrupt the organisation of specific genes. These 4 genes were chosen using data which demonstrate that their expression is indirectly affected by emerin, via β-catenin and the Wnt signalling pathway (van de Wetering et al., 2002; Markiewicz et al., 2006). If indeed changes in gene expression were detected, it would serve as a useful platform to investigate the relationship between gene positioning and transcriptional regulation.

4.4.2 Emerin's role in mediating genome organisation

4.4.2.1 Overview

While numerous previous studies have demonstrated that genome organisation is disrupted in disease (Bartova et al., 2000; Cremer et al., 2003; Bartova et al., 2005; Hanicarova et al., 2006; Meaburn et al., 2007; Murata et al., 2007; Meaburn and Mistelli., 2008; Wiech et al., 2009; Meaburn et al., 2009), research examining genome organisation in X-EDMD is limited. Meaburn et al. (2007) examined the interphase nuclear position of 4 chromosomes (4, 13, 18 and X) in an X-EDMD carrier, as well as in a number of laminopathy cell lines. It was demonstrated that in the X-EDMD carrier, chromosomes 13 and 18, the smaller chromosomes, occupied a more interior nuclear location than control fibroblasts, whereas, the locations of the larger chromosomes, 4 and X, remained normal. The positions occupied by chromosomes 13 and 18 were thus suggested to mimic those found in normal senescent cells (Meaburn et al., 2007). These results imply that the absence of emerin is not incompatible with the correct localisation of certain chromosomes. Indeed, when the positions of chromosomes were examined in several X-EDMD lymphoblastoid cell lines, no significant changes in

organisation were detected (Boyle et al., 2001; Meaburn et al., 2005). Taken together, this selective mis-positioning poses several questions: firstly, why are certain chromosomes affected while others are not? Is this due to emerin's involvement in tethering these specific, smaller chromosomes to the nuclear periphery in particular cell types?

4.4.2.2 Selected genes are aberrantly positioned in X-EDMD

Results from our study indicate that the absence of emerin does affect the positioning of selected genes in X-EDMD nuclei. Interestingly, the majority of differences between control and X-EDMD nuclei were seen in senescent rather than proliferating populations. Of the 4 genes, the positioning of *CCND1* and *CDH1* was particularly disrupted.

Our laboratory has previously demonstrated that chromosomes can change nuclear position on entry into quiescence or senescence (Bridger et al., 2000; Meaburn et al., 2007). It thus seemed pertinent to compare gene positioning in proliferating and senescent (senescent) cells. The genes positioned in this current chapter were located on 4 different human chromosomes: *CCND1* = 11q13 (Motokura et al., 1991); *CDH1* = 16q22.1 (Mansouri et al., 1988; Natt et al., 1989; Chen et al., 1991); *CTNNA1* = 5q31 (Furukawa et al., 1994); *C-MYC* = 8q24.12–q24.13 (Leder, 1982; Taub et al., 1982; Dalla-Favera et al., 1982; Takahashi et al., 1991). In our current study, 3 out of the four genes were observed to occupy similar positions in both proliferating and senescent control nuclei. The exception to this was *CCND1; s*ignificantly, *CCND1* was observed to statistically shift from an interior position in proliferating nuclei, to a more intermediate location in senescent populations. This was observed using both 2D and 3D analyses. Chromosome positioning demonstrates that HSA-11, which harbours *CCND1*, occupies an intermediate location in both proliferating and senescent nuclei (Meaburn et al., 2008; Mehta et al., unpublished data). Since 2D analysis revealed that *CCND1* is interiorly positioned in proliferating HDFs, this could suggest that in these cells, the gene loops away from its parent chromosome. It is possible that this change in position is either representative of a global re-organisation of chromosomes in senescence or due to a more specific re-positioning event; indeed, exploring the

relationship between positioning and transcriptional regulation is currently very topical (Elcock and Bridger, 2010).

Although *CDH1*, *CTNNA1* and *C-MYC* did not change position in senescent control nuclei, their nuclear locations differed from those documented for their respective parent chromosomes. While *CDH1* and its parent chromosome, HSA-16, are interiorly positioned in proliferating nuclei, their locations do not match in senescence; despite the fact that HSA-16 is intermediately placed, *CDH1* remains within the nuclear interior (this study; Boyle et al., 2001; Mehta et al., unpublished data). Furthermore, although *CTNNA1* occupied an intermediate location in senescent nuclei, its parent chromosome, HSA-5, is found peripherally positioned (Meaburn et al., 2008; Mehta et al., unpublished data). Finally, *C-MYC* was reported to be a peripheral gene in both pKi67+ and pKi67− populations, while its parent chromosome, HSA-8, is intermediate (this study; Boyle et al., 2001; Mehta et al., unpublished data). Since gene- and chromosome-specific FISH was not coupled in this study, it is not possible to verify whether or not these differences in chromosome and gene positioning are reflective of actual differences in location or an inherent error between the investigations. Nevertheless, such observations are worthy of note and future studies may reveal the looping of these specific genes, away from their parent chromosomes.

In X-EDMD HDFs, there were a number of statistical differences when comparing gene positioning in proliferating and senescent nuclei. KK exhibited differences in all four genes between the two proliferative states. Most significantly, like the control, *CCND1* was observed to change location in senescence in all 3 X-EDMD cell lines. In AP, *C-MYC* occupied different positions in proliferating and senescent nuclei; this was demonstrated using both 2D and 3D analyses.

The significance of this change in *CCND1* position in senescent nuclei requires further investigation; however, the observation that this re-positioning is still able to occur in X-EDMD cells, despite the absence of emerin, strengthens the view that local and global genome organisation is partly, but not entirely, disrupted in X-EDMD.

4.4.3 Emerin's involvement in the regulation of gene expression

The fact that no major changes in gene expression were detected in our study is intriguing in light of recent studies which demonstrate emerin's involvement in the canonical Wnt signalling pathway. Markiewicz et al. (2006) demonstrated that emerin interacts with β-catenin through an APC-like domain and importantly, regulates the flux of the protein into the nucleus. Significantly, in cells which harbour emerin lacking this APC-like domain, β-catenin accumulates in the nucleus. In line with this, β-catenin activity was found to be five-fold higher in the X-EDMD (emerin null) cells. In order to test whether this increase in activity resulted in the up-regulation of down-stream target genes, the expression of *C-MYC* was tested using RT-PCR; indeed, *C-MYC* was considerably up-regulated in the X-EDMD cells (Markiewicz et al., 2006).

The implication of the article (Markiewicz et al., 2006) is that the increased activity of β-catenin caused by the lack of regulation (due to emerin's absence) would result in the mis-expression of its down-stream target genes. It has been shown that the 4 genes investigated in our study are β-catenin target genes (van de Wetering et al., 2002). However, in our study, no change in gene expression was detected for any of the genes tested; there was no notable difference in expression levels when comparing control and X-EDMD. The fact that the levels of expression for all 4 genes were extremely similar for 3 emerin null cell lines and 2 control cell lines increases the likelihood that our data are both accurate and reproducible. In contrast, Markiewicz et al. (2006) displayed RT-PCR results for only one emerin null and a control cell line. The fibroblast cultures used by Markiewicz et al. (2006) had been, on average, through fewer passages (P6–12) than the cell lines used in our study (P9 and p19, control; P16–P21, emerin null). However, the proliferative capacities (% pKi67+) of the cultures used in both studies were similar. Furthermore, at the time of RNA extraction for RT-PCR in our study, the 3 X-EDMD cell lines each had differing pKi67 populations. Since the band intensities for all genes were very similar in all X-EDMD cell lines, this implies that the expression levels of the genes were not considerably different in proliferating and senescent nuclei.

4.4.4 How integral is emerin for normal cellular function?

The results from our study do raise some important points: how important is emerin as a structural protein and as a regulator of signalling pathways? Research does demonstrate that emerin is not essential for cell growth in mammalian cultured cells (Harborth et al., 2001) or for normal development in *C. elegans* (Gruenbaum et al., 2002). This indicates that emerin's role in cellular and nuclear activities are dispensable. Indeed, in our study, the absence of emerin does not appear to dramatically disrupt the expression or positioning of the genes tested, although there were moderate shifts in position. The fact that the changes in position were of significance perhaps suggests that emerin is involved in the 'fine-tuning' of global and local genome organisation, rather than the overall anchorage of genomic regions. Since chromosome positioning has only been examined in carrier, rather than patient, X-EDMD HDFs previously, the status of chromosome organisation has not been confirmed. The results presented in this chapter indicate that it is unlikely that global genome organisation is disrupted to a considerable extent in such nuclei. However, whether the differences in gene positioning were as a result of changes at the local level or indirectly due to disruptions in chromosome localisation is an area which requires further investigation. Despite these minor disruptions in gene positioning, this study did not reveal any changes in gene expression; this is an important finding. It reveals that the expression of the four genes analysed is not significantly perturbed in X-EDMD, which questions emerin's importance in the Wnt-signalling pathway. Nevertheless, this current study does not negate the possibility of a relationship between gene expression and positioning.

Emerin is evidently important enough for its loss to create a human disease phenotype in the form of X-EDMD. The key to understanding emerin's role in X-EDMD most probably lies in examining events occurring in those tissue types, i.e. skeletal and cardiac muscle, which are specifically affected in the disorder. While *emd* null mice show no overt muscle phenotype, muscle regeneration is perturbed as a result of disrupted pRb and MyoD pathways (Melcon et al., 2006). Rb-MyoD pathway disruption in X-EDMD has also been demonstrated using mRNA expression profiling analysis (Bakay et al., 2006). Furthermore, it has been reported that emerin binds β-catenin in

cardiomyocytes; importantly, in murine cells lacking emerin, both β-catenin signalling and intercalated disc function, are disordered (Wheeler et al., 2010). Taken together, these studies provide evidence of emerin's role in muscle regeneration and cardiac function, which aids understanding of why the pathogenesis of X-EDMD appears to be restricted to particular cell types.

4.4.5 Conclusion

In conclusion, the results of this study suggest that in the absence of emerin, some gene positioning is affected, while transcriptional regulation appears largely unchanged in fibroblasts. This study promotes the hypothesis that the impact of emerin's loss in X-EDMD is more severe in those cell types primarily affected in the disease i.e. myocytes.

5. Investigating the disease-causing mutations present in Atypical (type 2) HGPS patients

5.1 INTRODUCTION

5.1.1 X-linked Emery-Dreifuss Muscular Dystrophy (X-EDMD)

5.1.1.1 Overview

While autosomal EDMD can result from mutations in *EMD* and *LMNA*, X-EDMD is caused by *EMD* mutations (Bione et al., 1994; Bione et al., 1995). In the majority of X-EDMD cases, *EMD* mutations lead to an absence of the protein in patient cells; however, mutant forms of emerin can also cause X-EDMD (Yates et al., 1999). More recently, *EMD* mutations have also been demonstrated to cause limb-girdle muscular dystrophy (Ura et al., 2007) and familial atrial fibrillation (Karst et al., 2008).

5.1.1.2 Emerin

Emerin is a LEM domain-containing, type II integral nuclear membrane protein (Nagano et al., 1996) which is encoded by *EMD* (originally denoted *STA*). The gene, which comprises of 6 exons, is relatively small at 2 kb; the protein is a serine-rich molecule 34 kDa in size and 254 amino acids in length (Bione et al., 1994; Nagano et al., 1996; Manilal et al., 1996). The protein exists in four phosphorylated forms, three of which are associated with the cell cycle (Ellis et al., 1998). While the majority of the polypeptide resides in the nucleoplasm, its hydrophobic C-terminus anchors it to the nuclear membrane (Manilal et al., 1996). Although emerin expression is ubiquitous, levels are highest in cardiac and skeletal muscle (Bione et al., 1994). Importantly, correct emerin localisation is dependent on its interaction with A-type lamins (Vaughan et al., 2001).

5.1.1.3 X-EDMD carrier, ED5364

ED5364 is a HDF cell line derived from an X-EDMD carrier; previous work has been performed using this cell line (Meaburn et al., 2007). It is known that the disease-causing mutation resides in *EMD* (unpublished data, G. Morris); however, the specifics are unknown. In order to determine the nature and location of the mutation present in ED5364, *EMD* was amplified and sequenced using ED5364 genomic DNA. A

heterozygous point mutation was discovered in exon 4 of *EMD* (c.315T>G), which is predicted to lead to the substitution of tyrosine with a stop codon (p.Tyr105X).

5.1.2 Atypical Hutchinson-Gilford Progeria Syndrome (HGPS)

5.1.2.1 Overview

Hutchinson-Gilford Progeria syndrome (HGPS) is a rare, premature ageing disease caused by mutations in *LMNA* (De Sandre-Giovannoli et al., 2003; Eriksson et al., 2003). Numerous HGPS cell lines have been studied and in most cases, a mutation in *LMNA* is the source of disease (e.g. AG01972, AG11498, AG06297; Eriksson et al., 2003). However, in at least four HGPS patients (AG08466, AG11572, AG03199 and AG10578), a mutation in this gene has not been identified. Significantly, neither AG08466 nor AG11572 harbour a *LMNA* mutation (Dr. N. Levy; personal communication) which indicates that the genetic cause of the disease resides in another gene or other genes. Interestingly, in culture, these two cell lines act differently to *LMNA* mutated HGPS strains; they both exhibit a greater growth potential and lower fractions of abnormal nuclei (Bridger and Kill, 2004).

5.1.2.2 Candidate Genes

The mutation of several candidate genes could potentially result in the clinical phenotype exhibited by HGPS patients. These include *ZMPSTE2, LAP2* and *EMD*. As aforementioned in chapter 1, *ZMPSTE24,* encodes a zinc metalloproteinase involved in the processing of lamin A precursors (Pendas et al., 2002; Bergo et al., 2002; Navarro et al., 2005). Research has shown that mutated *Zmpste24* in mice causes HGPS-like symptoms (Fong et al., 2004). Furthermore, it has been postulated that HGPS and AR-MAD, a human disorder resulting from mutations in *ZMPSTE24*, could be variants of the same disease (Plasilova et al., 2004). Having said that, *ZMPSTE24* mutations also cause restrictive dermopathy; a laminopathy presenting with clinical phentotypes very disimilar to those seen in HGPS (Navarro et al., 2005; Levy et al., 2005; Mouslon et al., 2005). However, it has been demonstrated that there are two wild-type alleles for *ZMPSTE24* in both AG08466 and AG11572 (personal communication, Dr. N. Levy). This

leaves the two remaining candidate genes, *EMD* and *LAP2*; since EMD has been discussed previously (see 5.1.1), *LAP2* will now be discussed in more detail.

5.1.2.3 Lamina-associated polypeptide 2 alpha (LAP2α)

Through alternate splicing, the lamina-associated polypeptide 2 (*LAP2)* gene encodes 6 isoforms; α, β, β', γ, ε and δ (Foisner and Gerace, 1993; Harris et al., 1994; Berger et al., 1996). Though all 6 isoforms have been characterised in the mouse (Berger et al., 1996), this is only true of α, β and γ, in humans (Harris et al., 1994; Harris et al., 1995). The human *LAP2* gene, located on 12q22, is composed of 8 exons, which span 35 kb in total; the splicing of exons 1–4 produce LAP2α, while exons 1–3 and 5–8 encode LAP2β (see table 5.1.1; Harris et al., 1995). As a result, α and β exhibit distinct C-termini, while sharing a common, 187 residue N-terminal domain (Harris et al., 1994). Consequently, the two isoforms exhibit different nuclear localisation; LAP2α lacks a trans-membrane domain and is thus nucleoplasmic, whereas LAP2β is membrane bound (Foisner and Gerace, 1993; Harris et al., 1994; Dechat et al., 1998). Furthermore, they display different chromosomal associations (Vlcek et al., 1999).

Significantly, LAP2α is found to associate with lamin A; this interaction occurs between LAP2α's C-terminal 78 residues and amino acids 319–566 of lamin A/C (see figure 5.1.1; Dechat et al., 1998; Dechat et al., 2000a; Dechat et al., 2000b). Together, these proteins can be seen as intranuclear speckles, which are most prominent during G_1 (Dechat et al., 2000b). Furthermore, the presence of wildtype lamin A appears to be necessary for the correct localisation of LAP2α in the nucleus (Dechat et al., 2000b). Subsequently, Markiewicz et al. (2002) reported that these proteins are in fact involved in the nuclear tethering of the retinoblastoma protein (pRb). Indeed, the proteosomal degradation of pRb is regulated by these intranuclear protein complexes (Johnson et al., 2004).

Exon	Exon composition of LAP2 isoforms		
	α	β	γ
1	1–92	1–92	1–92
2	93–134	93–134	93–134
3	135–187	135–187	135–187
4	**188–693**	NP	NP
5	NP	188–220	188–220
6	NP	**221–329**	NP
7	NP	330–359	221–250
8	NP	362–453	251–344

Table 5.1.1: The exon composition of the LAP2 isoforms
Bold type indicates that the exon is specific to that isoform whereas NP (not present) signifies that the exon is not a component of the isoform's mRNA. The data displayed in this table has been derived from a research article by Harris et al. (1995).

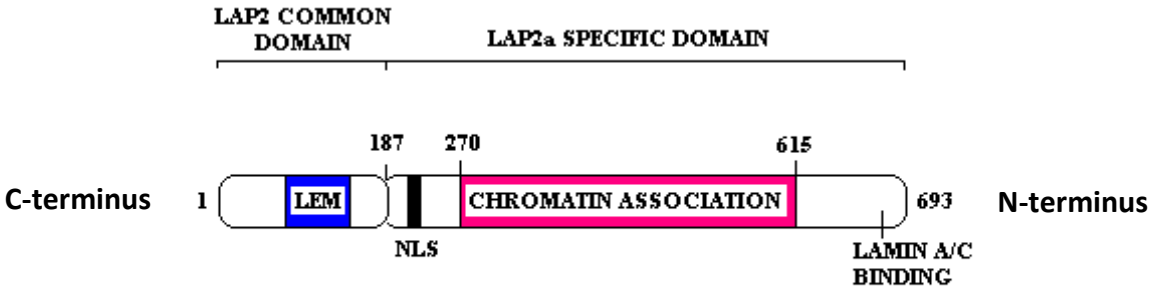

Figure 5.1.1: The structure of LAP2α

To put this into context, pRb's function within the cell must be considered. When hypo-phosphorylated, pRb binds to the transcription factor, E2F and blocks its transctivation domain (Mittnacht, 1998). However, when phosphorylated by the cyclin-dependent kinases, D and E, pRb releases E2F, allowing it to activate the transcription of S-phase specific genes; an event which eventually leads to cell proliferation (for review, see Yamasaki and Pagano, 2004; Frolov and Dyson, 2004). In agreement, a loss of lamin A from tumour strains is concomitant with their hyper-proliferation (Venables et al., 2001), while, the protein's up-regulation occurs when a proliferative cell

becomes quiescent (Pugh et al., 1997). In contrast, entry into quiescence is accompanied by the down-regulation of LAP2α expression (Pekovic et al., 2007).

Aside from LAP2α's participation in the regulation of cell cycle progression, it is also implicated in chromatin organisation. A stretch of ~350 amino acids in the protein's C-terminal mediates this interaction (Vlcek et al., 1999). Interestingly, its association with chromosomes is dependent on the protein's phosphorylative state (Dechat et al., 1998; Vlcek et al., 2002; Gajewski et al., 2004). During interphase, LAP2α is found dispersed throughout the nuclear interior, being absent from only nucleoli (Harris et al., 1994; Dechat et al., 1998) whereas in metaphase, it is cytoplasmic (Dechat et al., 2004). Furthermore, the protein sits at telomeres in a complex with BAF. This event is postulated to be necessary for chromosome repositioning during nuclear assembly (Dechat et al., 2004). In addition, the re-organisation of chromatin in apoptosis appears to be, in part, reliant on the early cleavage of LAPα (Gotzmann et al., 2000).

Unfortunately, LAP2α's expression in human tissues has not yet been fully characterised. However, studies suggest that its expression is altered during development, with high levels being reported during cardiac development (Taylor et al., 2005) and its down-regulation occurring in myogenesis (Markiewicz et al., 2005).

Adding further credence to the possibility that LAP2α is mutated in one of the two HGPS strains, Taylor et al. (2005) reported it as the molecular cause of DCM in two siblings. The heterozygous substitution led to the replacement of an arginine (hydrophilic and charged) with a cysteine (hydrophobic and uncharged) at codon 690 (Taylor et al., 2005). Significantly, the affected amino acid resides in the portion of the protein mediating an interaction with lamin A/C and as a result this association is weakened in these cells (Dechat et al., 2000b). Thus, it could be postulated that this aforementioned mutation results in the destabilisation of the lamin A-LAP2α-pRb complex, leading to the loss of cell cycle control.

5.1.2.4 Hypothesis

The difficulty with a mutation search such as this one is that the disease-causing mutations present could potentially reside in one of numerous genes. Therefore, a candidate gene approach has been selected. By assessing the literature, 2 such genes, *EMD* and *LAP2*, have been chosen on the basis of their respective protein's functional relationship with lamin A. Indeed, emerin is shown to interact with lamin A (Manilal et al., 1998; Clements et al., 2000; Vaughan et al., 2001; Lee et al., 2001) and this association is required for emerin's localisation at the NE (Sullivan et al., 1999; Burke and Stewart, 2002; Holaska et al., 2002; Muchir et al., 2003). Since LAP2α is observed to form a complex with A-type lamins, which acts to tether pRb in the nucleoplasm, it is thus plausible that a mutation in LAP2α could perturb lamin A function. Out of the two candidate genes chosen, the gene encoding LAP2α is most likely to be mutated in these two HGPS cell lines. Two main factors influenced this decision; firstly, the loss of functional LAP2α disrupts lamin A-LAP2α-pRb complexes, leading to deregulated cell cycle control (Markiewicz et al., 2002; Pekovic et al., 2007). Secondly, *EMD* mutations generally lead to muscle specific phenotypes; in AG11572 and AG08466, the patients show no signs of muscular dystrophy.

In order to test this hypothesis, both *EMD* and *LAP2* (exon 4) were amplified and sequenced in AG08466 and AG11572 using primers targeted to genomic DNA. Although, so far, this search has failed to reveal any mutations in either cell line for either gene, it has been an important study since it aids the elimination of *EMD* and *LAP2* (exon 4) from the list of candidate genes implicated in causing atypical HGPS.

5.2 METHODS AND MATERIALS

5.2.1 Cell Culture

Primary HDFs from HGPS patients AG08466 and AG11572 (both, Coriell cell repository) were grown in DMEM containing 15% (v/v) fetal bovine serum, 2% (v/v) penicillin/streptomycin and L-glutamine. Control and ED5364 HDFs were maintained as before (see sections 2.2 and 3.2).

5.2.2 DNA Extraction

To extract DNA, approximately 1 x 10^6 cells were incubated in Digest Mastermix, a solution of 400 µl of tail digestion buffer (100 mM Tris (pH 8.0), 5 mM EDTA, 200 mM NaCl, 0.2% (w/v) sodium dodecyl sulphate (SDS)) and 10 µl of Proteinase K (50mg/ml), for at least 2 hours at 55°C. Following this, the samples were briefly vortexed and spun at 500g for 5 minutes. Next, 1 ml of 100% (v/v) ethanol was added and the eppendorf inverted; this resulted in the formation of a precipitate. The solution was incubated at -80°C for 10 minutes and then, centrifuged (13,700 g) for 30 minutes at 4°C. Following the removal of the supernatant, the pellet was washed using 1 ml 70% (v/v) ethanol and centrifuged (13,700 g) for 20 minutes at 4°C. Finally, the remaining ethanol was discarded and the pellet re-suspended in 100 µl of 1 x Tris-EDTA buffer; this was stored at 4°C.

5.2.3 Polymerase Chain Reaction (PCR)

Before being added to a 0.2 ml thin-walled tube, all the PCR components were mixed and centrifuged. For the amplification of *EMD* components were: molecular grade double distilled water, 10 x PCR Amplification buffer (Invitrogen), PCR Enhancer Buffer (Invitrogen), de-oxynucleotides (dNTPs; 10 mM) (Eppendorf), forward and reverse primers (100 µM) (Sigma) (see tables 5.2.1 and 5.2.2), $MgSO_4$ (Invitrogen), Platinum *Taq* polymerase (5U/ µl) (Invitrogen) and genomic DNA. For *LAP2*, the KAPAHiFi^{TM} DNA Polymerase kit (KAPA BIOSYSTEMS) was used.

A number of different primers were employed to amplify *EMD* (table 5.2.1) and *LAP2* (exon 4; table 5.2.2). The reaction solutions were mixed and centrifuged, before being placed in the PCR cycler (GenePCR System 2400; Perkin Elmer). The PCR cycles required for *EMD* amplification are shown in tables 5.2.3 and 5.2.4.

Exon	Designated name	Forward Primer (5'–3')	Nucleotide position	Reverse Primer (5'–3')	Nucleotide position	Expected length (bp)
1	GEMD1F/R	AGCGGCCGTGA CGCGACAACG	−67 > −47	GAGGTCGCGAG GCGGAGC	253 > 236	320
2	GEMD2F/R	CGCGACCTCCCC GCTGCC	245 > 262	TGCCGCTCTCGA CCGGCC	507 > 490	262
3	GEMD3F/R	GTCGAGAGCGG CACTGGA	495 > 512	GTCTCAGGTCCT CCCTGTGAGC	1034 > 1014	232
4	GEMD4F/R	CCATCAGGCCA GGCGGGG	801 > 818	TAGGTTGTACCC AAGTACAGG	1034 > 1014	234
5	GEMD5F/R	GTGGGTTCCTG GCCTCTAACC	1257 > 1277	GGAGCCTGGAC C CAGAACC	1477 > 1459	221
6	GEMD6F/R	GCTCCTGGCCC ACTTGCTCC	1473 > 1492	CTAAGGCAGTC AGCCAGGAC	1888 > 1869	416

Table 5.2.1: Primer sequences used to amplify the six exons of *EMD*

Primers were designed as per Wulff et al., 1997.

Designated name	Forward Primer (5'–3')	Nucleotide position	Reverse Primer (5'–3')	Nucleotide position	Expected length (bp)
LAP2αintron /exon4	GCTTTGTCTACC AGGGCAAA	22726 > 22707*	CCAGTGGGGGC ATAGAGTTA	21929 > 21948*	798
LAP2α4.1	TCTTGTTGCCAC AAACTTGC	969 > 988[$]	GGCAGCCATCT TCACTTCAT	2124 > 2105[$]	1156
LAP2α4.2	CCAGGGTGGG GTAGGTAGTT	1362 > 1381[$]	AAATGCCAC AAAGGAACCTG	1548 > 1529[$]	187
LAP2α4.3	ACCTGGATCCG AACTGATGT	1557 > 1576[$]	CAGGCTTCCTA TCTACGCAAA	2490 > 2470[$]	934

Table 5.2.2: Primer sequences used to amplify *LAP2* (exon 4).

[$]Position in mRNA sequence derived from cDNA clones (NM_003276.1/U09086.1: Human thymopoietin alpha mRNA, complete cds; Harris et al., 1994). *Position in sequence

AC013418.32 (*Homo sapiens* 12 BAC RP11-181C3 (Roswell Park Cancer Institute Human BAC Library) complete sequence).

Phase	Temperature (°C)	Duration	Number of cycles
Initial denaturation	95	2 minutes	1
Denaturation	95	45 seconds	35
Annealing	60	30 seconds*	
Extension	68	1 minute	

Table 5.2.3: PCR cycle used to amplify *EMD*'s six exons.
***** varies for each primer pair (see table 3.2.4)

Exon	Designated name	Optimised PCR Enhancer Buffer Volume (µl)	Optimised Annealing Temperature (°C)
1	GEMD1F/R	0	61
2	GEMD2F/R	5	62
3	GEMD3F/R	0	60
4	GEMD4F/R	0	59
5	GEMD5F/R	5	60
6	GEMD6F/R	5	62

Table 5.2.4: Optimised PCR conditions for the 6 *EMD* primer pairs

Phase	Temperature (°C)	Duration	Number of cycles
Initial denaturation	95	2 minutes	1
Denaturation	98	20 seconds	35
Annealing	60	15 seconds	
Extension	68	30 seconds	
Final extension	68	3 minutes	1

Table 5.2.5: PCR cycle used to amplify *LAP2* exon 4

5.2.4 Agarose Gel Electrophoresis

Correctly sized bands were excised with a sterile scalpel and stored at −20°C until further use.

5.2.5 Gel Extraction and DNA Quantification

Following the excision of bands from the agarose gel, DNA contained within the gel was extracted and purified using a MinElute Gel Extraction Kit (Qiagen). The concentration of the extracted DNA was measured using a Qubit DNA/RNA quantification machine.

5.2.6 DNA Sequencing

The DNA sequencing was performed by the DNA Sequencing Service, MSI/WTB Complex at the University of Dundee (DNA Sequencing and Services, 2010) using an Applied Biosystems 3730 DNA Analyzer. In order for this to be done correctly, DNA samples and their respective primer pairs were provided at given concentrations (see table 5.2.6).

Size of PCR Product (bp)	DNA concentration required per reaction	Primer concentration required per reaction
100–200	1–3 ng	3.2 picomoles
200–500	3–10 ng	
500–1000	5–20 ng	

Table 5.2.6: The DNA concentrations required for efficient sequencing.
As specified by the DNA sequencing service in Dundee.

5.2.7 Western Blotting

After cells were grown in 10 cm^2 dishes to a known density, the medium was removed and the cells were washed 3 times with 1 x PBS. Following one wash with double distilled water, cells were scraped into 3 x sample buffer (186 mM Tris-HCl, 15% (v/v) glycerol, 6% (w/v) SDS, 0.01% (w/v) Bromophenol blue, 0.2% (v/v) β-mercaptoethanol). The samples were then boiled for 3 minutes and the required volume adjustments were made; at this point, the cells were stored at −20°C.

Samples were loaded on a gel (4–15% (w/v) Tris-HCl gradient ready gel (BioRad Laboratories)), at a density of 2 x 10^5 cells, per lane, alongside 10 µl of rainbow marker. The gels were run in tank buffer (25 mM Tris, 192 mM Glycine, 0.1% (w/v) SDS) using the Mini-PROTEAN II (BioRad Laboratories) electrophoresis equipment at 50V.

Following this, proteins from the gel were electrophoretically transferred onto a nitrocellulose membrane in transfer buffer (50 mM Tris, 380 mM Glycine, 0.1% (w/v) SDS, 20% (v/v) Methanol; pH 9.0–9.4) at 250 mA for an hour; this was performed at 4°C. Subsequently, the membranes were placed in block rinse buffer (10 mM Tris (pH 7.4), 150 mM NaCl, 1 mM EDTA, 0.1% Tween-20 (v/v)) and then, incubated in blocking buffer (4% (w/v) dried milk powder (Marvel)) at 4°C overnight or at room temperature for an hour. Once sufficient blocking has taken place, the buffer was removed and the blots were rinsed three times, with each rinse lasting 5 minutes, in block rinse buffer. Next, 10 ml primary antibody was added to each blot; the incubation time for this was 1 hour at room temperature. Primary antibodies used were: Novocastra anti-emerin (1:250), Novocastra anti-lamin A/C (1:100) and anti-LAP2α (1:200; a kind gift from R. Foisner). In order to eliminate excess antibody, the rinse steps were repeated. A second incubation, using 10 ml Alkaline Phosphatase-conjugated secondary antibodies (rabbit anti-mouse IgG, rabbit anti-goat IgG and swine anti-rabbit IgG (Sigma)) took place for 1 hour at room temperature. Following this, the blots were rinsed once again in blot rinse buffer three times. The membranes were then placed in colour development buffer (100 mM Tris; pH 9.4) for up to 5 minutes. Finally, the blots were incubated in colour reagent (5-bromo-4-chloro-3-indolyl-phosphate (BCIP) and nitroblue tetrazolium (NBT) until the bands had sufficiently developed. To stop the reaction, the membranes were washed in double distilled water. The molecular weights of the bands were determined using the rainbow marker (Sigma) as a reference.

5.3 RESULTS

5.3.1 The Amplification of *EMD* and *LAP2* (exon 4)

5.3.1.1 *EMD*

In order to successfully sequence *EMD,* several PCR conditions required optimisation. Since the genomic DNA in question is only 2 kb in length, it would be expected that amplification using a single primer pair would be straightforward; indeed, several other groups have done so (Bione et al., 1995). Here, attempts at this were unsuccessful and as a result, it was decided that the gene would be amplified using numerous primer pairs as per Wulff et al. (1997; see figure 5.3.1).

Since six different primer pairs were used to amplify the six individual exons, each pair had to be optimised in terms of the annealing temperature and the volume of enhancer buffer used. This turned out to be a lengthy process; however, the result of this optimisation process can be seen in the table below (table 5.3.1).

Exon	Designated name	Optimised PCR Enhancer Buffer Volume (µl)	Optimised Annealing Temperature (°C)
1	GEMD1F/R	0	61
2	GEMD2F/R	5	62
3	GEMD3F/R	0	60
4	GEMD4F/R	0	59
5	GEMD5F/R	5	60
6	GEMD6F/R	5	62

Table 5.3.1: The conditions required for successful amplification of the six *EMD* exons

5.3.1.2 *LAP2* (exon 4)

In contrast, exon 4 of *LAP2* was relatively simple to amplify. 4 different pairs of primers were employed to amplify *LAP2* exon 4 (see figure 5.3.2 and 5.3.3).

```
   1  GCGCGCAGGCCCCGCCCCTCTCACCCCGCCGCACGCCACAGGGTGACGTCTGGGCTCCCA
  61  GCCGCATCGCCCTGACTCCCGCGCGGGCCCCGCCCCCTGCCGCTAGCCAATCTGTGCGTT
 121  TGTGACTTTTGGGCCCGCAGCCCCGCCTGCTCCCACAGCGATACCGGTTTGCATTGCCCT
 181  GACTCCCGCGCGGGCCCCGCCCCCTACGCCGCTAGCCAATCCATGCATTAGTGGCGTCCG
 241  GGCTCGCAGTACCGCTCGCTCCCACCGCGAGACCTTCTGCTCCGCGCCCGCGCGGGCCCC
 301  TCCCCCTCCATCGCTAGCCAATCCCCGTTTTGTGACGTATGGGCTCGCGGCCCCGCTCGC
 361  TCCCACCGCGAGACCTTTTGCTCCGCGCCCGCGCGGGCCCCGCCCCCTCCATCACTAGCC
 421  AATCCCCGTGCTTGTGACATATGGGCTTGCGGCCCCGCCCGCTCCCATCGCGAGACCGGT
 481  TCCCACCGCCCTGACTCCCGGGCGGGCCCCGCCCTCTCCGCCGCTAGCCAATCCTCGCGT
 541  TGATGACGTTTGGGCTCGCGGCCCCAGCCTCCCAGCTCTCAGGGCACGGCCGGTCTGTGC
 601  CGGCTGCTCCCGCGGTTAGGTCCCGCCCCGCGCAGCGCGCGCAGCCTGCGGAGCCAGCGG
 661  CCGTGACGCGACAACGATTCGGCTGTGACGCGACAACGATTCGGCTGTGACGCGAGCGCG
 721  GCCGCTCCCGATGCGCTCGTGCCGCCCCCGCCGTGCTCCTCGGCAGCCGTTGCTCGGCCG
 781  GTTTTGGTAGGCCCGGGCCGCCGCCAGGCCTCCGCCTGAGCCCGCACCCGCCATGGACAA   E1
 841  CTACGCAGATCTTTCGGATACCGAGCTGACCACCTTGCTGCGCCGGTACAACATCCCGCA
 901  CGGGCCTGTAGTAGGTACGCGGCGGCGGGCGGGACCCCTTCCGGGCCCCCTCCTCGTGCT
 961  CCGCCTCGCGACCTCCCCGCTGCCCTCCCCGCGCGCCTTCCCCGGCCCGCGGCCCTGACC
1021  GCCCCGTGTCCGGCCAGGATCAACTCGTAGGCTTTACGAGAAGAAGATCTTCGAGTACGA   E2
1081  GACCCAGAGGCGGCGGCTCTCGCCCCCCAGCTCGTCCGCCGCCTCCTCTTATAGCTTCTC
1141  TGGTGAGAGCCTCGCCTGTGGGGACAGCCTGGGACGCGGGGAGGATGGGGTCGCGAGGGT
1201  GTGGCAGGGGGGCCGGTCGAGAGCGGCACTGGAGAAAGGGGAGGGAAGTCTGGGGGGGCA
1261  AACAGTTCTGTCTCCTCCTTTCAATCCAGACTTGAATTCGACTAGAGGGGATGCAGATAT   E3
1321  GTATGATCTTCCCAAGAAAGAGGACGCTTTACTCTACCAGAGCAAGGGTAAGGCAGGGGT
1381  TGGGTGGGCACGCTGGCACCTTCACCCGACTTCGTCAGGGACCCCGCTCACAGGGAGGAC
1441  CTGAGACCTCAGTCCCAACCACTCCAGCAGCCTTAGGAGGGAGAAACTGTTACAGGTCCC
1501  GAAATGGGATTCAGATTAGGGCCATCAGGCCAGGCGGGGCACACCGATGCCCCCTCTGCT
1561  ACCGCTGCCCCCCTTCCCAAGGCTACAATGACGACTACTATGAAGAGAGCTACTTCACCA   E4
1621  CCAGGACTTATGGGGAGCCCGAGTCTGCCGGCCCGTCCAGGGCTGTCCGCCAGTCAGTGA
1681  CTTCATTCCCAGATGCTGACGCTTTCCATCACCAGGTGAGCTGGCTGGCAGGCGTCCTGT
1741  ACTTGGGTACAACCTAGGGGATCGCGGCTGTGTTTGGATAAATCCAGGGGGGCACTGGGT
1801  ACAAATGGTGGCTCTTGGGCCTCCGGGGAGACTCTGTGTGACTAGAGCACCCTGGTCTGG
1861  GATCTAGGCTCAGACTCTTCCTGAGAGTCCTGGGGGCAAAAGGGGATGCTGGGGCATGAG
1921  CACAAGTGGCAAGGCCCCATGGATAAAGGGCTGAACACCCAGAGCCATTCAGGAGGGTGT
1981  GGGTTCCTGGCCTCTAACCAAAGGTCAGAGGGGACTGGCTGGGGAAGTTTGGACTGAGGG
2041  ACATGACAGGGCCATGGTGGCCCTGCCAGCCAGTCCCCTCGCCCTGACTCTCTTCTGCAG
2101  GTGCATGATGACGATCTTTTGTCTTCTTCTGAAGAGGAGTGCAAGGATAGGTGCGTAGTG   E5
2161  GGGGAGCCCAGGGACGGGCTGGTTCTGGGTCCAGGCTCCTGGCCCACTTGCTCCCCTCTT
2221  TTGCCTCAGGGAACGCCCCATGTACGGCCGGGACAGTGCCTACCAGAGCATCACGCACTA
2281  CCGCCCTGTTTCAGCCTCCAGGAGCTCCCTGGACCTGTCCTATTATCCTACTTCCTCCTC
2341  CACCTCTTTTATGTCCTCCTCATCATCTTCCTCTTCATGGCTCACCCGCCGTGCCATCCG   E6
2401  GCCTGAAAACCGTGCTCCTGGGGCTGGGCTGGGCCAGGATCGCCAGGTCCCGCTCTGGGG
2461  CCAGCTGCTGCTTTTCCTGGTCTTTGTGATCGTCCTCTTCTTCATTTACCACTTCATGCA
2521  GGCTGAAGAAGGCAACCCCTTCTAGAGGGAGCCATGAGGGTCTGGGCTTCAGAGCTAGGT
2581  CTTTGGGGAAGTCCTGGCTGACTGCCTTAGCAGTGGGGGTGGGGGTGGGGGCAGGGGCAG
2641  GGGCTTTATGTGTTTTTGCTTGGGGGGCGCTGGGCCTAGCCCAGAGTAGTGCTTGCTCCC
2701  CCTGCCTTGTCCCACCAGGGAGGCAGCAGACTCAGGCCCTCCATGGTCCTCTTTGTCATT
2761  TTGTTGACATGCATTCCTCCTTTTGTCATCTTGTTGGGGGGAGGGGATTAACCAAAGGCC
2821  ACCCTGACTTTGTTTTTGTGGACACACAATAAAAGCCCCGTTTATTTGTAATGCGTTGGC
2881  TCTTCCTGGAGGAGAGGGTTGGGCTCCCATGGCAAGGGCCTCTGCGTCTTGGGGCTCCAG
2941  GATTGCAATCCGGCTTTGTTGGGTCCGCATTTTTGCTTTAGTCTGGGGATAGGAATCAAA
3001  TGTTACCCAGAGATGTTTGTGTTTTGTTTGGGAGTTTTATTCCCTAACTCATTCCCCAAA
3061  GCACGTGTAACTGCTTATACATATAATCGTGGTACAACAAGGTATATACAGAGAACCCAC
3121  TTGGAAATTCAGGCAAAGCTGCATGCACGCTACCAGCAGTCTGCGGGTGTTTTAACTGGA
3181  AAAAGCTGAAGTCCACCTCGGTGTCCAATGGCATGGGGATGGAAAGAAAATGAGGCGTCT
3241  CTGGCACATCATTCTCAGCTCCTGGAACTGCTGCTTGTTTAACATGGGAGAAAAGCTCCA
3301  AAGGCTGAAATGCCCCATCATCCCTGGGTGATTGAATTC
```

Figure 5.3.1 *EMD* genomic DNA sequence

Figure 5.3.1 *EMD* genomic DNA sequence

Sequence derived from PubMed (X86810.1). Gene information sourced from Bione et al., (1994; 1995). Start (ATG) and stop (TAG) codons are underlined. Protein coding cDNA sequence is highlighted in dark grey (as per Bione et al., 1994). Non-protein coding cDNA sequence is highlighted in light grey (as per Bione et al., 1995). Forward primers for each exon are highlighted in green, while reverse primers are highlighted in red. Overlapping primer sequences are highlighted in dark green. Primers as per Wulff et al. (1997). E = exon.

```
1    GTTCGTAGTTCGGCTCTGGGGTCTTTTGTGTCCGGGTCTGGCTTGGCTTTGTGTCCGCGA
61   GTTTTTGTTCCGCTCCGCAGCGCTCTTCCCGGGCAGGAGCCGTGAGGCTCGGAGGCGGCA
121  GCGCGGTCCCCGGCCAGGAGCAAGCGCGCCGGCGTGAGCGGCGGCGGCAAAGGCTGTGGG
181  GAGGGGGCTTCGCAGATCCCCGAGATGCCGGAGTTCCTGGAAGACCCCTCGGTCCTGACA
241  AAAGACAAGTTGAAGAGTGAGTTGGTCGCCAACAATGTGACGCTGCCGGCCGGGGAGCAG
301  CGCAAAGACGTGTACGTCCAGCTCTACCTGCAGCACCTCACGGCTCGCAACCGGCCGCCG
361  CTCCCCGCCGGCACCAACAGCAAGGGGCCCCCGGACTTCTCCAGTGACGAAGAGCGCGAG
421  CCCACCCCGGTCCTCGGCTCTGGGGCCGCCGCCGCGGGCCGGAGCCGAGCAGCCGTCGGC
481  AGGAAAGCCACAAAAAAAACTGATAAACCCAGACAAGAAGATAAAGATGATCTAGATGTA
541  ACAGAGCTCACTAATGAAGATCTTTTGGATCAGCTTGTGAAATACGGAGTGAATCCTGGT
601  CCTATTGTGGGAACAACCAGGAAGCTATATGAGAAAAAGCTTTTGAAACTGAGGGAACAA
661  GGAACAGAATCAAGATCTTCTACTCCTCTGCCAACAATTTCTTCTTCAGCAGAAAATACA
721  AGGCAGAATGGAAGTAATGATTCTGACAGATACAGTGACAATGAAGAAGGAAAGAAGAAA
781  GAACACAAGAAAGTGAAGTCCACTAGGGATATTGTTCCTTTTTCTGAACTTGGAACTACT
841  CCCTCTGGTGGTGGATTTTTTCAGGGTATTTCTTTTCCTGAAATCTCCACCCGTCCTCCT
901  TTGGGCAGTACCGAACTACAGGCAGCTAAGAAAGTACATACTTCTAAGGGAGACCTACCT
961  AGGGAGCCTCTTGTTGCCACAAACTTGCCTGGCAGGGGACAGTTGCAGAAGTTAGCCTCT
1021 GAAAGGAATTTGTTTATTTCATGCAAGTCTAGCCATGATAGGTGTTTAGAGAAAAGTTCT
1081 TCGTCATCTTCTCAGCCTGAACACAGTGCCATGTTGGTCTCTACTGCAGCTTCTCCTTCA
1141 CTGATTAAAGAAACCACCACTGGTTACTATAAAGACATAGTAGAAAATATTTGCGGTAGA
1201 GAGAAAAGTGGAATTCAACCATTATGTCCTGAGAGGTCCCATATTTCAGATCAATCGCCT
1261 CTCTCCAGTAAAAGGAAAGCACTAGAAGAGTCTGAGAGCTCACAACTAATTTCTCCGCCA
1321 CTTGCCCAGGCAATCAGAGATTATGTCAATTCTCTGTTGGTCCAGGGTGGGGTAGGTAGT
1381 TTGCCTGGAACTTCTAACTCTATGCCCCCACTGGATGTAGAAAACATACAGAAGAGAATT
1441 GATCAGTCTAAGTTTCAAGAAACTGAATTCCTGTCTCCTCCAAGAAAAGTCCCTAGACTG
1501 AGTGAGAAGTCAGTGGAGGAAAGGGATTCAGGTTCCTTTGTGGCATTTCAGAACATACCT
1561 GGATCCGAACTGATGTCTTCTTTTGCCAAAACTGTTGTCTCTCATTCACTCACTACCTTA
1621 GGTCTAGAAGTGGCTAAGCAATCACAGCATGATAAAATAGATGCCTCAGAACTATCTTTT
1681 CCCTTCCATGAATCTATTTTAAAAGTAATTGAAGAAGAATGGCAGCAAGTTGACAGGCAG
1741 CTGCCTTCACTGGCATGCAAATATCCAGTTTCTTCCAGGGAGGCAACACAGATATTATCA
1801 GTTCCAAAAGTAGATGATGAAATCCTAGGGTTTATTTCTGAAGCCACTCCACTAGGAGGT
1861 ATTCAAGCAGCCTCCACTGAGTCTTGCAATCAGCAGTTGGACTTAGCACTCTGTAGAGCA
1921 TATGAAGCTGCAGCATCAGCATTGCAGATTGCAACTCACACTGCCTTTGTAGCTAAGGCT
1981 ATGCAGGCAGACATTAGTCAAGCTGCACAGATTCTTAGCTCAGATCCTAGTCGTACCCAC
2041 CAAGCGCTTGGGATTCTGAGCAAAACATATGATGCAGCCTCATATATTTGTGAAGCTGCA
2101 TTTGATGAAGTGAAGATGGCTGCCCATACCATGGGAAATGCCACTGTAGGTCGTCGATAC
2161 CTCTGGCTGAAGGATTGCAAAATTAATTTAGCTTCTAAGAATAAGCTGGCTTCCACTCCC
2221 TTTAAAGGTGGAACATTATTTGGAGGAGAAGTATGCAAAGTAATTAAAAAGCGTGGAAAT
2281 AAACACTAGTAAAATTAAGGACAAAAAGACATCTATCTTATCTTTCAGGTACTTTATGCC
2341 AACATTTTCTTTTCTGTTAAGGTTGTTTTAGTTTCCAGATAGGGCTAATTACAAAATGTT
2401 AAGCTTCTACCCATCAAATTACAGTATAAAAGTAATTGCCTGTGTAGAACTACTTGTCTT
2461 TTCTAAAGATTTGCGTAGATAGGAAGCCTG
```

Figure 5.3.2: *LAP2* exon 4 cDNA sequence

LAP2 sequence derived from PubMed (NM_003276; *Homo sapiens* thymopoietin (TMPO), transcript variant 1, mRNA). Nucleotides highlighted in teal code for exons 1–3, while those highlighted in dark grey code for exon 4. ATG: start of exon 1; GGA: start of exon 4; TAG: end

of exon 4. Additional information regarding gene sequence and structure was sourced from Harris et al. (1994). 3 different sets of primers used to amplify the exon 4 of *LAP2* have been colour coded:
LAP2α4.1F/R:TCTTGTTGCCACAAACTTGC/GGCAGCCATCTTCACTTCAT
LAP2α4.2F/RCCAGGGTGGGGTAGGTAGTT/AAATGCCACAAAGGAACCTG
LAP2α4.3F/R:ACCTGGATCCGAACTGATGT/CAGGCTTCCTATCTACGCAAA

```
20761 TTTTGGAGAATTGTAAAAACATAAGTAAAGCAGGAAACAGAAAACAACTTAGAGACTAAT
20821 ATGTGATCTAGAAAGCGTTAAATTGTTTGTACCAGGCTTCCTATCTACGCAAATCTTTAG
20881 AAAAGACAAGTAGTTCTACACAGGCAATTACTTTTATACTGTAATTTGATGGGTAGAAGC
20941 TTAACATTTTGTAATTAGCCCTATCTGGAAACTAAAACAACCTTAACAGAAAAGAAAATG
21001 TTGGCATAAAGTACCTGAAAGATAAGATAGATGTCTTTTTGTCCTTAATTTTACTAGTGT
21061 TTATTTCCACGCTTTTTAATTACTTTGCATACTTCTCCTCCAAATAATGTTCCACCTTTA
21121 AAGGGAGTGGAAGCCAGCTTATTCTTAGAAGCTAAATTAATTTTGCAATCCTTCAGCCAG
21181 AGGTATCGACGACCTACAGTGGCATTTCCCATGGTATGGGCAGCCATCTTCACTTCATCA
21241 AATGCAGCTTCACAAATATATGAGGCTGCATCATATGTTTTGCTCAGAATCCCAAGCGCT
21301 TGGTGGGTACGACTAGGATCTGAGCTAAGAATCTGTGCAGCTTGACTAATGTCTGCCTGC
21361 ATAGCCTTAGCTACAAAGGCAGTGTGAGTTGCAATCTGCAATGCTGATGCTGCAGCTTCA
21421 TATGCTCTACAGAGTGCTAAGTCCAACTGCTGATTGCAAGACTCAGTGGAGGCTGCTTGA
21481 ATACCTCCTAGTGGAGTGGCTTCAGAAATAAACCCTAGGATTTCATCATCTACTTTTGGA
21541 ACTGATAATATCTGTGTTGCCTCCCTGGAAGAAACTGGATATTTGCATGCCAGTGAAGGC
21601 AGCTGCCTGTCAACTTGCTGCCATTCTTCTTCAATTACTTTTAAAATAGATTCATGGAAG
21661 GGAAAAGATAGTTCTGAGGCATCTATTTTATCATGCTGTGATTGCTTAGCCACTTCTAGA
21721 CCTAAGGTAGTGAGTGAATGAGAGACAACAGTTTTGGCAAAAGAAGACATCAGTTCGGAT
21781 CCAGGTATGTTCTGAAATGCCACAAAGGAACCTGAATCCCTTTCCTCCACTGACTTCTCA
21841 CTCAGTCTAGGGACTTTTCTTGGAGGAGACAGGAATTCAGTTTCTTGAAACTTAGACTGA
21901 TCAATTCTCTTCTGTATGTTTTCTACATCCAGTGGGGGCATAGAGTTAGAAGTTCCAGGC
21961 AAACTACCTACCCCACCCTGGACCAACAGAGAATTGACATAATCTCTGATTGCCTGGGCA
22021 AGTGGCGGAGAAATTAGTTGTGAGCTCTCAGACTCTTCTAGTGCTTTCCTTTTACTGGAG
22081 AGAGGCGATTGATCTGAAATATGGGACCTCTCAGGACATAATGGTTGAATTCCACTTTTC
22141 TCTCTACCGCAAATATTTTCTACTATGTCTTTATAGTAACCAGTGGTGGTTTCTTTAATC
22201 AGTGAAGGAGAAGCTGCAGTAGAGACCAACATGGCACTGTGTTCAGGCTGAGAAGATGAC
22261 GAAGAACTTTTCTCTAAACACCTATCATGGCTAGACTTGCATGAAATAAACAAATTCCTT
22321 TCAGAGGCTAACTTCTGCAACTGTCCCCTGCCAGGCAAGTTTGTGGCAACAAGAGGCTCC
22381 CTAGGTAGGTCTCCCTTAGAAGTATGTACTTTCTTAGCTGCCTGTAGTTCGGTACTGCCC
22441 AAAGGAGGACGGGTGGAGATTTCAGGAAAAGAAATACCCTGAAAAAATCCACCACCAGAG
22501 GGAGTAGTTCCAAGTTCAGAAAAAGGAACAATATCCCTAGTGGACTTCACTTTCTTGTGT
22561 TCTTTCTTCTTTCCTGTAGAGGCAAAAGAGGCAGGAAGTTTAAGCATTACCTGTGTTTGA
22621 GCTGATTTTATTCTTTGCCTCTTTGCTAAAAATAGTGCTGTCAAAGGAAAAGACTATAAT
22681 TTCATATTCTGAACTAATCTGCCAGATTTGCCCTGGTAGACAAAGCTTATTGAGATATAA
22741 ACAATCTGGATCAAAATAAATAATCACAAGTCATATTAATTAAAAGTTTACAAAAATCAA
```

Figure 5.3.3: *LAP2* exon 4 genomic DNA sequence

Sequence derived from PubMed (selected region of AC013418; *Homo sapiens* 12 BAC RP11-181C3 (Roswell Park Cancer Institute Human BAC Library) complete sequence). Note that the sequence is in reverse orientation to the *LAP2* exon 4 cDNA (i.e. exons are coded in descending order). Gene information sourced from Harris et al., (1994; 1995). Protein coding nucleotide sequence is highlighted in dark grey (as per Harris et al., 1994). 5' exon/ intron boundary is denoted by the black arrow. Primer pairs used to amplify exon 4 plus the 5'exon/ intron boundary have been colour coded:

LAP2αintron/exon4F/R; GCTTTGTCTACCAGGGCAAA/ CCAGTGGGGGCATAGAGTTA
LAP2α4.1F/R:TCTTGTTGCCACAAACTTGC/GGCAGCCATCTTCACTTCAT
LAP2α4.2F/RCCAGGGTGGGGTAGGTAGTT/AAATGCCACAAAGGAACCTG
LAP2α4.3F/R:ACCTGGATCCGAACTGATGT/CAGGCTTCCTATCTACGCAAA

5.3.2 Sequencing

Once exon amplification was successful, the bands were extracted from the agarose gel; from this gel, DNA was isolated and sent away for sequencing as per the description in the methods and materials section, 5.2. For each DNA sample, the sequencing was performed twice, using both forward and reverse primers. Thus, any discrepancies present in both forward and reverse sequences were unlikely to be as a consequence of inaccurate sequencing. On receiving the results, a BLAST search was performed; this system compares the sequence against those in the database and highlights those identical or most similar to the sequence in the human genome.

Unfortunately, sequencing did not always produce a positive result. This was not due to contamination but to lack of DNA; this is likely to be as a result of using an inaccurate DNA quantification system. As a result, at times, far higher concentrations than required have been sent away for sequencing.

5.3.3 Determining the *EMD* mutation present in X-EDMD carrier, ED5364

In order to determine the location and nature of the *EMD* mutation present in ED5364, genomic DNA from this cell line was extracted and then employed to sequence *EMD*. A summary of sequencing results for ED5364 exon 4 can be seen in figure 5.3.4; full details can be found in Appendix (ED5364: *EMD*).

This mutation search was successful; a heterozygous point mutation (c.315T>G) was discovered in exon 4 of *EMD*. This can be seen by the presence of half-peaks in both forward and reverse readings at position 315 (see figure 5.3.5). At the amino acid level, this mutation is predicted to lead to tyrosine (TAT) being replaced by a stop codon (TAG) at residue 105 (p.Tyr105X). The presence of the mutation was confirmed twice.

```
   1  GCGCGCAGGCCCCGCCCCTCTCACCCCGCCGCACGCCACAGGGTGACGTCTGGGCTCCCA
  61  GCCGCATCGCCCTGACTCCCGCGCGGGCCCCGCCCCCTGCCGCTAGCCAATCTGTGCGTT
 121  TGTGACTTTTGGGCCCGCAGCCCCGCCTGCTCCCACAGCGATACCGGTTTGCATTGCCCT
 181  GACTCCCGCGCGGGCCCCGCCCCCTACGCCGCTAGCCAATCCATGCATTAGTGGCGTCCG
 241  GGCTCGCAGTACCGCTCGCTCCCACCGCGAGACCTTCTGCTCCGCGCCCGCGCGGGCCCC
 301  TCCCCCTCCATCGCTAGCCAATCCCCGTTTTGTGACGTATGGGCTCGCGGCCCCGCTCGC
 361  TCCCACCGCGAGACCTTTTGCTCCGCGCCCGCGCGGGCCCCGCCCCCTCCATCACTAGCC
 421  AATCCCCGTGCTTGTGACATATGGGCTTGCGGCCCCGCCCGCTCCCATCGCGAGACCGGT
 481  TCCCACCGCCCTGACTCCCGGGCGGGCCCCGCCCTCTCCGCCGCTAGCCAATCCTCGCGT
 541  TGATGACGTTTGGGCTCGCGGCCCCAGCCTCCCAGCTCTCAGGGCACGGCCGGTCTGTGC
 601  CGGCTGCTCCCGCGGTTAGGTCCCGCCCCGCGCAGCGCGCGCAGCCTGCGGAGCCAGCGG
 661  CCGTGACGCGACAACGATTCGGCTGTGACGCGACAACGATTCGGCTGTGACGCGAGCGCG
 721  GCCGCTCCCGATGCGCTCGTGCCGCCCCCGCCGTGCTCCTCGGCAGCCGTTGCTCGGCCG
 781  GTTTTGGTAGGCCCGGGCCGCCGCCAGGCCTCCGCCTGAGCCCGCACCCGCCATGGACAA
 841  CTACGCAGATCTTTCGGATACCGAGCTGACCACCTTGCTGCGCCGGTACAACATCCCGCA
 901  CGGGCCTGTAGTAGGTACGCGGCGGCGGGCGGGACCCCTTCCGGGCCCCCTCCTCGTGCT
 961  CCGCCTCGCGACCTCCCCGCTGCCCTCCCCGCGCGCCTTCCCCGGCCCGCGGCCCTGACC
1021  GCCCCGTGTCCGGCCAGGATCAACTCGTAGGCTTTACGAGAAGAAGATCTTCGAGTACGA
1081  GACCCAGAGGCGGCGGCTCTCGCCCCCCAGCTCGTCCGCCGCCTCCTCTTATAGCTTCTC
1141  TGGTGAGAGCCTCGCCTGTGGGGACAGCCTGGGACGCGGGGAGGATGGGGTCGCGAGGGT
1201  GTGGCAGGGGGGCCGGTCGAGAGCGGCACTGGAGAAAGGGGAGGGAAGTCTGGGGGGGCA
1261  AACAGTTCTGTCTCCTCCTTTCAATCCAGACTTGAATTCGACTAGAGGGGATGCAGATAT
1321  GTATGATCTTCCCAAGAAAGAGGACGCTTTACTCTACCAGAGCAAGGGTAAGGCAGGGGT
1381  TGGGTGGGCACGCTGGCACCTTCACCCGACTTCGTCAGGGACCCCGCTCACAGGGAGGAC
1441  CTGAGACCTCAGTCCCAACCACTCCAGCAGCCTTAGGAGGGAGAAACTGTTACAGGTCCC
1501  GAAATGGGATTCAGATTAGGGCCATCAGGCCAGGCGGGGCACACCGATGCCCCCTCTGCT
1561  ACCGCTGCCCCCCTTCCCAAGGCTACAATGACGACTACTATGAAGAGAGCTACTTCACCA
1621  CCAGGACTTATGGGGAGCCCGAGTCTGCCGGCCCGTCCAGGGCTGTCCGCCAGTCAGTGA
1681  CTTCATTCCCAGATGCTGACGCTTTCCATCACCAGGTGAGCTGGCTGGCAGGCGTCCTGT
1741  ACTTGGGTACAACCTAGGGGATCGCGGCTGTGTTTGGATAAATCCAGGGGGGCACTGGGT
1801  ACAAATGGTGGCTCTTGGGCCTCCGGGGAGACTCTGTGTGACTAGAGCACCCTGGTCTGG
1861  GATCTAGGCTCAGACTCTTCCTGAGAGTCCTGGGGGCAAAAGGGGATGCTGGGGCATGAG
1921  CACAAGTGGCAAGGCCCCATGGATAAAGGGCTGAACACCCAGAGCCATTCAGGAGGGTGT
1981  GGGTTCCTGGCCTCTAACCAAAGGTCAGAGGGGACTGGCTGGGGAAGTTTGGACTGAGGG
2041  ACATGACAGGGCCATGGTGGCCCTGCCAGCCAGTCCCCTCGCCCTGACTCTCTTCTGCAG
2101  GTGCATGATGACGATCTTTTGTCTTCTTCTGAAGAGGAGTGCAAGGATAGGTGCGTAGTG
2161  GGGGAGCCCAGGGACGGGCTGGTTCTGGGTCCAGGCTCCTGGCCCACTTGCTCCCCTCTT
2221  TTGCCTCAGGGAACGCCCCATGTACGGCCGGGACAGTGCCTACCAGAGCATCACGCACTA
2281  CCGCCCTGTTTCAGCCTCCAGGAGCTCCCTGGACCTGTCCTATTATCCTACTTCCTCCTC
2341  CACCTCTTTTATGTCCTCCTCATCATCTTCCTCTTCATGGCTCACCCGCCGTGCCATCCG
2401  GCCTGAAAACCGTGCTCCTGGGGCTGGGCTGGGCCAGGATCGCCAGGTCCCGCTCTGGGG
2461  CCAGCTGCTGCTTTTCCTGGTCTTTGTGATCGTCCTCTTCTTCATTTACCACTTCATGCA
2521  GGCTGAAGAAGGCAACCCCTTCTAGAGGGAGCCATGAGGGTCTGGGCTTCAGAGCTAGGT
2581  CTTTGGGGAAGTCCTGGCTGACTGCCTTAGCAGTGGGGGTGGGGGTGGGGGCAGGGGCAG
2641  GGGCTTTATGTGTTTTTGCTTGGGGGGCGCTGGGCCTAGCCCAGAGTAGTGCTTGCTCCC
2701  CCTGCCTTGTCCCACCAGGGAGGCAGCAGACTCAGGCCCTCCATGGTCCTCTTTGTCATT
2761  TTGTTGACATGCATTCCTCCTTTTGTCATCTTGTTGGGGGGAGGGGATTAACCAAAGGCC
2821  ACCCTGACTTTGTTTTTGTGGACACACAATAAAAGCCCCGTTTATTTGTAATGCGTTGGC
2881  TCTTCCTGGAGGAGAGGGTTGGGCTCCCATGGCAAGGGCCTCTGCGTCTTGGGGCTCCAG
2941  GATTGCAATCCGGCTTTGTTGGGTCCGCATTTTTGCTTTAGTCTGGGGATAGGAATCAAA
3001  TGTTACCCAGAGATGTTTGTGTTTTGTTTGGGAGTTTTATTCCCTAACTCATTCCCCAAA
3061  GCACGTGTAACTGCTTATACATATAATCGTGGTACAACAAGGTATATACAGAGAACCCAC
3121  TTGGAAATTCAGGCAAAGCTGCATGCACGCTACCAGCAGTCTGCGGGTGTTTTAACTGGA
3181  AAAAGCTGAAGTCCACCTCGGTGTCCAATGGCATGGGGATGGAAAGAAAATGAGGCGTCT
3241  CTGGCACATCATTCTCAGCTCCTGGAACTGCTGCTTGTTTAACATGGGAGAAAAGCTCCA
3301  AAGGCTGAAATGCCCCATCATCCCTGGGTGATTGAATTC
```

E1 E2 E3 E4 E5 E6

Figure 5.3.4: Sequencing of *EMD* in ED5364

Sequence derived from PubMed (X86810.1). Gene information sourced from Bione et al., (1994; 1995). Forward primers for each exon are highlighted in green, while reverse primers

are highlighted in red. Overlapping primer sequences are highlighted in dark green. Sequenced regions are highlighted in turquoise. A database discrepancy is highlighted in yellow. A confirmed heterozygous mutation is highlighted in black. Nucleotides highlighted in dark grey are protein coding bases which have not been successfully sequenced. Non-protein coding cDNA sequence is highlighted in light grey. E = exon.

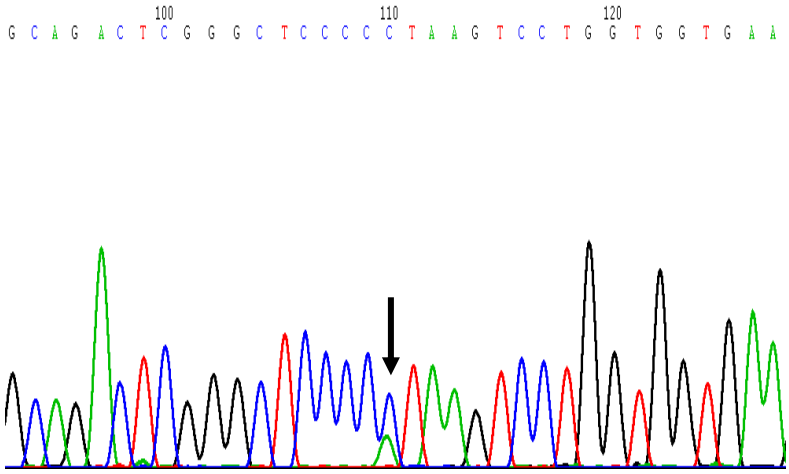

Figure 5.3.5: The identification of an *EMD* mutation in the X-EDMD carrier.
The arrow highlights the presence of a heterozygous point mutation at nucleotide 315 (c.315T>G) of *EMD*; this affects residue 105 (p.Tyr105X) of the protein and results in the production of a premature stop codon.

5.3.4 Attempting to determine the disease-causing mutation present in atypical HGPS cell lines, AG08466 and AG11572

5.3.4.1 Overview

Since neither of the atypical HGPS cell lines, AG08466 or AG11572, harbour a *LMNA* mutation, both *EMD* and *LAP2* (exon 4) were selected for sequencing. Both proteins are binding partners of lamin A and indeed, are documented to cause laminopathy-based disease when defective. Thus, the aim of this section was to determine whether either cell line exhibits an *EMD* or *LAP2* (exon 4) mutation.

5.3.4.2 *EMD*

The majority of the 6 *EMD* exons have been successfully sequenced in both AG08466 and AG11572; however, so far no mutations have been detected. A database discrepancy has been observed; at positions 1581–1583, the mRNA sequence

(X86810.1) predicts GGG; however, in all cell lines examined (i.e. AG08466, AG11572 and ED5364), there appears to be only 2 (nucleotide highlighted in yellow; see figures 5.3.4, 5.3.6 and 5.3.7). A summary of sequencing results for AG08466 and AG11572 can be seen in figures 5.3.6 and 5.3.7, respectively; full details can be found in Appendix (AG08466: *EMD* and AG11572: *EMD*).

```
   1  GCGCGCAGGCCCCGCCCCTCTCACCCCGCCGCACGCCACAGGGTGACGTCTGGGCTCCCA
  61  GCCGCATCGCCCTGACTCCCGCGCGGGCCCCGCCCCCTGCCGCTAGCCAATCTGTGCGTT
 121  TGTGACTTTTGGGCCCGCAGCCCCGCCTGCTCCCACAGCGATACCGGTTTGCATTGCCCT
 181  GACTCCCGCGCGGGCCCCGCCCCCTACGCCGCTAGCCAATCCATGCATTAGTGGCGTCCG
 241  GGCTCGCAGTACCGCTCGCTCCCACCGCGAGACCTTCTGCTCCGCGCCCGCGCGGGCCCC
 301  TCCCCCTCCATCGCTAGCCAATCCCCGTTTTGTGACGTATGGGCTCGCGGCCCCGCTCGC
 361  TCCCACCGCGAGACCTTTTGCTCCGCGCCCGCGCGGGCCCCGCCCCCTCCATCACTAGCC
 421  AATCCCCGTGCTTGTGACATATGGGCTTGCGGCCCCGCCCGCTCCCATCGCGAGACCGGT
 481  TCCCACCGCCCTGACTCCCGGGCGGGCCCCGCCCTCTCCGCCGCTAGCCAATCCTCGCGT
 541  TGATGACGTTTGGGCTCGCGGCCCCAGCCTCCCAGCTCTCAGGGCACGGCCGGTCTGTGC
 601  CGGCTGCTCCCGCGGTTAGGTCCCGCCCCGCGCAGCGCGCGCAGCCTGCGGAGCCAGCGG
 661  CCGTGACGCGACAACGATTCGGCTGTGACGCGACAACGATTCGGCTGTGACGCGAGCGCG
 721  GCCGCTCCCGATGCGCTCGTGCCGCCCCCGCCGTGCTCCTCGGCAGCCGTTGCTCGGCCG
 781  GTTTTGGTAGGCCCGGGCCGCCGCCAGGCCTCCGCCTGAGCCCGCACCCGCCATGGACAA
 841  CTACGCAGATCTTTCGGATACCGAGCTGACCACCTTGCTGCGCCGGTACAACATCCCGCA
 901  CGGGCCTGTAGTAGGTACGCGGCGGCGGGCGGGACCCCTTCCGGGCCCCCTCCTCGTGCT
 961  CCGCCTCGCGACCTCCCCGCTGCCCTCCCCGCGCGCCTTCCCCGGCCCGCGGCCCTGACC
1021  GCCCCGTGTCCGGCCAGGATCAACTCGTAGGCTTTACGAGAAGAAGATCTTCGAGTACGA
1081  GACCCAGAGGCGGCGGCTCTCGCCCCCCAGCTCGTCCGCCGCCTCCTCTTATAGCTTCTC
1141  TGGTGAGAGCCTCGCCTGTGGGGACAGCCTGGGACGCGGGGAGGATGGGGTCGCGAGGGT
1201  GTGGCAGGGGGGCCGGTCGAGAGCGGCACTGGAGAAAGGGGAGGGAAGTCTGGGGGGGCA
1261  AACAGTTCTGTCTCCTCCTTTCAATCCAGACTTGAATTCGACTAGAGGGGATGCAGATAT
1321  GTATGATCTTCCCAAGAAAGAGGACGCTTTACTCTACCAGAGCAAGGGTAAGGCAGGGGT
1381  TGGGTGGGCACGCTGGCACCTTCACCCGACTTCGTCAGGGACCCCGCTCACAGGGAGGAC
1441  CTGAGACCTCAGTCCCAACCACTCCAGCAGCCTTAGGAGGGAGAAACTGTTACAGGTCCC
1501  GAAATGGGATTCAGATTAGGGCCATCAGGCCAGGCGGGGCACACCGATGCCCCCTCTGCT
1561  ACCGCTGCCCCCCTTCCCAAGGCTACAATGACGACTACTATGAAGAGAGCTACTTCACCA
1621  CCAGGACTTATGGGGAGCCCGAGTCTGCCGGCCCGTCCAGGGCTGTCCGCCAGTCAGTGA
1681  CTTCATTCCCAGATGCTGACGCTTTCCATCACCAGGTGAGCTGGCTGGCAGGCGTCCTGT
1741  ACTTGGGTACAACCTAGGGGATCGCGGCTGTGTTTGGATAAATCCAGGGGGGCACTGGGT
1801  ACAAATGGTGGCTCTTGGGCCTCCGGGGAGACTCTGTGTGACTAGAGCACCCTGGTCTGG
1861  GATCTAGGCTCAGACTCTTCCTGAGAGTCCTGGGGGCAAAAGGGGATGCTGGGGCATGAG
1921  CACAAGTGGCAAGGCCCCATGGATAAAGGGCTGAACACCCAGAGCCATTCAGGAGGGTGT
1981  GGGTTCCTGGCCTCTAACCAAAGGTCAGAGGGGACTGGCTGGGGAAGTTTGGACTGAGGG
2041  ACATGACAGGGCCATGGTGGCCCTGCCAGCCAGTCCCCTCGCCCTGACTCTCTTCTGCAG
2101  GTGCATGATGACGATCTTTTGTCTTCTTCTGAAGAGGAGTGCAAGGATAGGTGCGTAGTG
2161  GGGGAGCCCAGGGACGGGCTGGTTCTGGGTCCAGGCTCCTGGCCCACTTGCTCCCCTCTT
2221  TTGCCTCAGGGAACGCCCCATGTACGGCCGGGACAGTGCCTACCAGAGCATCACGCACTA
2281  CCGCCCTGTTTCAGCCTCCAGGAGCTCCCTGGACCTGTCCTATTATCCTACTTCCTCCTC
2341  CACCTCTTTTATGTCCTCCTCATCATCTTCCTCTTCATGGCTCACCCGCCGTGCCATCCG
2401  GCCTGAAAACCGTGCTCCTGGGGCTGGGCTGGGCCAGGATCGCCAGGTCCCGCTCTGGGG
2461  CCAGCTGCTGCTTTTCCTGGTCTTTGTGATCGTCCTCTTCTTCATTTACCACTTCATGCA
2521  GGCTGAAGAAGGCAACCCCTTCTAGAGGGAGCCATGAGGGTCTGGGCTTCAGAGCTAGGT
2581  CTTTGGGGAAGTCCTGGCTGACTGCCTTAGCAGTGGGGGTGGGGGTGGGGGCAGGGGCAG
2641  GGGCTTTATGTGTTTTTGCTTGGGGGGCGCTGGGCCTAGCCCAGAGTAGTGCTTGCTCCC
2701  CCTGCCTTGTCCCACCAGGGAGGCAGCAGACTCAGGCCCTCCATGGTCCTCTTTGTCATT
2761  TTGTTGACATGCATTCCTCCTTTTGTCATCTTGTTGGGGGGAGGGGATTAACCAAAGGCC
2821  ACCCTGACTTTGTTTTTGTGGACACACAATAAAAGCCCCGTTTATTTGTAATGCGTTGGC
2881  TCTTCCTGGAGGAGAGGGTTGGGCTCCCATGGCAAGGGCCTCTGCGTCTTGGGGCTCCAG
2941  GATTGCAATCCGGCTTTGTTGGGTCCGCATTTTTGCTTTAGTCTGGGGATAGGAATCAAA
```

E1 E2 E3 E4 E5 E6

```
3001 TGTTACCCAGAGATGTTTGTGTTTTGTTTGGGAGTTTTATTCCCTAACTCATTCCCCAAA
3061 GCACGTGTAACTGCTTATACATATAATCGTGGTACAACAAGGTATATACAGAGAACCCAC
3121 TTGGAAATTCAGGCAAAGCTGCATGCACGCTACCAGCAGTCTGCGGGTGTTTTAACTGGA
3181 AAAAGCTGAAGTCCACCTCGGTGTCCAATGGCATGGGGATGGAAAGAAAATGAGGCGTCT
3241 CTGGCACATCATTCTCAGCTCCTGGAACTGCTGCTTGTTTAACATGGGAGAAAAGCTCCA
3301 AAGGCTGAAATGCCCCATCATCCCTGGGTGATTGAATTC
```

Figure 5.3.6: Sequencing of *EMD* in AG08466

Sequence derived from PubMed (X86810.1). Gene information sourced from Bione et al., (1994; 1995). Forward primers for each exon are highlighted in green, while reverse primers are highlighted in red. Overlapping primer sequences are highlighted in dark green. Sequenced regions are highlighted in turquoise. A database discrepancy is highlighted in yellow. Nucleotides highlighted in dark grey are protein coding bases which have not been successfully sequenced. Non-protein coding cDNA sequence is highlighted in light grey. E = exon.

```
   1 GCGCGCAGGCCCCGCCCCTCTCACCCCGCCGCACGCCACAGGGTGACGTCTGGGCTCCCA
  61 GCCGCATCGCCCTGACTCCCGCGCGGGCCCCGCCCCCTGCCGCTAGCCAATCTGTGCGTT
 121 TGTGACTTTTGGGCCCGCAGCCCCGCCTGCTCCCACAGCGATACCGGTTTGCATTGCCCT
 181 GACTCCCGCGCGGGCCCCGCCCCCTACGCCGCTAGCCAATCCATGCATTAGTGGCGTCCG
 241 GGCTCGCAGTACCGCTCGCTCCCACCGCGAGACCTTCTGCTCCGCGCCCGCGCGGGCCCC
 301 TCCCCCTCCATCGCTAGCCAATCCCCGTTTTGTGACGTATGGGCTCGCGGCCCCGCTCGC
 361 TCCCACCGCGAGACCTTTTGCTCCGCGCCCGCGCGGGCCCCGCCCCCTCCATCACTAGCC
 421 AATCCCCGTGCTTGTGACATATGGGCTTGCGGCCCCGCCCGCTCCCATCGCGAGACCGGT
 481 TCCCACCGCCCTGACTCCCGGGCGGGCCCCGCCCTCTCCGCCGCTAGCCAATCCTCGCGT
 541 TGATGACGTTTGGGCTCGCGGCCCCAGCCTCCCAGCTCTCAGGGCACGGCCGGTCTGTGC
 601 CGGCTGCTCCCGCGGTTAGGTCCCGCCCCGCGCAGCGCGCGCAGCCTGCGGAGCCAGCGG
 661 CCGTGACGCGACAACGATTCGGCTGTGACGCGACAACGATTCGGCTGTGACGCGAGCGCG
 721 GCCGCTCCCGATGCGCTCGTGCCGCCCCCGCCGTGCTCCTCGGCAGCCGTTGCTCGGCCG
 781 GTTTTGGTAGGCCCGGGCCGCCGCCAGGCCTCCGCCTGAGCCCGCACCCGCCATGGACAA
 841 CTACGCAGATCTTTCGGATACCGAGCTGACCACCTTGCTGCGCCGGTACAACATCCCGCA
 901 CGGGCCTGTAGTAGGTACGCGGCGGCGGGCGGGACCCCTTCCGGGCCCCCTCCTCGTGCT
 961 CCGCCTCGCGACCTCCCCGCTGCCCTCCCCGCGCGCCTTCCCCGGCCCGCGGCCCTGACC
1021 GCCCCGTGTCCGGCCAGGATCAACTCGTAGGCTTTACGAGAAGAAGATCTTCGAGTACGA
1081 GACCCAGAGGCGGCGGCTCTCGCCCCCCAGCTCGTCCGCCGCCTCCTCTTATAGCTTCTC
1141 TGGTGAGAGCCTCGCCTGTGGGGACAGCCTGGGACGCGGGGAGGATGGGGTCGCGAGGGT
1201 GTGGCAGGGGGGCCGGTCGAGAGCGGCACTGGAGAAAGGGGAGGGAAGTCTGGGGGGGCA
1261 AACAGTTCTGTCTCCTCCTTTCAATCCAGACTTGAATTCGACTAGAGGGGATGCAGATAT
1321 GTATGATCTTCCCAAGAAAGAGGACGCTTTACTCTACCAGAGCAAGGGTAAGGCAGGGGT
1381 TGGGTGGGCACGCTGGCACCTTCACCCGACTTCGTCAGGGACCCCGCTCACAGGGAGGAC
1441 CTGAGACCTCAGTCCCAACCACTCCAGCAGCCTTAGGAGGGAGAAACTGTTACAGGTCCC
1501 GAAATGGGATTCAGATTAGGGCCATCAGGCCAGGCGGGGCACACCGATGCCCCCTCTGCT
1561 ACCGCTGCCCCCCTTCCCAAGGCTACAATGACGACTACTATGAAGAGAGCTACTTCACCA
1621 CCAGGACTTATGGGGAGCCCGAGTCTGCCGGCCCGTCCAGGGCTGTCCGCCAGTCAGTGA
1681 CTTCATTCCCAGATGCTGACGCTTTCCATCACCAGGTGAGCTGGCTGGCAGGCGTCCTGT
1741 ACTTGGGTACAACCTAGGGGATCGCGGCTGTGTTTGGATAAATCCAGGGGGGCACTGGGT
1801 ACAAATGGTGGCTCTTGGGCCTCCGGGGAGACTCTGTGTGACTAGAGCACCCTGGTCTGG
1861 GATCTAGGCTCAGACTCTTCCTGAGAGTCCTGGGGGCAAAAGGGGATGCTGGGGCATGAG
1921 CACAAGTGGCAAGGCCCCATGGATAAAGGGCTGAACACCCAGAGCCATTCAGGAGGGTGT
1981 GGGTTCCTGGCCTCTAACCAAAGGTCAGAGGGGACTGGCTGGGGAAGTTTGGACTGAGGG
2041 ACATGACAGGGCCATGGTGGCCCTGCCAGCCAGTCCCCTCGCCCTGACTCTCTTCTGCAG
2101 GTGCATGATGACGATCTTTTGTCTTCTTCTGAAGAGGAGTGCAAGGATAGGTGCGTAGTG
2161 GGGGAGCCCAGGGACGGGCTGGTTCTGGGTCCAGGCTCCTGGCCCACTTGCTCCCCTCTT
2221 TTGCCTCAGGGAACGCCCCATGTACGGCCGGGACAGTGCCTACCAGAGCATCACGCACTA
2281 CCGCCCTGTTTCAGCCTCCAGGAGCTCCCTGGACCTGTCCTATTATCCTACTTCCTCCTC
2341 CACCTCTTTTATGTCCTCCTCATCATCTTCCTCTTCATGGCTCACCCGCCGTGCCATCCG
2401 GCCTGAAAACCGTGCTCCTGGGGCTGGGCTGGGCCAGGATCGCCAGGTCCCGCTCTGGGG
2461 CCAGCTGCTGCTTTTCCTGGTCTTTGTGATCGTCCTCTTCTTCATTTACCACTTCATGCA
2521 GGCTGAAGAAGGCAACCCCTTCTAGAGGGAGCCATGAGGGTCTGGGCTTCAGAGCTAGGT
```

E1 E2 E3 E4 E5 E6

```
2581 CTTTGGGGAAGTCCTGGCTGACTGCCTTAGCAGTGGGGGTGGGGGTGGGGGCAGGGGCAG
2641 GGGCTTTATGTGTTTTTGCTTGGGGGGCGCTGGGCCTAGCCCAGAGTAGTGCTTGCTCCC
2701 CCTGCCTTGTCCCACCAGGGAGGCAGCAGACTCAGGCCCTCCATGGTCCTCTTTGTCATT
2761 TTGTTGACATGCATTCCTCCTTTTGTCATCTTGTTGGGGGGAGGGGATTAACCAAAGGCC
2821 ACCCTGACTTTGTTTTTGTGGACACACAATAAAAGCCCCGTTTATTTGTAATGCGTTGGC
2881 TCTTCCTGGAGGAGAGGGTTGGGCTCCCATGGCAAGGGCCTCTGCGTCTTGGGGCTCCAG
2941 GATTGCAATCCGGCTTTGTTGGGTCCGCATTTTTGCTTTAGTCTGGGGATAGGAATCAAA
3001 TGTTACCCAGAGATGTTTGTGTTTTGTTTGGGAGTTTTATTCCCTAACTCATTCCCCAAA
3061 GCACGTGTAACTGCTTATACATATAATCGTGGTACAACAAGGTATATACAGAGAACCCAC
3121 TTGGAAATTCAGGCAAAGCTGCATGCACGCTACCAGCAGTCTGCGGGTGTTTTAACTGGA
3181 AAAAGCTGAAGTCCACCTCGGTGTCCAATGGCATGGGGATGGAAAGAAAATGAGGCGTCT
3241 CTGGCACATCATTCTCAGCTCCTGGAACTGCTGCTTGTTTAACATGGGAGAAAAGCTCCA
3301 AAGGCTGAAATGCCCCATCATCCCTGGGTGATTGAATTC
```

Figure 5.3.7: Sequencing of *EMD* in AG11572

Sequence derived from PubMed (X86810.1). Gene information sourced from Bione et al., (1994; 1995). Forward primers for each exon are highlighted in green, while reverse primers are highlighted in red. Overlapping primer sequences are highlighted in dark green. Sequenced regions are highlighted in turquoise. A database discrepancy is highlighted in yellow. Nucleotides highlighted in dark grey are protein coding bases which have not been successfully sequenced. Non-protein coding cDNA sequence is highlighted in light grey. E = exon.

5.3.4.3 *LAP2*

Part of exon 4 *LAP2* has been successfully sequenced in AG08466 (see figure 5.3.8); so far, no mutations have been observed. The whole of exon 4 *LAP2* (including the 5' intron and exon boundary) has been sequenced in AG11572 (see figures 5.3.9 and 5.3.10); again, no mutations have been identified. Full details of sequencing results can be found in Appendix (AG08466: *LAP2* exon 4 and AG11572: *LAP2* exon 4).

```
1    GTTCGTAGTTCGGCTCTGGGGTCTTTTGTGTCCGGGTCTGGCTTGGCTTTGTGTCCGCGA
61   GTTTTTGTTCCGCTCCGCAGCGCTCTTCCCGGGCAGGAGCCGTGAGGCTCGGAGGCGGCA
121  GCGCGGTCCCCGGCCAGGAGCAAGCGCGCCGGCGTGAGCGGCGGCGGCAAAGGCTGTGGG
181  GAGGGGGCTTCGCAGATCCCCGAGATGCCGGAGTTCCTGGAAGACCCCTCGGTCCTGACA
241  AAAGACAAGTTGAAGAGTGAGTTGGTCGCCAACAATGTGACGCTGCCGGCCGGGGAGCAG
301  CGCAAAGACGTGTACGTCCAGCTCTACCTGCAGCACCTCACGGCTCGCAACCGGCCGCCG
361  CTCCCCGCCGGCACCAACAGCAAGGGGCCCCCGGACTTCTCCAGTGACGAAGAGCGCGAG
421  CCCACCCCGGTCCTCGGCTCTGGGGCCGCCGCCGCGGGCCGGAGCCGAGCAGCCGTCGGC
481  AGGAAAGCCACAAAAAAAACTGATAAACCCAGACAAGAAGATAAAGATGATCTAGATGTA
541  ACAGAGCTCACTAATGAAGATCTTTTGGATCAGCTTGTGAAATACGGAGTGAATCCTGGT
601  CCTATTGTGGGAACAACCAGGAAGCTATATGAGAAAAAGCTTTTGAAACTGAGGGAACAA
661  GGAACAGAATCAAGATCTTCTACTCCTCTGCCAACAATTTCTTCTTCAGCAGAAAATACA
721  AGGCAGAATGGAAGTAATGATTCTGACAGATACAGTGACAATGAAGAAGGAAAGAAGAAA
781  GAACACAAGAAAGTGAAGTCCACTAGGGATATTGTTCCTTTTTCTGAACTTGGAACTACT
841  CCCTCTGGTGGTGGATTTTTTCAGGGTATTTCTTTTCCTGAAATCTCCACCCGTCCTCCT
901  TTGGGCAGTACCGAACTACAGGCAGCTAAGAAAGTACATACTTCTAAGGGAGACCTACCT
961  AGGGAGCCTCTTGTTGCCACAAACTTGCCTGGCAGGGGACAGTTGCAGAAGTTAGCCTCT
1021 GAAAGGAATTTGTTTATTTCATGCAAGTCTAGCCATGATAGGTGTTTAGAGAAAAGTTCT
1081 TCGTCATCTTCTCAGCCTGAACACAGTGCCATGTTGGTCTCTACTGCAGCTTCTCCTTCA
1141 CTGATTAAAGAAACCACCACTGGTTACTATAAAGACATAGTAGAAAATATTTGCGGTAGA
```

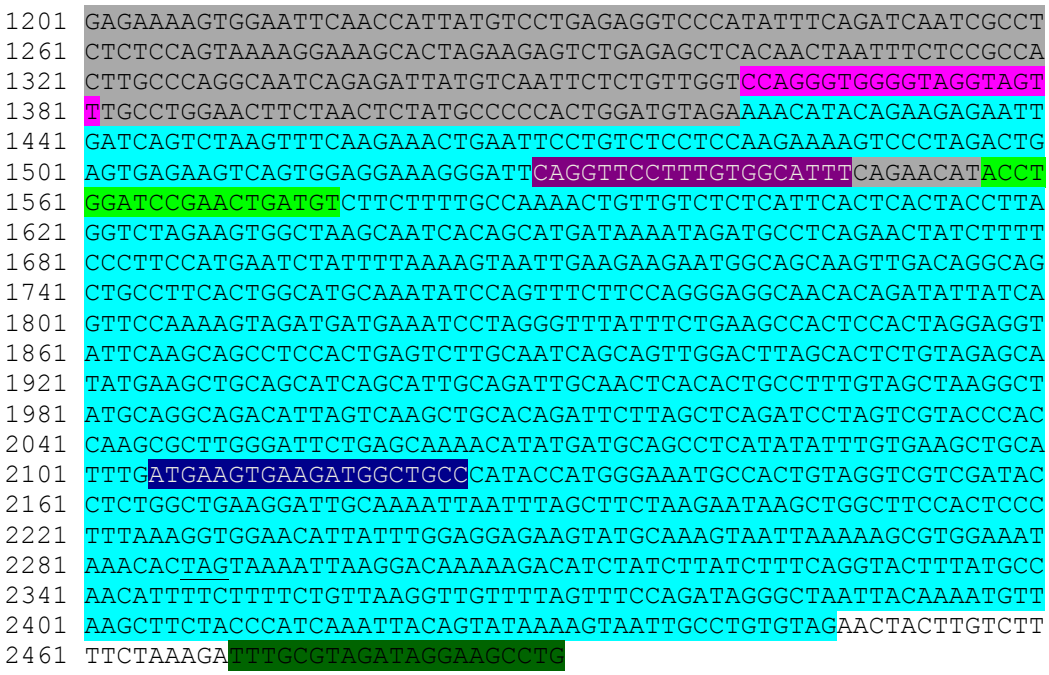

Figure 5.3.8: Sequencing of *LAP2* exon 4 in AG08466

LAP2 sequence derived from PubMed (NM_003276; *Homo sapiens* thymopoietin (TMPO), transcript variant 1, mRNA). Nucleotides highlighted in black code for exons 1–3. Successfully sequenced nucleotides are highlighted in turquoise. Nucleotides highlighted in dark grey are protein coding bases which have not been successfully sequenced. ATG: start of exon 1; GGA: start of exon 4; TAG: end of exon 4. 3 different sets of primers used to amplify the exon 4 of *LAP2* have been colour coded:

LAP2α4.1F/R:TCTTGTTGCCACAAACTTGC/GGCAGCCATCTTCACTTCAT
LAP2α4.2F/RCCAGGGTGGGGTAGGTAGTT/AAATGCCACAAAGGAACCTG
LAP2α4.3F/R:ACCTGGATCCGAACTGATGT/CAGGCTTCCTATCTACGCAAA

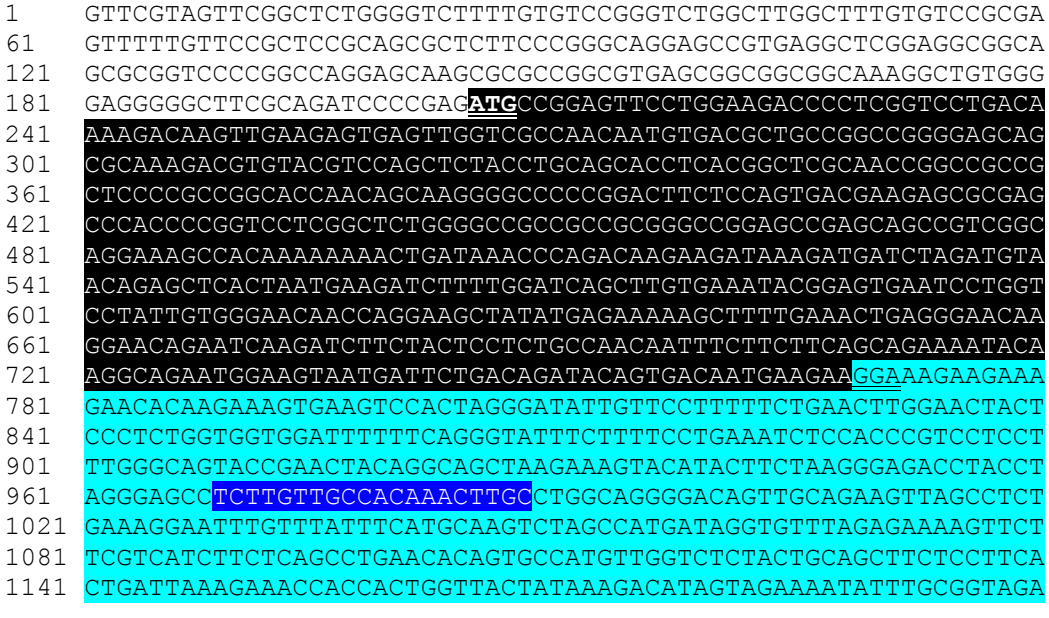

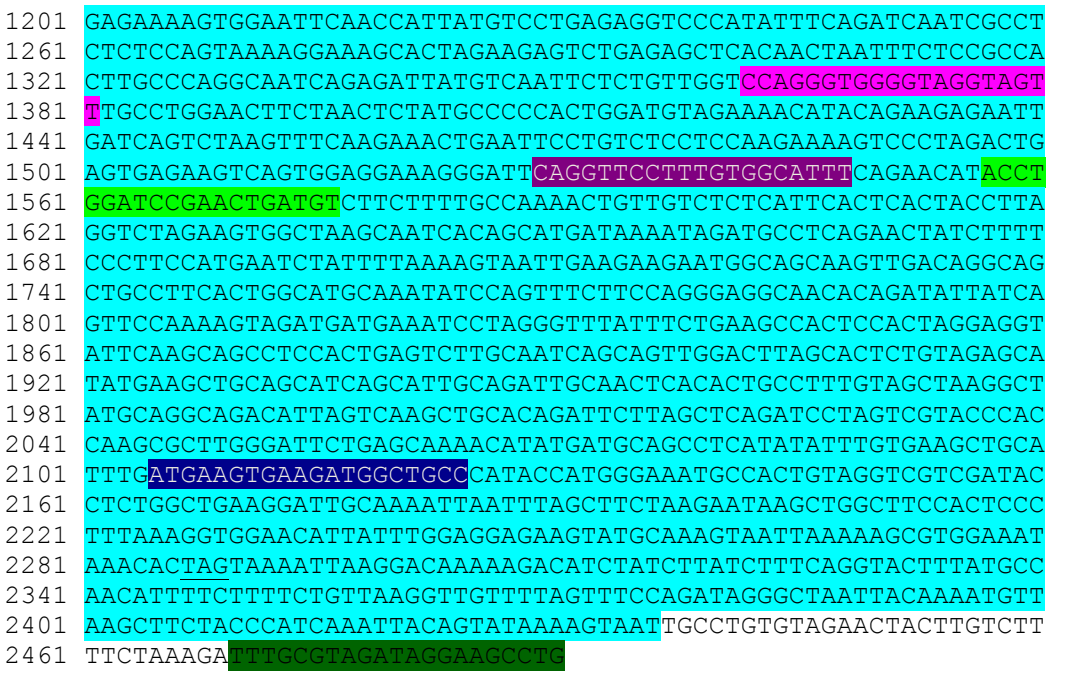

Figure 5.3.9: Sequencing of *LAP2* exon 4 in AG11572

LAP2 sequence derived from PubMed (NM_003276; *Homo sapiens* thymopoietin (TMPO), transcript variant 1, mRNA). Nucleotides highlighted in black code for exons 1-3. Successfully sequenced nucleotides are highlighted in turquoise; primers used to amplify and sequence the 5' intron/exon boundary can be seen in figure 5.3.10. ATG: start of exon 1; GGA: start of exon 4; TAG: end of exon 4. 3 different sets of primers used to amplify the exon 4 of *LAP2* have been colour coded:

LAP2α4.1F/R:TCTTGTTGCCACAAACTTGC/GGCAGCCATCTTCACTTCAT
LAP2α4.2F/RCCAGGGTGGGGTAGGTAGTT/AAATGCCACAAAGGAACCTG
LAP2α4.3F/R:ACCTGGATCCGAACTGATGT/CAGGCTTCCTATCTACGCAAA

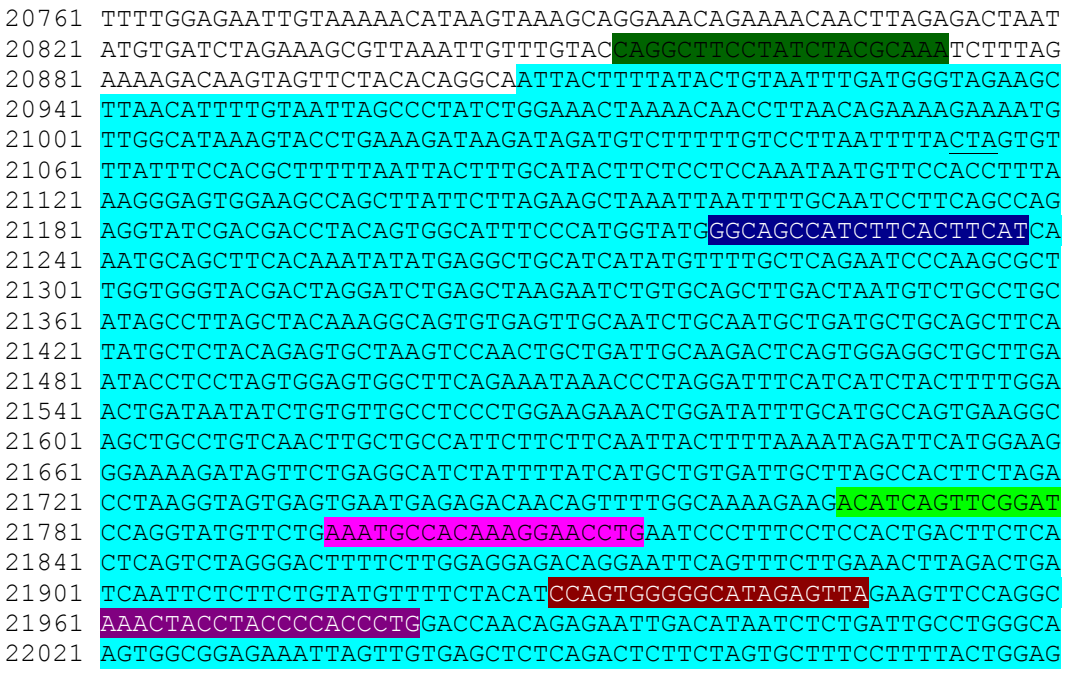

Figure 5.3.10 Sequencing of *LAP2* in AG11572

Sequence derived from PubMed (selected region of AC013418; *Homo sapiens* 12 BAC RP11-181C3 (Roswell Park Cancer Institute Human BAC Library) complete sequence). Note that the sequence is in reverse orientation to the *LAP2* exon 4 cDNA (i.e. exons are coded in descending order). Successfully sequenced nucleotides are highlighted in turquoise. Gene information sourced from Harris et al., (1994; 1995). 5' exon/ intron boundary is denoted by the black arrow. Primer pairs used to amplify exon 4 plus the 5'intron/ exon boundary have been colour coded:

LAP2αintron/exon4F/R; GCTTTGTCTACCAGGGCAAA/ CCAGTGGGGGCATAGAGTTA
LAP2α4.1F/R:TCTTGTTGCCACAAACTTGC/GGCAGCCATCTTCACTTCAT
LAP2α4.2F/RCCAGGGTGGGGTAGGTAGTT/AAATGCCACAAAGGAACCTG
LAP2α4.3F/R:ACCTGGATCCGAACTGATGT/CAGGCTTCCTATCTACGCAAA

5.3.4.4 Western Blotting

In order to determine the presence and load of emerin and LAP2α proteins in the two atypical HGPS cell lines, Western blotting was performed. The size and level of lamin A/C were also examined, with the aim of confirming that lamin A/C production was normal. Whole cell lysates were sampled from a control HDF cell line (2DD) plus, the two aforementioned HGPS cultures. The loading volumes of each lysate were adjusted according to the approximate cell numbers. The Western blots results can be seen in figure 5.3.11. For all three proteins, respective bands of the correct size were observed with minimal or undetectable nonspecific staining. The protein loads for each protein were similar for all cell lines, with the exception of LAP2α in AG11572; in this case, the band was very faint, albeit, visible (figure 5.3.11). The results of these Western blot experiments appear to further reduce the possibility that *EMD* is mutated in either or both atypical HGPS cell lines. The normal size and protein levels of lamin A/C also

confirm the previous observation that *LMNA* is wild-type in such cells. Lastly, these blots indicate that LAP2α is the correct size in both AG08466 and AG11572, suggesting that if mutations were present in exon of *LAP2,* they do not result in the production of a truncated protein. The normal level of LAP2α in AG08466 indicates that any mutation present would affect protein interactions. The implications of the decreased LAP2α protein load observed are possibly suggestive of a mutation. However, this is less likely in view of the sequencing results presented in this chapter. These findings are duly considered and discussed in the next section of this chapter (5.4).

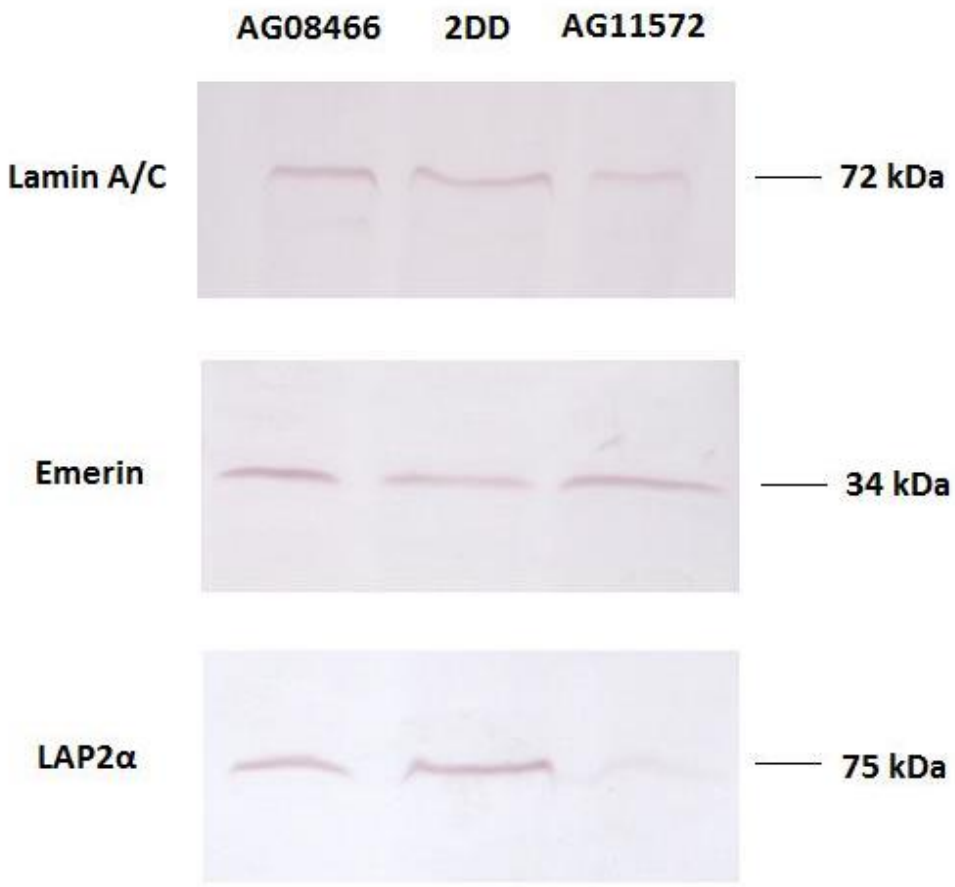

Figure 5.3.11 Western Blot Analysis of proteins extracted from normal and HGPS fibroblasts

Anti-lamin A/C, anti-emerin and anti-LAP2α antibodies were used to identify lamin A/C, emerin and LAP2α in control (2DD) and atypical HGPS (AG08466 and AG11572) HDF cell lines.

5.3.4.5 Accumulated population doublings (APD)

The rates of cell growth (at the time of protein preparation), were analyzed by determining the accumulated population doublings; this was calculated using the formula: (log *H*–log *S*)/log2.0 where log *H* is the logarithm of the number of cells harvested and log *S* is the logarithm of the number of cells seeded). APD values were plotted for all 3 cell lines (figure 5.3.12). As the graph depicts, the rates of population doubling were similar for 2DD, AG08466 and AG11572.

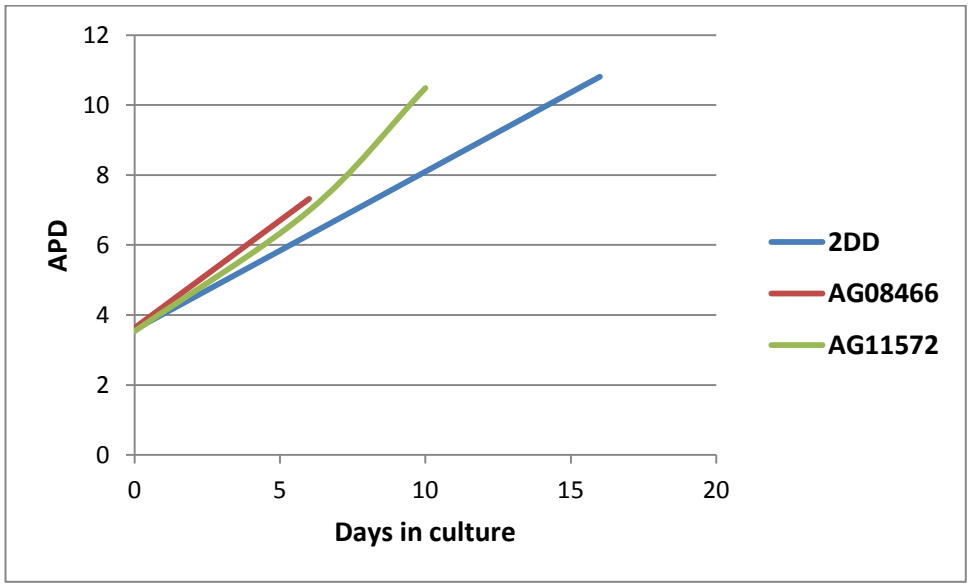

Figure 5.3.12 Comparing APD values for control and atypical HGPS cells at the time of protein preparation

5.4 DISCUSSION

5.4.1 ED5364

DNA sequencing of *EMD* in the X-EDMD carrier revealed the presence of a heterozygous point mutation (c.315T>G) in exon 4. At the amino acid level, this mutation exchanges tyrosine for a premature stop codon at residue 105 (p.Tyr105X). This mutation has previously been reported in 4 individuals and results in the loss of the DdeI restriction site (Muntoni et al., 1998). The EMD mutation database (last updated 2007), which can be found at www.umd.be/EMD/ (The EMD mutations database, 2007), is a great source of information regarding reported *EMD* mutations. It is possible to determine mutation frequency for all exons. As of 2007, the details of 203 X-EDMD cases (splice mutations excluded) had been reported. Of these, 37 mutations (excluding intronic mutations) were detected in exon 4. 32.5% of all mutations in exon 4 were nonsense mutations. Exon 4 encodes 45 codons and out of these, 13 potential stop codons exist; one of which is tyrosine 105. Of the 20 reported mutations affecting residue 105 of exon 4, the majority (16/20; 80%) are deletions (314_315delAT); nonsense mutations at this amino acid account for only 20% (4/20). Mutations affecting residue 105 account for approximately 54% of all exon 4 mutations.

Importantly, the *EMD* mutation presented in this study leads to the absence of emerin in affected cells. Indeed, the majority of X-EDMD mutations lead to the total absence of emerin (Yates et al., 1999). Since the individual is an X-EDMD carrier, the remaining population produce functional emerin; this is due to the random nature of X-inactivation. Why does the presence of this stop codon inhibit the detection of emerin in affected cells? Muntoni et al. (1998) hypothesised that it produces an unstable mutant protein. Post-translationally, emerin is found to enter the ER before diffusing to the nuclear envelope; importantly, the protein's C-terminal transmembrane domain is required for such events (Soullam and Worman, 1995; Cartegni et al., 1997; Ellis et al., 1998). It is suggested that the loss of this domain prevents the correct targeting of the protein to the ER and as a result, the protein is degraded rapidly (Yates et al., 1999).

While X-EDMD is largely characterised by lack of emerin expression, the disease can also be caused by missense mutations and in-frame shifts. Yates et al. (1999) reported 2 in-frame *EMD* deletions, both of which resulted in reduced emerin levels (as compared to wildtype). It is suggested that these mutations lead to impaired NE targeting. This paper also documented a novel missense mutation; cells harbouring this mutation produced emerin at normal amounts. Interestingly, genotype-phenotype analysis revealed that the in-frame deletions produced a similar phenotype to emerin null X-EDMD cells, while the missense mutation produced a milder phenotype.

5.4.2 Atypical HGPS

5.4.2.1 *EMD*

So far, the sequencing of both *EMD* and *LAP2* (exon 4) in the atypical HGPS patients has failed to reveal any mutations. The Western blotting experiments performed demonstrate that if the aforementioned atypical HGPS cell lines do harbour mutations in *EMD*, they do not lead to the loss of emerin expression. The results also indicate that a splicing mutation is unlikely since the size of the protein is very similar to that seen in the control. Therefore, if an emerin mutation were present in either of the cell lines, it is most probable that it would interfere with the protein's structure or capacity to bind to protein partners. However, the phenotypes displayed by AG08466 and AG11572 patients at the point of diagnosis are not suggestive of *EMD* mutations. While patients with disease-causing *EMD* mutations generally present with early contractures and muscle wasting and weakness (Emery, 2000), neither AG08466 nor AG11572 exhibited evidence of muscular problems (ccr.coriell.org).

Since both cell lines were derived from female patients, it is unlikely that mutations in *EMD* are the sole cause of disease in these two patients. Why? Due to X-inactivation, a heterozygous *EMD* mutation in a female would lead to a mosaic pattern of expression; one population of cells would produce functional emerin while the other would produce a mutant variant of the protein. Thus, the female would be a carrier of the disease rather than a sufferer of the disease. The other scenario is that both copies of chromosome X harbour mutations in *EMD*. This is highly improbable since it would

require that the mother be a carrier of the disease and the father a sufferer. However, it is possible that 2 independent mutations, one within *EMD* and the other in another gene, exist in the patient cells. Indeed, double mutations in *LMNA* and *EMD* have been reported in patients (Ben Yaou et al., 2007).

5.4.2.2 *LAP2*

Sequencing of *LAP2* exon 4 (specific to the LAP2α isoform) in AG08466 and AG11572 has not yet revealed any mutations. Western blot analysis demonstrated that LAP2α protein levels were barely detectable in AG11572, while in AG08466, expression was on a par with control. There are two possible explanations for this; either (1) the gene encoding LAP2α is mutated, causing low-level expression or (2) the culture, from which the AG11572 sample was derived, was senescent. Indeed, a mutation in exon 4 of *LAP2* has been demonstrated to reduce LAP2α levels in human DCM (Taylor et al., 2005). While the symptoms displayed by these 2 DCM patients primarily affected the heart, it is unknown whether the patient from whom AG11572 was derived displayed cardiac involvement. Since reports of disease causing *LAP2* mutations are rare, it is difficult to hypothesise whether a spectrum of clinical phenotypes can be caused by different *LAP2* exon 4 mutations.

The other possible cause for reduced LAP2α expression in AG11572 is if the proliferative status of the culture was different to that of AG08466 and control. Indeed, there is a correlation between LAP2α expression and cell cycle status (Markiewicz et al., 2002; Pekovic et al., 2007). On entry into serum-starvation induced quiescence, LAP2α is down-regulated; expression levels begin to increase after re-stimulation (Markiewicz et al., 2002; Pekovic et al., 2007). Conversely, lamin A is up-regulated in quiescence (Pugh et al., 1997). Indeed, siRNA knock-down of LAP2α in HDFs leads cell cycle arrest (Pekovic et al., 2007). Thus, Pekovic et al. (2007) hypothesize that the loss of LAP2α may play a role in driving cellular senescence. Taken together, these findings suggest that LAP2α expression may be down-regulated in senescence and as a result, cultures which are composed of mainly senescent cells are likely to contain lower levels of LAP2α protein than largely proliferating cultures.

Unfortunately pKi67 counts were not taken at the time of protein preparation. However, APD graphs demonstrated that AG11572 was growing at a rate similar to control and AG08466 cell lines in culture. This suggests that the proliferative capacity of the cultures at the time of protein preparation were comparable and thus, none of cultures were quiescent or senescent.

The observation that AG11572 fibroblasts display a period of hyper-proliferation (Bridger and Kill, 2004) questions the likelihood that mutant LAP2α, at low-levels, is a direct cause of disease in these cells. The DCM causing mutation in *LAP2* disrupts the formation of LAP2α-lamin A complexes (Taylor et al., 2005); such complexes are reported to maintain a cell's proliferative state (Pekovic et al., 2007). Therefore, the loss of LAP2α function is likely to induce cell cycle arrest (Pekovic et al., 2007) rather than drive the high rates of proliferation observed in AG11572 (Bridger and Kill, 2004).

Although this study has failed to reveal a mutation in exon 4 of *LAP2* in AG11572, the fact that LAP2α protein levels are reduced suggests that the sequencing results presented require further verification. Another possibility is that the disease-causing mutation resides in one of the other exons which encode LAP2α, exons 1–3. While there are no documented cases of human disease resulting from mutations affecting these exons, the possibility cannot be ruled out. If this were the case, the other LAP2 isoforms, LAP2β and LAP2γ, would be affected since they are also encoded by these exons (Harris et al., 1995). Since I have not investigated either LAP2β or LAP2γ, I cannot state whether levels of these proteins are normal. In light of this, it may be pertinent to investigate these proteins before further sequencing of other genes.

5.4.2.3 Additional candidate genes

If neither *EMD* nor *LAP2* mutations are responsible for the HGPS symptoms in AG08466 and AG11572 patients, what are the other candidate genes? Interestingly, when analyzing the karyotypic profile of four HGPS cell lines, Corso et al. (2005) repeatedly observed the amplification of 11q13 ~ q23 in the culture, AG08466. This is potentially interesting since it is home to *farnesylated protein-converting enzyme 2*

(*FACE-2)*, a gene which encodes an enzyme involved in the proteolytic maturation of farnesylated proteins (Otto et al., 1999; Freije et al., 1999). This is important because a similar protein, FACE-1 (otherwise known as ZMPSTE24), is shown to be mutated in laminopathy-based disease (Navarro et al., 2004; Moulson et al., 2005; Navarro et al., 2005). Although, FACE-2 has not yet been demonstrated to be involved in the processing of lamin proteins, it is certainly worthy of investigation.

Both AG08466 and AG11572 were sourced from the Coriell Cell Repository; it was from here that any details regarding clinical presentation were derived. Since the start of this project, the clinical features of patient AG08466 have been updated to include that 'Marfan features have also developed'. This is intriguing since Marfan syndrome is a connective tissue disease caused by mutations in the *FBN1* gene (Dietz et al., 1991). *FBN1* encodes profibrillin-1, which is then processed to form fibrillin, an extracellular glycoprotein (Frydman, 2008). There are a range of symptoms displayed by Marfan syndrome patients (Frydman, 2008); interestingly, some of which overlap with the clinical features reported for both AG08466 and AG11572. Although it is likely that symptoms observed in Marfan syndrome overlap with a number of other disorders, it would be pertinent to investigate fibrillin in both these atypical HGPS cell lines.

Lastly, it must be considered that the protein or proteins affected in these atypical HGPS patients have yet to be characterized. Indeed, Schirmer et al. (2003) report that in addition to the 13 known NE proteins, 67 uncharacterised others exist. This is an exciting but daunting prospect for a mutation search such as this present one; a number of these 67 proteins could potentially be the cause of disease in AG08466 and AG11572. In fact, there are hundreds of instances where the genetic cause of a dystrophy has not yet been identified in patients. Of the 67 proteins discovered, the corresponding genes of 23 have been mapped to chromosome regions previously linked to 14 human dystrophies (Schirmer et al., 2003).

5.4.3 Adopting another approach to identify disease-causing mutations

The attempt to determine the specific *EMD* mutation in ED5364 has been successful. However, the search for the disease-causing mutations in the atypical HGPS cell lines proved much more difficult and high-risk. The ED5364 search was considerably easier since previous work demonstrated that the mutation affected the *EMD* gene; while, with the atypical HGPS patients, only a small number of genes could be eliminated with certainty. In hindsight, perhaps it would have been more efficient to perform heteroduplex analysis of the PCR products before sequencing the exons. In heteroduplex analysis, the region of interest is subjected to denaturation and annealing steps, post-PCR; if a mutation is present in one of the alleles, heteroduplexes will be formed in solution. Heteroduplexes consist of a wild-type DNA strand and a mutated strand; homoduplexes are composed wholly of normal DNA. Since the electrophoretic mobility of these heteroduplexes is retarded, they can be differentiated from homoduplexes using specialized gels (for review, see Nataraj et al., 1999). The use of heteroduplex analysis in this present study would have indicated to the presence or absence of a mutation without the need for complete sequencing.

Rather than continuing to sequence candidate genes, selected primarily on the basis of their reported functions and interactions, which can be an expensive and time-consuming process, it would be perhaps sensible to use a different approach in order to identify the mutated genes. One approach could be functional complementation, whereby microcell-mediated chromosome transfer (MMCT) would be used to introduce single copies of chromosomes into disease cell lines. A panel of human:rodent somatic cell hybrids such as that developed by Cuthbert et al. (1995) would be employed. By monitoring each clone, the chromosome which rescues or improves the disease phenotype is then investigated in terms of candidate genes. Only then would such genes be amplified and then subjected to heteroduplex analysis and sequencing.

5.4.4 Conclusion

In conclusion, the findings of this study suggest that *EMD* is unlikely to be the site of the disease-causing mutation in AG08466 and AG11572. While sequencing has failed to reveal any mutations in exon 4 of *LAP2* in either cell line, Western blotting indicates that LAP2α levels are normal in AG08466 and reduced in AG11572. As a result, the sequencing of *LAP2* exon 4 in AG11572 requires further verification to confirm that no mutations exist in this specific exon. It is also plausible that other *LAP2* exons are the source of the disease-causing mutation.

6. Exploring nuclear structure in *LMNA*, *EMD* and *LBR* mutant fibroblasts

6.1 INTRODUCTION

6.1.1 Overview of the NE and NPCs

Within eukaryotic organisms, nuclear and cytoplasmic activities are separated by the NE. While the outer nuclear membrane is continuous with the ER, the inner face of the nuclear membrane is lined by the NL (Gerace and Burke, 1988). The NE is perforated with NPCs which mediate nucleocytoplasmic transport (Allen et al., 2000). While small molecules can diffuse freely through the NPCs, larger molecules (>40 kDa) require the assistance of receptor proteins such as importins (for review, see Lim et al., 2008). NPCs are large, multi-protein complexes; proteomic analysis reveals that both yeast and mammalian NPCs are composed of 29 different nucleoporins (Rout et al., 2000; Cronshaw et al., 2002). The vertebrate NPC exhibits a tripartite architecture, with an hour-glass shaped, central framework at the core. This component, also known as the spoke complex, spans the membrane and exhibits an octagonal symmetry. The cytoplasmic face of this central framework is known as the cytoplasmic ring moiety and is connected to protruding cytoplasmic filaments. On the inner face of the NE, the corresponding nuclear ring moiety anchors a nuclear basket, which is composed of eight filaments and a distal ring (Stoffler et al., 2003; for reviews see Fahrenhrog and Aebi, 2003; Lim et al., 2008). Human NPCs are reported to have an outer diameter of 120 nm and an inner diameter of 50 nm (Elad et al., 2009). While the outer diameter of NPCs in *Xenopus* oocytes are of comparable size to humans (110–120 nm; Goldberg and Allen, 1996), this diameter is slightly reduced in tobacco BY-2 plant cells (~ 105 nm; Fiserova et al., 2009) and smaller still in yeast (~95 nm; Kiseleva et al., 2004).

6.1.2 Lamin organisation

Since the NL is largely inaccessible due to its tight association with chromatin, the *in vivo* organisation of the NL in vertebrates is poorly understood (Goldberg et al., 2008a). Our comprehension of lamin organisation is largely based on work performed using *Xenopus* oocytes, whose NL is primarily composed of LIII/lamin B3 (Krohne et al., 1981; Stick., 1988). Goldberg et al. (2008b) used *Xenopus* oocytes to examine the organisation of somatic lamins. This is a useful system since exogenously expressed lamins are not incorporated into the endogenous lamina; instead, they form structures on top of the existing lamina (Ralle et al., 2004). While the expression of A-type lamins

produced thick lamin filaments and increased the rigidity of the NE, the expression of B-type lamins resulted in the formation of single filament layers (Goldberg et al., 2008b).

6.1.3 A link between the NL and NPCs

Evidence demonstrates that there is a link between NPCs and the NL (Goldberg and Allen, 1996; Liu et al., 2000; Daigle et al., 2001). Indeed, nucleoporins are found to interact directly and indirectly with lamin proteins (Smythe et al., 2000; Hubner et al., 2006; Pan et al., 2007). It has been suggested that lamin proteins anchor NPCs via binding to NUP153 (Smythe et al., 2000). Significantly, lamins are found to regulate NPC formation and distribution (Lenz-Bohme et al., 1997; Maeshima et al., 2006). In line with this, NPC clustering has been reported in late-passage HGPS cells (Goldman et al., 2004). Furthermore, nuclear import appears reduced in cells expressing lamin A mutants (Busch et al., 2009). These studies strengthen the link between mutant lamin A and an ageing phenotype since there is a reported reduction in NPC integrity (D'Angelo et al., 2009) and nuclear protein import (Pujol et al., 2002) with age.

6.1.4 Inner NM structure

6.1.4.1 Preparations employed to visualise inner NM/NS structure

The methodologies employed to isolate and visualise the structure of the NM/NS vary. Traditionally, they involve a combination of non-ionic detergents and hypertonic salt concentrations to extract soluble proteins and digested or non-NM associated DNA (Berezney and Coffey, 1974; He et al., 1990; Nickerson et al., 1997; for review, see Nickerson, 2001). Critics of such preparations suggest that these harsh preparations induce the formation of artefacts within the nucleus, which are misinterpreted as evidence for a NM/NS (Pederson, 2000). However, a number of modified preparations have been developed which produce structures similar to those revealed by traditional methodologies (Jackson and Cook, 1988; Nickerson et al., 1997; Wan et al., 1999). The DNA halo preparation as described in previous chapters (2 and 3) involves the extraction of histones and other soluble proteins using Triton X-100, digitonin, and high salt molarities (as per Bridger and Lichter, 1999). Since this protocol is useful for

studying DNA interactions with the residual nuclear structure, the use of DNase I is omitted (e.g. Gerdes et al., 1994). In contrast, variations of another methodology, the NM extraction, have been primarily used to study the structural basis of the inner NM (e.g. He et al., 1990; Nickerson et al., 1992; Nickerson et al., 1997; Wan et al., 1999). Since, unlike the DNA halo preparation, it uses nuclease treatment followed by ammonium sulphate elution to remove the bulk of attached DNA, an examination of underlying NM filaments can be performed.

6.1.4.2 EM studies analysing NM/NS structure

Using resinless sections of HeLa cells for EM, He et al. (1990) described the presence of thick polymorphic fibres which overlay core filaments with diameters of 9–13nm. It is these filaments that are suggested to link the internal NM with the peripheral NL (Nickerson et al., 2001). A similar structure has been reported by other labs (Hozak et al,. 1995; Nickerson et al., 1997). Furthermore, Hozak et al. (1995) confirmed using EM, earlier observations which suggested that lamin proteins were components of the internal NM (Goldman et al., 1992; Bridger et al., 1993).

One of the major gaps in NM research is knowledge of the NMPs which form the NM filaments observed by EM. While it is known that hundreds of NM associated proteins exist (Mika and Rost, 2005), a full molecular characterisation of the NM/NS has yet to be performed. In 2001, Nickerson and colleagues discussed the need for a characterisation of this nature and suggested the structural composition rather than the functional relevance of the NM should be the focus of future NM research. Nearly ten years later, it is still not understood how and which proteins form these NM filaments.

6.1.5 Examining nuclear structure in control and disease HDFs

6.1.5.1 Examining nuclear structure during and following two NM extraction protocols using Field Emission Scanning Electron Microscopy (feSEM)

The DNA halo preparation has been used extensively in previous chapters in order to examine interactions between different genomic elements and the NM. It thus seemed pertinent to follow the progress of this extraction using feSEM. Indeed, feSEM is a

useful tool for studying nuclear structure (Goldberg et al., 2008b) since it provides clear images at extremely high resolutions, with minimal sample damage; it is thus, superior to conventional SEM (Hitachi High Technologies America, 2010). In order to attempt to visualise the structure of the underlying residual nucleus produced by this preparation, which is usually obscured by dense chromatin, it was, at times, also combined with nuclease digestion. Cells were subjected to another NM extraction, known as the NM preparation (as per Dyer et al., 1997), allowing resulting nuclear morphologies to be compared. Normal HDFs were grown on silicon chips, taken through either preparation and then prepared for feSEM. At different stages of each methodology, silicon chips were removed and treated accordingly; this allowed the progress of the extraction to be observed.

Analysis of specimens fixed following Triton X-100 extraction in both protocols revealed the NL perforated with structures resembling NPCs. However, the interior of residual nuclei was only observed in cells extracted using the DNA halo preparation. In DNA halo prepared nuclei treated with DNase I, filaments, which were assumed to be of the inner NM, were exposed in places. Such filaments exhibited a mean diameter very similar to those measurements presented previously (He et al., 1990; Nickerson et al., 1997; Nickerson et al., 1999). The morphology of these filaments was also analogous to those presented by Hozak et al. (1995).

6.1.5.2 The absence of both lamin A and emerin disrupt the structural integrity of the NE

In order to examine nuclear ultrastructure in cells lacking functional NE proteins such as lamin A, emerin and LBR, disease fibroblasts were subjected to either one or both of the aforementioned NM extraction protocols. Unlike the lamin A mutant cells studied in previous chapters, the cell line used in this section was derived from a patient with a homozygous Y259X *LMNA* nonsense mutation (van Engelen et al., 2005; Pekovic et al., 2007). The phenotype was lethal and hence, the sample was obtained during an autopsy. In the heterozygous form, this mutation, which was present in a family member, produces classical LGMD1B (van Engelen et al., 2005). The cells used to study

the impact of emerin loss were sourced from previously described X-EDMD patients (KK and AP; chapter 4).

The importance of LBR in maintaining nuclear structure was also examined. LBR is an evolutionarily conserved, inner nuclear membrane protein, which binds chromatin and B-type lamins via its N-terminus (Worman et al., 1988; Meier and Georgatos, 1994; Pyrpasopoulou et al., 1996; Kawahire et al., 1997; Duband-Goulet and Courvalin, 2000; Makatsori et al., 2004; Wagner et al., 2004). Significantly, mutations in *LBR* are found to produce two human diseases; Greenberg Dysplasia (Waterham et al., 2003) and PHA (Hoffmann et al., 2002). While the former is an autosomal recessive, fatal disorder (Waterham et al., 2003), the latter, autosomal dominant disease generates a far milder phenotype (Hoffmann et al., 2002). In this study, cells were derived from two PHA patients; one of which harboured a heterozygous mutation, while the other was homozygous.

Examination of the nucleus following the permeabilisation of the cellular and nuclear membranes revealed that in cells lacking lamin A and emerin, the NL was irregular and disordered. While $EMD^{-/Y}$ cells exhibited slight disruptions, $LMNA^{-/-}$ nuclei were highly compromised and displayed evidence of NPC clustering. Neither NL disruption nor NPC clustering were detected in *LBR* mutant nuclei. The dimensions of residual NPCs were similar in all control and disease cell lines; however, the largest dimensions were recorded in those cells extracted in the presence of RNase inhibitors.

While the findings documented in this section are more suggestive than conclusive due to the absence of immunolabelling, the use of these NM extraction protocols have revealed some interesting structures which without doubt require further investigation.

6.2 METHODS AND MATERIALS

6.2.1 Cell Culture

All primary HDF cell lines (table 6.2.1) were maintained in 10% NCS in conditions described in previous chapters (2.2.1 and 4.2.1).

Phenotype	Cell line	Genotype
Normal	HDF	Normal
X-EDMD	KK	$EMD^{-/Y}$ (hemizygous)
	AP	
LGMD1B (fatal)	Y259X	$LMNA^{-/-}$ (homozygous)
LBR	99P0598	$LBR^{-/+}$ (heterozygous)
	99P0599	$LBR^{-/-}$ (homozygous)

Table 6.2.1: The primary HDF cell lines used and their corresponding phenotypes
All primary HDFs cell lines were provided by Professor CJ Hutchison.

Cells were grown on ethanol-sterilised 5 mm x 5 mm silicon chips (Agar Scientific Ltd) in 6-well plates; each well contained 2 silicon chips and was seeded with ~0.5–1 x 10^5 cells. Since the Y259X cells did not grow well on plain silicon chips, the chips used for this cell line were coated with 0.01 mg/ml Poly-D-lysine (Sigma) overnight and then were left to dry for two hours before use.

6.2.2 Preparation of Nuclear Matrices

This procedure, originally sourced from Nickerson et al. (1992), was modified by Dyer et al. (1997). All of the following buffers included 1% (v/v) of a protease inhibitor cocktail (Sigma). In some cases, RNase inhibitors (40 U/µl) (Sigma) were also added to all buffers. Cells grown on silicon chips were washed with PBS and then washed 3 times in ice-cold CSK buffer (10 mM Pipes (pH 6.8), 100 mM NaCl, 300 mM sucrose, 3 mM $MgCl_2$, 1 mM EGTA). Next, cells were incubated in CSK buffer plus 0.5% (v/v) Triton X-100 for 10 minutes at 4°C. Following this, they were rinsed three times in ice-cold RSB buffer (42.5 mM Tris-HCl (pH 8.7), 8.5 mM NaCl, 2.6 mM $MgCl_2$) and incubated in RSB Magik (RSB containing 1% (v/v) Tween 20 and 0.5% (v/v) sodium

deoxycholate) for 10 minutes at 4°C. The cells were then rinsed twice in ice-cold digestion buffer (10 mM Pipes pH 8.3, 50 mM NaCl, 300 mM sucrose, 3 mM $MgCl_2$, 1 mM EGTA). In order to remove DNA, the cells were incubated in digestion buffer containing DNase I (500 U/ml) (Sigma) for 30 minutes at room temperature. To this solution, 1 M $(NH_4)_2$ SO_4 was slowly added to give a final concentration of 0.25 M; this was incubated for 5 minutes at 4°C and removed the digested material.

6.2.3 DNA halo extraction

Chips were taken through the DNA halo preparation as per chapter 2.2. For selected cell lines, cells were incubated in DNase I (500 U/ml) (Sigma) for 30 minutes at room temperature after PBS and ethanol rows.

6.2.4 Sample preparation

The chips were removed at different stages throughout both extraction procedures and then placed and stored in fixative (3% (v/v) glutaraldehyde, 1% (w/v) PFA in 0.1M sodium cacodylate buffer). The chips were next washed in 0.2 M sodium cacodylate buffer and incubated in 1% (w/v) osmium tetroxide (OsO_4) for 15 minutes at room temperature. Following this, the chips were placed in distilled water and taken straight-through an ethanol row of 50%, 70%, 95% and 100% (v/v). Specimens were critical point dried with CO_2 using a Bal-Tec CPD 030 (BAL-TEC) machine. A Cressington Coating System 308R (Ted Pella, Inc) was then used to sputter coat the chips with either platinum or chromium (1–3 nm). The specimens were viewed using a Hitachi Model S-5200 feSEM (Hitachi High-Technologies) at various accelerating voltages.

6.3 RESULTS

6.3.1 Examining nuclear structure during and following NM extraction in normal fibroblasts

6.3.1.1 Using feSEM to visualise nuclear structure during NM extraction

Normal HDFs were subjected to either the DNA halo preparation (as per Bridger and Lichter, 1999; see figure 6.3.1) or the NM preparation (as per Dyer et al., 1997; see figure 6.3.2). At different stages of the preparations, chips were removed, fixed and prepared for feSEM. Both methodologies employed the early use of Triton X-100 which functions to permeabilise cellular and nuclear membranes (Jackson and Cook, 1988). Importantly, such detergent treatment extracts both inner and outer nuclear membranes (Aaronson and Blobel, 1974). Indeed, Triton X-100 is documented to solubilise approximately 95% of nuclear phospholipids and 10% of nuclear proteins (Aaronson and Blobel, 1974). After normal HDFs were subjected to Triton X-100 permeabilisation, a membrane-like structure remained (figure 6.3.3). Since the phospholipid element of the inner and outer nuclear membranes is largely removed following Triton X-100 incubation (Aaronson and Blobel, 1974) and the NL resists such extraction (Gerace et al., 1984; He et al., 1990; Hozak et al., 1995; Ma et al., 1999; Markiewicz et al., 2002), the remnant structure is likely to be composed of the outer face of the NL and any insoluble nuclear proteins. In DNA halo prepared nuclei; this surface was composed of a mesh-like structure, which exhibited no apparent symmetry or order (figure 6.3.3d). A similar structure was exposed in nuclei extracted using the NM preparation, however, the mesh-like composition was not as evident. The surface of the NL was also covered by structures which appeared to be ribosomal-like; indeed, they exhibited a diameter of 20–25 nm, a value similar to that documented for ribosomes in unextracted cells (Brakmann et al., 2010). Of further note were the filaments which overlaid the NL surface; evidence of these was observed with both extraction methodologies (figure 6.3.1). Since cytoskeletal IFs are anchored by the NL and remain after 2M NaCl extraction (He et al., 1990), it is likely that these filaments were IFs of cytoskeletal origin and are composed of vimentin (Franke et al., 1978). In order to identify the exact identity of these IFs, feSEM would need to be coupled with immunolabelling.

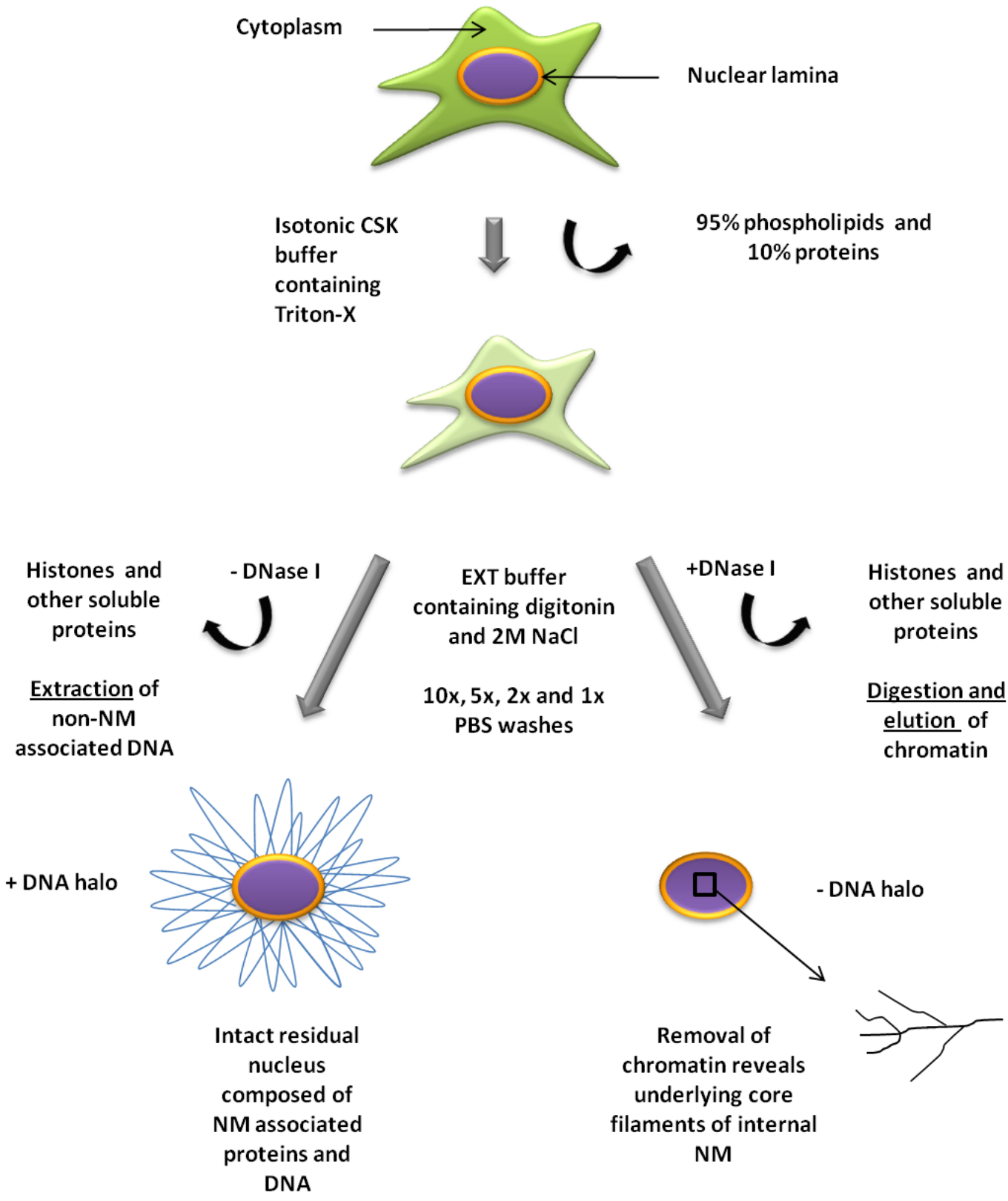

Figure 6.3.1: An overview of the DNA halo preparation

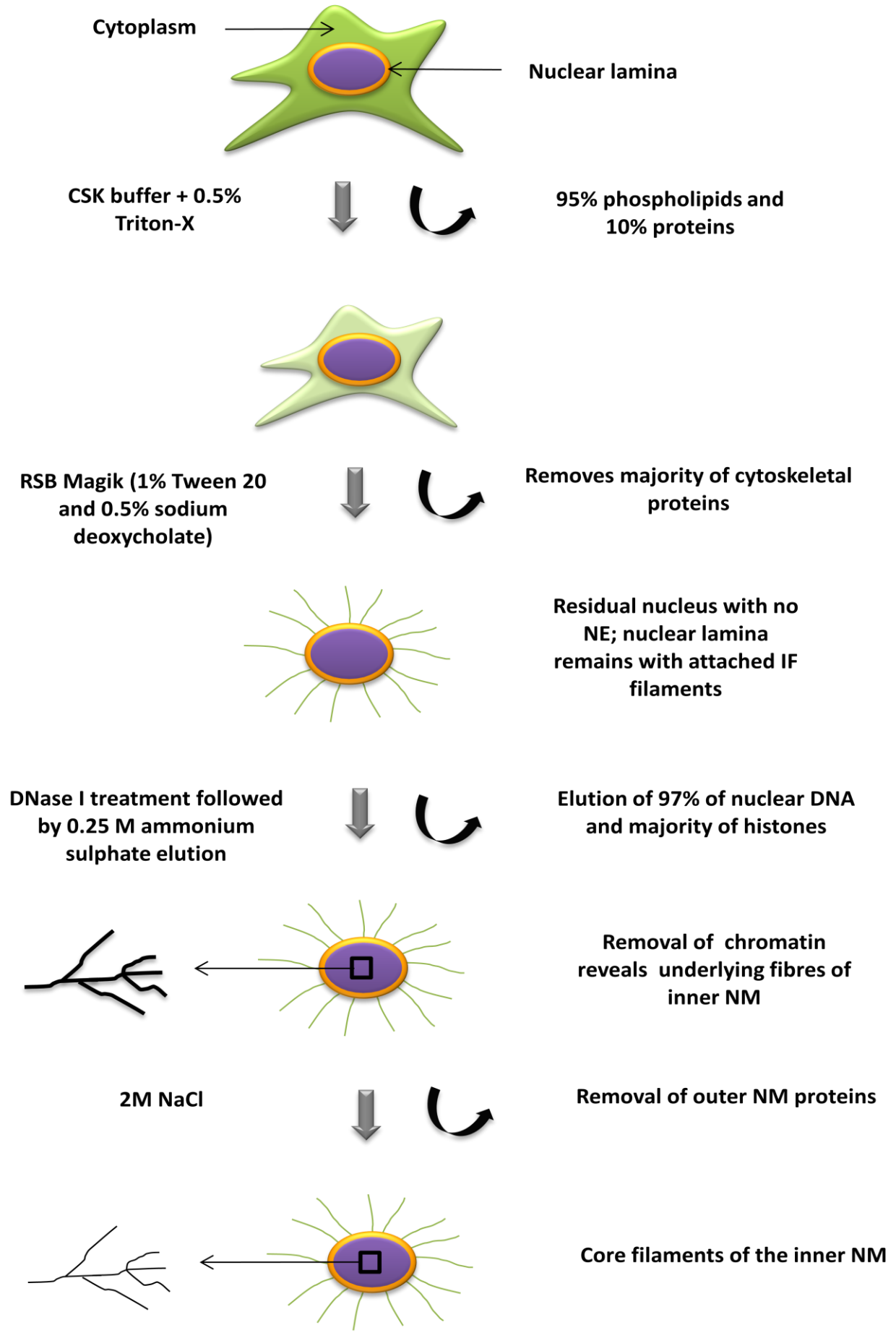

Figure 6.3.2: An overview of the NM preparation

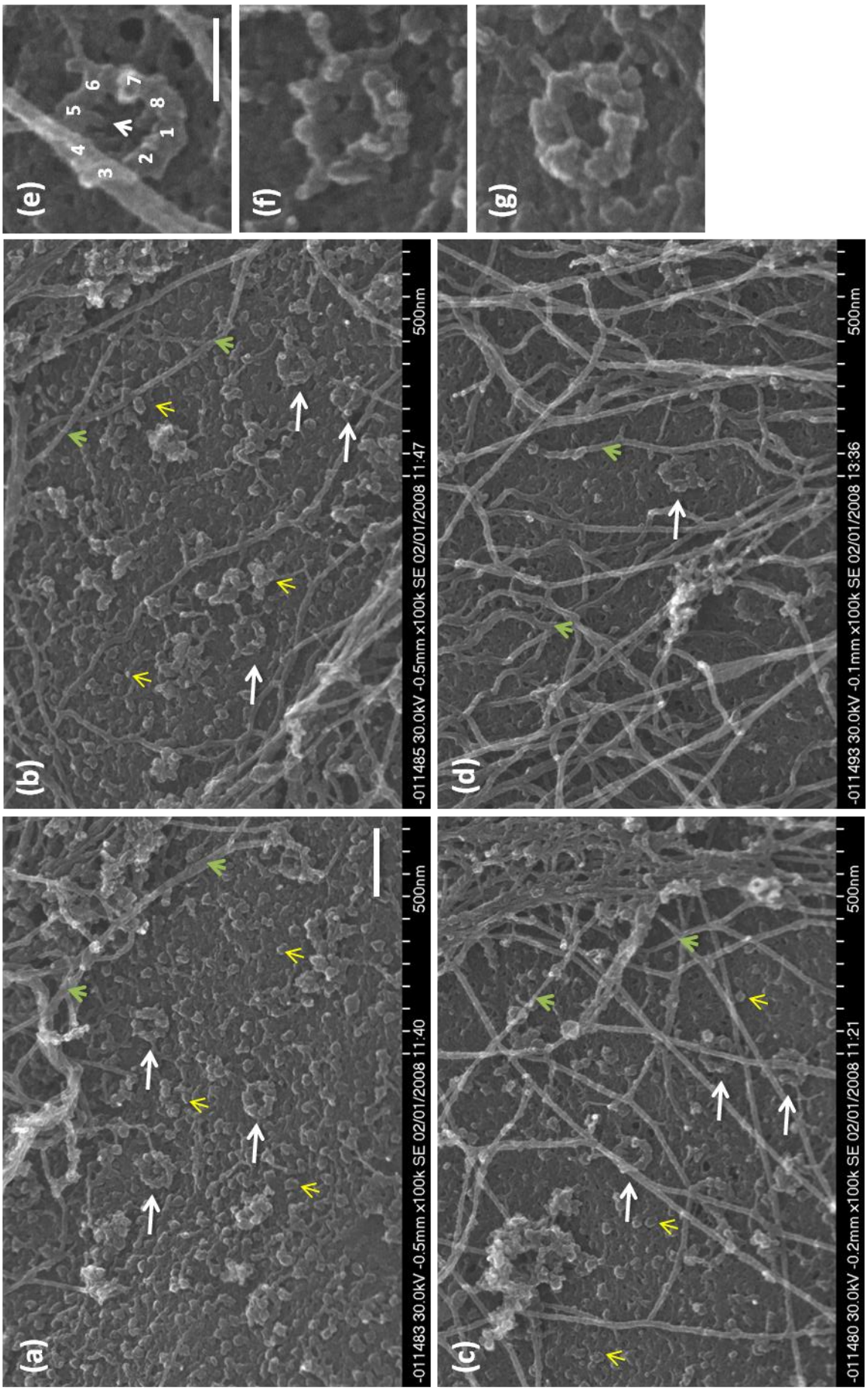

Figure 6.3.3: Nuclear morphology in control HDFs revealed by feSEM following cytoskeleton extraction

Figure 6.3.1: An overview of the DNA halo preparation

Whole cells grown on silicon chips are subjected to 3 rinses in 1 x PBS; following this, they are incubated in CSK buffer for 15 minutes at 4°C. The detergent activity of Triton X-100 extracts the majority of phosopholipids present in the plasma and nuclear membranes (Aaronson and Blobel, 1974; Fey et al., 1974). Furthermore, 65% of total cellular proteins are released (Fey et al., 1974) and of these 10% are nuclear proteins (Aaronson and Blobel, 1974). The residual structure is rinsed in 1 x PBS and then placed in EXT buffer, which contains digitonin and 2M NaCl, for 4 minutes. Following this incubation, cells are taken through 10x, 5x, 2x and 1x PBS for 1 minute/concentration. This process (mainly 2M NaCl) results in the release of histones and other soluble proteins, including outer NM proteins. Furthermore, non-NM associated DNA is extracted into the area surrounding the residual nucleus, while being tethered to the NM via MARs (at the base of the loops). After such treatment, these residual nuclei consist primarily of the peripheral NL and the core filaments of the inner NM, although both structures are obscured by DNA (He et al., 1990; Gerdes et al. 1994; Ma et al., 1999). A variation of this methodology has also been used in this chapter; using DNase I, DNA is digested before incubation in EXT buffer. As a result, the majority of DNA, histones and other soluble proteins are eluted during the following extraction steps and consequently, the core filaments of the inner NM can be visualised.

Figure 6.3.2: An overview of the NM preparation

Whole cells were washed 3 times in ice-cold CSK buffer and then incubated in CSK buffer (plus 0.5% Triton X-100) for 10 minutes at 4°C. As for the DNA halo preparation, Triton X-100 removes soluble proteins and the majority of phospholipids; thus, extracting the majority of plasma and nuclear membranes. The residual structures were rinsed 3 times in ice-cold RSB buffer and incubated in RSB-Magik (which contains 1% Tween 20 and 0.5% sodium deoxycholate) for 10 minutes at 4°C. This removes the majority of cytoskeletal proteins which leaves a residual nucleus with attached IFs (Nickerson et al., 1992). Following 2 rinses with ice-cold digestion buffer, the residual structures are placed in DNase I (in digestion buffer) for 30 minutes at room temperature. This digests the DNA. To this solution, 1M $(NH_4)_2\,SO_4$ is slowly added to obtain a final concentration of 0.25M and is incubated for 5 minutes at 4°C. This elutes the cleaved DNA and also extracts histones and other soluble proteins. As a result, the polymorphic fibres of the inner NM are revealed. Although not performed in this study, 2M NaCl can then be employed to visualise the core filaments of the inner NM (as per He et al., 1990).

Figure 6.3.3: Nuclear morphology in control HDFs revealed by feSEM following cytoskeleton extraction

The morphology of the outer NE following the removal of the cytoskeleton using **(a–c)** the NM preparation (chips were removed after the ice-cold RSB buffer rinse) and **(d)** the DNA halo preparation (chips removed after the CSK buffer). Magnification = 100k; scale bar = 150 nm (images 25% of actual size). White arrowheads indicate residual NPCs, while structures assumed to be ribosomes are marked using yellow arrowheads. Green arrowheads indicate filaments most likely to be the intermediate filament, vimentin. **(e–f)** The morphology of residual NPCs following the NM preparation; in **(e)** the eight constituent elements of the

octagonal spoke complex have been numbered and the white arrowhead indicates to a structure which resembles a nuclear basket. Magnification = 100k; scale bar = 50 nm.

The surface of NL appeared to be perforated with complexes resembling NPCs. These complexes exhibited an octagonal morphology and in selected NPCs, an attached basket-type structure was observed, which is probably representative of a nuclear basket (figure 6.3.3e). Indeed, since NPCs interact with and are anchored by the NL (Goldberg and Allen, 1996; Lenz-Bohme et al., 1997; Liu et al., 2000; Smythe et al., 2000; Daigle et al., 2001; Maeshima et al., 2006; Hubner et al., 2006; Pan et al., 2007) and thus, remain following 2M NaCl extraction (Gerdes et al., 1994), their presence after Triton X-100 treatment is unsurprising. There was variation in the preservation of NPC morphology in a sample and also when comparing these complexes in cells extracted using either the NM or the DNA halo preparation. NPC structure preservation was superior in those cells subjected to the NM preparation; a possible explanation for this is that protease inhibitors were used throughout this extraction procedure while they were not employed in the DNA halo methodology. Significantly, in places, a network of filaments was observed to be radiating from NPCs which can be most clearly seen in figure 6.3.3e. Once again, without immunolabelling, it is difficult to determine the composition of such filaments; however, it is probable that they are lamin filaments since they appear to be embedded in the NL. In order to determine the dimensions of these NPCs, the mean inner and outer diameters of the residual NPCs were recorded. For the NM preparation, the mean inner and outer diameters of the NPCs were 39.1 nm (± 5.4 (± standard deviation); n (NPCs) = 17) and 81.7 nm (± 3.6; n = 17), while for the DNA halo preparation, these diameters were 34.5 nm (± 7.0; n = 2) and 74.6 nm (± 8.0; n = 2). NPCs in cells extracted using the primary stages of the DNA halo preparation were on average smaller than those NPCs in NM preparations (table 6.3.1).

Cell line	Genotype	Extraction method	Number of NPCs analysed	Mean inner diameter in nm (SD)	Mean outer diameter in nm (SD)
HDF	Normal	NM	17	39.1 (5.4)	81.7 (3.6)
		DNA halo	2	34.5 (7.0)	74.6 (8.0)
Y259X	*LMNA* $^{-/-}$	DNA halo	13	35.6 (5.9)	89.9 (5.9)
KK	*EMD* $^{-/Y}$	NM	21	42.9 (4.6)	90.7 (5.6)
		DNA halo	24	41.0 (4.2)	89.2 (4.2)
AP	*EMD* $^{-/Y}$	NM	18	37.5 (4.2)	79.3 (3.6)
99P0598	*LBR*$^{-/+}$	NM	10	43.1 (5.7)	87.3 (3.0)
		NM (plus RNase inhibitors)	11	46.1 (5.6)	91.1 (8.5)
99P0599	*LBR*$^{-/-}$	NM	5	37.8 (6.2)	87.7 (4.0)

Table 6.3.1 Dimensions of residual NPCs in control and disease HDFs
The mean inner and outer diameters of residual NPCs were determined for control and disease HDFs. SD = standard deviation.

6.3.1.2 Using feSEM to visualise residual nuclei following the DNA halo preparation

The genome is proposed to be organised into repeating loops of DNA through its interaction with the NM; such loops are predicted to be 50–200 kb in length. Those sequences which anchor DNA to the NM are known as MARs or SARs (Laemmli et al., 1992; Heng et al., 2004). Following the DNA halo preparation, only inextractable elements of the nucleus are demonstrated to remain. Indeed, this includes a residual nucleus, which contains the inner NM and the peripheral NL; attached to this structure, via MARs, are loops of DNA which radiate from the residual nucleus and form a DNA halo (Gerdes et al., 1994). In order to visualise the residual nucleus following a NM extraction using feSEM, normal HDFs were subjected to the entire DNA halo preparation. As expected, a mass of DNA appeared to be attached to the underlying residual nucleus; surrounding which, was a halo of extracted DNA (figure

6.3.4). Thus, this concurred with observations of DNA halos using UV microscopy (see chapters 2 and 3). Significantly, the DNA fibres composing this halo exhibited a mean diameter of 10.3 nm (± 2.3; n (fibres) = 30); since DNA has a helical diameter of 2.2-2.6 nm (Mandelkern et al., 1981), this suggested that the DNA was not fully extended and instead, was partially supercoiled.

6.3.1.3 Visualisation of residual filaments following extraction by the DNA halo preparation

In an attempt to observe the structure of the internal NM, cells were taken through a modified version of the DNA halo preparation, which included the additional step of DNase I digestion. By following such DNase I digestion with 2M NaCl extraction, the digested DNA, associated histones and other soluble proteins were eluted. The removal of chromatin allowed the visualisation of the underlying structure, in places (figure 6.3.5). Indeed, NM extraction methodologies involving 2M NaCl are reported to extract the outer NM proteins and reveal a highly branched and heterogeneous network of core filaments (He et al., 1990). The morphology of the filaments remaining after extraction in this study was not unlike this description. These residual filaments exhibited a mean diameter of 9.0 nm (± 2.3; n (filaments) = 74) which is in line with the published diameter of core filaments (He et al., 1990). However, in the study by He et al. (1990), the ionic strength employed to reveal such filaments was increased gradually (i.e. 0.25 M ammonium sulphate followed by 2M NaCl); while in this present study, the ionic strength was rapidly increased (i.e. 2M NaCl) following DNase I digestion. He et al. (1990) demonstrate that such a rapid increase in ionic strength preserves the morphology of the core filaments less efficiently than a gradual rise and results in their aggregation (He et al., 1990). In fact, the residual structure seen in figure 6.3.5a is not dissimilar to that presented on page 573 of the paper by He et al. (1990), which was revealed following DNase I–2M NaCl treatment. Thus, it is likely that the filaments observed in 6.3.5 represent a partial aggregation of core filaments. Without immunolabelling or the use of mass spectrometry, it is impossible to conclude the composition of the residual filaments presented in this study. However, it is likely that they are RNA-rich since 67% of nuclear RNA is said to be retained in core filaments of the NM and also, RNase A treatment is demonstrated to destroy filament integrity

(He et al., 1990). Furthermore, it is probable that these filaments are composed of actin and NuMA since both are demonstrated to be are proteins of core filaments (He et al., 1990; Zeng et al., 1994).

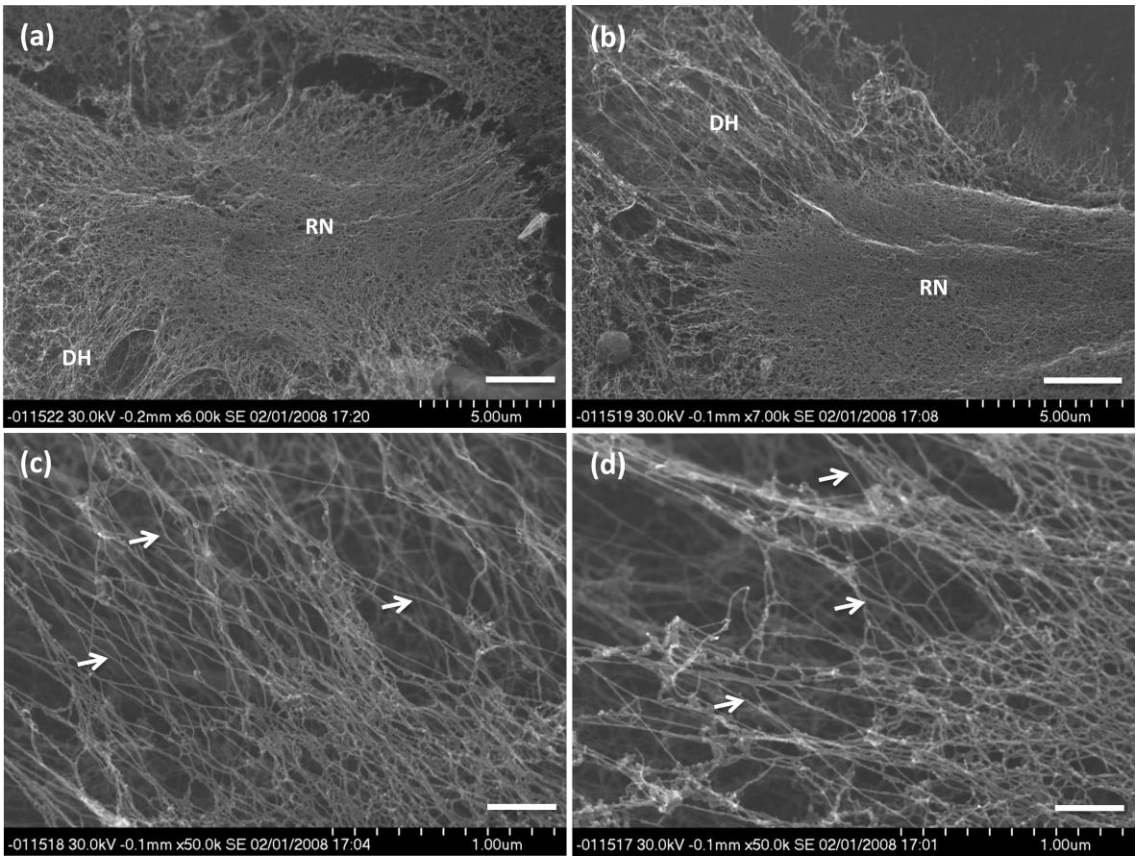

Figure 6.3.4: Residual nuclei surrounded by a halo of DNA visualised by feSEM
(a–b) The morphology of the residual nucleus (RN) and surrounding DNA halo (DH) in control HDFs following extraction by the DNA halo preparation. Magnification = 6k (a) and 7k (b); scale bar = 2.5 µm. **(c–d)** Extracted, supercoiled DNA (white arrowheads); scale bar 300 nm.

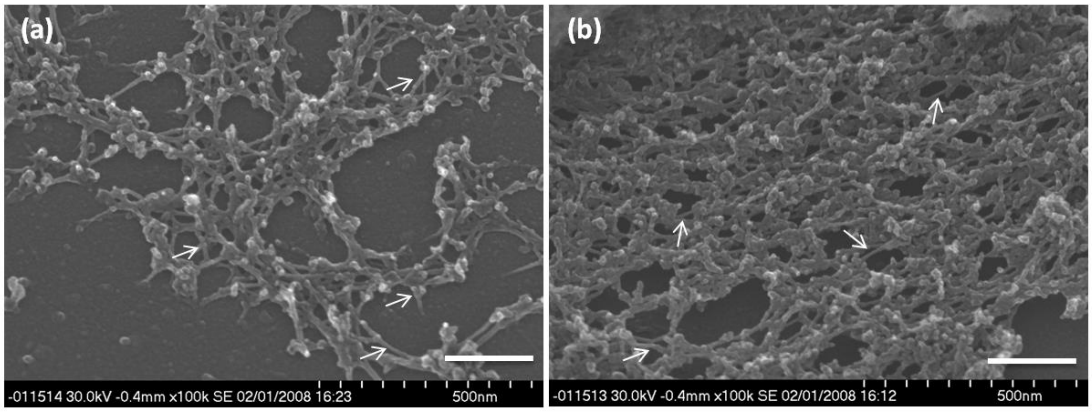

Figure 6.3.5: Residual NM filaments following extraction by the DNA halo preparation and DNase I digestion
(a–b) The morphology of residual NM filaments in control HDFs following extraction by the DNA halo preparation and DNase I digestion. White arrowheads indicate filaments which are assumed to be constituents of the inner NM. Magnification = 100k; scale bar = 200 nm.

6.3.2 Examining nuclear structure during NM extraction in diseased fibroblasts

Nuclear structure is perturbed in human and murine cells harbouring *LMNA*/*Lmna* (Fidzianska and Hausmanowa-Petrusewicz, 2003; Goldman et al., 2004; Columbaro et al., 2005; Scaffidi and Misteli, 2005; Filesi et al., 2005; Capell et al., 2005; Yang et al., 2005; Meaburn et al., 2007; Verstraeten et al., 2008; Park et al., 2009), *EMD*/*Emd* (Lammerding et al., 2005; Ozawa et al., 2006) and *LBR* (Hoffmann et al., 2002) mutations. In light of this, nuclear morphology was examined and compared in cells derived from patients that were either $LMNA^{-/-}$, $EMD^{-/Y}$, $LBR^{-/+}$ or $LBR^{-/-}$. Due to time restrictions as a visiting scientist, only selected cell lines were subjected to both NM extraction procedures; the remaining cell lines were extracted with one or the other. Since evidence demonstrates that the NM is RNA-rich and that RNase degradation destroys filament integrity (He et al., 1990), certain extractions were performed in the presence of RNase inhibitors.

In view of the fact that $LMNA^{-/-}$ and $EMD^{-/Y}$ cells were extracted using the DNA halo preparation, while the *LBR* mutants were subjected to the NM preparation, respective nuclear structures cannot be directly compared. However, such morphology for each disease cell line can be assessed according to control images produced using the same extraction technique. In cells harbouring *LMNA* (Y259X) or *EMD* (KK and AP) mutations, the outer face of the NL was disrupted (figure 6.3.6c and d, respectively); this was particularly true in Y259X, where the structural integrity of the NL appeared to be extremely compromised. In these $LMNA^{-/-}$ HDFs, the NL exhibited a ruffled morphology and appeared highly disordered (figure 6.3.6c). In cells with heterozygous or homozygous *LBR* mutations, the morphology of the NL was similar to controls. Significantly, there was evidence of NPC clustering in Y259X (figure 6.3.6c), which appears to be as a consequence of NL disorder; however, this was not detected in the *EMD* or *LBR* mutants. In order to determine whether the use of RNase inhibitors made a visible difference to nuclear morphology, cells extracted in the presence and absence of RNase inhibitors were compared. The most obvious difference between the two populations was an expected one; in those cells that were extracted in the presence of RNase inhibitors, an increase in the number of ribosomal-like structures on the surface of the outer face of the NL, was reported (figure 6.3.7).

The inner and outer diameters of NPC structures were recorded for control and disease cell lines (table 6.3.1). Mean inner pore diameters ranged from 34.5 (HDF; DNA halo) to 46.1 nm (99PO598; nuclear extraction (plus RNase inhibitors)), while mean outer pore diameters ranged from 74.6 (HDF; DNA halo) to 91.1 nm (99PO598; nuclear extraction (plus RNase inhibitors)). The largest mean inner and outer pore diameters were recorded in 99PO598 fibroblasts extracted in the presence of RNase inhibitors; thus, this suggests that inhibiting RNase activity preserves NPCs more effectively. Significantly, there were no consistent differences between control and disease cells with respect to NPC dimensions (table 6.3.1).

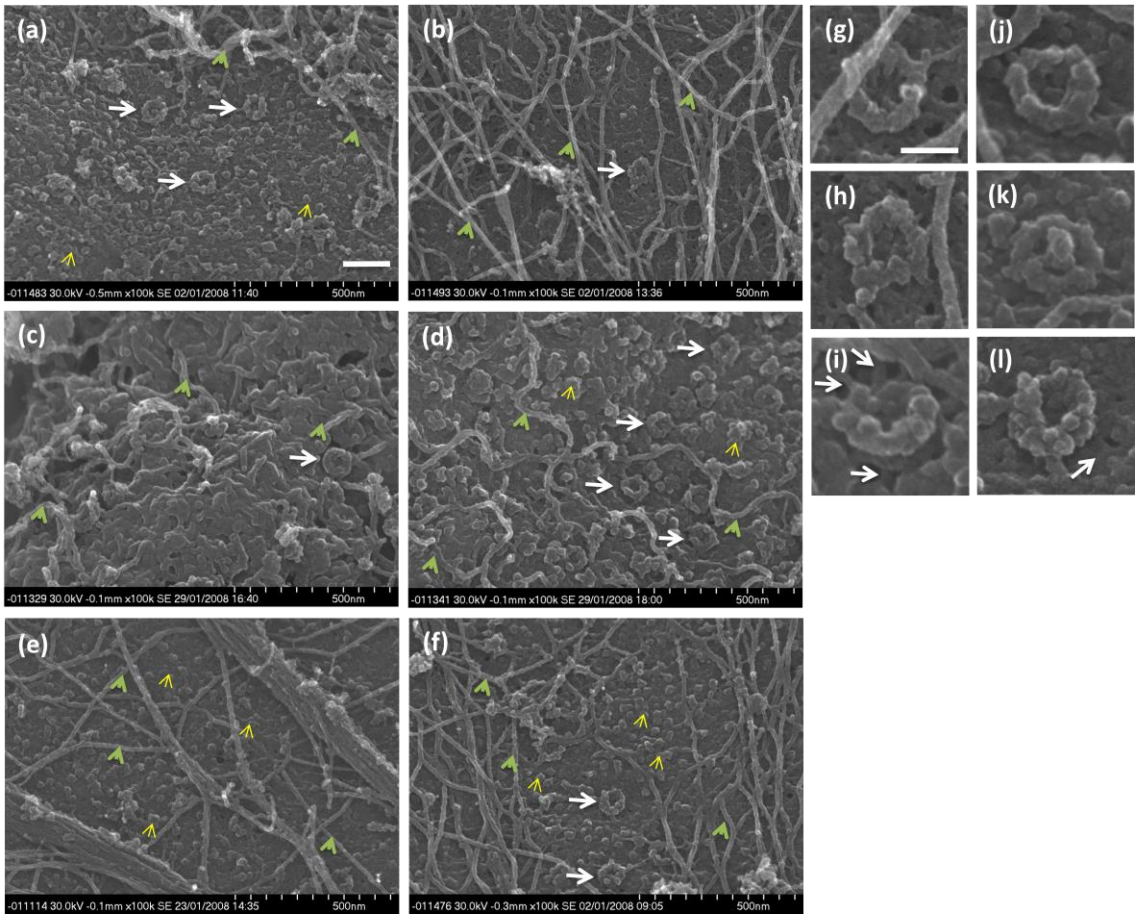

Figure 6.3.6: Nuclear morphology in control and disease HDFs following cytoskeleton extraction

In order to visualise the NL, HDFs were subjected to the primary stages of the NM preparation **(a, e, g, f, k, l)** or the DNA halo preparation **(b, c, d, h, i, j).** The morphology of the outer NL in **(a, b)** control, **(c)** *LMNA*$^{-/-}$, **(d)** *EMD*$^{-/-}$, **(e)** *LBR*$^{+/-}$ and **(f)** *LBR*$^{-/-}$ HDFs. White arrowheads indicate residual NPCs, while structures assumed to be ribosomes are marked using yellow arrowheads. Green arrowheads indicate filaments most likely to be the intermediate filament, vimentin. Magnification = 100k; scale bar = 150 nm (images 25% of actual size). The morphology of

residual NPCs in **(g, h)** control, **(i)** *LMNA*$^{-/-}$, **(j)** *EMD*$^{-/-}$, **(k)** *LBR*$^{+/-}$ and **(l)** *LBR*$^{-/-}$ HDFs. Magnification = 100k; scale bar = 50 nm. White arrowheads highlight filamentous structures that appear to radiate from the NPCs in *LBR* mutants.

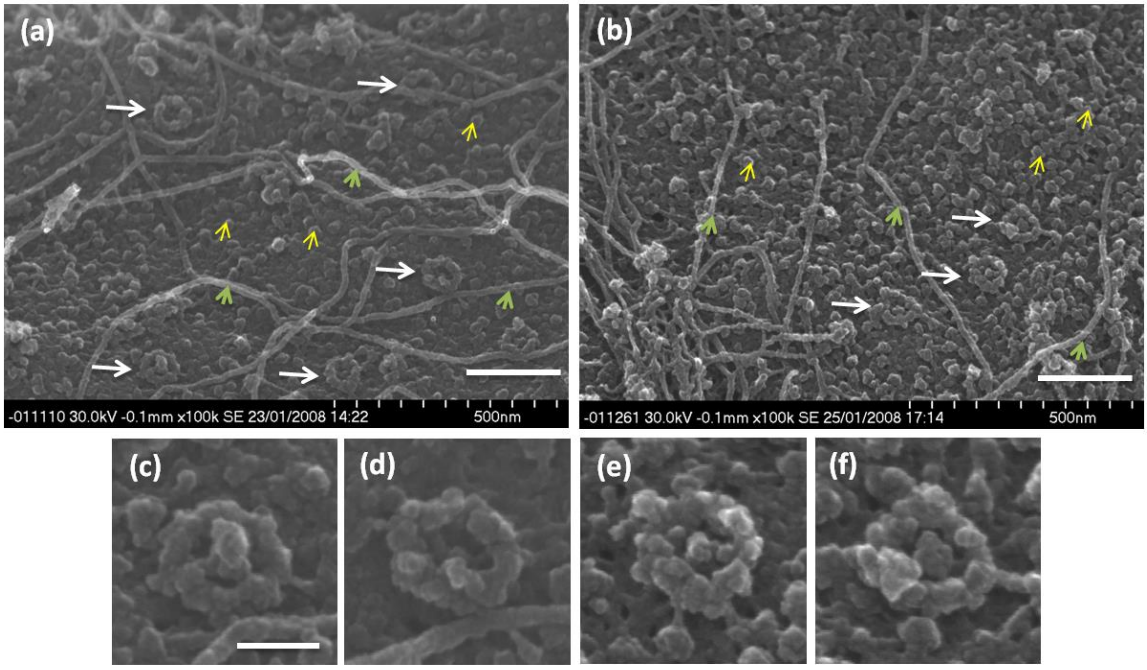

Figure 6.3.7: A comparison of nuclear morphology in *LBR*$^{+/-}$ HDFs following cytoskeleton extraction in the presence and absence of RNase inhibitors

NM preparations performed in the absence **(a, c, d)** and presence **(b, e, f)** of RNase inhibitors. The morphology of **(a, b)** the outer NL; magnification = 100k; scale bar = 200 nm and **(c–f)** residual NPCs; magnification = 100k; scale bar = 50 nm. White arrowheads indicate residual NPCs, while structures assumed to be ribosomes are marked using yellow arrowheads. Green arrowheads indicate filaments most likely to be the intermediate filament, vimentin.

6.4 DISCUSSION

6.4.1 Delineating the ultrastructure of the DNA halo prepared residual nuclei

The DNA observed following *in situ* NM preparations is highly supercoiled (Cook and Brazell, 1975; Berezney and Buchholtz, 1981). The methodologies employed to produce DNA halos act to relax such supercoiling by using ethanol dehydration and/or airdrying steps (Ma et al., 1999). However, although the degree of supercoiling is less extensive in DNA halos, the DNA still exhibits partial supercoiling (Comings and Okada, 1976; Vogelstein et al., 1980). Indeed, in this study, the mean diameter of the DNA extracted into the halo was approximately 10 nm; since DNA has a helical diameter of 2.2–2.6 nm (Mandelkern et al., 1981), this suggested that the DNA was not fully extended and instead, exhibited supercoiling.

The removal of DNA using DNase I allowed the observation of the underlying residual nucleus. In places, an array of filaments, approximately 9 nm in diameter, were recorded. This is intriguing since it is purported that the internal NM is composed of core filaments with a diameter of 10 nm, which underlie thick polymorphic fibres of varying sizes (He et al., 1990). Furthermore, the filaments presented in this chapter look similar to those presented previously (He et al., 1990). The obvious criticism of this present study is that these underlying filaments could be remnants of a collapsed NL. In order to interpret these structures correctly, EM would need to be coupled with the immunolabelling of A- and B-type lamins. Since evidence demonstrates that the core filaments of the internal NM are not enriched with lamin proteins (Hozak et al., 1995), this would aid in determining whether or not the filaments originated from the NL. Antibodies raised against cellular proteins such as vimentin would also help to delineate the structure.

6.4.2 The integrity of the NL is disrupted in cells harbouring *LMNA* and *EMD* mutations

By permeabilising the cellular and nuclear membranes of control and disease fibroblasts, a membrane-like structure was revealed. Since Triton X-100 is documented to disrupt and remove the inner and outer nuclear membranes (Aaronson and Blobel,

1974), it is likely that this remnant structure was the NL. Indeed, the NL is found to be insoluble and resistant to such extraction (Gerace et al., 1984; He et al., 1990; Hozak et al., 1995; Ma et al., 1999; Markiewicz et al., 2002). The observation that this structure was perforated with NPCs concurs with the notion that the nuclear membrane is not necessarily required for the anchorage of these complexes within the nucleus (Aaronson and Blobel, 1974). It also reinforces the previously documented link between lamin proteins, the NL and NPCs (Goldberg and Allen, 1996; Smythe et al., 2000; Liu et al., 2000; Daigle et al., 2001; Hubner et al., 2006; Pan et al., 2007).

The structural integrity of the NL appeared to be compromised to varying extents in disease fibroblasts. The severest disruption was observed in *LMNA*$^{-/-}$ cells; in these, the NL was highly irregular and disordered. This is to be expected since the NL, of which lamin A is a constituent, is assumed to be weakened is such cells. Indeed, there have been numerous reports of abnormal nuclear morphology in cells with *LMNA* mutations (Sullivan et al., 1999; Novelli et al., 2002; Bechert et al., 2003; Glynn and Glover, 2003, Bridger and Kill, 2004; Muchir et al., 2004; Goldman et al., 2004; Paradisi et al., 2005; Wang et al., 2006). Thus, it has been hypothesised that in cells harbouring *LMNA* mutations, the NL is weakened which in turn compromises the structural mechanics of the nucleus (Lammerding et al., 2004; Broers et al., 2004). A recent study suggests that lamin A is required to maintain the 'internal inertia' of the nucleus (De Vos et al., 2010). Therefore, it is logical to suggest that when lamin A is missing or mutant, the rigidity of the NL is partially lost and as a result, the NL becomes more flaccid and disorganised. This is probably a contributing factor to the abnormal clustering of NPCs evident in *LMNA*$^{-/-}$ cells. Such clustering of NPCs has been described previously in *Drosophila* and human lamin mutants (Lenz-Bohme et al., 1997; Goldman et al., 2004). Indeed, lamins and nucleoporins interact (Smythe et al., 2000; Hubner et al., 2006; Pan et al., 2007) and as a result, it has been hypothesised that lamin proteins have a role in anchoring NPCs (Smythe et al., 2000). Thus, it appears that in *LMNA*$^{-/-}$ nuclei, NPC organisation is disrupted in two ways: firstly, due to the irregularity of the NL and secondly, as a result of the perturbed or lost interaction with lamin proteins.

The electron micrographs revealed that the NL was also perturbed in X-EDMD nuclei, concurring with previous observations of abnormal nuclear morphology in *EMD*

mutant cells (Lammerding et al., 2005; Ozawa et al., 2006). However, the extent of this disorganisation was not as extreme as in *LMNA*$^{-/-}$ nuclei. Furthermore, the clustering of NPCs was not detected in these emerin null fibroblasts. This agrees with previous work which shows that while lamin A/C is important for NPC formation and localisation, emerin is not (Maeshima et al., 2006). This disparity in the disturbance of NL integrity is reflective of the difference in disease severity seen in mice that are either lamin A or emerin null. In humans, heterozygous *EMD* mutations are not sufficient to cause X-EDMD; thus, heterozygous females (*EMD*$^{+/-}$) are carriers while the disease pathology is observed in hemizygous males (*EMD*$^{-/Y}$; Bione et al., 1994; Yates et al., 1999). Disease-causing *LMNA* mutations are most common in the heterozygous state (Bonne et al., 1999; Eriksson et al., 2003; De Sandre-Giovannoli et al., 2003); while homozygous *LMNA* mutations do exist, they are rare, cause more severe phenotypes and can be fatal (Raffaele di Barletta et al., 2000; De Sandre - Giovannoli et al., 2002; van Engelen et al., 2005).

Although *EMD* mutant mouse models do not fully reflect the X-EDMD disease phenotype, it does reinforce the notion that *LMNA* and *EMD* mutations exhibit differing disease causing capacities. Emerin deficient mice display a mild clinical phenotype which does not affect growth rate or fertility (Ozawa et al., 2006), whereas mice null for lamin A are growth retarded and die prematurely (Sullivan et al., 1999). In addition, *Lmna* $^{-/-}$ mice exhibit skeletal and cardiac dysfunction (Sullivan et al., 1999) while *Emd* $^{-/Y}$ mice are largely unaffected by such disorders (Ozawa et al., 2006).

The outer surface of the NL appeared to be normal in both heterozygous and homozygous *LBR* mutants. LBR is found at the nuclear periphery; this is likely due to the protein's interaction with lamin B (Worman et al., 1988; Ye and Worman, 1994; Reichart et al., 2004). Importantly, LBR appears to have at least two distinct functions. Firstly, it is implicated in chromatin organisation through its association with DNA and HP1 (Ye and Worman, 1994; 1996; Ye et al., 1997). Furthermore, the protein also exhibits cholesterol biosynthetic enzymatic activity (Waterham et al., 2003). In humans, heterozygous *LBR* mutations lead to PHA which is a benign disease characterised primarily by the hypolobulated nuclei of blood granulocytes; chromatin organisation is also perturbed (Hoffmann et al., 2002). The aberrant shape in

granulocytes is caused by the failure of nuclear lobes to develop correctly. In the homozygous form, *LBR* mutations can cause a spectrum of disease severity; with AR-PHA at the mild end and Greenberg skeletal dysplasia, at the other (Hoffmann et al., 2002; Waterham et al., 2003). In granulocytes derived from AR-PHA, nuclei are round and non-segmented (Hoffmann et al., 2002). While NL disruption was not observed in cells harbouring *LBR* mutants, it is possible that such perturbations were so subtle that they could not be detected visually. It could be suggested that LBR is more actively involved in the formation or maintenance of nuclear shape in granulocytes than in fibroblasts; however, the overexpression of *LBR* has been demonstrated to result in NE invaginations in non-leukocytes (Ma et al., 2007).

Significantly, the inner and outer pore diameters were similar in all cell lines (control and disease) using both extraction techniques. This is important since it indicates that there is consistency in the nuclear structure and morphology revealed by extraction procedures performed on different days. The measurements for inner and outer pore diameters (34.5–46.1 nm and 74.6–91.1 nm, respectively) were significantly smaller than those reported for the human NPC (outer diameter 120 nm, inner diameter 50 nm; Elad et al., 2009). However, this is perhaps expected since the extraction procedures used in this chapter most probably resulted in the collapse and shrinkage of the cell/nucleus. Indeed, differences in dimensions and observed structure have been reported in native versus detergent-extracted NPCs (Fahrenkrog and Aebi, 2003).

6.4.3 Concluding remarks

Interpreting the results produced by such harsh, non-physiological extraction procedures is fraught with difficulty, mainly because the remnant nucleus does not represent any *in vivo* structure. However, as long as investigations using these methodologies are comparative, they can aid in our understanding of nuclear structure in normal cells and the disruption of such structure in diseased cells. Without coupling EM with immunolabelling, it would be incorrect to derive any firm conclusions from this study; nonetheless, the findings do confirm the observations of previous studies regarding the fragility of the NL in the absence of functional lamin A and emerin. These findings also reinforce the notion that the NL and NPC network is highly integrated.

7. General Discussion

7.1 Examining the nature of NM-genome interactions using the DNA halo assay

The NM or NS is a permanent network of core filaments, underlying thicker fibres, present regardless of transcriptional activity (Jackson and Cook, 1988; He et al., 1990; Hozak et al., 1995; Philimonenko et al., 2001; Nickerson et al., 2001). It is found to be both RNA and protein rich; indeed, treatment with RNase A destroys filament integrity (He et al., 1990). Significantly, the NM is proposed to organise the genome; indeed, chromosomes (Ma et al., 1999; Croft et al., 2001), genes (Tocharoentanaphol et al., 1994; Repping et al., 2003; Iarovaia et al., 2004) and telomeres (de Lange, 1992; Luderus et al., 1996) are demonstrated to be anchored to this structure. Therefore, it was logical to hypothesize that if the NM is dysfunctional its capacity to perform such function is restricted. In order to test this, it was necessary to develop an assay which allowed NM-genome interactions to be examined. As a result, the DNA halo preparation was selected. The residual nuclei remaining following such an extraction procedure represents a salt-resistant structure termed the NM. Since the use of DNA digestion is omitted, NM-associated DNA is anchored to the NM, while DNA which does not interact with the NM is extracted into the surrounding space to form a halo of DNA. By coupling the DNA halo preparation with different variants of FISH, it was possible to visualise interactions between the NM and specific parts of the genome. Significantly, chapter 2 demonstrated that the majority of chromosomes, telomeres and genes are anchored to this salt-resistant structure. Furthermore, these studies revealed that there was no significant difference in such NM-associations between proliferating and senescent HDFs; however, this anchorage did differ in quiescence. Importantly, these studies show that the DNA halo assay employed to examine such interactions, generates consistent and reproducible results.

7.2 Perturbed genome organisation in disease

7.2.1 NM-genome interactions

In light of this, it seemed pertinent to examine whether mutations in certain NM-associated proteins affect the capacity of the NM to tether chromatin within the interphase nucleus. Since both lamin A (Hozak et al., 1995; Barboro et al., 2002) and emerin (Squarzoni et al., 1998; Ellis et al., 1998; Takata et al., 2009) are NM proteins,

cells harbouring mutations in the genes encoding these proteins, presented an excellent opportunity to examine this hypothesis. In chapter 3, NM-genome interactions were investigated, using the DNA halo assay, in a variety of HGPS and X-EDMD cell lines, which exhibit mutations in *LMNA* and *EMD,* respectively. Chromosome anchorage by the NM was analysed in HGPS and significantly, half of the chromosomes examined displayed disrupted NM interactions. Subsequently, NM-telomere associations were investigated in HGPS and X-EDMD fibroblasts; indeed, these studies revealed a reduction in telomere anchorage for all disease cell lines. Since HGPS telomeres exhibit considerably shorter telomeres than those found in controls (Allsopp et al., 1992; Decker et al., 2009), it seemed necessary to question whether the activation of telomerase in these cells would affect telomere binding to the NM. To do this, classical HGPS cells, previously immortalised by the stable transfection of hTERT, were subjected to the DNA halo assay and telomere-PNA FISH. Surprisingly, this appeared to increase the number of NM-telomere interactions to a level statistically similar to control cells, which indicates that by immortalising HGPS HDFs, some telomere-related phenotypes can be rescued in lamin A mutant cells. These findings posed another question: what is the nature of NM-telomere interactions in cancer cell lines, which are consistently immortalised? To tackle this question, telomere anchorage by the NM was assessed in two melanoma cell lines (one highly tumourigenic, the other non-tumourigenic) using the DNA halo assay. Significantly, although the DNA halos generated from the melanoma cells were the most extensive of all the cell lines studied, telomere anchorage was similar to control HDFs. Taken together, these experiments using immortalised HGPS and melanoma cell lines suggest that telomerase activation most probably affects telomere binding to the NM.

7.2.2 Interphase gene positioning in non-extracted fibroblasts

While evidence linking *LMNA* mutations and disorganised genome organisation is quite extensive (Sewry et al., 2001; Fidzianska and Hausmanowa, 2003; Goldman et al., 2004; Filesi et al., 2005; Maraldi et al., 2006; Meaburn et al., 2007; Lattanzi et al., 2007; Hakelien et al., 2008; Park et al., 2009), the same cannot be said for *EMD* (Fidzianska et al., 1998; Ognibene et al., 1999; Meaburn et al., 2007). Therefore, to test whether *EMD*

mutations disrupt gene positioning, the locations of 4 genes were examined in control and 3 X-EDMD patient cell lines using 2D and 3D FISH. To determine if such positioning changes in senescent cells, both proliferating (pKi67+) and non-proliferating (pKi67−) populations were studied. Since previous research has reported that one of these genes (*C-MYC*) is up-regulated in X-EDMD (Markiewicz et al., 2006), this gave the study a dual aim. Firstly, to test whether the locations of these four genes were disrupted in X-EDMD and secondly, to examine whether any modifications in such positioning correlated with any changes in the expression of these genes by RT-PCR. Importantly, while there were subtle changes in gene positioning, there was no evidence of dysregulated transcription.

7.2.3 The role of lamin A and emerin in mediating genome organisation and structural integrity

By using the DNA halo assay, it has been demonstrated that telomere binding to the NM is weakened in *LMNA* and *EMD* mutant HDFs. Importantly, while cells lacking emerin exhibited perturbed telomere anchorage, such interactions were more severely affected in dominant-negative lamin A mutants. This fits with the previously observed trend regarding differences in disease severity; emerin's absence is less disruptive than the presence of lamin A mutants. Indeed, the loss of emerin did not appear to significantly affect the positioning of 4 selected genes in X-EDMD. What does this suggest? Firstly, it indicates that lamin A is more important for tethering chromatin within the nucleus than emerin. Indeed, lamin A is demonstrated to interact with DNA directly (Shoeman and Traub, 1990; Taniura et al., 1995; Stierle et al., 2003), while emerin's association with chromatin is likely to be indirectly mediated by BAF (Lin et al., 2000; Lee et al., 2001; Segura-Totten and Wilson, 2004). It is interesting that telomere anchorage is perturbed in extracted X-EDMD cells, while gene positioning in non-extracted cells lacks signs of significant disruption. Perhaps this indicates that while emerin is involved in the NM-complexes which tether telomeres to the NM, the protein is less implicated in those complexes which tether genome-wide MARs. This would thus suggest a differentiation between telomeric MARs and other MARs throughout the genome.

In addition to demonstrating that NM-genome associations are disrupted in *LMNA* and *EMD* mutants, the results presented in this thesis also indicate that in such cells, nuclear integrity is compromised. In chapter 6, control and disease HDFs were gradually extracted using either the DNA halo preparation or another procedure. This study revealed that the absence of functional lamin A more severely disrupted the integrity of the NL than emerin. This was not a surprising finding since lamin A is a major component of the NL, while emerin is tethered to the NP via its interaction with lamin A. However, the observation that emerin's absence weakened the NL is an important observation.

Taken together, these chapters demonstrate that while both lamin A and emerin are important for organising the genome and maintaining nuclear structural integrity, lamin A is less dispensable to the cell than emerin.

7.3 Delineating the effects of a dysfunctional NM

7.3.1 Transcription

Since *LMNA* and *EMD* mutations perturb the NM's ability to anchor chromatin within the interphase nucleus, it is necessary to consider the possible implications of such dysfunction on the nucleus. One possible consequence could be the deregulation of transcription. Indeed, the NM provides the foundation upon which transcription factories operate (Iborra et al., 1996). Thus, the effect of mutant lamin A or emerin on transcription could be multifaceted. Firstly, the presence of dominant-negative lamin A mutants or the absence of emerin contributes to NM dysfunction by failing to anchor MARs correctly. If genes are incorrectly positioned, their normal local environment may change significantly and therefore, altering the type of transcription factories available in the vicinity. As a result of this, gene expression could be mis-regulated, with genes either not participating in transcription or being forced to use sub-optimal factories. In line with this, transcription deregulation has been reported in both HGPS (Ly et al., 2000; Csoka et al., 2004) and X-EDMD (Tsukahara et al., 2002) cell lines. Mutant forms of lamin A and emerin may affect transcription in additional ways; indeed, if lamin proteins are missing or mutant, this nuclear process is perturbed. Spann et al. (2001) reported that the presence of mutant lamin A inhibits the activity

of RNA polymerase. Furthermore, depleting lamin B1 levels by interference technology significantly disrupts RNA synthesis (Tang et al., 2008).

7.3.2 DNA repair

In addition to the NM's role in transcription, the nuclear structure is implicated in co-ordinating DNA damage signalling (McCready and Cook, 1984; Harless and Hewitt, 1987; Koehler and Hanawalt, 1996; Jiang et al., 2001; Kamiuchi et al., 2002; Mladenov et al., 2009). Significantly, p53 binding to the NM increases in response to DNA damage (Jiang et al., 2001); it is thus plausible that if p53 cannot interact correctly due to a dysfunctional NM, such signalling becomes disordered. In line with this, p53 signalling is up-regulated in cells harbouring mutant lamin A (Varela et al., 2005). Furthermore, Rad51, a key homologous recombination protein, forms NM-associated foci in response to DNA damage (Mladenov et al., 2006, 2007, and 2009); in HGPS, there is evidence that the recruitment of this protein is perturbed (Liu et al., 2005). Therefore, it is likely that mutant lamin A hampers the NM's capacity to recruit such proteins, thus, impairing the DNA damage response.

What accounts for the shorter telomeres reported in HGPS patients (Allsopp et al., 1992; Decker et al., 2009)? It is suggested that compromised DNA damage pathways are possibly the cause of this phenomenon in HGPS. It is thus likely that in HGPS, damaged telomeres are not efficiently repaired and as a result, they are eroded at varying speeds; this could account for the wide variation seen in HGPS telomeric length (Decker et al., 2009). Consequently, HGPS telomeres reach a critical length far quicker than normal and as a result, these chromosome ends are recognised as DNA damage, leading to senescence or apoptosis (Decker et al., 2009). This increased proportion of senescent cells due to telomere dysfunction could illicit a compensatory response in the remaining pool of cells, in the form of enhanced proliferation (Decker et al., 2009). Indeed, hyper-proliferation and increased rates of apoptosis have been observed previously in HGPS (Bridger and Kill, 2004).

Does the incorrect telomere anchorage seen in HGPS and X-EDMD merely reflect the effect of *LMNA* and *EMD* mutations on NM function or does it contribute to the

disease phenotype seen in these patients? If the latter is the case, how does perturbed NM-telomere binding affect telomere biology on a larger scale? Since telomeres are vitally important for chromosome stability (Blackburn et al., 2001), it is likely that their anchorage to the NM contributes to this function. In light of the fact that the NM mediates DNA replication and repair processes, this seems especially logical. The binding of telomeres to this nuclear structure may also aid in the prevention of telomere fusions. Therefore, in HGPS and X-EDMD, it is possible that the reduction in telomere anchorage by the NM impairs the replication and repair of telomeres and as a result, increases genome instability through telomere erosion.

This discussion suggests that a sub-optimal NM contributes to the dysfunctional telomere biology observed in HGPS in different ways. Firstly, by the inefficient recruitment of proteins involved in DNA repair to the NM and secondly, by failing to anchor telomeres correctly. Furthermore, perhaps the inability of the lamin A mutant-NM to mediate telomere binding is also a contributing factor to the accelerated telomere erosion documented in HGPS. The study of telomeres in HGPS appears to be central to elucidating the mechanisms involved in premature ageing, particularly since signs of telomere dysfunction and DNA damage are found to increase with age (Jiang et al., 2008).

7.4 Summary

Taken together, the results presented in this thesis demonstrate the importance of lamin A, emerin and the NM in mediating correct genome organisation. Indeed, in cells harbouring mutant forms of these NM proteins, the structure's ability to tether chromosomes and telomeres, is perturbed. These findings further strengthen the view that the NM is a significant nuclear structure which participates and regulates numerous nuclear processes.

References

Aaronson RP and Blobel G (1975) Isolation of nuclear pore complexes in association with a lamina. *Proceedings of the National Academy of Sciences of the United States of America,* **72** (3), 1007-1011.

Aaronson RP and Blobel G (1974) On the attachment of the nuclear pore complex. *The Journal of cell biology,* **62** (3), 746-754.

Adachi Y, Kas E and Laemmli UK (1989) Preferential, cooperative binding of DNA topoisomerase II to scaffold-associated regions. *The EMBO journal,* **8** (13), 3997-4006.

Aebi U, Cohn J, Buhle L and Gerace L (1986) The nuclear lamina is a meshwork of intermediate-type filaments. *Nature,* **323** (6088), 560-564.

Agarwal AK, Fryns JP, Auchus RJ and Garg A (2003) Zinc metalloproteinase, ZMPSTE24, is mutated in mandibuloacral dysplasia. *Human molecular genetics,* **12** (16), 1995-2001.

Akhtar A and Gasser SM (2007) The nuclear envelope and transcriptional control. *Nature reviews. Genetics,* **8** (7), 507-517.

Alexander RB, Greene GL and Barrack ER (1987) Estrogen receptors in the nuclear matrix: direct demonstration using monoclonal antireceptor antibody. *Endocrinology,* **120** (5), 1851-1857.

Allen GC, Hall G,Jr, Michalowski S, Newman W, Spiker S, Weissinger AK and Thompson WF (1996) High-level transgene expression in plant cells: effects of a strong scaffold attachment region from tobacco. *The Plant Cell,* **8** (5), 899-913.

Allen TD, Cronshaw JM, Bagley S, Kiseleva E and Goldberg MW (2000) The nuclear pore complex: mediator of translocation between nucleus and cytoplasm. *Journal of cell science,* **113** (Pt 10), 1651-1659.

Allsopp RC, Vaziri H, Patterson C, Goldstein S, Younglai EV, Futcher AB, Greider CW and Harley CB (1992) Telomere length predicts replicative capacity of human fibroblasts. *Proceedings of the National Academy of Sciences of the United States of America,* **89** (21), 10114-10118.

Alsheimer M and Benavente R (1996) Change of karyoskeleton during mammalian spermatogenesis: expression pattern of nuclear lamin C2 and its regulation. *Experimental cell research,* **228** (2), 181-188.

Amati F, Biancolella M, D'Apice MR, Gambardella S, Mango R, Sbraccia P, D'Adamo M, Margiotti K, Nardone A, Lewis M and Novelli G (2004) Gene expression profiling of fibroblasts from a human progeroid disease (mandibuloacral dysplasia, MAD #248370) through cDNA microarrays. *Gene expression,* **12** (1), 39-47.

Amin D, Cornell SA, Gustafson SK, Needle SJ, Ullrich JW, Bilder GE and Perrone MH (1992) Bisphosphonates used for the treatment of bone disorders inhibit squalene

synthase and cholesterol biosynthesis. *Journal of lipid research,* **33** (11), 1657-1663.

Anachkova B, Djeliova V and Russev G (2005) Nuclear matrix support of DNA replication. *Journal of cellular biochemistry,* **96** (5), 951-961.

Antes TJ, Namciu SJ, Fournier RE and Levy-Wilson B (2001) The 5' boundary of the human apolipoprotein B chromatin domain in intestinal cells. *Biochemistry,* **40** (23), 6731-6742.

Arimura T, Helbling-Leclerc A, Massart C, Varnous S, Niel F, Lacene E, Fromes Y, Toussaint M, Mura AM, Keller DI, Amthor H, Isnard R, Malissen M, Schwartz K and Bonne G (2005) Mouse model carrying H222P-Lmna mutation develops muscular dystrophy and dilated cardiomyopathy similar to human striated muscle laminopathies. *Human molecular genetics,* **14** (1), 155-169.

Bakay M, Wang Z, Melcon G, Schiltz L, Xuan J, Zhao P, Sartorelli V, Seo J, Pegoraro E, Angelini C, Shneiderman B, Escolar D, Chen YW, Winokur ST, Pachman LM, Fan C, Mandler R, Nevo Y, Gordon E, Zhu Y, Dong Y, Wang Y and Hoffman EP (2006) Nuclear envelope dystrophies show a transcriptional fingerprint suggesting disruption of Rb-MyoD pathways in muscle regeneration. *Brain: a journal of neurology,* **129** (Pt 4), 996-1013.

Baker PB, Baba N and Boesel CP (1981) Cardiovascular abnormalities in progeria. Case report and review of the literature. *Archives of Pathology & Laboratory Medicine,* **105** (7), 384-386.

Bao X, Zhang W, Krencik R, Deng H, Wang Y, Girton J, Johansen J and Johansen KM (2005) The JIL-1 kinase interacts with lamin Dm0 and regulates nuclear lamina morphology of Drosophila nurse cells. *Journal of cell science,* **118** (Pt 21), 5079-5087.

Bar DZ, Neufeld E, Feinstein N and Gruenbaum Y (2009) Gliotoxin reverses age-dependent nuclear morphology phenotypes, ameliorates motility, but fails to affect lifespan of adult Caenorhabditis elegans. *Cell motility and the cytoskeleton,* **66** (10), 791-797.

Barboro P, D'Arrigo C, Diaspro A, Mormino M, Alberti I, Parodi S, Patrone E and Balbi C (2002) Unraveling the organization of the internal nuclear matrix: RNA-dependent anchoring of NuMA to a lamin scaffold. *Experimental cell research,* **279** (2), 202-218.

Barrack ER (1987) Steroid hormone receptor localization in the nuclear matrix: interaction with acceptor sites. *Journal of steroid biochemistry,* **27** (1-3), 115-121.

Bartek J, Bartkova J and Lukas J (1996) The retinoblastoma protein pathway and the restriction point. *Current opinion in cell biology,* **8** (6), 805-814.

Bartova E, Harnicarova A, Pachernik J and Kozubek S (2005) Nuclear topography and expression of the BCR/ABL fusion gene and its protein level influenced by cell differentiation and RNA interference. *Leukemia research,* **29** (8), 901-913.

Bartova E, Kozubek S, Kozubek M, Jirsova P, Lukasova E, Skalnikova M, Cafourkova A and Koutna I (2000) Nuclear topography of the c-myc gene in human leukemic cells. *Gene,* **244** (1-2), 1-11.

Bechert K, Lagos-Quintana M, Harborth J, Weber K and Osborn M (2003) Effects of expressing lamin A mutant protein causing Emery-Dreifuss muscular dystrophy and familial partial lipodystrophy in HeLa cells. *Experimental cell research,* **286** (1), 75-86.

Beck LA, Hosick TJ and Sinensky M (1990) Isoprenylation is required for the processing of the lamin A precursor. *The Journal of cell biology,* **110** (5), 1489-1499.

Ben Yaou R, Toutain A, Arimura T, Demay L, Massart C, Peccate C, Muchir A, Llense S, Deburgrave N, Leturcq F, Litim KE, Rahmoun-Chiali N, Richard P, Babuty D, Recan-Budiartha D and Bonne G (2007) Multitissular involvement in a family with LMNA and EMD mutations: Role of digenic mechanism? *Neurology,* **68** (22), 1883-1894.

Berezney R and Buchholtz LA (1981) Dynamic association of replicating DNA fragments with the nuclear matrix of regenerating liver. *Experimental cell research,* **132** (1), 1-13.

Berezney R and Coffey DS (1975) Nuclear protein matrix: association with newly synthesized DNA. *Science (New York, N.Y.),* **189** (4199), 291-293.

Berezney R and Coffey DS (1974) Identification of a nuclear protein matrix. *Biochemical and biophysical research communications,* **60** (4), 1410-1417.

Berger R, Theodor L, Shoham J, Gokkel E, Brok-Simoni F, Avraham KB, Copeland NG, Jenkins NA, Rechavi G and Simon AJ (1996) The characterization and localization of the mouse thymopoietin/lamina-associated polypeptide 2 gene and its alternatively spliced products. *Genome research,* **6** (5), 361-370.

Bergo MO, Gavino B, Ross J, Schmidt WK, Hong C, Kendall LV, Mohr A, Meta M, Genant H, Jiang Y, Wisner ER, Van Bruggen N, Carano RA, Michaelis S, Griffey SM and Young SG (2002) Zmpste24 deficiency in mice causes spontaneous bone fractures, muscle weakness, and a prelamin A processing defect. *Proceedings of the National Academy of Sciences of the United States of America,* **99** (20), 13049-13054.

Biamonti G, Giacca M, Perini G, Contreas G, Zentilin L, Weighardt F, Guerra M, Della Valle G, Saccone S and Riva S (1992) The gene for a novel human lamin maps at a highly transcribed locus of chromosome 19 which replicates at the onset of S-phase. *Molecular and cellular biology,* **12** (8), 3499-3506.

Bidwell JP, van Wijnen AJ, Fey EG, Merriman H, Penman S, Stein JL, Stein GS and Lian JB (1994) Subnuclear distribution of the vitamin D receptor. *Journal of cellular biochemistry,* **54** (4), 494-500.

Bione S, Maestrini E, Rivella S, Mancini M, Regis S, Romeo G and Toniolo D (1994) Identification of a novel X-linked gene responsible for Emery-Dreifuss muscular dystrophy. *Nature genetics,* **8** (4), 323-327.

Bione S, Small K, Aksmanovic VM, D'Urso M, Ciccodicola A, Merlini L, Morandi L, Kress W, Yates JR and Warren ST (1995) Identification of new mutations in the Emery-Dreifuss muscular dystrophy gene and evidence for genetic heterogeneity of the disease. *Human molecular genetics,* **4** (10), 1859-1863.

Blackburn EH (2001) Switching and signaling at the telomere. *Cell,* **106** (6), 661-673.

Blackburn EH (1994) Telomeres: no end in sight. *Cell,* **77** (5), 621-623.

Blasquez VC, Xu M, Moses SC and Garrard WT (1989) Immunoglobulin kappa gene expression after stable integration. I. Role of the intronic MAR and enhancer in plasmacytoma cells. *The Journal of biological chemistry,* **264** (35), 21183-21189.

Blobel G (1985) Gene gating: a hypothesis. *Proceedings of the National Academy of Sciences of the United States of America,* **82** (24), 8527-8529.

Blomen VA and Boonstra J (2007) Cell fate determination during G1 phase progression. *Cellular and molecular life sciences : CMLS,* **64** (23), 3084-3104.

Bode J, Benham C, Knopp A and Mielke C (2000) Transcriptional augmentation: modulation of gene expression by scaffold/matrix-attached regions (S/MAR elements). *Critical reviews in eukaryotic gene expression,* **10** (1), 73-90.

Bode J, Goetze S, Heng H, Krawetz SA and Benham C (2003) From DNA structure to gene expression: mediators of nuclear compartmentalization and dynamics. *Chromosome research: an international journal on the molecular, supramolecular and evolutionary aspects of chromosome biology,* **11** (5), 435-445.

Bode J, Kohwi Y, Dickinson L, Joh T, Klehr D, Mielke C and Kohwi-Shigematsu T (1992) Biological significance of unwinding capability of nuclear matrix-associating DNAs. *Science (New York, N.Y.),* **255** (5041), 195-197.

Bode J and Maass K (1988) Chromatin domain surrounding the human interferon-beta gene as defined by scaffold-attached regions. *Biochemistry,* **27** (13), 4706-4711.

Bodnar AG, Ouellette M, Frolkis M, Holt SE, Chiu CP, Morin GB, Harley CB, Shay JW, Lichtsteiner S and Wright WE (1998) Extension of life-span by introduction of telomerase into normal human cells. *Science (New York, N.Y.),* **279** (5349), 349-352.

Bolzer A, Kreth G, Solovei I, Koehler D, Saracoglu K, Fauth C, Muller S, Eils R, Cremer C, Speicher MR and Cremer T (2005) Three-dimensional maps of all chromosomes in human male fibroblast nuclei and prometaphase rosettes. *PLoS biology,* **3** (5), e157.

Bonne G, Di Barletta MR, Varnous S, Becane HM, Hammouda EH, Merlini L, Muntoni F, Greenberg CR, Gary F, Urtizberea JA, Duboc D, Fardeau M, Toniolo D and Schwartz K (1999) Mutations in the gene encoding lamin A/C cause autosomal dominant Emery-Dreifuss muscular dystrophy. *Nature genetics,* **21** (3), 285-288.

Bonne G, Mercuri E, Muchir A, Urtizberea A, Becane HM, Recan D, Merlini L, Wehnert M, Boor R, Reuner U, Vorgerd M, Wicklein EM, Eymard B, Duboc D, Penisson-Besnier I, Cuisset JM, Ferrer X, Desguerre I, Lacombe D, Bushby K, Pollitt C, Toniolo D, Fardeau M, Schwartz K and Muntoni F (2000) Clinical and molecular genetic spectrum of autosomal dominant Emery-Dreifuss muscular dystrophy due to mutations of the lamin A/C gene. *Annals of Neurology,* **48** (2), 170-180.

Boulikas T (1995) Chromatin domains and prediction of MAR sequences. *International review of cytology,* **162A,** 279-388.

Boyle S, Gilchrist S, Bridger JM, Mahy NL, Ellis JA and Bickmore WA (2001) The spatial organization of human chromosomes within the nuclei of normal and emerin-mutant cells. *Human molecular genetics,* **10** (3), 211-219.

Brakmann S (2010) Single-molecule analysis: A ribosome in action. *Nature,* **464** (7291), 987-988.

Branco MR and Pombo A (2006) Intermingling of chromosome territories in interphase suggests role in translocations and transcription-dependent associations. *PLoS biology,* **4** (5), e138.

Bridger JM and Lichter P (1999) Analysis of mammalian interphase chromosomes by FISH and immunofluorescence. In *Chromosome Structural Analysis: a practical approach*. Edited by Dr. Wendy Bickmore (IRL Press).

Bridger JM, Boyle S, Kill IR and Bickmore WA (2000) Re-modelling of nuclear architecture in quiescent and senescent human fibroblasts. *Current biology : CB,* **10** (3), 149-152.

Bridger JM and Kill IR (2004) Aging of Hutchinson-Gilford progeria syndrome fibroblasts is characterised by hyperproliferation and increased apoptosis. *Experimental gerontology,* **39** (5), 717-724.

Bridger JM, Kill IR, O'Farrell M and Hutchison CJ (1993) Internal lamin structures within G1 nuclei of human dermal fibroblasts. *Journal of cell science,* **104 (Pt 2)** (Pt 2), 297-306.

Broers JL, Machiels BM, van Eys GJ, Kuijpers HJ, Manders EM, van Driel R and Ramaekers FC (1999) Dynamics of the nuclear lamina as monitored by GFP-tagged A-type lamins. *Journal of cell science,* **112 (Pt 20)** (Pt 20), 3463-3475.

Broers JL, Peeters EA, Kuijpers HJ, Endert J, Bouten CV, Oomens CW, Baaijens FP and Ramaekers FC (2004) Decreased mechanical stiffness in LMNA-/- cells is caused by defective nucleo-cytoskeletal integrity: implications for the development of laminopathies. *Human molecular genetics,* **13** (21), 2567-2580.

Broers JL, Raymond Y, Rot MK, Kuijpers H, Wagenaar SS and Ramaekers FC (1993) Nuclear A-type lamins are differentially expressed in human lung cancer subtypes. *The American journal of pathology,* **143** (1), 211-220.

Brown CA, Lanning RW, McKinney KQ, Salvino AR, Cherniske E, Crowe CA, Darras BT, Gominak S, Greenberg CR, Grosmann C, Heydemann P, Mendell JR, Pober BR, Sasaki T, Shapiro F, Simpson DA, Suchowersky O and Spence JE (2001) Novel and recurrent mutations in lamin A/C in patients with Emery-Dreifuss muscular dystrophy. *American Journal of Medical Genetics,* **102** (4), 359-367.

Brown KE, Amoils S, Horn JM, Buckle VJ, Higgs DR, Merkenschlager M and Fisher AG (2001) Expression of alpha- and beta-globin genes occurs within different nuclear domains in haemopoietic cells. *Nature cell biology,* **3** (6), 602-606.

Buendia B, Courvalin JC and Collas P (2001) Dynamics of the nuclear envelope at mitosis and during apoptosis. *Cellular and molecular life sciences : CMLS,* **58** (12-13), 1781-1789.

Burke B and Stewart CL (2002) Life at the edge: the nuclear envelope and human disease. *Nature reviews.Molecular cell biology,* **3** (8), 575-585.

Busch A, Kiel T, Heupel WM, Wehnert M and Hubner S (2009) Nuclear protein import is reduced in cells expressing nuclear envelopathy-causing lamin A mutants. *Experimental cell research,* **315** (14), 2373-2385.

Cai M, Huang Y, Ghirlando R, Wilson KL, Craigie R and Clore GM (2001) Solution structure of the constant region of nuclear envelope protein LAP2 reveals two LEM-domain structures: one binds BAF and the other binds DNA. *The EMBO journal,* **20** (16), 4399-4407.

Cao H and Hegele RA (2003) LMNA is mutated in Hutchinson-Gilford progeria (MIM 176670) but not in Wiedemann-Rautenstrauch progeroid syndrome (MIM 264090). *Journal of human genetics,* **48** (5), 271-274.

Cao H and Hegele RA (2000) Nuclear lamin A/C R482Q mutation in canadian kindreds with Dunnigan-type familial partial lipodystrophy. *Human molecular genetics,* **9** (1), 109-112.

Capanni C, Cenni V, Mattioli E, Sabatelli P, Ognibene A, Columbaro M, Parnaik VK, Wehnert M, Maraldi NM, Squarzoni S and Lattanzi G (2003) Failure of lamin A/C to functionally assemble in R482L mutated familial partial lipodystrophy fibroblasts: altered intermolecular interaction with emerin and implications for gene transcription. *Experimental cell research,* **291** (1), 122-134.

Capanni C, Mattioli E, Columbaro M, Lucarelli E, Parnaik VK, Novelli G, Wehnert M, Cenni V, Maraldi NM, Squarzoni S and Lattanzi G (2005) Altered pre-lamin A processing is a common mechanism leading to lipodystrophy. *Human molecular genetics,* **14** (11), 1489-1502.

Capco DG, Wan KM and Penman S (1982) The nuclear matrix: three-dimensional architecture and protein composition. *Cell,* **29** (3), 847-858.

Capell BC and Collins FS (2006) Human laminopathies: nuclei gone genetically awry. *Nature reviews.Genetics,* **7** (12), 940-952.

Capell BC, Erdos MR, Madigan JP, Fiordalisi JJ, Varga R, Conneely KN, Gordon LB, Der CJ, Cox AD and Collins FS (2005) Inhibiting farnesylation of progerin prevents the characteristic nuclear blebbing of Hutchinson-Gilford progeria syndrome. *Proceedings of the National Academy of Sciences of the United States of America,* **102** (36), 12879-12884.

Capell BC, Olive M, Erdos MR, Cao K, Faddah DA, Tavarez UL, Conneely KN, Qu X, San H, Ganesh SK, Chen X, Avallone H, Kolodgie FD, Virmani R, Nabel EG and Collins FS (2008) A farnesyltransferase inhibitor prevents both the onset and late progression of cardiovascular disease in a progeria mouse model. *Proceedings of the National Academy of Sciences of the United States of America,* **105** (41), 15902-15907.

Caron H, van Schaik B, van der Mee M, Baas F, Riggins G, van Sluis P, Hermus MC, van Asperen R, Boon K, Voute PA, Heisterkamp S, van Kampen A and Versteeg R (2001) The human transcriptome map: clustering of highly expressed genes in chromosomal domains. *Science (New York, N.Y.),* **291** (5507), 1289-1292.

Cartegni L, di Barletta MR, Barresi R, Squarzoni S, Sabatelli P, Maraldi N, Mora M, Di Blasi C, Cornelio F, Merlini L, Villa A, Cobianchi F and Toniolo D (1997) Heart-specific localization of emerin: new insights into Emery-Dreifuss muscular dystrophy. *Human molecular genetics,* **6** (13), 2257-2264.

Chen L, Lee L, Kudlow BA, Dos Santos HG, Sletvold O, Shafeghati Y, Botha EG, Garg A, Hanson NB, Martin GM, Mian IS, Kennedy BK and Oshima J (2003) LMNA mutations in atypical Werner's syndrome. *Lancet,* **362** (9382), 440-445.

Chen LZ, Harris PC, Apostolou S, Baker E, Holman K, Lane SA, Nancarrow JK, Whitmore SA, Stallings RL and Hildebrand CE (1991) A refined physical map of the long arm of human chromosome 16. *Genomics,* **10** (2), 308-312.

Cheung VG and Nelson SF (1996) Whole genome amplification using a degenerate oligonucleotide primer allows hundreds of genotypes to be performed on less than one nanogram of genomic DNA. *Proceedings of the National Academy of Sciences of the United States of America,* **93** (25), 14676-14679.

Chitayat D, Gruber H, Mullen BJ, Pauzner D, Costa T, Lachman R and Rimoin DL (1993) Hydrops-ectopic calcification-moth-eaten skeletal dysplasia (Greenberg

dysplasia): prenatal diagnosis and further delineation of a rare genetic disorder. *American Journal of Medical Genetics,* **47** (2), 272-277.

Chong L, van Steensel B, Broccoli D, Erdjument-Bromage H, Hanish J, Tempst P and de Lange T (1995) A human telomeric protein. *Science (New York, N.Y.),* **270** (5242), 1663-1667.

Chuang CH, Carpenter AE, Fuchsova B, Johnson T, de Lanerolle P and Belmont AS (2006) Long-range directional movement of an interphase chromosome site. *Current biology : CB,* **16** (8), 825-831.

Ciejek EM, Tsai MJ and O'Malley BW (1983) Actively transcribed genes are associated with the nuclear matrix. *Nature,* **306** (5943), 607-609.

Clements L, Manilal S, Love DR and Morris GE (2000) Direct interaction between emerin and lamin A. *Biochemical and biophysical research communications,* **267** (3), 709-714.

Cockerill PN and Garrard WT (1986) Chromosomal loop anchorage sites appear to be evolutionarily conserved. *FEBS letters,* **204** (1), 5-7.

Coller HA, Sang L and Roberts JM (2006) A new description of cellular quiescence. *PLoS biology,* **4** (3), e83.

Columbaro M, Capanni C, Mattioli E, Novelli G, Parnaik VK, Squarzoni S, Maraldi NM and Lattanzi G (2005) Rescue of heterochromatin organization in Hutchinson-Gilford progeria by drug treatment. *Cellular and molecular life sciences : CMLS,* **62** (22), 2669-2678.

Comings DE and Okada TA (1976) Nuclear proteins. III. The fibrillar nature of the nuclear matrix. *Experimental cell research,* **103** (2), 341-360.

Cook PR (1999) The organization of replication and transcription. *Science (New York, N.Y.),* **284** (5421), 1790-1795.

Cook PR and Brazell IA (1975) Supercoils in human DNA. *Journal of cell science,* **19** (2), 261-279.

Coradeghini R, Barboro P, Rubagotti A, Boccardo F, Parodi S, Carmignani G, D'Arrigo C, Patrone E and Balbi C (2006) Differential expression of nuclear lamins in normal and cancerous prostate tissues. *Oncology reports,* **15** (3), 609-613.

Corso C, Parry EM, Faragher RG, Seager A, Green MH and Parry JM (2005) Molecular cytogenetic insights into the ageing syndrome Hutchinson-Gilford Progeria (HGPS). *Cytogenetic and genome research,* **111** (1), 27-33.

Cremer M, Kupper K, Wagler B, Wizelman L, von Hase J, Weiland Y, Kreja L, Diebold J, Speicher MR and Cremer T (2003) Inheritance of gene density-related higher order chromatin arrangements in normal and tumor cell nuclei. *The Journal of cell biology,* **162** (5), 809-820.

Cremer T, Cremer C, Schneider T, Baumann H, Hens L and Kirsch-Volders M (1982) Analysis of chromosome positions in the interphase nucleus of Chinese hamster cells by laser-UV-microirradiation experiments. *Human genetics,* **62** (3), 201-209.

Cremer T, Kreth G, Koester H, Fink RH, Heintzmann R, Cremer M, Solovei I, Zink D and Cremer C (2000) Chromosome territories, interchromatin domain compartment, and nuclear matrix: an integrated view of the functional nuclear architecture. *Critical reviews in eukaryotic gene expression,* **10** (2), 179-212.

Cremer T, Kurz A, Zirbel R, Dietzel S, Rinke B, Schrock E, Speicher MR, Mathieu U, Jauch A, Emmerich P, Scherthan H, Ried T, Cremer C and Lichter P (1993) Role of chromosome territories in the functional compartmentalization of the cell nucleus. *Cold Spring Harbor symposia on quantitative biology,* **58**777-792.

Crisp M, Liu Q, Roux K, Rattner JB, Shanahan C, Burke B, Stahl PD and Hodzic D (2006) Coupling of the nucleus and cytoplasm: role of the LINC complex. *The Journal of cell biology,* **172** (1), 41-53.

Croft JA, Bridger JM, Boyle S, Perry P, Teague P and Bickmore WA (1999) Differences in the localization and morphology of chromosomes in the human nucleus. *The Journal of cell biology,* **145** (6), 1119-1131.

Cronshaw JM, Krutchinsky AN, Zhang W, Chait BT and Matunis MJ (2002) Proteomic analysis of the mammalian nuclear pore complex. *The Journal of cell biology,* **158** (5), 915-927.

Cuthbert AP, Trott DA, Ekong RM, Jezzard S, England NL, Themis M, Todd CM and Newbold RF (1995) Construction and characterization of a highly stable human: rodent monochromosomal hybrid panel for genetic complementation and genome mapping studies. *Cytogenetics and cell genetics,* **71** (1), 68-76.

d'Adda di Fagagna F, Reaper PM, Clay-Farrace L, Fiegler H, Carr P, Von Zglinicki T, Saretzki G, Carter NP and Jackson SP (2003) A DNA damage checkpoint response in telomere-initiated senescence. *Nature,* **426** (6963), 194-198.

Dahl KN, Kahn SM, Wilson KL and Discher DE (2004) The nuclear envelope lamina network has elasticity and a compressibility limit suggestive of a molecular shock absorber. *Journal of cell science,* **117** (Pt 20), 4779-4786.

Daigle N, Beaudouin J, Hartnell L, Imreh G, Hallberg E, Lippincott-Schwartz J and Ellenberg J (2001) Nuclear pore complexes form immobile networks and have a very low turnover in live mammalian cells. *The Journal of cell biology,* **154** (1), 71-84.

Dalla-Favera R, Bregni M, Erikson J, Patterson D, Gallo RC and Croce CM (1982) Human c-myc onc gene is located on the region of chromosome 8 that is translocated in Burkitt lymphoma cells. *Proceedings of the National Academy of Sciences of the United States of America,* **79** (24), 7824-7827.

D'Angelo MA, Raices M, Panowski SH and Hetzer MW (2009) Age-dependent deterioration of nuclear pore complexes causes a loss of nuclear integrity in postmitotic cells. *Cell,* **136** (2), 284-295.

D'Apice MR, Tenconi R, Mammi I, van den Ende J and Novelli G (2004) Paternal origin of LMNA mutations in Hutchinson-Gilford progeria. *Clinical genetics,* **65** (1), 52-54.

de Lange T (1992) Human telomeres are attached to the nuclear matrix. *The EMBO journal,* **11** (2), 717-724.

De Sandre-Giovannoli A, Bernard R, Cau P, Navarro C, Amiel J, Boccaccio I, Lyonnet S, Stewart CL, Munnich A, Le Merrer M and Levy N (2003) Lamin a truncation in Hutchinson-Gilford progeria. *Science (New York, N.Y.),* **300** (5628), 2055.

De Sandre-Giovannoli A, Chaouch M, Kozlov S, Vallat JM, Tazir M, Kassouri N, Szepetowski P, Hammadouche T, Vandenberghe A, Stewart CL, Grid D and Levy N (2002) Homozygous defects in LMNA, encoding lamin A/C nuclear-envelope proteins, cause autosomal recessive axonal neuropathy in human (Charcot-Marie-Tooth disorder type 2) and mouse. *American Journal of Human Genetics,* **70** (3), 726-736.

De Vos WH, Houben F, Hoebe RA, Hennekam R, van Engelen B, Manders EM, Ramaekers FC, Broers JL and Van Oostveldt P (2010) Increased plasticity of the nuclear envelope and hypermobility of telomeres due to the loss of A-type lamins. *Biochimica et biophysica acta,* **1800** (4), 448-458.

Dean R, Kim SS and Delgado D (1986) Expression of c-myc oncogene in human fibroblasts during in vitro senescence. *Biochemical and biophysical research communications,* **135** (1), 105-109.

DeBusk FL (1972) The Hutchinson-Gilford progeria syndrome. Report of 4 cases and review of the literature. *The Journal of pediatrics,* **80** (4), 697-724.

Dechat T, Gajewski A, Korbei B, Gerlich D, Daigle N, Haraguchi T, Furukawa K, Ellenberg J and Foisner R (2004) LAP2alpha and BAF transiently localize to telomeres and specific regions on chromatin during nuclear assembly. *Journal of cell science,* **117** (Pt 25), 6117-6128.

Dechat T, Gotzmann J, Stockinger A, Harris CA, Talle MA, Siekierka JJ and Foisner R (1998) Detergent-salt resistance of LAP2alpha in interphase nuclei and phosphorylation-dependent association with chromosomes early in nuclear assembly implies functions in nuclear structure dynamics. *The EMBO journal,* **17** (16), 4887-4902.

Dechat T, Korbei B, Vaughan OA, Vlcek S, Hutchison CJ and Foisner R (2000) Lamina-associated polypeptide 2alpha binds intranuclear A-type lamins. *Journal of cell science,* **113 Pt 19**3473-3484.

Dechat T, Vlcek S and Foisner R (2000) Review: lamina-associated polypeptide 2 isoforms and related proteins in cell cycle-dependent nuclear structure dynamics. *Journal of structural biology,* **129** (2-3), 335-345.

Decker ML, Chavez E, Vulto I and Lansdorp PM (2009) Telomere length in Hutchinson-Gilford progeria syndrome. *Mechanisms of ageing and development,* **130** (6), 377-383.

Deloukas P, Schuler GD, Gyapay G, Beasley EM, Soderlund C, Rodriguez-Tome P, Hui L, Matise TC, McKusick KB, Beckmann JS, Bentolila S, Bihoreau M, Birren BB, Browne J, Butler A, Castle AB, Chiannilkulchai N, Clee C, Day PJ, Dehejia A, Dibling T, Drouot N, Duprat S, Fizames C, Fox S, Gelling S, Green L, Harrison P, Hocking R, Holloway E, Hunt S, Keil S, Lijnzaad P, Louis-Dit-Sully C, Ma J, Mendis A, Miller J, Morissette J, Muselet D, Nusbaum HC, Peck A, Rozen S, Simon D, Slonim DK, Staples R, Stein LD, Stewart EA, Suchard MA, Thangarajah T, Vega-Czarny N, Webber C, Wu X, Hudson J, Auffray C, Nomura N, Sikela JM, Polymeropoulos MH, James MR, Lander ES, Hudson TJ, Myers RM, Cox DR, Weissenbach J, Boguski MS and Bentley DR (1998) A physical map of 30,000 human genes. *Science (New York, N.Y.),* **282** (5389), 744-746.

Denecke J, Brune T, Feldhaus T, Robenek H, Kranz C, Auchus RJ, Agarwal AK and Marquardt T (2006) A homozygous ZMPSTE24 null mutation in combination with a heterozygous mutation in the LMNA gene causes Hutchinson-Gilford progeria syndrome (HGPS): insights into the pathophysiology of HGPS. *Human mutation,* **27** (6), 524-531.

Deniaud E and Bickmore WA (2009) Transcription and the nuclear periphery: edge of darkness? *Current opinion in genetics & development,* **19** (2), 187-191.

Dickinson LA and Kohwi-Shigematsu T (1995) Nucleolin is a matrix attachment region DNA-binding protein that specifically recognizes a region with high base-unpairing potential. *Molecular and cellular biology,* **15** (1), 456-465.

Dickinson P, Cook PR and Jackson DA (1990) Active RNA polymerase I is fixed within the nucleus of HeLa cells. *The EMBO journal,* **9** (7), 2207-2214.

Dietz HC, Cutting GR, Pyeritz RE, Maslen CL, Sakai LY, Corson GM, Puffenberger EG, Hamosh A, Nanthakumar EJ and Curristin SM (1991) Marfan syndrome caused by a recurrent de novo missense mutation in the fibrillin gene. *Nature,* **352** (6333), 337-339.

Dieudonne M, Maiuri P, Biancotto C, Knezevich A, Kula A, Lusic M and Marcello A (2009) Transcriptional competence of the integrated HIV-1 provirus at the nuclear periphery. *The EMBO journal,* **28** (15), 2231-2243.

Djeliova V, Russev G and Anachkova B (2001a) Dynamics of association of origins of DNA replication with the nuclear matrix during the cell cycle. *Nucleic acids research,* **29** (15), 3181-3187.

Djeliova V, Russev G and Anachkova B (2001b) Distribution of DNA replication origins between matrix-attached and loop DNA in mammalian cells. *Journal of cellular biochemistry,* **80** (3), 353-359.

DNA Sequencing & Services (2010). Available at: http://www.dnaseq.co.uk/. Last accessed: 5th November 2010.

Dowdy SF, Hinds PW, Louie K, Reed SI, Arnold A and Weinberg RA (1993) Physical interaction of the retinoblastoma protein with human D cyclins. *Cell,* **73** (3), 499-511.

Dreuillet C, Harper M, Tillit J, Kress M and Ernoult-Lange M (2008) Mislocalization of human transcription factor MOK2 in the presence of pathogenic mutations of lamin A/C. *Biology of the cell / under the auspices of the European Cell Biology Organization,* **100** (1), 51-61.

Dreuillet C, Tillit J, Kress M and Ernoult-Lange M (2002) In vivo and in vitro interaction between human transcription factor MOK2 and nuclear lamin A/C. *Nucleic acids research,* **30** (21), 4634-4642.

Duband-Goulet IandCourvalin JC (2000) Inner nuclear membrane protein LBR preferentially interacts with DNA secondary structures and nucleosomal linker. *Biochemistry,* **39** (21), 6483-6488.

Dundr M, Ospina JK, Sung MH, John S, Upender M, Ried T, Hager GL and Matera AG (2007) Actin-dependent intranuclear repositioning of an active gene locus in vivo. *The Journal of cell biology,* **179** (6), 1095-1103.

Dunn KL, Zhao H and Davie JR (2003) The insulator binding protein CTCF associates with the nuclear matrix. *Experimental cell research,* **288** (1), 218-223.

Dunnigan MG, Cochrane MA, Kelly A and Scott JW (1974) Familial lipoatrophic diabetes with dominant transmission. A new syndrome. *The Quarterly journal of medicine,* **43** (169), 33-48.

Dyer JA, Kill IR, Pugh G, Quinlan RA, Lane EB and Hutchison CJ (1997) Cell cycle changes in A-type lamin associations detected in human dermal fibroblasts using monoclonal antibodies. *Chromosome research : an international journal on the molecular, supramolecular and evolutionary aspects of chromosome biology,* **5** (6), 383-394.

Eisenberg LM and Eisenberg CA (2006) Wnt signal transduction and the formation of the myocardium. *Developmental biology,* **293** (2), 305-315.

Elad N, Maimon T, Frenkiel-Krispin D, Lim RY and Medalia O (2009) Structural analysis of the nuclear pore complex by integrated approaches. *Current opinion in structural biology,* **19** (2), 226-232.

Elcock LS and Bridger JM (2010) Exploring the relationship between interphase gene positioning, transcriptional regulation and the nuclear matrix. *Biochemical Society transactions,* **38** (Pt 1), 263-267.

Elcock LS and Bridger JM (2008) Exploring the effects of a dysfunctional nuclear matrix. *Biochemical Society transactions,* **36** (Pt 6), 1378-1383.

Eldridge R, Anayiotos CP, Schlesinger S, Cowen D, Bever C, Patronas N and McFarland H (1984) Hereditary adult-onset leukodystrophy simulating chronic progressive multiple sclerosis. *The New England journal of medicine,* **311** (15), 948-953.

Ellis DJ, Jenkins H, Whitfield WG and Hutchison CJ (1997) GST-lamin fusion proteins act as dominant negative mutants in Xenopus egg extract and reveal the function of the lamina in DNA replication. *Journal of cell science,* **110** (Pt 20), 2507-2518.

Ellis JA, Craxton M, Yates JR and Kendrick-Jones J (1998) Aberrant intracellular targeting and cell cycle-dependent phosphorylation of emerin contribute to the Emery-Dreifuss muscular dystrophy phenotype. *Journal of cell science,* **111** (Pt 6), 781-792.

Emerson LJ, Holt MR, Wheeler MA, Wehnert M, Parsons M and Ellis JA (2009) Defects in cell spreading and ERK1/2 activation in fibroblasts with lamin A/C mutations. *Biochimica et biophysica acta,* **1792** (8), 810-821.

Emery AE and Dreifuss FE (1966) Unusual type of benign x-linked muscular dystrophy. *Journal of neurology, neurosurgery, and psychiatry,* **29** (4), 338-342.

Eriksson M, Brown WT, Gordon LB, Glynn MW, Singer J, Scott L, Erdos MR, Robbins CM, Moses TY, Berglund P, Dutra A, Pak E, Durkin S, Csoka AB, Boehnke M, Glover TW and Collins FS (2003) Recurrent de novo point mutations in lamin A cause Hutchinson-Gilford progeria syndrome. *Nature,* **423** (6937), 293-298.

Ewen ME, Sluss HK, Sherr CJ, Matsushime H, Kato J and Livingston DM (1993) Functional interactions of the retinoblastoma protein with mammalian D-type cyclins. *Cell,* **73** (3), 487-497.

Fackelmayer FO, Dahm K, Renz A, Ramsperger U and Richter A (1994) Nucleic-acid-binding properties of hnRNP-U/SAF-A, a nuclear-matrix protein which binds DNA and RNA in vivo and in vitro. *European journal of biochemistry / FEBS,* **221** (2), 749-757.

Fackelmayer FO and Richter A (1994) Purification of two isoforms of hnRNP-U and characterization of their nucleic acid binding activity. *Biochemistry,* **33** (34), 10416-10422.

Fahrenkrog B and Aebi U (2003) The nuclear pore complex: nucleocytoplasmic transport and beyond. *Nature reviews.Molecular cell biology,* **4** (10), 757-766.

Fajas L, Fruchart JC and Auwerx J (1998) Transcriptional control of adipogenesis. *Current opinion in cell biology,* **10** (2), 165-173.

Farrell CM, West AG and Felsenfeld G (2002) Conserved CTCF insulator elements flank the mouse and human beta-globin loci. *Molecular and cellular biology,* **22** (11), 3820-3831.

Fatkin D, MacRae C, Sasaki T, Wolff MR, Porcu M, Frenneaux M, Atherton J, Vidaillet HJ,Jr, Spudich S, De Girolami U, Seidman JG, Seidman C, Muntoni F, Muehle G, Johnson W and McDonough B (1999) Missense mutations in the rod domain of the lamin A/C gene as causes of dilated cardiomyopathy and conduction-system disease. *The New England journal of medicine,* **341** (23), 1715-1724.

Favreau C, Higuet D, Courvalin JC and Buendia B (2004) Expression of a mutant lamin A that causes Emery-Dreifuss muscular dystrophy inhibits in vitro differentiation of C2C12 myoblasts. *Molecular and cellular biology,* **24** (4), 1481-1492.

Fey EG, Wan KM and Penman S (1984) Epithelial cytoskeletal framework and nuclear matrix-intermediate filament scaffold: three-dimensional organization and protein composition. *The Journal of cell biology,* **98** (6), 1973-1984.

Fidzianska A and Hausmanowa-Petrusewicz I (2003) Architectural abnormalities in muscle nuclei. Ultrastructural differences between X-linked and autosomal dominant forms of EDMD. *Journal of the neurological sciences,* **210** (1-2), 47-51.

Fidzianska A, Toniolo D and Hausmanowa-Petrusewicz I (1998) Ultrastructural abnormality of sarcolemmal nuclei in Emery-Dreifuss muscular dystrophy (EDMD). *Journal of the neurological sciences,* **159** (1), 88-93.

Filesi I, Gullotta F, Lattanzi G, D'Apice MR, Capanni C, Nardone AM, Columbaro M, Scarano G, Mattioli E, Sabatelli P, Maraldi NM, Biocca S and Novelli G (2005) Alterations of nuclear envelope and chromatin organization in mandibuloacral dysplasia, a rare form of laminopathy. *Physiological genomics,* **23** (2), 150-158.

Finlan LE, Sproul D, Thomson I, Boyle S, Kerr E, Perry P, Ylstra B, Chubb JR and Bickmore WA (2008) Recruitment to the nuclear periphery can alter expression of genes in human cells. *PLoS genetics,* **4** (3), e1000039.

Fiserova J, Kiseleva E and Goldberg MW (2009) Nuclear envelope and nuclear pore complex structure and organization in tobacco BY-2 cells. *The Plant Journal : for cell and molecular biology,* **59** (2), 243-255.

Fisher DZ, Chaudhary N and Blobel G (1986) cDNA sequencing of nuclear lamins A and C reveals primary and secondary structural homology to intermediate filament proteins. *Proceedings of the National Academy of Sciences of the United States of America,* **83** (17), 6450-6454.

Foisner R and Gerace L (1993) Integral membrane proteins of the nuclear envelope interact with lamins and chromosomes, and binding is modulated by mitotic phosphorylation. *Cell,* **73** (7), 1267-1279.

Fong LG, Ng JK, Lammerding J, Vickers TA, Meta M, Cote N, Gavino B, Qiao X, Chang SY, Young SR, Yang SH, Stewart CL, Lee RT, Bennett CF, Bergo MO and Young SG (2006) Prelamin A and lamin A appear to be dispensable in the nuclear lamina. *The Journal of clinical investigation,* **116** (3), 743-752.

Fong LG, Ng JK, Meta M, Cote N, Yang SH, Stewart CL, Sullivan T, Burghardt A, Majumdar S, Reue K, Bergo MO and Young SG (2004) Heterozygosity for Lmna deficiency eliminates the progeria-like phenotypes in Zmpste24-deficient mice. *Proceedings of the National Academy of Sciences of the United States of America,* **101** (52), 18111-18116.

Foster HA, Abeydeera LR, Griffin DK and Bridger JM (2005) Non-random chromosome positioning in mammalian sperm nuclei, with migration of the sex chromosomes during late spermatogenesis. *Journal of cell science,* **118** (Pt 9), 1811-1820.

Foster HA and Bridger JM (2005) The genome and the nucleus: a marriage made by evolution. Genome organisation and nuclear architecture. *Chromosoma,* **114** (4), 212-229.

Foster HA, Stokes P, Forsey K, Leese HJ and Bridger JM (2007) Lamins A and C are present in the nuclei of early porcine embryos, with lamin A being distributed in large intranuclear foci. *Chromosome research : an international journal on the molecular, supramolecular and evolutionary aspects of chromosome biology,* **15** (2), 163-174.

Foster KA and Collins JM (1985) The interrelation between DNA synthesis rates and DNA polymerases bound to the nuclear matrix in synchronized HeLa cells. *The Journal of biological chemistry,* **260** (7), 4229-4235.

Franke WW, Schmid E, Osborn M and Weber K (1978) Different intermediate-sized filaments distinguished by immunofluorescence microscopy. *Proceedings of the National Academy of Sciences of the United States of America,* **75** (10), 5034-5038.

Freidenberg GR, Cutler DL, Jones MC, Hall B, Mier RJ, Culler F, Jones KL, Lozzio C and Kaufmann S (1992) Severe insulin resistance and diabetes mellitus in mandibuloacral dysplasia. *American Journal of Diseases of Children (1960),* **146** (1), 93-99.

Freije JM, Blay P, Pendas AM, Cadinanos J, Crespo P and Lopez-Otin C (1999) Identification and chromosomal location of two human genes encoding enzymes potentially involved in proteolytic maturation of farnesylated proteins. *Genomics,* **58** (3), 270-280.

Frey MR, Bailey AD, Weiner AM and Matera AG (1999) Association of snRNA genes with coiled bodies is mediated by nascent snRNA transcripts. *Current biology : CB,* **9** (3), 126-135.

Frock RL, Kudlow BA, Evans AM, Jameson SA, Hauschka SD and Kennedy BK (2006) Lamin A/C and emerin are critical for skeletal muscle satellite cell differentiation. *Genes & development,* **20** (4), 486-500.

Frolov MV and Dyson NJ (2004) Molecular mechanisms of E2F-dependent activation and pRB-mediated repression. *Journal of cell science,* **117** (Pt 11), 2173-2181.

Frydman M (2008) The Marfan syndrome. *The Israel Medical Association journal : IMAJ,* **10** (3), 175-178.

Fukami J, Anno K, Ueda K, Takahashi T and Ide T (1995) Enhanced expression of cyclin D1 in senescent human fibroblasts. *Mechanisms of ageing and development,* **81** (2-3), 139-157.

Fukami-Kobayashi JandMitsui Y (1998) The regulation of cyclin D1 expression in senescent human fibroblasts. *Experimental cell research,* **241** (2), 435-444.

Furukawa Y, Nakatsuru S, Nagafuchi A, Tsukita S, Muto T, Nakamura Y and Horii A (1994) Structure, expression and chromosome assignment of the human catenin (cadherin-associated protein) alpha 1 gene (CTNNA1). *Cytogenetics and cell genetics,* **65** (1-2), 74-78.

Gajewski A, Csaszar E and Foisner R (2004) A phosphorylation cluster in the chromatin-binding region regulates chromosome association of LAP2alpha. *The Journal of biological chemistry,* **279** (34), 35813-35821.

Galiova G, Bartova E and Kozubek S (2004) Nuclear topography of beta-like globin gene cluster in IL-3-stimulated human leukemic K-562 cells. *Blood cells, molecules & diseases,* **33** (1), 4-14.

Gasser SM and Laemmli UK (1986) The organisation of chromatin loops: characterization of a scaffold attachment site. *The EMBO journal,* **5** (3), 511-518.

Gately DP, Hittle JC, Chan GK and Yen TJ (1998) Characterization of ATM expression, localization, and associated DNA-dependent protein kinase activity. *Molecular biology of the cell,* **9** (9), 2361-2374.

Gaudy-Marqueste C, Roll P, Esteves-Vieira V, Weiller PJ, Grob JJ, Cau P, Levy N and De Sandre-Giovannoli A (2010) LBR mutation and nuclear envelope defects in a patient affected with Reynolds syndrome. *Journal of medical genetics,* **47** (6), 361-370.

Gerace L, Blum A and Blobel G (1978) Immunocytochemical localization of the major polypeptides of the nuclear pore complex-lamina fraction. Interphase and mitotic distribution. *The Journal of cell biology,* **79** (2 Pt 1), 546-566.

Gerace L and Burke B (1988) Functional organization of the nuclear envelope. *Annual Review of Cell Biology,* **4**335-374.

Gerace L, Comeau C and Benson M (1984) Organization and modulation of nuclear lamina structure. *Journal of cell science.Supplement,* **1**137-160.

Gerdes J, Lelle RJ, Pickartz H, Heidenreich W, Schwarting R, Kurtsiefer L, Stauch G and Stein H (1986) Growth fractions in breast cancers determined in situ with monoclonal antibody Ki-67. *Journal of clinical pathology,* **39** (9), 977-980.

Gerdes J, Lemke H, Baisch H, Wacker HH, Schwab U and Stein H (1984) Cell cycle analysis of a cell proliferation-associated human nuclear antigen defined by the monoclonal antibody Ki-67. *Journal of immunology (Baltimore, Md.: 1950),* **133** (4), 1710-1715.

Gerdes MG, Carter KC, Moen PT,Jr and Lawrence JB (1994) Dynamic changes in the higher-level chromatin organization of specific sequences revealed by in situ hybridization to nuclear halos. *The Journal of cell biology,* **126** (2), 289-304.

Gierman HJ, Indemans MH, Koster J, Goetze S, Seppen J, Geerts D, van Driel R and Versteeg R (2007) Domain-wide regulation of gene expression in the human genome. *Genome research,* **17** (9), 1286-1295.

Gilford H (1904) Progeria; A form of senilism. *The Practitioner,* **73**, 188 - 217.

Glynn MW and Glover TW (2005) Incomplete processing of mutant lamin A in Hutchinson-Gilford progeria leads to nuclear abnormalities, which are reversed by farnesyltransferase inhibition. *Human molecular genetics,* **14** (20), 2959-2969.

Goetze S, Baer A, Winkelmann S, Nehlsen K, Seibler J, Maass K and Bode J (2005) Performance of genomic bordering elements at predefined genomic loci. *Molecular and cellular biology,* **25** (6), 2260-2272.

Goetze S, Mateos-Langerak J, Gierman HJ, de Leeuw W, Giromus O, Indemans MH, Koster J, Ondrej V, Versteeg R and van Driel R (2007) The three-dimensional structure of human interphase chromosomes is related to the transcriptome map. *Molecular and cellular biology,* **27** (12), 4475-4487.

Gohring F and Fackelmayer FO (1997) The scaffold/matrix attachment region binding protein hnRNP-U (SAF-A) is directly bound to chromosomal DNA in vivo: a chemical cross-linking study. *Biochemistry,* **36** (27), 8276-8283.

Goldberg M, Jenkins H, Allen T, Whitfield WG and Hutchison CJ (1995) Xenopus lamin B3 has a direct role in the assembly of a replication competent nucleus: evidence from cell-free egg extracts. *Journal of cell science,* **108** (Pt 11), 3451-3461.

Goldberg MW and Allen TD (1996) The nuclear pore complex and lamina: three-dimensional structures and interactions determined by field emission in-lens scanning electron microscopy. *Journal of Molecular Biology,* **257** (4), 848-865.

Goldberg MW, Fiserova J, Huttenlauch I and Stick R (2008a) A new model for nuclear lamina organization. *Biochemical Society transactions,* **36** (Pt 6), 1339-1343.

Goldberg MW, Huttenlauch I, Hutchison CJ and Stick R (2008b) Filaments made from A- and B-type lamins differ in structure and organization. *Journal of cell science,* **121** (Pt 2), 215-225.

Goldman AE, Moir RD, Montag-Lowy M, Stewart M and Goldman RD (1992) Pathway of incorporation of microinjected lamin A into the nuclear envelope. *The Journal of cell biology,* **119** (4), 725-735.

Goldman RD, Goldman AE and Shumaker DK (2005) Nuclear lamins: building blocks of nuclear structure and function. *Novartis Foundation symposium,* **264**3-16; discussion 16-21, 227-30.

Goldman RD, Shumaker DK, Erdos MR, Eriksson M, Goldman AE, Gordon LB, Gruenbaum Y, Khuon S, Mendez M, Varga R and Collins FS (2004) Accumulation of mutant lamin A causes progressive changes in nuclear architecture in Hutchinson-Gilford progeria syndrome. *Proceedings of the National Academy of Sciences of the United States of America,* **101** (24), 8963-8968.

Gonzalez JM, Navarro-Puche A, Casar B, Crespo P and Andres V (2008) Fast regulation of AP-1 activity through interaction of lamin A/C, ERK1/2, and c-Fos at the nuclear envelope. *The Journal of cell biology,* **183** (4), 653-666.

Gonzalez-Suarez I, Redwood AB, Perkins SM, Vermolen B, Lichtensztejin D, Grotsky DA, Morgado-Palacin L, Gapud EJ, Sleckman BP, Sullivan T, Sage J, Stewart CL, Mai S and Gonzalo S (2009) Novel roles for A-type lamins in telomere biology and the DNA damage response pathway. *The EMBO journal,* **28** (16), 2414-2427.

Goto M, Imamura O, Kuromitsu J, Matsumoto T, Yamabe Y, Tokutake Y, Suzuki N, Mason B, Drayna D, Sugawara M, Sugimoto M and Furuichi Y (1997) Analysis of helicase gene mutations in Japanese Werner's syndrome patients. *Human genetics,* **99** (2), 191-193.

Goto M, Tanimoto K, Horiuchi Y and Sasazuki T (1981) Family analysis of Werner's syndrome: a survey of 42 Japanese families with a review of the literature. *Clinical genetics,* **19** (1), 8-15.

Gotzmann J, Vlcek S and Foisner R (2000) Caspase-mediated cleavage of the chromosome-binding domain of lamina-associated polypeptide 2 alpha. *Journal of cell science,* **113 Pt 21**3769-3780.

Grasser F, Neusser M, Fiegler H, Thormeyer T, Cremer M, Carter NP, Cremer T and Muller S (2008) Replication-timing-correlated spatial chromatin arrangements in cancer and in primate interphase nuclei. *Journal of cell science,* **121** (Pt 11), 1876-1886.

Greider CW and Blackburn EH (1989) A telomeric sequence in the RNA of Tetrahymena telomerase required for telomere repeat synthesis. *Nature,* **337** (6205), 331-337.

Gruenbaum Y, Lee KK, Liu J, Cohen M and Wilson KL (2002) The expression, lamin-dependent localization and RNAi depletion phenotype for emerin in C. elegans. *Journal of cell science,* **115** (Pt 5), 923-929.

Gruenbaum Y, Margalit A, Goldman RD, Shumaker DK and Wilson KL (2005) The nuclear lamina comes of age. *Nature reviews.Molecular cell biology,* **6** (1), 21-31.

Guelen L, Pagie L, Brasset E, Meuleman W, Faza MB, Talhout W, Eussen BH, de Klein A, Wessels L, de Laat W and van Steensel B (2008) Domain organization of human chromosomes revealed by mapping of nuclear lamina interactions. *Nature,* **453** (7197), 948-951.

Gurudatta BV, Shashidhara LS and Parnaik VK (2010) Lamin C and chromatin organization in Drosophila. *Journal of genetics,* **89** (1), 37-49.

Habermann FA, Cremer M, Walter J, Kreth G, von Hase J, Bauer K, Wienberg J, Cremer C, Cremer T and Solovei I (2001) Arrangements of macro- and microchromosomes in chicken cells. *Chromosome research : an international journal on the molecular, supramolecular and evolutionary aspects of chromosome biology,* **9** (7), 569-584.

Hakelien AM, Delbarre E, Gaustad KG, Buendia B and Collas P (2008) Expression of the myodystrophic R453W mutation of lamin A in C2C12 myoblasts causes promoter-specific and global epigenetic defects. *Experimental cell research,* **314** (8), 1869-1880.

Han X, Feng X, Rattner JB, Smith H, Bose P, Suzuki K, Soliman MA, Scott MS, Burke BE and Riabowol K (2008) Tethering by lamin A stabilizes and targets the ING1 tumour suppressor. *Nature cell biology,* **10** (11), 1333-1340.

Hancock R (2000) A new look at the nuclear matrix. *Chromosoma,* **109** (4), 219-225.

Haque F, Lloyd DJ, Smallwood DT, Dent CL, Shanahan CM, Fry AM, Trembath RC and Shackleton S (2006) SUN1 interacts with nuclear lamin A and cytoplasmic nesprins to provide a physical connection between the nuclear lamina and the cytoskeleton. *Molecular and cellular biology,* **26** (10), 3738-3751.

Haraguchi T, Holaska JM, Yamane M, Koujin T, Hashiguchi N, Mori C, Wilson KL and Hiraoka Y (2004) Emerin binding to Btf, a death-promoting transcriptional repressor, is disrupted by a missense mutation that causes Emery-Dreifuss muscular dystrophy. *European journal of biochemistry / FEBS,* **271** (5), 1035-1045.

Harborth J, Elbashir SM, Bechert K, Tuschl T and Weber K (2001) Identification of essential genes in cultured mammalian cells using small interfering RNAs. *Journal of cell science,* **114** (Pt 24), 4557-4565.

Harless J and Hewitt RR (1987) Intranuclear localization of UV-induced DNA repair in human VA13 cells. *Mutation research,* **183** (2), 177-184.

Harley CB, Futcher AB and Greider CW (1990) Telomeres shorten during ageing of human fibroblasts. *Nature,* **345** (6274), 458-460.

Harnicarova A, Kozubek S, Pachernik J, Krejci J and Bartova E (2006) Distinct nuclear arrangement of active and inactive c-myc genes in control and differentiated colon carcinoma cells. *Experimental cell research,* **312** (20), 4019-4035.

Harris CA, Andryuk PJ, Cline S, Chan HK, Natarajan A, Siekierka JJ and Goldstein G (1994) Three distinct human thymopoietins are derived from alternatively spliced mRNAs. *Proceedings of the National Academy of Sciences of the United States of America,* **91** (14), 6283-6287.

Harris CA, Andryuk PJ, Cline SW, Mathew S, Siekierka JJ and Goldstein G (1995) Structure and mapping of the human thymopoietin (TMPO) gene and relationship of human TMPO beta to rat lamin-associated polypeptide 2. *Genomics,* **28** (2), 198-205.

Hassan AB and Cook PR (1993) Visualization of replication sites in unfixed human cells. *Journal of cell science,* **105** (Pt 2), 541-550.

Hayflick L and moorhead PS (1961) The serial cultivation of human diploid cell strains. *Experimental cell research,* **25,** 585-621.

He D, Zeng C and Brinkley BR (1995) Nuclear matrix proteins as structural and functional components of the mitotic apparatus. *International review of cytology,* **162B,** 1-74.

He DC, Nickerson JA and Penman S (1990) Core filaments of the nuclear matrix. *The Journal of cell biology,* **110** (3), 569-580.

Hegele RA, Cao H, Liu DM, Costain GA, Charlton-Menys V, Rodger NW and Durrington PN (2006) Sequencing of the reannotated LMNB2 gene reveals novel mutations in patients with acquired partial lipodystrophy. *American Journal of Human Genetics,* **79** (2), 383-389.

Henderson AS, Warburton D and Atwood KC (1972) Location of ribosomal DNA in the human chromosome complement. *Proceedings of the National Academy of Sciences of the United States of America,* **69** (11), 3394-3398.

Heng HH, Goetze S, Ye CJ, Liu G, Stevens JB, Bremer SW, Wykes SM, Bode J and Krawetz SA (2004) Chromatin loops are selectively anchored using scaffold/matrix-attachment regions. *Journal of cell science,* **117** (Pt 7), 999-1008.

Heng HH, Krawetz SA, Lu W, Bremer S, Liu G and Ye CJ (2001) Re-defining the chromatin loop domain. *Cytogenetics and cell genetics,* **93** (3-4), 155-161.

Heng HH, Squire J and Tsui LC (1992) High-resolution mapping of mammalian genes by in situ hybridization to free chromatin. *Proceedings of the National Academy of Sciences of the United States of America,* **89** (20), 9509-9513.

Hennekes H and Nigg EA (1994) The role of isoprenylation in membrane attachment of nuclear lamins. A single point mutation prevents proteolytic cleavage of the lamin A precursor and confers membrane binding properties. *Journal of cell science,* **107** (Pt 4), 1019-1029.

Hepperger C, Mannes A, Merz J, Peters J and Dietzel S (2008) Three-dimensional positioning of genes in mouse cell nuclei. *Chromosoma,* **117** (6), 535-551.

Herbig U, Jobling WA, Chen BP, Chen DJ and Sedivy JM (2004) Telomere shortening triggers senescence of human cells through a pathway involving ATM, p53, and p21(CIP1), but not p16(INK4a). *Molecular cell,* **14** (4), 501-513.

Herrmann H, Bar H, Kreplak L, Strelkov SV and Aebi U (2007) Intermediate filaments: from cell architecture to nanomechanics. *Nature reviews.Molecular cell biology,* **8** (7), 562-573.

Hewitt SL, High FA, Reiner SL, Fisher AG and Merkenschlager M (2004) Nuclear repositioning marks the selective exclusion of lineage-inappropriate transcription factor loci during T helper cell differentiation. *European journal of immunology,* **34** (12), 3604-3613.

Hitachi High Technologies America (2010). Available at: http://www.hitachi-hta.com. Last accessed: 5th November 2010.

Hoffmann K, Dreger CK, Olins AL, Olins DE, Shultz LD, Lucke B, Karl H, Kaps R, Muller D, Vaya A, Aznar J, Ware RE, Sotelo Cruz N, Lindner TH, Herrmann H, Reis A and Sperling K (2002) Mutations in the gene encoding the lamin B receptor produce an altered nuclear morphology in granulocytes (Pelger-Huet anomaly). *Nature genetics,* **31** (4), 410-414.

Holaska JM, Kowalski AK and Wilson KL (2004) Emerin caps the pointed end of actin filaments: evidence for an actin cortical network at the nuclear inner membrane. *PLoS biology,* **2** (9), E231.

Holaska JM, Lee KK, Kowalski AK and Wilson KL (2003) Transcriptional repressor germ cell-less (GCL) and barrier to autointegration factor (BAF) compete for binding to emerin in vitro. *The Journal of biological chemistry,* **278** (9), 6969-6975.

Holaska JM and Wilson KL (2006) Multiple roles for emerin: implications for Emery-Dreifuss muscular dystrophy. *The anatomical record. Part A, Discoveries in molecular, cellular, and evolutionary biology,* **288** (7), 676-680.

Holaska JM, Wilson KL and Mansharamani M (2002) The nuclear envelope, lamins and nuclear assembly. *Current opinion in cell biology,* **14** (3), 357-364.

Holtz D, Tanaka RA, Hartwig J and McKeon F (1989) The CaaX motif of lamin A functions in conjunction with the nuclear localization signal to target assembly to the nuclear envelope. *Cell,* **59** (6), 969-977.

Hornbeck P, Huang KP and Paul WE (1988) Lamin B is rapidly phosphorylated in lymphocytes after activation of protein kinase C. *Proceedings of the National Academy of Sciences of the United States of America,* **85** (7), 2279-2283.

Hozak P, Hassan AB, Jackson DA and Cook PR (1993) Visualization of replication factories attached to nucleoskeleton. *Cell,* **73** (2), 361-373.

Hozak P, Jackson DA and Cook PR (1994) Replication factories and nuclear bodies: the ultrastructural characterization of replication sites during the cell cycle. *Journal of cell science,* **107** (Pt 8), 2191-2202.

Hozak P, Sasseville AM, Raymond Y and Cook PR (1995) Lamin proteins form an internal nucleoskeleton as well as a peripheral lamina in human cells. *Journal of cell science,* **108** (Pt 2), 635-644.

Huang S, Risques RA, Martin GM, Rabinovitch PS and Oshima J (2008) Accelerated telomere shortening and replicative senescence in human fibroblasts overexpressing mutant and wild-type lamin A. *Experimental cell research,* **314** (1), 82-91.

Huber LJ and Chodosh LA (2005) Dynamics of DNA repair suggested by the subcellular localization of Brca1 and Brca2 proteins. *Journal of cellular biochemistry,* **96** (1), 47-55.

Hubner S, Eam JE, Hubner A and Jans DA (2006) Laminopathy-inducing lamin A mutants can induce redistribution of lamin binding proteins into nuclear aggregates. *Experimental cell research,* **312** (2), 171-183.

Hutchinson J (1886) Congenital absence of hair and mammary glands with atrophic condition of the skin and is appendages in a boy whose mother had been almost wholly bald from alopecia areata from the age of six. *Med Chirurg Trans,* **69**, 473 - 477.

Hutchison CJ (2002) Lamins: building blocks or regulators of gene expression? *Nature reviews.Molecular cell biology,* **3** (11), 848-858.

Hutchison CJ and Worman HJ (2004) A-type lamins: guardians of the soma? *Nature cell biology,* **6** (11), 1062-1067.

Iarovaia OV, Akopov SB, Nikolaev LG, Sverdlov ED and Razin SV (2005) Induction of transcription within chromosomal DNA loops flanked by MAR elements causes an association of loop DNA with the nuclear matrix. *Nucleic acids research,* **33** (13), 4157-4163.

Iarovaia OV, Bystritskiy A, Ravcheev D, Hancock R and Razin SV (2004) Visualization of individual DNA loops and a map of loop domains in the human dystrophin gene. *Nucleic acids research,* **32** (7), 2079-2086.

Iborra FJ, Pombo A, Jackson DA and Cook PR (1996) Active RNA polymerases are localized within discrete transcription "factories' in human nuclei. *Journal of cell science,* **109** (Pt 6), 1427-1436.

Ivorra C, Kubicek M, Gonzalez JM, Sanz-Gonzalez SM, Alvarez-Barrientos A, O'Connor JE, Burke B and Andres V (2006) A mechanism of AP-1 suppression through interaction of c-Fos with lamin A/C. *Genes & development,* **20** (3), 307-320.

Jackson DA and Cook PR (1993) Transcriptionally active minichromosomes are attached transiently in nuclei through transcription units. *Journal of cell science,* **105** (Pt 4), 1143-1150.

Jackson DA and Cook PR (1988) Visualization of a filamentous nucleoskeleton with a 23 nm axial repeat. *The EMBO journal,* **7** (12), 3667-3677.

Jackson DA and Cook PR (1985) Transcription occurs at a nucleoskeleton. *The EMBO journal,* **4** (4), 919-925.

Jacob KN and Garg A (2006) Laminopathies: multisystem dystrophy syndromes. *Molecular genetics and metabolism,* **87** (4), 289-302.

Jagatheesan G, Thanumalayan S, Muralikrishna B, Rangaraj N, Karande AA and Parnaik VK (1999) Colocalization of intranuclear lamin foci with RNA splicing factors. *Journal of cell science,* **112** (Pt 24), 4651-4661.

Jiang M, Axe T, Holgate R, Rubbi CP, Okorokov AL, Mee T and Milner J (2001) P53 Binds the Nuclear Matrix in Normal Cells: Binding Involves the Proline-Rich Domain of P53 and Increases Following Genotoxic Stress. *Oncogene,* **20** (39), 5449-5458.

Johnson BR, Nitta RT, Frock RL, Mounkes L, Barbie DA, Stewart CL, Harlow E and Kennedy BK (2004) A-type lamins regulate retinoblastoma protein function by promoting subnuclear localization and preventing proteasomal degradation. *Proceedings of the National Academy of Sciences of the United States of America,* **101** (26), 9677-9682.

Kalos M and Fournier RE (1995) Position-independent transgene expression mediated by boundary elements from the apolipoprotein B chromatin domain. *Molecular and cellular biology,* **15** (1), 198-207.

Kamiuchi S, Saijo M, Citterio E, de Jager M, Hoeijmakers JH and Tanaka K (2002) Translocation of Cockayne syndrome group A protein to the nuclear matrix: possible relevance to transcription-coupled DNA repair. *Proceedings of the National Academy of Sciences of the United States of America,* **99** (1), 201-206.

Kandert S, Luke Y, Kleinhenz T, Neumann S, Lu W, Jaeger VM, Munck M, Wehnert M, Muller CR, Zhou Z, Noegel AA, Dabauvalle MC and Karakesisoglou I (2007) Nesprin-2 giant safeguards nuclear envelope architecture in LMNA S143F progeria cells. *Human molecular genetics,* **16** (23), 2944-2959.

Karst ML, Herron KJ and Olson TM (2008) X-linked nonsyndromic sinus node dysfunction and atrial fibrillation caused by emerin mutation. *Journal of cardiovascular electrophysiology,* **19** (5), 510-515.

Kas E and Chasin LA (1987) Anchorage of the Chinese hamster dihydrofolate reductase gene to the nuclear scaffold occurs in an intragenic region. *Journal of Molecular Biology,* **198** (4), 677-692.

Kasper EK, Agema WR, Hutchins GM, Deckers JW, Hare JM and Baughman KL (1994) The causes of dilated cardiomyopathy: a clinicopathologic review of 673 consecutive patients. *Journal of the American College of Cardiology,* **23** (3), 586-590.

Kaufmann SH, Mabry M, Jasti R and Shaper JH (1991) Differential expression of nuclear envelope lamins A and C in human lung cancer cell lines. *Cancer research,* **51** (2), 581-586.

Kawahire S, Takeuchi M, Gohshi T, Sasagawa S, Shimada M, Takahashi M, Abe TK, Ueda T, Kuwano R, Hikawa A, Ichimura T, Omata S and Horigome T (1997) cDNA cloning of nuclear localization signal binding protein NBP60, a rat homologue of lamin B receptor, and identification of binding sites of human lamin B receptor for nuclear localization signals and chromatin. *Journal of Biochemistry,* **121** (5), 881-889.

Keller RK and Fliesler SJ (1999) Mechanism of aminobisphosphonate action: characterization of alendronate inhibition of the isoprenoid pathway. *Biochemical and biophysical research communications,* **266** (2), 560-563.

Kill IR (1996) Localisation of the Ki-67 antigen within the nucleolus. Evidence for a fibrillarin-deficient region of the dense fibrillar component. *Journal of cell science,* **109** (Pt 6), 1253-1263.

Kim SH, McQueen PG, Lichtman MK, Shevach EM, Parada LA and Misteli T (2004) Spatial genome organization during T-cell differentiation. *Cytogenetic and genome research,* **105** (2-4), 292-301.

Kimura H, Sugaya K and Cook PR (2002) The transcription cycle of RNA polymerase II in living cells. *The Journal of cell biology,* **159** (5), 777-782.

Kipp M, Gohring F, Ostendorp T, van Drunen CM, van Driel R, Przybylski M and Fackelmayer FO (2000) SAF-Box, a conserved protein domain that specifically recognizes scaffold attachment region DNA. *Molecular and cellular biology,* **20** (20), 7480-7489.

Kirschner J, Brune T, Wehnert M, Denecke J, Wasner C, Feuer A, Marquardt T, Ketelsen UP, Wieacker P, Bonnemann CG and Korinthenberg R (2005) p.S143F mutation in lamin A/C: a new phenotype combining myopathy and progeria. *Annals of Neurology,* **57** (1), 148-151.

Kiseleva E, Allen TD, Rutherford S, Bucci M, Wente SR and Goldberg MW (2004) Yeast nuclear pore complexes have a cytoplasmic ring and internal filaments. *Journal of structural biology,* **145** (3), 272-288.

Koehler DR and Hanawalt PC (1996) Recruitment of damaged DNA to the nuclear matrix in hamster cells following ultraviolet irradiation. *Nucleic acids research,* **24** (15), 2877-2884.

Kosak ST and Groudine M (2002) The undiscovered country: chromosome territories and the organization of transcription. *Developmental cell,* **2** (6), 690-692.

Kosak ST, Scalzo D, Alworth SV, Li F, Palmer S, Enver T, Lee JS and Groudine M (2007) Coordinate gene regulation during hematopoiesis is related to genomic organization. *PLoS biology,* **5** (11), e309.

Krohne G, Dabauvalle MC and Franke WW (1981) Cell type-specific differences in protein composition of nuclear pore complex-lamina structures in oocytes and erythrocytes of Xenopus laevis. *Journal of Molecular Biology,* **151** (1), 121-141.

Kudlow BA, Stanfel MN, Burtner CR, Johnston ED and Kennedy BK (2008) Suppression of proliferative defects associated with processing-defective lamin A mutants by hTERT or inactivation of p53. *Molecular biology of the cell,* **19** (12), 5238-5248.

Kumaran RI and Spector DL (2008) A genetic locus targeted to the nuclear periphery in living cells maintains its transcriptional competence. *The Journal of cell biology,* **180** (1), 51-65.

Laemmli UK, Kas E, Poljak L and Adachi Y (1992) Scaffold-associated regions: cis-acting determinants of chromatin structural loops and functional domains. *Current opinion in genetics & development,* **2** (2), 275-285.

Laguri C, Gilquin B, Wolff N, Romi-Lebrun R, Courchay K, Callebaut I, Worman HJ and Zinn-Justin S (2001) Structural characterization of the LEM motif common to three human inner nuclear membrane proteins. *Structure (London, England : 1993),* **9** (6), 503-511.

Lammerding J, Hsiao J, Schulze PC, Kozlov S, Stewart CL and Lee RT (2005) Abnormal nuclear shape and impaired mechanotransduction in emerin-deficient cells. *The Journal of cell biology,* **170** (5), 781-791.

Lammerding J, Schulze PC, Takahashi T, Kozlov S, Sullivan T, Kamm RD, Stewart CL and Lee RT (2004) Lamin A/C deficiency causes defective nuclear mechanics and mechanotransduction. *The Journal of clinical investigation,* **113** (3), 370-378.

Lanctot C, Cheutin T, Cremer M, Cavalli G and Cremer T (2007) Dynamic genome architecture in the nuclear space: regulation of gene expression in three dimensions. *Nature reviews. Genetics,* **8** (2), 104-115.

Lansdorp PM, Verwoerd NP, van de Rijke FM, Dragowska V, Little MT, Dirks RW, Raap AK and Tanke HJ (1996) Heterogeneity in telomere length of human chromosomes. *Human molecular genetics,* **5** (5), 685-691.

Lattanzi G, Columbaro M, Mattioli E, Cenni V, Camozzi D, Wehnert M, Santi S, Riccio M, Del Coco R, Maraldi NM, Squarzoni S, Foisner R and Capanni C (2007) Pre-Lamin A processing is linked to heterochromatin organization. *Journal of cellular biochemistry,* **102** (5), 1149-1159.

Lee J, Mehta K, Blick MB, Gutterman JU and Lopez-Berestein G (1987) Expression of c-fos, c-myb, and c-myc in human monocytes: correlation with monocytic differentiation. *Blood,* **69** (5), 1542-1545.

Lee KK, Haraguchi T, Lee RS, Koujin T, Hiraoka Y and Wilson KL (2001) Distinct functional domains in emerin bind lamin A and DNA-bridging protein BAF. *Journal of cell science,* **114** (Pt 24), 4567-4573.

Lee MS and Craigie R (1998) A previously unidentified host protein protects retroviral DNA from autointegration. *Proceedings of the National Academy of Sciences of the United States of America,* **95** (4), 1528-1533.

Lee SH and Hurwitz J (1990) Mechanism of elongation of primed DNA by DNA polymerase delta, proliferating cell nuclear antigen, and activator 1. *Proceedings of the National Academy of Sciences of the United States of America,* **87** (15), 5672-5676.

Lehner CF, Stick R, Eppenberger HM and Nigg EA (1987) Differential expression of nuclear lamin proteins during chicken development. *The Journal of cell biology,* **105** (1), 577-587.

Leman ES and Getzenberg RH (2008) Nuclear structure as a source of cancer specific biomarkers. *Journal of cellular biochemistry,* **104** (6), 1988-1993.

Lenz-Bohme B, Wismar J, Fuchs S, Reifegerste R, Buchner E, Betz H and Schmitt B (1997) Insertional mutation of the Drosophila nuclear lamin Dm0 gene results in defective nuclear envelopes, clustering of nuclear pore complexes, and accumulation of annulate lamellae. *The Journal of cell biology,* **137** (5), 1001-1016.

Lever E and Sheer D (2010) The role of nuclear organization in cancer. *The Journal of pathology,* **220** (2), 114-125.

Levy MZ, Allsopp RC, Futcher AB, Greider CW and Harley CB (1992) Telomere end-replication problem and cell aging. *Journal of Molecular Biology,* **225** (4), 951-960.

Levy N, Lopez-Otin C and Hennekam RC (2005) Defective prelamin A processing resulting from LMNA or ZMPSTE24 mutations as the cause of restrictive dermopathy. *Archives of Dermatology,* **141** (11), 1473-4; author reply 1474.

Lim RY, Aebi U and Fahrenkrog B (2008) Towards reconciling structure and function in the nuclear pore complex. *Histochemistry and cell biology,* **129** (2), 105-116.

Lin F, Blake DL, Callebaut I, Skerjanc IS, Holmer L, McBurney MW, Paulin-Levasseur M and Worman HJ (2000) MAN1, an inner nuclear membrane protein that shares the LEM domain with lamina-associated polypeptide 2 and emerin. *The Journal of biological chemistry,* **275** (7), 4840-4847.

Lin F and Worman HJ (1995) Structural organization of the human gene (LMNB1) encoding nuclear lamin B1. *Genomics,* **27** (2), 230-236.

Lin F and Worman HJ (1993) Structural organization of the human gene encoding nuclear lamin A and nuclear lamin C. *The Journal of biological chemistry,* **268** (22), 16321-16326.

Lin St and Fu YH (2009) miR-23 regulation of lamin B1 is crucial for oligodendrocyte development and myelination. *Disease models & mechanisms,* **2** (3-4), 178-188.

Liu B, Wang J, Chan KM, Tjia WM, Deng W, Guan X, Huang JD, Li KM, Chau PY, Chen DJ, Pei D, Pendas AM, Cadinanos J, Lopez-Otin C, Tse HF, Hutchison C, Chen J, Cao Y, Cheah KS, Tryggvason K and Zhou Z (2005) Genomic instability in laminopathy-based premature aging. *Nature medicine,* **11** (7), 780-785.

Liu J, Rolef Ben-Shahar T, Riemer D, Treinin M, Spann P, Weber K, Fire A and Gruenbaum Y (2000) Essential roles for Caenorhabditis elegans lamin gene in nuclear organization, cell cycle progression, and spatial organization of nuclear pore complexes. *Molecular biology of the cell,* **11** (11), 3937-3947.

Liu Y, Rusinol A, Sinensky M, Wang Y and Zou Y (2006) DNA damage responses in progeroid syndromes arise from defective maturation of prelamin A. *Journal of cell science,* **119** (Pt 22), 4644-4649.

Lloyd DJ, Trembath RC and Shackleton S (2002) A novel interaction between lamin A and SREBP1: implications for partial lipodystrophy and other laminopathies. *Human molecular genetics,* **11** (7), 769-777.

Londono-Vallejo JA, DerSarkissian H, Cazes L and Thomas G (2001) Differences in telomere length between homologous chromosomes in humans. *Nucleic acids research,* **29** (15), 3164-3171.

Lourim D and Lin JJ (1989) Expression of nuclear lamin A and muscle-specific proteins in differentiating muscle cells in ovo and in vitro. *The Journal of cell biology,* **109** (2), 495-504.

Luderus ME, de Graaf A, Mattia E, den Blaauwen JL, Grande MA, de Jong L and van Driel R (1992) Binding of matrix attachment regions to lamin B1. *Cell,* **70** (6), 949-959.

Luderus ME, den Blaauwen JL, de Smit OJ, Compton DA and van Driel R (1994) Binding of matrix attachment regions to lamin polymers involves single-stranded regions and the minor groove. *Molecular and cellular biology,* **14** (9), 6297-6305.

Luderus ME, van Steensel B, Chong L, Sibon OC, Cremers FF and de Lange T (1996) Structure, subnuclear distribution, and nuclear matrix association of the mammalian telomeric complex. *The Journal of cell biology,* **135** (4), 867-881.

Lutz RJ, Trujillo MA, Denham KS, Wenger L and Sinensky M (1992) Nucleoplasmic localization of prelamin A: implications for prenylation-dependent lamin A assembly into the nuclear lamina. *Proceedings of the National Academy of Sciences of the United States of America,* **89** (7), 3000-3004.

Lyon MF (1961) Gene action in the X-chromosome of the mouse (Mus musculus L.). *Nature,* **190,** 372-373.

Ma H, Siegel AJ and Berezney R (1999) Association of chromosome territories with the nuclear matrix. Disruption of human chromosome territories correlates with the release of a subset of nuclear matrix proteins. *The Journal of cell biology,* **146** (3), 531-542.

Maeshima K, Yahata K, Sasaki Y, Nakatomi R, Tachibana T, Hashikawa T, Imamoto F and Imamoto N (2006) Cell-cycle-dependent dynamics of nuclear pores: pore-free islands and lamins. *Journal of cell science,* **119** (Pt 21), 4442-4451.

Mahy NL, Perry PE, Gilchrist S, Baldock RA and Bickmore WA (2002) Spatial organization of active and inactive genes and noncoding DNA within chromosome territories. *The Journal of cell biology,* **157** (4), 579-589.

Makatsori D, Kourmouli N, Polioudaki H, Shultz LD, McLean K, Theodoropoulos PA, Singh PB and Georgatos SD (2004) The inner nuclear membrane protein lamin B receptor forms distinct microdomains and links epigenetically marked chromatin to the nuclear envelope. *The Journal of biological chemistry,* **279** (24), 25567-25573.

Malhas A, Lee CF, Sanders R, Saunders NJ and Vaux DJ (2007) Defects in lamin B1 expression or processing affect interphase chromosome position and gene expression. *The Journal of cell biology,* **176** (5), 593-603.

Malhas AN, Lee CF and Vaux DJ (2009) Lamin B1 controls oxidative stress responses via Oct-1. *The Journal of cell biology,* **184** (1), 45-55.

Mallampalli MP, Huyer G, Bendale P, Gelb MH and Michaelis S (2005) Inhibiting farnesylation reverses the nuclear morphology defect in a HeLa cell model for Hutchinson-Gilford progeria syndrome. *Proceedings of the National Academy of Sciences of the United States of America,* **102** (40), 14416-14421.

Mancini MA, Shan B, Nickerson JA, Penman S and Lee WH (1994) The retinoblastoma gene product is a cell cycle-dependent, nuclear matrix-associated protein. *Proceedings of the National Academy of Sciences of the United States of America,* **91** (1), 418-422.

Mandelkern M, Elias JG, Eden D and Crothers DM (1981) The dimensions of DNA in solution. *Journal of Molecular Biology,* **152** (1), 153-161.

Manilal S, Nguyen TM and Morris GE (1998) Colocalization of emerin and lamins in interphase nuclei and changes during mitosis. *Biochemical and biophysical research communications,* **249** (3), 643-647.

Manilal S, Nguyen TM, Sewry CA and Morris GE (1996) The Emery-Dreifuss muscular dystrophy protein, emerin, is a nuclear membrane protein. *Human molecular genetics,* **5** (6), 801-808.

Manilal S, Recan D, Sewry CA, Hoeltzenbein M, Llense S, Leturcq F, Deburgrave N, Barbot J, Man N, Muntoni F, Wehnert M, Kaplan J and Morris GE (1998) Mutations in Emery-Dreifuss muscular dystrophy and their effects on emerin protein expression. *Human molecular genetics,* **7** (5), 855-864.

Manilal S, Sewry CA, Man N, Muntoni F and Morris GE (1997) Diagnosis of X-linked Emery-Dreifuss muscular dystrophy by protein analysis of leucocytes and skin with monoclonal antibodies. *Neuromuscular disorders : NMD,* **7** (1), 63-66.

Mansouri A, Spurr N, Goodfellow PN and Kemler R (1988) Characterization and chromosomal localization of the gene encoding the human cell adhesion molecule uvomorulin. *Differentiation; research in biological diversity,* **38** (1), 67-71.

Maraldi NM, Lattanzi G, Capanni C, Columbaro M, Merlini L, Mattioli E, Sabatelli P, Squarzoni S and Manzoli FA (2006) Nuclear envelope proteins and chromatin arrangement: a pathogenic mechanism for laminopathies. *European journal of histochemistry : EJH,* **50** (1), 1-8.

Marella NV, Bhattacharya S, Mukherjee L, Xu J and Berezney R (2009) Cell type specific chromosome territory organization in the interphase nucleus of normal and cancer cells. *Journal of cellular physiology,* **221** (1), 130-138.

Margalit A, Brachner A, Gotzmann J, Foisner R and Gruenbaum Y (2007) Barrier-to-autointegration factor--a BAFfling little protein. *Trends in cell biology,* **17** (4), 202-208.

Margalit A, Segura-Totten M, Gruenbaum Y and Wilson KL (2005) Barrier-to-autointegration factor is required to segregate and enclose chromosomes within the nuclear envelope and assemble the nuclear lamina. *Proceedings of the National Academy of Sciences of the United States of America,* **102** (9), 3290-3295.

Mariappan I, Gurung R, Thanumalayan S and Parnaik VK (2007) Identification of cyclin D3 as a new interaction partner of lamin A/C. *Biochemical and biophysical research communications,* **355** (4), 981-985.

Marji J, O'Donoghue SI, McClintock D, Satagopam VP, Schneider R, Ratner D, J Worman H, Gordon LB and Djabali K (2010) Defective lamin A-Rb signaling in Hutchinson-Gilford Progeria Syndrome and reversal by farnesyltransferase inhibition. *PloS one,* **5** (6), e11132.

Markiewicz E, Dechat T, Foisner R, Quinlan RA and Hutchison CJ (2002) Lamin A/C binding protein LAP2alpha is required for nuclear anchorage of retinoblastoma protein. *Molecular biology of the cell,* **13** (12), 4401-4413.

Markiewicz E, Ledran M and Hutchison CJ (2005) Remodelling of the nuclear lamina and nucleoskeleton is required for skeletal muscle differentiation in vitro. *Journal of cell science,* **118** (Pt 2), 409-420.

Markiewicz E, Tilgner K, Barker N, van de Wetering M, Clevers H, Dorobek M, Hausmanowa-Petrusewicz I, Ramaekers FC, Broers JL, Blankesteijn WM, Salpingidou G, Wilson RG, Ellis JA and Hutchison CJ (2006) The inner nuclear membrane protein emerin regulates beta-catenin activity by restricting its accumulation in the nucleus. *The EMBO journal,* **25** (14), 3275-3285.

Markiewicz E, Venables R, Mauricio-Alvarez-Reyes, Quinlan R, Dorobek M, Hausmanowa-Petrucewicz I and Hutchison C (2002) Increased solubility of lamins and redistribution of lamin C in X-linked Emery-Dreifuss muscular dystrophy fibroblasts. *Journal of structural biology,* **140** (1-3), 241-253.

Martelli AM, Capitani S and Neri LM (1998) Prereplicative increase of nuclear matrix-bound DNA polymerase-alpha and primase activities in HeLa S3 cells following dilution of long-term cultures. *Journal of cellular biochemistry,* **71** (1), 11-20.

Martins RP, Ostermeier GC and Krawetz SA (2004) Nuclear matrix interactions at the human protamine domain: a working model of potentiation. *The Journal of biological chemistry,* **279** (50), 51862-51868.

Martins S, Eikvar S, Furukawa K and Collas P (2003) HA95 and LAP2 beta mediate a novel chromatin-nuclear envelope interaction implicated in initiation of DNA replication. *The Journal of cell biology,* **160** (2), 177-188.

Mattern KA, Humbel BM, Muijsers AO, de Jong L and van Driel R (1996) hnRNP proteins and B23 are the major proteins of the internal nuclear matrix of HeLa S3 cells. *Journal of cellular biochemistry,* **62** (2), 275-289.

Mattioli E, Columbaro M, Capanni C, Santi S, Maraldi NM, D'Apice MR, Novelli G, Riccio M, Squarzoni S, Foisner R and Lattanzi G (2008) Drugs affecting prelamin A processing: effects on heterochromatin organization. *Experimental cell research,* **314** (3), 453-462.

Mayer R, Brero A, von Hase J, Schroeder T, Cremer T and Dietzel S (2005) Common themes and cell type specific variations of higher order chromatin arrangements in the mouse. *BMC cell biology,* **6**44.

McClintock D, Gordon LB and Djabali K (2006) Hutchinson-Gilford progeria mutant lamin A primarily targets human vascular cells as detected by an anti-Lamin A G608G antibody. *Proceedings of the National Academy of Sciences of the United States of America,* **103** (7), 2154-2159.

McCready SJ and Cook PR (1984) Lesions induced in DNA by ultraviolet light are repaired at the nuclear cage. *Journal of cell science,* **70,** 189-196.

McKeon FD, Kirschner MW and Caput D (1986) Homologies in both primary and secondary structure between nuclear envelope and intermediate filament proteins. *Nature,* **319** (6053), 463-468.

Meaburn KJ, Cabuy E, Bonne G, Levy N, Morris GE, Novelli G, Kill IR and Bridger JM (2007) Primary laminopathy fibroblasts display altered genome organization and apoptosis. *Aging cell,* **6** (2), 139-153.

Meaburn KJ, Gudla PR, Khan S, Lockett SJ and Misteli T (2009) Disease-specific gene repositioning in breast cancer. *The Journal of cell biology,* **187** (6), 801-812.

Meaburn KJ, Levy N, Toniolo D and Bridger JM (2005) Chromosome positioning is largely unaffected in lymphoblastoid cell lines containing emerin or A-type lamin mutations. *Biochemical Society transactions,* **33** (Pt 6), 1438-1440.

Meaburn KJ and Misteli T (2008) Locus-specific and activity-independent gene repositioning during early tumorigenesis. *The Journal of cell biology,* **180** (1), 39-50.

Meaburn KJ, Newbold RF and Bridger JM (2008) Positioning of human chromosomes in murine cell hybrids according to synteny. *Chromosoma,* **117** (6), 579-591.

Mehta IS, Amira M, Harvey AJ and Bridger JM (2010) Rapid chromosome territory relocation by nuclear motor activity in response to serum removal in primary human fibroblasts. *Genome biology,* **11** (1), R5.

Mehta IS, Bridger JM and Kill IR (2010) Progeria, the nucleolus and farnesyltransferase inhibitors. *Biochemical Society transactions,* **38** (Pt 1), 287-291.

Mehta IS, Elcock LS, Amira M, Kill IR and Bridger JM (2008) Nuclear motors and nuclear structures containing A-type lamins and emerin: is there a functional link? *Biochemical Society transactions,* **36** (Pt 6), 1384-1388.

Mehta IS, Figgitt M, Clements CS, Kill IR and Bridger JM (2007) Alterations to nuclear architecture and genome behavior in senescent cells. *Annals of the New York Academy of Sciences,* **1100,** 250-263.

Meier J, Campbell KH, Ford CC, Stick R and Hutchison CJ (1991) The role of lamin LIII in nuclear assembly and DNA replication, in cell-free extracts of Xenopus eggs. *Journal of cell science,* **98** (Pt 3), 271-279.

Meier J and Georgatos SD (1994) Type B lamins remain associated with the integral nuclear envelope protein p58 during mitosis: implications for nuclear reassembly. *The EMBO journal,* **13** (8), 1888-1898.

Melcon G, Kozlov S, Cutler DA, Sullivan T, Hernandez L, Zhao P, Mitchell S, Nader G, Bakay M, Rottman JN, Hoffman EP and Stewart CL (2006) Loss of emerin at the nuclear envelope disrupts the Rb1/E2F and MyoD pathways during muscle regeneration. *Human molecular genetics,* **15** (4), 637-651.

Metzger DA and Korach KS (1990) Cell-free interaction of the estrogen receptor with mouse uterine nuclear matrix: evidence of saturability, specificity, and resistance to KCl extraction. *Endocrinology,* **126** (4), 2190-2195.

Michishita E, Kurahashi T, Suzuki T, Fukuda M, Fujii M, Hirano H and Ayusawa D (2002) Changes in nuclear matrix proteins during the senescence-like phenomenon induced by 5-chlorodeoxyuridine in HeLa cells. *Experimental gerontology,* **37** (7), 885-890.

Mika S and Rost B (2005) NMPdb: Database of Nuclear Matrix Proteins. *Nucleic acids research,* **33** (Database issue), D160-3.

Mirkovitch J, Mirault ME and Laemmli UK (1984) Organization of the higher-order chromatin loop: specific DNA attachment sites on nuclear scaffold. *Cell,* **39** (1), 223-232.

Mislow JM, Holaska JM, Kim MS, Lee KK, Segura-Totten M, Wilson KL and McNally EM (2002) Nesprin-1alpha self-associates and binds directly to emerin and lamin A in vitro. *FEBS letters,* **525** (1-3), 135-140.

Mittnacht S (1998) Control of pRB phosphorylation. *Current opinion in genetics & development,* **8** (1), 21-27.

Mittnacht SandWeinberg RA (1991) G1/S phosphorylation of the retinoblastoma protein is associated with an altered affinity for the nuclear compartment. *Cell,* **65** (3), 381-393.

Mladenov E, Anachkova B and Tsaneva I (2006) Sub-nuclear localization of Rad51 in response to DNA damage. *Genes to cells : devoted to molecular & cellular mechanisms,* **11** (5), 513-524.

Mladenov E, Tsaneva I and Anachkova B (2007) Cell cycle-dependent association of Rad51 with the nuclear matrix. *DNA and cell biology,* **26** (1), 36-43.

Mladenov EV, Kalev PS and Anachkova BB (2009) Nuclear matrix binding site in the Rad51 recombinase. *Journal of cellular physiology,* **219** (1), 202-208.

Moir RD, Montag-Lowy M and Goldman RD (1994) Dynamic properties of nuclear lamins: lamin B is associated with sites of DNA replication. *The Journal of cell biology,* **125** (6), 1201-1212.

Moir RD, Spann TP, Herrmann H and Goldman RD (2000) Disruption of nuclear lamin organization blocks the elongation phase of DNA replication. *The Journal of cell biology,* **149** (6), 1179-1192.

Mora L, Sanchez I, Garcia M and Ponsa M (2006) Chromosome territory positioning of conserved homologous chromosomes in different primate species. *Chromosoma,* **115** (5), 367-375.

Morel CF, Thomas MA, Cao H, O'Neil CH, Pickering JG, Foulkes WD and Hegele RA (2006) A LMNA splicing mutation in two sisters with severe Dunnigan-type familial partial lipodystrophy type 2. *The Journal of clinical endocrinology and metabolism,* **91** (7), 2689-2695.

Morey C, Kress C and Bickmore WA (2009) Lack of bystander activation shows that localization exterior to chromosome territories is not sufficient to up-regulate gene expression. *Genome research,* **19** (7), 1184-1194.

Moss SF, Krivosheyev V, de Souza A, Chin K, Gaetz HP, Chaudhary N, Worman HJ and Holt PR (1999) Decreased and aberrant nuclear lamin expression in gastrointestinal tract neoplasms. *Gut,* **45** (5), 723-729.

Motokura T, Bloom T, Kim HG, Juppner H, Ruderman JV, Kronenberg HM and Arnold A (1991) A novel cyclin encoded by a bcl1-linked candidate oncogene. *Nature,* **350** (6318), 512-515.

Moulson CL, Go G, Gardner JM, van der Wal AC, Smitt JH, van Hagen JM and Miner JH (2005) Homozygous and compound heterozygous mutations in ZMPSTE24 cause the laminopathy restrictive dermopathy. *The Journal of investigative dermatology,* **125** (5), 913-919.

Mounkes LC, Kozlov S, Hernandez L, Sullivan T and Stewart CL (2003) A progeroid syndrome in mice is caused by defects in A-type lamins. *Nature,* **423** (6937), 298-301.

Mounkes LC, Kozlov SV, Rottman JN and Stewart CL (2005) Expression of an LMNA-N195K variant of A-type lamins results in cardiac conduction defects and death in mice. *Human molecular genetics,* **14** (15), 2167-2180.

Muchir A, Bonne G, van der Kooi AJ, van Meegen M, Baas F, Bolhuis PA, de Visser M and Schwartz K (2000) Identification of mutations in the gene encoding lamins A/C in autosomal dominant limb girdle muscular dystrophy with atrioventricular conduction disturbances (LGMD1B). *Human molecular genetics,* **9** (9), 1453-1459.

Muchir A, Medioni J, Laluc M, Massart C, Arimura T, van der Kooi AJ, Desguerre I, Mayer M, Ferrer X, Briault S, Hirano M, Worman HJ, Mallet A, Wehnert M, Schwartz K and Bonne G (2004) Nuclear envelope alterations in fibroblasts from patients with muscular dystrophy, cardiomyopathy, and partial lipodystrophy carrying lamin A/C gene mutations. *Muscle & nerve,* **30** (4), 444-450.

Muchir A, Pavlidis P, Bonne G, Hayashi YK and Worman HJ (2007a) Activation of MAPK in hearts of EMD null mice: similarities between mouse models of X-linked and autosomal dominant Emery Dreifuss muscular dystrophy. *Human molecular genetics,* **16** (15), 1884-1895.

Muchir A, Pavlidis P, Decostre V, Herron AJ, Arimura T, Bonne G and Worman HJ (2007b) Activation of MAPK pathways links LMNA mutations to cardiomyopathy in Emery-Dreifuss muscular dystrophy. *The Journal of clinical investigation,* **117** (5), 1282-1293.

Muchir A, van Engelen BG, Lammens M, Mislow JM, McNally E, Schwartz K and Bonne G (2003) Nuclear envelope alterations in fibroblasts from LGMD1B patients carrying nonsense Y259X heterozygous or homozygous mutation in lamin A/C gene. *Experimental cell research,* **291** (2), 352-362.

Mukherjee AB and Costello C (1998) Aneuploidy analysis in fibroblasts of human premature aging syndromes by FISH during in vitro cellular aging. *Mechanisms of ageing and development,* **103** (2), 209-222.

Mullenders LH, van Kesteren van Leeuwen AC, van Zeeland AA and Natarajan AT (1988) Nuclear matrix associated DNA is preferentially repaired in normal human fibroblasts, exposed to a low dose of ultraviolet light but not in Cockayne's syndrome fibroblasts. *Nucleic acids research,* **16** (22), 10607-10622.

Muntoni F, Lichtarowicz-Krynska EJ, Sewry CA, Manilal S, Recan D, Llense S, Taylor J, Morris GE and Dubowitz V (1998) Early presentation of X-linked Emery-Dreifuss muscular dystrophy resembling limb-girdle muscular dystrophy. *Neuromuscular disorders : NMD,* **8** (2), 72-76.

Muralikrishna B, Dhawan J, Rangaraj N and Parnaik VK (2001) Distinct changes in intranuclear lamin A/C organization during myoblast differentiation. *Journal of cell science,* **114** (Pt 22), 4001-4011.

Murata S, Nakazawa T, Ohno N, Terada N, Iwashina M, Mochizuki K, Kondo T, Nakamura N, Yamane T, Iwasa S, Ohno S and Katoh R (2007) Conservation and alteration of chromosome territory arrangements in thyroid carcinoma cell nuclei. *Thyroid : official journal of the American Thyroid Association,* **17** (6), 489-496.

Nagano A, Koga R, Ogawa M, Kurano Y, Kawada J, Okada R, Hayashi YK, Tsukahara T and Arahata K (1996) Emerin deficiency at the nuclear membrane in patients with Emery-Dreifuss muscular dystrophy. *Nature genetics,* **12** (3), 254-259.

Nagele RG, Freeman T, McMorrow L, Thomson Z, Kitson-Wind K and Lee H (1999) Chromosomes exhibit preferential positioning in nuclei of quiescent human cells. *Journal of cell science,* **112** (Pt 4), 525-535.

Namciu SJ, Blochlinger KB and Fournier RE (1998) Human matrix attachment regions insulate transgene expression from chromosomal position effects in Drosophila melanogaster. *Molecular and cellular biology,* **18** (4), 2382-2391.

Natt E, Magenis RE, Zimmer J, Mansouri A and Scherer G (1989) Regional assignment of the human loci for uvomorulin (UVO) and chymotrypsinogen B (CTRB) with the help of two overlapping deletions on the long arm of chromosome 16. *Cytogenetics and cell genetics,* **50** (2-3), 145-148.

Navarro CL, Cadinanos J, De Sandre-Giovannoli A, Bernard R, Courrier S, Boccaccio I, Boyer A, Kleijer WJ, Wagner A, Giuliano F, Beemer FA, Freije JM, Cau P, Hennekam RC, Lopez-Otin C, Badens C and Levy N (2005) Loss of ZMPSTE24 (FACE-1) causes autosomal recessive restrictive dermopathy and accumulation of Lamin A precursors. *Human molecular genetics,* **14** (11), 1503-1513.

Navarro CL, De Sandre-Giovannoli A, Bernard R, Boccaccio I, Boyer A, Genevieve D, Hadj-Rabia S, Gaudy-Marqueste C, Smitt HS, Vabres P, Faivre L, Verloes A, Van Essen T, Flori E, Hennekam R, Beemer FA, Laurent N, Le Merrer M, Cau P and Levy N (2004) Lamin A and ZMPSTE24 (FACE-1) defects cause nuclear disorganization and identify restrictive dermopathy as a lethal neonatal laminopathy. *Human molecular genetics,* **13** (20), 2493-2503.

Negrini S, Gorgoulis VG and Halazonetis TD (2010) Genomic instability--an evolving hallmark of cancer. *Nature reviews.Molecular cell biology,* **11** (3), 220-228.

Neusser M, Schubel V, Koch A, Cremer T and Muller S (2007) Evolutionarily conserved, cell type and species-specific higher order chromatin arrangements in interphase nuclei of primates. *Chromosoma,* **116** (3), 307-320.

Newport JW, Wilson KL and Dunphy WG (1990) A lamin-independent pathway for nuclear envelope assembly. *The Journal of cell biology,* **111** (6 Pt 1), 2247-2259.

Nickerson J (2001) Experimental observations of a nuclear matrix. *Journal of cell science,* **114** (Pt 3), 463-474.

Nickerson JA, Krockmalnic G, Wan KM and Penman S (1997) The nuclear matrix revealed by eluting chromatin from a cross-linked nucleus. *Proceedings of the National Academy of Sciences of the United States of America,* **94** (9), 4446-4450.

Nickerson JA and Penman S (1992) Localization of nuclear matrix core filament proteins at interphase and mitosis. *Cell biology international reports,* **16** (8), 811-826.

Nielsen AL, Ortiz JA, You J, Oulad-Abdelghani M, Khechumian R, Gansmuller A, Chambon P and Losson R (1999) Interaction with members of the heterochromatin protein 1 (HP1) family and histone deacetylation are differentially involved in transcriptional silencing by members of the TIF1 family. *The EMBO journal,* **18** (22), 6385-6395.

Nikolova V, Leimena C, McMahon AC, Tan JC, Chandar S, Jogia D, Kesteven SH, Michalicek J, Otway R, Verheyen F, Rainer S, Stewart CL, Martin D, Feneley MP and Fatkin D (2004) Defects in nuclear structure and function promote dilated

cardiomyopathy in lamin A/C-deficient mice. *The Journal of clinical investigation,* **113** (3), 357-369.

Nili E, Cojocaru GS, Kalma Y, Ginsberg D, Copeland NG, Gilbert DJ, Jenkins NA, Berger R, Shaklai S, Amariglio N, Brok-Simoni F, Simon AJ and Rechavi G (2001) Nuclear membrane protein LAP2beta mediates transcriptional repression alone and together with its binding partner GCL (germ-cell-less). *Journal of cell science,* **114** (Pt 18), 3297-3307.

Nitta RT, Jameson SA, Kudlow BA, Conlan LA and Kennedy BK (2006) Stabilization of the retinoblastoma protein by A-type nuclear lamins is required for INK4A-mediated cell cycle arrest. *Molecular and cellular biology,* **26** (14), 5360-5372.

Novelli G, Muchir A, Sangiuolo F, Helbling-Leclerc A, D'Apice MR, Massart C, Capon F, Sbraccia P, Federici M, Lauro R, Tudisco C, Pallotta R, Scarano G, Dallapiccola B, Merlini L and Bonne G (2002) Mandibuloacral dysplasia is caused by a mutation in LMNA-encoding lamin A/C. *American Journal of Human Genetics,* **71** (2), 426-431.

Ognibene A, Sabatelli P, Petrini S, Squarzoni S, Riccio M, Santi S, Villanova M, Palmeri S, Merlini L and Maraldi NM (1999) Nuclear changes in a case of X-linked Emery-Dreifuss muscular dystrophy. *Muscle & nerve,* **22** (7), 864-869.

Okabe J, Eguchi A, Masago A, Hayakawa T and Nakanishi M (2000) TRF1 is a critical trans-acting factor required for de novo telomere formation in human cells. *Human molecular genetics,* **9** (18), 2639-2650.

Okabe J, Eguchi A, Wadhwa R, Rakwal R, Tsukinoki R, Hayakawa T and Nakanishi M (2004) Limited capacity of the nuclear matrix to bind telomere repeat binding factor TRF1 may restrict the proliferation of mortal human fibroblasts. *Human molecular genetics,* **13** (3), 285-293.

Oosterwijk JC, Mansour S, van Noort G, Waterham HR, Hall CM and Hennekam RC (2003) Congenital abnormalities reported in Pelger-Huet homozygosity as compared to Greenberg/HEM dysplasia: highly variable expression of allelic phenotypes. *Journal of medical genetics,* **40** (12), 937-941.

Osborne CS, Chakalova L, Brown KE, Carter D, Horton A, Debrand E, Goyenechea B, Mitchell JA, Lopes S, Reik W and Fraser P (2004) Active genes dynamically colocalize to shared sites of ongoing transcription. *Nature genetics,* **36** (10), 1065-1071.

Osborne CS, Chakalova L, Mitchell JA, Horton A, Wood AL, Bolland DJ, Corcoran AE and Fraser P (2007) Myc dynamically and preferentially relocates to a transcription factory occupied by Igh. *PLoS biology,* **5** (8), e192.

Otto JC, Kim E, Young SG and Casey PJ (1999) Cloning and characterization of a mammalian prenyl protein-specific protease. *The Journal of biological chemistry,* **274** (13), 8379-8382.

Ozaki T, Saijo M, Murakami K, Enomoto H, Taya Y and Sakiyama S (1994) Complex formation between lamin A and the retinoblastoma gene product: identification of the domain on lamin A required for its interaction. *Oncogene,* **9** (9), 2649-2653.

Ozawa R, Hayashi YK, Ogawa M, Kurokawa R, Matsumoto H, Noguchi S, Nonaka I and Nishino I (2006) Emerin-lacking mice show minimal motor and cardiac dysfunctions with nuclear-associated vacuoles. *The American journal of pathology,* **168** (3), 907-917.

Padiath QS, Saigoh K, Schiffmann R, Asahara H, Yamada T, Koeppen A, Hogan K, Ptacek LJ and Fu YH (2006) Lamin B1 duplications cause autosomal dominant leukodystrophy. *Nature genetics,* **38** (10), 1114-1123.

Padmakumar VC, Libotte T, Lu W, Zaim H, Abraham S, Noegel AA, Gotzmann J, Foisner R and Karakesisoglou I (2005) The inner nuclear membrane protein Sun1 mediates the anchorage of Nesprin-2 to the nuclear envelope. *Journal of cell science,* **118** (Pt 15), 3419-3430.

Pan Y, Garg A and Agarwal AK (2007) Mislocalization of prelamin A Tyr646Phe mutant to the nuclear pore complex in human embryonic kidney 293 cells. *Biochemical and biophysical research communications,* **355** (1), 78-84.

Parada L and Misteli T (2002) Chromosome positioning in the interphase nucleus. *Trends in cell biology,* **12** (9), 425-432.

Paradisi M, McClintock D, Boguslavsky RL, Pedicelli C, Worman HJ and Djabali K (2005) Dermal fibroblasts in Hutchinson-Gilford progeria syndrome with the lamin A G608G mutation have dysmorphic nuclei and are hypersensitive to heat stress. *BMC cell biology***,** 627.

Park YE, Hayashi YK, Goto K, Komaki H, Hayashi Y, Inuzuka T, Noguchi S, Nonaka I and Nishino I (2009) Nuclear changes in skeletal muscle extend to satellite cells in autosomal dominant Emery-Dreifuss muscular dystrophy/limb-girdle muscular dystrophy 1B. *Neuromuscular disorders: NMD,* **19** (1), 29-36.

Parris CN, Harris JD, Griffin DK, Cuthbert AP, Silver AJ and Newbold RF (1999) Functional evidence of novel tumor suppressor genes for cutaneous malignant melanoma. *Cancer research,* **59** (3), 516-520.

Parry DA and Steinert PM (1999) Intermediate filaments: molecular architecture, assembly, dynamics and polymorphism. *Quarterly reviews of biophysics,* **32** (2), 99-187.

Pederson T (2000) Half a century of "the nuclear matrix". *Molecular biology of the cell,* **11** (3), 799-805.

Pekovic V, Harborth J, Broers JL, Ramaekers FC, van Engelen B, Lammens M, von Zglinicki T, Foisner R, Hutchison C and Markiewicz E (2007) Nucleoplasmic LAP2alpha-lamin A complexes are required to maintain a proliferative state in human fibroblasts. *The Journal of cell biology,* **176** (2), 163-172.

Pendas AM, Zhou Z, Cadinanos J, Freije JM, Wang J, Hultenby K, Astudillo A, Wernerson A, Rodriguez F, Tryggvason K and Lopez-Otin C (2002) Defective prelamin A processing and muscular and adipocyte alterations in Zmpste24 metalloproteinase-deficient mice. *Nature genetics,* **31** (1), 94-99.

Pereira S, Bourgeois P, Navarro C, Esteves-Vieira V, Cau P, De Sandre-Giovannoli A and Levy N (2008) HGPS and related premature aging disorders: from genomic identification to the first therapeutic approaches. *Mechanisms of ageing and development,* **129** (7-8), 449-459.

Philimonenko AA, Hodny Z, Jackson DA and Hozak P (2006) The microarchitecture of DNA replication domains. *Histochemistry and cell biology,* **125** (1-2), 103-117.

Philimonenko VV, Flechon JE and Hozak P (2001) The nucleoskeleton: a permanent structure of cell nuclei regardless of their transcriptional activity. *Experimental cell research,* **264** (2), 201-210.

Pickersgill H, Kalverda B, de Wit E, Talhout W, Fornerod M and van Steensel B (2006) Characterization of the Drosophila melanogaster genome at the nuclear lamina. *Nature genetics,* **38** (9), 1005-1014.

Piercy RJ, Zhou H, Feng L, Pombo A, Muntoni F and Brown SC (2007) Desmin immunolocalisation in autosomal dominant Emery-Dreifuss muscular dystrophy. *Neuromuscular disorders : NMD,* **17** (4), 297-305.

Plasilova M, Chattopadhyay C, Pal P, Schaub NA, Buechner SA, Mueller H, Miny P, Ghosh A and Heinimann K (2004) Homozygous missense mutation in the lamin A/C gene causes autosomal recessive Hutchinson-Gilford progeria syndrome. *Journal of medical genetics,* **41** (8), 609-614.

Platts AE, Quayle AK and Krawetz SA (2006) In-silico prediction and observations of nuclear matrix attachment. *Cellular & Molecular Biology Letters,* **11** (2), 191-213.

Puckelwartz MJ, Kessler E, Zhang Y, Hodzic D, Randles KN, Morris G, Earley JU, Hadhazy M, Holaska JM, Mewborn SK, Pytel P and McNally EM (2009) Disruption of nesprin-1 produces an Emery Dreifuss muscular dystrophy-like phenotype in mice. *Human molecular genetics,* **18** (4), 607-620.

Pugh GE, Coates PJ, Lane EB, Raymond Y and Quinlan RA (1997) Distinct nuclear assembly pathways for lamins A and C lead to their increase during quiescence in Swiss 3T3 cells. *Journal of cell science,* **110** (Pt 19), 2483-2493.

Pujol G, Soderqvist H and Radu A (2002) Age-associated reduction of nuclear protein import in human fibroblasts. *Biochemical and biophysical research communications,* **294** (2), 354-358.

Pyrpasopoulou A, Meier J, Maison C, Simos G and Georgatos SD (1996) The lamin B receptor (LBR) provides essential chromatin docking sites at the nuclear envelope. *The EMBO journal,* **15** (24), 7108-7119.

Radichev I, Parashkevova A and Anachkova B (2005) Initiation of DNA replication at a nuclear matrix-attached chromatin fraction. *Journal of cellular physiology,* **203** (1), 71-77.

Raffaele Di Barletta M, Ricci E, Galluzzi G, Tonali P, Mora M, Morandi L, Romorini A, Voit T, Orstavik KH, Merlini L, Trevisan C, Biancalana V, Housmanowa-Petrusewicz I, Bione S, Ricotti R, Schwartz K, Bonne G and Toniolo D (2000) Different mutations in the LMNA gene cause autosomal dominant and autosomal recessive Emery-Dreifuss muscular dystrophy. *American Journal of Human Genetics,* **66** (4), 1407-1412.

Ragnauth CD, Warren DT, Liu Y, McNair R, Tajsic T, Figg N, Shroff R, Skepper J and Shanahan CM (2010) Prelamin A acts to accelerate smooth muscle cell senescence and is a novel biomarker of human vascular aging. *Circulation,* **121** (20), 2200-2210.

Ragoczy T, Bender MA, Telling A, Byron R and Groudine M (2006) The locus control region is required for association of the murine beta-globin locus with engaged transcription factories during erythroid maturation. *Genes & development,* **20** (11), 1447-1457.

Ragoczy T, Telling A, Sawado T, Groudine M and Kosak ST (2003) A genetic analysis of chromosome territory looping: diverse roles for distal regulatory elements. *Chromosome research : an international journal on the molecular, supramolecular and evolutionary aspects of chromosome biology,* **11** (5), 513-525.

Raj A, Peskin CS, Tranchina D, Vargas DY and Tyagi S (2006) Stochastic mRNA synthesis in mammalian cells. *PLoS biology,* **4** (10), e309.

Ralle T, Grund C, Franke WW and Stick R (2004) Intranuclear membrane structure formations by CaaX-containing nuclear proteins. *Journal of cell science,* **117** (Pt 25), 6095-6104.

Ratsch A, Joos S, Kioschis P and Lichter P (2002) Topological organization of the MYC/IGK locus in Burkitt's lymphoma cells assessed by nuclear halo preparations. *Experimental cell research,* **273** (1), 12-20.

Raz V, Vermolen BJ, Garini Y, Onderwater JJ, Mommaas-Kienhuis MA, Koster AJ, Young IT, Tanke H and Dirks RW (2008) The nuclear lamina promotes telomere aggregation and centromere peripheral localization during senescence of human mesenchymal stem cells. *Journal of cell science,* **121** (Pt 24), 4018-4028.

Reddel CJ and Weiss AS (2004) Lamin A expression levels are unperturbed at the normal and mutant alleles but display partial splice site selection in Hutchinson-Gilford progeria syndrome. *Journal of medical genetics,* **41** (9), 715-717.

Reddy KL, Zullo JM, Bertolino E and Singh H (2008) Transcriptional repression mediated by repositioning of genes to the nuclear lamina. *Nature,* **452** (7184), 243-247.

Reichart B, Klafke R, Dreger C, Kruger E, Motsch I, Ewald A, Schafer J, Reichmann H, Muller CR and Dabauvalle MC (2004) Expression and localization of nuclear proteins in autosomal-dominant Emery-Dreifuss muscular dystrophy with LMNA R377H mutation. *BMC cell biology,* 512.

Renz A and Fackelmayer FO (1996) Purification and molecular cloning of the scaffold attachment factor B (SAF-B), a novel human nuclear protein that specifically binds to S/MAR-DNA. *Nucleic acids research,* **24** (5), 843-849.

Repping S, de Vries JW, van Daalen SK, Korver CM, Leschot NJ and van der Veen F (2003) The use of sperm HALO-FISH to determine DAZ gene copy number. *Molecular human reproduction,* **9** (4), 183-188.

Ris H (1997) High-resolution field-emission scanning electron microscopy of nuclear pore complex. *Scanning,* **19** (5), 368-375.

Rober RA, Sauter H, Weber K and Osborn M (1990) Cells of the cellular immune and hemopoietic system of the mouse lack lamins A/C: distinction versus other somatic cells. *Journal of cell science,* **95** (Pt 4), 587-598.

Rober RA, Weber K and Osborn M (1989) Differential timing of nuclear lamin A/C expression in the various organs of the mouse embryo and the young animal: a developmental study. *Development (Cambridge, England),* **105** (2), 365-378.

Romig H, Fackelmayer FO, Renz A, Ramsperger U and Richter A (1992) Characterization of SAF-A, a novel nuclear DNA binding protein from HeLa cells with high affinity for nuclear matrix/scaffold attachment DNA elements. *The EMBO journal,* **11** (9), 3431-3440.

Rothmann C, Cohen AM and Malik Z (1997) Chromatin condensation in erythropoiesis resolved by multipixel spectral imaging: differentiation versus apoptosis. *The journal of histochemistry and cytochemistry : official journal of the Histochemistry Society,* **45** (8), 1097-1108.

Rout MP, Aitchison JD, Suprapto A, Hjertaas K, Zhao Y and Chait BT (2000) The yeast nuclear pore complex: composition, architecture, and transport mechanism. *The Journal of cell biology,* **148** (4), 635-651.

Sabatelli P, Lattanzi G, Ognibene A, Columbaro M, Capanni C, Merlini L, Maraldi NM and Squarzoni S (2001) Nuclear alterations in autosomal-dominant Emery-Dreifuss muscular dystrophy. *Muscle & nerve,* **24** (6), 826-829.

Scaffidi P and Misteli T (2008) Lamin A-dependent misregulation of adult stem cells associated with accelerated ageing. *Nature cell biology,* **10** (4), 452-459.

Scaffidi P and Misteli T (2006) Lamin A-dependent nuclear defects in human aging. *Science (New York, N.Y.),* **312** (5776), 1059-1063.

Scaffidi P and Misteli T (2005) Reversal of the cellular phenotype in the premature aging disease Hutchinson-Gilford progeria syndrome. *Nature medicine,* **11** (4), 440-445.

Schatten G, Maul GG, Schatten H, Chaly N, Simerly C, Balczon R and Brown DL (1985) Nuclear lamins and peripheral nuclear antigens during fertilization and embryogenesis in mice and sea urchins. *Proceedings of the National Academy of Sciences of the United States of America,* **82** (14), 4727-4731.

Scheuermann MO, Tajbakhsh J, Kurz A, Saracoglu K, Eils R and Lichter P (2004) Topology of genes and nontranscribed sequences in human interphase nuclei. *Experimental cell research,* **301** (2), 266-279.

Schiffmann Randvan der Knaap MS (2004) The latest on leukodystrophies. *Current opinion in neurology,* **17** (2), 187-192.

Schirmer EC, Florens L, Guan T, Yates JR,3rd and Gerace L (2003) Nuclear membrane proteins with potential disease links found by subtractive proteomics. *Science (New York, N.Y.),* **301** (5638), 1380-1382.

Schubeler D, Mielke C, Maass K and Bode J (1996) Scaffold/matrix-attached regions act upon transcription in a context-dependent manner. *Biochemistry,* **35** (34), 11160-11169.

Segura-Totten M and Wilson KL (2004) BAF: roles in chromatin, nuclear structure and retrovirus integration. *Trends in cell biology,* **14** (5), 261-266.

Sewry CA, Brown SC, Mercuri E, Bonne G, Feng L, Camici G, Morris GE and Muntoni F (2001) Skeletal muscle pathology in autosomal dominant Emery-Dreifuss muscular dystrophy with lamin A/C mutations. *Neuropathology and applied neurobiology,* **27** (4), 281-290.

Shackleton S, Lloyd DJ, Jackson SN, Evans R, Niermeijer MF, Singh BM, Schmidt H, Brabant G, Kumar S, Durrington PN, Gregory S, O'Rahilly S and Trembath RC (2000) LMNA, encoding lamin A/C, is mutated in partial lipodystrophy. *Nature genetics,* **24** (2), 153-156.

Shoeman RL and Traub P (1990) The in vitro DNA-binding properties of purified nuclear lamin proteins and vimentin. *The Journal of biological chemistry,* **265** (16), 9055-9061.

Shumaker DK, Dechat T, Kohlmaier A, Adam SA, Bozovsky MR, Erdos MR, Eriksson M, Goldman AE, Khuon S, Collins FS, Jenuwein T and Goldman RD (2006) Mutant nuclear lamin A leads to progressive alterations of epigenetic control in premature aging. *Proceedings of the National Academy of Sciences of the United States of America,* **103** (23), 8703-8708.

Shumaker DK, Solimando L, Sengupta K, Shimi T, Adam SA, Grunwald A, Strelkov SV, Aebi U, Cardoso MC and Goldman RD (2008) The highly conserved nuclear

lamin Ig-fold binds to PCNA: its role in DNA replication. *The Journal of cell biology,* **181** (2), 269-280.

Silve S, Dupuy PH, Ferrara P and Loison G (1998) Human lamin B receptor exhibits sterol C14-reductase activity in Saccharomyces cerevisiae. *Biochimica et biophysica acta,* **1392** (2-3), 233-244.

Simha VandGarg A (2002) Body fat distribution and metabolic derangements in patients with familial partial lipodystrophy associated with mandibuloacral dysplasia. *The Journal of clinical endocrinology and metabolism,* **87** (2), 776-785.

Simonis M, Klous P, Splinter E, Moshkin Y, Willemsen R, de Wit E, van Steensel B and de Laat W (2006) Nuclear organization of active and inactive chromatin domains uncovered by chromosome conformation capture-on-chip (4C). *Nature genetics,* **38** (11), 1348-1354.

Sinensky M, Beck LA, Leonard S and Evans R (1990) Differential inhibitory effects of lovastatin on protein isoprenylation and sterol synthesis. *The Journal of biological chemistry,* **265** (32), 19937-19941.

Sinensky M, Fantle K, Trujillo M, McLain T, Kupfer A and Dalton M (1994) The processing pathway of prelamin A. *Journal of cell science,* **107** (Pt 1), 61-67.

Sjakste N, Sjakste T and Vikmanis U (2004) Role of the nuclear matrix proteins in malignant transformation and cancer diagnosis. *Experimental oncology,* **26** (3), 170-178.

Smith HC and Berezney R (1983) Dynamic domains of DNA polymerase alpha in regenerating rat liver. *Biochemistry,* **22** (13), 3042-3046.

Smith HC and Berezney R (1982) Nuclear matrix-bound deoxyribonucleic acid synthesis: an in vitro system. *Biochemistry,* **21** (26), 6751-6761.

Smith HC and Berezney R (1980) DNA polymerase alpha is tightly bound to the nuclear matrix of actively replicating liver. *Biochemical and biophysical research communications,* **97** (4), 1541-1547.

Smythe C, Jenkins HE and Hutchison CJ (2000) Incorporation of the nuclear pore basket protein nup153 into nuclear pore structures is dependent upon lamina assembly: evidence from cell-free extracts of Xenopus eggs. *The EMBO journal,* **19** (15), 3918-3931.

Solovei I, Kreysing M, Lanctot C, Kosem S, Peichl L, Cremer T, Guck J and Joffe B (2009) Nuclear architecture of rod photoreceptor cells adapts to vision in mammalian evolution. *Cell,* **137** (2), 356-368.

Solovei I, Schermelleh L, During K, Engelhardt A, Stein S, Cremer C and Cremer T (2004) Differences in centromere positioning of cycling and postmitotic human cell types. *Chromosoma,* **112** (8), 410-423.

Somech R, Shaklai S, Geller O, Amariglio N, Simon AJ, Rechavi G and Gal-Yam EN (2005) The nuclear-envelope protein and transcriptional repressor LAP2beta interacts with HDAC3 at the nuclear periphery, and induces histone H4 deacetylation. *Journal of cell science,* **118** (Pt 17), 4017-4025.

Song K, Dube MP, Lim J, Hwang I, Lee I and Kim JJ (2007) Lamin A/C mutations associated with familial and sporadic cases of dilated cardiomyopathy in Koreans. *Experimental & molecular medicine,* **39** (1), 114-120.

Soullam B and Worman HJ (1995) Signals and structural features involved in integral membrane protein targeting to the inner nuclear membrane. *The Journal of cell biology,* **130** (1), 15-27.

Spann TP, Goldman AE, Wang C, Huang S and Goldman RD (2002) Alteration of nuclear lamin organization inhibits RNA polymerase II-dependent transcription. *The Journal of cell biology,* **156** (4), 603-608.

Speckman RA, Garg A, Du F, Bennett L, Veile R, Arioglu E, Taylor SI, Lovett M and Bowcock AM (2000) Mutational and haplotype analyses of families with familial partial lipodystrophy (Dunnigan variety) reveal recurrent missense mutations in the globular C-terminal domain of lamin A/C. *American Journal of Human Genetics,* **66** (4), 1192-1198.

Squarzoni S, Sabatelli P, Ognibene A, Toniolo D, Cartegni L, Cobianchi F, Petrini S, Merlini L and Maraldi NM (1998) Immunocytochemical detection of emerin within the nuclear matrix. *Neuromuscular disorders: NMD,* **8** (5), 338-344.

Stacey DW (2003) Cyclin D1 serves as a cell cycle regulatory switch in actively proliferating cells. *Current opinion in cell biology,* **15** (2), 158-163.

Stewart SA and Weinberg RA (2006) Telomeres: cancer to human aging. *Annual Review of Cell and Developmental Biology,* **22,** 531-557.

Stick R (1988) cDNA cloning of the developmentally regulated lamin LIII of Xenopus laevis. *The EMBO journal,* **7** (10), 3189-3197.

Stick R and Hausen P (1985) Changes in the nuclear lamina composition during early development of Xenopus laevis. *Cell,* **41** (1), 191-200.

Stierle V, Couprie J, Ostlund C, Krimm I, Zinn-Justin S, Hossenlopp P, Worman HJ, Courvalin JC and Duband-Goulet I (2003) The carboxyl-terminal region common to lamins A and C contains a DNA binding domain. *Biochemistry,* **42** (17), 4819-4828.

Stoffler D, Feja B, Fahrenkrog B, Walz J, Typke D and Aebi U (2003) Cryo-electron tomography provides novel insights into nuclear pore architecture: implications for nucleocytoplasmic transport. *Journal of Molecular Biology,* **328** (1), 119-130.

Strelkov SV, Schumacher J, Burkhard P, Aebi U and Herrmann H (2004) Crystal structure of the human lamin A coil 2B dimer: implications for the head-to-tail association of nuclear lamins. *Journal of Molecular Biology,* **343** (4), 1067-1080.

Sullivan GJ, Bridger JM, Cuthbert AP, Newbold RF, Bickmore WA and McStay B (2001) Human acrocentric chromosomes with transcriptionally silent nucleolar organizer regions associate with nucleoli. *The EMBO journal,* **20** (11), 2867-2874.

Sullivan T, Escalante-Alcalde D, Bhatt H, Anver M, Bhat N, Nagashima K, Stewart CL and Burke B (1999) Loss of A-type lamin expression compromises nuclear envelope integrity leading to muscular dystrophy. *The Journal of cell biology,* **147** (5), 913-920.

Sun HB, Shen J and Yokota H (2000) Size-dependent positioning of human chromosomes in interphase nuclei. *Biophysical journal,* **79** (1), 184-190.

Sun S, Xu MZ, Poon RT, Day PJ and Luk JM (2010) Circulating Lamin B1 (LMNB1) biomarker detects early stages of liver cancer in patients. *Journal of proteome research,* **9** (1), 70-78.

Suzuki T, Michishita E, Ogino H, Fujii M and Ayusawa D (2002) Synergistic induction of the senescence-associated genes by 5-bromodeoxyuridine and AT-binding ligands in HeLa cells. *Experimental cell research,* **276** (2), 174-184.

Suzuki T, Minagawa S, Michishita E, Ogino H, Fujii M, Mitsui Y and Ayusawa D (2001) Induction of senescence-associated genes by 5-bromodeoxyuridine in HeLa cells. *Experimental gerontology,* **36** (3), 465-474.

Szczerbal I, Foster HA and Bridger JM (2009) The spatial repositioning of adipogenesis genes is correlated with their expression status in a porcine mesenchymal stem cell adipogenesis model system. *Chromosoma,* **118** (5), 647-663.

Takahashi E, Hori T, O'Connell P, Leppert M and White R (1991) Mapping of the MYC gene to band 8q24.12----q24.13 by R-banding and distal to fra(8)(q24.11), FRA8E, by fluorescence in situ hybridization. *Cytogenetics and cell genetics,* **57** (2-3), 109-111.

Takata H, Nishijima H, Ogura S, Sakaguchi T, Bubulya PA, Mochizuki T and Shibahara K (2009) Proteome analysis of human nuclear insoluble fractions. *Genes to cells : devoted to molecular & cellular mechanisms,* **14** (8), 975-990.

Takizawa T, Gudla PR, Guo L, Lockett S and Misteli T (2008) Allele-specific nuclear positioning of the monoallelically expressed astrocyte marker GFAP. *Genes & development,* **22** (4), 489-498.

Tanabe H, Habermann FA, Solovei I, Cremer M and Cremer T (2002) Non-random radial arrangements of interphase chromosome territories: evolutionary considerations and functional implications. *Mutation research,* **504** (1-2), 37-45.

Tanabe H, Muller S, Neusser M, von Hase J, Calcagno E, Cremer M, Solovei I, Cremer C and Cremer T (2002) Evolutionary conservation of chromosome territory arrangements in cell nuclei from higher primates. *Proceedings of the National Academy of Sciences of the United States of America,* **99** (7), 4424-4429.

Tang CW, Maya-Mendoza A, Martin C, Zeng K, Chen S, Feret D, Wilson SA and Jackson DA (2008) The integrity of a lamin-B1-dependent nucleoskeleton is a fundamental determinant of RNA synthesis in human cells. *Journal of cell science,* **121** (Pt 7), 1014-1024.

Tang K, Finley RL,Jr, Nie D and Honn KV (2000) Identification of 12-lipoxygenase interaction with cellular proteins by yeast two-hybrid screening. *Biochemistry,* **39** (12), 3185-3191.

Taniura H, Glass C and Gerace L (1995) A chromatin binding site in the tail domain of nuclear lamins that interacts with core histones. *The Journal of cell biology,* **131** (1), 33-44.

Taub R, Kirsch I, Morton C, Lenoir G, Swan D, Tronick S, Aaronson S and Leder P (1982) Translocation of the c-myc gene into the immunoglobulin heavy chain locus in human Burkitt lymphoma and murine plasmacytoma cells. *Proceedings of the National Academy of Sciences of the United States of America,* **79** (24), 7837-7841.

Taylor MR, Slavov D, Gajewski A, Vlcek S, Ku L, Fain PR, Carniel E, Di Lenarda A, Sinagra G, Boucek MM, Cavanaugh J, Graw SL, Ruegg P, Feiger J, Zhu X, Ferguson DA, Bristow MR, Gotzmann J, Foisner R, Mestroni L and Familial Cardiomyopathy Registry Research Group (2005) Thymopoietin (lamina-associated polypeptide 2) gene mutation associated with dilated cardiomyopathy. *Human mutation,* **26** (6), 566-574.

Telenius H, Carter NP, Bebb CE, Nordenskjold M, Ponder BA and Tunnacliffe A (1992) Degenerate oligonucleotide-primed PCR: general amplification of target DNA by a single degenerate primer. *Genomics,* **13** (3), 718-725.

The EMD mutations database (2007). Available at: http://www.umd.be/EMD/. Last accessed: 5th November 2010.

Thisted M, Just T, Pluzek K-J, Hyldig-Nielsen J-J, Nielsen KV, Mollerup TA, Stender H, Rasmussen OF, Adelhorst K and Godtfredsen SE (1999) Application of peptide nucleic acid probes for in situ hybridization. In: P.E. Nielsen and M. Egholm, Editors, *Peptide Nucleic Acids: Protocols and Application*, Horizon Scientific Press, Wymondham, UK, pp. 99–117 (Chap. 3.2).

Thompson M, Haeusler RA, Good PD and Engelke DR (2003) Nucleolar clustering of dispersed tRNA genes. *Science (New York, N.Y.),* **302** (5649), 1399-1401.

Tocharoentanaphol C, Cremer M, Schrock E, Blonden L, Kilian K, Cremer T and Ried T (1994) Multicolor fluorescence in situ hybridization on metaphase chromosomes and interphase Halo-preparations using cosmid and YAC clones for the simultaneous high resolution mapping of deletions in the dystrophin gene. *Human genetics,* **93** (3), 229-235.

Toth JI, Yang SH, Qiao X, Beigneux AP, Gelb MH, Moulson CL, Miner JH, Young SG and Fong LG (2005) Blocking protein farnesyltransferase improves nuclear shape in fibroblasts from humans with progeroid syndromes. *Proceedings of the*

National Academy of Sciences of the United States of America, **102** (36), 12873-12878.

Tsukahara T, Tsujino S and Arahata K (2002) CDNA microarray analysis of gene expression in fibroblasts of patients with X-linked Emery-Dreifuss muscular dystrophy. *Muscle & nerve,* **25** (6), 898-901.

Tubo RA and Berezney R (1987a) Identification of 100 and 150 S DNA polymerase alpha-primase megacomplexes solubilized from the nuclear matrix of regenerating rat liver. *The Journal of biological chemistry,* **262** (12), 5857-5865.

Tubo RA and Berezney R (1987b) Nuclear matrix-bound DNA primase. Elucidation of an RNA priming system in nuclear matrix isolated from regenerating rat liver. *The Journal of biological chemistry,* **262** (14), 6637-6642.

Tubo RA and Berezney R (1987c) Pre-replicative association of multiple replicative enzyme activities with the nuclear matrix during rat liver regeneration. *The Journal of biological chemistry,* **262** (3), 1148-1154.

Tyner SD, Venkatachalam S, Choi J, Jones S, Ghebranious N, Igelmann H, Lu X, Soron G, Cooper B, Brayton C, Hee Park S, Thompson T, Karsenty G, Bradley A and Donehower LA (2002) P53 Mutant Mice that Display Early Ageing-Associated Phenotypes. *Nature,* **415** (6867), 45-53.

Ura S, Hayashi YK, Goto K, Astejada MN, Murakami T, Nagato M, Ohta S, Daimon Y, Takekawa H, Hirata K, Nonaka I, Noguchi S and Nishino I (2007) Limb-girdle muscular dystrophy due to emerin gene mutations. *Archives of Neurology,* **64** (7), 1038-1041.

van de Wetering M, Sancho E, Verweij C, de Lau W, Oving I, Hurlstone A, van der Horn K, Batlle E, Coudreuse D, Haramis AP, Tjon-Pon-Fong M, Moerer P, van den Born M, Soete G, Pals S, Eilers M, Medema R and Clevers H (2002) The beta-catenin/TCF-4 complex imposes a crypt progenitor phenotype on colorectal cancer cells. *Cell,* **111** (2), 241-250.

van der Kooi AJ, Barth PG, Busch HF, de Haan R, Ginjaar HB, van Essen AJ, van Hooff LJ, Howeler CJ, Jennekens FG, Jongen P, Oosterhuis HJ, Padberg GW, Spaans F, Wintzen AR, Wokke JH, Bakker E, van Ommen GJ, Bolhuis PA and de Visser M (1996) The clinical spectrum of limb girdle muscular dystrophy. A survey in The Netherlands. *Brain : a journal of neurology,* **119** (Pt 5), 1471-1480.

van Engelen BG, Muchir A, Hutchison CJ, van der Kooi AJ, Bonne G and Lammens M (2005) The lethal phenotype of a homozygous nonsense mutation in the lamin A/C gene. *Neurology,* **64** (2), 374-376.

van Riggelen J, Yetil A and Felsher DW (2010) MYC as a regulator of ribosome biogenesis and protein synthesis. *Nature reviews. Cancer,* **10** (4), 301-309.

van Steensel B, van Haarst AD, de Kloet ER and van Driel R (1991) Binding of corticosteroid receptors to rat hippocampus nuclear matrix. *FEBS letters,* **292** (1-2), 229-231.

Varela I, Cadinanos J, Pendas AM, Gutierrez-Fernandez A, Folgueras AR, Sanchez LM, Zhou Z, Rodriguez FJ, Stewart CL, Vega JA, Tryggvason K, Freije JM and Lopez-Otin C (2005) Accelerated ageing in mice deficient in Zmpste24 protease is linked to p53 signalling activation. *Nature,* **437** (7058), 564-568.

Varela I, Pereira S, Ugalde AP, Navarro CL, Suarez MF, Cau P, Cadinanos J, Osorio FG, Foray N, Cobo J, de Carlos F, Levy N, Freije JM and Lopez-Otin C (2008) Combined treatment with statins and aminobisphosphonates extends longevity in a mouse model of human premature aging. *Nature medicine,* **14** (7), 767-772.

Vaughan A, Alvarez-Reyes M, Bridger JM, Broers JL, Ramaekers FC, Wehnert M, Morris GE, Whitfield WGF and Hutchison CJ (2001) Both emerin and lamin C depend on lamin A for localization at the nuclear envelope. *Journal of cell science,* **114** (Pt 14), 2577-2590.

Vaughn JP, Dijkwel PA, Mullenders LH and Hamlin JL (1990) Replication forks are associated with the nuclear matrix. *Nucleic acids research,* **18** (8), 1965-1969.

Venables RS, McLean S, Luny D, Moteleb E, Morley S, Quinlan RA, Lane EB and Hutchison CJ (2001) Expression of individual lamins in basal cell carcinomas of the skin. *British journal of cancer,* **84** (4), 512-519.

Verloes A, Mulliez N, Gonzales M, Laloux F, Hermanns-Le T, Pierard GE and Koulischer L (1992) Restrictive dermopathy, a lethal form of arthrogryposis multiplex with skin and bone dysplasias: three new cases and review of the literature. *American Journal of Medical Genetics,* **43** (3), 539-547.

Versteeg R, van Schaik BD, van Batenburg MF, Roos M, Monajemi R, Caron H, Bussemaker HJ and van Kampen AH (2003) The human transcriptome map reveals extremes in gene density, intron length, GC content, and repeat pattern for domains of highly and weakly expressed genes. *Genome research,* **13** (9), 1998-2004.

Verstraeten VL, Ji JY, Cummings KS, Lee RT and Lammerding J (2008) Increased mechanosensitivity and nuclear stiffness in Hutchinson-Gilford progeria cells: effects of farnesyltransferase inhibitors. *Aging cell,* **7** (3), 383-393.

Vishwanatha JK, Jindal HK and Davis RG (1992) The role of primer recognition proteins in DNA replication: association with nuclear matrix in HeLa cells. *Journal of cell science,* **101** (Pt 1), 25-34.

Visser AE and Aten JA (1999) Chromosomes as well as chromosomal subdomains constitute distinct units in interphase nuclei. *Journal of cell science,* **112** (Pt 19), 3353-3360.

Visser AE, Jaunin F, Fakan S and Aten JA (2000) High resolution analysis of interphase chromosome domains. *Journal of cell science,* **113** (Pt 14), 2585-2593.

Vlcek S, Just H, Dechat T and Foisner R (1999) Functional diversity of LAP2alpha and LAP2beta in postmitotic chromosome association is caused by an alpha-specific nuclear targeting domain. *The EMBO journal,* **18** (22), 6370-6384.

Vogelstein B, Pardoll DM and Coffey DS (1980) Supercoiled loops and eucaryotic DNA replicaton. *Cell,* **22** (1 Pt 1), 79-85.

Volpi EV and Bridger JM (2008) FISH glossary: an overview of the fluorescence in situ hybridization technique. *BioTechniques,* **45** (4), 385-6, 388, 390 passim.

Volpi EV, Chevret E, Jones T, Vatcheva R, Williamson J, Beck S, Campbell RD, Goldsworthy M, Powis SH, Ragoussis J, Trowsdale J and Sheer D (2000) Large-scale chromatin organization of the major histocompatibility complex and other regions of human chromosome 6 and its response to interferon in interphase nuclei. *Journal of cell science,* **113** (Pt 9), 1565-1576.

Wagner N, Weber D, Seitz S and Krohne G (2004) The lamin B receptor of Drosophila melanogaster. *Journal of cell science,* **117** (Pt 10), 2015-2028.

Wallis CV, Sheerin AN, Green MH, Jones CJ, Kipling D and Faragher RG (2004) Fibroblast clones from patients with Hutchinson-Gilford progeria can senesce despite the presence of telomerase. *Experimental gerontology,* **39** (4), 461-467.

Wan KM, Nickerson JA, Krockmalnic G and Penman S (1999) The nuclear matrix prepared by amine modification. *Proceedings of the National Academy of Sciences of the United States of America,* **96** (3), 933-938.

Wansink DG, Schul W, van der Kraan I, van Steensel B, van Driel R and de Jong L (1993) Fluorescent labeling of nascent RNA reveals transcription by RNA polymerase II in domains scattered throughout the nucleus. *The Journal of cell biology,* **122** (2), 283-293.

Waterham HR, Koster J, Mooyer P, Noort Gv G, Kelley RI, Wilcox WR, Wanders RJ, Hennekam RC and Oosterwijk JC (2003) Autosomal recessive HEM/Greenberg skeletal dysplasia is caused by 3 beta-hydroxysterol delta 14-reductase deficiency due to mutations in the lamin B receptor gene. *American Journal of Human Genetics,* **72** (4), 1013-1017.

Weipoltshammer K, Schofer C, Almeder M, Philimonenko VV, Frei K, Wachtler F and Hozak P (1999) Intranuclear anchoring of repetitive DNA sequences: centromeres, telomeres, and ribosomal DNA. *The Journal of cell biology,* **147** (7), 1409-1418.

Weissman IL, Anderson DJ and Gage F (2001) Stem and progenitor cells: origins, phenotypes, lineage commitments, and transdifferentiations. *Annual Review of Cell and Developmental Biology,* **17,** 387-403.

Wheeler MA, Davies JD, Zhang Q, Emerson LJ, Hunt J, Shanahan CM and Ellis JA (2007) Distinct functional domains in nesprin-1alpha and nesprin-2beta bind directly to emerin and both interactions are disrupted in X-linked Emery-Dreifuss muscular dystrophy. *Experimental cell research,* **313** (13), 2845-2857.

Wheeler MA, Warley A, Roberts RG, Ehler E and Ellis JA (2010) Identification of an emerin-beta-catenin complex in the heart important for intercalated disc architecture and beta-catenin localisation. *Cellular and molecular life sciences : CMLS,* **67** (5), 781-796.

Wiech T, Stein S, Lachenmaier V, Schmitt E, Schwarz-Finsterle J, Wiech E, Hildenbrand G, Werner M and Hausmann M (2009) Spatial allelic imbalance of BCL2 genes and chromosome 18 territories in nonneoplastic and neoplastic cervical squamous epithelium. *European biophysics journal: EBJ,* **38** (6), 793-806.

Wiegant J, Kalle W, Mullenders L, Brookes S, Hoovers JM, Dauwerse JG, van Ommen GJ and Raap AK (1992) High-resolution in situ hybridization using DNA halo preparations. *Human molecular genetics,* **1** (8), 587-591.

Wilkinson FL, Holaska JM, Zhang Z, Sharma A, Manilal S, Holt I, Stamm S, Wilson KL and Morris GE (2003) Emerin interacts in vitro with the splicing-associated factor, YT521-B. *European journal of biochemistry / FEBS,* **270** (11), 2459-2466.

Williams RR, Azuara V, Perry P, Sauer S, Dvorkina M, Jorgensen H, Roix J, McQueen P, Misteli T, Merkenschlager M and Fisher AG (2006) Neural induction promotes large-scale chromatin reorganisation of the Mash1 locus. *Journal of cell science,* **119** (Pt 1), 132-140.

Willis ND, Cox TR, Rahman-Casans SF, Smits K, Przyborski SA, van den Brandt P, van Engeland M, Weijenberg M, Wilson RG, de Bruine A and Hutchison CJ (2008) Lamin A/C is a risk biomarker in colorectal cancer. *PloS one,* **3** (8), e2988.

Wilson KL (2000) The nuclear envelope, muscular dystrophy and gene expression. *Trends in cell biology,* **10** (4), 125-129.

Wilson KL and Foisner R (2010) Lamin-binding Proteins. *Cold Spring Harbor perspectives in biology,* **2** (4), a000554.

Witt DR, Hayden MR, Holbrook KA, Dale BA, Baldwin VJ and Taylor GP (1986) Restrictive dermopathy: a newly recognized autosomal recessive skin dysplasia. *American Journal of Medical Genetics,* **24** (4), 631-648.

Wolff N, Gilquin B, Courchay K, Callebaut I, Worman HJ and Zinn-Justin S (2001) Structural analysis of emerin, an inner nuclear membrane protein mutated in X-linked Emery-Dreifuss muscular dystrophy. *FEBS letters,* **501** (2-3), 171-176.

Worman HJ and Bonne G (2007) "Laminopathies": a wide spectrum of human diseases. *Experimental cell research,* **313** (10), 2121-2133.

Worman HJ, Yuan J, Blobel G and Georgatos SD (1988) A lamin B receptor in the nuclear envelope. *Proceedings of the National Academy of Sciences of the United States of America,* **85** (22), 8531-8534.

Woynarowski JM, Trevino AV, Rodriguez KA, Hardies SC and Benham CJ (2001) AT-rich islands in genomic DNA as a novel target for AT-specific DNA-reactive antitumor drugs. *The Journal of biological chemistry,* **276** (44), 40555-40566.

Wright WE, Tesmer VM, Huffman KE, Levene SD and Shay JW (1997) Normal human chromosomes have long G-rich telomeric overhangs at one end. *Genes & development,* **11** (21), 2801-2809.

Wulff K, Parrish JE, Herrmann FH and Wehnert M (1997) Six novel mutations in the emerin gene causing X-linked Emery-Dreifuss muscular dystrophy. *Human mutation,* **9** (6), 526-530.

Wuyts W, Biervliet M, Reyniers E, D'Apice MR, Novelli G and Storm K (2005) Somatic and gonadal mosaicism in Hutchinson-Gilford progeria. *American journal of medical genetics. Part A,* **135** (1), 66-68.

Xu M and Cook PR (2008) Similar active genes cluster in specialized transcription factories. *The Journal of cell biology,* **181** (4), 615-623.

Yamasaki L and Pagano M (2004) Cell cycle, proteolysis and cancer. *Current opinion in cell biology,* **16** (6), 623-628.

Yang K, Hitomi M and Stacey DW (2006) Variations in cyclin D1 levels through the cell cycle determine the proliferative fate of a cell. *Cell division,* 132.

Yang SH, Bergo MO, Toth JI, Qiao X, Hu Y, Sandoval S, Meta M, Bendale P, Gelb MH, Young SG and Fong LG (2005) Blocking protein farnesyltransferase improves nuclear blebbing in mouse fibroblasts with a targeted Hutchinson-Gilford progeria syndrome mutation. *Proceedings of the National Academy of Sciences of the United States of America,* **102** (29), 10291-10296.

Yang SH, Qiao X, Fong LG and Young SG (2008) Treatment with a farnesyltransferase inhibitor improves survival in mice with a Hutchinson-Gilford progeria syndrome mutation. *Biochimica et biophysica acta,* **1781** (1-2), 36-39.

Yaron Y, Kramer JA, Gyi K, Ebrahim SA, Evans MI, Johnson MP and Krawetz SA (1998) Centromere sequences localize to the nuclear halo of human spermatozoa. *International journal of andrology,* **21** (1), 13-18.

Yates JR, Bagshaw J, Aksmanovic VM, Coomber E, McMahon R, Whittaker JL, Morrison PJ, Kendrick-Jones J and Ellis JA (1999) Genotype-phenotype analysis in X-linked Emery-Dreifuss muscular dystrophy and identification of a missense mutation associated with a milder phenotype. *Neuromuscular disorders : NMD,* **9** (3), 159-165.

Ye Q, Callebaut I, Pezhman A, Courvalin JC and Worman HJ (1997) Domain-specific interactions of human HP1-type chromodomain proteins and inner nuclear membrane protein LBR. *The Journal of biological chemistry,* **272** (23), 14983-14989.

Ye Q and Worman HJ (1996) Interaction between an integral protein of the nuclear envelope inner membrane and human chromodomain proteins homologous to Drosophila HP1. *The Journal of biological chemistry,* **271** (25), 14653-14656.

Ye Q and Worman HJ (1994) Primary structure analysis and lamin B and DNA binding of human LBR, an integral protein of the nuclear envelope inner membrane. *The Journal of biological chemistry,* **269** (15), 11306-11311.

Young LW, Radebaugh JF, Rubin P, Sensenbrenner JA, Fiorelli G and McKusick VA (1971) New syndrome manifested by mandibular hypoplasia, acroosteolysis, stiff joints and cutaneous atrophy (mandibuloacral dysplasia) in two unrelated boys. *Birth defects original article series,* **7** (7), 291-297.

Young SG, Meta M, Yang SH and Fong LG (2006) Prelamin A farnesylation and progeroid syndromes. *The Journal of biological chemistry,* **281** (52), 39741-39745.

Yu CE, Oshima J, Fu YH, Wijsman EM, Hisama F, Alisch R, Matthews S, Nakura J, Miki T, Ouais S, Martin GM, Mulligan J and Schellenberg GD (1996) Positional cloning of the Werner's syndrome gene. *Science (New York, N.Y.),* **272** (5259), 258-262.

Yusufzai TMandFelsenfeld G (2004) The 5'-HS4 chicken beta-globin insulator is a CTCF-dependent nuclear matrix-associated element. *Proceedings of the National Academy of Sciences of the United States of America,* **101** (23), 8620-8624.

Zakian VA (1995) Telomeres: beginning to understand the end. *Science (New York, N.Y.),* **270** (5242), 1601-1607.

Zeitlin S, Parent A, Silverstein S and Efstratiadis A (1987) Pre-mRNA splicing and the nuclear matrix. *Molecular and cellular biology,* **7** (1), 111-120.

Zeitlin S, Wilson RC and Efstratiadis A (1989) Autonomous splicing and complementation of in vivo-assembled spliceosomes. *The Journal of cell biology,* **108** (3), 765-777.

Zeng C, He D and Brinkley BR (1994) Localization of NuMA protein isoforms in the nuclear matrix of mammalian cells. *Cell motility and the cytoskeleton,* **29** (2), 167-176.

Zhang Q, Bethmann C, Worth NF, Davies JD, Wasner C, Feuer A, Ragnauth CD, Yi Q, Mellad JA, Warren DT, Wheeler MA, Ellis JA, Skepper JN, Vorgerd M, Schlotter-Weigel B, Weissberg PL, Roberts RG, Wehnert M and Shanahan CM (2007) Nesprin-1 and -2 are involved in the pathogenesis of Emery Dreifuss muscular

dystrophy and are critical for nuclear envelope integrity. *Human molecular genetics,* **16** (23), 2816-2833.

Zink D, Amaral MD, Englmann A, Lang S, Clarke LA, Rudolph C, Alt F, Luther K, Braz C, Sadoni N, Rosenecker J and Schindelhauer D (2004) Transcription-dependent spatial arrangements of CFTR and adjacent genes in human cell nuclei. *The Journal of cell biology,* **166** (6), 815-825.

Zink D, Bornfleth H, Visser A, Cremer C and Cremer T (1999) Organization of early and late replicating DNA in human chromosome territories. *Experimental cell research,* **247** (1), 176-188.

Zink D, Cremer T, Saffrich R, Fischer R, Trendelenburg MF, Ansorge W and Stelzer EH (1998) Structure and dynamics of human interphase chromosome territories in vivo. *Human genetics,* **102** (2), 241-251.

Zirbel RM, Mathieu UR, Kurz A, Cremer T and Lichter P (1993) Evidence for a nuclear compartment of transcription and splicing located at chromosome domain boundaries. *Chromosome research : an international journal on the molecular, supramolecular and evolutionary aspects of chromosome biology,* **1** (2), 93-106.

Appendix

Appendix I

Key to sequencing data

Forward primer

Reverse primer

Successfully sequenced: BLAST matched

Discrepancy

Database discrepancy

Mutation

>.....<:denotes exon

ED5364: *EMD*

1. Exon 1

a. Forward sequence (BLAST)

>ref|NM_000117.2| Homo sapiens emerin (EMD), mRNA
Length=1370

GENE ID: 2010 EMD | emerin [Homo sapiens] (Over 10 PubMed links)

Score = 398 bits (215), Expect = 2e-108
Identities = 222/225 (98%), Gaps = 2/225 (0%)
Strand=Plus/Plus

```
Query  6    CGAC-ACGATTCGGCTGTGA-GCGAGCGCGGCCGCTCCCGATGCGCTCGTGCCGCCCCCG  63
            ||||  ||||||||||||||  |||||||||||||||||||||||||||||||||||||
Sbjct  107  CGACAACGATTCGGCTGTGACGCGAGCGCGGCCGCTCCCGATGCGCTCGTGCCGCCCCCG  166

Query  64   CCGTGCTCCTCGGCAGCCGTTGCTCGGCCGGTTTTGGTAGGCCCGGGCCGCCGCCAGGCC  123
            ||||||||||||||||||||||||||||||||||||||||||||||||||||||||||||
Sbjct  167  CCGTGCTCCTCGGCAGCCGTTGCTCGGCCGGTTTTGGTAGGCCCGGGCCGCCGCCAGGCC  226

Query  124  CCCGCCTGAGCCCGCACCCGCCATGGACAACTACGCAGATCTTTCGGATACCGAGCTGAC  183
             ||||||||||||||||||||||||||||||||||||||||||||||||||||||||||||
Sbjct  227  TCCGCCTGAGCCCGCACCCGCCATGGACAACTACGCAGATCTTTCGGATACCGAGCTGAC  286

Query  184  CACCTTGCTGCGCCGGTACAACATCCCGCACGGGCCTGTAGTAGG  228
            |||||||||||||||||||||||||||||||||||||||||||||
Sbjct  287  CACCTTGCTGCGCCGGTACAACATCCCGCACGGGCCTGTAGTAGG  331
```

b. Forward sequence (vs. X86810.1)

```
601 CGGCTGCTCCCGCGGTTAGGTCCCGCCCCGCGCAGCGCGCGCAGCCTGCGGAGCCAGCGG

661 CCGTGACGCGACAACGATTCGGCTGTGACGCGACAACGATTCGGCTGTGACGCGAGCGCG

721 GCCGCTCCCGATGCGCTCGTGCCGCCCCCGCCGTGCTCCTCGGCAGCCGTTGCTCGGCCG
     >.....

781 GTTTTGGTAGGCCCGGGCCGCCGCCAGGCCTCCGCCTGAGCCCGCACCCGCCATGGACAA
    .....

841 CTACGCAGATCTTTCGGATACCGAGCTGACCACCTTGCTGCGCCGGTACAACATCCCGCA
    .....

901 CGGGCCTGTAGTAGGTACGCGGCGGCGGGCGGGACCCCTTCCGGGCCCCCTCCTCGTGCT
    ..................<

961 CCGCCTCGCGACCTCCCCGCTGCCCTCCCCGCGCGCCTTCCCCGGCCCGCGGCCCTGACC
```

c. Reverse sequence (BLAST)

>ref|NM_000117.2| Homo sapiens emerin (EMD), mRNA
Length=1370

GENE ID: 2010 EMD | emerin [Homo sapiens] (Over 10 PubMed links)

Score = 462 bits (250), Expect = 6e-128
Identities = 254/256 (99%), Gaps = 0/256 (0%)
Strand=Plus/Minus

```
Query  33   CCTACTACAGGCCCGTGCGGGATGTTGTACCGGCGCAGCAAGGTGGTCAGCTCGGTATCC  92
            ||||||||||||||||||||||||||||||||||||||||||||||||||||||||||||
Sbjct  331  CCTACTACAGGCCCGTGCGGGATGTTGTACCGGCGCAGCAAGGTGGTCAGCTCGGTATCC  272

Query  93   GAAAGATCTGCGTAGTTGTCCATGGCGGGTGCGGGCTCAGGCGGAGGCCTGGCGGCGGCC  152
            ||||||||||||||||||||||||||||||||||||||||||||||||||||||||||||
Sbjct  271  GAAAGATCTGCGTAGTTGTCCATGGCGGGTGCGGGCTCAGGCGGAGGCCTGGCGGCGGCC  212

Query  153  CGGGCCTACCAAAACCGGCCGAGCAACGGCTGCCGAGGAGCACGGCGGGGGCGGCACGAG  212
            ||||||||||||||||||||||||||||||||||||||||||||||||||||||||||||
Sbjct  211  CGGGCCTACCAAAACCGGCCGAGCAACGGCTGCCGAGGAGCACGGCGGGGGCGGCACGAG  152

Query  213  CGCATCGGGAGCGGCCGCGCTCGCGTCACAGCCGAATCGTTGTCGCGTCACAGCCGAAAC  272
            |||||||||||||||||||||||||||||||||||||||||||||||||||||||||| |
Sbjct  151  CGCATCGGGAGCGGCCGCGCTCGCGTCACAGCCGAATCGTTGTCGCGTCACAGCCGAATC  92

Query  273  GTTGTCGCGTCCCGGC  288
            |||||||||||| ||||
Sbjct  91   GTTGTCGCGTCACGGC  76
```

d. Reverse sequence (vs. X86810.1)

```
601 CGGCTGCTCCCGCGGTTAGGTCCCGCCCCGCGCAGCGCGCGCAGCCTGCGGAGCCAGCGG

661 CCGTGACGCGACAACGATTCGGCTGTGACGCGACAACGATTCGGCTGTGACGCGAGCGCG

721 GCCGCTCCCGATGCGCTCGTGCCGCCCCCGCCGTGCTCCTCGGCAGCCGTTGCTCGGCCG
    >.....

781 GTTTTGGTAGGCCCGGGCCGCCGCCAGGCCTCCGCCTGAGCCCGCACCCGCCATGGACAA
    ....................................................................

841 CTACGCAGATCTTTCGGATACCGAGCTGACCACCTTGCTGCGCCGGTACAACATCCCGCA
    ....................................................................

901 CGGGCCTGTAGTAGGTACGCGGCGGCGGGCGGGACCCCTTCCGGGCCCCCTCCTCGTGCT
    ..................<

961 CCGCCTCGCGACCTCCCCGCTGCCCTCCCCGCGCGCCTTCCCCGGCCCGCGGCCCTGACC
```

e. Combined sequencing (forward and reverse sequences)

```
  601 CGGCTGCTCCCGCGGTTAGGTCCCGCCCCGCGCAGCGCGCGCAGCCTGCGGAGCCAGCGG

  661 CCGTGACGCGACAACGATTCGGCTGTGACGCGACAACGATTCGGCTGTGACGCGAGCGCG

  721 GCCGCTCCCGATGCGCTCGTGCCGCCCCCGCCGTGCTCCTCGGCAGCCGTTGCTCGGCCG
      >.....

  781 GTTTTGGTAGGCCCGGGCCGCCGCCAGGCCTCCGCCTGAGCCCGCACCCGCCATGGACAA
      .....

  841 CTACGCAGATCTTTCGGATACCGAGCTGACCACCTTGCTGCGCCGGTACAACATCCCGCA
      .....

  901 CGGGCCTGTAGTAGGTACGCGGCGGCGGGCGGGACCCCTTCCGGGCCCCCTCCTCGTGCT
      .....<

  961 CCGCCTCGCGACCTCCCCGCTGCCCTCCCCGCGCGCCTTCCCCGGCCCGCGGCCCTGACC
```

2. Exon 2

a. Forward sequence (BLAST)

```
>  ref|NM_000117.2|  Homo sapiens emerin (EMD), mRNA
Length=1370

 GENE ID: 2010 EMD | emerin [Homo sapiens] (Over 10 PubMed links)


 Score =  198 bits (107),  Expect = 1e-48
 Identities = 107/107 (100%), Gaps = 0/107 (0%)
 Strand=Plus/Plus

Query  35   AGGATCAACTCGTAGGCTTTACGAGAAGAAGATCTTCGAGTACGAGACCCAGAGGCGGCG  94
            ||||||||||||||||||||||||||||||||||||||||||||||||||||||||||||
Sbjct  329  AGGATCAACTCGTAGGCTTTACGAGAAGAAGATCTTCGAGTACGAGACCCAGAGGCGGCG  388

Query  95   GCTCTCGCCCCCCAGCTCGTCCGCCGCCTCCTCTTATAGCTTCTCTG  141
            |||||||||||||||||||||||||||||||||||||||||||||||
Sbjct  389  GCTCTCGCCCCCCAGCTCGTCCGCCGCCTCCTCTTATAGCTTCTCTG  435
```

b. Forward sequence (vs. X86810.1)

```
  961 CCGCCTCGCGACCTCCCCGCTGCCCTCCCCGCGCGCCTTCCCCGGCCCGCGGCCCTGACC

 1021 GCCCCGTGTCCGGCCAGGATCAACTCGTAGGCTTTACGAGAAGAAGATCTTCGAGTACGA
                      >.....
```

```
1081 GACCCAGAGGCGGCGGCTCTCGCCCCCCAGCTCGTCCGCCGCCTCCTCTTATAGCTTCTC
     ..................................................................

1141 TGGTGAGAGCCTCGCCTGTGGGGACAGCCTGGGACGCGGGGAGGATGGGGTCGCGAGGGT
     ...<

1201 GTGGCAGGGGGGCCGGTCGAGAGCGGCACTGGAGAAAGGGGAGGGAAGTCTGGGGGGGCA
```

c. Reverse sequence (BLAST)

```
>  ref|NM_000117.2|  Homo sapiens emerin (EMD), mRNA
Length=1370

 GENE ID: 2010 EMD | emerin [Homo sapiens] (Over 10 PubMed links)


 Score =  198 bits (107),  Expect = 1e-48
 Identities = 107/107 (100%), Gaps = 0/107 (0%)
 Strand=Plus/Minus

Query  48   CAGAGAAGCTATAAGAGGAGGCGGCGGACGAGCTGGGGGGCGAGAGCCGCCGCCTCTGGG  107
            ||||||||||||||||||||||||||||||||||||||||||||||||||||||||||||
Sbjct  435  CAGAGAAGCTATAAGAGGAGGCGGCGGACGAGCTGGGGGGCGAGAGCCGCCGCCTCTGGG  376

Query  108  TCTCGTACTCGAAGATCTTCTTCTCGTAAAGCCTACGAGTTGATCCT  154
            |||||||||||||||||||||||||||||||||||||||||||||
Sbjct  375  TCTCGTACTCGAAGATCTTCTTCTCGTAAAGCCTACGAGTTGATCCT  329
```

d. Reverse sequence (vs. X86810.1)

```
 961 CCGCCTCGCGACCTCCCCGCTGCCCTCCCCGCGCGCCTTCCCCGGCCCGCGGCCCTGACC


1021 GCCCCGTGTCCGGCCAGGATCAACTCGTAGGCTTTACGAGAAGAAGATCTTCGAGTACGA
                     >..........................................................

1081 GACCCAGAGGCGGCGGCTCTCGCCCCCCAGCTCGTCCGCCGCCTCCTCTTATAGCTTCTC
     ..................................................................

1141 TGGTGAGAGCCTCGCCTGTGGGGACAGCCTGGGACGCGGGGAGGATGGGGTCGCGAGGGT
     ...<

1201 GTGGCAGGGGGGCCGGTCGAGAGCGGCACTGGAGAAAGGGGAGGGAAGTCTGGGGGGGCA
```

e. Combined sequencing (forward and reverse sequences)

```
 961 CCGCCTCGCGACCTCCCCGCTGCCCTCCCCGCGCGCCTTCCCCGGCCCGCGGCCCTGACC

1021 GCCCCGTGTCCGGCCAGGATCAACTCGTAGGCTTTACGAGAAGAAGATCTTCGAGTACGA
                     >.....

1081 GACCCAGAGGCGGCGGCTCTCGCCCCCCAGCTCGTCCGCCGCCTCCTCTTATAGCTTCTC
     .....

1141 TGGTGAGAGCCTCGCCTGTGGGGACAGCCTGGGACGCGGGGAGGATGGGGTCGCGAGGGT
     ...<

1201  GTGGCAGGGGGGCCGGTCGAGAGCGGCACTGGAGAAAGGGGAGGGAAGTCTGGGGGGGCA
```

3. Exon 3

a. Forward sequence (BLAST)

> ref|NM_000117.2| Homo sapiens emerin (EMD), mRNA
Length=1370

GENE ID: 2010 EMD | emerin [Homo sapiens] (Over 10 PubMed links)

```
 Score =  148 bits (80),  Expect = 2e-33
 Identities = 80/80 (100%), Gaps = 0/80 (0%)
 Strand=Plus/Plus

Query  49   GACTTGAATTCGACTAGAGGGGATGCAGATATGTATGATCTTCCCAAGAAAGAGGACGCT  108
            ||||||||||||||||||||||||||||||||||||||||||||||||||||||||||||
Sbjct  435  GACTTGAATTCGACTAGAGGGGATGCAGATATGTATGATCTTCCCAAGAAAGAGGACGCT  494

Query  109  TTACTCTACCAGAGCAAGGG  128
            ||||||||||||||||||||
Sbjct  495  TTACTCTACCAGAGCAAGGG  514
```

b. Forward sequence (vs. X86810.1)

```
1201 GTGGCAGGGGGGCCGGTCGAGAGCGGCACTGGAGAAAGGGGAGGGAAGTCTGGGGGGGCA

1261 AACAGTTCTGTCTCCTCCTTTCAATCCAGACTTGAATTCGACTAGAGGGGATGCAGATAT
                                  >.....

1321 GTATGATCTTCCCAAGAAAGAGGACGCTTTACTCTACCAGAGCAAGGGTAAGGCAGGGGT
     .....<
```

1381 TGGGTGGGCACGCTGGCACCTTCACCCGACTTCGTCAGGGACCCCGCTCACAGGGAGGAC

1441 CTGAGACCTCAGTCCCAACCACTCCAGCAGCCTTAGGAGGGAGAAACTGTTACAGGTCCC

c. Reverse sequence (BLAST)

> ref|NM_000117.2| Homo sapiens emerin (EMD), mRNA
Length=1370

GENE ID: 2010 EMD | emerin [Homo sapiens] (Over 10 PubMed links)

Score = 148 bits (80), Expect = 4e-35
Identities = 80/80 (100%), Gaps = 0/80 (0%)
Strand=Plus/Minus

```
Query  55   CCCTTGCTCTGGTAGAGTAAAGCGTCCTCTTTCTTGGGAAGATCATACATATCTGCATCC  114
            ||||||||||||||||||||||||||||||||||||||||||||||||||||||||||||
Sbjct  514  CCCTTGCTCTGGTAGAGTAAAGCGTCCTCTTTCTTGGGAAGATCATACATATCTGCATCC  455

Query  115  CCTCTAGTCGAATTCAAGTC  134
            ||||||||||||||||||||
Sbjct  454  CCTCTAGTCGAATTCAAGTC  435
```

d. Reverse sequence (vs. X86810.1)

1201 GTGGCAGGGGGGCCGGTCGAGAGCGGCACTGGAGAAAGGGGAGGGAAGTCTGGGGGGGCA

1261 AACAGTTCTGTCTCCTCCTTTCAATCCAGACTTGAATTCGACTAGAGGGGATGCAGATAT
>.....

1321 GTATGATCTTCCCAAGAAAGAGGACGCTTTACTCTACCAGAGCAAGGGTAAGGCAGGGGT
.....<

1381 TGGGTGGGCACGCTGGCACCTTCACCCGACTTCGTCAGGGACCCCGCTCACAGGGAGGAC

1441 CTGAGACCTCAGTCCCAACCACTCCAGCAGCCTTAGGAGGGAGAAACTGTTACAGGTCCC

e. Combined sequencing (forward and reverse sequences)

1201 GTGGCAGGGGGGCCGGTCGAGAGCGGCACTGGAGAAAGGGGAGGGAAGTCTGGGGGGGCA

1261 AACAGTTCTGTCTCCTCCTTTCAATCCAGACTTGAATTCGACTAGAGGGGATGCAGATAT
>.....

```
1321 GTATGATCTTCCCAAGAAAGAGGACGCTTTACTCTACCAGAGCAAGGGTAAGGCAGGGGT
     ……….<

1381 TGGGTGGGCACGCTGGCACCTTCACCCGACTTCGTCAGGGACCCCGCTCACAGGGAGGAC


1441  CTGAGACCTCAGTCCCAACCACTCCAGCAGCCTTAGGAGGGAGAAACTGTTACAGGTCCC
```

4. Exon 4

a. Forward sequence 1 (BLAST)

>ref|NM_000117.2| Homo sapiens emerin (EMD), mRNA
Length=1370

GENE ID: 2010 EMD | emerin [Homo sapiens] (Over 10 PubMed links)

Score = 255 bits (138), Expect = 7e-66
Identities = 141/142 (99%), Gaps = 1/142 (0%)
Strand=Plus/Plus

```
Query  22   CAA-GGCTACAATGACGACTACTATGAAGAGAGCTACTTCACCACCAGGACTTATGGGGA  80
            ||| ||||||||||||||||||||||||||||||||||||||||||||||||||||||||
Sbjct  509  CAAGGGCTACAATGACGACTACTATGAAGAGAGCTACTTCACCACCAGGACTTATGGGGA  568

Query  81   GCCCGAGTCTGCCGGCCCGTCCAGGGCTGTCCGCCAGTCAGTGACTTCATTCCCAGATGC  140
            ||||||||||||||||||||||||||||||||||||||||||||||||||||||||||||
Sbjct  569  GCCCGAGTCTGCCGGCCCGTCCAGGGCTGTCCGCCAGTCAGTGACTTCATTCCCAGATGC  628

Query  141  TGACGCTTTCCATCACCAGGTG  162
            ||||||||||||||||||||||
Sbjct  629  TGACGCTTTCCATCACCAGGTG  650
```

b. Forward sequence 1 (vs. X86810.1)

```
1501 GAAATGGGATTCAGATTAGGGCCATCAGGCCAGGCGGGGCACACCGATGCCCCCTCTGCT


1561 ACCGCTGCCCCCCTTCCCAAGGCTACAATGACGACTACTATGAAGAGAGCTACTTCACCA
                          >……

1621 CCAGGACTTATGGGGAGCCCGAGTCTGCCGGCCCGTCCAGGGCTGTCCGCCAGTCAGTGA
     ……

1681 CTTCATTCCCAGATGCTGACGCTTTCCATCACCAGGTGAGCTGGCTGGCAGGCGTCCTGT
     ……<

1741 ACTTGGGTACAACCTAGGGGATCGCGGCTGTGTTTGGATAAATCCAGGGGGGCACTGGGT
```

c. Forward sequence 2 (BLAST)

```
>  ref|NM_000117.2|  Homo sapiens emerin (EMD), mRNA
Length=1370

 GENE ID: 2010 EMD | emerin [Homo sapiens] (Over 10 PubMed links)


 Score =  255 bits (138),  Expect = 5e-66
 Identities = 141/142 (99%), Gaps = 1/142 (0%)
 Strand=Plus/Plus

Query  32   CAA-GGCTACAATGACGACTACTATGAAGAGAGCTACTTCACCACCAGGACTTATGGGGA  90
            ||| ||||||||||||||||||||||||||||||||||||||||||||||||||||||||
Sbjct  509  CAAGGGCTACAATGACGACTACTATGAAGAGAGCTACTTCACCACCAGGACTTATGGGGA  568

Query  91   GCCCGAGTCTGCCGGCCCGTCCAGGGCTGTCCGCCAGTCAGTGACTTCATTCCCAGATGC  150
            ||||||||||||||||||||||||||||||||||||||||||||||||||||||||||||
Sbjct  569  GCCCGAGTCTGCCGGCCCGTCCAGGGCTGTCCGCCAGTCAGTGACTTCATTCCCAGATGC  628

Query  151  TGACGCTTTCCATCACCAGGTG  172
            ||||||||||||||||||||||
Sbjct  629  TGACGCTTTCCATCACCAGGTG  650
```

d. Forward sequence 2 (vs. X86810.1)

```
1501 GAAATGGGATTCAGATTAGGGCCATCAGGCCAGGCGGGGCACACCGATGCCCCCTCTGCT


1561 ACCGCTGCCCCCCTTCCCAAGGCTACAATGACGACTACTATGAAGAGAGCTACTTCACCA
                          >..........................................

1621 CCAGGACTTATGGGGAGCCCGAGTCTGCCGGCCCGTCCAGGGCTGTCCGCCAGTCAGTGA
     ..........................................................................

1681 CTTCATTCCCAGATGCTGACGCTTTCCATCACCAGGTGAGCTGGCTGGCAGGCGTCCTGT
     ..................................................................<

1741 ACTTGGGTACAACCTAGGGGATCGCGGCTGTGTTTGGATAAATCCAGGGGGGCACTGGGT
```

e. Reverse sequence 2 (BLAST)

```
>  ref|NM_000117.2|  Homo sapiens emerin (EMD), mRNA
Length=1370

 GENE ID: 2010 EMD | emerin [Homo sapiens] (Over 10 PubMed links)

 Score =  239 bits (129),  Expect = 8e-61
 Identities = 136/139 (97%), Gaps = 2/139 (1%)
 Strand=Plus/Minus
```

```
Query  27   CTGGTGATGG-AAGCGTCAGCATCTGGGAATGAAGTCACTGACTGGCGGACAGCCCTGGA  85
           |||||||||| ||||||||||||||||||||||||||||||||||||||||||||||||||
Sbjct  647  CTGGTGATGGAAAGCGTCAGCATCTGGGAATGAAGTCACTGACTGGCGGACAGCCCTGGA  588

Query  86   CGGGCCGGCAGACTCGGGCTCCCCCTAAGTCCTGGTGGTGAAGTAGCTCTCTTCATAGTA  145
           |||||||||||||||||||||| ||||||||||||||||||||||||||||||||||||||
Sbjct  587  CGGGCCGGCAGACTCGGGCTCCCCATAAGTCCTGGTGGTGAAGTAGCTCTCTTCATAGTA  528

Query  146  GTCGTCATTGTAGCC-TTG  163
           ||||||||||||||| |||
Sbjct  527  GTCGTCATTGTAGCCCTTG  509
```

f. Reverse sequence 2 (vs. X86810.1)

```
1501 GAAATGGGATTCAGATTAGGGCCATCAGGCCAGGCGGGGCACACCGATGCCCCCTCTGCT

1561 ACCGCTGCCCCCCTTCCCAAGGCTACAATGACGACTACTATGAAGAGAGCTACTTCACCA
                          >..........................................

1621 CCAGGACTTATGGGGAGCCCGAGTCTGCCGGCCCGTCCAGGGCTGTCCGCCAGTCAGTGA
     ..........................................................................

1681 CTTCATTCCCAGATGCTGACGCTTTCCATCACCAGGTGAGCTGGCTGGCAGGCGTCCTGT
     ..................................................<

1741 ACTTGGGTACAACCTAGGGGATCGCGGCTGTGTTTGGATAAATCCAGGGGGGCACTGGGT
```

g. Combined sequencing (forward and reverse sequences)

```
1501 GAAATGGGATTCAGATTAGGGCCATCAGGCCAGGCGGGGCACACCGATGCCCCCTCTGCT

1561 ACCGCTGCCCCCCTTCCCAAGGCTACAATGACGACTACTATGAAGAGAGCTACTTCACCA
                          >..........................................

1621 CCAGGACTTATGGGGAGCCCGAGTCTGCCGGCCCGTCCAGGGCTGTCCGCCAGTCAGTGA
     ..........................................................................

1681 CTTCATTCCCAGATGCTGACGCTTTCCATCACCAGGTGAGCTGGCTGGCAGGCGTCCTGT
     ..................................................<

1741 ACTTGGGTACAACCTAGGGGATCGCGGCTGTGTTTGGATAAATCCAGGGGGGCACTGGGT
```

5. Exon 5

a. Forward sequence (BLAST)

> ref|NM_000117.2| Homo sapiens emerin (EMD), mRNA
Length=1370

GENE ID: 2010 EMD | emerin [Homo sapiens] (Over 10 PubMed links)

Score = 100 bits (54), Expect = 4e-19
Identities = 54/54 (100%), Gaps = 0/54 (0%)
Strand=Plus/Plus

```
Query  85   CAGGTGCATGATGACGATCTTTTGTCTTCTTCTGAAGAGGAGTGCAAGGATAGG  138
            ||||||||||||||||||||||||||||||||||||||||||||||||||||||
Sbjct  645  CAGGTGCATGATGACGATCTTTTGTCTTCTTCTGAAGAGGAGTGCAAGGATAGG  698
```

b. Forward sequence (vs. X86810.1)

```
1921 CACAAGTGGCAAGGCCCCATGGATAAAGGGCTGAACACCCAGAGCCATTCAGGAGGGTGT

1981 GGGTTCCTGGCCTCTAACCAAAGGTCAGAGGGGACTGGCTGGGGAAGTTTGGACTGAGGG

2041 ACATGACAGGGCCATGGTGGCCCTGCCAGCCAGTCCCCTCGCCCTGACTCTCTTCTGCAG

2101 GTGCATGATGACGATCTTTTGTCTTCTTCTGAAGAGGAGTGCAAGGATAGGTGCGTAGTG
     >.....<

2161 GGGGAGCCCAGGGACGGGCTGGTTCTGGGTCCAGGCTCCTGGCCCACTTGCTCCCCTCTT
```

c. Reverse sequence (BLAST)

> ref|NM_000117.2| Homo sapiens emerin (EMD), mRNA
Length=1370

GENE ID: 2010 EMD | emerin [Homo sapiens] (Over 10 PubMed links)

Score = 100 bits (54), Expect = 3e-19
Identities = 54/54 (100%), Gaps = 0/54 (0%)
Strand=Plus/Minus

```
Query  16   CCTATCCTTGCACTCCTCTTCAGAAGAAGACAAAAGATCGTCATCATGCACCTG  69
            ||||||||||||||||||||||||||||||||||||||||||||||||||||||
Sbjct  698  CCTATCCTTGCACTCCTCTTCAGAAGAAGACAAAAGATCGTCATCATGCACCTG  645
```

d. Reverse sequence (vs. X86810.1)

```
1921 CACAAGTGGCAAGGCCCCATGGATAAAGGGCTGAACACCCAGAGCCATTCAGGAGGGTGT

1981 GGGTTCCTGGCCTCTAACCAAAGGTCAGAGGGGACTGGCTGGGGAAGTTTGGACTGAGGG

2041 ACATGACAGGGCCATGGTGGCCCTGCCAGCCAGTCCCCTCGCCCTGACTCTCTTCTGCAG

2101 GTGCATGATGACGATCTTTTGTCTTCTTCTGAAGAGGAGTGCAAGGATAGGTGCGTAGTG
     >.....<

2161 GGGGAGCCCAGGGACGGGCTGGTTCTGGGTCCAGGCTCCTGGCCCACTTGCTCCCCTCTT
```

e. Combined sequencing (forward and reverse sequences)

```
1921 CACAAGTGGCAAGGCCCCATGGATAAAGGGCTGAACACCCAGAGCCATTCAGGAGGGTGT

1981 GGGTTCCTGGCCTCTAACCAAAGGTCAGAGGGGACTGGCTGGGGAAGTTTGGACTGAGGG

2041 ACATGACAGGGCCATGGTGGCCCTGCCAGCCAGTCCCCTCGCCCTGACTCTCTTCTGCAG

2101 GTGCATGATGACGATCTTTTGTCTTCTTCTGAAGAGGAGTGCAAGGATAGGTGCGTAGTG
     >.....<

2161 GGGGAGCCCAGGGACGGGCTGGTTCTGGGTCCAGGCTCCTGGCCCACTTGCTCCCCTCTT
```

AG08466: *EMD*

1. Exon 1

a. Forward sequence (BLAST)

ref|NM_000117.2| Homo sapiens emerin (EMD), mRNA
Length=1370

GENE ID: 2010 EMD | emerin [Homo sapiens] (Over 10 PubMed links)

Score = 401 bits (217), Expect = 9e-110
Identities = 233/240 (97%), Gaps = 3/240 (1%)
Strand=Plus/Plus

```
Query  1    ATTTGGCGGTGA-GCG-CCACGATTTCGGCTGTGACGCGAGCGCGGCCGCTCCCGATGCG  58
            ||| ||| |||| ||| | |||| ||||||||||||||||||||||||||||||||||||
Sbjct  93   ATTCGGCTGTGACGCGACAACGA-TTCGGCTGTGACGCGAGCGCGGCCGCTCCCGATGCG  151

Query  59   CTCGTGCCGCCCCCGCCGTGCTCCTCGGCAGCCGTTGCTCGGCCGGTTTTGGTAGGCCCG  118
            ||||||||||||||||||||||||||||||||||||||||||||||||||||||||||||
Sbjct  152  CTCGTGCCGCCCCCGCCGTGCTCCTCGGCAGCCGTTGCTCGGCCGGTTTTGGTAGGCCCG  211

Query  119  GGCCGCCGCCAGGCCTCCGCCTGAGCCCGCACCCGCCATGGACAACTACGCAAATCTTTC  178
            |||||||||||||||||||||||||||||||||||||||||||||||||| |||||||
Sbjct  212  GGCCGCCGCCAGGCCTCCGCCTGAGCCCGCACCCGCCATGGACAACTACGCAGATCTTTC  271

Query  179  GGATACCGAGCTGACCACCTTGCTGCGCCGGTACAACATCCCGCACGGGCCTGTAGTAGG  238
            ||||||||||||||||||||||||||||||||||||||||||||||||||||||||||||
Sbjct  272  GGATACCGAGCTGACCACCTTGCTGCGCCGGTACAACATCCCGCACGGGCCTGTAGTAGG  331
```

b. Forward sequence (vs. X86810.1)

```
601 CGGCTGCTCCCGCGGTTAGGTCCCGCCCCGCGCAGCGCGCGCAGCCTGCGGAGCCAGCGG

661 CCGTGACGCGACAACGATTCGGCTGTGACGCGACAACGATTCGGCTGTGACGCGAGCGCG

721 GCCGCTCCCGATGCGCTCGTGCCGCCCCCGCCGTGCTCCTCGGCAGCCGTTGCTCGGCCG
      >.....

781 GTTTTGGTAGGCCCGGGCCGCCGCCAGGCCTCCGCCTGAGCCCGCACCCGCCATGGACAA
    .....

841 CTACGCAGATCTTTCGGATACCGAGCTGACCACCTTGCTGCGCCGGTACAACATCCCGCA
    .....

901 CGGGCCTGTAGTAGGTACGCGGCGGCGGGCGGGACCCCTTCCGGGCCCCCTCCTCGTGCT
    .....<

961 CCGCCTCGCGACCTCCCCGCTGCCCTCCCCGCGCGCCTTCCCCGGCCCGCGGCCCTGACC
```

c. Reverse sequence (BLAST)

> ref|NM_000117.2| Homo sapiens emerin (EMD), mRNA
Length=1370

GENE ID: 2010 EMD | emerin [Homo sapiens] (Over 10 PubMed links)

Score = 300 bits (162), Expect = 3e-79
Identities = 186/198 (93%), Gaps = 0/198 (0%)
Strand=Plus/Minus

```
Query  44   CCTACTACAGGCCCGTGCGGGATGTTGTACCGGCGCAGCATGGTGGTCAGCTCGGTATCC  103
            ||||||||||||||||||||||||||||||||||||||| ||||||||||||||||||
Sbjct  331  CCTACTACAGGCCCGTGCGGGATGTTGTACCGGCGCAGCAAGGTGGTCAGCTCGGTATCC  272

Query  104  GAAAGATCTGCGTAGTTGTCCTTGGCGGGTGCGGGCTCAGGCGGAGGCCTGGCGGCGGCC  163
            |||||||||||||||||| ||||||||||||||||||||||||||||||||||||||||
Sbjct  271  GAAAGATCTGCGTAGTTGTCCATGGCGGGTGCGGGCTCAGGCGGAGGCCTGGCGGCGGCC  212

Query  164  CGGGCCTACCAAAACCGGCCGAGCAACGGCTGTTGTGGAGCACGGGGGGGGCTGTACGAG  223
            |||||||||||||||||||||||||||||  | ||||||||| |||||| | |||||
Sbjct  211  CGGGCCTACCAAAACCGGCCGAGCAACGGCTGCCGAGGAGCACGGCGGGGGCGGCACGAG  152

Query  224  TTCATCGGTAGCGGTCGC  241
              |||||| ||||| |||
Sbjct  151  CGCATCGGGAGCGGCCGC  134
```

d. Reverse sequence (vs. X86810.1)

```
601 CGGCTGCTCCCGCGGTTAGGTCCCGCCCCGCGCAGCGCGCGCAGCCTGCGGAGCCAGCGG

661 CCGTGACGCGACAACGATTCGGCTGTGACGCGACAACGATTCGGCTGTGACGCGAGCGCG

721 GCCGCTCCCGATGCGCTCGTGCCGCCCCCGCCGTGCTCCTCGGCAGCCGTTGCTCGGCCG
      >.....

781 GTTTTGGTAGGCCCGGGCCGCCGCCAGGCCTCCGCCTGAGCCCGCACCCGCCATGGACAA
    .....

841 CTACGCAGATCTTTCGGATACCGAGCTGACCACCTTGCTGCGCCGGTACAACATCCCGCA
    .....

901 CGGGCCTGTAGTAGGTACGCGGCGGCGGGCGGGACCCCTTCCGGGCCCCCTCCTCGTGCT
    .....<

961 CCGCCTCGCGACCTCCCCGCTGCCCTCCCCGCGCGCCTTCCCCGGCCCGCGGCCCTGACC
```

e. Combined sequencing (forward and reverse sequences)

```
601 CGGCTGCTCCCGCGGTTAGGTCCCGCCCCGCGCAGCGCGCGCAGCCTGCGGAGCCAGCGG

661 CCGTGACGCGACAACGATTCGGCTGTGACGCGACAACGATTCGGCTGTGACGCGAGCGCG

721 GCCGCTCCCGATGCGCTCGTGCCGCCCCCGCCGTGCTCCTCGGCAGCCGTTGCTCGGCCG
      >.....

781 GTTTTGGTAGGCCCGGGCCGCCGCCAGGCCTCCGCCTGAGCCCGCACCCGCCATGGACAA
    .....
```

```
  841 CTACGCAGATCTTTCGGATACCGAGCTGACCACCTTGCTGCGCCGGTACAACATCCCGCA
      ..................................................................

  901 CGGGCCTGTAGTAGGTACGCGGCGGCGGGCGGGACCCCTTCCGGGCCCCCTCCTCGTGCT
      ..................................<

  961 CCGCCTCGCGACCTCCCCGCTGCCCTCCCCGCGCGCCTTCCCCGGCCCGCGGCCCTGACC
```

2. Exon 2

a. Forward sequence (BLAST)

```
>  ref|NM_000117.2|  Homo sapiens emerin (EMD), mRNA
Length=1370

 GENE ID: 2010 EMD | emerin [Homo sapiens] (Over 10 PubMed links)


 Score =  169 bits (91),  Expect = 9e-40
 Identities = 102/107 (95%), Gaps = 1/107 (0%)
 Strand=Plus/Plus

Query  47   AGGATCAACTCGTAGGCTTTACGAGAAGAAGA-CTTCGAGTACGAGACCCAGAGGCGGCG  105
            ||||||||||||||||||||||||||||||| |||||||||||||||||||||||||||
Sbjct  329  AGGATCAACTCGTAGGCTTTACGAGAAGAAGATCTTCGAGTACGAGACCCAGAGGCGGCG  388

Query  106  GCTCTCGCCCCCTTGCTCGTCCGCCGCCTCCTCTTATTGTTTCTCTG  152
            ||||||||||||  |||||||||||||||||||| | |||||||
Sbjct  389  GCTCTCGCCCCCCAGCTCGTCCGCCGCCTCCTCTTATAGCTTCTCTG  435
```

b. Forward sequence (vs. X86810.1)

```
961 CCGCCTCGCGACCTCCCCGCTGCCCTCCCCGCGCGCCTTCCCCGGCCCGCGGCCCTGACC


 1021 GCCCCGTGTCCGGCCAGGATCAACTCGTAGGCTTTACGAGAAGAAGATCTTCGAGTACGA
                      >..................................................

 1081 GACCCAGAGGCGGCGGCTCTCGCCCCCCAGCTCGTCCGCCGCCTCCTCTTATAGCTTCTC
      ..................................................................

 1141 TGGTGAGAGCCTCGCCTGTGGGGACAGCCTGGGACGCGGGGAGGATGGGGTCGCGAGGGT
      …<

 1201 GTGGCAGGGGGGCCGGTCGAGAGCGGCACTGGAGAAAGGGGAGGGAAGTCTGGGGGGGCA
```

c. Reverse sequence (BLAST)

```
>  ref|NM_000117.2|  Homo sapiens emerin (EMD), mRNA
Length=1370

 GENE ID: 2010 EMD | emerin [Homo sapiens] (Over 10 PubMed links)


 Score =  198 bits (107),  Expect = 9e-49
 Identities = 107/107 (100%), Gaps = 0/107 (0%)
 Strand=Plus/Minus
```

```
Query  60   CAGAGAAGCTATAAGAGGAGGCGGCGGACGAGCTGGGGGGCGAGAGCCGCCGCCTCTGGG  119
            ||||||||||||||||||||||||||||||||||||||||||||||||||||||||||||
Sbjct  435  CAGAGAAGCTATAAGAGGAGGCGGCGGACGAGCTGGGGGGCGAGAGCCGCCGCCTCTGGG  376

Query  120  TCTCGTACTCGAAGATCTTCTTCTCGTAAAGCCTACGAGTTGATCCT  166
             |||||||||||||||||||||||||||||||||||||||||||||
Sbjct  375  TCTCGTACTCGAAGATCTTCTTCTCGTAAAGCCTACGAGTTGATCCT  329
```

d. Reverse sequence (vs. X86810.1)

```
  961 CCGCCTCGCGACCTCCCCGCTGCCCTCCCCGCGCGCCTTCCCCGGCCCGCGGCCCTGACC

 1021 GCCCCGTGTCCGGCCAGGATCAACTCGTAGGCTTTACGAGAAGAAGATCTTCGAGTACGA
                       >.....

 1081 GACCCAGAGGCGGCGGCTCTCGCCCCCCAGCTCGTCCGCCGCCTCCTCTTATAGCTTCTC
      .....

 1141 TGGTGAGAGCCTCGCCTGTGGGGACAGCCTGGGACGCGGGGAGGATGGGGTCGCGAGGGT
      ...<

 1201  GTGGCAGGGGGGCCGGTCGAGAGCGGCACTGGAGAAAGGGGAGGGAAGTCTGGGGGGGCA
```

e. Combined sequencing (forward and reverse sequences)

```
 961 CCGCCTCGCGACCTCCCCGCTGCCCTCCCCGCGCGCCTTCCCCGGCCCGCGGCCCTGACC

1021 GCCCCGTGTCCGGCCAGGATCAACTCGTAGGCTTTACGAGAAGAAGATCTTCGAGTACGA
                       >.....

1081 GACCCAGAGGCGGCGGCTCTCGCCCCCCAGCTCGTCCGCCGCCTCCTCTTATAGCTTCTC
     .....

1141 TGGTGAGAGCCTCGCCTGTGGGGACAGCCTGGGACGCGGGGAGGATGGGGTCGCGAGGGT
     ...<

1201 GTGGCAGGGGGGCCGGTCGAGAGCGGCACTGGAGAAAGGGGAGGGAAGTCTGGGGGGGCA
```

3. Exon 3

4. Exon 4

a. Forward sequence (BLAST)

```
ref|NM_000117.2|  Homo sapiens emerin (EMD), mRNA
Length=1370

 GENE ID: 2010 EMD | emerin [Homo sapiens] (Over 10 PubMed links)


 Score =  255 bits (138),  Expect = 5e-66
 Identities = 141/142 (99%), Gaps = 1/142 (0%)
 Strand=Plus/Plus

Query  32   CAA-GGCTACAATGACGACTACTATGAAGAGAGCTACTTCACCACCAGGACTTATGGGGA  90
            ||| ||||||||||||||||||||||||||||||||||||||||||||||||||||||||
Sbjct  509  CAAGGGCTACAATGACGACTACTATGAAGAGAGCTACTTCACCACCAGGACTTATGGGGA  568
```

```
Query  91   GCCCGAGTCTGCCGGCCCGTCCAGGGCTGTCCGCCAGTCAGTGACTTCATTCCCAGATGC  150
           ||||||||||||||||||||||||||||||||||||||||||||||||||||||||||||
Sbjct  569  GCCCGAGTCTGCCGGCCCGTCCAGGGCTGTCCGCCAGTCAGTGACTTCATTCCCAGATGC  628

Query  151  TGACGCTTTCCATCACCAGGTG  172
           ||||||||||||||||||||||
Sbjct  629  TGACGCTTTCCATCACCAGGTG  650
```

b. Forward sequence (vs. X86810.1)

```
1501 GAAATGGGATTCAGATTAGGGCCATCAGGCCAGGCGGGGCACACCGATGCCCCCTCTGCT

1561 ACCGCTGCCCCCCTTCCCAAGGCTACAATGACGACTACTATGAAGAGAGCTACTTCACCA
                          >.....

1621 CCAGGACTTATGGGGAGCCCGAGTCTGCCGGCCCGTCCAGGGCTGTCCGCCAGTCAGTGA
     .....

1681 CTTCATTCCCAGATGCTGACGCTTTCCATCACCAGGTGAGCTGGCTGGCAGGCGTCCTGT
     .....<

1741 ACTTGGGTACAACCTAGGGGATCGCGGCTGTGTTTGGATAAATCCAGGGGGGCACTGGGT
```

c. Reverse sequence (BLAST)

```
>  ref|NM_000117.2|  Homo sapiens emerin (EMD), mRNA
Length=1370

 GENE ID: 2010 EMD | emerin [Homo sapiens] (Over 10 PubMed links)


 Score =  244 bits (132),  Expect = 1e-62
 Identities = 137/139 (98%), Gaps = 2/139 (1%)
 Strand=Plus/Minus

Query  17   CTGGTGATGG-AAGCGTCAGCATCTGGGAATGAAGTCACTGACTGGCGGACAGCCCTGGA  75
           |||||||||| ||||||||||||||||||||||||||||||||||||||||||||||||||
Sbjct  647  CTGGTGATGGAAAGCGTCAGCATCTGGGAATGAAGTCACTGACTGGCGGACAGCCCTGGA  588

Query  76   CGGGCCGGCAGACTCGGGCTCCCCATAAGTCCTGGTGGTGAAGTAGCTCTCTTCATAGTA  135
           ||||||||||||||||||||||||||||||||||||||||||||||||||||||||||||
Sbjct  587  CGGGCCGGCAGACTCGGGCTCCCCATAAGTCCTGGTGGTGAAGTAGCTCTCTTCATAGTA  528

Query  136  GTCGTCATTGTAGCC-TTG  153
           ||||||||||||||| |||
Sbjct  527  GTCGTCATTGTAGCCCTTG  509
```

d. Reverse sequence (vs. X86810.1)

```
1501 GAAATGGGATTCAGATTAGGGCCATCAGGCCAGGCGGGGCACACCGATGCCCCCTCTGCT

1561 ACCGCTGCCCCCCTTCCCAAGGCTACAATGACGACTACTATGAAGAGAGCTACTTCACCA
                          >.....

1621 CCAGGACTTATGGGGAGCCCGAGTCTGCCGGCCCGTCCAGGGCTGTCCGCCAGTCAGTGA
     .....
```

```
1681 CTTCATTCCCAGATGCTGACGCTTTCCATCACCAGGTGAGCTGGCTGGCAGGCGTCCTGT
     ..........................................................<

   1741 ACTTGGGTACAACCTAGGGGATCGCGGCTGTGTTTGGATAAATCCAGGGGGGCACTGGGT
```

e. Combined sequencing (forward and reverse sequences)

```
1501 GAAATGGGATTCAGATTAGGGCCATCAGGCCAGGCGGGGCACACCGATGCCCCCTCTGCT

1561 ACCGCTGCCCCCCTTCCCAAGGCTACAATGACGACTACTATGAAGAGAGCTACTTCACCA
                          >..........................................

1621 CCAGGACTTATGGGGAGCCCGAGTCTGCCGGCCCGTCCAGGGCTGTCCGCCAGTCAGTGA
     ..........................................................

1681 CTTCATTCCCAGATGCTGACGCTTTCCATCACCAGGTGAGCTGGCTGGCAGGCGTCCTGT
     ..........................................................<

1741 ACTTGGGTACAACCTAGGGGATCGCGGCTGTGTTTGGATAAATCCAGGGGGGCACTGGGT
```

5. Exon 5

a. Forward sequence (BLAST)

> ref|NM_000117.2| Homo sapiens emerin (EMD), mRNA
Length=1370

GENE ID: 2010 EMD | emerin [Homo sapiens] (Over 10 PubMed links)

Score = 100 bits (54), Expect = 2e-19
Identities = 54/54 (100%), Gaps = 0/54 (0%)
Strand=Plus/Plus

```
Query  93   CAGGTGCATGATGACGATCTTTTGTCTTCTTCTGAAGAGGAGTGCAAGGATAGG  146
           ||||||||||||||||||||||||||||||||||||||||||||||||||||||
Sbjct  645  CAGGTGCATGATGACGATCTTTTGTCTTCTTCTGAAGAGGAGTGCAAGGATAGG  698
```

b. Forward sequence (vs. X86810.1)

```
1921 CACAAGTGGCAAGGCCCCATGGATAAAGGGCTGAACACCCAGAGCCATTCAGGAGGGTGT

1981 GGGTTCCTGGCCTCTAACCAAAGGTCAGAGGGGACTGGCTGGGGAAGTTTGGACTGAGGG

2041 ACATGACAGGGCCATGGTGGCCCTGCCAGCCAGTCCCCTCGCCCTGACTCTCTTCTGCAG

2101 GTGCATGATGACGATCTTTTGTCTTCTTCTGAAGAGGAGTGCAAGGATAGGTGCGTAGTG
     >..........................................................<

2161 GGGGAGCCCAGGGACGGGCTGGTTCTGGGTCCAGGCTCCTGGCCCACTTGCTCCCCTCTT
```

c. Reverse sequence (BLAST)

>ref|NM_000117.2| Homo sapiens emerin (EMD), mRNA
Length=1370

GENE ID: 2010 EMD | emerin [Homo sapiens] (Over 10 PubMed links)

Score = 100 bits (54), Expect = 8e-21
Identities = 54/54 (100%), Gaps = 0/54 (0%)
Strand=Plus/Minus

```
Query  25   CCTATCCTTGCACTCCTCTTCAGAAGAAGACAAAAGATCGTCATCATGCACCTG  78
            ||||||||||||||||||||||||||||||||||||||||||||||||||||||
Sbjct  698  CCTATCCTTGCACTCCTCTTCAGAAGAAGACAAAAGATCGTCATCATGCACCTG  645
```

d. Reverse sequence (vs. X86810.1)

```
1921 CACAAGTGGCAAGGCCCCATGGATAAAGGGCTGAACACCCAGAGCCATTCAGGAGGGTGT

1981 GGGTTCCTGGCCTCTAACCAAAGGTCAGAGGGGACTGGCTGGGGAAGTTTGGACTGAGGG

2041 ACATGACAGGGCCATGGTGGCCCTGCCAGCCAGTCCCCTCGCCCTGACTCTCTTCTGCAG

2101 GTGCATGATGACGATCTTTTGTCTTCTTCTGAAGAGGAGTGCAAGGATAGGTGCGTAGTG
     >.....<

2161 GGGGAGCCCAGGGACGGGCTGGTTCTGGGTCCAGGCTCCTGGCCCACTTGCTCCCCTCTT
```

e. Combined sequencing (forward and reverse sequences)

```
1921 CACAAGTGGCAAGGCCCCATGGATAAAGGGCTGAACACCCAGAGCCATTCAGGAGGGTGT

1981 GGGTTCCTGGCCTCTAACCAAAGGTCAGAGGGGACTGGCTGGGGAAGTTTGGACTGAGGG

2041 ACATGACAGGGCCATGGTGGCCCTGCCAGCCAGTCCCCTCGCCCTGACTCTCTTCTGCAG

2101 GTGCATGATGACGATCTTTTGTCTTCTTCTGAAGAGGAGTGCAAGGATAGGTGCGTAGTG
     >.....<

2161 GGGGAGCCCAGGGACGGGCTGGTTCTGGGTCCAGGCTCCTGGCCCACTTGCTCCCCTCTT
```

6. Exon 6

a. Forward sequence 1 (BLAST)

>ref|NM_000117.2| Homo sapiens emerin (EMD), mRNA
Length=1370

GENE ID: 2010 EMD | emerin [Homo sapiens] (Over 10 PubMed links)

```
 Score =  446 bits (241),  Expect = 2e-124
 Identities = 330/373 (88%), Gaps = 5/373 (1%)
 Strand=Plus/Plus

Query  21    ATGTACGGCCTGGA-AGTGCCTACCAGAGCAACACGCACTACCGCCCTG-TTCAATTTTA  78
             |||||||||| ||| ||||||||||||||| |||||||||||||||| ||||   |
Sbjct  708   ATGTACGGCCGGGACAGTGCCTACCAGAGCATCACGCACTACCGCCCTGTTTCAGCCTCC  767

Query  79    AGAAGAGCTCCCAGGACCTGTCCTATTATCCTACTTCCTCCTCCACCTCTCTAATGTCCT  138
             ||  |||||||| ||||||||||||||||||||||||||||||||||| | |||||||
Sbjct  768   AG--GAGCTCCCTGGACCTGTCCTATTATCCTACTTCCTCCTCCACCTCTTTTATGTCCT  825

Query  139   ACTCATCATCTTCCTCTTCATGGCTCACCCGCCGTGCCATCCGGCATGAAAACCGTGCTC  198
              |||||||||||||||||||||||||||||||||||||||||| ||||||||||||||
Sbjct  826   CCTCATCATCTTCCTCTTCATGGCTCACCCGCCGTGCCATCCGGCCTGAAAACCGTGCTC  885

Query  199   CTGGGGCTGGGCTGGGCCAGGATCGCCAGGCCCCTCTCTGGGTCCACCTGCTGCTTTTCC  258
             |||||||||||||||||||||||||||| ||| ||||||| ||| ||||||||||||||
Sbjct  886   CTGGGGCTGGGCTGGGCCAGGATCGCCAGGTCCCGCTCTGGGGCCAGCTGCTGCTTTTCC  945

Query  259   TGGTCTTTGTGATCGTCCTTTTCTTCATTTACCACTTCCTGCAAGCTGAACAAAGCAAAA  318
             |||||||||||||||||| |||||||||||||||| |||| |||||| || ||||
Sbjct  946   TGGTCTTTGTGATCGTCCTCTTCTTCATTTACCACTTCATGCAGGCTGAAGAAGGCAACC  1005

Query  319   CCTTCCAGATGTAGCTATGAGGGTATGAGCTTCACATCAACGTTTTTGGAAAAAATCCTG  378
             ||||| ||| | ||| |||||||| || |||||| | | | || |||||  ||  |||||
Sbjct  1006  CCTTCTAGAGGGAGCCATGAGGGTCTGGGCTTCAGAGCTAGGTCTTTGGGGAAG-TCCTG  1064

Query  379   GCTAACTGCCTTA  391
             ||| |||||||||
Sbjct  1065  GCTGACTGCCTTA  1077
```

b. Forward sequence 1 (vs. X86810.1)

```
2161 GGGGAGCCCAGGGACGGGCTGGTTCTGGGTCCAGGCTCCTGGCCCACTTGCTCCCCTCTT

2221 TTGCCTCAGGGAACGCCCCATGTACGGCCGGGACAGTGCCTACCAGAGCATCACGCACTA

2281 CCGCCCTGTTTCAGCCTCCAGGAGCTCCCTGGACCTGTCCTATTATCCTACTTCCTCCTC

2341 CACCTCTTTTATGTCCTCCTCATCATCTTCCTCTTCATGGCTCACCCGCCGTGCCATCCG

2401 GCCTGAAAACCGTGCTCCTGGGGCTGGGCTGGGCCAGGATCGCCAGGTCCCGCTCTGGGG

2461 CCAGCTGCTGCTTTTCCTGGTCTTTGTGATCGTCCTCTTCTTCATTTACCACTTCATGCA

2521 GGCTGAAGAAGGCAACCCCTTCTAGAGGGAGCCATGAGGGTCTGGGCTTCAGAGCTAGGT

2581 CTTTGGGGAAGTCCTGGCTGACTGCCTTAGCAGTGGGGGTGGGGGTGGGGGCAGGGGCAG
```

c. Forward sequence 2 (BLAST)

>ref|NM_000117.2| Homo sapiens emerin (EMD), mRNA
Length=1370

GENE ID: 2010 EMD | emerin [Homo sapiens] (Over 10 PubMed links)

Score = 678 bits (367), Expect = 0.0
Identities = 372/374 (99%), Gaps = 2/374 (0%)
Strand=Plus/Plus

```
Query  4     CCCATGTACGGCCGGGA-AGTGCCTACCAGAGCATCACGCACTACCGCCCTGTTTCAGCC  62
             ||||||||||||||||| ||||||||||||||||||||||||||||||||||||||||||
Sbjct  705   CCCATGTACGGCCGGGACAGTGCCTACCAGAGCATCACGCACTACCGCCCTGTTTCAGCC  764

Query  63    TCCAGGAGCTCCCTGGACCTGTCCTATTATCCTACTTCCTCCTCCACCTCTTTTATGTCC  122
             ||||||||||||||||||||||||||||||||||||||||||||||||||||||||||||
Sbjct  765   TCCAGGAGCTCCCTGGACCTGTCCTATTATCCTACTTCCTCCTCCACCTCTTTTATGTCC  824

Query  123   TCCTCATCATCTTCCTCTTCATGGCTCACCCGCCGTGCCATCCGGCCTGAAAACCGTGCT  182
             ||||||||||||||||||||||||||||||||||||||||||||||||||||||||||||
Sbjct  825   TCCTCATCATCTTCCTCTTCATGGCTCACCCGCCGTGCCATCCGGCCTGAAAACCGTGCT  884

Query  183   CCTGGGGCTGGGCTGGGCCAGGATCGCCAGGTCCCGCTCTGGGGCCAGCTGCTGCTTTTC  242
             ||||||||||||||||||||||||||||||||||||||||||||||||||||||||||||
Sbjct  885   CCTGGGGCTGGGCTGGGCCAGGATCGCCAGGTCCCGCTCTGGGGCCAGCTGCTGCTTTTC  944

Query  243   CTGGTCTTTGTGATCGTCCTCTTCTTCATTTACCACTTCATGCAGGCTGAAGAAGGCAAC  302
             ||||||||||||||||||||||||||||||||||||||||||||||||||||||||||||
Sbjct  945   CTGGTCTTTGTGATCGTCCTCTTCTTCATTTACCACTTCATGCAGGCTGAAGAAGGCAAC  1004

Query  303   CCCTTCTAGAGGGAGCCATGAGGGTCTGGGCTTCAGAGCTAGGTCTTTGGGGAAGTCCTG  362
             ||||||||||||||||||||||||||||||||||||||||||||||||||||||||||||
Sbjct  1005  CCCTTCTAGAGGGAGCCATGAGGGTCTGGGCTTCAGAGCTAGGTCTTTGGGGAAGTCCTG  1064

Query  363   GCTGA-TGCCTTAG  375
             ||||| ||||||||
Sbjct  1065  GCTGACTGCCTTAG  1078
```

d. Forward sequence 2 (vs. X86810.1)

```
2161 GGGGAGCCCAGGGACGGGCTGGTTCTGGGTCCAGGCTCCTGGCCCACTTGCTCCCCTCTT

2221 TTGCCTCAGGGAACGCCCCATGTACGGCCGGGACAGTGCCTACCAGAGCATCACGCACTA

2281 CCGCCCTGTTTCAGCCTCCAG>GAGCTCCCTGGACCTGTCCTATTATCCTACTTCCTCCTC

2341 CACCTCTTTTATGTCCTCCTCATCATCTTCCTCTTCATGGCTCACCCGCCGTGCCATCCG

2401 GCCTGAAAACCGTGCTCCTGGGGCTGGGCTGGGCCAGGATCGCCAGGTCCCGCTCTGGGG

2461 CCAGCTGCTGCTTTTCCTGGTCTTTGTGATCGTCCTCTTCTTCATTTACCACTTCATGCA

2521 GGCTGAAGAAGGCAACCCCTTCTAGAGGGAGCCATGAGGGTCTGGGCTTCAGAGCTAGGT
```

2581 CTTTGGGGAAGTCCTGGCTGACTGCCTTAGCAGTGGGGGTGGGGGTGGGGGCAGGGGCAG

e. Reverse sequence 1 (BLAST)

> ref|NM_000117.2| Homo sapiens emerin (EMD), mRNA
Length=1370

GENE ID: 2010 EMD | emerin [Homo sapiens] (Over 10 PubMed links)

Score = 377 bits (204), Expect = 1e-102
Identities = 241/259 (93%), Gaps = 2/259 (0%)
Strand=Plus/Minus

```
Query  21    CCAGACCCTCTTGGCTCCCTCTAGAAGGGGTTGCCTTCTTCAGCCTGCATGAAGTGGTAA  80
             |||||||||| ||||||||||||||||||||||||||||||||||||||||||||||||||
Sbjct  1033  CCAGACCCTCATGGCTCCCTCTAGAAGGGGTTGCCTTCTTCAGCCTGCATGAAGTGGTAA  974

Query  81    ATGAAGACGAGGACGATCATTT-GACCAGGAAAAGCTGCAGCTGGCCCCACAGCGGGACC  139
             ||||||| |||||||||||    |||||||||||| |||||||||||| |||||||||
Sbjct  973   ATGAAGAAGAGGACGATCACAAAGACCAGGAAAAGCAGCAGCTGGCCCCAGAGCGGGACC  914

Query  140   TGGCGATCCTGGCCCAGCCCATCCCCATGAGCACGGTTTTCAGGCCTGATGGCACGGCGG  199
             |||||||||||||||||||| ||||| |||||||||||||||| ||||||||||||
Sbjct  913   TGGCGATCCTGGCCCAGCCCAGCCCCAGGAGCACGGTTTTCAGGCCGGATGGCACGGCGG  854

Query  200   GTGAGCCTTGAAGAGGAATATGATGAGGAGGACATATA-GAGGTGGATGAGGAAGTAGGA  258
             ||||||| |||||||||| |||||||||||||||| | |||||||| ||||||||||||
Sbjct  853   GTGAGCCATGAAGAGGAAGATGATGAGGAGGACATAAAAGAGGTGGAGGAGGAAGTAGGA  794

Query  259   TAATATGACAGGTCCTGGG  277
             ||||| ||||||||| |||
Sbjct  793   TAATAGGACAGGTCCAGGG  775
```

f. Reverse sequence 1 (vs. X86810.1)

2161 GGGGAGCCCAGGGACGGGCTGGTTCTGGGTCCAGGCTCCTGGCCCACTTGCTCCCCTCTT

2221 TTGCCTCAGGGAACGCCCCATGTACGGCCGGGACAGTGCCTACCAGAGCATCACGCACTA

2281 CCGCCCTGTTTCAGCCTCCAG>GAGCTCCCTGGACCTGTCCTATTATCCTACTTCCTCCTC

2341 CACCTCTTTTATGTCCTCCTCATCATCTTCCTCTTCATGGCTCACCCGCCGTGCCATCCG

2401 GCCTGAAAACCGTGCTCCTGGGGCTGGGCTGGGCCAGGATCGCCAGGTCCCGCTCTGGGG

2461 CCAGCTGCTGCTTTTCCTGGTCTTTGTGATCGTCCTCTTCTTCATTTACCACTTCATGCA

2521 GGCTGAAGAAGGCAACCCCTTCTAGAGGGAGCCATGAGGGTCTGGGCTTCAGAGCTAGGT

2581 CTTTGGGGAAGTCCTGGCTGACTGCCTTAGCAGTGGGGGTGGGGGTGGGGGCAGGGGCAG

g. Reverse sequence 2 (BLAST)

ref|NM_000117.2| Homo sapiens emerin (EMD), mRNA
Length=1370

GENE ID: 2010 EMD | emerin [Homo sapiens] (Over 10 PubMed links)

Score = 623 bits (337), Expect = 4e-176
Identities = 337/337 (100%), Gaps = 0/337 (0%)
Strand=Plus/Minus

```
Query  8     CAGACCCTCATGGCTCCCTCTAGAAGGGGTTGCCTTCTTCAGCCTGCATGAAGTGGTAAA  67
             ||||||||||||||||||||||||||||||||||||||||||||||||||||||||||||
Sbjct  1032  CAGACCCTCATGGCTCCCTCTAGAAGGGGTTGCCTTCTTCAGCCTGCATGAAGTGGTAAA  973

Query  68    TGAAGAAGAGGACGATCACAAAGACCAGGAAAAGCAGCAGCTGGCCCCAGAGCGGGACCT  127
             ||||||||||||||||||||||||||||||||||||||||||||||||||||||||||||
Sbjct  972   TGAAGAAGAGGACGATCACAAAGACCAGGAAAAGCAGCAGCTGGCCCCAGAGCGGGACCT  913

Query  128   GGCGATCCTGGCCCAGCCCAGCCCCAGGAGCACGGTTTTCAGGCCGGATGGCACGGCGGG  187
             ||||||||||||||||||||||||||||||||||||||||||||||||||||||||||||
Sbjct  912   GGCGATCCTGGCCCAGCCCAGCCCCAGGAGCACGGTTTTCAGGCCGGATGGCACGGCGGG  853

Query  188   TGAGCCATGAAGAGGAAGATGATGAGGAGGACATAAAAGAGGTGGAGGAGGAAGTAGGAT  247
             ||||||||||||||||||||||||||||||||||||||||||||||||||||||||||||
Sbjct  852   TGAGCCATGAAGAGGAAGATGATGAGGAGGACATAAAAGAGGTGGAGGAGGAAGTAGGAT  793

Query  248   AATAGGACAGGTCCAGGGAGCTCCTGGAGGCTGAAACAGGGCGGTAGTGCGTGATGCTCT  307
             ||||||||||||||||||||||||||||||||||||||||||||||||||||||||||||
Sbjct  792   AATAGGACAGGTCCAGGGAGCTCCTGGAGGCTGAAACAGGGCGGTAGTGCGTGATGCTCT  733

Query  308   GGTAGGCACTGTCCCGGCCGTACATGGGGCGTTCCCT  344
             |||||||||||||||||||||||||||||||||||||
Sbjct  732   GGTAGGCACTGTCCCGGCCGTACATGGGGCGTTCCCT  696
```

h. Reverse sequence 2 (vs. X86810.1)

```
2161 GGGGAGCCCAGGGACGGGCTGGTTCTGGGTCCAGGCTCCTGGCCCACTTGCTCCCCTCTT

2221 TTGCCTCAGGGAACGCCCCATGTACGGCCGGGACAGTGCCTACCAGAGCATCACGCACTA

2281 CCGCCCTGTTTCAGCCTCCAG>GAGCTCCCTGGACCTGTCCTATTATCCTACTTCCTCCTC

2341 CACCTCTTTTATGTCCTCCTCATCATCTTCCTCTTCATGGCTCACCCGCCGTGCCATCCG

2401 GCCTGAAAACCGTGCTCCTGGGGCTGGGCTGGGCCAGGATCGCCAGGTCCCGCTCTGGGG

2461 CCAGCTGCTGCTTTTCCTGGTCTTTGTGATCGTCCTCTTCTTCATTTACCACTTCATGCA

2521 GGCTGAAGAAGGCAACCCCTTCTAGAGGGAGCCATGAGGGTCTGGGCTTCAGAGCTAGGT

2581 CTTTGGGGAAGTCCTGGCTGACTGCCTTAGCAGTGGGGGTGGGGGTGGGGGCAGGGGCAG
```

i. Combined sequencing (forward and reverse sequences)

2161 GGGGAGCCCAGGGACGGGCTGGTTCTGGGTCCAGGCTCCTGGCCCACTTGCTCCCCTCTT

2221 TTGCCTCAGGGAACGCCCCATGTACGGCCGGGACAGTGCCTACCAGAGCATCACGCACTA

2281 CCGCCCTGTTTCAGCCTCCAGGAGCTCCCTGGACCTGTCCTATTATCCTACTTCCTCCTC

2341 CACCTCTTTTATGTCCTCCTCATCATCTTCCTCTTCATGGCTCACCCGCCGTGCCATCCG

2401 GCCTGAAAACCGTGCTCCTGGGGCTGGGCTGGGCCAGGATCGCCAGGTCCCGCTCTGGGG

2461 CCAGCTGCTGCTTTTCCTGGTCTTTGTGATCGTCCTCTTCTTCATTTACCACTTCATGCA

2521 GGCTGAAGAAGGCAACCCCTTCTAGAGGGAGCCATGAGGGTCTGGGCTTCAGAGCTAGGT

2581 CTTTGGGGAAGTCCTGGCTGACTGCCTTAGCAGTGGGGGTGGGGGTGGGGGCAGGGGCAG

AG11572: *EMD*

1. Exon 1

a. Forward sequence (BLAST)

>ref|NM_000117.2| Homo sapiens emerin (EMD), mRNA
Length=1370

GENE ID: 2010 EMD | emerin [Homo sapiens] (Over 10 PubMed links)

Score = 161 bits (87), Expect = 1e-37
Identities = 147/176 (83%), Gaps = 4/176 (2%)
Strand=Plus/Plus

```
Query  8    TGCGGCTCGTTGCCGCCCCCGCTGGGAAACAGGGGGAGCCGTTGCTCGGCCGGTTTTGGT  67
            ||| ||||| ||||||||||||  |  |   |   || ||||||||||||||||||||||
Sbjct  148  TGC-GCTCG-TGCCGCCCCCGCCGTG-CTCCTCGGCAGCCGTTGCTCGGCCGGTTTTGGT  204

Query  68   AGGCCCGGATCATAAAACAGGCCTCCGACTGAGCCCGCACTCGCCATGGATAACTACTCA  127
            ||||||||  |      |||||||||| |||||||||||  ||||||||| ||||||  ||
Sbjct  205  AGGCCCGGGCCGCCGC-CAGGCCTCCGCCTGAGCCCGCACCCGCCATGGACAACTACGCA  263

Query  128  CATCTTTCGGATACCGATCTTTCTACCTTGCTGCGCCGGTACAACATCCCCCACGG  183
             ||||||||||||||| ||  | ||||||||||||||||||||||||| |||||
Sbjct  264  GATCTTTCGGATACCGAGCTGACCACCTTGCTGCGCCGGTACAACATCCCGCACGG  319
```

b. Forward sequence (vs. X86810.1)

```
  601 CGGCTGCTCCCGCGGTTAGGTCCCGCCCCGCGCAGCGCGCGCAGCCTGCGGAGCCAGCGG

  661 CCGTGACGCGACAACGATTCGGCTGTGACGCGACAACGATTCGGCTGTGACGCGAGCGCG

  721 GCCGCTCCCGATGCGCTCGTGCCGCCCCCGCCGTGCTCCTCGGCAGCCGTTGCTCGGCCG
        >.....

  781 GTTTTGGTAGGCCCGGGCCGCCGCCAGGCCTCCGCCTGAGCCCGCACCCGCCATGGACAA
      .....

  841 CTACGCAGATCTTTCGGATACCGAGCTGACCACCTTGCTGCGCCGGTACAACATCCCGCA
      .....

  901 CGGGCCTGTAGTAGGTACGCGGCGGCGGGCGGGACCCCTTCCGGGCCCCCTCCTCGTGCT
      ..................................<

  961 CCGCCTCGCGACCTCCCCGCTGCCCTCCCCGCGCGCCTTCCCCGGCCCGCGGCCCTGACC
```

c. Reverse sequence (BLAST)

>ref|NM_000117.2| Homo sapiens emerin (EMD), mRNA
Length=1370

GENE ID: 2010 EMD | emerin [Homo sapiens] (Over 10 PubMed links)

```
 Score =  329 bits (178),  Expect = 4e-88
 Identities = 208/223 (93%), Gaps = 0/223 (0%)
 Strand=Plus/Minus

Query  43   CTACTACAGGCCCGTGCGGGATGTTGTACCGGCGCAAAAAGGTGGGCAGCTCGGTATCCG  102
            |||||||||||||||||||||||||||||||||||  |||||||  ||||||||||||||
Sbjct  330  CTACTACAGGCCCGTGCGGGATGTTGTACCGGCGCAGCAAGGTGGTCAGCTCGGTATCCG  271

Query  103  AAAGATCTGCGTAGTTGTCCATGGCGGGTGCGGGCTCAGGCGGAGGCCTGGCGGCGGCCC  162
            ||||||||||||||||||||||||||||||||||||||||||||||||||||||||||||
Sbjct  270  AAAGATCTGCGTAGTTGTCCATGGCGGGTGCGGGCTCAGGCGGAGGCCTGGCGGCGGCCC  211

Query  163  GGGCCTACCAAAACCGGTCGAGCAACGGCTGCCGAGGAACACGGCGGGGGCGGCACAAGC  222
            |||||||||||||||| |||||||||||||||||| ||||||||||||||| |||
Sbjct  210  GGGCCTACCAAAACCGGCCGAGCAACGGCTGCCGAGGAGCACGGCGGGGGCGGCACGAGC  151

Query  223  GCATCGGTATCGGTCGCTCTCCCTTCACAACCGAATAATTGTC  265
            ||||||| | ||| ||| ||| | ||||| ||||||  |||||
Sbjct  150  GCATCGGGAGCGGCCGCGCTCGCGTCACAGCCGAATCGTTGTC  108
```

d. Reverse sequence (vs. X86810.1)

```
601 CGGCTGCTCCCGCGGTTAGGTCCCGCCCCGCGCAGCGCGCGCAGCCTGCGGAGCCAGCGG

661 CCGTGACGCGACAACGATTCGGCTGTGACGCGACAACGATTCGGCTGTGACGCGAGCGCG

721 GCCGCTCCCGATGCGCTCGTGCCGCCCCCGCCGTGCTCCTCGGCAGCCGTTGCTCGGCCG
      >.....

781 GTTTTGGTAGGCCCGGGCCGCCGCCAGGCCTCCGCCTGAGCCCGCACCCGCCATGGACAA
    .....

841 CTACGCAGATCTTTCGGATACCGAGCTGACCACCTTGCTGCGCCGGTACAACATCCCGCA
    .....

901 CGGGCCTGTAGTAGGTACGCGGCGGCGGGCGGGACCCCTTCCGGGCCCCCTCCTCGTGCT
    ..............................<

961 CCGCCTCGCGACCTCCCCGCTGCCCTCCCCGCGCGCCTTCCCCGGCCCGCGGCCCTGACC
```

e. Combined sequencing (forward and reverse sequences)

```
601 CGGCTGCTCCCGCGGTTAGGTCCCGCCCCGCGCAGCGCGCGCAGCCTGCGGAGCCAGCGG

661 CCGTGACGCGACAACGATTCGGCTGTGACGCGACAACGATTCGGCTGTGACGCGAGCGCG

721 GCCGCTCCCGATGCGCTCGTGCCGCCCCCGCCGTGCTCCTCGGCAGCCGTTGCTCGGCCG
      >.....

781 GTTTTGGTAGGCCCGGGCCGCCGCCAGGCCTCCGCCTGAGCCCGCACCCGCCATGGACAA
    .....

841 CTACGCAGATCTTTCGGATACCGAGCTGACCACCTTGCTGCGCCGGTACAACATCCCGCA
    .....

901 CGGGCCTGTAGTAGGTACGCGGCGGCGGGCGGGACCCCTTCCGGGCCCCCTCCTCGTGCT
    ..............................<
```

961 CCGCCTCGCGACCTCCCCGCTGCCCTCCCCGCGCGCCTTCCCCGGCCCGCGGCCCTGACC

2. Exon 2

a. Forward sequence (BLAST)

> ref|NM_000117.2| Homo sapiens emerin (EMD), mRNA
Length=1370

GENE ID: 2010 EMD | emerin [Homo sapiens] (Over 10 PubMed links)

Score = 106 bits (57), Expect = 8e-21
Identities = 68/73 (93%), Gaps = 2/73 (2%)
Strand=Plus/Plus

```
Query  43   AGGATCAACTCGTAGGCTTTACGAGAAGAAGATCTTCGAGTACGAGACCCATGAGGCGTT  102
            |||||||||||||||||||||||||||||||||||||||||||||||||||| ||||||
Sbjct  329  AGGATCAACTCGTAGGCTTTACGAGAAGAAGATCTTCGAGTACGAGACCCA-GAGGCGGC  387

Query  103  GGCTCT-GACCCC  114
            |||||| | ||||
Sbjct  388  GGCTCTCGCCCCC  400
```

b. Forward sequence (vs. X86810.1)

961 CCGCCTCGCGACCTCCCCGCTGCCCTCCCCGCGCGCCTTCCCCGGCCCGCGGCCCTGACC

1021 GCCCCGTGTCCGGCCAGGATCAACTCGTAGGCTTTACGAGAAGAAGATCTTCGAGTACGA
>.....

1081 GACCCAGAGGCGGCGGCTCTCGCCCCCCAGCTCGTCCGCCGCCTCCTCTTATAGCTTCTC
.....

1141 TGGTGAGAGCCTCGCCTGTGGGGACAGCCTGGGACGCGGGGAGGATGGGGTCGCGAGGGT
…<

1201 GTGGCAGGGGGGCCGGTCGAGAGCGGCACTGGAGAAAGGGGAGGGAAGTCTGGGGGGGCA

c. Reverse sequence (BLAST)

> ref|NM_000117.2| Homo sapiens emerin (EMD), mRNA
Length=1370

GENE ID: 2010 EMD | emerin [Homo sapiens] (Over 10 PubMed links)

Score = 198 bits (107), Expect = 2e-48
Identities = 107/107 (100%), Gaps = 0/107 (0%)
Strand=Plus/Minus

```
Query  59   CAGAGAAGCTATAAGAGGAGGCGGCGGACGAGCTGGGGGGCGAGAGCCGCCGCCTCTGGG  118
            ||||||||||||||||||||||||||||||||||||||||||||||||||||||||||||
Sbjct  435  CAGAGAAGCTATAAGAGGAGGCGGCGGACGAGCTGGGGGGCGAGAGCCGCCGCCTCTGGG  376

Query  119  TCTCGTACTCGAAGATCTTCTTCTCGTAAAGCCTACGAGTTGATCCT  165
            |||||||||||||||||||||||||||||||||||||||||||||||
Sbjct  375  TCTCGTACTCGAAGATCTTCTTCTCGTAAAGCCTACGAGTTGATCCT  329
```

d. Reverse sequence (vs. X86810.1)

```
  961 CCGCCTCGCGACCTCCCCGCTGCCCTCCCCGCGCGCCTTCCCCGGCCCGCGGCCCTGACC

 1021 GCCCCGTGTCCGGCCAGGATCAACTCGTAGGCTTTACGAGAAGAAGATCTTCGAGTACGA
                       >.....

 1081 GACCCAGAGGCGGCGGCTCTCGCCCCCCAGCTCGTCCGCCGCCTCCTCTTATAGCTTCTC
      .....

 1141 TGGTGAGAGCCTCGCCTGTGGGGACAGCCTGGGACGCGGGGAGGATGGGGTCGCGAGGGT
      ...<

 1201 GTGGCAGGGGGGCCGGTCGAGAGCGGCACTGGAGAAAGGGGAGGGAAGTCTGGGGGGGCA
```

e. Combined sequencing (forward and reverse sequences)

```
  961 CCGCCTCGCGACCTCCCCGCTGCCCTCCCCGCGCGCCTTCCCCGGCCCGCGGCCCTGACC

 1021 GCCCCGTGTCCGGCCAGGATCAACTCGTAGGCTTTACGAGAAGAAGATCTTCGAGTACGA
                       >.....

 1081 GACCCAGAGGCGGCGGCTCTCGCCCCCCAGCTCGTCCGCCGCCTCCTCTTATAGCTTCTC
      .....

 1141 TGGTGAGAGCCTCGCCTGTGGGGACAGCCTGGGACGCGGGGAGGATGGGGTCGCGAGGGT
      ...<

 1201 GTGGCAGGGGGGCCGGTCGAGAGCGGCACTGGAGAAAGGGGAGGGAAGTCTGGGGGGGCA
```

3. Exon 3

a. Forward sequence (BLAST)

```
>  ref|NM_000117.2|  Homo sapiens emerin (EMD), mRNA
Length=1370

 GENE ID: 2010 EMD | emerin [Homo sapiens] (Over 10 PubMed links)


 Score =  143 bits (77),  Expect = 4e-32
 Identities = 79/80 (98%), Gaps = 0/80 (0%)
 Strand=Plus/Plus

Query  47   GACTTGAATTCGACTAGAGGGGATGCAGATTTGTATGATCTTCCCAAGAAAGAGGACGCT  106
            |||||||||||||||||||||||||||| ||||||||||||||||||||||||||||||
Sbjct  435  GACTTGAATTCGACTAGAGGGGATGCAGATATGTATGATCTTCCCAAGAAAGAGGACGCT  494

Query  107  TTACTCTACCAGAGCAAGGG  126
            ||||||||||||||||||||
Sbjct  495  TTACTCTACCAGAGCAAGGG  514
```

b. Forward sequence (vs. X86810.1)

```
1201 GTGGCAGGGGGGCCGGTCGAGAGCGGCACTGGAGAAAGGGGAGGGAAGTCTGGGGGGGCA

1261 AACAGTTCTGTCTCCTCCTTTCAATCCAGACTTGAATTCGACTAGAGGGGATGCAGATAT
                                  >..................................

1321 GTATGATCTTCCCAAGAAAGAGGACGCTTTACTCTACCAGAGCAAGGGTAAGGCAGGGGT
     ..................................................................<

1381 TGGGTGGGCACGCTGGCACCTTCACCCGACTTCGTCAGGGACCCCGCTCACAGGGAGGAC

1441 CTGAGACCTCAGTCCCAACCACTCCAGCAGCCTTAGGAGGGAGAAACTGTTACAGGTCCC
```

c. Reverse sequence (BLAST)

ref|NM_000117.2| Homo sapiens emerin (EMD), mRNA
Length=1370

GENE ID: 2010 EMD | emerin [Homo sapiens] (Over 10 PubMed links)

```
 Score =  148 bits (80),  Expect = 8e-34
 Identities = 80/80 (100%), Gaps = 0/80 (0%)
 Strand=Plus/Minus

Query  57   CCCTTGCTCTGGTAGAGTAAAGCGTCCTCTTTCTTGGGAAGATCATACATATCTGCATCC  116
            ||||||||||||||||||||||||||||||||||||||||||||||||||||||||||||
Sbjct  514  CCCTTGCTCTGGTAGAGTAAAGCGTCCTCTTTCTTGGGAAGATCATACATATCTGCATCC  455

Query  117  CCTCTAGTCGAATTCAAGTC  136
            ||||||||||||||||||||
Sbjct  454  CCTCTAGTCGAATTCAAGTC  435
```

d. Reverse sequence (vs. X86810.1)

```
1201 GTGGCAGGGGGGCCGGTCGAGAGCGGCACTGGAGAAAGGGGAGGGAAGTCTGGGGGGGCA

1261 AACAGTTCTGTCTCCTCCTTTCAATCCAGACTTGAATTCGACTAGAGGGGATGCAGATAT
                                  >..................................

1321 GTATGATCTTCCCAAGAAAGAGGACGCTTTACTCTACCAGAGCAAGGGTAAGGCAGGGGT
     ..................................................................<

1381 TGGGTGGGCACGCTGGCACCTTCACCCGACTTCGTCAGGGACCCCGCTCACAGGGAGGAC

1441 CTGAGACCTCAGTCCCAACCACTCCAGCAGCCTTAGGAGGGAGAAACTGTTACAGGTCCC
```

e. Combined sequencing (forward and reverse sequences)

```
1201 GTGGCAGGGGGGCCGGTCGAGAGCGGCACTGGAGAAAGGGGAGGGAAGTCTGGGGGGGCA

1261 AACAGTTCTGTCTCCTCCTTTCAATCCAGACTTGAATTCGACTAGAGGGGATGCAGATAT
                                  >.....

1321 GTATGATCTTCCCAAGAAAGAGGACGCTTTACTCTACCAGAGCAAGGGTAAGGCAGGGGT
     .....<

1381 TGGGTGGGCACGCTGGCACCTTCACCCGACTTCGTCAGGGACCCCGCTCACAGGGAGGAC
1441 CTGAGACCTCAGTCCCAACCACTCCAGCAGCCTTAGGAGGGAGAAACTGTTACAGGTCCC
```

4. Exon 4

a. Forward sequence (BLAST)

```
>  ref|NM_000117.2|  Homo sapiens emerin (EMD), mRNA
Length=1370

 GENE ID: 2010 EMD | emerin [Homo sapiens] (Over 10 PubMed links)


 Score =  141 bits (76),  Expect = 1e-31
 Identities = 122/143 (85%), Gaps = 7/143 (4%)
 Strand=Plus/Plus


Query  36   CAA-GGCTACAATGACGACTACTATGAAGAGAGCTACTTCAAAAAAAAGAAGGGATGGGG  94
            ||| ||||||||||||||||||||||||||||||||||  |  | ||    ||||||
Sbjct  509  CAAGGGCTACAATGACGACTACTATGAAGAGAGCTACTTCACCACCAGGACTT-ATGGGG  567

Query  95   AGCCCGAGTCTGCCGGCCCGTCCAGC-CTTTTGTCCGCCACCCCCCCGACTTCATTCCCA  153
            |||||||||||||||||||||||||  ||   ||||||||  |    ||||||||||||
Sbjct  568  AGCCCGAGTCTGCCGGCCCGTCCAGGGCT---GTCCGCCAGTCAGT-GACTTCATTCCCA  623

Query  154  GATGCTGACGCTTTCCATCACCA  176
            |||||||||||||||||||||||
Sbjct  624  GATGCTGACGCTTTCCATCACCA  646
```

b. Forward sequence (vs. X86810.1)

```
1501 GAAATGGGATTCAGATTAGGGCCATCAGGCCAGGCGGGGCACACCGATGCCCCCTCTGCT

1561 ACCGCTGCCCCCCTTCCCAAGGCTACAATGACGACTACTATGAAGAGAGCTACTTCACCA
                           >.....

1621 CCAGGACTTATGGGGAGCCCGAGTCTGCCGGCCCGTCCAGGGCTGTCCGCCAGTCAGTGA
     .....

1681 CTTCATTCCCAGATGCTGACGCTTTCCATCACCAGGTGAGCTGGCTGGCAGGCGTCCTGT
     .....<

1741 ACTTGGGTACAACCTAGGGGATCGCGGCTGTGTTTGGATAAATCCAGGGGGGCACTGGGT
```

c. Reverse sequence (BLAST)

>ref|NM_000117.2| Homo sapiens emerin (EMD), mRNA
Length=1370

GENE ID: 2010 EMD | emerin [Homo sapiens] (Over 10 PubMed links)

Score = 241 bits (130), Expect = 1e-61
Identities = 138/141 (97%), Gaps = 3/141 (2%)
Strand=Plus/Minus

```
Query  17   ACCTGGTG-TGG-AAGCGTCAGCATCTGGGAATGAAGTCACTGACTGGCGGACAGCCCTG  74
            |||||||| ||| ||||||||||||||||||||||||||||||||||||||||||||||
Sbjct  649  ACCTGGTGATGGAAAGCGTCAGCATCTGGGAATGAAGTCACTGACTGGCGGACAGCCCTG  590

Query  75   GACGGGCCGGCAGACTCGGGCTCCCCATAAGTCCTGGTGGTGAAGTAGCTCTCTTCATAG  134
            ||||||||||||||||||||||||||||||||||||||||||||||||||||||||||||
Sbjct  589  GACGGGCCGGCAGACTCGGGCTCCCCATAAGTCCTGGTGGTGAAGTAGCTCTCTTCATAG  530

Query  135  TAGTCGTCATTGTAGCC-TTG  154
            |||||||||||||||| |||
Sbjct  529  TAGTCGTCATTGTAGCCCTTG  509
```

d. Reverse sequence (vs. X86810.1)

```
1501 GAAATGGGATTCAGATTAGGGCCATCAGGCCAGGCGGGGCACACCGATGCCCCCTCTGCT

1561 ACCGCTGCCCCCCTTCCCAAGGCTACAATGACGACTACTATGAAGAGAGCTACTTCACCA
                          >.....

1621 CCAGGACTTATGGGGAGCCCGAGTCTGCCGGCCCGTCCAGGGCTGTCCGCCAGTCAGTGA
     .....

1681 CTTCATTCCCAGATGCTGACGCTTTCCATCACCAGGTGAGCTGGCTGGCAGGCGTCCTGT
     .....<

1741  ACTTGGGTACAACCTAGGGGATCGCGGCTGTGTTTGGATAAATCCAGGGGGGCACTGGGT
```

e. Combined sequencing (forward and reverse sequences)

```
1501 GAAATGGGATTCAGATTAGGGCCATCAGGCCAGGCGGGGCACACCGATGCCCCCTCTGCT

1561 ACCGCTGCCCCCCTTCCCAAGGCTACAATGACGACTACTATGAAGAGAGCTACTTCACCA
                          >.....

1621 CCAGGACTTATGGGGAGCCCGAGTCTGCCGGCCCGTCCAGGGCTGTCCGCCAGTCAGTGA
     .....

1681 CTTCATTCCCAGATGCTGACGCTTTCCATCACCAGGTGAGCTGGCTGGCAGGCGTCCTGT
     .....<

1740 ACTTGGGTACAACCTAGGGGATCGCGGCTGTGTTTGGATAAATCCAGGGGGGCACTGGGT
```

5. Exon 5

a. Forward sequence (BLAST)

```
>  ref|NM_000117.2|  Homo sapiens emerin (EMD), mRNA
Length=1370

 GENE ID: 2010 EMD | emerin [Homo sapiens] (Over 10 PubMed links)


 Score =  100 bits (54),  Expect = 5e-19
 Identities = 54/54 (100%), Gaps = 0/54 (0%)
 Strand=Plus/Plus

Query  92   CAGGTGCATGATGACGATCTTTTGTCTTCTTCTGAAGAGGAGTGCAAGGATAGG  145
            ||||||||||||||||||||||||||||||||||||||||||||||||||||||
Sbjct  645  CAGGTGCATGATGACGATCTTTTGTCTTCTTCTGAAGAGGAGTGCAAGGATAGG  698
```

b. Forward sequence (vs. X86810.1)

```
1921 CACAAGTGGCAAGGCCCCATGGATAAAGGGCTGAACACCCAGAGCCATTCAGGAGGGTGT

1981 GGGTTCCTGGCCTCTAACCAAAGGTCAGAGGGGACTGGCTGGGGAAGTTTGGACTGAGGG

2041 ACATGACAGGGCCATGGTGGCCCTGCCAGCCAGTCCCCTCGCCCTGACTCTCTTCTGCAG

2101 GTGCATGATGACGATCTTTTGTCTTCTTCTGAAGAGGAGTGCAAGGATAGGTGCGTAGTG
     >.....<

2161 GGGGAGCCCAGGGACGGGCTGGTTCTGGGTCCAGGCTCCTGGCCCACTTGCTCCCCTCTT
```

c. Reverse sequence (BLAST)

```
ref|NT_167198.1|  Homo sapiens chromosome X genomic contig, GRCh37
reference primary
assembly
Length=6178498

 Features in this part of subject sequence:
   emerin


 Score =  292 bits (158),  Expect = 8e-77
 Identities = 177/186 (95%), Gaps = 2/186 (1%)
 Strand=Plus/Minus

Query  14       CACTACGCA-CTATCCTTGCACTCCTCTTCAGAAG-AGACAAAAGATCGTCATCATGCAC  71
                ||||||||| |||||||||||||||||||||||| |||||||||||||||||||||||||
Sbjct  4527110  CACTACGCACCTATCCTTGCACTCCTCTTCAGAAGAAGACAAAAGATCGTCATCATGCAC
4527051

Query  72       CTGCAGAAGAGAGTCAGGGCGAGGGGACTGGCTGGCAGGGCCACCATGGCCCTGTCATGT  131
                ||||||||||||||||||||||||||||||||||||||||||||||||||||||||||||
Sbjct  4527050  CTGCAGAAGAGAGTCAGGGCGAGGGGACTGGCTGGCAGGGCCACCATGGCCCTGTCATGT
4526991

Query  132      CCCTCAGTCCAAACTTCCCCAGCCAGTCCCCTCGGACCTTTGGTTGGAGCCCCCGACCCC  191
                |||||||||||||||||||||||||||||||| |||||||||| ||| ||  || |||
```

```
Sbjct  4526990  CCCTCAGTCCAAACTTCCCCAGCCAGTCCCCTCTGACCTTTGGTTAGAGGCCAGGAACCC
4526931

Query  192      ACTCCC  197
                 || |||
Sbjct  4526930  ACACCC  4526925
```

d. Reverse sequence (vs. X86810.1)

```
1921 CACAAGTGGCAAGGCCCCATGGATAAAGGGCTGAACACCCAGAGCCATTCAGGAGGGTGT

1981 GGGTTCCTGGCCTCTAACCAAAGGTCAGAGGGGACTGGCTGGGGAAGTTTGGACTGAGGG

2041 ACATGACAGGGCCATGGTGGCCCTGCCAGCCAGTCCCCTCGCCCTGACTCTCTTCTGCAG

2101 GTGCATGATGACGATCTTTTGTCTTCTTCTGAAGAGGAGTGCAAGGATAGGTGCGTAGTG
     >.....<

2161 GGGGAGCCCAGGGACGGGCTGGTTCTGGGTCCAGGCTCCTGGCCCACTTGCTCCCCTCTT
```

e. Combined sequencing (forward and reverse sequences)

```
1921 CACAAGTGGCAAGGCCCCATGGATAAAGGGCTGAACACCCAGAGCCATTCAGGAGGGTGT

1981 GGGTTCCTGGCCTCTAACCAAAGGTCAGAGGGGACTGGCTGGGGAAGTTTGGACTGAGGG

2041 ACATGACAGGGCCATGGTGGCCCTGCCAGCCAGTCCCCTCGCCCTGACTCTCTTCTGCAG

2101 GTGCATGATGACGATCTTTTGTCTTCTTCTGAAGAGGAGTGCAAGGATAGGTGCGTAGTG
     >.....<

2161 GGGGAGCCCAGGGACGGGCTGGTTCTGGGTCCAGGCTCCTGGCCCACTTGCTCCCCTCTT
```

AG08466: *LAP2* exon 4

1. Primer pair: LAP2α4.2

a. Forward sequence (BLAST)

ef|NM_003276.1| Homo sapiens thymopoietin (TMPO), transcript variant 1, mRNA
Length=2490

Score = 252 bits (127), Expect = 8e-65
Identities = 127/127 (100%), Gaps = 0/127 (0%)
Strand=Plus/Plus

```
Query  5     AAACATACAGAAGAGAATTGATCAGTCTAAGTTTCAAGAAACTGAATTCCTGTCTCCTCC  64
             ||||||||||||||||||||||||||||||||||||||||||||||||||||||||||||
Sbjct  1422  AAACATACAGAAGAGAATTGATCAGTCTAAGTTTCAAGAAACTGAATTCCTGTCTCCTCC  1481

Query  65    AAGAAAAGTCCCTAGACTGAGTGAGAAGTCAGTGGAGGAAAGGGATTCAGGTTCCTTTGT  124
             ||||||||||||||||||||||||||||||||||||||||||||||||||||||||||||
Sbjct  1482  AAGAAAAGTCCCTAGACTGAGTGAGAAGTCAGTGGAGGAAAGGGATTCAGGTTCCTTTGT  1541

Query  125   GGCATTT  131
             |||||||
Sbjct  1542  GGCATTT  1548
```

b. Forward sequence (vs. NM_003276.1)

```
1321 CTTGCCCAGGCAATCAGAGATTATGTCAATTCTCTGTTGGTCCAGGGTGGGGTAGGTAGT
1381 TTGCCTGGAACTTCTAACTCTATGCCCCCACTGGATGTAGAAAACATACAGAAGAGAATT
1441 GATCAGTCTAAGTTTCAAGAAACTGAATTCCTGTCTCCTCCAAGAAAAGTCCCTAGACTG
1501 AGTGAGAAGTCAGTGGAGGAAAGGGATTCAGGTTCCTTTGTGGCATTTCAGAACATACCT
```

2. Primer pair: LAP2α4.3

a. Forward sequence (BLAST)

> ref|NM_003276.1| Homo sapiens thymopoietin (TMPO), transcript variant 1, mRNA
Length=2490

GENE ID: 7112 TMPO | thymopoietin [Homo sapiens] (Over 10 PubMed links)

Score = 1620 bits (877), Expect = 0.0
Identities = 891/897 (99%), Gaps = 4/897 (0%)
Strand=Plus/Plus

```
Query  5     AAACCTGTTTGTCTCTC-TTC-CTCACTACCTTAGGTCTAGAAGTGGCTAAGCAATCACA  62
             ||| ||| |||||||||| ||| ||||||||||||||||||||||||||||||||||||
Sbjct  1588  AAAACTG-TTGTCTCTCATTCACTCACTACCTTAGGTCTAGAAGTGGCTAAGCAATCACA  1646

Query  63    GCATGATAAAATAGATGCCTCAGAACTATCTTTTCCCTTCCATGAATCTATTTTAAAAGT  122
             ||||||||||||||||||||||||||||||||||||||||||||||||||||||||||||
Sbjct  1647  GCATGATAAAATAGATGCCTCAGAACTATCTTTTCCCTTCCATGAATCTATTTTAAAAGT  1706

Query  123   AATTGAAGAAGAATGGCAGCAAGTTGACAGGCAGCTGCCTTCACTGGCATGCAAATATCC  182
             ||||||||||||||||||||||||||||||||||||||||||||||||||||||||||||
Sbjct  1707  AATTGAAGAAGAATGGCAGCAAGTTGACAGGCAGCTGCCTTCACTGGCATGCAAATATCC  1766
```

```
Query  183   AGTTTCTTCCAGGGAGGCAACACAGATATTATCAGTTCCAAAAGTAGATGATGAAATCCT  242
             ||||||||||||||||||||||||||||||||||||||||||||||||||||||||||||
Sbjct  1767  AGTTTCTTCCAGGGAGGCAACACAGATATTATCAGTTCCAAAAGTAGATGATGAAATCCT  1826

Query  243   AGGGTTTATTTCTGAAGCCACTCCACTAGGAGGTATTCAAGCAGCCTCCACTGAGTCTTG  302
             ||||||||||||||||||||||||||||||||||||||||||||||||||||||||||||
Sbjct  1827  AGGGTTTATTTCTGAAGCCACTCCACTAGGAGGTATTCAAGCAGCCTCCACTGAGTCTTG  1886

Query  303   CAATCAGCAGTTGGACTTAGCACTCTGTAGAGCATATGAAGCTGCAGCATCAGCATTGCA  362
             ||||||||||||||||||||||||||||||||||||||||||||||||||||||||||||
Sbjct  1887  CAATCAGCAGTTGGACTTAGCACTCTGTAGAGCATATGAAGCTGCAGCATCAGCATTGCA  1946

Query  363   GATTGCAACTCACACTGCCTTTGTAGCTAAGGCTATGCAGGCAGACATTAGTCAAGCTGC  422
             ||||||||||||||||||||||||||||||||||||||||||||||||||||||||||||
Sbjct  1947  GATTGCAACTCACACTGCCTTTGTAGCTAAGGCTATGCAGGCAGACATTAGTCAAGCTGC  2006

Query  423   ACAGATTCTTAGCTCAGATCCTAGTCGTACCCACCAAGCGCTTGGGATTCTGAGCAAAAC  482
             ||||||||||||||||||||||||||||||||||||||||||||||||||||||||||||
Sbjct  2007  ACAGATTCTTAGCTCAGATCCTAGTCGTACCCACCAAGCGCTTGGGATTCTGAGCAAAAC  2066

Query  483   ATATGATGCAGCCTCATATATTTGTGAAGCTGCATTTGATGAAGTGAAGATGGCTGCCCA  542
             ||||||||||||||||||||||||||||||||||||||||||||||||||||||||||||
Sbjct  2067  ATATGATGCAGCCTCATATATTTGTGAAGCTGCATTTGATGAAGTGAAGATGGCTGCCCA  2126

Query  543   TACCATGGGAAATGCCACTGTAGGTCGTCGATACCTCTGGCTGAAGGATTGCAAAATTAA  602
             ||||||||||||||||||||||||||||||||||||||||||||||||||||||||||||
Sbjct  2127  TACCATGGGAAATGCCACTGTAGGTCGTCGATACCTCTGGCTGAAGGATTGCAAAATTAA  2186

Query  603   TTTAGCTTCTAAGAATAAGCTGGCTTCCACTCCCTTTAAAGGTGGAACATTATTTGGAGG  662
             ||||||||||||||||||||||||||||||||||||||||||||||||||||||||||||
Sbjct  2187  TTTAGCTTCTAAGAATAAGCTGGCTTCCACTCCCTTTAAAGGTGGAACATTATTTGGAGG  2246

Query  663   AGAAGTATGCAAAGTAATTAAAAAGCGTGGAAATAAACACTAGTAAAATTAAGGACAACA  722
             |||||||||||||||||||||||||||||||||||||||||||||||||||||||||| |
Sbjct  2247  AGAAGTATGCAAAGTAATTAAAAAGCGTGGAAATAAACACTAGTAAAATTAAGGACAAAA  2306

Query  723   AGACATCTATCTTATCTTTCAGGTACTTTATGCCAACATTTTCTTTTCTGTTAAGGTTGT  782
             ||||||||||||||||||||||||||||||||||||||||||||||||||||||||||||
Sbjct  2307  AGACATCTATCTTATCTTTCAGGTACTTTATGCCAACATTTTCTTTTCTGTTAAGGTTGT  2366

Query  783   TTTAGTTTCCAGATAGGGCTAATTACAAAATGTTAAGCTTCTACCCATCAAATTACAGTA  842
             ||||||||||||||||||||||||||||||||||||||||||||||||||||||||||||
Sbjct  2367  TTTAGTTTCCAGATAGGGCTAATTACAAAATGTTAAGCTTCTACCCATCAAATTACAGTA  2426

Query  843   TAAAAGTAATTGCCTGTGTAGAACTACTTGTCTTTTCTAAAGATTTGCGTAG-TAGG  898
             ||||||||||||||||||||||||||||||||||||||||||||||||||| ||||
Sbjct  2427  TAAAAGTAATTGCCTGTGTAGAACTACTTGTCTTTTCTAAAGATTTGCGTAGATAGG  2483
```

b. Forward sequence (vs. NM_003276.1)

```
1501 AGTGAGAAGTCAGTGGAGGAAAGGGATTCAGGTTCCTTTGTGGCATTTCAGAACATACCT
1561 GGATCCGAACTGATGTCTTCTTTTGCCAAAACTGTTGTCTCTCATTCACTCACTACCTTA
1621 GGTCTAGAAGTGGCTAAGCAATCACAGCATGATAAAATAGATGCCTCAGAACTATCTTTT
1681 CCCTTCCATGAATCTATTTTAAAAGTAATTGAAGAAGAATGGCAGCAAGTTGACAGGCAG
1741 CTGCCTTCACTGGCATGCAAATATCCAGTTTCTTCCAGGGAGGCAACACAGATATTATCA
1801 GTTCCAAAAGTAGATGATGAAATCCTAGGGTTTATTTCTGAAGCCACTCCACTAGGAGGT
1861 ATTCAAGCAGCCTCCACTGAGTCTTGCAATCAGCAGTTGGACTTAGCACTCTGTAGAGCA
1921 TATGAAGCTGCAGCATCAGCATTGCAGATTGCAACTCACACTGCCTTTGTAGCTAAGGCT
1981 ATGCAGGCAGACATTAGTCAAGCTGCACAGATTCTTAGCTCAGATCCTAGTCGTACCCAC
2041 CAAGCGCTTGGGATTCTGAGCAAAACATATGATGCAGCCTCATATATTTGTGAAGCTGCA
2101 TTTGATGAAGTGAAGATGGCTGCCCATACCATGGGAAATGCCACTGTAGGTCGTCGATAC
2161 CTCTGGCTGAAGGATTGCAAAATTAATTTAGCTTCTAAGAATAAGCTGGCTTCCACTCCC
2221 TTTAAAGGTGGAACATTATTTGGAGGAGAAGTATGCAAAGTAATTAAAAAGCGTGGAAAT
2281 AAACACTAGTAAAATTAAGGACAAAAAGACATCTATCTTATCTTTCAGGTACTTTATGCC
2341 AACATTTTCTTTTCTGTTAAGGTTGTTTTAGTTTCCAGATAGGGCTAATTACAAAATGTT
2401 AAGCTTCTACCCATCAAATTACAGTATAAAAGTAATTGCCTGTGTAGAACTACTTGTCTT
2461 TTCTAAAGATTTGCGTAGATAGGAAGCCTG
```

c. Reverse sequence (BLAST)

ref|NM_003276.1| Homo sapiens thymopoietin (TMPO), transcript variant 1, mRNA
Length=2490

GENE ID: 7112 TMPO | thymopoietin [Homo sapiens] (Over 10 PubMed links)

Score = 1629 bits (882), Expect = 0.0
Identities = 891/895 (99%), Gaps = 1/895 (0%)
Strand=Plus/Minus

```
Query  6     AAGTAGTGGCTACACAGGCAATTACTTTTATACTGTAATTTGATGGGTAGAAGCTTAACA  65
             |||||||  ||||||||||||||||||||||||||||||||||||||||||||||||||||
Sbjct  2455  AAGTAGT-TCTACACAGGCAATTACTTTTATACTGTAATTTGATGGGTAGAAGCTTAACA  2397

Query  66    TTTTGTAATTAGCCCTATCTGGAAACTAAAACAACCTTAACAGAAAAGAAAATGTTGGCA  125
             ||||||||||||||||||||||||||||||||||||||||||||||||||||||||||||
Sbjct  2396  TTTTGTAATTAGCCCTATCTGGAAACTAAAACAACCTTAACAGAAAAGAAAATGTTGGCA  2337

Query  126   TAAAGTACCTGAAAGATAAGATAGATGTCTTTTTGTCCTTAATTTTACTAGTGTTTATTT  185
             ||||||||||||||||||||||||||||||||||||||||||||||||||||||||||||
Sbjct  2336  TAAAGTACCTGAAAGATAAGATAGATGTCTTTTTGTCCTTAATTTTACTAGTGTTTATTT  2277

Query  186   CCACGCTTTTTAATTACTTTGCATACTTCTCCTCCAAATAATGTTCCACCTTTAAAGGGA  245
             ||||||||||||||||||||||||||||||||||||||||||||||||||||||||||||
Sbjct  2276  CCACGCTTTTTAATTACTTTGCATACTTCTCCTCCAAATAATGTTCCACCTTTAAAGGGA  2217

Query  246   GTGGAAGCCAGCTTATTCTTAGAAGCTAAATTAATTTTGCAATCCTTCAGCCAGAGGTAT  305
             ||||||||||||||||||||||||||||||||||||||||||||||||||||||||||||
Sbjct  2216  GTGGAAGCCAGCTTATTCTTAGAAGCTAAATTAATTTTGCAATCCTTCAGCCAGAGGTAT  2157

Query  306   CGACGACCTACAGTGGCATTTCCCATGGTATGGGCAGCCATCTTCACTTCATCAAATGCA  365
             ||||||||||||||||||||||||||||||||||||||||||||||||||||||||||||
Sbjct  2156  CGACGACCTACAGTGGCATTTCCCATGGTATGGGCAGCCATCTTCACTTCATCAAATGCA  2097

Query  366   GCTTCACAAATATATGAGGCTGCATCATATGTTTTGCTCAGAATCCCAAGCGCTTGGTGG  425
             ||||||||||||||||||||||||||||||||||||||||||||||||||||||||||||
Sbjct  2096  GCTTCACAAATATATGAGGCTGCATCATATGTTTTGCTCAGAATCCCAAGCGCTTGGTGG  2037

Query  426   GTACGACTAGGATCTGAGCTAAGAATCTGTGCAGCTTGACTAATGTCTGCCTGCATAGCC  485
             ||||||||||||||||||||||||||||||||||||||||||||||||||||||||||||
Sbjct  2036  GTACGACTAGGATCTGAGCTAAGAATCTGTGCAGCTTGACTAATGTCTGCCTGCATAGCC  1977

Query  486   TTAGCTACAAAGGCAGTGTGAGTTGCAATCTGCAATGCTGATGCTGCAGCTTCATATGCT  545
             ||||||||||||||||||||||||||||||||||||||||||||||||||||||||||||
Sbjct  1976  TTAGCTACAAAGGCAGTGTGAGTTGCAATCTGCAATGCTGATGCTGCAGCTTCATATGCT  1917

Query  546   CTACAGAGTGCTAAGTCCAACTGCTGATTGCAAGACTCAGTGGAGGCTGCTTGAATACCT  605
             ||||||||||||||||||||||||||||||||||||||||||||||||||||||||||||
Sbjct  1916  CTACAGAGTGCTAAGTCCAACTGCTGATTGCAAGACTCAGTGGAGGCTGCTTGAATACCT  1857

Query  606   CCTAGTGGAGTGGCTTCAGAAATAAACCCTAGGATTTCATCATCTACTTTTGGAACTGAT  665
             ||||||||||||||||||||||||||||||||||||||||||||||||||||||||||||
Sbjct  1856  CCTAGTGGAGTGGCTTCAGAAATAAACCCTAGGATTTCATCATCTACTTTTGGAACTGAT  1797

Query  666   AATATCTGTGTTGCCTCCCTGGAAGAAACTGGATATTTGCATGCCAGTGAAGGCAGCTGC  725
             ||||||||||||||||||||||||||||||||||||||||||||||||||||||||||||
Sbjct  1796  AATATCTGTGTTGCCTCCCTGGAAGAAACTGGATATTTGCATGCCAGTGAAGGCAGCTGC  1737

Query  726   CTGTCAACTTGCTGCCATTCTTCTTCAATTACTTTTAAAATAGATTCATGGAAGGGAAAA  785
             ||||||||||||||||||||||||||||||||||||||||||||||||||||||||||||
Sbjct  1736  CTGTCAACTTGCTGCCATTCTTCTTCAATTACTTTTAAAATAGATTCATGGAAGGGAAAA  1677

Query  786   GATAGTTCTGAGGCATCTATTTTATCATGCTGTGATTGCTTAGCCACTTCTAGACCTAAG  845
             ||||||||||||||||||||||||||||||||||||||||||||||||||||||||||||
Sbjct  1676  GATAGTTCTGAGGCATCTATTTTATCATGCTGTGATTGCTTAGCCACTTCTAGACCTAAG  1617
```

```
Query  846   GTAGTGAGTGAATGAGAGACAACAGTTTTGGCAAAAGAAGACATCAGATCAGATC  900
              ||||||||||||||||||||||||||||||||||||||||||||| || ||||
Sbjct  1616  GTAGTGAGTGAATGAGAGACAACAGTTTTGGCAAAAGAAGACATCAGTTCGGATC  1562
```

d. Reverse sequence (vs. NM_003276.1)

```
1501 AGTGAGAAGTCAGTGGAGGAAAGGGATTCAGGTTCCTTTGTGGCATTTCAGAACATACCT
1561 GGATCCGAACTGATGTCTTCTTTTGCCAAAACTGTTGTCTCTCATTCACTCACTACCTTA
1621 GGTCTAGAAGTGGCTAAGCAATCACAGCATGATAAAATAGATGCCTCAGAACTATCTTTT
1681 CCCTTCCATGAATCTATTTTAAAAGTAATTGAAGAAGAATGGCAGCAAGTTGACAGGCAG
1741 CTGCCTTCACTGGCATGCAAATATCCAGTTTCTTCCAGGGAGGCAACACAGATATTATCA
1801 GTTCCAAAAGTAGATGATGAAATCCTAGGGTTTATTTCTGAAGCCACTCCACTAGGAGGT
1861 ATTCAAGCAGCCTCCACTGAGTCTTGCAATCAGCAGTTGGACTTAGCACTCTGTAGAGCA
1921 TATGAAGCTGCAGCATCAGCATTGCAGATTGCAACTCACACTGCCTTTGTAGCTAAGGCT
1981 ATGCAGGCAGACATTAGTCAAGCTGCACAGATTCTTAGCTCAGATCCTAGTCGTACCCAC
2041 CAAGCGCTTGGGATTCTGAGCAAAACATATGATGCAGCCTCATATATTTGTGAAGCTGCA
2101 TTTGATGAAGTGAAGATGGCTGCCCATACCATGGGAAATGCCACTGTAGGTCGTCGATAC
2161 CTCTGGCTGAAGGATTGCAAAATTAATTTAGCTTCTAAGAATAAGCTGGCTTCCACTCCC
2221 TTTAAAGGTGGAACATTATTTGGAGGAGAAGTATGCAAAGTAATTAAAAAGCGTGGAAAT
2281 AAACACTAGTAAAATTAAGGACAAAAAGACATCTATCTTATCTTTCAGGTACTTTATGCC
2341 AACATTTTCTTTTCTGTTAAGGTTGTTTTAGTTTCCAGATAGGGCTAATTACAAAATGTT
2401 AAGCTTCTACCCATCAAATTACAGTATAAAAGTAATTGCCTGTGTAGAACTACTTGTCTT
2461 TTCTAAAGATTTGCGTAGATAGGAAGCCTG
```

e. Combined sequencing (forward and reverse sequences)

```
1501 AGTGAGAAGTCAGTGGAGGAAAGGGATTCAGGTTCCTTTGTGGCATTTCAGAACATACCT
1561 GGATCCGAACTGATGTCTTCTTTTGCCAAAACTGTTGTCTCTCATTCACTCACTACCTTA
1621 GGTCTAGAAGTGGCTAAGCAATCACAGCATGATAAAATAGATGCCTCAGAACTATCTTTT
1681 CCCTTCCATGAATCTATTTTAAAAGTAATTGAAGAAGAATGGCAGCAAGTTGACAGGCAG
1741 CTGCCTTCACTGGCATGCAAATATCCAGTTTCTTCCAGGGAGGCAACACAGATATTATCA
1801 GTTCCAAAAGTAGATGATGAAATCCTAGGGTTTATTTCTGAAGCCACTCCACTAGGAGGT
1861 ATTCAAGCAGCCTCCACTGAGTCTTGCAATCAGCAGTTGGACTTAGCACTCTGTAGAGCA
1921 TATGAAGCTGCAGCATCAGCATTGCAGATTGCAACTCACACTGCCTTTGTAGCTAAGGCT
1981 ATGCAGGCAGACATTAGTCAAGCTGCACAGATTCTTAGCTCAGATCCTAGTCGTACCCAC
2041 CAAGCGCTTGGGATTCTGAGCAAAACATATGATGCAGCCTCATATATTTGTGAAGCTGCA
2101 TTTGATGAAGTGAAGATGGCTGCCCATACCATGGGAAATGCCACTGTAGGTCGTCGATAC
2161 CTCTGGCTGAAGGATTGCAAAATTAATTTAGCTTCTAAGAATAAGCTGGCTTCCACTCCC
2221 TTTAAAGGTGGAACATTATTTGGAGGAGAAGTATGCAAAGTAATTAAAAAGCGTGGAAAT
2281 AAACACTAGTAAAATTAAGGACAAAAAGACATCTATCTTATCTTTCAGGTACTTTATGCC
2341 AACATTTTCTTTTCTGTTAAGGTTGTTTTAGTTTCCAGATAGGGCTAATTACAAAATGTT
2401 AAGCTTCTACCCATCAAATTACAGTATAAAAGTAATTGCCTGTGTAGAACTACTTGTCTT
2461 TTCTAAAGATTTGCGTAGATAGGAAGCCTG
```

AG11572: *LAP2* exon 4

1. Primer pair: LAP2αintron/exon4

a. Forward sequence (BLAST)

>ref|NT_029419.12| Homo sapiens chromosome 12 genomic contig, GRCh37 reference primary assembly
Length=71516776

Features in this part of subject sequence:
thymopoietin isoform beta
thymopoietin isoform gamma

Score = 1362 bits (737), Expect = 0.0
Identities = 744/747 (99%), Gaps = 2/747 (0%)
Strand=Plus/Plus

```
Query  13        ATATGGAATTATAGTCTTTTCCTTTGACAGCACTATTTTTAGCAAAGAGGCAAAGAATAA  72
                 |||||.|||||||||||||||||||||||||||||||||||||||||||||||||||||
Sbjct  61069793  ATATGAAATTATAGTCTTTTCCTTTGACAGCACTATTTTTAGCAAAGAGGCAAAGAATAA
61069852

Query  73        AATCAGCTCAAACACAGGTAATGCTTAAACTTCCTGCCTCTTTTGCCTCTACAGGAAAGA
132
                 ||||||||||||||||||||||||||||||||||||||||||||||||||||||||||||
Sbjct  61069853  AATCAGCTCAAACACAGGTAATGCTTAAACTTCCTGCCTCTTTTGCCTCTACAGGAAAGA
61069912

Query  133       AGAAAGAACACAAGAAAGTGAAGTCCACTAGGGATATTGTTCCTTTTTCTGAACTTGGAA
192
                 ||||||||||||||||||||||||||||||||||||||||||||||||||||||||||||
Sbjct  61069913  AGAAAGAACACAAGAAAGTGAAGTCCACTAGGGATATTGTTCCTTTTTCTGAACTTGGAA
61069972

Query  193       CTACTCCCTCTGGTGGTGGATTTTTTCAGGGTATTTCTTTTCCTGAAATCTCCACCCGTC
252
                 ||||||||||||||||||||||||||||||||||||||||||||||||||||||||||||
Sbjct  61069973  CTACTCCCTCTGGTGGTGGATTTTTTCAGGGTATTTCTTTTCCTGAAATCTCCACCCGTC
61070032

Query  253       CTCCTTTGGGCAGTACCGAACTACAGGCAGCTAAGAAAGTACATACTTCTAAGGGAGACC
312
                 ||||||||||||||||||||||||||||||||||||||||||||||||||||||||||||
Sbjct  61070033  CTCCTTTGGGCAGTACCGAACTACAGGCAGCTAAGAAAGTACATACTTCTAAGGGAGACC
61070092

Query  313       TACCTAGGGAGCCTCTTGTTGCCACAAACTTGCCTGGCAGGGGACAGTTGCAGAAGTTAG
372
                 ||||||||||||||||||||||||||||||||||||||||||||||||||||||||||||
Sbjct  61070093  TACCTAGGGAGCCTCTTGTTGCCACAAACTTGCCTGGCAGGGGACAGTTGCAGAAGTTAG
61070152

Query  373       CCTCTGAAAGGAATTTGTTTATTTCATGCAAGTCTAGCCATGATAGGTGTTTAGAGAAAA
432
                 ||||||||||||||||||||||||||||||||||||||||||||||||||||||||||||
Sbjct  61070153  CCTCTGAAAGGAATTTGTTTATTTCATGCAAGTCTAGCCATGATAGGTGTTTAGAGAAAA
61070212

Query  433       GTTCTTCGTCATCTTCTCAGCCTGAACACAGTGCCATGTTGGTCTCTACTGCAGCTTCTC
492
                 ||||||||||||||||||||||||||||||||||||||||||||||||||||||||||||
Sbjct  61070213  GTTCTTCGTCATCTTCTCAGCCTGAACACAGTGCCATGTTGGTCTCTACTGCAGCTTCTC
61070272
```

```
Query  493       CTTCACTGATTAAAGAAACCACCACTGGTTACTATAAAGACATAGTAGAAAATATTTGCG
552
                  ||||||||||||||||||||||||||||||||||||||||||||||||||||||||||||
Sbjct  61070273  CTTCACTGATTAAAGAAACCACCACTGGTTACTATAAAGACATAGTAGAAAATATTTGCG
61070332

Query  553       GTAGAGAGAAAAGTGGAATTCAACCATTATGTCCTGAGAGGTCCCATATTTCAGATCAAT
612
                  ||||||||||||||||||||||||||||||||||||||||||||||||||||||||||||
Sbjct  61070333  GTAGAGAGAAAAGTGGAATTCAACCATTATGTCCTGAGAGGTCCCATATTTCAGATCAAT
61070392

Query  613       CGCCTCTCTCCAGTAAAAGGAAAGCACTAGAAGAGTCTGAGAGCTCACAACTAATTTCTC
672
                  ||||||||||||||||||||||||||||||||||||||||||||||||||||||||||||
Sbjct  61070393  CGCCTCTCTCCAGTAAAAGGAAAGCACTAGAAGAGTCTGAGAGCTCACAACTAATTTCTC
61070452

Query  673       CGCCACTTGCCCAGGCAATCAGAGATTATGTCAATTCTCTGTTGGTCCAGGGTGGG-TAG
731
                  |||||||||||||||||||||||||||||||||||||||||||||||||||||| |||
Sbjct  61070453  CGCCACTTGCCCAGGCAATCAGAGATTATGTCAATTCTCTGTTGGTCCAGGGTGGGGTAG
61070512

Query  732       GGTAGTTTGCCTGGAACTTCTAACTCT  758
                  | ||||||||||||||||||||||||
Sbjct  61070513  G-TAGTTTGCCTGGAACTTCTAACTCT  61070538
```

b. Forward sequence (vs. AC013418.32)

```
21901 TCAATTCTCT TCTGTATGTT TTCTACATCC AGTGGGGGCA TAGAGTTAGA AGTTCCAGGC
21961 AAACTACCTA CCCCACCCTG GACCAACAGA GAATTGACAT AATCTCTGAT TGCCTGGGCA
22021 AGTGGCGGAG AAATTAGTTG TGAGCTCTCA GACTCTTCTA GTGCTTTCCT TTTACTGGAG
22081 AGAGGCGATT GATCTGAAAT ATGGGACCTC TCAGGACATA ATGGTTGAAT TCCACTTTTC
22141 TCTCTACCGC AAATATTTTC TACTATGTCT TTATAGTAAC CAGTGGTGGT TTCTTTAATC
22201 AGTGAAGGAG AAGCTGCAGT AGAGACCAAC ATGGCACTGT GTTCAGGCTG AGAAGATGAC
22261 GAAGAACTTT TCTCTAAACA CCTATCATGG CTAGACTTGC ATGAAATAAA CAAATTCCTT
22321 TCAGAGGCTA ACTTCTGCAA CTGTCCCCTG CCAGGCAAGT TTGTGGCAAC AAGAGGCTCC
22381 CTAGGTAGGT CTCCCTTAGA AGTATGTACT TTCTTAGCTG CCTGTAGTTC GGTACTGCCC
22441 AAAGGAGGAC GGGTGGAGAT TTCAGGAAAA GAAATACCCT GAAAAAATCC ACCACCAGAG
22501 GGAGTAGTTC CAAGTTCAGA AAAAGGAACA ATATCCCTAG TGGACTTCAC TTTCTTGTGT
22561 TCTTTCTTCT TTCCTGTAGA GGCAAAAGAG GCAGGAAGTT TAAGCATTAC CTGTGTTTGA
22621 GCTGATTTTA TTCTTTGCCT CTTTGCTAAA AATAGTGCTG TCAAAGGAAA AGACTATAAT
22681 TTCATATTCT GAACTAATCT GCCAGATTTG CCCTGGTAGA CAAAGCTTAT TGAGATATAA
```

c. Reverse sequence (BLAST)

> ref|NT_029419.12| Homo sapiens chromosome 12 genomic contig, GRCh37 reference primary assembly
Length=71516776

Features in this part of subject sequence:
thymopoietin isoform beta
thymopoietin isoform gamma

```
 Score = 1406 bits (761),  Expect = 0.0
 Identities = 764/765 (99%), Gaps = 1/765 (0%)
 Strand=Plus/Minus

Query  8          ACTACCTACCCCACCCTGGACCAACAGAGAATTGACATAATCTCTGATTGCCTGGGCAAG
67
                  ||||||||||||||||||||||||||||||||||||||||||||||||||||||||||||
Sbjct  61070517  ACTACCTACCCCACCCTGGACCAACAGAGAATTGACATAATCTCTGATTGCCTGGGCAAG
61070458

Query  68        TGGCGGAGAAATTAGTTGTGAGCTCTCAGACTCTTCTAGTGCTTTCCTTTTACTGGAGAG
127
                  ||||||||||||||||||||||||||||||||||||||||||||||||||||||||||||
Sbjct  61070457  TGGCGGAGAAATTAGTTGTGAGCTCTCAGACTCTTCTAGTGCTTTCCTTTTACTGGAGAG
61070398

Query  128       AGGCGATTGATCTGAAATATGGGACCTCTCAGGACATAATGGTTGAATTCCACTTTTCTC
187
                  ||||||||||||||||||||||||||||||||||||||||||||||||||||||||||||
Sbjct  61070397  AGGCGATTGATCTGAAATATGGGACCTCTCAGGACATAATGGTTGAATTCCACTTTTCTC
61070338

Query  188       TCTACCGCAAATATTTTCTACTATGTCTTTATAGTAACCAGTGGTGGTTTCTTTAATCAG
247
                  ||||||||||||||||||||||||||||||||||||||||||||||||||||||||||||
Sbjct  61070337  TCTACCGCAAATATTTTCTACTATGTCTTTATAGTAACCAGTGGTGGTTTCTTTAATCAG
61070278

Query  248       TGAAGGAGAAGCTGCAGTAGAGACCAACATGGCACTGTGTTCAGGCTGAGAAGATGACGA
307
                  ||||||||||||||||||||||||||||||||||||||||||||||||||||||||||||
Sbjct  61070277  TGAAGGAGAAGCTGCAGTAGAGACCAACATGGCACTGTGTTCAGGCTGAGAAGATGACGA
61070218

Query  308       AGAACTTTTCTCTAAACACCTATCATGGCTAGACTTGCATGAAATAAACAAATTCCTTTC
367
                  ||||||||||||||||||||||||||||||||||||||||||||||||||||||||||||
Sbjct  61070217  AGAACTTTTCTCTAAACACCTATCATGGCTAGACTTGCATGAAATAAACAAATTCCTTTC
61070158

Query  368       AGAGGCTAACTTCTGCAACTGTCCCCTGCCAGGCAAGTTTGTGGCAACAAGAGGCTCCCT
427
                  ||||||||||||||||||||||||||||||||||||||||||||||||||||||||||||
Sbjct  61070157  AGAGGCTAACTTCTGCAACTGTCCCCTGCCAGGCAAGTTTGTGGCAACAAGAGGCTCCCT
61070098

Query  428       AGGTAGGTCTCCCTTAGAAGTATGTACTTTCTTAGCTGCCTGTAGTTCGGTACTGCCCAA
487
                  ||||||||||||||||||||||||||||||||||||||||||||||||||||||||||||
Sbjct  61070097  AGGTAGGTCTCCCTTAGAAGTATGTACTTTCTTAGCTGCCTGTAGTTCGGTACTGCCCAA
61070038

Query  488       AGGAGGACGGGTGGAGATTTCAGGAAAAGAAATACCCTGAAAAAATCCACCACCAGAGGG
547
                  ||||||||||||||||||||||||||||||||||||||||||||||||||||||||||||
Sbjct  61070037  AGGAGGACGGGTGGAGATTTCAGGAAAAGAAATACCCTGAAAAAATCCACCACCAGAGGG
61069978

Query  548       AGTAGTTCCAAGTTCAGAAAAAGGAACAATATCCCTAGTGGACTTCACTTTCTTGTGTTC
607
                  ||||||||||||||||||||||||||||||||||||||||||||||||||||||||||||
Sbjct  61069977  AGTAGTTCCAAGTTCAGAAAAAGGAACAATATCCCTAGTGGACTTCACTTTCTTGTGTTC
61069918

Query  608       TTTCTTCTTTCCTGTAGAGGCAAAAGAGGCAGGAAGTTTAAGCATTACCTGTGTTTGAGC
667
                  ||||||||||||||||||||||||||||||||||||||||||||||||||||||||||||
Sbjct  61069917  TTTCTTCTTTCCTGTAGAGGCAAAAGAGGCAGGAAGTTTAAGCATTACCTGTGTTTGAGC
61069858
```

```
Query  668       TGATTTTATTCTTTGCCTCTTTGCTAAAAATAGTGCTGTCAAAGGAAAAGACTATAATTT
727
                  ||||||||||||||||||||||||||||||||||||||||||||||||||||||||||||
Sbjct  61069857  TGATTTTATTCTTTGCCTCTTTGCTAAAAATAGTGCTGTCAAAGGAAAAGACTATAATTT
61069798

Query  728       CATATTCTGAACTAATCTGCCAGATTTGCCCTGGTAAGACAAAGC  772
                  |||||||||||||||||||||||||||||||| ||||||||
Sbjct  61069797  CATATTCTGAACTAATCTGCCAGATTTGCCCTGGTA-GACAAAGC  61069754
```

d. Reverse sequence (vs. AC013418.32)

```
21901 TCAATTCTCT TCTGTATGTT TTCTACATCC AGTGGGGGCA TAGAGTTAGA AGTTCCAGGC
21961 AAACTACCTA CCCCACCCTG GACCAACAGA GAATTGACAT AATCTCTGAT TGCCTGGGCA
22021 AGTGGCGGAG AAATTAGTTG TGAGCTCTCA GACTCTTCTA GTGCTTTCCT TTTACTGGAG
22081 AGAGGCGATT GATCTGAAAT ATGGGACCTC TCAGGACATA ATGGTTGAAT TCCACTTTTC
22141 TCTCTACCGC AAATATTTTC TACTATGTCT TTATAGTAAC CAGTGGTGGT TTCTTTAATC
22201 AGTGAAGGAG AAGCTGCAGT AGAGACCAAC ATGGCACTGT GTTCAGGCTG AGAAGATGAC
22261 GAAGAACTTT TCTCTAAACA CCTATCATGG CTAGACTTGC ATGAAATAAA CAAATTCCTT
22321 TCAGAGGCTA ACTTCTGCAA CTGTCCCCTG CCAGGCAAGT TTGTGGCAAC AAGAGGCTCC
22381 CTAGGTAGGT CTCCCTTAGA AGTATGTACT TTCTTAGCTG CCTGTAGTTC GGTACTGCCC
22441 AAAGGAGGAC GGGTGGAGAT TTCAGGAAAA GAAATACCCT GAAAAAATCC ACCACCAGAG
22501 GGAGTAGTTC CAAGTTCAGA AAAAGGAACA ATATCCCTAG TGGACTTCAC TTTCTTGTGT
22561 TCTTTCTTCT TTCCTGTAGA GGCAAAAGAG GCAGGAAGTT TAAGCATTAC CTGTGTTTGA
22621 GCTGATTTTA TTCTTTGCCT CTTTGCTAAA AATAGTGCTG TCAAAGGAAA AGACTATAAT
22681 TTCATATTCT GAACTAATCT GCCAGATTTG CCCTGGTAGA CAAAGCTTAT TGAGATATAA
```

e. Combined sequencing (forward and reverse sequences)

```
21901 TCAATTCTCT TCTGTATGTT TTCTACATCC AGTGGGGGCA TAGAGTTAGA AGTTCCAGGC
21961 AAACTACCTA CCCCACCCTG GACCAACAGA GAATTGACAT AATCTCTGAT TGCCTGGGCA
22021 AGTGGCGGAG AAATTAGTTG TGAGCTCTCA GACTCTTCTA GTGCTTTCCT TTTACTGGAG
22081 AGAGGCGATT GATCTGAAAT ATGGGACCTC TCAGGACATA ATGGTTGAAT TCCACTTTTC
22141 TCTCTACCGC AAATATTTTC TACTATGTCT TTATAGTAAC CAGTGGTGGT TTCTTTAATC
22201 AGTGAAGGAG AAGCTGCAGT AGAGACCAAC ATGGCACTGT GTTCAGGCTG AGAAGATGAC
22261 GAAGAACTTT TCTCTAAACA CCTATCATGG CTAGACTTGC ATGAAATAAA CAAATTCCTT
22321 TCAGAGGCTA ACTTCTGCAA CTGTCCCCTG CCAGGCAAGT TTGTGGCAAC AAGAGGCTCC
22381 CTAGGTAGGT CTCCCTTAGA AGTATGTACT TTCTTAGCTG CCTGTAGTTC GGTACTGCCC
22441 AAAGGAGGAC GGGTGGAGAT TTCAGGAAAA GAAATACCCT GAAAAAATCC ACCACCAGAG
22501 GGAGTAGTTC CAAGTTCAGA AAAAGGAACA ATATCCCTAG TGGACTTCAC TTTCTTGTGT
22561 TCTTTCTTCT TTCCTGTAGA GGCAAAAGAG GCAGGAAGTT TAAGCATTAC CTGTGTTTGA
22621 GCTGATTTTA TTCTTTGCCT CTTTGCTAAA AATAGTGCTG TCAAAGGAAA AGACTATAAT
22681 TTCATATTCT GAACTAATCT GCCAGATTTG CCCTGGTAGA CAAAGCTTAT TGAGATATAA
```

2. Primer pair: LAP2α4.1

a. Forward sequence (BLAST)

>ref|NM_003276.1| Homo sapiens thymopoietin (TMPO), transcript variant 1, mRNA
Length=2490

GENE ID: 7112 TMPO | thymopoietin [Homo sapiens] (Over 10 PubMed links)

Score = 1868 bits (1011), Expect = 0.0
Identities = 1050/1067 (98%), Gaps = 9/1067 (0%)
Strand=Plus/Plus

```
Query  3
GGGGGC-GTTGC-G-AGTTAGCCTCTG-AAGG-ATTTGTTTATTTCATGCAAGTCTAGCC  57
|||| | ||||| | ||||||||||||  |||| ||||||||||||||||||||||||||
Sbjct  995   GGGGACAGTTGCAGAAGTTAGCCTCTGAAAGGAATTTGTTTATTTCATGCAAGTCTAGCC  1054

Query  58    ATGATAGGTGTTTAGAGAAAAGTTCTTCGTCATCTTCTCAGCCTGAACACAGTGCCATGT  117
             ||||||||||||||||||||||||||||||||||||||||||||||||||||||||||||
Sbjct  1055  ATGATAGGTGTTTAGAGAAAAGTTCTTCGTCATCTTCTCAGCCTGAACACAGTGCCATGT  1114

Query  118   TGGTCTCTACTGCAGCTTCTCCTTCACTGATTAAAGAAACCACCACTGGTTACTATAAAG  177
             ||||||||||||||||||||||||||||||||||||||||||||||||||||||||||||
Sbjct  1115  TGGTCTCTACTGCAGCTTCTCCTTCACTGATTAAAGAAACCACCACTGGTTACTATAAAG  1174

Query  178   ACATAGTAGAAAATATTTGCGGTAGAGAGAAAAGTGGAATTCAACCATTATGTCCTGAGA  237
             ||||||||||||||||||||||||||||||||||||||||||||||||||||||||||||
Sbjct  1175  ACATAGTAGAAAATATTTGCGGTAGAGAGAAAAGTGGAATTCAACCATTATGTCCTGAGA  1234

Query  238   GGTCCCATATTTCAGATCAATCGCCTCTCTCCAGTAAAAGGAAAGCACTAGAAGAGTCTG  297
             ||||||||||||||||||||||||||||||||||||||||||||||||||||||||||||
Sbjct  1235  GGTCCCATATTTCAGATCAATCGCCTCTCTCCAGTAAAAGGAAAGCACTAGAAGAGTCTG  1294

Query  298   AGAGCTCACAACTAATTTCTCCGCCACTTGCCCAGGCAATCAGAGATTATGTCAATTCTC  357
             ||||||||||||||||||||||||||||||||||||||||||||||||||||||||||||
Sbjct  1295  AGAGCTCACAACTAATTTCTCCGCCACTTGCCCAGGCAATCAGAGATTATGTCAATTCTC  1354

Query  358   TGTTGGTCCAGGGTGGGGTAGGTAGTTTGCCTGGAACTTCTAACTCTATGCCCCCACTGG  417
             ||||||||||||||||||||||||||||||||||||||||||||||||||||||||||||
Sbjct  1355  TGTTGGTCCAGGGTGGGGTAGGTAGTTTGCCTGGAACTTCTAACTCTATGCCCCCACTGG  1414

Query  418   ATGTAGAAAACATACAGAAGAGAATTGATCAGTCTAAGTTTCAAGAAACTGAATTCCTGT  477
             ||||||||||||||||||||||||||||||||||||||||||||||||||||||||||||
Sbjct  1415  ATGTAGAAAACATACAGAAGAGAATTGATCAGTCTAAGTTTCAAGAAACTGAATTCCTGT  1474

Query  478   CTCCTCCAAGAAAAGTCCCTAGACTGAGTGAGAAGTCAGTGGAGGAAAGGGATTCAGGTT  537
             ||||||||||||||||||||||||||||||||||||||||||||||||||||||||||||
Sbjct  1475  CTCCTCCAAGAAAAGTCCCTAGACTGAGTGAGAAGTCAGTGGAGGAAAGGGATTCAGGTT  1534

Query  538   CCTTTGTGGCATTTCAGAACATACCTGGATCCGAACTGATGTCTTCTTTTGCCAAAACTG  597
             ||||||||||||||||||||||||||||||||||||||||||||||||||||||||||||
Sbjct  1535  CCTTTGTGGCATTTCAGAACATACCTGGATCCGAACTGATGTCTTCTTTTGCCAAAACTG  1594

Query  598   TTGTCTCTCATTCACTCACTACCTTAGGTCTAGAAGTGGCTAAGCAATCACAGCATGATA  657
             ||||||||||||||||||||||||||||||||||||||||||||||||||||||||||||
Sbjct  1595  TTGTCTCTCATTCACTCACTACCTTAGGTCTAGAAGTGGCTAAGCAATCACAGCATGATA  1654

Query  658   AAATAGATGCCTCAGAACTATCTTTTCCCTTCCATGAATCTATTTTAAAAGTAATTGAAG  717
             ||||||||||||||||||||||||||||||||||||||||||||||||||||||||||||
Sbjct  1655  AAATAGATGCCTCAGAACTATCTTTTCCCTTCCATGAATCTATTTTAAAAGTAATTGAAG  1714

Query  718   AAGAATGGCAGCAAGTTGACAGGCAGCTGCCTTCACTGGCATGCAAATATCCAGTTTCTT  777
```

```
                ||||||||||||||||||||||||||||||||||||||||||||||||||||||||||||
Sbjct  1715  AAGAATGGCAGCAAGTTGACAGGCAGCTGCCTTCACTGGCATGCAAATATCCAGTTTCTT  1774

Query  778   CCAGGGAGGCAACACAGATATTATCAGTTCCAAAAGTAGATGATGAAATCCTAGGGTTTA  837
              ||||||||||||||||||||||||||||||||||||||||||||||||||||||||||||
Sbjct  1775  CCAGGGAGGCAACACAGATATTATCAGTTCCAAAAGTAGATGATGAAATCCTAGGGTTTA  1834

Query  838   TTTCTGAAGCCACTCCACTAGGAGGTATTCAAGCAGCCTCCACTGAGTCTTGCAATCAGC  897
              ||||||||||||||||||||||||||||||||||||||||||||||||||||||||||||
Sbjct  1835  TTTCTGAAGCCACTCCACTAGGAGGTATTCAAGCAGCCTCCACTGAGTCTTGCAATCAGC  1894

Query  898   AGTTGGACTTAGCACTCTGTAGAGCATATGAAGCTGCAGCATCAGCATTGCGGATTGCGA  957
|||||||||||||||||||||||||||||||||||||||||||||||||| ||||||  |
Sbjct  1895  AGTTGGACTTAGCACTCTGTAGAGCATATGAAGCTGCAGCATCAGCATTGCAGATTGCAA  1954

Query  958
CTCACACTGCCTTTGTAGCTAAGGCTATGCAGACAGACATAAGTCAAGCTGC-CAGATTC  1016
|||||||||||||||||||||||||||||| ||||||| |||||||||||| |||||||
Sbjct  1955  CTCACACTGCCTTTGTAGCTAAGGCTATGCAGGCAGACATTAGTCAAGCTGCACAGATTC  2014

Query  1017  TTAACTCAGATCCAAGTCGTACCC-CCAAGCGCCTGG-ATTTCTGAG  1061
              ||| ||||||||| |||||||||| |||||||| ||| ||| |||||
Sbjct  2015  TTAGCTCAGATCCTAGTCGTACCCACCAAGCGCTTGGGATT-CTGAG  2060
```

b. Forward sequence (vs. NM_003276.1)

```
961   AGGGAGCCTCTTGTTGCCACAAACTTGCCTGGCAGGGGACAGTTGCAGAAGTTAGCCTCT
1021  GAAAGGAATTTGTTTATTTCATGCAAGTCTAGCCATGATAGGTGTTTAGAGAAAAGTTCT
1081  TCGTCATCTTCTCAGCCTGAACACAGTGCCATGTTGGTCTCTACTGCAGCTTCTCCTTCA
1141  CTGATTAAAGAAACCACCACTGGTTACTATAAAGACATAGTAGAAAATATTTGCGGTAGA
1201  GAGAAAAGTGGAATTCAACCATTATGTCCTGAGAGGTCCCATATTTCAGATCAATCGCCT
1261  CTCTCCAGTAAAAGGAAAGCACTAGAAGAGTCTGAGAGCTCACAACTAATTTCTCCGCCA
1321  CTTGCCCAGGCAATCAGAGATTATGTCAATTCTCTGTTGGTCCAGGGTGGGGTAGGTAGT
1381  TTGCCTGGAACTTCTAACTCTATGCCCCCACTGGATGTAGAAAACATACAGAAGAGAATT
1441  GATCAGTCTAAGTTTCAAGAAACTGAATTCCTGTCTCCTCCAAGAAAAGTCCCTAGACTG
1501  AGTGAGAAGTCAGTGGAGGAAAGGGATTCAGGTTCCTTTGTGGCATTTCAGAACATACCT
1561  GGATCCGAACTGATGTCTTCTTTTGCCAAAACTGTTGTCTCTCATTCACTCACTACCTTA
1621  GGTCTAGAAGTGGCTAAGCAATCACAGCATGATAAAATAGATGCCTCAGAACTATCTTTT
1681  CCCTTCCATGAATCTATTTTAAAAGTAATTGAAGAAGAATGGCAGCAAGTTGACAGGCAG
1741  CTGCCTTCACTGGCATGCAAATATCCAGTTTCTTCCAGGGAGGCAACACAGATATTATCA
1801  GTTCCAAAAGTAGATGATGAAATCCTAGGGTTTATTTCTGAAGCCACTCCACTAGGAGGT
1861  ATTCAAGCAGCCTCCACTGAGTCTTGCAATCAGCAGTTGGACTTAGCACTCTGTAGAGCA
1921  TATGAAGCTGCAGCATCAGCATTGCAGATTGCAACTCACACTGCCTTTGTAGCTAAGGCT
1981  ATGCAGGCAGACATTAGTCAAGCTGCACAGATTCTTAGCTCAGATCCTAGTCGTACCCAC
2041  CAAGCGCTTGGGATTCTGAGCAAAACATATGATGCAGCCTCATATATTTGTGAAGCTGCA
2101  TTTGATGAAGTGAAGATGGCTGCCCATACCATGGGAAATGCCACTGTAGGTCGTCGATAC
```

c. Reverse sequence (BLAST)

> ref|NM_003276.1| Homo sapiens thymopoietin (TMPO), transcript variant 1, mRNA
Length=2490

GENE ID: 7112 TMPO | thymopoietin [Homo sapiens] (Over 10 PubMed links)

Score = 1930 bits (1045), Expect = 0.0
Identities = 1082/1098 (98%), Gaps = 9/1098 (0%)
Strand=Plus/Minus

```
Query  9     AAATATATGAGGCTGCATCATATGTTTTGCTCAGAATCCCAAGCGCTTGGTGGGTACGAC  68
             ||||||||||||||||||||||||||||||||||||||||||||||||||||||||||||
Sbjct  2089  AAATATATGAGGCTGCATCATATGTTTTGCTCAGAATCCCAAGCGCTTGGTGGGTACGAC  2030

Query  69    TAGGATCTGAGCTAAGAATCTGTGCAGCTTGACTAATGTCTGCCTGCATAGCCTTAGCTA  128
             ||||||||||||||||||||||||||||||||||||||||||||||||||||||||||||
Sbjct  2029  TAGGATCTGAGCTAAGAATCTGTGCAGCTTGACTAATGTCTGCCTGCATAGCCTTAGCTA  1970

Query  129   CAAAGGCAGTGTGAGTTGCAATCTGCAATGCTGATGCTGCAGCTTCATATGCTCTACAGA  188
             ||||||||||||||||||||||||||||||||||||||||||||||||||||||||||||
Sbjct  1969  CAAAGGCAGTGTGAGTTGCAATCTGCAATGCTGATGCTGCAGCTTCATATGCTCTACAGA  1910

Query  189   GTGCTAAGTCCAACTGCTGATTGCAAGACTCAGTGGAGGCTGCTTGAATACCTCCTAGTG  248
             ||||||||||||||||||||||||||||||||||||||||||||||||||||||||||||
Sbjct  1909  GTGCTAAGTCCAACTGCTGATTGCAAGACTCAGTGGAGGCTGCTTGAATACCTCCTAGTG  1850

Query  249   GAGTGGCTTCAGAAATAAACCCTAGGATTTCATCATCTACTTTTGGAACTGATAATATCT  308
             ||||||||||||||||||||||||||||||||||||||||||||||||||||||||||||
Sbjct  1849  GAGTGGCTTCAGAAATAAACCCTAGGATTTCATCATCTACTTTTGGAACTGATAATATCT  1790

Query  309   GTGTTGCCTCCCTGGAAGAAACTGGATATTTGCATGCCAGTGAAGGCAGCTGCCTGTCAA  368
             ||||||||||||||||||||||||||||||||||||||||||||||||||||||||||||
Sbjct  1789  GTGTTGCCTCCCTGGAAGAAACTGGATATTTGCATGCCAGTGAAGGCAGCTGCCTGTCAA  1730

Query  369   CTTGCTGCCATTCTTCTTCAATTACTTTTAAAATAGATTCATGGAAGGGAAAAGATAGTT  428
             ||||||||||||||||||||||||||||||||||||||||||||||||||||||||||||
Sbjct  1729  CTTGCTGCCATTCTTCTTCAATTACTTTTAAAATAGATTCATGGAAGGGAAAAGATAGTT  1670

Query  429   CTGAGGCATCTATTTTATCATGCTGTGATTGCTTAGCCACTTCTAGACCTAAGGTAGTGA  488
             ||||||||||||||||||||||||||||||||||||||||||||||||||||||||||||
Sbjct  1669  CTGAGGCATCTATTTTATCATGCTGTGATTGCTTAGCCACTTCTAGACCTAAGGTAGTGA  1610

Query  489   GTGAATGAGAGACAACAGTTTTGGCAAAAGAAGACATCAGTTCGGATCCAGGTATGTTCT  548
             ||||||||||||||||||||||||||||||||||||||||||||||||||||||||||||
Sbjct  1609  GTGAATGAGAGACAACAGTTTTGGCAAAAGAAGACATCAGTTCGGATCCAGGTATGTTCT  1550

Query  549   GAAATGCCACAAAGGAACCTGAATCCCTTTCCTCCACTGACTTCTCACTCAGTCTAGGGA  608
             ||||||||||||||||||||||||||||||||||||||||||||||||||||||||||||
Sbjct  1549  GAAATGCCACAAAGGAACCTGAATCCCTTTCCTCCACTGACTTCTCACTCAGTCTAGGGA  1490

Query  609   CTTTTCTTGGAGGAGACAGGAATTCAGTTTCTTGAAACTTAGACTGATCAATTCTCTTCT  668
             ||||||||||||||||||||||||||||||||||||||||||||||||||||||||||||
Sbjct  1489  CTTTTCTTGGAGGAGACAGGAATTCAGTTTCTTGAAACTTAGACTGATCAATTCTCTTCT  1430

Query  669   GTATGTTTTCTACATCCAGTGGGGGCATAGAGTTAGAAGTTCCAGGCAAACTACCTACCC  728
             ||||||||||||||||||||||||||||||||||||||||||||||||||||||||||||
Sbjct  1429  GTATGTTTTCTACATCCAGTGGGGGCATAGAGTTAGAAGTTCCAGGCAAACTACCTACCC  1370

Query  729   CACCCTGGACCAACAGAGAATTGACATAATCTCTGATTGCCTGGGCAAGTGGCGGAGAAA  788
             ||||||||||||||||||||||||||||||||||||||||||||||||||||||||||||
Sbjct  1369  CACCCTGGACCAACAGAGAATTGACATAATCTCTGATTGCCTGGGCAAGTGGCGGAGAAA  1310

Query  789   TTAGTTGTGAGCTCTCAGACTCTTCTAGTGCTTTCCTTTTACTGGAGAGAGGCGATTGAT  848
             ||||||||||||||||||||||||||||||||||||||||||||||||||||||||||||
Sbjct  1309  TTAGTTGTGAGCTCTCAGACTCTTCTAGTGCTTTCCTTTTACTGGAGAGAGGCGATTGAT  1250
```

```
Query  849   CTGAAATATGGGACCTCTCAGGACATAATGGTTGAATTCCACTTTTCTCTCTACCGCAAA  908
              ||||||||||||||||||||||||||||||||||||||||||||||||||||||||||||
Sbjct  1249  CTGAAATATGGGACCTCTCAGGACATAATGGTTGAATTCCACTTTTCTCTCTACCGCAAA  1190

Query  909   TATTTTCTACTATGTCTTTATAGTAACCAGTGGTGGTTTCTTTAATCAGTGAAGGAGAAG  968
              ||||||||||||||||||||||||||||||||||||||||||||||||||||||||||||
Sbjct  1189  TATTTTCTACTATGTCTTTATAGTAACCAGTGGTGGTTTCTTTAATCAGTGAAGGAGAAG  1130

Query  969   CTGCAGTACAGACCAACATGGCACTGTGTTCAGGCTGAGAAGATGACGAAGAACTTTTCT  1028
              |||||||| ||||||||||||||||||||||||||||||||||||||||||||||||||||
Sbjct  1129  CTGCAGTAGAGACCAACATGGCACTGTGTTCAGGCTGAGAAGATGACGAAGAACTTTTCT  1070

Query  1029  CTAA-CACCTATCATG-CTAGCCTTGCATGAA-TGACCGA-TTCCTT-CAG---CTA-CT  1079
              |||| |||||||||| |||| |||||||||| | | | | |||||| |||   ||| ||
Sbjct  1069  CTAAACACCTATCATGGCTAGACTTGCATGAAATAAACAAATTCCTTTCAGAGGCTAACT  1010

Query  1080  TCTGCAACTGTACTCTGC  1097
              ||||||||||| | ||||
Sbjct  1009  TCTGCAACTGTCCCCTGC  992
```

d. Reverse sequence (vs. NM_003276.1)

```
961   AGGGAGCCTCTTGTTGCCACAAACTTGCCTGGCAGGGGACAGTTGCAGAAGTTAGCCTCT
1021  GAAAGGAATTTGTTTATTTCATGCAAGTCTAGCCATGATAGGTGTTTAGAGAAAAGTTCT
1081  TCGTCATCTTCTCAGCCTGAACACAGTGCCATGTTGGTCTCTACTGCAGCTTCTCCTTCA
1141  CTGATTAAAGAAACCACCACTGGTTACTATAAAGACATAGTAGAAAATATTTGCGGTAGA
1201  GAGAAAAGTGGAATTCAACCATTATGTCCTGAGAGGTCCCATATTTCAGATCAATCGCCT
1261  CTCTCCAGTAAAAGGAAAGCACTAGAAGAGTCTGAGAGCTCACAACTAATTTCTCCGCCA
1321  CTTGCCCAGGCAATCAGAGATTATGTCAATTCTCTGTTGGTCCAGGGTGGGGTAGGTAGT
1381  TTGCCTGGAACTTCTAACTCTATGCCCCCACTGGATGTAGAAAACATACAGAAGAGAATT
1441  GATCAGTCTAAGTTTCAAGAAACTGAATTCCTGTCTCCTCCAAGAAAAGTCCCTAGACTG
1501  AGTGAGAAGTCAGTGGAGGAAAGGGATTCAGGTTCCTTTGTGGCATTTCAGAACATACCT
1561  GGATCCGAACTGATGTCTTCTTTTGCCAAAACTGTTGTCTCTCATTCACTCACTACCTTA
1621  GGTCTAGAAGTGGCTAAGCAATCACAGCATGATAAAATAGATGCCTCAGAACTATCTTTT
1681  CCCTTCCATGAATCTATTTTAAAAGTAATTGAAGAAGAATGGCAGCAAGTTGACAGGCAG
1741  CTGCCTTCACTGGCATGCAAATATCCAGTTTCTTCCAGGGAGGCAACACAGATATTATCA
1801  GTTCCAAAAGTAGATGATGAAATCCTAGGGTTTATTTCTGAAGCCACTCCACTAGGAGGT
1861  ATTCAAGCAGCCTCCACTGAGTCTTGCAATCAGCAGTTGGACTTAGCACTCTGTAGAGCA
1921  TATGAAGCTGCAGCATCAGCATTGCAGATTGCAACTCACACTGCCTTTGTAGCTAAGGCT
1981  ATGCAGGCAGACATTAGTCAAGCTGCACAGATTCTTAGCTCAGATCCTAGTCGTACCCAC
2041  CAAGCGCTTGGGATTCTGAGCAAAACATATGATGCAGCCTCATATATTTGTGAAGCTGCA
2101  TTTGATGAAGTGAAGATGGCTGCCCATACCATGGGAAATGCCACTGTAGGTCGTCGATAC
```

e. Combined sequencing (forward and reverse sequences)

```
961   AGGGAGCCTCTTGTTGCCACAAACTTGCCTGGCAGGGGACAGTTGCAGAAGTTAGCCTCT
1021  GAAAGGAATTTGTTTATTTCATGCAAGTCTAGCCATGATAGGTGTTTAGAGAAAAGTTCT
1081  TCGTCATCTTCTCAGCCTGAACACAGTGCCATGTTGGTCTCTACTGCAGCTTCTCCTTCA
1141  CTGATTAAAGAAACCACCACTGGTTACTATAAAGACATAGTAGAAAATATTTGCGGTAGA
1201  GAGAAAAGTGGAATTCAACCATTATGTCCTGAGAGGTCCCATATTTCAGATCAATCGCCT
```

1261 CTCTCCAGTAAAAGGAAAGCACTAGAAGAGTCTGAGAGCTCACAACTAATTTCTCCGCCA

1321 CTTGCCCAGGCAATCAGAGATTATGTCAATTCTCTGTTGGTCCAGGGTGGGGTAGGTAGT

1381 TTGCCTGGAACTTCTAACTCTATGCCCCCACTGGATGTAGAAAACATACAGAAGAGAATT

1441 GATCAGTCTAAGTTTCAAGAAACTGAATTCCTGTCTCCTCCAAGAAAAGTCCCTAGACTG

1501 AGTGAGAAGTCAGTGGAGGAAAGGGATTCAGGTTCCTTTGTGGCATTTCAGAACATACCT

1561 GGATCCGAACTGATGTCTTCTTTTGCCAAAACTGTTGTCTCTCATTCACTCACTACCTTA

1621 GGTCTAGAAGTGGCTAAGCAATCACAGCATGATAAAATAGATGCCTCAGAACTATCTTTT

1681 CCCTTCCATGAATCTATTTTAAAAGTAATTGAAGAAGAATGGCAGCAAGTTGACAGGCAG

1741 CTGCCTTCACTGGCATGCAAATATCCAGTTTCTTCCAGGGAGGCAACACAGATATTATCA

1801 GTTCCAAAAGTAGATGATGAAATCCTAGGGTTTATTTCTGAAGCCACTCCACTAGGAGGT

1861 ATTCAAGCAGCCTCCACTGAGTCTTGCAATCAGCAGTTGGACTTAGCACTCTGTAGAGCA

1921 TATGAAGCTGCAGCATCAGCATTGCAGATTGCAACTCACACTGCCTTTGTAGCTAAGGCT

1981 ATGCAGGCAGACATTAGTCAAGCTGCACAGATTCTTAGCTCAGATCCTAGTCGTACCCAC

2041 CAAGCGCTTGGGATTCTGAGCAAAACATATGATGCAGCCTCATATATTTGTGAAGCTGCA

2101 TTTGATGAAGTGAAGATGGCTGCCCATACCATGGGAAATGCCACTGTAGGTCGTCGATAC

3. Primer pair: LAP2α4.2

a. Forward sequence (BLAST)

ref|NM_003276.1| Homo sapiens thymopoietin (TMPO), transcript variant 1, mRNA
Length=2490

Score = 252 bits (127), Expect = 8e-65
Identities = 127/127 (100%), Gaps = 0/127 (0%)
Strand=Plus/Plus

```
Query  5     AAACATACAGAAGAGAATTGATCAGTCTAAGTTTCAAGAAACTGAATTCCTGTCTCCTCC  64
             ||||||||||||||||||||||||||||||||||||||||||||||||||||||||||||
Sbjct  1422  AAACATACAGAAGAGAATTGATCAGTCTAAGTTTCAAGAAACTGAATTCCTGTCTCCTCC  1481

Query  65    AAGAAAAGTCCCTAGACTGAGTGAGAAGTCAGTGGAGGAAAGGGATTCAGGTTCCTTTGT  124
             ||||||||||||||||||||||||||||||||||||||||||||||||||||||||||||
Sbjct  1482  AAGAAAAGTCCCTAGACTGAGTGAGAAGTCAGTGGAGGAAAGGGATTCAGGTTCCTTTGT  1541

Query  125   GGCATTT  131
             |||||||
Sbjct  1542  GGCATTT  1548
```

b. Forward sequence (vs. NM_003276.1)

1321 CTTGCCCAGGCAATCAGAGATTATGTCAATTCTCTGTTGGTCCAGGGTGGGGTAGGTAGT

1381 TTGCCTGGAACTTCTAACTCTATGCCCCCACTGGATGTAGAAAACATACAGAAGAGAATT

1441 GATCAGTCTAAGTTTCAAGAAACTGAATTCCTGTCTCCTCCAAGAAAAGTCCCTAGACTG

1501 AGTGAGAAGTCAGTGGAGGAAAGGGATTCAGGTTCCTTTGTGGCATTTCAGAACATACCT

4. Primer pair: LAP2α4.3

a. Forward sequence (BLAST)

>ref|NM_003276.1| Homo sapiens thymopoietin (TMPO), transcript variant 1, mRNA
Length=2490

GENE ID: 7112 TMPO | thymopoietin [Homo sapiens] (Over 10 PubMed links)

Score = 1640 bits (888), Expect = 0.0
Identities = 896/899 (99%), Gaps = 3/899 (0%)
Strand=Plus/Plus

```
Query  5     AACTGTTGTCTCTCATTC-CTCACTACCTTAGGTCTAGAAGTGGCTAAGCAATCACAGCA  63
             |||||||||||||||||| ||||||||||||||||||||||||||||||||||||||||
Sbjct  1590  AACTGTTGTCTCTCATTCACTCACTACCTTAGGTCTAGAAGTGGCTAAGCAATCACAGCA  1649

Query  64    TGATAAAATAGATGCCTCAGAACTATCTTTTCCCTTCCATGAATCTATTTTAAAAGTAAT  123
             ||||||||||||||||||||||||||||||||||||||||||||||||||||||||||||
Sbjct  1650  TGATAAAATAGATGCCTCAGAACTATCTTTTCCCTTCCATGAATCTATTTTAAAAGTAAT  1709

Query  124   TGAAGAAGAATGGCAGCAAGTTGACAGGCAGCTGCCTTCACTGGCATGCAAATATCCAGT  183
             ||||||||||||||||||||||||||||||||||||||||||||||||||||||||||||
Sbjct  1710  TGAAGAAGAATGGCAGCAAGTTGACAGGCAGCTGCCTTCACTGGCATGCAAATATCCAGT  1769

Query  184   TTCTTCCAGGGAGGCAACACAGATATTATCAGTTCCAAAAGTAGATGATGAAATCCTAGG  243
             ||||||||||||||||||||||||||||||||||||||||||||||||||||||||||||
Sbjct  1770  TTCTTCCAGGGAGGCAACACAGATATTATCAGTTCCAAAAGTAGATGATGAAATCCTAGG  1829

Query  244   GTTTATTTCTGAAGCCACTCCACTAGGAGGTATTCAAGCAGCCTCCACTGAGTCTTGCAA  303
             ||||||||||||||||||||||||||||||||||||||||||||||||||||||||||||
Sbjct  1830  GTTTATTTCTGAAGCCACTCCACTAGGAGGTATTCAAGCAGCCTCCACTGAGTCTTGCAA  1889

Query  304   TCAGCAGTTGGACTTAGCACTCTGTAGAGCATATGAAGCTGCAGCATCAGCATTGCAGAT  363
             ||||||||||||||||||||||||||||||||||||||||||||||||||||||||||||
Sbjct  1890  TCAGCAGTTGGACTTAGCACTCTGTAGAGCATATGAAGCTGCAGCATCAGCATTGCAGAT  1949

Query  364   TGCAACTCACACTGCCTTTGTAGCTAAGGCTATGCAGGCAGACATTAGTCAAGCTGCACA  423
             ||||||||||||||||||||||||||||||||||||||||||||||||||||||||||||
Sbjct  1950  TGCAACTCACACTGCCTTTGTAGCTAAGGCTATGCAGGCAGACATTAGTCAAGCTGCACA  2009

Query  424   GATTCTTAGCTCAGATCCTAGTCGTACCCACCAAGCGCTTGGGATTCTGAGCAAAACATA  483
             ||||||||||||||||||||||||||||||||||||||||||||||||||||||||||||
Sbjct  2010  GATTCTTAGCTCAGATCCTAGTCGTACCCACCAAGCGCTTGGGATTCTGAGCAAAACATA  2069

Query  484   TGATGCAGCCTCATATATTTGTGAAGCTGCATTTGATGAAGTGAAGATGGCTGCCCATAC  543
             ||||||||||||||||||||||||||||||||||||||||||||||||||||||||||||
Sbjct  2070  TGATGCAGCCTCATATATTTGTGAAGCTGCATTTGATGAAGTGAAGATGGCTGCCCATAC  2129

Query  544   CATGGGAAATGCCACTGTAGGTCGTCGATACCTCTGGCTGAAGGATTGCAAAATTAATTT  603
             ||||||||||||||||||||||||||||||||||||||||||||||||||||||||||||
Sbjct  2130  CATGGGAAATGCCACTGTAGGTCGTCGATACCTCTGGCTGAAGGATTGCAAAATTAATTT  2189

Query  604   AGCTTCTAAGAATAAGCTGGCTTCCACTCCCTTTAAAGGTGGAACATTATTTGGAGGAGA  663
             ||||||||||||||||||||||||||||||||||||||||||||||||||||||||||||
Sbjct  2190  AGCTTCTAAGAATAAGCTGGCTTCCACTCCCTTTAAAGGTGGAACATTATTTGGAGGAGA  2249

Query  664   AGTATGCAAAGTAATTAAAAAGCGTGGAAATAAACACTAGTAAAATTAAGGACAAAAAGA  723
             ||||||||||||||||||||||||||||||||||||||||||||||||||||||||||||
Sbjct  2250  AGTATGCAAAGTAATTAAAAAGCGTGGAAATAAACACTAGTAAAATTAAGGACAAAAAGA  2309

Query  724   CATCTATCTTATCTTTCAGGTACTTTATGCCAACATTTTCTTTTCTGTTAAGGTTGTTTT  783
             ||||||||||||||||||||||||||||||||||||||||||||||||||||||||||||
Sbjct  2310  CATCTATCTTATCTTTCAGGTACTTTATGCCAACATTTTCTTTTCTGTTAAGGTTGTTTT  2369

Query  784   AGTTTCCAGATAGGGCTAATTACAAAATGTTAAGCTTCTACCCATCAAATTACAGTATAA  843
             ||||||||||||||||||||||||||||||||||||||||||||||||||||||||||||
```

```
Sbjct  2370  AGTTTCCAGATAGGGCTAATTACAAAATGTTAAGCTTCTACCCATCAAATTACAGTATAA  2429

Query  844   AAGTAATTGCCTGTGTAGAACTACTTGTCTTTTCTAAAGATTTGCGTAG-TAGGGAAGC  901
             ||||||||||||||||||||||||||||||||||||||||||||||||| |||| ||||
Sbjct  2430  AAGTAATTGCCTGTGTAGAACTACTTGTCTTTTCTAAAGATTTGCGTAGATAGG-AAGC  2487
```

b. Forward sequence (vs. NM_003276.1)

```
1501 AGTGAGAAGTCAGTGGAGGAAAGGGATTCAGGTTCCTTTGTGGCATTTCAGAACATACCT
1561 GGATCCGAACTGATGTCTTCTTTTGCCAAAACTGTTGTCTCTCATTCACTCACTACCTTA
1621 GGTCTAGAAGTGGCTAAGCAATCACAGCATGATAAAATAGATGCCTCAGAACTATCTTTT
1681 CCCTTCCATGAATCTATTTTAAAAGTAATTGAAGAAGAATGGCAGCAAGTTGACAGGCAG
1741 CTGCCTTCACTGGCATGCAAATATCCAGTTTCTTCCAGGGAGGCAACACAGATATTATCA
1801 GTTCCAAAAGTAGATGATGAAATCCTAGGGTTTATTTCTGAAGCCACTCCACTAGGAGGT
1861 ATTCAAGCAGCCTCCACTGAGTCTTGCAATCAGCAGTTGGACTTAGCACTCTGTAGAGCA
1921 TATGAAGCTGCAGCATCAGCATTGCAGATTGCAACTCACACTGCCTTTGTAGCTAAGGCT
1981 ATGCAGGCAGACATTAGTCAAGCTGCACAGATTCTTAGCTCAGATCCTAGTCGTACCCAC
2041 CAAGCGCTTGGGATTCTGAGCAAAACATATGATGCAGCCTCATATATTTGTGAAGCTGCA
2101 TTTGATGAAGTGAAGATGGCTGCCCATACCATGGGAAATGCCACTGTAGGTCGTCGATAC
2161 CTCTGGCTGAAGGATTGCAAAATTAATTTAGCTTCTAAGAATAAGCTGGCTTCCACTCCC
2221 TTTAAAGGTGGAACATTATTTGGAGGAGAAGTATGCAAAGTAATTAAAAAGCGTGGAAAT
2281 AAACACTAGTAAAATTAAGGACAAAAAGACATCTATCTTATCTTTCAGGTACTTTATGCC
2341 AACATTTTCTTTTCTGTTAAGGTTGTTTTAGTTTCCAGATAGGGCTAATTACAAAATGTT
2401 AAGCTTCTACCCATCAAATTACAGTATAAAAGTAATTGCCTGTGTAGAACTACTTGTCTT
2461 TTCTAAAGATTTGCGTAGATAGGAAGCCTG
```

c. Reverse sequence (BLAST)

> ref|NM_003276.1| Homo sapiens thymopoietin (TMPO), transcript variant 1, mRNA
Length=2490

GENE ID: 7112 TMPO | thymopoietin [Homo sapiens] (Over 10 PubMed links)

Score = 1626 bits (880), Expect = 0.0
Identities = 895/901 (99%), Gaps = 5/901 (0%)
Strand=Plus/Minus

```
Query  4     AAGA-AGGTAGTTTCTACACAGGC-ATTACTTTTATACTGTAATTTGATGGGTAGAAGCT  61
             |||| | |||| |||||||||||| ||||||||||||||||||||||||||||||||||
Sbjct  2460  AAGACAAGTAG-TTCTACACAGGCAATTACTTTTATACTGTAATTTGATGGGTAGAAGCT  2402

Query  62    TAACATTTTGTAATTAGCCCTATCTGGAAACTAAAACAACCTTAACAGAAAAGAAAATGT  121
             ||||||||||||||||||||||||||||||||||||||||||||||||||||||||||||
Sbjct  2401  TAACATTTTGTAATTAGCCCTATCTGGAAACTAAAACAACCTTAACAGAAAAGAAAATGT  2342

Query  122   TGGCATAAAGTACCTGAAAGATAAGATAGATGTCTTTTTGTCCTTAATTTTACTAGTGTT  181
             ||||||||||||||||||||||||||||||||||||||||||||||||||||||||||||
Sbjct  2341  TGGCATAAAGTACCTGAAAGATAAGATAGATGTCTTTTTGTCCTTAATTTTACTAGTGTT  2282

Query  182   TATTTCCACGCTTTTTAATTACTTTGCATACTTCTCCTCCAAATAATGTTCCACCTTTAA  241
             ||||||||||||||||||||||||||||||||||||||||||||||||||||||||||||
Sbjct  2281  TATTTCCACGCTTTTTAATTACTTTGCATACTTCTCCTCCAAATAATGTTCCACCTTTAA  2222
```

```
Query  242   AGGGAGTGGAAGCCAGCTTATTCTTAGAAGCTAAATTAATTTTGCAATCCTTCAGCCAGA  301
             ||||||||||||||||||||||||||||||||||||||||||||||||||||||||||||
Sbjct  2221  AGGGAGTGGAAGCCAGCTTATTCTTAGAAGCTAAATTAATTTTGCAATCCTTCAGCCAGA  2162

Query  302   GGTATCGACGACCTACAGTGGCATTTCCCATGGTATGGGCAGCCATCTTCACTTCATCAA  361
             ||||||||||||||||||||||||||||||||||||||||||||||||||||||||||||
Sbjct  2161  GGTATCGACGACCTACAGTGGCATTTCCCATGGTATGGGCAGCCATCTTCACTTCATCAA  2102

Query  362   ATGCAGCTTCACAAATATATGAGGCTGCATCATATGTTTTGCTCAGAATCCCAAGCGCTT  421
             ||||||||||||||||||||||||||||||||||||||||||||||||||||||||||||
Sbjct  2101  ATGCAGCTTCACAAATATATGAGGCTGCATCATATGTTTTGCTCAGAATCCCAAGCGCTT  2042

Query  422   GGTGGGTACGACTAGGATCTGAGCTAAGAATCTGTGCAGCTTGACTAATGTCTGCCTGCA  481
             ||||||||||||||||||||||||||||||||||||||||||||||||||||||||||||
Sbjct  2041  GGTGGGTACGACTAGGATCTGAGCTAAGAATCTGTGCAGCTTGACTAATGTCTGCCTGCA  1982

Query  482   TAGCCTTAGCTACAAAGGCAGTGTGAGTTGCAATCTGCAATGCTGATGCTGCAGCTTCAT  541
             ||||||||||||||||||||||||||||||||||||||||||||||||||||||||||||
Sbjct  1981  TAGCCTTAGCTACAAAGGCAGTGTGAGTTGCAATCTGCAATGCTGATGCTGCAGCTTCAT  1922

Query  542   ATGCTCTACAGAGTGCTAAGTCCAACTGCTGATTGCAAGACTCAGTGGAGGCTGCTTGAA  601
             ||||||||||||||||||||||||||||||||||||||||||||||||||||||||||||
Sbjct  1921  ATGCTCTACAGAGTGCTAAGTCCAACTGCTGATTGCAAGACTCAGTGGAGGCTGCTTGAA  1862

Query  602   TACCTCCTAGTGGAGTGGCTTCAGAAATAAACCCTAGGATTTCATCATCTACTTTTGGAA  661
             ||||||||||||||||||||||||||||||||||||||||||||||||||||||||||||
Sbjct  1861  TACCTCCTAGTGGAGTGGCTTCAGAAATAAACCCTAGGATTTCATCATCTACTTTTGGAA  1802

Query  662   CTGATAATATCTGTGTTGCCTCCCTGGAAGAAACTGGATATTTGCATGCCAGTGAAGGCA  721
             ||||||||||||||||||||||||||||||||||||||||||||||||||||||||||||
Sbjct  1801  CTGATAATATCTGTGTTGCCTCCCTGGAAGAAACTGGATATTTGCATGCCAGTGAAGGCA  1742

Query  722   GCTGCCTGTCAACTTGCTGCCATTCTTCTTCAATTACTTTTAAAATAGATTCATGGAAGG  781
             ||||||||||||||||||||||||||||||||||||||||||||||||||||||||||||
Sbjct  1741  GCTGCCTGTCAACTTGCTGCCATTCTTCTTCAATTACTTTTAAAATAGATTCATGGAAGG  1682

Query  782   GAAAAGATAGTTCTGAGGCATCTATTTTATCATGCTGTGATTGCTTAGCCACTTCTAGAC  841
             ||||||||||||||||||||||||||||||||||||||||||||||||||||||||||||
Sbjct  1681  GAAAAGATAGTTCTGAGGCATCTATTTTATCATGCTGTGATTGCTTAGCCACTTCTAGAC  1622

Query  842   CTAAGGTAGTGAGTGAATGAGAGACAACAGTTTTGGCAAAAGAAGACATCAGT-CGGGAT  900
             ||||||||||||||||||||||||||||||||||||||||||||||||||| ||| ||
Sbjct  1621  CTAAGGTAGTGAGTGAATGAGAGACAACAGTTTTGGCAAAAGAAGACATCAGTTCGG-AT  1563

Query  901   C  901
             |
Sbjct  1562  C  1562
```

d. Reverse sequencing (vs. NM_003276.1)

```
1501 AGTGAGAAGTCAGTGGAGGAAAGGGATTCAGGTTCCTTTGTGGCATTTCAGAACATACCT
1561 GGATCCGAACTGATGTCTTCTTTTGCCAAAACTGTTGTCTCTCATTCACTCACTACCTTA
1621 GGTCTAGAAGTGGCTAAGCAATCACAGCATGATAAAATAGATGCCTCAGAACTATCTTTT
1681 CCCTTCCATGAATCTATTTTAAAAGTAATTGAAGAAGAATGGCAGCAAGTTGACAGGCAG
1741 CTGCCTTCACTGGCATGCAAATATCCAGTTTCTTCCAGGGAGGCAACACAGATATTATCA
1801 GTTCCAAAAGTAGATGATGAAATCCTAGGGTTTATTTCTGAAGCCACTCCACTAGGAGGT
1861 ATTCAAGCAGCCTCCACTGAGTCTTGCAATCAGCAGTTGGACTTAGCACTCTGTAGAGCA
1921 TATGAAGCTGCAGCATCAGCATTGCAGATTGCAACTCACACTGCCTTTGTAGCTAAGGCT
1981 ATGCAGGCAGACATTAGTCAAGCTGCACAGATTCTTAGCTCAGATCCTAGTCGTACCCAC
2041 CAAGCGCTTGGGATTCTGAGCAAAACATATGATGCAGCCTCATATATTTGTGAAGCTGCA
2101 TTTGATGAAGTGAAGATGGCTGCCCATACCATGGGAAATGCCACTGTAGGTCGTCGATAC
```

```
2161 CTCTGGCTGAAGGATTGCAAAATTAATTTAGCTTCTAAGAATAAGCTGGCTTCCACTCCC
2221 TTTAAAGGTGGAACATTATTTGGAGGAGAAGTATGCAAAGTAATTAAAAAGCGTGGAAAT
2281 AAACACTAGTAAAATTAAGGACAAAAAGACATCTATCTTATCTTTCAGGTACTTTATGCC
2341 AACATTTTCTTTTCTGTTAAGGTTGTTTTAGTTTCCAGATAGGGCTAATTACAAAATGTT
2401 AAGCTTCTACCCATCAAATTACAGTATAAAAGTAATTGCCTGTGTAGAACTACTTGTCTT
2461 TTCTAAAGATTTGCGTAGATAGGAAGCCTG
```

e. Combined sequencing (forward and reverse sequences)

```
1501 AGTGAGAAGTCAGTGGAGGAAAGGGATTCAGGTTCCTTTGTGGCATTTCAGAACATACCT
1561 GGATCCGAACTGATGTCTTCTTTTGCCAAAACTGTTGTCTCTCATTCACTCACTACCTTA
1621 GGTCTAGAAGTGGCTAAGCAATCACAGCATGATAAAATAGATGCCTCAGAACTATCTTTT
1681 CCCTTCCATGAATCTATTTTAAAAGTAATTGAAGAAGAATGGCAGCAAGTTGACAGGCAG
1741 CTGCCTTCACTGGCATGCAAATATCCAGTTTCTTCCAGGGAGGCAACACAGATATTATCA
1801 GTTCCAAAAGTAGATGATGAAATCCTAGGGTTTATTTCTGAAGCCACTCCACTAGGAGGT
1861 ATTCAAGCAGCCTCCACTGAGTCTTGCAATCAGCAGTTGGACTTAGCACTCTGTAGAGCA
1921 TATGAAGCTGCAGCATCAGCATTGCAGATTGCAACTCACACTGCCTTTGTAGCTAAGGCT
1981 ATGCAGGCAGACATTAGTCAAGCTGCACAGATTCTTAGCTCAGATCCTAGTCGTACCCAC
2041 CAAGCGCTTGGGATTCTGAGCAAAACATATGATGCAGCCTCATATATTTGTGAAGCTGCA
2101 TTTGATGAAGTGAAGATGGCTGCCCATACCATGGGAAATGCCACTGTAGGTCGTCGATAC
2161 CTCTGGCTGAAGGATTGCAAAATTAATTTAGCTTCTAAGAATAAGCTGGCTTCCACTCCC
2221 TTTAAAGGTGGAACATTATTTGGAGGAGAAGTATGCAAAGTAATTAAAAAGCGTGGAAAT
2281 AAACACTAGTAAAATTAAGGACAAAAAGACATCTATCTTATCTTTCAGGTACTTTATGCC
2341 AACATTTTCTTTTCTGTTAAGGTTGTTTTAGTTTCCAGATAGGGCTAATTACAAAATGTT
2401 AAGCTTCTACCCATCAAATTACAGTATAAAAGTAATTGCCTGTGTAGAACTACTTGTCTT
2461 TTCTAAAGATTTGCGTAGATAGGAAGCCTG
```

Appendix II

List of Publications

- **Elcock LS** and Bridger JM (2010) Exploring the relationship between interphase gene positioning, transcriptional regulation and the nuclear matrix. *Biochemical Society Transactions* 38 (Pt 1):263-7.
- **Elcock LS** and Bridger JM (2008) Exploring the effects of a dysfunctional nuclear matrix. *Biochemical Society Transactions* 36 (Pt 6):1378-83.
- Mehta IS, **Elcock LS**, Amira M, Kill IR and Bridger JM (2008) Nuclear Motors and Nuclear Structures containing A-type lamins and emerin: is there a functional link? *Biochemical Society Transactions* 36 (Pt 6):1384-88.
- **Elcock LS** and Bridger JM (in press) FISH extended chromatin fibres and DNA halos. In E Volpi and JM Bridger, ed. *Methods in Molecular Biology*. Humana Press.